# Physiological Assessment of Coronary Stenoses and the Microcirculation

Javier Escaned
Justin Davies
*Editors*

Springer

Physiological Assessment of Coronary Stenoses and the Microcirculation

Javier Escaned
Justin Davies
*Editors*

# Physiological Assessment of Coronary Stenoses and the Microcirculation

Springer

*Editors*
**Javier Escaned**
Hospital Clínico San Carlos
Universidad Complutense de Madrid
Madrid
Spain

**Justin Davies**
Imperial College London
London
UK

ISBN 978-1-4471-5244-6 ISBN 978-1-4471-5245-3 (eBook)
DOI 10.1007/978-1-4471-5245-3

Library of Congress Control Number: 2017940189



Printed on acid-free paper

This Springer imprint is published by Springer Nature
The registered company is Springer-Verlag London Ltd.
The registered company address is: 236 Gray's Inn Road, London WC1X 8HB, United Kingdom

# Preface

This book was completed in 2016, when coronary physiology probably reached its maturity.

Forty years had passed since the publication of the landmark articles linking stenosis severity and coronary flow impairment. The impact of this research was enormous and triggered the development of numerous invasive and non-invasive technologies aimed at interrogating the coronary circulation with a new index, coronary flow reserve.

Twenty years later, fractional flow reserve (FFR) demonstrated its diagnostic utility as a pressure-derived index of stenosis severity. Over the next decades, FFR was used in clinical trials to demonstrate the importance of functional guidance of coronary revascularization and demonstrated, this time without any residual doubt, that angiography is a deceptive technique in assessing functional relevance of coronary stenoses.

Today, two decades later, a new revolution in coronary physiology is occurring applying computational fluid dynamics and in silico simulations to coronary imaging with the aim of calculating FFR-like indices without the need for intracoronary instrumentation. Furthermore, new indices such as the instantaneous wave free ratio (iFR) have been developed to facilitate easier pressure guidewire interrogation of the coronary arteries and hopefully increase its use.

Despite this progress and the growing interest generated by these developments, adoption of coronary physiology in clinical practice is still lagging. The main aim of this book is to serve both as an introduction to coronary physiology for all those interested in the field of cardiovascular disease and as a companion for practicing clinical and interventional cardiologists.

In that regard, this book provides a comprehensive approach to the interrogation of different domains of the coronary circulation. In 2016, coronary physiology is still largely stenosis centered. Assessment of the coronary microcirculation is seldom performed in the catheterization laboratory, and few centers routinely perform coronary vasomotion tests. This occurs despite growing information on the implications that microcirculatory and vasomotion disorders have for both patient's symptoms and prognosis. It is quite likely that a more extensive interest in these topics will foster the development and availability of diagnostic methods to interrogate the coronary circulation beyond the stenoses. And if this happens, surely new avenues for research and patient care will follow.

We are extremely grateful to all the authors for sharing their expertise in the topics covered in the many chapters of this book. We are also indebted to our Deputy Editors Hernán Mejía-Rentería, MD, and Nicola Ryan, MB, BCh, for their support throughout the edition of this book, and to Sara Fernández, MSc, for valuable technical assistance.

Madrid, Spain — Javier Escaned
London, UK — Justin Davies

# Contents

## V Indices of Coronary Resistance



## VI Fractional Flow Reserve (FFR)



## VII Instantaneous Wave Free Ratio (iFR)



## VIII Multimodality Assessment of the Coronary Circulation



## IX Wave Intensity Analysis



## X Assessment of Endothelial Dysfunction

## XI Research Models

# Contributors


**Diego Arroyo**
Department of Cardiology
Fribourg University and Hospital
Fribourg, Switzerland

**Sérgio Baptista**
Hospital do Espírito Santo Évora
Evora, Portugal
sergio.b.baptista@gmail.com

**Christopher J. Broyd**
Interventional Cardiology Unit
Department of Cardiology
Hospital Clínico San Carlos
Madrid, Spain

Imperial College London
London, UK
c.broyd@imperial.ac.uk

**Lorena Casadonte**
Department of Biomedical Engineering and Physics
Academic Medical Center
University of Amsterdam
Amsterdam, The Netherlands
l.casadonte@amc.uva.nl

**Carlos A. Collet**
Cardiology
Academic Medical Center
Amsterdam, The Netherlands
carloscollet@gmail.com

**Stéphane Cook**
Department of Cardiology
Fribourg University & Hospital
Fribourg, Switzerland
stephane.cook@unifr.ch

**Justin Davies**
Imperial College London
London, UK
justindavies@heart123.com

**Harry R. Davis**
CVPath Institute, Inc
Gaithersburg, MD, USA

**Pedro de Araújo Gonçalves**
Hospital do Espírito Santo Évora
Evora, Portugal
paraujogoncalves@yahoo.co.uk

**Guus A. de Waard**
Department of Cardiology
VU University Medical Center
Institute for Cardiovascular Research
Amsterdam, The Netherlands
g.dewaard@vumc.nl

**María Del Trigo**
Interventional Cardiology Unit
Department of Cardiology
Hospital Clínico San Carlos
Madrid, Spain
mariadeltrigo@hotmail.com

**Fernando Dominguez**
Heart Failure and Inherited Cardiac Diseases Unit
Department of Cardiology
Hospital Universitario Puerta de Hierro
Madrid, Spain
fdominguezrodriguez@gmail.com

**Dirk J. Duncker**
Division of Experimental Cardiology
Department of Cardiology
Thoraxcenter
Erasmus MC
University Medical Center Rotterdam
Rotterdam, The Netherlands
d.duncker@erasmusmc.nl

**Mauro Echavarría-Pinto**
Interventional Cardiology Unit
Department of Cardiology
Hospital Clínico San Carlos
Madrid, Spain
mauroep@hotmail.com

**Javier Escaned**
Interventional Cardiology Unit
Department of Cardiology
Hospital Clínico San Carlos
Madrid, Spain
escaned@secardiologia.es

**Aloke V. Finn**
CVPath Institute, Inc
Gaithersburg, MD, USA
afinn@cvpath.org

**Pablo Garcia-Pavia**
Heart Failure and Inherited Cardiac Diseases Unit
Department of Cardiology
Hospital Universitario Puerta de Hierro
Madrid, Spain
pablogpavia@yahoo.es

**Chrysafios Girasis**
Department of Cardiology
Onassis Cardiac Surgery Center
Athens, FL, Greece
chrisgirasis@gmail.com

**Nieves Gonzalo**
Interventional Cardiology Unit
Department of Cardiology
Hospital Clínico San Carlos
Madrid, Spain
Nieves_gonzalo@yahoo.es

**Ilkka H. A. Heinonen**
Division of Experimental Cardiology
Department of Cardiology
Thoraxcenter
Erasmus MC
University Medical Center Rotterdam
Rotterdam, The Netherlands

Turku PET Centre
Turku, Finland

Department of Clinical Physiology and Nuclear Medicine
University of Turku and Turku University Hospital
Turku, Finland
ilkka.heinonen@utu.fi

**Maurits R. Hollander**
Department of Cardiology
VU University Medical Center
Amsterdam, The Netherlands
m.hollander@vumc.nl

**Pilar Jiménez-Quevedo**
Interventional Cardiology Unit
Department of Cardiology
Hospital Clínico San Carlos
Madrid, Spain
pjimenezq@salud.madrid.org

**Michael Joner**
CVPath Institute, Inc
Gaithersburg, MD, USA
joner@dhm.mhn.de

**Morton J. Kern**
Long Beach Veterans Affairs Medical Center
University of California
Irvine Medical Center
Long Beach, CA, USA
mkern@uci.edu

**Frank D. Kolodgie**
CVPath Institute, Inc
Gaithersburg, MD, USA

**Antonio Maria Leone**
Institute of Cardiology
Catholic University of the Sacred Heart
Rome, Italy
antoniomarialeone@gmail.com

**Amir Lerman**
Cardiovascular Institute Hospital Clínico San Carlos
Madrid, Spain
lerman.amir@mayo.edu

**Fernando Macaya**
Interventional Cardiology Unit
Department of Cardiology
Hospital Clínico San Carlos
Madrid, Spain
webjazzler@gmail.com

**Koen M. Marques**
Department of Cardiology
VU University Medical Center
Institute for Cardiovascular Research
Amsterdam, The Netherlands
km.marques@vumc.nl

**Yasushi Matsuzawa**
Cardiovascular Institute Hospital Clínico San Carlos
Madrid, Spain
matsuzawa-yuji@sumitomo-hp.or.jp

**Hernán Mejía-Rentería**
Interventional Cardiology Unit
Department of Cardiology
Hospital Clinico San Carlos
Madrid, Spain
hernan_m_r@yahoo.com

**Daphne Merkus**
Division of Experimental Cardiology
Department of Cardiology
Thoraxcenter
Erasmus MC
University Medical Center Rotterdam
Rotterdam, The Netherlands

**Hiroyoshi Mori**
CVPath Institute, Inc
Gaithersburg, MD, USA

**David Neves**
Hospital do Espírito Santo Évora
Evora, Portugal
dneves@hevora.min-saude.pt

**Giampaolo Niccoli**
Institute of Cardiology
Catholic University of the Sacred Heart
Rome, Italy
gniccoli73@hotmail.it

**Sukhjinder Nijjer**
Hammersmith Hospital
Imperial College Healthcare NHS Trust
London, UK
s.nijjer@yahoo.co.uk

**Luis Nombela-Franco**
Interventional Cardiology Unit
Department of Cardiology
Hospital Clínico San Carlos
Madrid, Spain
luisnombela@yahoo.com

**Ivan Nuñéz-Gil**
Interventional Cardiology Unit
Department of Cardiology
Hospital Clínico San Carlos
Madrid, Spain
ibnsky@yahoo.es

**Peter Ong**
Department of Cardiology
Robert-Bosch Krankenhaus
Stuttgart, Germany
Peter.Ong@rbk.de

**Yoshinobu Onuma**
Department of Cardiology, Erasmus Medical Center
Madrid, Spain
yoshinobuonuma@gmail.com

**Kim Parker**
Imperial College London
London, UK
k.parker@imperial.ac.uk

**Ricardo Petraco**
Imperial College London
London, Uk
r.petraco@imperial.ac.uk

**Jan J. Piek**
AMC Heart Centre
Academic Medical Centre
University of Amsterdam
Amsterdam, The Netherlands
j.j.piek@amc.nl

**Serban Puricel**
Department of Cardiology
Fribourg University & Hospital
Fribourg, Switzerland
serbanpurciel@icloud.com

**Alicia Quirós**
Interventional Cardiology Unit
Department of Cardiology
Hospital Clínico San Carlos
Madrid, Spain
alicia.quiros@unileon.es

**Ruben Ramos**
Hospital do Espírito Santo Évora
Evora, Portugal
ruben.a.b.ramos@gmail.com

**Luís Raposo**
Hospital do Espírito Santo Évora
Evora, Portugal
lfor.md@gmail.com

**Vera Rodriguez**
Interventional Cardiology Unit
Department of Cardiology
Hospital Clínico San Carlos
Madrid, Spain
verarodriguez@yahoo.com

**Nicola Ryan**
Interventional Cardiology Unit
Department of Cardiology
Hospital Clínico San Carlos
Madrid, Spain
nicolaryan@gmail.com

**Giancarla Scalone**
Institute of Cardiology
Catholic University of the Sacred Heart
Rome, Italy
gcarlascl@gmail.com

**Udo Sechtem**
Department of Cardiology
Robert-Bosch Krankenhaus
Stuttgart, Germany
Udo.Sechtem@rbk.de

**Christian Seiler**
Department of Cardiology
University Hospital
Bern, Switzerland
christian.seiler@insel.ch

**Patrick W. Serruys**
International Centre for Circulatory Health NHLI
Imperial College of London
Rotterdam, The Netherlands
Patrick.w.j.c.serruys@gmail.com

**Arnold H. Seto**
Long Beach Veterans Affairs Medical Center
University of California
Irvine Medical Center
Long Beach, CA, USA
Arnold.seto@va.gov

**Murat Sezer**
Istanbul Faculty of Medicine
Department of Cardiology
Istanbul University
Istanbul, Turkey
sezermr@gmail.com

**Maria Siebes**
Department of Biomedical Engineering and Physics
Academic Medical Center
University of Amsterdam
Amsterdam, The Netherlands
m.siebes@amc.uva.nl

**Oana Sorop**
Division of Experimental Cardiology
Department of Cardiology
Thoraxcenter
Erasmus MC
University Medical Center Rotterdam
Rotterdam, The Netherlands
o.sorop@erasmusmc.nl

**Charles Taylor**
Cardiovascular Institute Hospital Clínico San Carlos
Madrid, Spain
taylor@heartflow.com

**Mario Togni**
Department of Cardiology
Fribourg University and Hospital
Fribourg, Switzerland
mario.togni@unifr.ch

**Sabahattin Umman**
Istanbul Faculty of Medicine
Department of Cardiology
Istanbul University
Istanbul, Turkey
ummans@e-kolay.net

**Luis Felipe Valenzuela-García**
Cardiovascular Institute Hospital Clínico San Carlos
Madrid, Spain
lfvgmjrh1@yahoo.es

**Tim P. van de Hoef**
AMC Heart Centre
Academic Medical Centre
University of Amsterdam
Amsterdam, The Netherlands
t.p.vandehoef@amc.uva.nl

**Nina W. van der Hoeven**
Department of Cardiology
VU University Medical Center
Amsterdam, The Netherlands
ni.vanderhoeven@vumc.nl

**Niels van Royen**
Department of Cardiology
VU University Medical Center
Institute for Cardiovascular Research
Amsterdam, The Netherlands
n.vanroyen@vumc.nl

**Renu Virmani**
CVPath Institute, Inc
Gaithersburg, MD, USA
rvirmani@cvpath.org

**Nicolaas Westerhof**
Department of Cardiology
VU University Medical Center
Institute for Cardiovascular Research
Amsterdam, The Netherlands
n.westerhof@vumc.nl

# The Physiology of the Coronary Circulation

Contents

# Hemodynamic Effects of Epicardial Stenoses

*Lorena Casadonte and Maria Siebes*




J. Escaned, J. Davies (eds.), *Physiological Assessment of Coronary Stenoses and the Microcirculation*,
DOI 10.1007/978-1-4471-5245-3_1

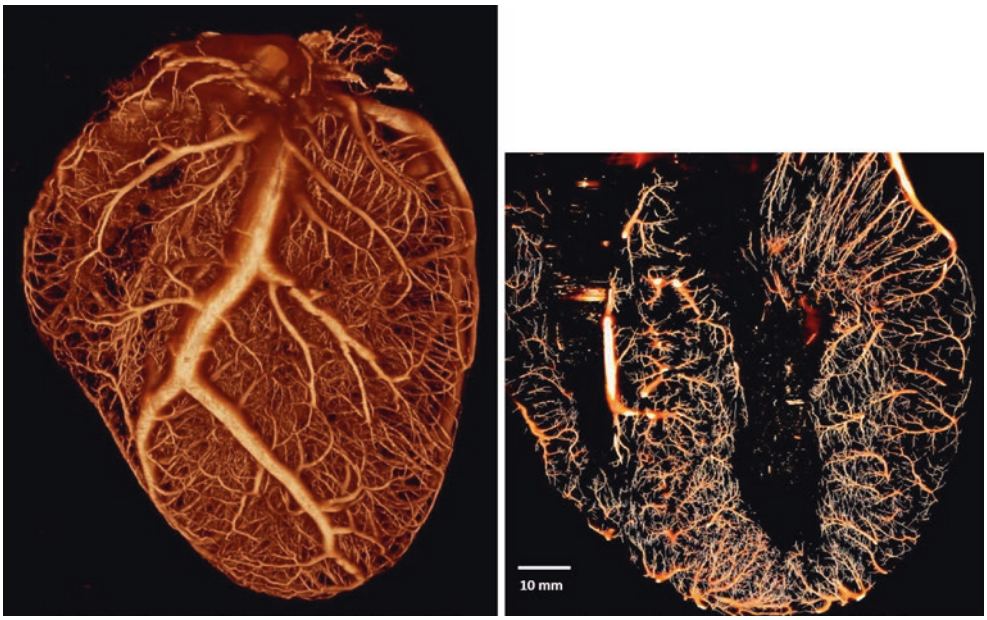


**Fig. 1.1** 3D image of coronary arteries of a dog heart obtained by a novel cryomicrotome technique with epifluorescence imaging. The vessels were filled with fluorescent cast material, and the frozen heart was alternately sliced at 40 μm and the bulk surface imaged with a high-resolution CCD camera [4]. The right panel shows a longitudinal cross section of a 2-mm-thick maximal intensity projection of transmural vessels (partially skeletonized) where the branching pattern of penetrating vessels is clearly visible

## 1.1 Principles of Coronary Physiology

A comprehensive understanding of coronary physiology is fundamental to aid in the interpretation of coronary pressure and flow signals obtained in patients with coronary artery disease. The heart is perfused by an intricate network of arteries that supply oxygen and nutrients to this continuously active muscle. Multiple branching vessels arise from epicardial conduit arteries (Fig. 1.1) and perfuse small volumes at the subepicardial layer of the myocardium, whereas the subendocardium is perfused by penetrating arteries that pass through the outer layers of the myocardium and only branch out into numerous vessels once they have reached the inner layer, where they supply larger volumes of myocardial tissue [1–4].

From a physical standpoint, minimal vascular resistance is principally determined by the segmental dimensions (length and diameter) of the distributed maximally dilated network. Thus, in the absence of epicardial coronary artery stenosis, maximal coronary flow is a function of the coronary driving pressure and of the maximal surface area of the dilated coronary resistance vessels. In this respect it is important to recall that all blood vessels are essentially elastic tubes when active smooth muscle tone is minimal. Once coronary arterioles are maximally dilated, they passively react to changes in distending and extravascular pressure, i.e., their diameter becomes pressure dependent [5–7].

**Coronary pressure-flow relations** Oxygen extraction from the coronary circulation is near maximal at rest, and raised myocardial oxygen demand is met by a corresponding change in coronary blood flow. The dynamic match to oxygen consumption at constant arterial pressure is denoted as metabolic flow adaptation or functional hyperemia. For a given cardiac workload, coronary blood flow remains constant over a wide range of arterial perfusion pressures (typically from about 60 to 140 mmHg) by an intrinsic mechanism denoted as autoregulation [8]. This entails coronary resistance changes in a direction parallel to the change in perfusion pressure. Importantly, autoregulation fails at higher pressures in subendocardial than subepicardial vessels [9, 10]. All arteries and arterioles contribute to flow control by changing their smooth muscle tone. Resistance to flow is negligible in large epicardial vessels, and most of coronary resistance resides in the intramural microvessels smaller than approximately 300 μm in diameter [11]. The regulation of coronary microvascular resistance includes integrative mechanisms of metabolic, myogenic, and flow-dependent vascular control, discussed in more detail elsewhere in this book. Distributed vasodilation decreases local microvascular resistance in the normal heart to maintain resting flow at the autoregulatory level as coronary pressure falls, e.g., in the presence of an epicardial coronary stenosis [12]. Substantial vasodilator reserve exists to increase flow above resting level during exercise, and values of 4–5 times above resting flow levels have been reported for humans [13–17]. Vasodilation results in a substantial redistribution of microvascular resistance compared to baseline conditions. Chilian and colleagues [11] reported that the resistance of arterial microvessels (<170 μm diameter) decreased nearly 15-fold for a sixfold increase in flow after dipyridamole administration, while papaverine caused preferential vasodilation of larger arterioles (>200 μm diameter) [18].

At low pressures the pressure-flow curve declines in a convex fashion toward the flow axis, and actual zero-flow pressure ($P_{zf}$) is only 2–4 mmHg above coronary sinus pressure at steady state [19]. The curvature reflects the progressive increase in resistance that results from the decrease in vascular transmural pressure. The curvilinear shape of this

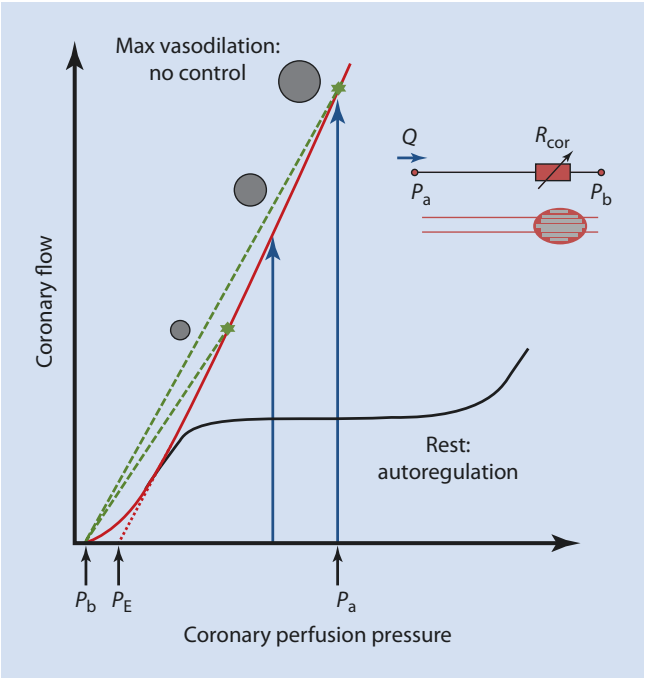


**Fig. 1.2** Coronary pressure-flow relations in the absence of a stenosis. At rest, flow (*Q*) is maintained over a large range of arterial perfusion pressures. At maximal vasodilation (*red line*), flow can increase 4–5 times at normal arterial pressure ($P_a$); however, control is exhausted and flow reserve depends on pressure (blue arrows). The line curves at low pressures toward a zero flow intercept, which is the effective back pressure ($P_b$) to flow and only slightly above venous pressure. $P_E$ is obtained by linear extrapolation of the straight part of the pressure-flow curve. As pressure falls, the diameter of the passive resistance vessels decreases (*circles*), and microvascular resistance ($R_{cor}$) gradually increases. The *dashed lines* (*green*) indicate pressure-flow lines at constant minimal resistance, shown here for a normal and a reduced perfusion pressure (*stars*). The inverse of the slope of these lines represents minimal resistance

pressure-flow curve is important in defining coronary vascular resistance, and the influence of distributed capacitive effects should be kept in mind when approximating zero-flow pressure by linear extrapolation to the pressure axis from data obtained after cessation of flow in epicardial vessels [19]. Moreover, data in isolated maximally dilated dog hearts suggest that $P_{zf}$ is likely distributed across the left ventricular wall rather than being a function of global flow [20].

Typical coronary pressure-flow relations at autoregulation and at maximal vasodilation are schematically shown in Fig. 1.2.

The coronary pressure-flow relation at maximal vasodilation is a steep line with a nonzero pressure intercept, and flow is now a function of perfusion pressure. Although the pressure-flow curve at vasodilation (without control) appears relatively straight at pressures above about 40 mmHg, this line is likely the result of interacting mechanisms which are obscured from signals obtained at the epicardial arteries [21]. These include time constants involved in emptying microvascular compliance and coronary resistance changes that are affected by the greater narrowing of microvessels at the lower pressure range due to the strong nonlinear pressure-distensibility relation for vessels with relaxed smooth muscle tone [6, 22–26].

Coronary blood flow is principally determined by the driving pressure and the resistance of the coronary vascular bed. In the absence of an epicardial stenosis, the driving pressure is the difference between aortic input pressure $P_a$ and the effective back pressure $P_b$ at which flow becomes zero. Since steady-state $P_b$ is difficult to assess in humans, venous pressure can be used as a reasonable approximation. In equivalence to Ohm's law, the resistance *R* of a vascular compartment is defined as the pressure drop $\Delta P$ across that compartment divided by flow *Q*:

$$R = \Delta P / Q \qquad \textbf{(1.1)}$$

By analogy, coronary resistance at vasodilation is then the inverse slope of the line connecting $P_b$ on the pressure axis with the data point on the pressure-flow line at a certain arterial pressure (star symbol in Fig. 1.2). The decreasing slope of these lines reflects the increased coronary resistance at lower perfusion pressure, e.g., distal to a stenosis.

At vasodilation, coronary pressure and flow are *not* linearly related and do not pass through the origin. The intercept on the pressure axis makes this relation incremental linear, and the change in flow is not proportional to the change in pressure [26, 27]. Hence, the inverse slope of the hyperaemic pressure-flow line is not a measure of coronary resistance. Although the units are those of resistance, the inverse slope is the change in pressure divided by the *change* in flow. For example, the parallel rightward shift of this relationship from the arrested to the beating heart [28] clearly implies an increase in resistance due to cardiac contraction, but resistance determined from the slope would remain constant. Minimal coronary resistance has been shown to increase with decreasing perfusion pressure (and vice versa) in animals and humans [5, 6, 29, 30], and models that assume a pressure-independent microvascular resistance at maximal dilation are rather unrealistic.

Other influences can independently alter the coronary pressure-flow relationships illustrated schematically in Fig. 1.3.

An increase in oxygen consumption at rest shifts the autoregulatory plateau upward (1), which implies that autoregulation fails at higher pressure. Additionally, an increased resistance with lower maximal flow at the same pressure ensues when the slope of the pressure-flow relation for maximally dilated vessels decreases (2), as with left ventricular hypertrophy, increased blood viscosity in polycythemia, or small vessel disease due to, e.g., hypertension [31, 32]. Notably, a rise in myocardial wall stress due to cardiac contraction induces a rightward shift of the hyperemic pressure-flow curve. This parallel shift between a non-beating and a beating heart was shown to amount to half of the mean left ventricular pressure [26, 28]. Several other factors can raise zero-flow pressure (3), such as elevated left ventricular end-diastolic pressure or coronary venous pressure [33, 34], and collateral flow, which tends to decrease the curvature at the low-pressure range [35, 36]. It is possible for several factors to operate

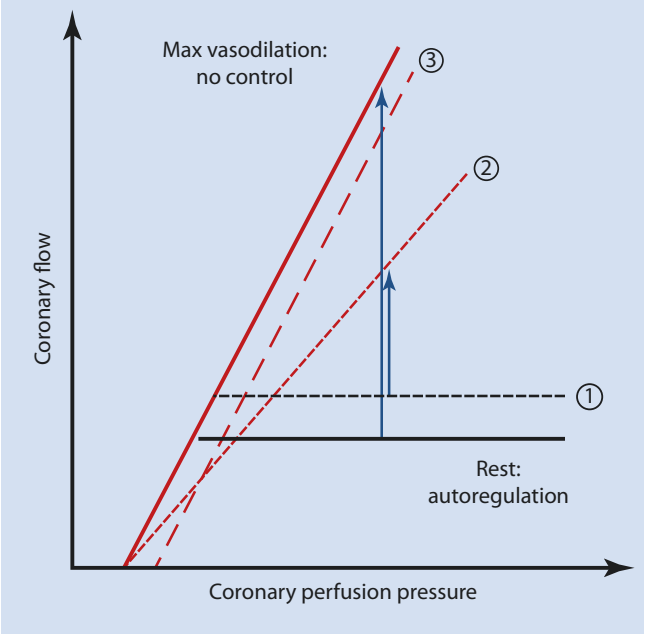


**Fig. 1.3** Factors that decrease coronary flow reserve at any perfusion pressure. (*1*) A raised autoregulated flow, e.g., due to increased oxygen consumption. (*2*) When the slope of the pressure-flow line during maximal vasodilation is reduced, the maximum flow falls. (*3*) A parallel shift to the right of the pressure-flow relationship during vasodilation increases zero-flow pressure. Note that autoregulation fails at higher pressures for each condition

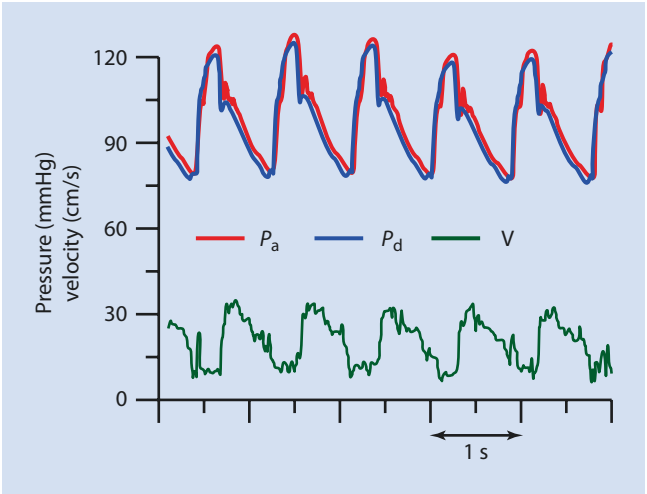


**Fig. 1.4** Typical pressure and flow velocity waveforms obtained in a normal coronary artery at rest. Coronary flow is maximal during the diastolic phase. $P_a$ aortic pressure, $P_d$ distal coronary pressure, *v* flow velocity

synergistically, leading to a more pronounced reduction in flow reserve for any given perfusion pressure and to failure of autoregulation at a higher pressure. These concepts have been summarized in several publications [10, 26, 32, 37, 38].

**Determinants of coronary blood flow** The main cause for the pulsatile behavior of coronary blood flow is cardiac contraction. In contrast to the systemic circulation, coronary inflow is low in systole despite higher input pressure and highest in diastole when aortic input pressure declines (Fig. 1.4).

The forces exerted by the squeezing action of the heart muscle on the compressible vessels embedded in the myocardium vary the intramural blood volume throughout a heartbeat and lead to an impediment of systolic inflow and augmentation of venous outflow during systole. The out-of-phase behavior of these signals can be explained by the intramyocardial pump model [22, 23, 39] and varying elastance concept [40]. Basically, the transmural tissue pressure gradient generated by the intramyocardial pump that acts on the intramyocardial compliance is modulated by the time-varying elastance of the myocardium and vessels during the cardiac cycle [25, 41]. Both models assume that coronary resistance is volume dependent. The distensibility of the intramural vessels in interaction with the surrounding myocardial tissue constitutes the so-called intramyocardial compliance. The rate of volume exchange between systole and diastole (capacitive flow) modifies the microvascular inflow and outflow resistances [42, 43]. Due to the longtime constants involved in changing the blood volume of the large intramyocardial compliance, microvascular resistance is varying throughout the cardiac cycle and cannot simply be divided into systolic and diastolic components.

**Transmural flow and subendocardial vulnerability** A dense network of branching elastic vessels delivers blood flow across the myocardium; however, the flow distribution across the myocardium is not uniform. Studies in animals and humans have demonstrated a profound perfusion heterogeneity both across and within layers [44–46], which makes it difficult to assess subendocardial perfusion from epicardial intracoronary measurements.

Several mechanisms contribute to the subendocardial vulnerability to ischemia [47]. The impeding effect of extravascular compression during cardiac contraction is stronger at the subendocardium. This is partially compensated by the larger total volume of the resistance vessels in the inner than the outer layer of the heart wall, yielding a lower intrinsic resistance at full dilation [48]. Subendocardial perfusion was shown to be about 50 % higher than at the subepicardium in the non-beating dog heart [2]. Transmural perfusion during maximal coronary vasodilation was nearly uniform at a heart rate of 100 bpm, whereas subendocardial flow was about half of subepicardial flow at a heart rate of about 200 bpm [49]. This implies that over heart rates ranging from 0 to 200 bpm, heart contraction may reduce subendocardial flow by a factor of 3, while subepicardial flow may even slightly increase at elevated heart rates [50].

Clearly, factors that affect the rate of filling of intramural vessels in diastole, such as perfusion pressure and the duration of diastole [51], modulate microvascular conductance at the subendocardium. Perfusion pressure is generally lower in the subendocardial layer due to the longer path length (greater longitudinal pressure drop) for blood to reach the subendocardium via transmural penetrating vessels. A decreased perfusion pressure tends to redistribute blood flow

away from the subendocardium and causes a reduction of the subendocardial/subepicardial blood flow ratio [52]. Further reduction in perfusion pressure distal to a stenosis decreases the diameter of subendocardial arterioles more than the subepicardial arterioles, and additionally, a stenosis selectively decreases the dilatory response of subendocardial arterioles [53]. Another confounding factor is inadequate perfusion time, expressed as the diastolic time fraction, DTF, which leads to insufficient flow to subendocardium, while the more superficial layers may still be adequately perfused. Moreover, the effect of DTF on subendocardial blood flow is exacerbated at low perfusion pressure distal to a stenosis [54–56]. Interestingly, DTF was shown to be prolonged at reduced coronary pressure distal to a stenosis, which may act as a protective regulatory mechanism when vasodilatory reserve is exhausted [57].

## 1.2 Stenosis Hemodynamics

This section provides an overview of stenosis fluid dynamics and its mathematical description as derived from in vitro and in vivo experiments.

**Stenosis pressure drop-flow (Δ*P*-*Q*) characteristics** Pressure is lost due to viscous friction, when blood flows through a vessel. For steady and laminar flow, the pressure drop $\Delta P$ over a uniform tube of length $L$ is given by Poiseuille's law as

$$\Delta P = \frac{32\ \mu L}{D^2} v \tag{1.2}$$

where $\mu$ is the viscosity, $D$ is the diameter of the tube, and $v$ is the mean cross-sectional velocity. In terms of volume flow $Q$ and diameter $D$, this equation becomes

$$\Delta P = \frac{128\ \mu L}{\pi D^4} Q \tag{1.3}$$

This implies that for a given tube dimension and length, the resistance $R = \Delta P/Q$ is constant. Viscous shear determines viscous energy losses along the entire length of an artery. The pressure drop increases with the inverse fourth power of the tube diameter, i.e., when the diameter is reduced by factor of 2, the resistance increases 16 times for the same flow and unit length. This relationship clearly shows the dominant influence of vessel diameter, and both active and passive mechanisms can substantially change vessel resistance and flow.

The main assumptions for Poiseuille's law are (1) a rigid, straight tube of uniform cross section, (2) steady, laminar flow with a parabolic velocity profile, and (3) constant viscosity, i.e., blood is considered a Newtonian fluid. These assumptions are far from true in curved, branching, and compliant vessels with pulsatile blood flow, but Poiseuille's law can serve as a first-order approximation.

For a change in diameter along the tube, conservation of mass applied to fluid transport comes into play. Conservation of mass states that the volume of blood entering a vessel per unit time is equal to the rate at which it leaves the vessel. This is described by the so-called continuity equation, with $A$ the cross-sectional area:

$$Q = A_1 v_1 = A_2 v_2 = \text{constant} \tag{1.4}$$

Bernoulli's law relates blood pressure to flow velocity $v$ and is based on the conservation of energy and conservation of momentum. It states that the sum of static pressure, hydrostatic pressure (potential energy), and dynamic pressure (kinetic energy) remains constant:

$$P_{tot} = P + \rho g h + \tfrac{1}{2}\rho v^2 = \text{constant} \tag{1.5}$$

where ρ is the blood density, $g$ is the gravitational acceleration, and $h$ is the height of the fluid column above a reference level. Pressure losses due to friction are neglected (inviscid flow is assumed), and the fluid is considered incompressible, with constant density. Note that for a blood density of 1.06 g/cm$^3$, a difference in hydrostatic pressure (mmHg) is related to a change in the height (h, cm) by $\Delta P = \Delta h \cdot 0.78$. If the height is constant, then Eq. 1.5 reduces to

$$P_1 + \tfrac{1}{2}\rho v_1^2 = P_2 + \tfrac{1}{2}\rho v_2^2 \tag{1.6}$$

As blood enters a narrowed section, the velocity $v$ increases proportional to the decrease in cross-sectional area of the vessel, and pressure is lost ($P_2 < P_1$) due to convective acceleration ($v_2 > v_1$), with conversion of pressure to kinetic energy, as depicted in Fig. 1.5. In addition, there is a pressure drop due to viscous losses as blood moves through the stenosis.

Under ideal circumstances, pressure would be recovered once the diverging section is reached where the flow decelerates. However, blood emerges from the stenosis as an inertial jet, leading to flow separation and formation of a recirculation zone, with eddies and viscous shear stresses between slow and fast moving fluid particles. The extent of this recirculation zone depends on stenosis area reduction and varies with flow [58, 59]. In addition, significant irreversible losses are incurred due to viscous friction along the length of the converging and narrowed section, which can be approximated by Poiseuille's law for the reduced diameter in the narrowed section. As a result, pressure is lowest inside the narrowed stenosis section, close to the point of flow separation, and only a small portion of kinetic energy is converted back to pressure energy downstream of the stenosis.

Based on a series of experiments with steady and pulsatile flows through models of concentric and eccentric stenoses in the 1970s, Young and co-workers [60–62] developed an empirical relationship describing the pressure drop across as a function of stenosis geometry. In essence, the total pressure drop across a stenosis is a quadratic function of flow and equals the sum of viscous losses along the entrance and throat of the stenosis, $\Delta P_v$, that are linearly related to flow and inertial losses at the exit of the stenosis, $\Delta P_e$, that scale with the square of the flow:

$$\Delta P = \Delta P_v + \Delta P_e \tag{1.7}$$

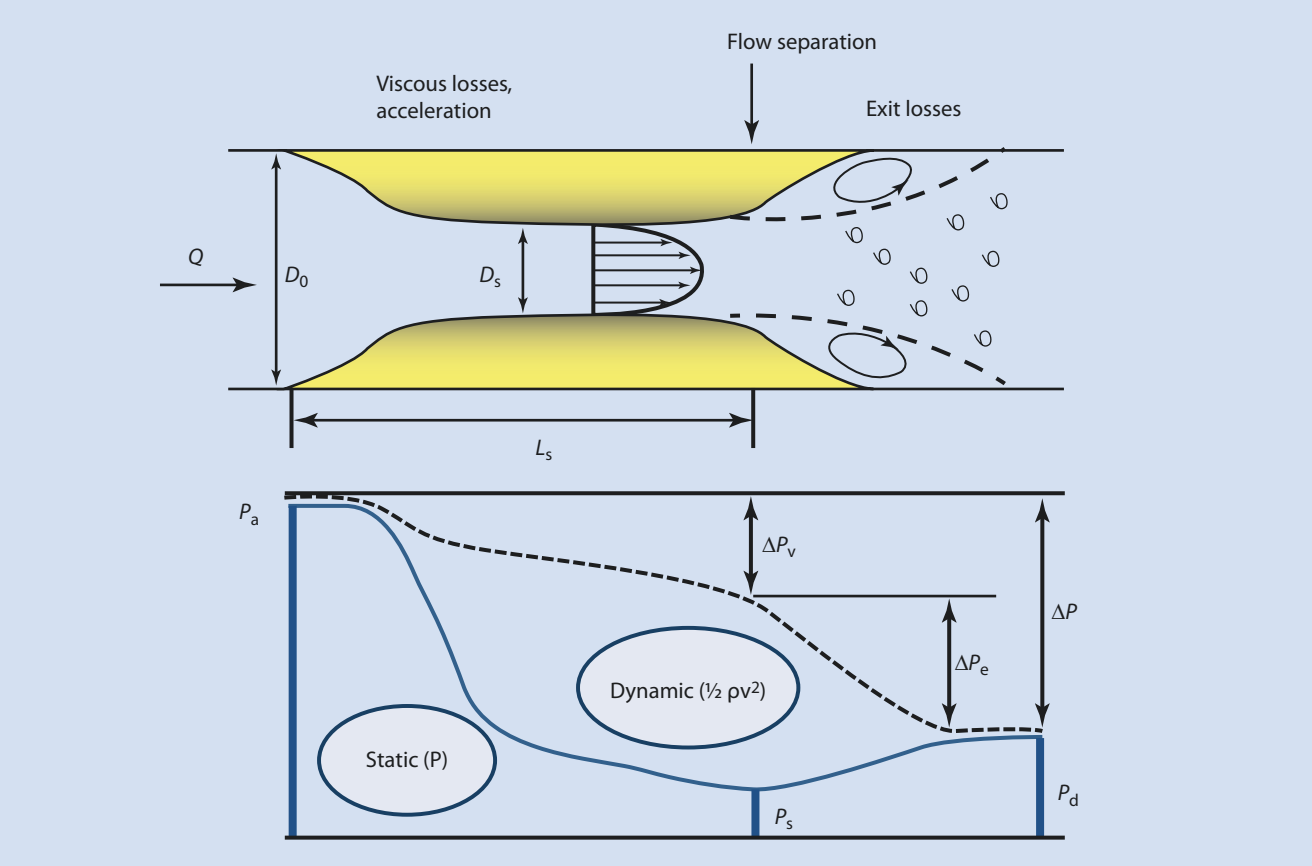


**Fig. 1.5** Stenosis flow field (*top*) and energy loss (*bottom*). Pressure is lost by viscous friction along the converging and narrowed section. The convective acceleration due to diameter reduction causes conversion from static pressure energy to kinetic energy, with minimal pressure close to the point of flow separation. Exit losses are incurred at the expansion zone where the high-velocity jet leaving the narrowed section leads to formation of eddies and energy is converted to heat. The total pressure drop ($\Delta P$) is the sum of viscous losses ($\Delta P_v$) that scale linearly with flow and exit losses ($\Delta P_e$) that increase with the square of flow. $D_0$ *and* $D_s$ normal and stenosis diameter, resp., $L_s$ length of converging section and throat up to the point of flow separation, $Q$ flow rate, $P_a$ aortic input pressure, $P_s$ minimal stenosis pressure, $P_d$ distal pressure, $v$ velocity, $\rho$ fluid density

Or expressed in terms of flow, $Q$

$$\Delta P = AQ + BQ^2 \tag{1.8}$$

where A and B are constants that derive from stenosis geometry and rheological properties of blood:

$$A = 32\frac{L_s}{D_0}\left(\frac{A_0}{A_s}\right)^2\frac{\mu}{A_0 D_0} \tag{1.8a}$$

$$B = \frac{\rho}{2}\frac{k_e}{A_0^2}\left(\frac{A_0}{A_s}-1\right)^2 \tag{1.8b}$$

where $k_e$ is an exit coefficient that was originally determined to average 1.52 for blunt-ended stenoses with $L_s/D_0$=2 [60]. A series of additional experiments in the 1980s [63, 64] has shown that not only the stenosis area reduction $A_0/A_s$ and length $L_s$ but also the shape of the entrance and exit sections influence the overall pressure drop by altering the velocity profile as it develops along the entrance and throat of the constriction. This boundary-layer growth from the inlet to the outlet of a stenosis could empirically be accounted for by adjusting $L_s/D_0$ in Eq. 1.8a to

$$L_s'/D_0 = 0.45 + 0.86\left(L_s/D_0\right) \tag{1.8c}$$

and by expressing the exit loss coefficient $k_e$ in Eq. 1.8b as a function of $L_s/D_0$:

$$k_e = 1.21 + 0.08\left(L_s/D_0\right) \tag{1.8d}$$

The gradually changing area reduction along the stenosis can be taken into account by integration of differential viscous losses over the stenosis length. The effect of the stenosis entrance region was also more recently investigated by Huo et al. [65] who proposed a second-order polynomial to determine the diffusive energy loss coefficients for different uniform (blunt/parabolic) velocity profiles at the entrance and outlet region.

Because resistance is per definition equal to pressure drop divided by the flow, Eq. 1.8 implies that stenosis resistance is given by

$$R_S = A + BQ \tag{1.9}$$

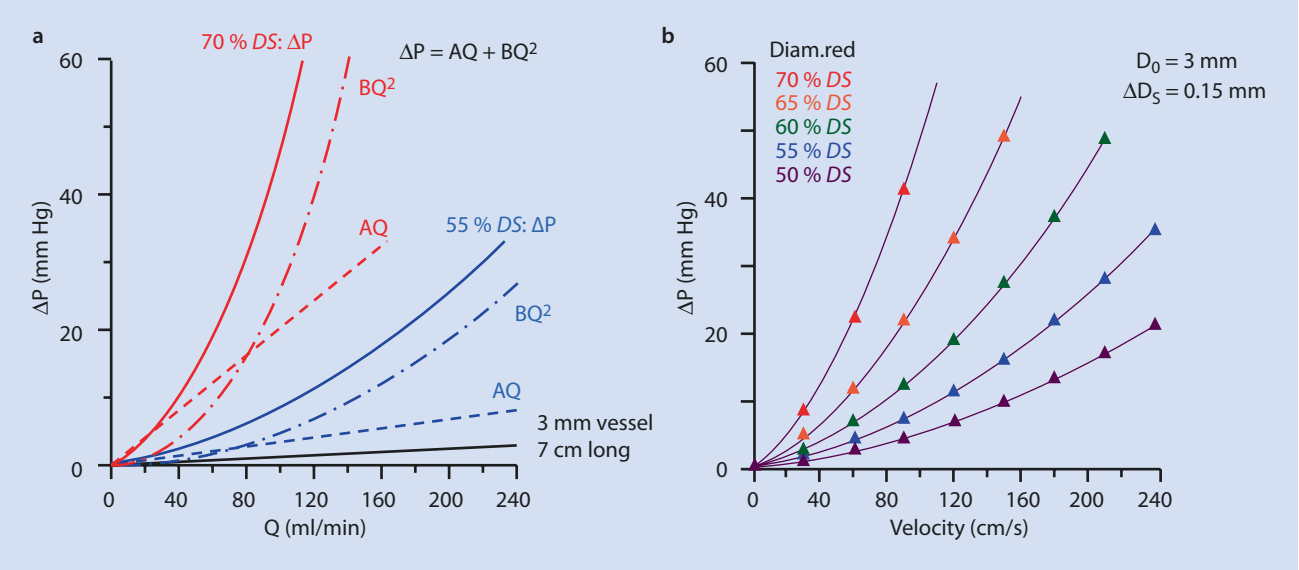


**Fig. 1.6** Illustrations of stenosis pressure drop-flow relationship. **a** The total pressure gradient ($\Delta P$) is the sum of linear viscous pressure losses (AQ) and quadratic exit losses ($BQ^2$). Theoretical relationships are shown for a 55 % and a 70 % diameter stenosis in a 3-mm vessel. The lower black line indicates pressure loss in the unobstructed vessel. **b** Effect of small changes in stenosis diameter ($\Delta D_s$) in a vessel with 3-mm normal diameter ($D_0$). The pressure drop for a given flow rate increases progressively with each reduction in stenosis diameter by 0.15 mm

The first term on the right represents the viscous resistance which is constant for a given stenosis geometry, and the second term relates to exit losses that increase with flow.

The two additive components of stenosis pressure drop (Eq. 1.7) are graphically shown in Fig. 1.6a for a moderate and severe lesion with $L_s/D_0 = 2$ in a 3-mm vessel. Note that viscous losses dominate at low flow rates, while the nonlinear exit losses grow more quickly with increasing flow through the stenosis and makes up the larger contribution to the total pressure drop at elevated flow. The major geometric factor is the minimum stenosis diameter, which enters with its inverse fourth power into both terms of the $\Delta P$-$Q$ relationship. Even small changes in stenosis dimensions can have a large effect, as is illustrated in Fig. 1.6b. The difference between the $\Delta P$-$Q$ curves stems from a reduction in stenosis diameter by <0.2 mm, which produces a progressively larger incremental rise in pressure drop with increasing stenosis severity, even for moderate flow. This example highlights the influence of a small thrombus in the narrowed section, or the effect of passive changes in stenosis dimensions with variations in intraluminal pressure when a compliant plaque or wall section is present (see below).

The mean value of pulsatile flow (time averaged over a cardiac cycle) was shown to differ less than 5 % from the steady-state value in the coronary circulation [62, 65], and the general quadratic equation relating pressure drop to flow (Eq. 1.8) is applicable to both steady and pulsatile flow. Studies of coronary stenoses in unsedated dogs have shown that throughout diastole and mid-systole, the measured instantaneous data followed the theoretical form and that inertial effects due to rapid flow deceleration and acceleration during the cycle were limited to brief periods at the end of systole and beginning of diastole [66]. The general form of Eq. 1.8 has been used to derive hemodynamic characteristics of coronary artery stenoses in patients based on per-beat averages of pressure drop and flow velocity throughout the hyperemic response to a vasodilator stimulus [67]. Stenosis pressure drop-velocity relations also served to successfully assess hemodynamic stenosis severity by evaluating the pressure gradient at a fixed flow velocity of 50 cm/s for instantaneous diastolic flow and at 30 cm/s for cycle-averaged flow velocity [68, 69]. The advantage of this approach is that maximal vasodilation is not required (e.g., contrast injection can be used to increase flow), and potential pitfalls of baseline measurements associated with autoregulation or measurement errors are avoided.

## 1.3 Effects of Stenosis on Coronary Blood Flow

As outlined above, maximum myocardial perfusion depends on the sum of all resistances, and distal coronary pressure is the major determinant of microvascular perfusion. An epicardial stenosis represents an additional resistance to flow in the coronary system (Fig. 1.7). It is important to realize that stenosis resistance is directly dependent on flow and hence is variable, even for a stenosis of fixed geometry. Moreover, coronary microvascular resistance includes an active component governed by mechanisms of flow control and a passive component that is pressure dependent and determines minimal resistance of the dilated vessels without tone. Hence, all resistances are variable and functions of flow and pressure.

The hemodynamic effect of an epicardial stenosis in the context of coronary perfusion is schematically illustrated in Fig. 1.8, where the stenosis $\Delta P$-$Q$ relationship is combined with the pressure-flow relations of the coronary circulation at rest and at maximal vasodilation. The x-axis represents (distal) coronary perfusion pressure, and flow is shown on the y-axis.

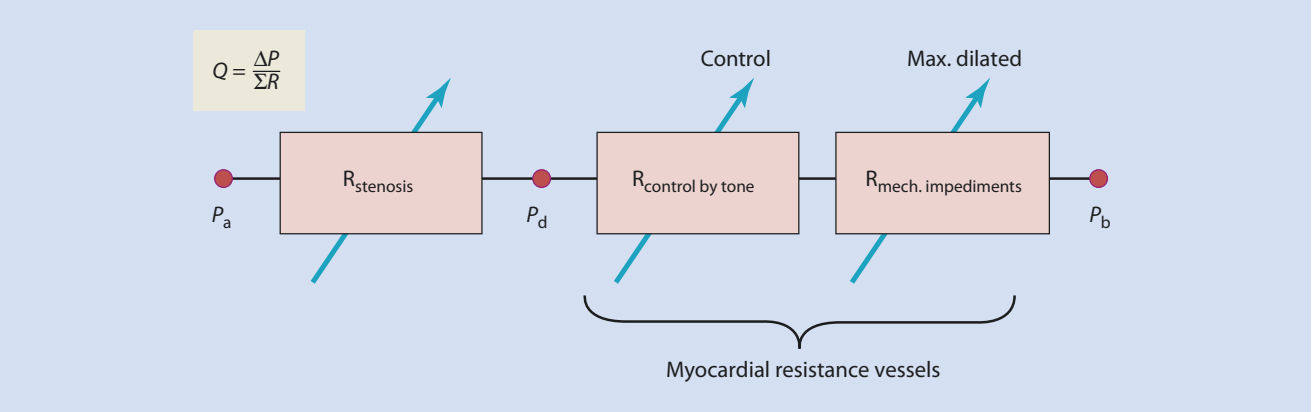


**Fig. 1.7** Stenosis resistance is in series with microvascular resistance. Flow ($Q$) in a stenosed artery is determined by the total pressure gradient ($\Delta P = P_a - P_b$) divided by the sum of all resistances. Myocardial resistance vessels include a resistance that is controlled by tone and a minimum resistance at maximal vasodilation that is determined by the structure of the vascular tree and altered by mechanical impediments. $P_d$ is the perfusion pressure for the microcirculation downstream of the stenosis. Note that all resistances are variable

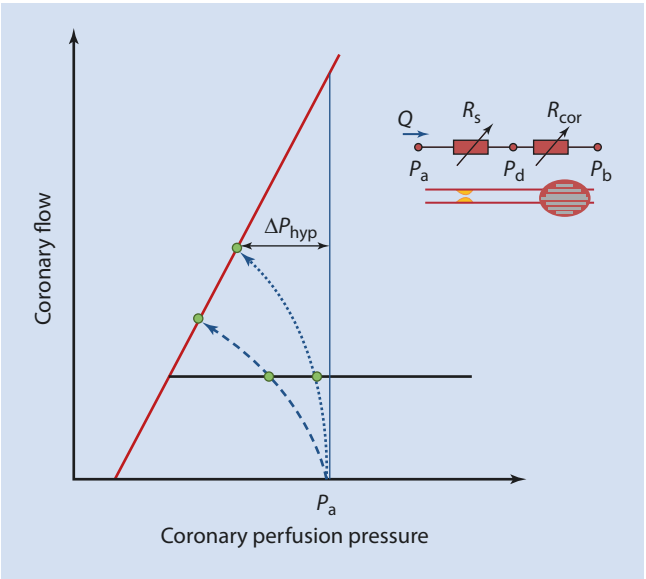


**Fig. 1.8** Coronary pressure-flow relation and stenosis pressure drop-flow relations (*dashed lines*) shown for two stenoses of different severities. While the pressure drop at rest is compensated by a reduction in microvascular resistance, maximal flow is reduced with increasing stenosis severity (*dotted vs. dashed curve*), with an increase in hyperemic pressure drop ($\Delta P_{hyp}$)

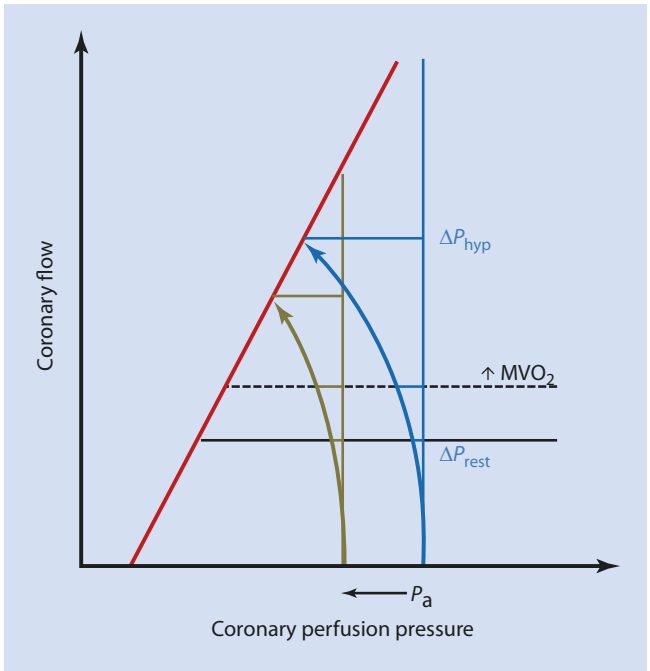


**Fig. 1.9** Effect of decreasing perfusion pressure and increased resting flow on stenosis resistance for a given stenosis. The stenosis pressure drop-flow relation shifts to the left (*blue to brown*) when aortic pressure is reduced ($P_a$). The hyperemic pressure gradient ($\Delta P_{hyp}$) is reduced because of a lower maximal flow that can be achieved, while pressure gradient at baseline ($\Delta P_{rest}$) is unchanged. However, when resting flow is increased due to a higher oxygen consumption ($MVO_2$), resting pressure gradient is increased, while hyperemic pressure gradient is not affected. Note that stenosis resistance increases linearly with flow ($R_s = A + BQ$)

Starting from no-pressure drop at no flow ($P_d = P_a$), the curve representing stenosis pressure drop as a function of flow (Eq. 1.8) turns left toward lower distal perfusion pressure with increasing flow, reflecting the nonlinear loss in pressure across the stenosis with increasing flow. In order to maintain baseline flow at rest, the coronary microcirculation adapts to the presence of a stenosis and compensates for the additional pressure loss by lowering microvascular resistance, which in turn reduces the vasodilatory reserve. The maximal flow value is prescribed by the pressure-flow line at maximal vasodilation, which can turn downward or shift to the right in certain cardiovascular conditions, as discussed earlier. The difference between aortic pressure and the intersection with the hyperemic pressure-flow line is the stenosis pressure drop at maximal dilation.

If oxygen demand increases at rest, the intersection with the autoregulation plateau occurs at a higher flow (Fig. 1.9), which on fluid dynamic principles implies an increase in basal stenosis resistance commensurate with the nonlinear relationship between flow and stenosis pressure drop. Conversely, a

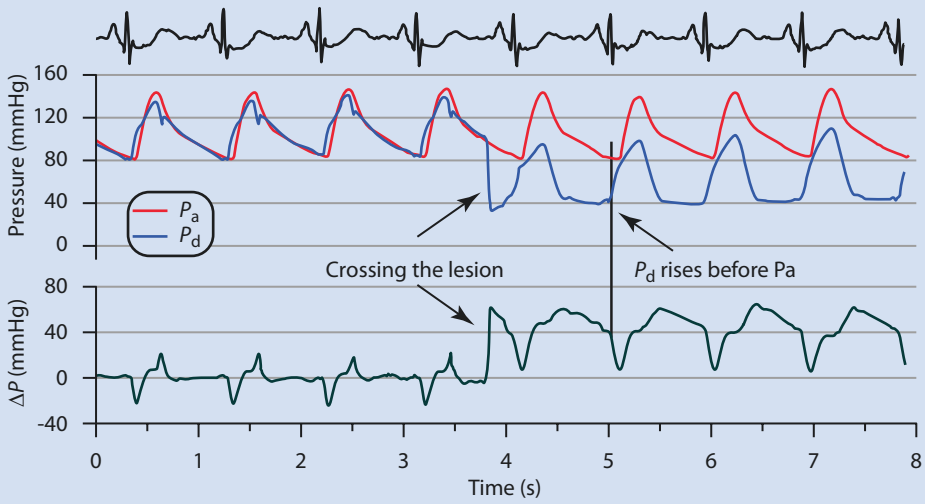


**Fig. 1.10** Phasic tracings of aortic ($P_a$) and distal pressure ($P_d$) obtained in a patient's left anterior descending artery with a 75 % diameter stenosis. As the stenosis is crossed, a substantial pressure gradient ($\Delta P$) is clearly seen that is higher during diastole. The distal pressure profile resembles a left ventricular pressure pattern. Note that coronary pressure downstream of the stenosis rises slightly before aortic pressure

decrease in aortic pressure will shift the pressure drop-flow relationship of this stenosis to the left resulting in a lower maximal flow, despite the same baseline resistance. Both examples entail a reduced capacity to increase flow above resting levels.

**Effect of stenosis on pulsatile flow and pressure signals** Development of an epicardial stenosis has a profound effect on pulsatile pressure and flow waveform patterns. An example obtained in a patient with a severe lesion (Fig. 1.10) shows how the pressure signal changes from an aortic to a ventricular pattern (not unlike that of the intramyocardial pump model) as the stenosis is crossed. This is explained by the higher diastolic flow and corresponding higher pressure loss during this part of the cardiac cycle. Note that the rise in distal pressure occurs earlier than the rise in aortic pressure. It is known from animal studies that distal pressure starts to increase during isovolumic contraction, whereas the pressure proximal to the stenosis rises with aortic pressure at the onset of aortic valve opening.

The availability of sensor-equipped guidewires allows the simultaneous acquisition of pulsatile coronary pressure and flow velocity data in patients. Figure 1.11 shows an example of coronary hemodynamic signals obtained in a left circumflex vessel with a severe lesion during increasing flow induced by intracoronary administration of adenosine, before (left) and after (right) percutaneous coronary intervention. In the presence of the stenosis, the distal pressure signal clearly reveals the hemodynamic stenosis severity. Although only a small increase in average flow velocity was attained during hyperemia (from 20 to 31 cm/s), the predominantly diastolic pressure gradient is exacerbated, with additionally a substantial pressure gradient during systole. Conversely, after revascularization, the distal pressure profile hardly changes despite a large rise in flow velocity (from 23 to 75 cm/s). The corresponding $\Delta P$-$Q$ relationships (lower panel) unequivocally illustrate the improvement in stenosis hemodynamics that was accomplished by revascularization, and the post-intervention $\Delta P$-$Q$ relationship closely approaches that obtained in an undiseased reference vessel of this patient. The solid lines represent least-squares quadratic fits through the data (Eq. 1.8). Note that the post-intervention and reference $\Delta P$-$Q$ relationships are almost straight, which indicates the dominance of viscous losses along the vessel (between the $P_a$ at the ostium and the location of distal pressure sensor). This implies a lack of energy losses due to convective acceleration in a narrowed section (second term in Eq. 1.8) and confirms a successful hemodynamic outcome without further constrictions along the interrogated vessel path.

**Compliant stenosis** Pathological studies and intravascular imaging have shown that only a minority of coronary artery stenoses is concentric with a fixed, rigid geometry. Most plaques develop at the inner curvature of the epicardial vessel or at bifurcations, with a D-shaped, concentric, or elliptical residual lumen [70–73]. The eccentric location of the plaque implies that in most cases, an arc of normal wall circumference is present which provides a mechanism whereby variations in intraluminal pressure or vasomotor tone can affect the luminal dimensions and thus alter flow resistance. Moreover, the plaque itself can be compliant [74–77]. The hemodynamic significance of dynamic changes in stenosis dimensions has received much attention in the past, and both active and passive mechanisms have been demonstrated in vivo [78–85]. Especially when vasomotor tone of epicardial vessels is minimized after giving nitroglycerin, a passive change in stenosis geometry can take place during the hyperemic response, when flow velocity increases at the expense of intraluminal pressure in the narrowed section [67, 84]. For a stenosis with an arc of compliant wall, the decrease in pressure may lead to extra narrowing by partial passive collapse, thereby worsening the situation.

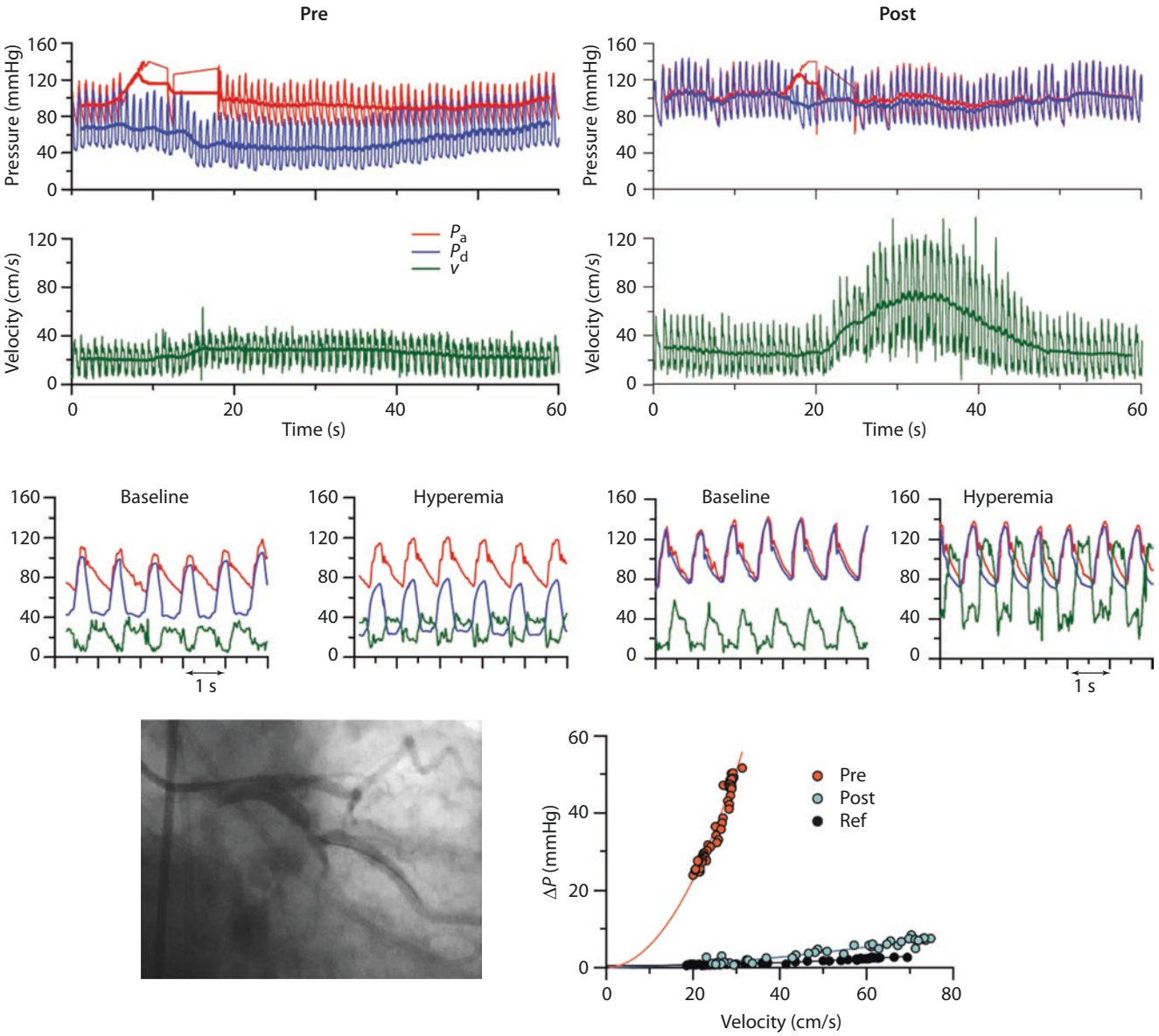


**Fig. 1.11** Hyperemic response to an intracoronary adenosine injection. Simultaneous pressure and velocity measurements were obtained in a 63-year-old patient with a 85 % diameter stenosis in the left circumflex artery (angiogram) before (pre, *left*) and after (post, *right*) interventional revascularization. Middle panels show proximal ($P_a$) and distal ($P_d$) pressure and flow velocity ($v$) at baseline and maximal hyperemia for each condition. On the lower right, the corresponding pressure drop ($\Delta P$)-velocity relations are shown for cycle-averaged values from baseline to hyperemia. Post intervention the ΔP-velocity relation closely approaches that of an undiseased reference vessel (Ref)

As outlined above (see Fig. 1.6b), even very small changes in minimum diameter can lead to large changes in pressure drop. In terms of the $\Delta P$-$Q$ relationship, stenosis hemodynamics is then no longer characterized by a single curve, but by a family of curves that reflect the changing stenosis geometry with time during the waxing and waning of flow [67]. The resulting $\Delta P$-$Q$ relationship of such a stenosis then displays in the form of a loop (Fig. 1.12), with two different pressure gradients at the same flow velocity, reflecting the passive dynamic change in stenosis dimensions.

**Serial lesions** Many lesions do not appear in isolation, but multiple stenoses are frequently present along a coronary artery. If the distance separating two lesions is sufficiently large, the overall pressure drop is simply the sum of the pressure drops across the individual stenoses. However, as the distance between the lesions decreases, interaction between the upstream and downstream lesion causes the overall pressure drop to be less than the sum. This interaction depends on the severity of the lesions, the distance between them, and the flow. At low flow rates, the expansion loss is small and two similar lesions act as a single lesion of summed length [60]. With increasing flow, two stenoses in series can undergo a transition from a single lesion of twice the length to two independent lesions with twice the overall pressure drop, as shown in Fig. 1.13. The flow rate at which this transition occurs decreases with increasing distance between the lesions, i.e., two lesions that are close together behave as a single lesion of twice

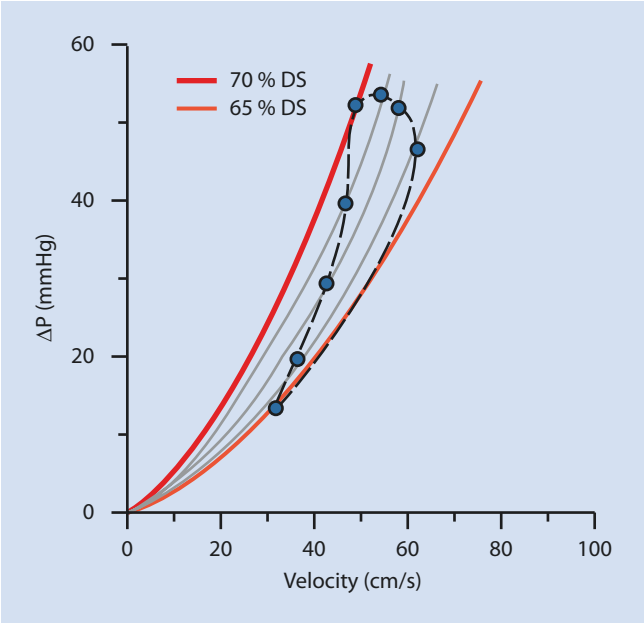


**Fig. 1.12** Effect of stenosis compliance on the pressure drop ($\Delta P$)-velocity relation. As intraluminal pressure declines with increasing velocity, partial collapse leads to a worsening of stenosis severity. The resulting loop is a composite of a family of unique curves that are traversed during the hyperemic response. Note that the change in stenosis geometry results in different pressure gradients for the same velocity

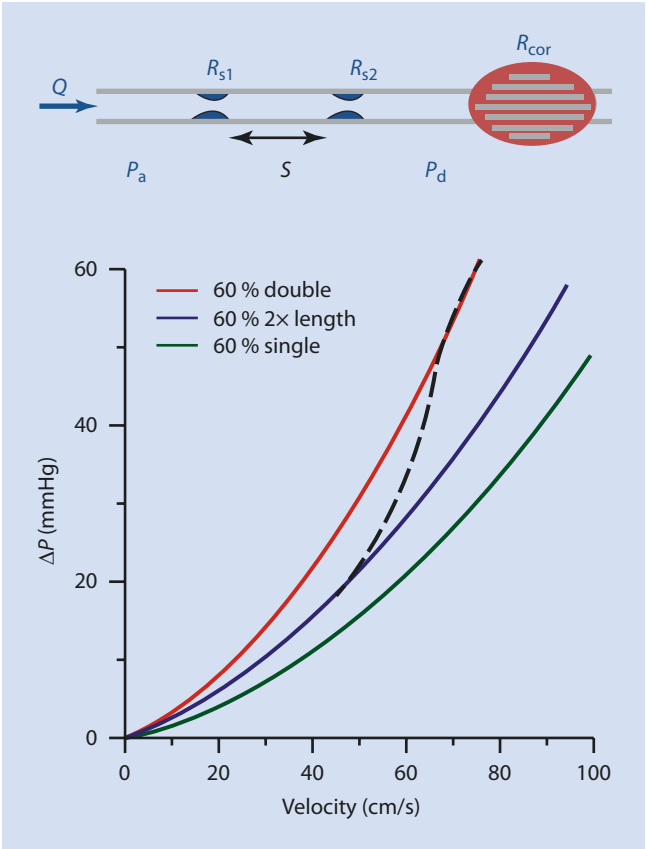


**Fig. 1.13** Effect of two 60 % diameter stenoses in series on the pressure drop ($\Delta P$)-velocity relation. A single stenosis is indicated by the *green line*. At low flow rates, two lesions act as a single lesion of twice the length (*blue line*). But with increasing flow, they undergo a transition (*dashed trajectory*) to two independent lesions with twice the pressure gradient (*red line*). This transition depends on the distance ($S$) between the lesions and on the sequence and severity of the stenoses. $Q$ flow, $R_s$ stenosis resistance, $R_{cor}$ coronary resistance, $P_a$ aortic pressure, $P_d$ distal pressure

the length over a larger flow range compared to lesions that are further apart [86].

For a given flow rate, the "critical" separation distance for two lesions to act independently depends on stenosis severity and distance. This is in line with the extent of the flow expansion zone of the upstream stenosis mentioned earlier. If the jet leaving the proximal lesion can fully expand before the distal lesion is encountered, the lesions are fluid dynamically independent, and pressure loss is maximal. This reattachment length is longer at elevated flow and for more severe lesions (up to 5–10 normal diameters). Intermediate lesions (55 % diameter reduction) at moderate flow (physiological range) tended to act independently when the distance between the lesions, $S$, exceeding six times the normal diameter, i.e., when $S/D_0$>6 [86]. For lesions that are closer together, the overall energy loss is reduced, since energy diffusion in the expanding jet is limited by the distal lesion and flow tends to remain more laminar [61]. Steady flow studies have shown that if a severe lesion is closely ($S/D_0$ =2) followed by a mild or moderate stenosis, the overall pressure drop was even less than that across the single severe stenosis [87]. If the upstream stenosis is compliant, increasing the severity of the downstream stenosis in a coronary artery can lead to expansion of the upstream stenosis lumen area, thereby decreasing its hemodynamic effect and increasing flow through both lesions [88, 89].

Selecting the most appropriate stenosis of serial lesions to be dilated is challenging. A method to predict the theoretical pressure drop across the remaining individual lesion after virtual stepwise revascularization is complicated and involves obtaining a wedge pressure requiring balloon inflation [90]. In the case of a left main stenosis in the presence of a downstream left anterior or circumflex lesion, it was proposed to measure distal pressure in the uninvolved epicardial artery instead [91]. However, both methods assume a constant hyperemic microvascular resistance regardless of distending pressure to the downstream myocardial bed, and the effect of distance between the lesions on mutual interaction was not investigated. A practical approach to identify the culprit lesion may be to determine sudden steps in pressure gradient by pressure wire pullback along the length of a coronary artery during hyperemia [92].

In summary, the overall effect of serial stenoses not only depends on the severity of the stenoses and the distance between them but also on the sequence of lesion severities, on stenosis compliance, and on flow. Clearly, more studies are needed in this area, but it is certain that multiple noncritical stenoses can cause a significant pressure loss, especially in the presence of underlying diffuse narrowing.

**Diffuse disease** The importance of diffuse coronary artery disease underlying a focal stenosis has long been recognized [93] and continues to be an active focus of research attention [94, 95]. A tandem development of focal and diffuse coronary artery disease is common and is associated with an increased risk of coronary events [17, 95, 96]. Recent studies using computed tomography imaging have shown that the cumulative plaque burden proximal to a focal stenosis plays an important role in determining the functional significance of that stenosis [97, 98].

Detection of diffuse disease by conventional angiographic imaging remains a problem for interventional cardiologists. The true extent of plaque accumulation cannot be appreciated by luminal angiography that may show smooth vessels, falsely suggesting the absence of atherosclerotic disease, and errors in angiographic assessment of plaque burden are exacerbated by the frequent occurrence of eccentric plaques that may present angiographically as a marginally narrowed circular lumen [99]. Yet the absence of focal disease does not imply the absence of increased flow resistance. Diffuse segmental narrowing can lead to substantial loss in distal perfusion pressure [100, 101] and can conceptually be modeled as a uniform relative reduction in normal segmental diameter with or without an overlaying focal obstruction [102]. Normal coronary artery size in humans is not easy to assess [103, 104]. Several approaches have employed length-area relations based on scaling laws that relate the size of the coronary tree to regional perfused mass via cumulative distal artery branch length [105, 106] or tried to assess the size of normal vessels via bifurcation analysis, where deviation from normal scaling law patterns can reveal the severity of diffuse disease [107–109]. Based on this approach, the extent of diffuse disease in the epicardial coronary artery tree of patients with metabolic syndrome was reflected by a 28 % decrease of mean cross-sectional area along the entire epicardial coronary artery tree and an 18% decrease of the sum of intravascular volume as a result of reduced cross-sectional area in distal coronary arteries [108].

*Recapitulating,* the hemodynamics of an epicardial stenosis can be summarized as follows:

1. Stenosis pressure drop (and therefore flow through the vessel) is influenced by stenosis geometry (shape of converging and diverging section, plaque location, length, lumen area of the stenosis, and lumen area of the vessel), velocity, blood viscosity and density, and blood flow waveform. Of these, the most important factors are flow velocity and minimum stenosis diameter.
2. The pressure drop varies nonlinearly with flow velocity, and the resistance of a stenosis is therefore not constant. For a fixed geometry, stenosis resistance increases linearly with velocity. In this regard, it should be recognized that microvascular resistance influences stenosis hemodynamics via its direct influence on flow velocity.
3. The major geometric factor influencing the pressure drop is the reduction in lumen area. This effect is relatively small for mild lesions, but escalates nonlinearly with increasing stenosis severity, where even a small worsening in stenosis diameter causes a steep rise in pressure drop.
4. Stenosis shape and lumen eccentricity do not strongly affect the pressure drop for moderate to severe lesions for which lumen reduction dominates. However, in case of partially compliant lesions (compliant plaque or an arc of flexible wall circumference), dynamic behavior can be introduced by small changes in effective lesion diameter with decreasing distending pressure, e.g., at elevated flow rates (passive) or induced by changes in tone (active).
5. The effect of multiple stenoses depends on the severity of the lesions, sequence of different severities, spacing between the lesions, and flow. If the distal lesion is close enough to the proximal one, it interferes with the expanding jet emerging from the upstream stenosis, thereby reducing its pressure loss. Based on experimental findings, sequential lesions can be regarded as independent (overall pressure drop is determined by the sum of individual lesions) when the distance between the lesions is greater than 6 times the adjacent vessel diameter.
6. Diffuse coronary artery disease underlying a focal lumen obstruction is common and independently modulates the physiological effect of an epicardial stenosis.

## 1.4 Distal Perfusion Beyond the Epicardial Lesion: Integrated Measures of Physiological Stenosis Severity

Considering that flow velocity is a major physiological determinant of epicardial stenosis hemodynamics for any given driving pressure, the level of microvascular resistance at the time of measurement is of paramount importance. After all, the value of basal and maximal flow during physiological lesion assessment determines the position along the stenosis $\Delta P$-$Q$ relationship, and clinically relevant functional parameters are derived from these values.

The power of conveying stenosis hemodynamics in terms of combined pressure and flow velocity information is further depicted in Fig. 1.14 showing stenosis $\Delta P$-$Q$ relationships for a selection of clinical cases. Data were obtained during a diagnostic procedure with intracoronary adenosine administration in coronary arteries of six patients with various degrees of anatomical stenosis severity.

In line with observations and simulations by others [94, 102], it becomes clear that percent diameter reduction alone is not a defining measure for the functional severity of a lesion. As shown in Fig. 1.14a, two lesions of 55 % DS (light blue and green) have very different $\Delta P$-$Q$ relationships (due to different diameters of the stenosed coronary vessel), whereas the fluid dynamic relationship of the 50 % DS (orange) is on the same curve as that of a 55 % DS (shown in green), albeit at a much lower flow velocity range. When pressure gradient is expressed in terms of aortic pressure ($1-\Delta P/P_a = P_d/P_a$), it can be seen

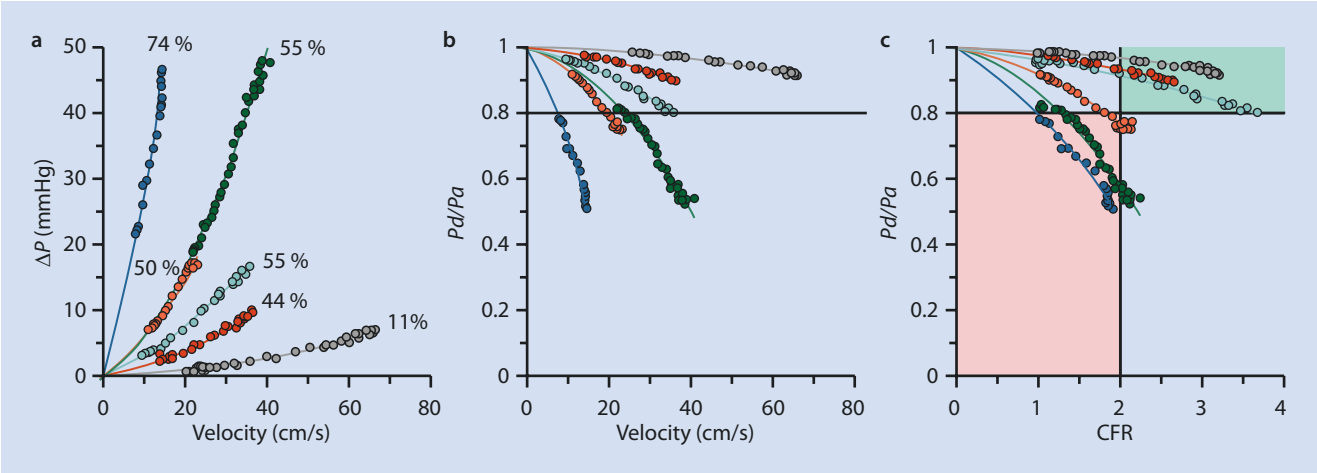


**Fig. 1.14** Combined pressure and velocity measurements during the hyperemic response to intracoronary adenosine. **a** Examples of pressure drop ($\Delta P$)-velocity relations obtained for different stenosis severities in coronary arteries of patients. It is clear that percent diameter reduction alone is not a defining measure of hemodynamic severity. **b** When the ratio of distal ($P_d$) to proximal ($P_a$) pressure is shown on the y-axis, three lesions cross the threshold of 0.8 for fractional flow reserve at maximal flow during hyperemia. **c** Expressing the x-axis in terms of coronary flow reserve (CFR) reveals that only the most severe lesion stays below the threshold value of 2.0. The vasodilatory capacity of all other lesions was sufficient to sustain an adequate flow reserve

(Fig. 1.14b) that three lesions cross the threshold of 0.8 for fractional flow reserve. Two of these lesions reduce distal perfusion pressure during vasodilation to about half of the aortic input pressure, although flow velocity for the 55 % DS (green) is much higher than for the 74 % DS. As discussed earlier, a decline in distending pressure of the dilated microvascular bed to low values will invariably lead to a passive diameter reduction of the relaxed microvessels, with consequentially (Poiseuille losses) an enhanced microvascular resistance compared to more normotensive distension pressures [30]. Finally, expressing hyperemic velocity as a multiple of basal velocity (Fig. 1.14c) reveals that only the most severe stenosis falls below the established cutoff value of 2.0 for coronary flow reserve. Obviously, other factors than percent diameter stenosis are influential in determining the physiological impact of a stenosis.

Note that the green 55 % DS was associated with the lowest hyperemic microvascular resistance (1.39 mmHg·cm$^{-1}$·s), suggesting that the vasodilatory capacity of that microvascular bed was sufficient to sustain an adequate flow reserve. In contrast, the hyperemic microvascular resistance distal to the 50 % DS (orange) was much higher (2.19 mmHg·cm$^{-1}$·s), which is corroborated by the low maximal velocity that was achieved. It is not known to which extent this HMR may reflect microvascular dysfunction, but removing the stenosis might still help this patient. Hoffman therefore proposed that threshold values for Pd/Pa should not be fixed, but should vary with the individual level of peripheral coronary resistance [32]. The same should likely be applied to flow velocity reserve, and this view was expressed in recommendations to adopt more integrated physiological measures [96, 110].

**Coronary stenosis physiology from anatomy** Despite the established fluid dynamic equations of an arterial stenosis, prediction of physiology from anatomy alone is subject to much scatter that limits agreement with observed functional indices in individual patients [17, 94]. The dissociation of anatomic and functional measures of stenosis severity is due not only to diffuse atherosclerosis but also to the influence of microvascular function that ultimately determines maximal flow and, hence, pressure gradient. Additionally, even quantitative angiography or computed tomography cannot assess stenosis dimensions with an accuracy that is adequate to enter with a fourth power relationship into the fluid dynamic equations [94]. Studies employing 3D computational fluid dynamics (CFD) assume population-based values for coupled reduced-order models describing the inlet and outlet boundary conditions of epicardial coronary arteries. Parameters of normal coronary models are applied to diseased models. Resistance values of the downstream vasculature are assumed to be dictated by their own anatomy (as derived from images) rather than by the upstream stenosis (which also modulates distal pressure and, hence, downstream resistance) [111]. Therefore, the application of classical fluid dynamic principles and 3D CFD as a tool for the patient-specific prediction of physiological stenosis severity from image-derived stenosis geometry still faces many challenges and limitations [94, 112].

**Coronary flow as physiological parameter of choice** The concept of "critical reduction in flow capacity" was introduced to aid in clinical interpretation of physiological severity [113]. The premise of this concept is that actual pressure and flow levels measured in epicardial vessels represent a continuum that is modulated by many external factors beyond the focal stenosis, including vasodilatory capacity (microvascular dysfunction), stress level, perfused mass (which is not accounted for with invasive measurements), vessel dimensions (diffuse disease), and distending pressure (input and distal pressure), as well as active and passive impeding mechanisms. A comprehensive approach termed "coronary flow capacity" was proposed by

Johnson, Gould, and colleagues [17, 114] that produces a 2D colored "physiological" scatterplot which takes into account both regional flow reserve and maximum stress flow (in ml/min/g) obtained by positron emission tomography as measures reflecting physiological stenosis severity, diffuse disease, and microvascular function. These data can be superimposed on left ventricular topographical depictions to yield a color-coded spatial distribution of coronary flow capacity. This concept has been "translated" to a "global" flow capacity map based on invasive measurements of flow velocity that also places the focus on the importance of coronary flow impairment for physiology-based decision-making in ischemic heart disease [115].

*In conclusion*, the hemodynamic characteristics of a coronary stenosis are governed by fluid dynamic laws that describe the quadratic relationship between pressure gradient and flow, based on (potentially variable) stenosis geometry and the rheological properties of blood. A coronary stenosis is proximally located in an epicardial curved, compliant, and moving vessel, with a downstream vascular network comprised of elastic branches whose resistance to flow is affected by active (tone) and passive (vasodilated) dimensional changes. This network is embedded in a continuously beating muscle that intrinsically regulates local myocardial perfusion based on oxygen demand at rest and during stress. All involved components can separately or together be diseased and malfunctioning to variable degrees. The physiological impact of an epicardial stenosis on perfusion impairment, therefore, derives from complex physical, biological, and pathophysiological interactions. Binary thresholding based on population-derived cutoff values of isolated epicardial physiological measurements obtained under pharmacologically simulated stress conditions should evolve toward integrating the accessible diagnostic information on multiple, individual factors of coronary artery disease into quantifiable criteria to optimize interventional decisions [116].

## References


1. Fulton WF. The dynamic factor in enlargement of coronary arterial anastomoses, and paradoxical changes in the subendocardial plexus. Br Heart J. 1964;26:39–50.
2. Wusten B, Buss DD, Deist H, Schaper W. Dilatory capacity of the coronary circulation and its correlation to the arterial vasculature in the canine left ventricle. Basic Res Cardiol. 1977;72(6):636–50.
3. Spaan JAE, Ter Wee R, Van Teeffelen JWGE, Streekstra G, Siebes M, Kolyva C, et al. Visualisation of intramural coronary vasculature by an imaging cryomicrotome suggests compartmentalisation of myocardial perfusion areas. Med Biol Eng Comput. 2005;43(4):431–5.
4. van Horssen P, van den Wijngaard JP, Brandt M, Hoefer IE, Spaan JA, Siebes M. Perfusion territories subtended by penetrating coronary arteries increase in size and decrease in number towards the subendocardium. Am J Physiol Heart Circ Physiol. 2014;306(4):H496–504.
5. Hanley FL, Messina LM, Grattan MT, Hoffman JIE. The effect of coronary inflow pressure on coronary vascular resistance in the isolated dog heart. Circ Res. 1984;54(6):760–72.
6. Kanatsuka H, Ashikawa K, Komaru T, Suzuki T, Takishima T. Diameter change and pressure-red blood cell velocity relations in coronary microvessels during long diastoles in the canine left ventricle. Circ Res. 1990;66:503–10.
7. Marcus M, Chilian W, Kanatsuka H, Dellsperger K, Eastham C, Lamping K. Understanding the coronary circulation through studies at the microvascular level. Circulation. 1990;82(1):1–7.
8. Mosher P, Ross Jr J, McFate PA, Shaw RF. Control of coronary blood flow by an autoregulatory mechanism. Circ Res. 1964;14:250–9.
9. Canty Jr JM. Coronary pressure-function and steady-state pressure-flow relations during autoregulation in the unanesthetized dog. Circ Res. 1988;63(4):821–36.
10. Duncker DJ, Koller A, Merkus D, Canty Jr JM. Regulation of coronary blood flow in health and ischemic heart disease. Prog Cardiovasc Dis. 2015;57(5):409–22.
11. Chilian WM, Layne SM, Klausner EC, Eastham CL, Marcus ML. Redistribution of coronary microvascular resistance produced by dipyridamole. Am J Physiol Heart Circ Physiol. 1989;256(2 Pt 2):H383–90.
12. Uren NG, Melin JA, De Bruyne B, Wijns W, Baudhuin T, Camici PG. Relation between myocardial blood flow and the severity of coronary-artery stenosis. N Engl J Med. 1994;330(25):1782–8.
13. Marcus ML, Doty DB, Hiratzka LF, Wright CB, Eastham CL. Decreased coronary reserve: a mechanism for angina pectoris in patients with aortic stenosis and normal coronary arteries. N Engl J Med. 1982;307(22):1362–6.
14. Wilson RF, Wyche K, Christensen BV, Zimmer S, Laxson DD. Effects of adenosine on human coronary arterial circulation. Circulation. 1990;82(5):1595–606.
15. Windecker S, Allemann Y, Billinger M, Pohl T, Hutter D, Orsucci T, et al. Effect of endurance training on coronary artery size and function in healthy men: an invasive followup study. Am J Physiol Heart Circ Physiol. 2002;282(6):H2216–23.
16. Sdringola S, Johnson NP, Kirkeeide RL, Cid E, Gould KL. Impact of unexpected factors on quantitative myocardial perfusion and coronary flow reserve in young, asymptomatic volunteers. JACC Cardiovasc Imaging. 2011;4(4):402–12.
17. Gould KL, Johnson NP, Bateman TM, Beanlands RS, Bengel FM, Bober R, et al. Anatomic versus physiologic assessment of coronary artery disease. Role of coronary flow reserve, fractional flow reserve, and positron emission tomography imaging in revascularization decision-making. J Am Coll Cardiol. 2013;62(18):1639–53.
18. Chilian WM, Eastham CL, Marcus ML. Microvascular distribution of coronary vascular resistance in beating left ventricle. Am J Physiol Heart Circ Physiol. 1986;251(4):H779–88.
19. Hoffman JI, Spaan JA. Pressure-flow relations in coronary circulation. Physiol Rev. 1990;70(2):331–90.
20. Aldea GS, Mori H, Husseini WK, Austin RE, Hoffman JIE. Effects of increased pressure inside or outside ventricles on total and regional myocardial blood flow. Am J Physiol Heart Circ Physiol. 2000;279(6):H2927–38.
21. Komaru T, Kanatsuka H, Shirato K. Coronary microcirculation: physiology and pharmacology. Pharmacol Ther. 2000;86(3):217–61.
22. Spaan JAE. Coronary diastolic pressure-flow relation and zero flow pressure explained on the basis of intramyocardial compliance. Circ Res. 1985;56:293–309.
23. Spaan JAE. Mechanical determinants of myocardial perfusion. Basic Res Cardiol. 1995;90(2):89–102.
24. Cornelissen AJM, Dankelman J, VanBavel E, Stassen HG, Spaan JAE. Myogenic reactivity and resistance distribution in the coronary arterial tree: a model study. Am J Physiol Heart Circ Physiol. 2000;278(5):H1490–9.
25. Spaan J, Siebes M, Piek J. Coronary circulation and hemodynamics. In: Sperelakis N, Kurachi Y, Terzic A, Cohen M, editors. Heart physiology and pathophysiology. 4th ed. San Diego: Academic Press; 2001. p. 19–44.
26. Spaan JAE, Piek JJ, Hoffman JIE, Siebes M. Physiological basis of clinically used coronary hemodynamic indices. Circulation. 2006;113(3):446–55.
27. Heusch G. Adenosine and maximum coronary vasodilation in humans: myth and misconceptions in the assessment of coronary reserve. Basic Res Cardiol. 2010;105(1):1–5.

28. Downey JM, Kirk ES. Inhibition of coronary blood flow by a vascular waterfall. Circ Res. 1975;36:753–60.
29. Verhoeff B, Siebes M, Meuwissen M, Koch KT, De Winter RJ, Kearney D, et al. Changes of coronary microvascular resistance before and after percutaneous coronary intervention. Eur Heart J. 2003;24:328.
30. Indermuehle A, Vogel R, Meier P, Zbinden R, Seiler C. Myocardial blood volume and coronary resistance during and after coronary angioplasty. Am J Physiol Heart Circ Physiol. 2011;300(3):H1119–H24.
31. Duncker DJ, Zhang J, Bache RJ. Coronary pressure-flow relation in left ventricular hypertrophy. Importance of changes in back pressure versus changes in minimum resistance. Circ Res. 1993;72(3):579–87.
32. Hoffman JIE. Problems of coronary flow reserve. Ann Biomed Eng. 2000;28:884–96.
33. Uhlig PN, Baer RW, Vlahakes GJ, Hanley FL, Messina LM, Hoffman JI. Arterial and venous coronary pressure-flow relations in anesthetized dogs. Evidence for a vascular waterfall in epicardial coronary veins. Circ Res. 1984;55(2):238–48.
34. Watanabe J, Maruyama Y, Satoh S, Keitoku M, Takishima T. Effects of the pericardium on the diastolic left coronary pressure-flow relationship in the isolated dog heart. Circulation. 1987;75(3):670–5.
35. Messina LM, Hanley FL, Uhlig PN, Baer RW, Grattan MT, Hoffman JIE. Effects of pressure gradients between branches of the left coronary artery on the pressure axis intercept and the shape of steady state circumflex pressure-flow relations in dogs. Circ Res. 1985;56:11–9.
36. Scheel KW, Mass H, Williams SE. Collateral influence on pressure-flow characteristics of coronary circulation. Am J Physiol Heart Circ Physiol. 1989;257(3 Pt 2):H717–H25.
37. Spaan JAE. Coronary blood flow. mechanics, distribution, and control. Dordrecht: Kluwer; 1991. p. 14–6. 166–168.
38. Tune JD. Coronary circulation. San Rafael: Biota Publishing; 2015.
39. Spaan JAE, Breuls NPW, Laird JD. Diastolic-systolic flow differences are caused by intramyocardial pump action in the anesthetized dog. Circ Res. 1981;49:584–93.
40. Krams R, Sipkema P, Westerhof N. Varying elastance concept may explain coronary systolic flow impediment. Am J Physiol Heart Circ Physiol. 1989;257(5 Pt 2):H1471–9.
41. Westerhof N, Boer C, Lamberts RR, Sipkema P. Cross-talk between cardiac muscle and coronary vasculature. Physiol Rev. 2006;86(4): 1263–308.
42. Bruinsma P, Arts T, Dankelman J, Spaan JAE. Model of the coronary circulation based on pressure dependence of coronary resistance and compliance. Basic Res Cardiol. 1988;83(5):510–24.
43. Spaan JAE, Cornelissen AJM, Chan C, Dankelman J, Yin FC. Dynamics of flow, resistance, and intramural vascular volume in canine coronary circulation. Am J Physiol Heart Circ Physiol. 2000;278:H383–403.
44. Austin Jr RE, Aldea GS, Coggins DL, Flynn AE, Hoffman JI. Profound spatial heterogeneity of coronary reserve. Discordance between patterns of resting and maximal myocardial blood flow. Circ Res. 1990;67(2):319–31.
45. Hoffman JI. Heterogeneity of myocardial blood flow. Basic Res Cardiol. 1995;90(2):103–11.
46. Chareonthaitawee P, Kaufmann PA, Rimoldi O, Camici PG. Heterogeneity of resting and hyperemic myocardial blood flow in healthy humans. Cardiovasc Res. 2001;50:151–61.
47. van de Hoef TP, Nolte F, Rolandi MC, Piek JJ, van den Wijngaard JPHM, Spaan JAE, et al. Coronary pressure-flow relations as basis for the understanding of coronary physiology. J Mol Cell Cardiol. 2012;52(4):786–93.
48. Chilian WM. Microvascular pressures and resistances in the left ventricular subepicardium and subendocardium. Circ Res. 1991;69(3):561–70.
49. Bache R, Cobb F. Effect of maximal coronary vasodilation on transmural myocardial perfusion during tachycardia in the awake dog. Circ Res. 1977;41(5):648–53.
50. Flynn AE, Coggins DL, Goto M, Aldea GS, Austin RE, Doucette JW, et al. Does systolic subepicardial perfusion come from retrograde subendocardial flow? Am J Physiol Heart Circ Physiol. 1992;262(6):H1759–69.
51. Boudoulas H. Diastolic time: the forgotten dynamic factor. Implications for myocardial perfusion. Acta Cardiol. 1991;46(1):61–71.
52. Bache RJ, Schwartz JS. Effect of perfusion pressure distal to coronary stenosis on transmural myocardial blood flow. Circulation. 1982;65:928–32.
53. Merkus D, Vergroesen I, Hiramatsu O, Tachibana H, Nakamoto H, Toyota E, et al. Stenosis differentially affects subendocardial and subepicardial arterioles in vivo. Am J Physiol Heart Circ Physiol. 2001;280(4):H1674–82.
54. Ferro G, Duilio C, Spinelli L, Liucci GA, Mazza F, Indolfi C. Relation between diastolic perfusion time and coronary artery stenosis during stress-induced myocardial ischemia. Circulation. 1995;92(3):342–7.
55. Ferro G, Spinelli L, Duilio C, Spadafora M, Guarnaccia F, Condorelli M. Diastolic perfusion time at ischemic threshold in patients with stress-induced ischemia. Circulation. 1991;84(1):49–56.
56. Fokkema DS, VanTeeffelen JWGE, Dekker S, Vergroesen I, Reitsma JB, Spaan JAE. Diastolic time fraction as a determinant of subendocardial perfusion. Am J Physiol Heart Circ Physiol. 2005;288(5):H2450–6.
57. Merkus D, Kajiya F, Vink H, Vergroesen I, Dankelman J, Goto M, et al. Prolonged diastolic time fraction protects myocardial perfusion when coronary blood flow is reduced. Circulation. 1999;100(1):75–81.
58. Roschke EJ, Back LH. The influence of upstream conditions on flow reattachment lengths downstream of an abrupt circular channel expansion. J Biomech. 1976;9(7):481–3.
59. Kirkeeide RL, Young DF, Cholvin NR. Wall vibrations induced by flow through simulated stenoses in models and arteries. J Biomech. 1977;10(7):431–7.
60. Seeley BD, Young DF. Effect of geometry on pressure losses across models of arterial stenoses. J Biomech. 1976;9:439–48.
61. Young DF. Fluid mechanics of arterial stenoses. J Biomech Eng. 1979;101(3):157–75.
62. Young DF, Cholvin NR, Kirkeeide RL, Roth AC. Hemodynamics of arterial stenoses at elevated flow rates. Circ Res. 1977;41(1):99–107.
63. Siebes M, Tjajahdi I, Gottwik M, Schlepper M. Influence of elliptical and eccentric area reduction on the pressure drop across stenoses. Z Kardiol. 1984;73:59.
64. Kirkeeide RL. Coronary obstructions, morphology and physiologic significance. In: Reiber JHC, Serruys PW, editors. Quantitative coronary arteriography. Dordrecht: Kluwer Academic Publishers; 1991. p. 229–44.
65. Huo Y, Svendsen M, Choy JS, Zhang Z-D, Kassab GS. A validated predictive model of coronary fractional flow reserve. J R Soc Interface. 2012;9(71):1325–38.
66. Gould KL. Pressure-flow characteristics of coronary stenoses in unsedated dogs at rest and during coronary vasodilation. Circ Res. 1978;43(2):242–53.
67. Siebes M, Verhoeff BJ, Meuwissen M, de Winter RJ, Spaan JAE, Piek JJ. Single-wire pressure and flow velocity measurement to quantify coronary stenosis hemodynamics and effects of percutaneous interventions. Circulation. 2004;109(6):756–62.
68. Nolte F, van de Hoef TP, de Klerk W, Baan Jr J, Lockie TP, Spaan JA, et al. Functional coronary stenosis severity assessed from the mean pressure gradient-velocity relationship obtained by contrast medium-induced submaximal hyperaemia. EuroIntervention. 2014;10(3):320–8.
69. Marques KMJ, Spruijt HJ, Boer C, Westerhof N, Visser CA, Visser FC. The diastolic flow-pressure gradient relation in coronary stenoses in humans. J Am Coll Cardiol. 2002;39(10):1630–6.
70. Vlodaver Z, Edwards JW. Pathology of coronary atherosclerosis. Prog Cardiovasc Dis. 1971;14:256–74.
71. Freudenberg H, Lichtlen PR. The normal wall segment in coronary stenoses – a postmortem study. Z Kardiol. 1981;70:863–9.
72. Waller BF. The eccentric coronary atherosclerotic plaque: morphologic observations and clinical relevance. Clin Cardiol. 1989;12(1):14–20.
73. Jeremias A, Huegel H, Lee DP, Hassan A, Wolf A, Yeung AC, et al. Spatial orientation of atherosclerotic plaque in non-branching coronary artery segments. Atherosclerosis. 2000;152(1):209–15.

74. Tang D, Yang C, Zheng J, Woodard PK, Saffitz JE, Petruccelli JD, et al. Local maximal stress hypothesis and computational plaque vulnerability index for atherosclerotic plaque assessment. Ann Biomed Eng. 2005;33(12):1789–801.
75. Sadat U, Teng Z, Gillard JH. Biomechanical structural stresses of atherosclerotic plaques. Expert Rev Cardiovasc Ther. 2010;8(10):1469–81.
76. Akyildiz AC, Speelman L, Gijsen FJ. Mechanical properties of human atherosclerotic intima tissue. J Biomech. 2014;47(4):773–83.
77. Ohayon J, Finet G, Le Floc'h S, Cloutier G, Gharib AM, Heroux J, et al. Biomechanics of atherosclerotic coronary plaque: site, stability and in vivo elasticity modeling. Ann Biomed Eng. 2014;42(2):269–79.
78. Logan SE. On the fluid mechanics of human coronary artery stenosis. IEEE Trans Biomed Eng. 1975;22(4):327–34.
79. Walinsky P, Santamore WP, Wiener L, Brest A. Dynamic changes in the haemodynamic severity of coronary artery stenosis in a canine model. Cardiovasc Res. 1979;13:113–8.
80. Schwartz JS, Carlyle PF, Cohn JN. Effect of coronary arterial pressure on coronary stenosis resistance. Circulation. 1980;61:70–6.
81. Gould KL. Dynamic coronary stenosis. Am J Cardiol. 1980;45(2):286–92.
82. Santamore WP, Kent RL, Carey RA, Bove AA. Synergistic effects of pressure, distal resistance, and vasoconstriction on stenosis. Am J Physiol Heart Circ Physiol. 1982;243(2):H236–42.
83. Brown BG, Lee AB, Bolson EL, Dodge HT. Reflex constriction of significant coronary stenosis as a mechanism contributing to ischemic left ventricular dysfunction during isometric exercise. Circulation. 1984;70(1):18–24.
84. Schwartz JS, Bache RJ. Effect of arteriolar dilation on coronary artery diameter distal to coronary stenoses. Am J Physiol Heart Circ Physiol. 1985;249(5 Pt 2):H981–8.
85. Siebes M, Campbell CS, D'Argenio DZ. Fluid dynamics of a partially collapsible stenosis in a flow model of the coronary circulation. J Biomech Eng. 1996;118(4):489–97.
86. Siebes M, Gottwik MG, Schlepper M. Experimental studies of the pressure drop across serial stenoses. Proceeding World Congress on Medical Physics and Biomedical Engineering. Hamburg: IFMBE; 1982. p. 2. 47.
87. Siebes M, Gottwik MG, Schlepper M. Hemodynamic effect of sequence and severity of serial stenoses. J Am Coll Cardiol. 1983;1(2):684.
88. Schwartz JS. Interaction of compliant coronary stenoses in series in a canine model. Am J Med Sci. 1985;289(5):192–9.
89. John B, Siebes M. Effects of stenosis compliance on flow through sequential stenoses. Adv Bioeng Am Soc Mech Eng. 1992;BED-22:383–6.
90. Pijls NHJ, De Bruyne B, Bech GJW, Liistro F, Heyndrickx GR, Bonnier HJRM, et al. Coronary pressure measurement to assess the hemodynamic significance of serial stenoses within one coronary artery: validation in humans. Circulation. 2000;102(19):2371–7.
91. Fearon WF, Yong AS, Lenders G, Toth GG, Dao C, Daniels DV, et al. The impact of downstream coronary stenosis on fractional flow reserve assessment of intermediate left main coronary artery diseasehuman validation. J Am Coll Cardiol Intv. 2015;8(3):398–403.
92. Kim H-L, Koo B-K, Nam C-W, Doh J-H, Kim J-H, Yang H-M, et al. Clinical and physiological outcomes of fractional flow reserve-guided percutaneous coronary intervention in patients with serial stenoses within one coronary artery. JACC Cardiovasc Interv. 2012;5(10):1013–8.
93. Marcus ML, Harrison DG, White CW, McPherson DD, Wilson RF, Kerber RE. Assessing the physiologic significance of coronary obstructions in patients: importance of diffuse undetected atherosclerosis. Prog Cardiovasc Dis. 1988;31(1):39–56.
94. Johnson NP, Kirkeeide RL, Gould KL. Coronary anatomy to predict physiology: fundamental limits. Circ Cardiovasc Imaging. 2013;6(5):817–32.
95. Gould KL, Johnson NP. Physiologic severity of diffuse coronary artery disease: hidden high risk. Circulation. 2015;131(1):4–6.
96. Gould KL, Johnson NP, Kaul S, Kirkeeide RL, Mintz GS, Rentrop KP, et al. Patient selection for elective revascularization to reduce myocardial infarction and mortality: new lessons from randomized trials, coronary physiology, and statistics. Circ Cardiovasc Imaging. 2015;8(5):e003099.
97. Nakazato R, Shalev A, Doh JH, Koo BK, Gransar H, Gomez MJ, et al. Aggregate plaque volume by coronary computed tomography angiography is superior and incremental to luminal narrowing for diagnosis of ischemic lesions of intermediate stenosis severity. J Am Coll Cardiol. 2013;62(5):460–7.
98. Abd TT, George RT. Association of coronary plaque burden with fractional flow reserve: should we keep attempting to derive physiology from anatomy? Cardiovasc Diagn Ther. 2015;5(1):67–70.
99. Narula J, Nakano M, Virmani R, Kolodgie FD, Petersen R, Newcomb R, et al. Histopathologic characteristics of atherosclerotic coronary disease and implications of the findings for the invasive and noninvasive detection of vulnerable plaques. J Am Coll Cardiol. 2013;61(10):1041–51.
100. De Bruyne B, Hersbach F, Pijls NHJ, Bartunek J, Bech J-W, Heyndrickx GR, et al. Abnormal epicardial coronary resistance in patients with diffuse atherosclerosis but "normal" coronary angiography. Circulation. 2001;104(20):2401–6.
101. Back LH, Cho YI, Crawford DW, Cuffel RF. Effect of mild atherosclerosis on flow resistance in a coronary artery casting of man. J Biomech Eng. 1984;106:48–53.
102. Johnson NP, Kirkeeide RL, Gould KL. Is discordance of coronary flow reserve and fractional flow reserve due to methodology or clinically relevant coronary pathophysiology? JACC Cardiovasc Imaging. 2012;5(2):193–202.
103. Dodge Jr J, Brown B, Bolson E, Dodge H. Lumen diameter of normal human coronary arteries. Influence of age, sex, anatomic variation, and left ventricular hypertrophy or dilation. Circulation. 1992;86(1):232–46.
104. Santamore WP, Bove AA. Why are arteries the size they are? J Appl Physiol. 2008;104(5):1259.
105. Seiler C, Kirkeeide RL, Gould KL. Basic structure-function relations of the epicardial coronary vascular tree. Basis of quantitative coronary arteriography for diffuse coronary artery disease. Circulation. 1992;85(6):1987–2003.
106. Gould KL, Nakagawa Y, Nakagawa K, Sdringola S, Hess MJ, Haynie M, et al. Frequency and clinical implications of fluid dynamically significant diffuse coronary artery disease manifest as graded, longitudinal, base-to-apex myocardial perfusion abnormalities by noninvasive positron emission tomography. Circulation. 2000;101(16):1931–54.
107. Choy JS, Kassab GS. Scaling of myocardial mass to flow and morphometry of coronary arteries. J Appl Physiol. 2008;104(5):1281–6.
108. Huo Y, Wischgoll T, Choy JS, Sola S, Navia JL, Teague SD, et al. CT-based diagnosis of diffuse coronary artery disease on the basis of scaling power laws. Radiology. 2013;268(3):694–701.
109. Kassab GS, Finet G. Anatomy and function relation in the coronary tree: from bifurcations to myocardial flow and mass. EuroIntervention. 2015;11(V):V13–V7.
110. Johnson NP, Toth GG, Lai D, Zhu H, Acar G, Agostoni P, et al. Prognostic value of fractional flow reserve: linking physiologic severity to clinical outcomes. J Am Coll Cardiol. 2014;64(16):1641–54.
111. Zhang JM, Zhong L, Su B, Wan M, Yap JS, Tham JP, et al. Perspective on CFD studies of coronary artery disease lesions and hemodynamics: a review. Int J Numer Method Biomed Eng. 2014;30(6):659–80.
112. Morris PD, van de Vosse FN, Lawford PV, Hose DR, Gunn JP. "Virtual" (Computed) fractional flow reserve current challenges and limitations. JACC Cardiovasc Interv. 2015;8:1009–17.
113. Gould KL. Does coronary flow trump coronary anatomy? JACC Cardiovasc Imaging. 2009;2(8):1009–23.
114. Johnson NP, Gould KL. Integrating noninvasive absolute flow, coronary flow reserve, and ischemic thresholds into a comprehensive map of physiological severity. JACC Cardiovasc Imaging. 2012;5(4):430–40.
115. van de Hoef TP, Siebes M, Spaan JA, Piek JJ. Fundamentals in clinical coronary physiology: why coronary flow is more important than coronary pressure. Eur Heart J. 2015; 36(47):3312-9.
116. Gould KL, Johnson NP. Physiologic stenosis severity, binary thinking, revascularization, and "hidden reality". Circ Cardiovasc Imaging. 2015;8(1):e002970.

# Pathological Changes in the Coronary Circulation

Contents

# Atherogenesis: The Development of Stable and Unstable Plaques

*Hiroyoshi Mori, Aloke V. Finn, Frank D. Kolodgie, Harry R. Davis, Michael Joner, and Renu Virmani*




J. Escaned, J. Davies (eds.), *Physiological Assessment of Coronary Stenoses and the Microcirculation*,
DOI 10.1007/978-1-4471-5245-3_2

2

## 2.1 Introduction

Cardiovascular diseases (CVDs) as reported by the World Health Organization (WHO) represent the foremost cause of death worldwide [1]. Recent estimates in 2012 indicate 17.5 million deaths from CVDs, corresponding to 31 % deaths worldwide. Of these, an estimated 7.4 million were attributed to coronary artery disease (CAD) and 6.7 million strokes, while assessments in 2000 were lower at 6 million for CAD and 5.7 million for stroke, thus indicating a substantial rise over the past decade. As society is aging, the number of CVD-related deaths is expected to increase further to 23.6 million by 2030 [2].

Acute coronary syndromes (ACS) represent a clinical spectrum of unstable angina, acute myocardial infarction (AMI) (ST or non-ST-segment elevation MI), and sudden coronary death (SCD). Most ACS are believed to stem from acute luminal thrombosis, which can arise from three distinct morphologies: plaque rupture, erosion, and calcified nodule [3]. In addition, SCD can also occur in the absence of acute thrombotic event, where severe underlying stenosis likely contributes to ischemic complications and lethal arrhythmias [4]. The concept of acute plaque rupture as a major cause of SCD was first introduced at the autopsy of the famous neoclassical Danish artist, Bertel Thorvaldsen, who died suddenly in the Royal Theatre in Copenhagen in 1844 [5]. It took many decades thereafter, however, before researchers like Clark, Koch, Friedman, and Constandinides in the early to mid-twentieth century to describe features of the culprit plaques that lead to sudden cardiac death and coined the terms "erosions" and "fissures" to describe some of the unique processes that occurred in these lesions [6–9]. Near the same time, the importance of intramural hemorrhage to coronary lesion progression was described by Wartman, Patterson, and Winternitz [9–11]. Meyer Friedman was the first to apply the approach of systematic serial sectioning to coronary lesions that revealed plaque rupture, as the underlying pathophysiology of luminal thrombosis. Leary's description of "necrotic core" was compared to "intramural atheromatous abscess," which helped to better understand the use of the term "atheromatous" a Greek word for "gruel-like material, a concept originally proposed by Virchow in 1858 [12]." Friedman laid the foundation for the understanding of the role of "necrotic core prolapse" leading to the disruption of luminal blood flow triggered from the cascade of pro-coagulation processes that results in complete or incomplete thrombotic obstruction of the coronary artery [13].

In the early 1980s, the Velicans added to existing knowledge of coronary artery atherosclerosis progression from an early-stage atherosclerotic process advancing into the late stages. They focused on the morphologic description of "fatty streak" to "fibroatheroma" and advanced plaque complicated by the presence of hemorrhage, calcification, ulceration, and thrombosis [14]. Michael Davies laid the foundation for the role of plaque rupture, thrombosis, and fissures as the triggers of sudden coronary death. These initial pioneering studies resulted in the assembly of scientists by the American Heart Association (AHA) headed by Stary that gave rise to consensus nomenclature introducing a numerical classification of atherosclerotic plaque (type I–VI) in the mid-1990s [15, 16]. The most severe, type VI lesions constituted a complicated plaque with surface defects, hemorrhage, and luminal thrombus. Davis et al. introduced the concept of intraplaque fissure, as an additional source of coronary thrombosis although actually occurring within the plaque, calling it "intra-intimal" thrombus [17]. Virmani et al. subsequently revised the classification proposed by Stary et al. providing a more comprehensive descriptive classification lead by distinct etiologies of coronary thrombosis and SCD, i.e., plaque rupture, plaque erosion, and calcified nodule [3]. In this context, stable coronary lesions (AHA type I–V) are replaced by terms of adaptive intimal thickening (AIT), intimal xanthoma (fatty streak), pathologic intimal thickening (PIT), and fibroatheroma, respectively, where the latter were further subcategorized into "early" and "late" stages of necrosis depending on the extent of extracellular matrix (high early/low late) and free cholesterol (low early/high late) within the necrotic core. Additional terminology was introduced to address lesions of silent episodic thrombosis: healed plaque rupture, intraplaque hemorrhage, and plaque fissures. Another important shortcoming of the AHA classification scheme was the lack of entities like healed thrombi called "healed plaque (HP) rupture" or "HP erosion." Furthermore, plaques inferring "stability" were also introduced, i.e., fibrous and fibrocalcific plaques.

## 2.2 Classification of Atherosclerosis According to Lesion Morphology

### 2.2.1 Intimal Thickening and Fatty Streaks

Intimal thickening (AHA type I) is the earliest vascular change, which consists of a focal accumulation of smooth muscle cells in an extracellular matrix. It is currently regarded as an adaptive change within the intima because the proliferation rate of smooth muscle cells is low, and the cells maintain an anti-apoptotic phenotype [18, 19]. On the other hand, it is also true that intimal thickening is more frequently recognized in atherosclerosis-prone arteries (coronary, carotid, abdominal and descending aorta, and iliac artery) [20].

Fatty streak or intimal xanthoma (AHA type II) is comprised of foamy macrophages along with lipid-laden smooth muscle cells (SMC) within the thickened intima. In the AHA classification, this lesion is referred to as the earliest atherosclerotic lesion; however, these lesions do not always progress to more advanced plaque. In humans, regression of fatty streak lesions has been observed in the thoracic aorta and the right coronary artery in young individuals aged between 15 and 30 years [21]. In keeping with this, studies of fatty streak lesions in rabbits support the notion of regression where a lipid-lowering diet resulted in a dynamic change in lesion morphology to reflect more fibrotic plaques [22].

### 2.2.2 Pathologic Intimal Thickening

In our view, pathologic intimal thickening (PIT, AHA type III lesion) represents the earliest of progressive atherosclerotic lesions characterized by smooth muscle cells and acellular proteoglycan and type III collagen-rich extracellular matrix involving lipid pools adjacent to the media [3]. The lipid pools are relative absent of smooth muscle cells (SMCs), and the extracellular matrix is mainly composed of hyaluronan and proteoglycans rich in versican [23, 24]. On the other hand, the earliest lesion of adaptive intimal thickening is mainly composed of SMCs embedded in proteoglycan matrix of biglycan and decorin. It is thought that PITs develop as the normal intima thickens over time, whereby SMCs undergo apoptosis evidenced by a persistent thickened basement membrane surrounding dead and the dying cells, as detected by PAS (periodic-acid Schiff) staining [25].

Macrophages occurring within PIT lesions when present begin to accumulate toward the lumen [24], and their presence is considered a more advanced stage of atherosclerosis. While the precise underlying mechanism of macrophage infiltration remains unknown, it is thought to involve oxidation of LDL present within lipid pools, as well as upregulation of endothelial selective adhesion molecule and monocyte chemotactic protein-1 (MCP-1) [26]. Free cholesterol in the form of fine crystalline structures has been observed in the lipid pools and is considered another cause of macrophage infiltration. Free cholesterol in PIT lesions is likely derived from cholesterol-rich membranes of dying smooth muscle cells or through the insudation of plasma lipoproteins [27–29]. Microcalcification within lipid pools is another important feature of PITs. Under transmission electron microscopy, apoptotic smooth muscle cell remnants, as well as calcium apatite crystals, are observed within the lipid pool. Although the source of this early calcification remains controversial, microcalcifications likely coalesce and gradually appear as calcified fragments with time [30].

### 2.2.3 Fibroatheroma

Fibroatheroma represents an advanced stage of atherosclerosis and is characterized by the presence of an acellular necrotic core. This is in contrast to the lipid pool of PIT in which distinct extracellular matrix proteins such as hyaluronan and proteoglycan versican are observed (AHA type IV lesion) [24]. We recently subclassified fibroatheromas into those with "early" and "late" necrotic cores. Early necrotic core is characterized by the presence of macrophage infiltration into the lipid pool that coincides with an increase in free cholesterol and breakdown of extracellular matrix [24]. Early necrotic cores show the focal absence of hyaluronan, versican, and biglycan matrix within the areas that eventually form the "late necrotic core" as observed in more advanced stages, which exhibit a complete absence of proteoglycans and collagen. Matrix-degrading enzymes produced by macrophages are thought to augment the breakdown of proteoglycans. The majority of macrophages within the necrotic core show features consistent with apoptosis as the necrotic core is enlarging. The necrotic core represents a "graveyard" of dead macrophages [31]. In fibroatheroma, there is an overlying layer of fibrous tissue (fibrous cap), mostly composed of type I and III collagen, proteoglycans, and interspersed smooth muscle cells. The fibrous cap plays a critical role in harboring the contents of the necrotic core. Thinning of the fibrous cap with the support of infiltrating macrophages may lead to the vulnerable plaque or thin-cap fibroatheroma (TCFA), a precursor lesion to rupture and thrombosis.

During the progression of early to late fibroatheroma, increased accumulation of free cholesterol is observed within the necrotic core resulting in a prominent histopathological appearance of empty clefts. The presence of free cholesterol in macrophages is in part regulated by a reesterification process involving acyl coenzyme A: acylcholesterol transferase, or ACAT1, which can be manipulated in animal models to promote the enlargement of the necrotic core [32].

### 2.2.4 Lipid Composition in Atheroma Progression

Classic studies of atherosclerotic lipid composition from the 1970s demonstrated significant increases in total cholesterol levels and changes in cholesterol esterification with lesion progression [29, 33]. In fatty streaks, the lipid is primarily intracellular, within foam cells, and the majority of cholesterol is esterified [33]. The fatty streaks have more cholesteryl oleate and less cholesteryl linoleate and arachidonate than advanced lesions [33]. As lesions progress to intermediate (PIT) and fibroatheromas with large necrotic cores, the amount of free cholesterol increased relative to cholesteryl esters (CE), with the appearance of cholesterol monohydrate crystals [33]. Total phospholipid levels increase with lesion progression, along with an increase in the sphingomyelin (SM)/phosphatidylcholine (PC) ratio, while triglycerides (TG) levels are low in atherosclerotic lesions and do not change with progression [33]. Recent arterial shotgun lipidomic studies, using mass spectrometry methods, detected 150 lipid species from nine different lipid classes where 24 were unique to plaques [34, 35]. These findings demonstrate an increase in cholesteryl esters (CE) and free cholesterol in plaques followed by SM > PC > ceramists, and TGs, which further corroborates earlier studies. The fatty acid content of the CEs is primarily linoleate and oleate, with additional long-chain fatty acid CEs [34]. Oxidized CEs and phospholipids were identified by lipidomics in lesions, which may have originated from oxidized LDL [34, 35]. Felton et al. [36] reported that the burden of free cholesterol was linked to lesion instability, with disrupted plaques showing an increase in total cholesterol and free-to-esterified cholesterol ratio, while triglyceride content is unchanged. Studies of coronary lesions at autopsy in our laboratory have shown the percentage of cholesterol clefts within necrotic cores was greater in lesions with rupture compared to eroded or stable plaques [3].

### 2.2.5 Macrophage Apoptosis Leading to Necrotic Core Expansion

Mechanism(s) underlying the recruitment of macrophages into lipid pools remains incomplete for translational studies of atherosclerotic lesion progression. Studies in genetically engineered mice revealed that the endoplasmic reticulum (ER) stress pathway is key in macrophage cell death, which may result in focal accumulation of apoptotic bodies resulting in increased demands of phagocytic clearance [37–39]. Macrophage apoptosis, as shown in murine models of atherosclerosis, may also be triggered by a combination of ER stress and engagement of the type A scavenger receptor, which is also demonstrated in human atheroma [40]. Signal transducer, in addition to decreased ability of phagocytic clearance (efferocytosis), has been forwarded as a crucial component to the removal of dead cells within the necrotic core [31, 41]. ER stress was suggested to induce apoptosis of smooth muscle cells and macrophages [39], while phagocytosis of apoptotic cells is severely impaired in advanced atherosclerotic plaques [41] (Fig. 2.1).

Several factors underlying the defective removal of apoptotic cells include oxidative stress, competitive inhibition of oxidized RBCs, and oxidized LDL [41]. Effective macrophage efferocytosis requires a well-balanced interaction between apoptotic cell ligands, phagocyte receptors, and supportive extracellular bridging molecules that link phagocytes to apoptotic cells [42]. Some important targets have been discussed in the past and found to be highly relevant: lack of milk fat globule-EGF factor 8 (Mfge8, also known as lactadherin) leads to apoptotic cell accumulation and accelerated atherosclerosis in mice [43]. This protein was further identified as a key extracellular regulator of apoptosis, phagocytic clearance, and secondary necrosis [44]. In a study performed in LDL receptor-deficient mice, bone marrow-derived cells form lactadherin-deficient mice were transplanted into aplastic mice, which resulted in a substantial increase in apoptotic cell death in the developing lesions [43]. Another

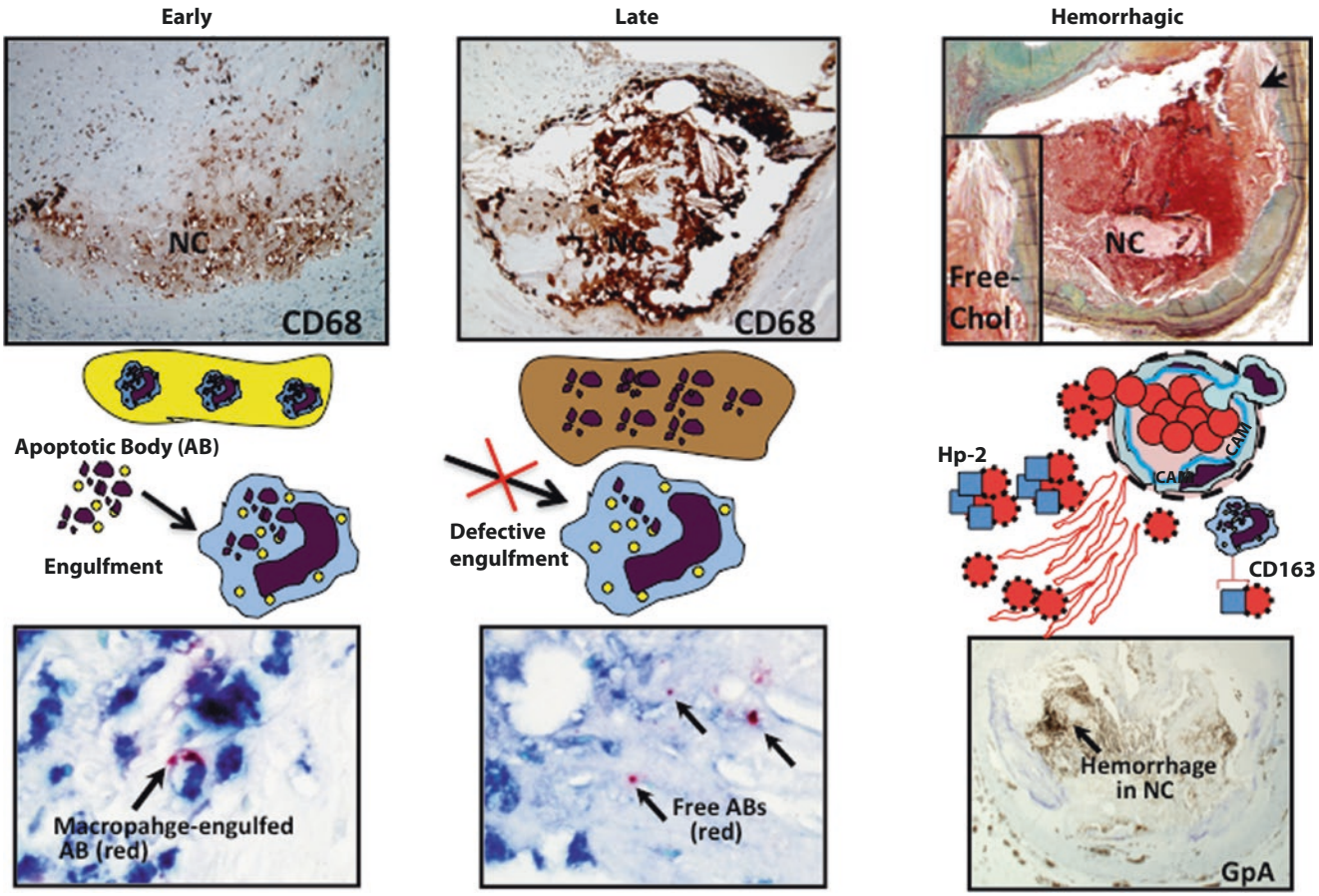


**Fig. 2.1** Putative mechanism(s) of necrotic core formation in humans, in part, guided by mouse models of atherosclerosis. A, shows representative micrographs of human coronary plaques illustrating early, late, and hemorrhagic necrosis. Early necrosis is marked by the infiltration of CD68-positive macrophages within lipid pools, whereas late necrosis is represented by increased macrophage death, cell lysis, and loss of extracellular matrix. Hemorrhagic necrosis is accompanied by accumulated free cholesterol (Free-Chol, *arrow*), presumably derived from erythrocyte membranes, and is thought to lead to the relatively rapid expansion of the necrotic core. B, diagrammatic representation of necrotic core formation and expansion, highlighted by defective efferocytosis (phagocytosis). *Left* normal engulfment of apoptotic bodies (ABs, *red*) within macrophages (*blue*), *middle* defective engulfment with free ABs, and *right* hemorrhagic necrosis with exposed heme, which is exacerbated by expression of the HP-2 haptoglobin protein type 2 allele (Reproduced with permission from Finn et al. [126] and Kolodgie et al. [127])

potential mediator implicated in defective efferocytosis is macrophage transglutaminase 2, a broadly expressed regulator of protein cross-linked to wound healing, and tissue fibrosis, that promotes both apoptotic cell clearance and ABCA1 (ATP-binding cassette subfamily A, member1) expression in vitro and limits atherosclerotic lesion size in vivo [45]. Mertk, a tyrosine kinase receptor, has been shown to be causally involved in αho5 integrin-mediated polymerization of the phagocyte cytoskeleton, thereby facilitating the internalization of apoptotic debris [46]. Mice deficient in Mertk show evidence of defective efferocytosis and susceptibility to a lupus-like autoimmune syndrome [46].

In addition to macrophages as predominant cell type involved in efferocytosis, dendritic cells (DC) expressing high levels of CD11c and MHC II also regulate immune responses related to atherosclerosis [47]. Recent evidence in human plaques suggests that the number of DCs increases with the lesion progression with the accumulation of mature DCs in rupture-prone vulnerable plaques [48]. Dendritic cells are known to progressively lose their capability of phagocytosis upon maturation [49], which may explain why DCs entrapped in advanced atherosclerotic lesions provide an insufficient level of efferocytosis and facilitate secondary necrosis [50]. DCs are also known to be involved in T-cell-mediated immune response, thus highlighting the complexity of efferocytosis in atherosclerotic lesions. It seems intuitive that pharmacological approaches to stimulate efferocytosis may become an important target in limiting progression of atherosclerosis. However, further studies are needed to elucidate the precise mechanisms of efferocytosis in vivo and designate molecular targets before selective treatment can be investigated.

The group led by Tabas et al. have recently reported that when macrophage autophagy is inhibited, apoptosis is increased and that this inhibition leads to apoptotic cells being less well recognized by efferocyte phagocytes. These findings link macrophage autophagy to two distinct cellular processes during atherosclerotic lesion progression and necrotic core enlargement, i.e., macrophage apoptosis and defective efferocytosis [51].

Although an association between defective efferocytosis and increased necrotic core size has been described in several mouse model of atherosclerosis, a direct cause and effect relationship remains unclear. Moreover, the contributions of efferocytosis in humans contribute to necrotic core expansion that remains to be determined. Conceivably, the effective clearance of apoptotic bodies could be used therapeutically to decrease secondary inflammation and atherosclerosis.

### 2.2.6 Intraplaque Hemorrhage

The concept of intraplaque hemorrhage (IPH) a major contributor to lesion progression was introduced in the first half of the twentieth century [9]. Constantinides et al. introduced the concept of cracks or fissures originating from the luminal surface as a source of IPH, which was later expanded by Davis et al. who described plaque fissure and intramural thrombosis, caused by the activation of coagulation pathways and fibrin deposition within the necrotic core [52, 53]. In an elaborate morphologic study of advanced coronary human coronary plaque, Barger et al. demonstrated an elaborate network of neoangiogenesis through injection of a vascular marker microfil [54]. Studies from our group showed that these neoangiogenic vessels were likely "leaky" leading to hemorrhage into a necrotic core recognized by a specific erythrocyte antibody (glycophorin A), which was most prevalent in advanced plaques prone to rupture [55]. The supply of plaque vasa vasorum is thought to extend into the intima from the adventitia [56] although intraluminal vasa vasorum have been identified (Fig. 2.2).

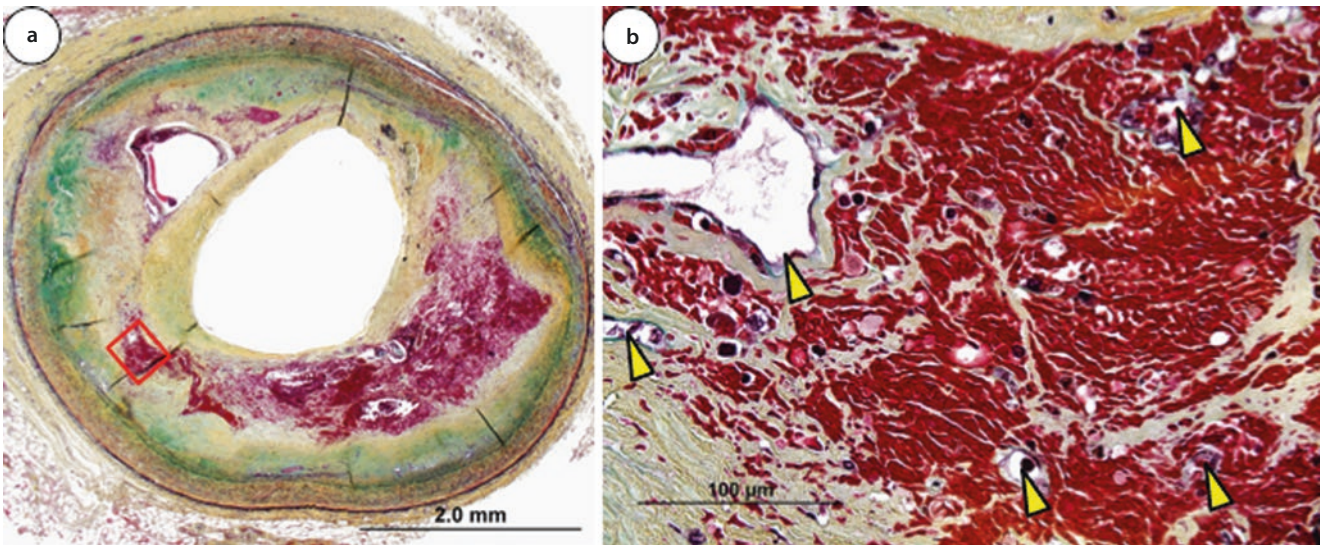


**Fig. 2.2** Coronary intraplaque hemorrhage. **a** Cross-sectional image of human coronary artery with extensive intraplaque hemorrhage into a necrotic core and severe luminal narrowing. **b** Higher-magnification image of the areas within the small *red box* in "**a**." Numerous neoangiogenic vessels with various sizes (*arrowheads*) are identified in the area of hemorrhage (Reproduced with permission from Falk et al. [106])

Apoptotic macrophages are unlikely to be the sole source of free cholesterol in plaques because foam cells contain mostly esterified cholesterol, while the necrotic core contains mostly free cholesterol [57]. Therefore, free cholesterol within the necrotic could be derived from other sources. IPH is commonly observed in advanced coronary atherosclerotic lesions that contain large amount of free cholesterol. Since erythrocyte membranes hold the highest free cholesterol of all the cells in the human body, the composition of the erythrocyte membrane is 40 % lipid in weight. Therefore, the accumulation of free cholesterol likely occurs through deposition of red blood cells as shown by glycophorin A along with iron staining for hemoglobin [55]. Moreover, there was also a linear relationship between necrotic core size and glycophorin A staining [38, 55, 58], and we also showed that leaky vasa vasorum were the main source of extravasated erythrocytes [55].

IPH can occur repeatedly over the years; thus, the amount of cholesterol derived from erythrocyte membranes is estimated to be substantial. In a clinical AMI study, the total cholesterol content of erythrocytesin circulation was assessed and found to be highest in patients presenting with ST-segment elevation myocardial infarction (STEMI), followed by non-ST-segment elevation ACS (NSTEAS) and stable angina pectoris (SAP), and was the least in control groups [59]. Moreover, rosuvastatin was shown to decrease the cholesterol content of erythrocyte membranes [59]. Small-angle X-ray diffraction analysis was used to compare arterial smooth muscle cell plasma membranes isolated from control and cholesterol-fed rabbits and provided evidence that excessive membrane cholesterol can phase separate and form a liquid-crystalline lipid bilayer consisting of pure cholesterol [27]. Deposition of free cholesterol can stimulate inflammation through activation of macrophages by stimulating caspase-1-activating NLRP3 inflammasomes, which leads to the cleavage and release of pro-inflammatory cytokines, such as interleukin-1 (IL-1) [60].

### 2.2.7 Heme Toxicity and Secondary Inflammation

Hemoglobin is composed of a globin protein core and an iron-containing heme. It is well established that heme/iron can support oxidative stress and directly interfere with the biology of other proteins and lipids, thereby amplifying the pro-inflammatory milieu encompassing the necrotic core [61, 62]. IPH can stimulate an inflammatory response by recruiting monocyte/macrophages into the plaque [63]. Moreover, denatured proteins such as coagulated blood likely augment inflammatory responses [64]. It has been reported that hydroperoxides, oxidized LDLs, and lipids from human atheromatous plaques can induce erythrocyte lysis [65]. These lipids are also capable of oxidizing Fe2 + hemoglobin to the more reactive Fe3 + hemoglobin, which easily dissociates from globin relative to Fe2+, thus releasing highly reactive heme/iron, which can be toxic to endothelial cells [65]. The elimination of free hemoglobins is mediated through binding to haptoglobin forming a hemoglobin/haptoglobin (H:H) complex, which is removed via CD163 receptors expressed on macrophages. The hemoglobin unit of the H:H complex is degraded by hemoxygenase (HO-1) and converted to free iron which is either utilized by the cell or exported via ferroportin and converted to a less toxic form ferric iron (Fe2+) as stated above.

Studies by Boyle et al. [66] and Finn et al. [67] implicate an alternative macrophage phenotype [Mhem or M(Hb)] derived from exposure to H:H complexes, which is also considered an anti-inflammatory due to its production of interleukin-10 (IL-10) via activating Th2 interleukins IL-4 and IL-13. M(Hb) macrophages therefore counter foam cell formation and are functionally different from classically activated pro-inflammatory M1 macrophages induced by Th1 cytokines like tumor necrosis factor α (TNF-α) and LPS. Clearly, there is a link between IPH, oxidative stress, and iron/lipid homeostasis that is directly related to macrophage phenotype, and a further understanding of this relationship represents an active area of research.

Haptoglobin (Hp) genotype/phenotype is also an important identifier of genetic risk factors in diabetic patients in humans; two classes of alleles for Hp exist. In the Western world, 16 % of the population is Hp 1-1 (homozygous for Hp 1 allele), 36 % is Hp 2-2 (homozygous for the Hp 2 allele), and 48 % is Hp 2-1 (heterozygote) [68]. Levy et al. reported that the odds of having CVD in DM with Hp 2-2 phenotype was 5.0 times greater than in DM with the Hp 1-1 phenotype ($p = 0.002$) [68]. Insertion of Hp 2-2 in the ApoE-deficient mouse model (ApoE−/−Hp 2-2) showed increased iron, lipid peroxidation, and macrophage accumulation as compared with ApoE−/− haptoglobin 1-1 mice [58]. To test the hypothesis that hemoglobin clearance may be deficient in diabetic atheroma from patients with Hp2-2, 40 patients with diabetes mellitus were genotyped, and their peripheral plaques are examined after atherectomy. Lesions from patients with the Hp 2-2 genotype had increased hemorrhage, iron content, and heme oxygenase-1 protein and reduced anti-inflammatory marker IL-10 and CD163 expression, although neovessel density was increase in haptoglobin 2-2 compared to controls [69]. Hemopexin is another inherent defense mechanism against heme toxicity, which is also capable of binding free hemoglobin and iron and, once combined, activates endocytotic clearance of bound hemoglobin [70].

### 2.2.8 Neoangiogenesis

The vascular network of small vessels in normal coronary arteries (vasa vasorum) is located in the adventitia and does not extend into the media or intima [71]. The majority of vasa vasorum are arterial in origin although venous connections have been reported [72, 73]. Coronary arteries show a higher vasa vasorum density as compared to renal and femoral arteries ($2.12 \pm 0.26 n/mm^2$ versus $0.61 \pm 0.06 n/mm^2$ and $0.66 \pm 0.11 n/mm^2$, respectively, $P < 0.05$ for both) [74]. With regard to their structure, vasa vasorum are usually composed

of a single layer of endothelial cells connected by tight adherent junctions with a well-formed basement membrane [75]. Supportive pericytes may be present as single or multiple layers, but the ratio of vessels stabilized by pericytes/SMCs is generally low within the adventitia and even lower within the developing plaque [76]. In general, the majority of intraplaque vasa vasorum are endothelialized under disease conditions but fail to show sufficient encasement with pericytes/SMCs. The relative shortage of mural cells along with incompetent endothelial junctions contributes to the leakiness of intraplaque vasa vasorum [77–79].

More recently Mulligan-Kehoe and Simons [80] have suggested two types of vasa vasorum in plaques, the "vasa vasorum interna," which originate from the luminal surface of the artery and branch into the adjacent artery wall, and "vasa vasorum externa," found mostly in the adventitia originating from adjoining vascular structures such as ascending aorta, intercostal vessels, etc. The arterial vasa vasorum are fewer and smaller in diameter (11.6–36.6 μm) as compared to the venous vasa vasorum, which are greater in number and larger in size (range from 11.1 to 200.3 μm). Under disease conditions, the arterial vasa vasorum expand in a disorderly pattern [80].

Intraplaque vasa vasorum from the adventitia follow a distinct pattern of arborization, where the entrance into the intimal space from the adventitia occurs specifically at breakpoints in the medial layer near sites of lipid pool and early necrotic core formation. Inflammation, especially by T-cells and macrophages, is associated with greater number of vasa vasorum within the plaque. Leukocyte adhesion molecules (vascular cell adhesion molecule 1 (VCAM-1), intercellular adhesion molecule 1 (ICAM-1), and E-selectin) in the arterial wall are reported higher for "vasa vasorum externa" than "vasa vasorum interna" [81]. There is a strong correlation between adventitial vasa vasorum and neointimal formation [82] and lesion progression [76]. Hypoxia is regarded as one of the primary stimuli for the induction of angiogenesis, as supported by studies in human carotid plaque where the marker of oxygen deprivation pimonidazole was commonly found in areas of macrophage infiltration, neoangiogenesis, and thrombosis [76]. T lymphocytes and macrophages have been shown to be a source of vascular endothelial cell growth factor (VEGF), which can stimulate neoangiogenesis [83]. Other important mediators involve CD40 and its ligand as a mechanism of VEGF release [84–87]. Similarly Toll-like receptors (TLRs) have also been implicated to induce neoangiogenesis by activating the pro-inflammatory transcription factor kB (NF-kB) and the mitogen-activated protein kinase pathway (MAPK), resulting in the production of pro-inflammatory cytokines. More recently, alternatively spliced tissue factor (asTF), a novel isoform of full-length tissue factor, was shown to promote neoangiogenesis supported by HIF-1α induction of VEGF, as demonstrated in lesions complicated by disruption, hemorrhage, and thrombosis as compared to uncomplicated fibroatheromatous plaques [88].

Neoangiogenesis has not only been reported to be a significant risk factor for atherosclerotic plaque progression in coronary arteries and subsequent cardiovascular events, but also for future stroke risk in patients with symptomatic carotid stenosis [89]. After combining two of the largest biobanks of atherosclerotic carotid plaques, Howard et al. showed that plaque thrombus, low fibrous content, macrophage infiltration, and high microvessel density were strong predictors of stroke risk [89]. However, there was no association in regard to cap thickness, calcification, intraplaque hemorrhage, or lymphocytic infiltration. Therefore, vasa vasorum play an important role during progression of atherosclerotic plaque and likely represent a promising target to establish more selective imaging protocols for patients undergoing risk stratification of stroke. Very recently, mast cells have also been implicated in plaque instability via induction of vasa vasorum [90]. Although mast cells have been well described in chronic immune responses to external pathogens and wound healing, an active involvement in plaque progression, particularly unstable coronary lesions, remains to be established.

### 2.2.9 Progression of Calcification and Vascular Remodeling

Complications of lesion calcification typically begin in middle age and are commonly observed in older individuals. The extent of calcification however shows substantial variability and correlates with the disease severity but not with plaque vulnerability [91]. Age, gender, renal function, diabetes mellitus, vitamin D levels and other aspects of bone metabolism, and genetic markers are all associated with vascular calcification [92–95].

Coronary calcification can be observed in progressive lesions originating from PIT but not in early fatty streaks. Apoptotic smooth muscle cells are considered one of the main early sources of calcification, which is best, appreciated by von Kossa staining. Others implicate early calcification to matrix vesicles released from vascular SMCs and macrophages reminiscent of bone matrix vesicles, which contain alkaline phosphatase and annexins that nucleate calcium mineral [30, 96]. We have observed microcalcifications in apoptotic macrophages, which appear as large punctate or blocky particles, while SMC apoptosis results in fine microcalcification (<5 micron in size). Apoptotic bodies serve as nucleation sites for calcium phosphate crystals. As these micro-calcium deposits coalesce, larger granules, fragments of calcium, and eventually sheets of calcium are observed, which can be recognized by standard histopathological stains. Nodular calcification is observed as small fragments of calcium interspersed with fibrin and represents a further advanced end stage of coronary calcification. Typically, nodular calcification is seen in tortuous arteries of older individuals, sometimes with ossification including marrow formation.

The most important determinant of coronary calcification is age [97], increasing with each decade and greater in white

males than women and African Americans [98]. Although the prevalence of calcification in sectional-based analysis of ruptured lesions is over 80 %, the severity of calcification is generally greater in stable fibrocalcific plaque with more than 75 % stenosis or in healed plaque ruptures. Moreover, clinical imaging studies in patients with acute coronary syndromes as well as autopsy observations in SCD victims have demonstrated less calcification in ruptured and vulnerable plaques as compared to stable plaques [91, 99]. Thus, the overall extent of calcification is a poor predictor of lesion vulnerability but is rather a strong indicator of plaque burden.

In 2003, Shaw and colleagues reported the relationship of coronary artery calcification to all-cause mortality in a large cohort study, followed for an average of 5 ± 3.5 years. Coronary artery calcification (CAC) as detected by CT was an independent predictor of death, and the risk increased proportionally to the baseline calcium scores (risk factor adjusted relative risk of 1.6, 1.7, 2.5, and 4 for CAC score 11–100, 101–400, 401–1000, and greater than 1000, respectively) [100, 101]. In terms of vulnerability, spotty calcification, positive remodeling, and low plaque density (Hounsfield unit <30 [HU]) are associated with acute coronary syndrome [91].

Sangiorgi et al. [102] correlated the extent of calcification with luminal narrowing and showed a strong interrelation with plaque burden, but an overall weak predictor of lumen narrowing. Compensatory vessel enlargement and other factors may contribute to this seemingly contradictory finding. Glagov et al. [103] showed that lumen area does not decrease until the lesion occupies ≥40 % of the internal elastic lamina area. Fibrosis and negative remodeling, as commonly found in highly calcified plaque, may partially explain the poor link between calcification and lumen size [103]. On the other hand, we have reported that prevalence of any calcification increases with luminal narrowing, which correlates with mean area of calcification [98], possibly because our coronary lesions had greater abundance of advanced atherosclerotic plaques (healed plaque rupture). In this autopsy study, the mean age was 51 years, individuals had varying degrees of calcification, and their direct impact on luminal narrowing could clearly be assessed [98].

## 2.3 Vulnerable Plaques as a Cause of Arterial Thrombosis

### 2.3.1 Thin-Cap Fibroatheroma and Plaque Rupture

The thin-cap fibroatheroma (TCFA) is morphologically reminiscent of ruptured plaque, although clearly there is absence of luminal thrombus [3] (Fig. 2.3). TCFAs are defined

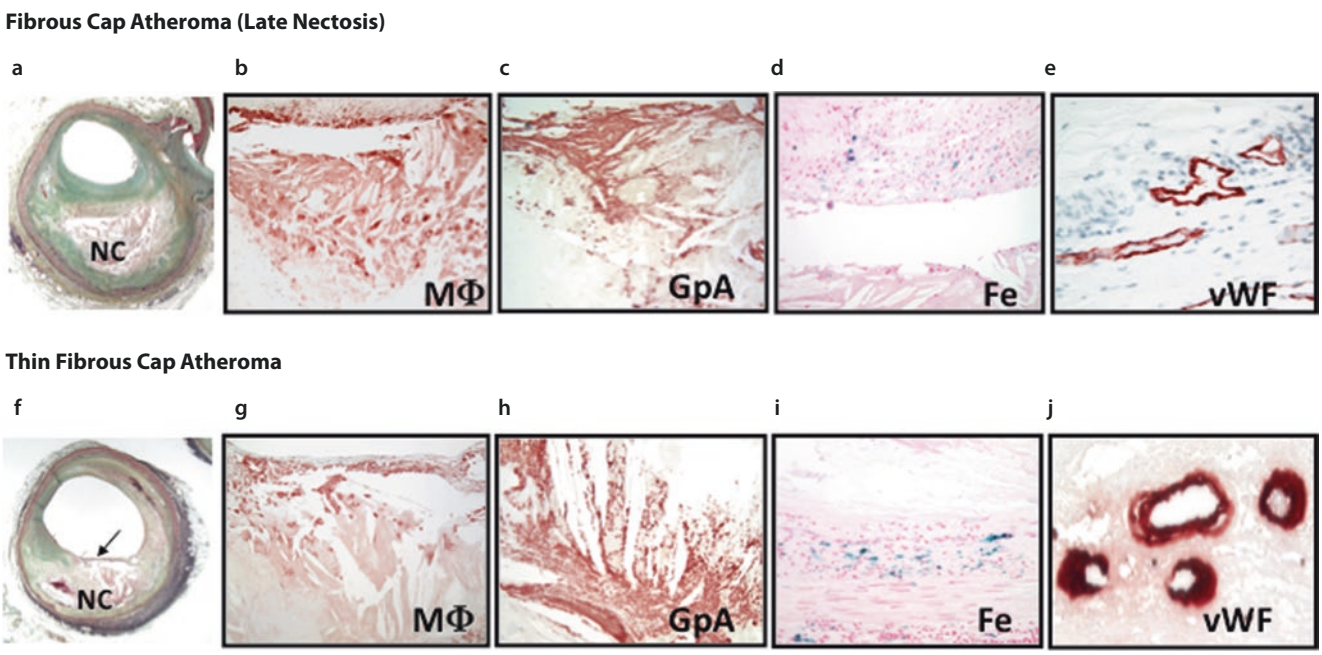


**Fig. 2.3** Intraplaque hemorrhage in fibroatheroma with late stage of necrosis (panels **a**, **b**, **c**, **d**, and **e**) and thin-cap fibroatheroma (panels **f**, **g**, **h**, **i**, and **j**). Fibroatheroma: panel **a** shows a low-power view of a fibroatheroma with a late-stage necrotic core (*NC*) (Movat pentachrome, ×20). Panel **b** shows intense staining of CD68-positive macrophages within the necrotic core (×200). Panel **c** shows extensive staining for glycophorin A, a sensitive marker for erythrocyte membranes shown aligned with numerous cholesterol clefts within the necrotic core (×200). Panel **d** shows iron deposits (*blue pigment*) within foam cells (Mallory's stain, ×200). Panel **e** shows microvessels bordering the necrotic core with perivascular deposition of von Willebrand factor (*vWF*) (×400). Thin-cap fibroatheroma: panel **f**, low-power view of a thin-cap (*arrow*) fibroatheroma overlying a relatively large necrotic core (Movat pentachrome, ×20). The fibrous cap is devoid of smooth muscle cells (not shown) and is heavily infiltrated by CD68-positive macrophages (panel **g**, ×200). Panel **h**, intense staining for glycophorin A in erythrocyte membranes within the necrotic core, together with intervening cholesterol clefts (×100). Panel **i**, adjacent coronary segment with iron deposits (*blue pigment*) in a macrophage-rich region deep within the plaque (Mallory's stain, ×200). Panel **j**, diffuse, perivascular deposits of von Willebrand factor in microvessels, indicating "leaky microvessels" near the necrotic core (×400). (Reproduced with permission from Kolodgie et al. [55])

lesions with a necrotic core and overlying thin intact fibrous cap, which is mainly composed of type I collagen with varying degrees infiltrating macrophages and lymphocytes. Smooth muscle cells within the thin fibrous cap are usually rare or absent. The thinnest portion of the remnant cap in ruptures measures 23 ± 19mwith 95 % of the ruptured caps measuring <65 μm. Therefore, the thickness of the fibrous cap in vulnerable plaque is defined as <65 μm [104] (Table 2.1). In comparison to ruptured plaques, TCFAs tend to have smaller necrotic cores less calcification and less macrophage infiltration (Table 2.1). Cross-sectional area luminal narrowing is also less in TCFAs as compared to ruptured plaques, with approximately 70 % of ruptured plaques having >75 % narrowing, as compared with TCFAs where approximately 40 % show similar narrowing. The best discriminators of potential for rupture were fibrous cap thickness (<55 μm), followed by % narrowing, and macrophage infiltration (area under the curve: TCFA 0.58 and PR 0.72) [105]. Overall, a large percentage of ruptured plaque with occlusive thrombi show greater underlying stenosis as compared to those without occlusive thrombi. TCFAs also show smaller necrotic core, fewer macrophages and cholesterol clefts, and less intimal vasa vasorum and accumulation of hemosiderin as compared with ruptures (Table 2.2). Similarly the length of the necrotic core tends to be longer in ruptures: mean 9 mm (2.5–22 mm) vs. 8 mm (2–17 mm) for TCFA and is the least for fibroatheromas 6 mm (1–18 mm) (Table 2.3) (Fig. 2.4).

The incidence of reported cases of plaque rupture, the most frequent cause of coronary thrombosis, varies between

**Table 2.1** Morphologic characteristics of plaque rupture and TCFA

| Plaque type | Necrotic core, % | Fibrous cap thickness, μm | Macrophages, % | SMCs, % | T lymphocytes | Calcification score |
|---|---|---|---|---|---|---|
| Rupture ($n = 25$) | 34 ± 17 | 23 ± 19 | 26 ± 20 | 0.002 ± 0.004 | 4.9 ± 4.3 | 1.53 ± 1.03 |
| TCFA ($n = 15$) | 23 ± 17 | <65 | 14 ± 10 | 6.6 ± 10.4 | 6.6 ± 10.4 | 0.97 ± 1.1 |
| *p* value | 0.05 | — | 0.005 | ns | ns | 0.014 |

Mean values represent ± SD. Reprinted, *SMC* smooth muscle cell, *TCFA* thin-cap fibroatheroma, with permission, from Kolodgie et al. [123]

**Table 2.2** Morphological characteristics of culprit and rupture-prone plaques in cases of sudden coronary death

| Plaque type | Necrotic core, % | Cholesterol clefts, % | Macrophages, % | Mean no. of sections with intraplaque hemorrhage |
|---|---|---|---|---|
| Rupture | 34 ± 17* | 12 ± 12† | 26 ± 20‡ | 2.5 ± 1.3§ |
| Thin fibrous cap atheroma | 23 ± 17 | 8 ± 9 | 14 ± 10 | … |
| Erosion | 14 ± 14 | 2 ± 5 | 10 ± 12 | 0 |
| Fibrocalcific | 15 ± 20 | 4 ± 6 | 6 ± 8 | 0.05 ± 0.6 |
| P | *0.003 vs. erosion, 0.01 vs. fibrocalcific | †0.002 vs. erosion, 0.04 vs. fibrocalcific | ‡ < 0.001 vs. erosion and stable plaque, 0.03 vs. thin fibrous cap atheroma | § < 0.01 vs. erosion and fibrocalcific plaque |

Reprinted, with permission from Virmani et al. [124]

**Table 2.3** Approximate sizes of necrotic core in fibroatheroma, thin-cap atheroma, and acute plaque rupture

| Dimension | Plaque type | | |
|---|---|---|---|
| | Fibrous cap atheroma ($n = 17$) | Thin-cap fibroatheroma ($n = 10$) | Acute plaque rupture ($n = 15$) |
| Mean length, mm (range) | 6 (1–18) | 8 (2–17) | 9 (2.5–22) |
| Necrotic core area, $mm^2$ | 1.2 ± 2.2 | 1.7 ± 1.1 | 3.8 ± 5.5 |
| Necrotic core, % | 15 ± 20 | 23 ± 17 | 34 ± 17 |

Reprinted, with permission from Virmani et al. [125]

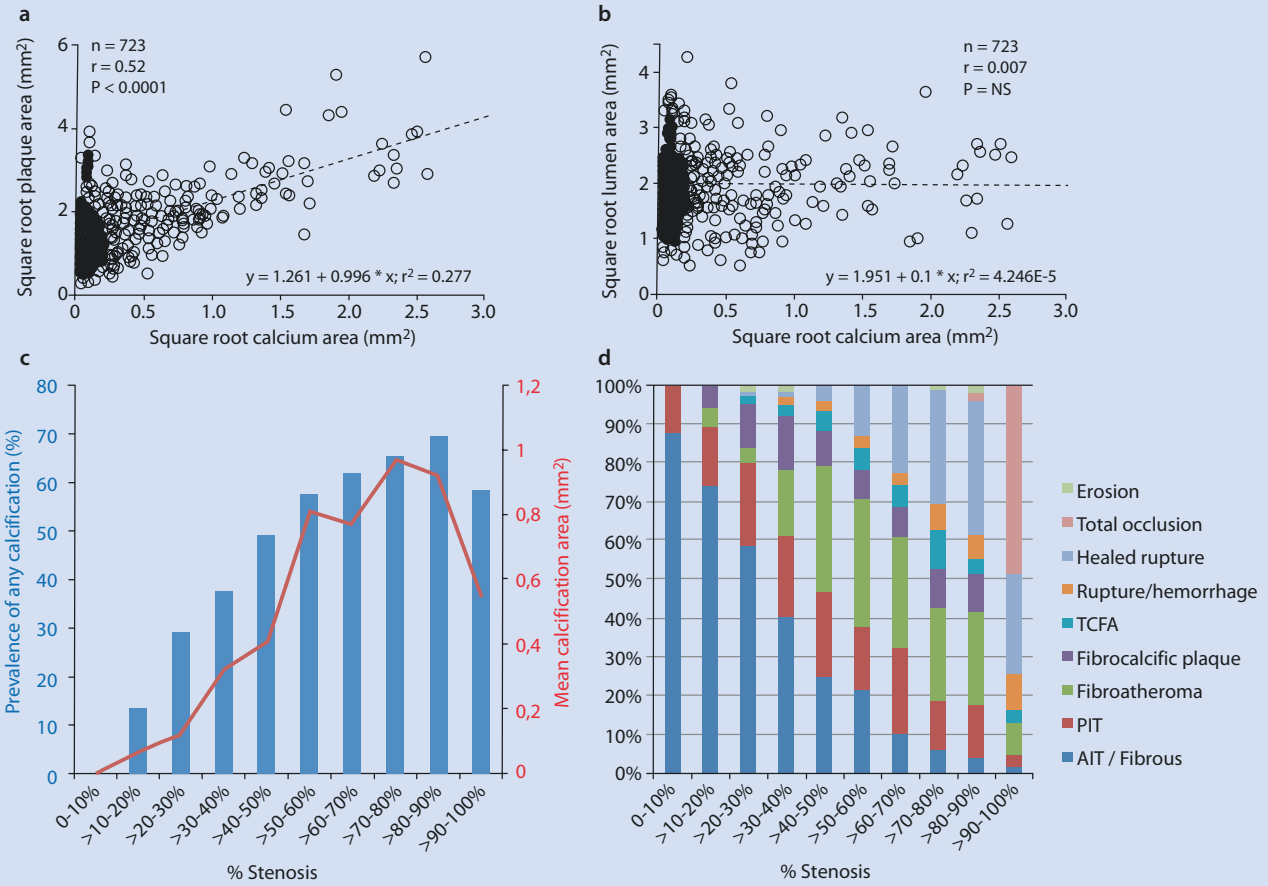


**Fig. 2.4** Analysis of lesion calcification by plaque area and stenosis. **a** Correlation between the square root of coronary calcium area ($mm^2$) detected by histopathologic and microradiographic analysis and square root of plaque area ($mm^2$), which includes analysis of 723 coronary artery segments from SCD victims. **b** Square root of coronary calcium area ($mm^2$) detected by histopathologic and microradiographic analysis versus square root of lumen area ($mm^2$) for each of the 723 coronary artery segments where no relation was identified. **c** Relationship between stenosis (%) and the degree of calcification. Each blue bar represents prevalence of any calcification (%), while the solid *red line* represents the mean calcification area ($mm^2$). **d** Prevalence of various coronary plaque morphologies at 10 % incremental cross-sectional area narrowing. Abbreviations: *AIT* adaptive intimal thickening, *TCFA* thin-cap fibroatheroma **a**, **b** are reproduced with permission from Sangiorgi et al. [102]. Data in **c**, **d** are from [128])

Europe and the USA. A European autopsy series compiled by Falk et al. reported a higher incidence of plaque rupture (73 %), which includes hospital-based AMI and SCDs from medical examiners, which is much greater than our experience (59 %) [106]. On the contrary, our series of 360SCDs solely representative of diagnostic medical examiner's cases is by far the largest and consists of relatively younger individuals (mean age = 48 years) specifically with no previous medical history of coronary heart disease. In an earlier autopsy series also medical examiner based by Davies in 1984, which included 100 SCDs with or without history of myocardial infarction or angina, the majority of subjects were greater than 65 years of age (all but one), and the reported incidence of intraluminal thrombi was 74 % and intra-intimal thrombus with or without fissure 21 %, with 5 % showing an absence of thrombi. Plaque fissure was defined by "an intra-intimal thrombus communicating with the lumen" further supported by postmortem coronary arteriography. For our cases, clarity of rupture is based on morphological characteristics, as postmortem angiography can artificially disrupt plaques depending on the viscosity of the barium/gelatin suspension and the pressure. The report by Davies and Thomas [107] showed a major thrombus that occluded more than 50 % in 60 % of cases, while the remaining had only minor thrombi, i.e., occupying less than 50 % of lumen with 64 % of the coronary arteries showing >75 % cross-sectional area narrowing. In our SCD series, plaque ruptures show greater luminal narrowing than erosions (78 ± 12 vs. 70 ± 11 %, respectively) with 18 % of plaque ruptures with <70 % narrowing relative to 37 % of erosions [108].

Although occlusive thrombi at sites of rupture and erosion are not always apparent, the thrombus composition is mainly of platelets and is typically described as "white thrombus," while the propagated thrombus proximal or distal to the site of rupture is typically rich in red blood cells with fibrin layering or the so-called red thrombus. Ruptured fibrous caps have been described in shoulder regions, which exhibit the greatest stress; however, some ruptures occur in the

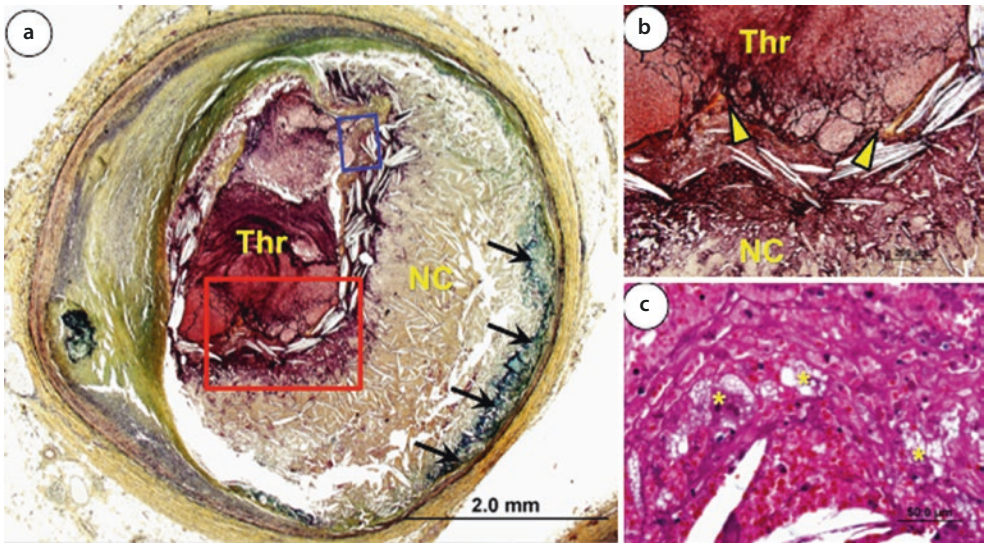


**Fig. 2.5** Histology of plaque rupture. **a** Cross-sectional histology of plaque rupture. A large necrotic core (*NC*) is identified in the underlying plaque with significant positive remodeling likely associated with medial atrophy. The lumen is occupied by an acute occlusive thrombus (*Thr*) rich in platelets. **b** Higher-magnification image of the rupture site represents the area with the *red box* in "A" where the thin fibrous cap is disrupted (*arrowheads*). **c** Higher-magnification image of remnant fibrous cap represented by the area within the *blue box* in "**a**," which is infiltrated by macrophages (*asterisks*) (Reproduced with permission from Falk et al. [106])

mid-region of the fibrous cap. Burke et al. reported a divergence of rupture sites with a greater occurrence at shoulder regions (65 %) during rest and mid-region of the fibrous cap (75 %), generally the thinnest portion in those with exercise [109]. Exercise-related ruptures had no evidence of acute myocardial infarction (AMI), while 13 % of those that died at rest had evidence of AMI. Thus, it is reasonable to speculate the occurrence of different processes, as determinants in the final event of plaque rupture. Increased collagenolysis by interstitial collagenease-1 (MMP-1 = matrix metalloproteinase-1), gelatinase (MMP-2 and MMP-9), and stromelysin (MMP-3) has been implicated in destabilization of the plaque and rupture [110]. Shear stress [111], microcalcification [112], and apoptotic macrophages [113] all likely play important roles in the initiation of rupture (Fig. 2.5).

### 2.3.2 Plaque Erosion

Until van der Wal et al. and Farb et al. separately reported on plaque erosion in the middle 1990s, plaque rupture was considered an exclusive mechanism of coronary thrombosis [108, 114]. This widely held paradigm was based on autopsy hearts in which postmortem angiography demonstrated the presence of dye (barium gelatin) within the lesion itself and was interpreted as rupture [107]. In the 20 original cases reported by van der Wal et al. 40 % showed "erosion," while 60 % of cases had plaque rupture. Plaque erosion was defined as coronary thrombosis in the absence of fibrous cap rupture. The intimal involving the thrombus was characterized by an eroded surface with an absence of endothelium together with injury of the superficial intimal layers intermixed with platelet/fibrin thrombi and inflammatory cells [114]. Overall 30–35 % of coronary thrombi occur from plaque erosion (Fig. 2.6).

Farb's report of 22 cases of erosion out of 50 SCD cases involving men and women showed superficial erosion/thrombosis defined in the absence of any communication with a necrotic core after serial sectioning [108]. Over 70 % of erosions occurred in women <50 years of age. Similarly, in another study of 189 men, with coronary thrombosis attributed to plaque rupture or erosion, 48 (25.4 %) had erosion in which 70 % were less than 50 years [115]. PIT or fibroatheromas with a thick fibrous caps with equally frequency best represent the underlying substrate for plaque erosion. Although the precise mechanism underlying the onset of erosion is unknown, coronary vasospasm may play an important role in its pathophysiology since the media is usually intact rich in smooth muscle cells. Eroded lesions show abundance of extracellular matrix consisting of versican, hyaluronan, and type III collagen, while ruptured or stable plaques are rich in type I collagen and biglycan and decorin [3, 116]. It has been suggested that hyaluronan may play a supportive role in the development of thrombosis in erosion through its CD44 receptor, which has been liked to platelet adhesion, inflammation, and vascular cell activation where ligation of hyaluronan could activate SMC through specific cell signaling [116]. Although van der Wal et al. reported inflammation consisting of macrophages and T lymphocytes at the eroded site, our experience shows usually minimum inflammation at the erosive site and less expression of inflammatory cell activators, such as human leukocyte class II antigen (HLA-DR) [108, 114].

Coronary risk factors for erosion appear different than those for rupture [117], as the occurrence is typically greater in young female smokers without significant elevated circulating cholesterol, body mass index, or glycohemoglobin levels. Smoking cessation is the most important risk factor modification for those susceptible to plaque erosion. Overall,

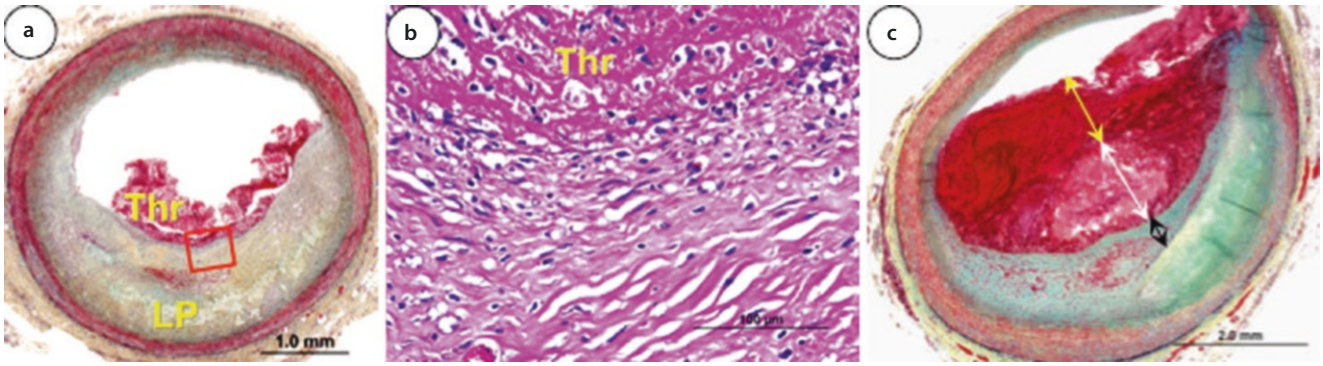


**Fig. 2.6** Histology of coronary plaque erosion. **a** Cross-sectional histology of plaque erosion (Movat pentachrome staining) shows a non-occlusive thrombus (*Thr*) on the plaque surface. Note, there is no connection between thrombus and the underlying lipid pool (*LP*) and the medial wall appears intact. **b** Higher-magnification H&E-stained section of the area represented by the *red box* in "**a**." The thrombus (*Thr*)/plaque interface shows an absence of surface endothelium with minimal inflammation. **c** Repeat thrombosis in plaque erosion. The oldest layer (*double black arrow*) represents an organizing thrombus replaced by proteoglycan (Reproduced with permission from Falk et al. [106])

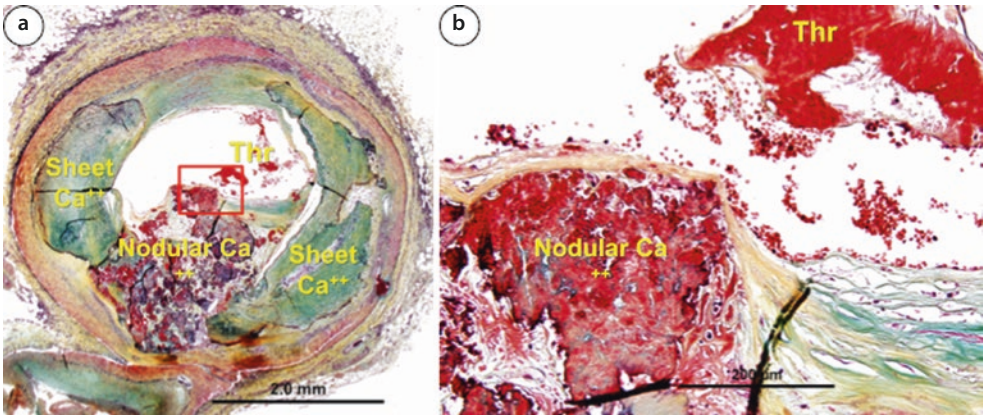


**Fig. 2.7** Histology of eruptive calcified nodule with luminal thrombosis. **a** Heavily calcified coronary plaque exhibiting calcified sheets flanking an area of nodular calcification (Ca + 2). **b** Higher-magnification image of the area represented by the *red box* in "**a**." The nodular calcification is nearly protruding into the lumen area with an overlying thrombus (*Thr*). All sections were stained by Movat pentachrome (Reproduced with permission from Falk et al. [106])

plaque erosions tend to be less stenotic and less calcified, as compared with ruptures [3]. The incidence of erosions and rupture in women can clearly be projected by age, as erosions in those <50 years of age account for 70 % of thrombi, while in women >50 years more commonly exhibit rupture.

Erosions more often give rise to downstream myocardial microemboli and microvascular obstruction, as observed in 71 % of cases as compared with 42% of ruptures [118]. Besides, 88 % of coronary thrombi in erosions showed later stages of healing (>1 days), whereas in rupture, only 54 % of coronary thrombi showed this stage of healing [119], pointing toward the fact that thrombus formation may follow an on-off phenomenon resulting in gradual expansion of the thrombosis. Moreover, coronary thrombi in erosions exhibit higher densities of myeloperoxidase-positive cells than those of ruptured plaque [120]. Eroded surfaces contain fewer macrophages (rupture 100 % vs. erosion 50 %, $P < 0.0001$) and T lymphocytes (rupture 75 % vs. erosion 32 %, $P < 0.0001$) as compared to ruptured plaques [108]. At present, no distinct morphological features exist for erosion-prone plaques, unlike the well-described morphological features of TCFA for plaque rupture.

### 2.3.3 Calcified Nodule

The calcified nodule is the least frequent cause of coronary thrombosis [3]. Generally, it occurs in heavily calcified arteries where small, calcified nodules appear to protrude into the lumen through fibrous tissue with and overlying platelet-rich luminal thrombus in the absence of surface endothelium. The nodules within the plaque are typically surrounded by fibrin and there may be interspersed macrophages/osteoclasts, and rarely bone- and a marrow-like substance have been observed [3]. Little is known about the mechanism of the nodular calcification; however, we believe this may be related to fractures within calcified sheets that result in multiple smaller fragments that can either protrude into the lumen or away from the lumen also causing disruption of the media where nodules of calcium have also been observed in the adventitia. Calcified nodules with thrombosis are typically observed in older individuals, males more frequent than females, and tend to occur in highly calcified tortuous coronary arteries like the middle right coronary where torsion stress is maximal. These lesions are also frequently observed in the carotid or lower extremity arteries where mechanical factors may be most important (Fig. 2.7).

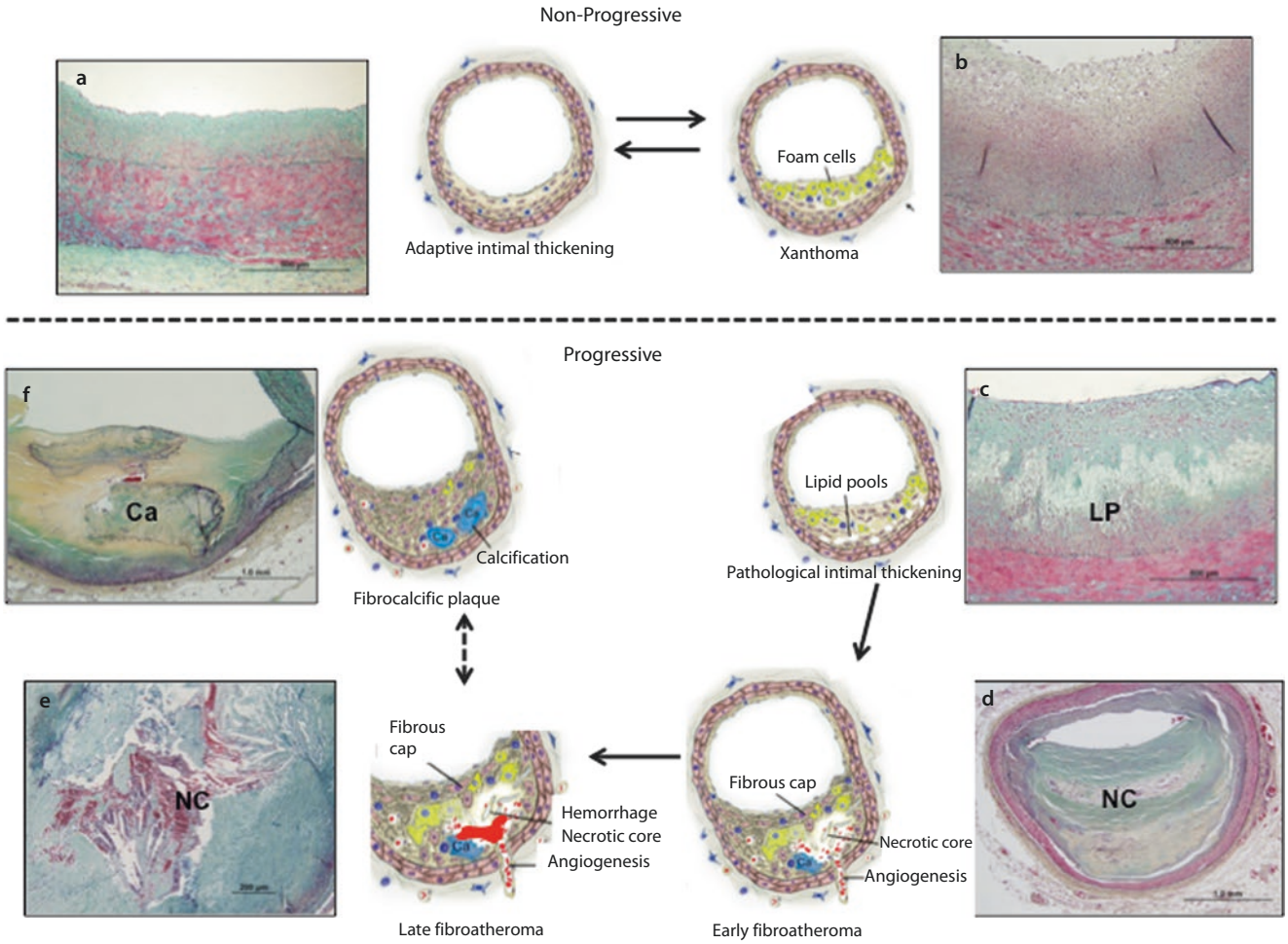


**Fig. 2.8** Proposed sequence of atherosclerotic lesion development in human disease. **a** Adaptive intimal thickening is characterized by smooth muscle cell accumulation within the intima. **b** Intimal xanthoma consisting predominantly macrophage-derived foam cells. Pathologic intimal thickening shown in **c** denotes the accumulation of extracellular lipid (*LP* lipid pool) in the absence of apparent necrosis. **d** Early fibroatheroma characterized by a necrotic core (*NC*) containing macrophages and extracellular matrix with limited cholesterol clefts an overlying thick fibrous cap. Neoangiogenesis within the developing lesion may lead to intraplaque hemorrhage resulting in a relatively rapid expansion of the NC as shown in **e**. The late fibroatheroma shows a hemorrhagic necrotic core with limited extracellular matrix and numerous cholesterol clefts. The necrotic core and surrounding tissue may eventually calcify, forming a more stable fibrocalcific plaque shown in. **f** Since some of the advanced lesion types (fibroatheromas and fibrocalcific plaques) evolve simultaneously in life, their interrelationships are difficult to resolve in autopsy studies. All histologic sections are stained by Movat pentachrome (Reproduced with permission from Bezton et al [129])

### 2.3.4 Healed Plaque Rupture

Healed plaque ruptures (HPR) are best recognized by connective tissue Movat pentachrome or picrosirius red collagen staining, with or without immunohistochemical detection of smooth muscle actin. Typically, there is a layering of collagen-rich buried fibrous cap(s) in the deeper regions of the plaque with more superficial proteoglycan (bluish-green on Movat) intermixed with SMCs and type III collagen recognized by sirius red staining under polarized light [121]. In the seminal study by Mann and Davies in 1999, HPRs were observed in 73 % of arteries showing more than 50 % cross-sectional area luminal stenosis, 19 % with 21 to 50 % area stenosis, and 16 % with stenosis <20 % [121]. Among our cases of SCD, we have reported an incidence of 61 % [122]. The prevalence of HPR was highest in stable plaques (80 %), followed by acute plaque rupture (75 %), and was least for plaque erosion (9 %). Multiple healed ruptures with layering were more common in proximal coronary vasculature, and there is an increase in the mean percent luminal narrowing relative to the number of HPRs for both acute and healed ruptures [122]. It is clear from these studies that repeated plaque rupture likely contributes significantly to increased luminal narrowing and may eventually become symptomatic, although these lesions are often clinically silent when observed in arteries not severely narrowed. As these lesion age, the type III collagen is replaced by type I collagen, and the underlying necrotic core tends to calcify forming a more stable plaque, which may or may not be severely narrowed but is rich in collagen and calcium. The incidence of silent ruptures in the clinical setting remains unknown, as these lesions cannot be identified even by more sophisticated intravascular modalities, like optical coherence tomography (OCT) (Fig. 2.8).

## 2.4 Stable and Unstable Plaques

Unstable plaques are plaques that are considered those with luminal thrombi from rupture, erosion, and calcified plaque in addition to those with severe hemorrhage, fissure, or TCFAs. Even early healed HPRs may go on to rupture and are also considered unstable, as they may progress to form another thin cap and eventually rupture. On the contrary, fairly common lesions such as fibroatheromas and PITs, which form the underlying plaque for erosions, are not considered unstable, as we today we cannot predict which lesion sites will develop into erosion. Highly calcified, i.e., fibrocalcific plaques, are stable plaques and if >75 % narrowed may cause stable angina but are less likely to thrombose unless they develop into calcified nodules.

## 2.5 Conclusion

The current understanding of the pathophysiology of atherosclerosis progression culminating in the development of stable and unstable lesions mainly extends from numerous human studies involving autopsy investigation as well as retrospective and prospective clinical trials and murine studies. The most critical discoveries include the consequence of macrophage-derived foam cells, intraplaque hemorrhage, and fibrous cap thinning, which are widely adopted morphologic features commonly used as endpoints in clinical studies particularly involving intravascular imaging modalities. Unraveling lipid metabolism and the role of inflammation have clearly added to the knowledge base of coronary disease, which have lead to promising clinical targets with the goal of improving clinical outcomes from this widespread disease. Further insights into the natural history of coronary atherosclerosis relative to a more firm understanding of the temporal change that occurs with lesion progression represents another key component that is lacking today, but with time and further improvement in intravascular imaging modalities would likely be valuable to clinical studies in order to conceive new therapeutic approaches for the prevention of disease progression.

## References


1. WHO. The top 10 causes of death: Fact sheet N°310 [Internet]. World Heal Organ. 2013. Available from: http://www.who.int/mediacentre/factsheets/fs310/en/.
2. Laslett LJ, Alagona P, Clark BA, Drozda JP, Saldivar F, Wilson SR, et al. The worldwide environment of cardiovascular disease: prevalence, diagnosis, therapy, and policy issues: a report from the American College of Cardiology. J Am Coll Cardiol. 2012;60:S1–49.
3. Virmani R, Kolodgie FD, Burke AP, Farb A, Schwartz SM. Lessons from sudden coronary death: a comprehensive morphological classification scheme for atherosclerotic lesions. Arterioscler Thromb Vasc Biol. 2000;20:1262–75.
4. Virmani R, Burke AP, Farb A. Sudden cardiac death. Cardiovasc Pathol. 2001;10:275–82.
5. Herrick JB. Clinical features of sudden obstruction of the coronary arteries. JAMA. 1912;LIX:2015.
6. Clark E, Graef I, Chasis H. Thrombosis of the aorta and coronary arteries with specific reference to the "fibrinoid" lesions. Arch Pathol. 1936;22:183–212.
7. Constantinides P. Plaque fissures in human coronary thrombosis (abstract). Fed Prox. 1964;23:443.
8. Koch W, Kong L. Uber die formen des coronarverschlusses, die anderungen im coronarkreislauf und die beziehungen zur angina pectoris. Beitr Path Anat. 1932;33:21–84.
9. Wartman WB. Occlusion of the coronary arteries by hemorrhage into their walls. Am Heart J. 1938;15:459–70.
10. Patterson J. The reaction of the arterial wall to intramural hemorrhage. Washington, DC:National Academy of Sciences 1954.
11. Winternitz M, Thomas R, LeCompte P. The relation of vascularity to disease of the vessel wall. In: Charles CT, editor. The biology of atherosclerosis. Springfield, Ill; 1938.
12. Leary T. Pathology of coronary sclerosis. Am Hear J. 1934;35:338–44.
13. Friedman M, Van den Bovernkamp G. The pathogenesis of a coronary thrombus. Am J Pathol. 1966;48:19–44.
14. Velican C, Velican D. Discrepancies between data on atherosclerotic involvement of human coronary arteries furnished by gross inspection and by light microscopy. Atherosclerosis. 1982;43:39–49.
15. Stary HC, Blankenhorn DH, Chandler AB, Glagov S, Insull W, Richardson M, et al. A definition of the intima of human arteries and of its atherosclerosis-prone regions. A report from the Committee on Vascular Lesions of the Council on Arteriosclerosis. Am Heart Assoc/Arterioscler Thromb Vasc Biol. 1992;12:120–34.
16. Stary HC, Chandler AB, Dinsmore RE, Fuster V, Glagov S, Insull W, et al. A definition of advanced types of atherosclerotic lesions and a histological classification of atherosclerosis. A report from the Committee on Vascular Lesions of the Council on Arteriosclerosis. Am Heart Assoc/Arterioscler Thromb Vasc Biol. 1995;15:1512–31.
17. Lendon C, Born GV, Davies MJ, Richardson PD. Plaque fissure: the link between atherosclerosis and thrombosis. Nouv Rev Fr Hematol. 1992;34:27–9.
18. Orekhov AN, Andreeva ER, Mikhailova IA, Gordon D. Cell proliferation in normal and atherosclerotic human aorta: proliferative splash in lipid-rich lesions. Atherosclerosis. 1998;139:41–8.
19. Imanishi T, McBride J, Ho Q, O'Brien KD, Schwartz SM, Han DK. Expression of cellular FLICE-inhibitory protein in human coronary arteries and in a rat vascular injury model. Am J Pathol. 2000;156:125–37.
20. Nakashima Y, Chen Y-X, Kinukawa N, Sueishi K. Distributions of diffuse intimal thickening in human arteries: preferential expression in atherosclerosis-prone arteries from an early age. Virchows Arch. 2002;441:279–88.
21. McGill HC, McMahan CA, Herderick EE, Tracy RE, Malcom GT, Zieske AW, et al. Effects of coronary heart disease risk factors on atherosclerosis of selected regions of the aorta and right coronary artery. PDAY Research Group. Pathobiological determinants of atherosclerosis in youth. Arterioscler Thromb Vasc Biol. 2000;20:836–45.
22. Aikawa M, Rabkin E, Okada Y, Voglic SJ, Clinton SK, Brinckerhoff CE, et al. Lipid lowering by diet reduces matrix metalloproteinase activity and increases collagen content of rabbit atheroma: a potential mechanism of lesion stabilization. Circulation. 1998;97:2433–44.
23. Kolodgie FD, Burke AP, Nakazawa G, Virmani R. Is pathologic intimal thickening the key to understanding early plaque progression in human atherosclerotic disease? Arterioscler Thromb Vasc Biol. 2007;27:986–9.
24. Otsuka F, Kramer MCA, Woudstra P, Yahagi K, Ladich E, Finn AV, et al. Natural progression of atherosclerosis from pathologic intimal thickening to late fibroatheroma in human coronary arteries: a pathology study. Atherosclerosis. 2015;241:772–82.
25. Schrijvers D, De Meyer G, Herman A, Martinet W. Phagocytosis in atherosclerosis: molecular mechanisms and implications for plaque progression and stability. Cardiovasc Res. 2007;73:470–80.

26. Newby AC, Zaltsman AB. Fibrous cap formation or destruction – the critical importance of vascular smooth muscle cell proliferation, migration and matrix formation. Cardiovasc Res. 1999;41:345–60.
27. Tulenko TN, Chen M, Mason PE, Mason RP. Physical effects of cholesterol on arterial smooth muscle membranes: evidence of immiscible cholesterol domains and alterations in bilayer width during atherogenesis. J Lipid Res. 1998;39:947–56.
28. Hoff HF, Bradley WA, Heideman CL, Gaubatz JW, Karagas MD, Gotto AM. Characterization of low density lipoprotein-like particle in the human aorta from grossly normal and atherosclerotic regions. Biochim Biophys Acta. 1979;573:361–74.
29. Smith EB, Slater RS. The microdissection of large atherosclerotic plaques to give morphologically and topographically defined fractions for analysis. 1. The lipids in the isolated fractions. Atherosclerosis. 1972;15:37–56.
30. New SEP, Goettsch C, Aikawa M, Marchini JF, Shibasaki M, Yabusaki K, et al. Macrophage-derived matrix vesicles: an alternative novel mechanism for microcalcification in atherosclerotic plaques. Circ Res. 2013;113:72–7.
31. Tabas I. Consequences and therapeutic implications of macrophage apoptosis in atherosclerosis: the importance of lesion stage and phagocytic efficiency. Arterioscler Thromb Vasc Biol. 2005;25:2255–64.
32. Dove DE, Su YR, Zhang W, Jerome WG, Swift LL, Linton MF, et al. ACAT1 deficiency disrupts cholesterol efflux and alters cellular morphology in macrophages. Arterioscler Thromb Vasc Biol. 2005;25:128–34.
33. Katz SS, Shipley GG, Small DM. Physical chemistry of the lipids of human atherosclerotic lesions. Demonstration of a lesion intermediate between fatty streaks and advanced plaques. J Clin Invest. 1976;58:200–11.
34. Stegemann C, Drozdov I, Shalhoub J, Humphries J, Ladroue C, Didangelos A, et al. Comparative lipidomics profiling of human atherosclerotic plaques. Circ Cardiovasc Genet. 2011;4:232–42.
35. Vorkas PA, Shalhoub J, Isaac G, Want EJ, Nicholson JK, Holmes E, et al. Metabolic phenotyping of atherosclerotic plaques reveals latent associations between free cholesterol and ceramide metabolism in atherogenesis. J Proteome Res. 2015;14:1389–99. 150223090903003.
36. Felton CV, Crook D, Davies MJ, Oliver MF. Relation of plaque lipid composition and morphology to the stability of human aortic plaques. Arterioscler Thromb Vasc Biol. 1997;17:1337–45.
37. Feng B, Yao PM, Li Y, Devlin CM, Zhang D, Harding HP, et al. The endoplasmic reticulum is the site of cholesterol-induced cytotoxicity in macrophages. Nat Cell Biol. 2003;5:781–92.
38. Hossain GS, Van Thienen JV, Werstuck GH, Zhou J, Sood SK, Dickhout JG, et al. TDAG51 is induced by homocysteine, promotes detachment-mediated programmed cell death, and contributes to the development of atherosclerosis in hyperhomocysteinemia. J Biol Chem. 2003;278:30317–27.
39. Myoishi M, Hao H, Minamino T, Watanabe K, Nishihira K, Hatakeyama K, et al. Increased endoplasmic reticulum stress in atherosclerotic plaques associated with acute coronary syndrome. Circulation. 2007;116:1226–33.
40. Lim W-S, Timmins JM, Seimon TA, Sadler A, Kolodgie FD, Virmani R, et al. Signal transducer and activator of transcription-1 is critical for apoptosis in macrophages subjected to endoplasmic reticulum stress in vitro and in advanced atherosclerotic lesions in vivo. Circulation. 2008;117:940–51.
41. Schrijvers DM, De Meyer GRY, Kockx MM, Herman AG, Martinet W. Phagocytosis of apoptotic cells by macrophages is impaired in atherosclerosis. Arterioscler Thromb Vasc Biol. 2005;25:1256–61.
42. Elliott MR, Ravichandran KS. Clearance of apoptotic cells: implications in health and disease. J Cell Biol. 2010;189:1059–70.
43. Ait-Oufella H, Kinugawa K, Zoll J, Simon T, Boddaert J, Heeneman S, et al. Lactadherin deficiency leads to apoptotic cell accumulation and accelerated atherosclerosis in mice. Circulation. 2007;115:2168–77.
44. Odegaard JI, Chawla A. Alternative macrophage activation and metabolism. Annu Rev Pathol. 2011;6:275–97.
45. Boisvert WA, Rose DM, Boullier A, Quehenberger O, Sydlaske A, Johnson KA, et al. Leukocyte transglutaminase 2 expression limits atherosclerotic lesion size. Arterioscler Thromb Vasc Biol. 2006;26:563–9.
46. Scott RS, McMahon EJ, Pop SM, Reap EA, Caricchio R, Cohen PL, et al. Phagocytosis and clearance of apoptotic cells is mediated by MER. Nature. 2001;411:207–11.
47. Alberts-Grill N, Denning TL, Rezvan A, Jo H. The role of the vascular dendritic cell network in atherosclerosis. Am J Physiol Cell Physiol. 2013;305:C1–21.
48. Yilmaz A, Reiss C, Tantawi O, Weng A, Stumpf C, Raaz D, et al. HMG-CoA reductase inhibitors suppress maturation of human dendritic cells: new implications for atherosclerosis. Atherosclerosis. 2004;172:85–93.
49. Shi Y, Evans JE, Rock KL. Molecular identification of a danger signal that alerts the immune system to dying cells. Nature. 2003;425:516–21.
50. Albert ML, Pearce SF, Francisco LM, Sauter B, Roy P, Silverstein RL, et al. Immature dendritic cells phagocytose apoptotic cells via alphavbeta5 and CD36, and cross-present antigens to cytotoxic T lymphocytes. J Exp Med. 1998;188:1359–68.
51. Liao X, Sluimer JC, Wang Y, Subramanian M, Brown K, Pattison JS, Robbins J, Martinez J, Tabas I. Macrophage autophagy plays a protective role in advanced atherosclerosis. Cell Metab. 2012;15(4):545–53. doi:10.1016/j.cmet.2012.01.022.
52. Kim-Shapiro DB, Schechter AN, Gladwin MT. Unraveling the reactions of nitric oxide, nitrite, and hemoglobin in physiology and therapeutics. Arterioscler Thromb Vasc Biol. 2006;26:697–705.
53. Graversen JH, Madsen M, Moestrup SK. CD163: a signal receptor scavenging haptoglobin-hemoglobin complexes from plasma. Int J Biochem Cell Biol. 2002;34:309–14.
54. Barger AC, Beeuwkes R, Lainey LL, Silverman KJ. Hypothesis: vasa vasorum and neovascularization of human coronary arteries. A possible role in the pathophysiology of atherosclerosis. N Engl J Med. 1984;310:175–7.
55. Kolodgie FD, Gold HK, Burke AP, Fowler DR, Kruth HS, Weber DK, et al. Intraplaque hemorrhage and progression of coronary atheroma. N Engl J Med. 2003;349:2316–25.
56. Van den Heuvel MM, Tensen CP, van As JH, Van den Berg TK, Fluitsma DM, Dijkstra CD, et al. Regulation of CD 163 on human macrophages: cross-linking of CD163 induces signaling and activation. J Leukoc Biol. 1999;66:858–66.
57. Tabas I. Consequences of cellular cholesterol accumulation: basic concepts and physiological implications. J Clin Invest. 2002;110:905–11.
58. Levy AP, Levy JE, Kalet-Litman S, Miller-Lotan R, Levy NS, Asaf R, et al. Haptoglobin genotype is a determinant of iron, lipid peroxidation, and macrophage accumulation in the atherosclerotic plaque. Arterioscler Thromb Vasc Biol. 2007;27:134–40.
59. Zhong Y, Tang H, Zeng Q, Wang X, Yi G, Meng K, et al. Total cholesterol content of erythrocyte membranes is associated with the severity of coronary artery disease and the therapeutic effect of rosuvastatin. Ups J Med Sci. 2012;117:390–8.
60. Duewell P, Kono H, Rayner KJ, Sirois CM, Vladimer G, Bauernfeind FG, et al. NLRP3 inflammasomes are required for atherogenesis and activated by cholesterol crystals. Nature. 2010;464:1357–61.
61. Balla G, Jacob HS, Eaton JW, Belcher JD, Vercellotti GM. Hemin: a possible physiological mediator of low density lipoprotein oxidation and endothelial injury. Arterioscler Thromb. 1991;11:1700–11.
62. Abraham NG, Lavrovsky Y, Schwartzman ML, Stoltz RA, Levere RD, Gerritsen ME, et al. Transfection of the human heme oxygenase gene into rabbit coronary microvessel endothelial cells: protective effect against heme and hemoglobin toxicity. Proc Natl Acad Sci U S A. 1995;92:6798–802.
63. Habib A, Finn AV. The role of iron metabolism as a mediator of macrophage inflammation and lipid handling in atherosclerosis. Front Pharmacol. 2014;5:195.

64. Davis GE. The Mac-1 and p150,95 beta 2 integrins bind denatured proteins to mediate leukocyte cell-substrate adhesion. Exp Cell Res. 1992;200:242–52.
65. Michel JB, Virmani R, Arbustini E, Pasterkamp G. Intraplaque haemorrhages as the trigger of plaque vulnerability. Eur Heart J. 2011;32:1977–85.
66. Boyle JJ, Harrington HA, Piper E, Elderfield K, Stark J, Landis RC, et al. Coronary intraplaque hemorrhage evokes a novel atheroprotective macrophage phenotype. Am J Pathol. 2009;174:1097–108.
67. Finn AV, Nakano M, Polavarapu R, Karmali V, Saeed O, Zhao X, et al. Hemoglobin directs macrophage differentiation and prevents foam cell formation in human atherosclerotic plaques. J Am Coll Cardiol. 2012;59:166–77.
68. Levy AP, Hochberg I, Jablonski K, Resnick HE, Lee ET, Best L, et al. Haptoglobin phenotype is an independent risk factor for cardiovascular disease in individuals with diabetes: the Strong Heart Study. J Am Coll Cardiol. 2002;40:1984–90.
69. Purushothaman M, Krishnan P, Purushothaman KR, Baber U, Tarricone A, Perez JS, et al. Genotype-dependent impairment of hemoglobin clearance increases oxidative and inflammatory response in human diabetic atherosclerosis. Arterioscler Thromb Vasc Biol. 2012;32:2769–75.
70. Miller YI, Smith A, Morgan WT, Shaklai N. Role of hemopexin in protection of low-density lipoprotein against hemoglobin-induced oxidation. Biochemistry. 1996;35:13112–7.
71. Vancov V. Structural basis of the microcirculation in the wall of arterial vessels. Bibl Anat. 1973;11:383–8.
72. Clarke JA. An x-ray microscopic study of the postnatal development of the vasa vasorum of normal human coronary arteries. Acta Anat (Basel). 1966;64:506–16.
73. Heistad DD, Marcus ML, Larsen GE, Armstrong ML. Role of vasa vasorum in nourishment of the aortic wall. Am J Physiol. 1981;240:H781–7.
74. Hildebrandt HA, Gossl M, Mannheim D, Versari D, Herrmann J, Spendlove D, et al. Differential distribution of vasa vasorum in different vascular beds in humans. Atherosclerosis. 2008;199:47–54.
75. Carmeliet P. Angiogenesis in life, disease and medicine. Nature. 2005;438:932–6.
76. Sluimer JC, Kolodgie FD, Bijnens APJJ, Maxfield K, Pacheco E, Kutys B, et al. Thin-walled microvessels in human coronary atherosclerotic plaques show incomplete endothelial junctions. Relevance of compromised structural integrity for intraplaque microvascular leakage. J Am Coll Cardiol. 2009;53:1517–27.
77. Jeziorska M, Woolley DE. Local neovascularization and cellular composition within vulnerable regions of atherosclerotic plaques of human carotid arteries. J Pathol. 1999;188:189–96.
78. Kockx MM, Cromheeke KM, Knaapen MWM, Bosmans JM, De Meyer GRY, Herman AG, et al. Phagocytosis and macrophage activation associated with hemorrhagic microvessels in human atherosclerosis. Arterioscler Thromb Vasc Biol. 2003;23:440–6.
79. Virmani R, Narula J, Farb A. When neoangiogenesis ricochets. Am Heart J. 1998;136:937–9.
80. Mulligan-Kehoe MJ, Simons M. Vasa vasorum in normal and diseased arteries. Circulation. 2014;129:2557–66.
81. O'Brien KD, McDonald TO, Chait A, Allen MD, Alpers CE. Neovascular expression of E-selectin, intercellular adhesion molecule-1, and vascular cell adhesion molecule-1 in human atherosclerosis and their relation to intimal leukocyte content. Circulation. 1996;93:672–82.
82. Cheema AN, Hong T, Nili N, Segev A, Moffat JG, Lipson KE, et al. Adventitial microvessel formation after coronary stenting and the effects of SU11218, a tyrosine kinase inhibitor. J Am Coll Cardiol. 2006;47:1067–75.
83. Hansson GK. Immune mechanisms in atherosclerosis. Arterioscler Thromb Vasc Biol. 2001;21:1876–90.
84. Russo S, Bussolati B, Deambrosis I, Mariano F, Camussi G. Platelet-activating factor mediates CD40-dependent angiogenesis and endothelial-smooth muscle cell interaction. J Immunol. 2003;171:5489–97.
85. Deregibus MC, Buttiglieri S, Russo S, Bussolati B, Camussi G. CD40-dependent activation of phosphatidylinositol 3-kinase/Akt pathway mediates endothelial cell survival and in vitro angiogenesis. J Biol Chem. 2003;278:18008–14.
86. Flaxenburg JA, Melter M, Lapchak PH, Briscoe DM, Pal S. The CD40-induced signaling pathway in endothelial cells resulting in the overexpression of vascular endothelial growth factor involves Ras and phosphatidylinositol 3-kinase. J Immunol. 2004;172:7503–9.
87. Monaco C, Andreakos E, Kiriakidis S, Feldmann M, Paleolog E. T-cell-mediated signalling in immune, inflammatory and angiogenic processes: the cascade of events leading to inflammatory diseases. Curr Drug Targets Inflamm Allergy. 2004;3:35–42.
88. Giannarelli C, Alique M, Rodriguez DT, Yang DK, Jeong D, Calcagno C, et al. Alternatively spliced tissue factor promotes plaque angiogenesis through the activation of hypoxia-inducible factor-1α and vascular endothelial growth factor signaling. Circulation. 2014;130:1274–86.
89. Howard DPJ, van Lammeren GW, Rothwell PM, Redgrave JN, Moll FL, de Vries J-PPM, et al. Symptomatic carotid atherosclerotic disease: correlations between plaque composition and ipsilateral stroke risk. Stroke. 2015;46:182–9.
90. Willems S, Vink A, Bot I, Quax PHA, de Borst GJ, de Vries J-PPM, et al. Mast cells in human carotid atherosclerotic plaques are associated with intraplaque microvessel density and the occurrence of future cardiovascular events. Eur Heart J. 2013;34:3699–706.
91. Motoyama S, Kondo T, Sarai M, Sugiura A, Harigaya H, Sato T, et al. Multislice computed tomographic characteristics of coronary lesions in acute coronary syndromes. J Am Coll Cardiol. 2007;50:319–26.
92. Burke AP, Farb A, Malcom G, Virmani R. Effect of menopause on plaque morphologic characteristics in coronary atherosclerosis. Am Heart J. 2001;141:S58–62.
93. Burke AP, Taylor A, Farb A, Malcom GT, Virmani R. Coronary calcification: insights from sudden coronary death victims. Z Kardiol. 2000;89 Suppl 2:49–53.
94. Watson KE, Abrolat ML, Malone LL, Hoeg JM, Doherty T, Detrano R, et al. Active serum vitamin D levels are inversely correlated with coronary calcification. Circulation. 1997;96:1755–60.
95. Keso T, Perola M, Laippala P, Ilveskoski E, Kunnas TA, Mikkelsson J, et al. Polymorphisms within the tumor necrosis factor locus and prevalence of coronary artery disease in middle-aged men. Atherosclerosis. 2001;154:691–7.
96. Demer LL, Tintut Y. Inflammatory, metabolic, and genetic mechanisms of vascular calcification. Arterioscler Thromb Vasc Biol. 2014;34:715–23.
97. Fernández-Friera L, Peñalvo JL, Fernández-Ortiz A, Ibañez B, López-Melgar B, Laclaustra M, et al. Prevalence, vascular distribution, and multiterritorial extent of subclinical atherosclerosis in a middle-aged cohort: the PESA (Progression of Early Subclinical Atherosclerosis) study. Circulation. 2015;131:2104–13.
98. Otsuka F, Sakakura K, Yahagi K, Joner M, Virmani R. Has our understanding of calcification in human coronary atherosclerosis progressed? Arterioscler Thromb Vasc Biol. 2014;34:724–36.
99. Huang H, Virmani R, Younis H, Burke AP, Kamm RD, Lee RT. The impact of calcification on the biomechanical stability of atherosclerotic plaques. Circulation. 2001;103:1051–6.
100. Shaw LJ, Raggi P, Schisterman E, Berman DS, Callister TQ. Prognostic value of cardiac risk factors and coronary artery calcium screening for all-cause mortality. Radiology. 2003;228:826–33.
101. Budoff MJ, Gul KM. Expert review on coronary calcium. Vasc Health Risk Manag. 2008;4:315–24.
102. Sangiorgi G, Rumberger JA, Severson A, Edwards WD, Gregoire J, Fitzpatrick LA, et al. Arterial calcification and not lumen stenosis is highly correlated with atherosclerotic plaque burden in humans: a histologic study of 723 coronary artery segments using nondecalcifying methodology. J Am Coll Cardiol. 1998;31:126–33.
103. Glagov S, Weisenberg E, Zarins CK, Stankunavicius R, Kolettis GJ. Compensatory enlargement of human atherosclerotic coronary arteries. N Engl J Med. 1987;316:1371–5.

104. Burke AP, Farb A, Malcom GT, Liang YH, Smialek J, Virmani R. Coronary risk factors and plaque morphology in men with coronary disease who died suddenly. N Engl J Med. 1997;336:1276–82.
105. Narula J, Nakano M, Virmani R, Kolodgie FD, Petersen R, Newcomb R, et al. Histopathologic characteristics of atherosclerotic coronary disease and implications of the findings for the invasive and noninvasive detection of vulnerable plaques. J Am Coll Cardiol. 2013;61:1041–51.
106. Falk E, Nakano M, Bentzon JF, Finn AV, Virmani R. Update on acute coronary syndromes: the pathologists' view. Eur Heart J. 2013;34:719–28.
107. Davies MJ, Thomas A. Thrombosis and acute coronary-artery lesions in sudden cardiac ischemic death. N Engl J Med. 1984;310:1137–40.
108. Farb A, Burke AP, Tang AL, Liang TY, Mannan P, Smialek J, et al. Coronary plaque erosion without rupture into a lipid core. A frequent cause of coronary thrombosis in sudden coronary death. Circulation. 1996;93:1354–63.
109. Burke AP, Farb A, Malcom GT, Liang Y, Smialek JE, Virmani R. Plaque rupture and sudden death related to exertion in men with coronary artery disease. JAMA. 1999;281:921–6.
110. Galis ZS, Sukhova GK, Lark MW, Libby P. Increased expression of matrix metalloproteinases and matrix degrading activity in vulnerable regions of human atherosclerotic plaques. J Clin Invest. 1994;94:2493–503.
111. Gijsen FJH, Wentzel JJ, Thury A, Mastik F, Schaar JA, Schuurbiers JCH, et al. Strain distribution over plaques in human coronary arteries relates to shear stress. Am J Physiol Heart Circ Physiol. 2008;295:H1608–14.
112. Vengrenyuk Y, Carlier S, Xanthos S, Cardoso L, Ganatos P, Virmani R, et al. A hypothesis for vulnerable plaque rupture due to stress-induced debonding around cellular microcalcifications in thin fibrous caps. Proc Natl Acad Sci U S A. 2006;103:14678–83.
113. Kolodgie FD, Narula J, Burke AP, Haider N, Farb A, Hui-Liang Y, et al. Localization of apoptotic macrophages at the site of plaque rupture in sudden coronary death. Am J Pathol. 2000;157:1259–68.
114. van der Wal AC, Becker AE, van der Loos CM, Das PK. Site of intimal rupture or erosion of thrombosed coronary atherosclerotic plaques is characterized by an inflammatory process irrespective of the dominant plaque morphology. Circulation. 1994;89:36–44.
115. Arbustini E, Dal Bello B, Morbini P, Burke AP, Bocciarelli M, Specchia G, et al. Plaque erosion is a major substrate for coronary thrombosis in acute myocardial infarction. Heart. 1999;82:269–72.
116. Kolodgie FD, Burke AP, Farb A, Weber DK, Kutys R, Wight TN, et al. Differential accumulation of proteoglycans and hyaluronan in culprit lesions: Insights into plaque erosion. Arterioscler Thromb Vasc Biol. 2002;22:1642–8.
117. Burke AP, Farb A, Malcom GT, Liang Y, Smialek J, Virmani R. Effect of risk factors on the mechanism of acute thrombosis and sudden coronary death in women. Circulation. 1998;97:2110–6.
118. Schwartz RS, Burke A, Farb A, Kaye D, Lesser JR, Henry TD, et al. Microemboli and microvascular obstruction in acute coronary thrombosis and sudden coronary death. Relation to epicardial plaque histopathology. J Am Coll Cardiol. 2009;54:2167–73. Elsevier Inc.
119. Kramer MCA, Rittersma SZH, de Winter RJ, Ladich ER, Fowler DR, Liang YH, et al. Relationship of thrombus healing to underlying plaque morphology in sudden coronary death. J Am Coll Cardiol. 2010;55:122–32. Elsevier Inc.
120. Ferrante G, Nakano M, Prati F, Niccoli G, Mallus MT, Ramazzotti V, et al. High levels of systemic myeloperoxidase are associated with coronary plaque erosion in patients with acute coronary syndromes: a clinicopathological study. Circulation. 2010;122:2505–13.
121. Mann J, Davies MJ. Mechanisms of progression in native coronary artery disease: role of healed plaque disruption. Heart. 1999;82:265–8.
122. Burke AP, Kolodgie FD, Farb A, Weber DK, Malcom GT, Smialek J, et al. Healed plaque ruptures and sudden coronary death: evidence that subclinical rupture has a role in plaque progression. Circulation. 2001;103:934–40.
123. Kolodgie FD, Burke AP, Farb A, Gold HK, Yuan J, Narula J, et al. The thin-cap fibroatheroma: a type of vulnerable plaque: the major precursor lesion to acute coronary syndromes. Curr Opin Cardiol. 2001;16:285–92.
124. Virmani R, Burke AP, Kolodgie FD, Farb A. Pathology of the thin-cap fibroatheroma: a type of vulnerable plaque. J Interv Cardiol. 2003;16:267–72.
125. Virmani R, Burke AP, Kolodgie FD, Farb A. Vulnerable plaque: the pathology of unstable coronary lesions. J Interv Cardiol. 2002;15:439–46.
126. Finn AV, Nakano M, Narula J, Kolodgie FD, Virmani R. Concept of vulnerable/unstable plaque. Arterioscler Thromb Vasc Biol. 2010;30:1282–92.
127. Kolodgie FD. Pathogenesis of atherosclerosis and the unstable plaque. In: Peter O, Kwiterovich J, (editors). Johns Hopkins Textbook of Dyslipidemia. Philadelphia: Lippincott Williams and Wilkins; 2009.
128. Burke AP, Weber DK, Kolodgie FD, Farb A, Taylor AJ, Virmani R. Pathophysiology of calcium deposition in coronary arteries. Herz. 2001;26:239–44.
129. Bentzon JF, Otsuka F, Virmani R, Falk E. Mechanisms of plaque formation and rupture. Circ Res. 2014;114:1852–66.

# Microcirculatory Dysfunction

*Nina W. van der Hoeven, Hernán Mejía-Rentería, Maurits R. Hollander, Niels van Royen, and Javier Escaned*




J. Escaned, J. Davies (eds.), *Physiological Assessment of Coronary Stenoses and the Microcirculation*,
DOI 10.1007/978-1-4471-5245-3_3

## 3.1 Introduction

Although microcirculatory dysfunction is linked to multiple cardiac and non-cardiac conditions, a conclusive diagnosis of microcirculatory dysfunction is rarely made in everyday clinical practice. As discussed below, assessment of the microcirculation may contribute to understanding the role of small vessel disease in the manifestations of chronic conditions, the direct impact of acute cardiac events on the microvasculature [1], or even to detect early anomalies in the coronary circulation occurring before the development of pathological changes in the large epicardial vessels [2].

Like the epicardial vascular compartment of the coronary circulation, the microcirculation can also be affected in different cardiac conditions. However, while the former can easily be explored with invasive and noninvasive angiography techniques, current imaging techniques cannot provide adequate visualization of the microvessels, and the techniques used to explore its functionality are relatively unknown and seldom applied in clinical practice. Furthermore, the mechanisms of microcirculatory dysfunction are multiple, including dysregulation, structural vessel remodeling, microvascular plugging, and extravascular compression. Due to this, a single diagnostic technique cannot explore all the mechanisms that may cause coronary microvascular dysfunction (CMVD).

In this chapter, we will describe the orchestrated mechanisms of the coronary microcirculation under physiological circumstances and review the different pathologies of the coronary microcirculation. Furthermore, we will discuss the clinical and prognostic implications of CMVD.

## 3.2 Functional Anatomy of the Coronary Microcirculation

The anatomy and physiology of the coronary microcirculation are strongly linked to specific functional characteristics of the myocardium and its requirements of blood supply. The constantly beating heart needs a significant amount of oxygen and nutrients [3], as shown by the high oxygen extraction of the myocardium (approximately 75 %, while in skeletal muscle only 20–30 %). Due to this, myocardial "resting" flow and capillary density are significantly higher in the coronary circulation compared to the circulation in skeletal muscles [4]. Paradoxically, extravascular compression of the collapsible elements of the microcirculation caused by myocardial contraction, predominantly of the left ventricle (LV), leads to a periodic decrease in blood supply during part of the systolic cardiac cycle. In addition, there is an intramural redistribution of myocardial flow over the cardiac cycle, driven by shifting transmural pressure gradients [5].

Broadly, the coronary microcirculation can be described as all vascular elements with a diameter <300 μm [6] that contribute to myocardial perfusion [7] and originate from larger epicardial conduit vessels. This includes the pre-arterioles (<300 μm), the arterioles (<200 μm), the capillaries, and the venules [8]. These vascular elements exhibit significant variances in their physiological behavior and pharmacological responses [9]. The microcirculatory network extends in the arterial wall both longitudinally and transmurally. The connection between the epicardial and transmural vascular network is made through small branches that penetrate the myocardium perpendicularly giving origin to short vessels with treelike structure (type I vessels) or long vessels running directly to the subendocardium (type II vessels) (Fig. 3.1). It is unclear whether the vascular network originating from these transmural arteries is continuous and interconnected, with more than one artery supplying the same network [10], or whether separate myocardial perfusion territories are outlined by the presence of capillary end loops [11]. Three-dimensional reconstruction of the transmural vasculature in the canine heart confirms the presence of a complex network, with a larger vascular volume density for subendocardial than for epicardial territories [12].

As a result of the transmural pressure gradient, subendocardial vessels are more susceptible to extravascular compression. However, this is compensated by a lower subendocardial vascular resistance, caused by an increased vessel density that facilitates its blood supply [13]. Also with the variations in resistance among the different transmural vessels, there are also transmural variations in myogenic response and autoregulation, which will be discussed in the next section.

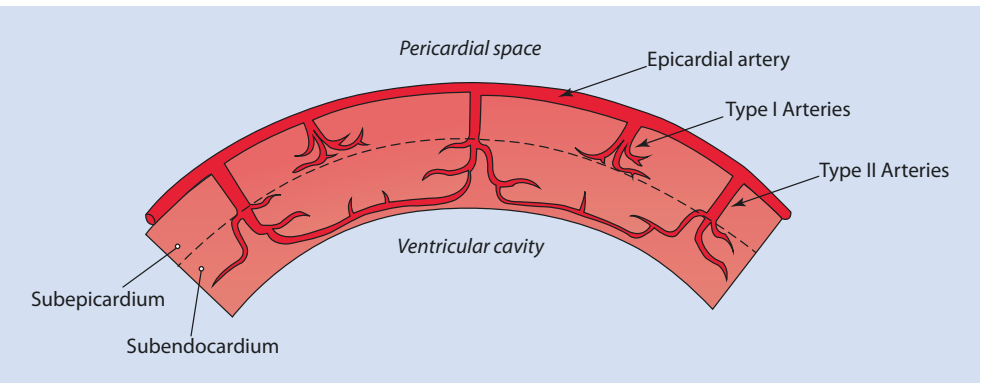


**Fig. 3.1** Transmural vascularization of the myocardium

### 3.2.1 Arterioles

Arterioles contain several layers of vascular smooth muscle cells (VSMC), which are responsible for vasoconstriction and vasodilatation. Arterioles are preceded by small extramyocardial vessels (occasionally called pre-arterioles) that account for 25 % of the coronary vascular resistance during hyperemia [14]. Arterioles are responsible for 55 % of the total coronary resistance. Among these arterioles, there are different types according to their size and mechanisms (◘ Fig. 3.2). The largest arterioles (100–200 μm) are most sensitive to flow-related stimuli (endothelial cell-mediated vasodilatation) [15]. The intermediate arterioles (40–100 μm) are most sensitive to intravascular pressure changes detected by VSMC stretch receptors. The so-called myogenic response, a key element of coronary autoregulation, consists of fast variations in arteriolar tone resulting from shifting intravascular pressure [16]. In these intermediate arterioles, there are also endothelial dependent mechanisms [17]. The small arterioles (<40 μm) are most sensitive to metabolic activity [18]. An increase in metabolic activity causes vasodilatation, and the subsequent increase in flow leads to upstream vasodilatation of larger arterioles via an endothelium-dependent mechanism [19]. These processes demonstrate the close interaction between different elements of the microcirculation.

### 3.2.2 Capillaries

Capillaries are the most abundant conduits in the heart, and their density is highest in the myocardium (about 2000–4000/mm$^2$), accounting for 90 % of the intramyocardial blood volume [20, 21]. As the capillaries are responsible for the exchange of oxygen, nutrients, and metabolites, its structure differs significantly from that of arterioles, consisting only of an endothelial layer over a basal lamina. The capillaries lie parallel to the cardiac muscle fibers, forming a network with inter-arterial connections following a Y-, T-, H-shape (due to intercapillary anastomoses) and hairpins [22]. Capillaries are collapsible structures and thus susceptible to extravascular compression by either intramyocardial or intraventricular pressures.

### 3.2.3 Venules

Like the capillaries, postcapillary venules are small vascular structures (8–30 μm), made up of VSMC, with a structure consisting of endothelial cells and pericytes, and collapsible in nature [8]. Venules drain into collecting venules (30–50 μm) that ultimately merge in larger cardiac veins.

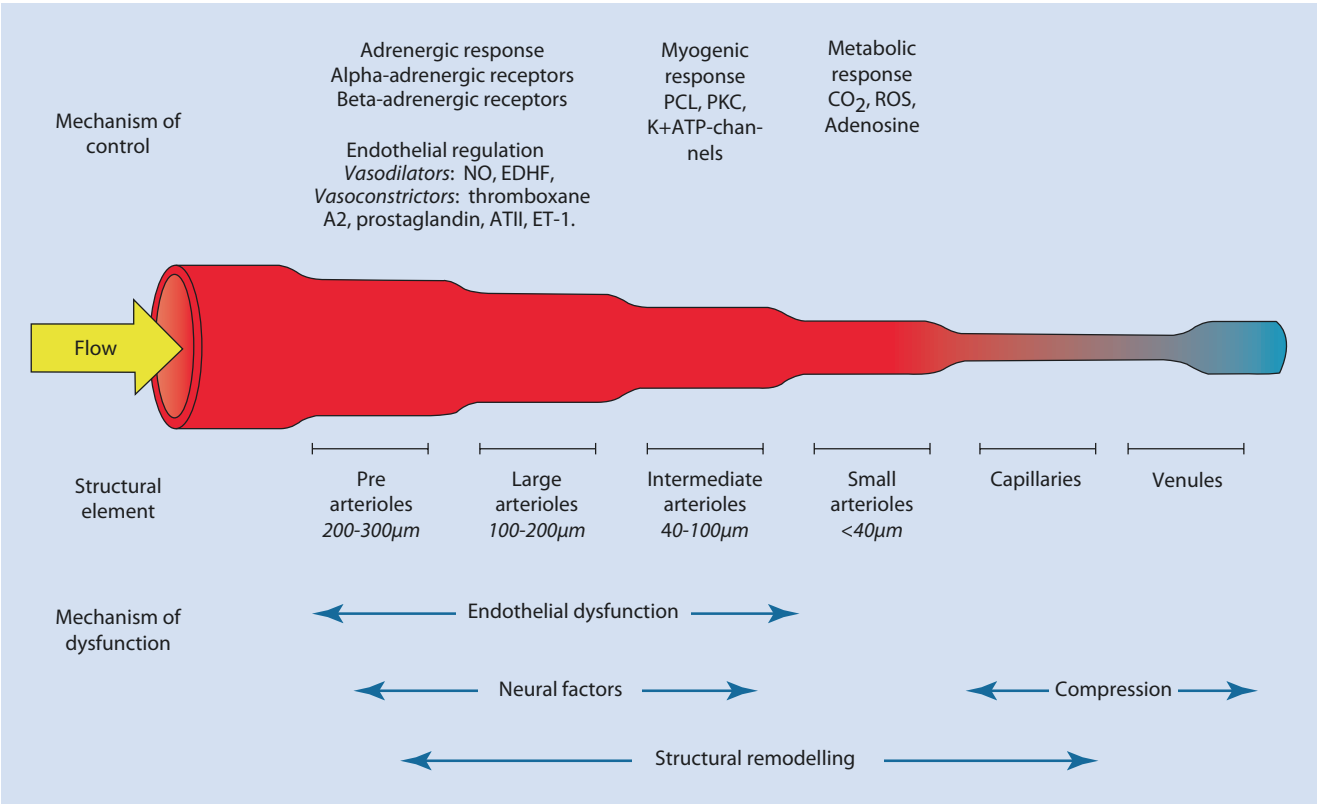


◘ **Fig. 3.2** Different physiologic mechanisms involved in microcirculatory autoregulation ATII angiotensin II, CO2 carbon dioxide, EDHF endothelial derived relaxation factor, ET-1 endothelin-1, K+ATP-channels Kalium-Adenosine triphosphate channels, NO nitric oxygen, PCL phospholipase C, PKC protein kinase C, ROS reactive oxygen species, SMC smooth muscle cell

## 3.3 Orchestrated Regulatory Mechanisms of the Coronary Microcirculation

While the coronary circulation is often seen as a stiff and static vascular network, in reality it is an extremely dynamic system in which numerous physiologic mechanisms are involved (Fig. 3.2). These mechanisms are heterogeneously distributed in the different subdomains of the coronary microcirculation (large and small arterioles, capillaries) [23, 24] and are triggered by specific stimuli (pressure, metabolites, flow, etc.) to ensure coronary autoregulation. Furthermore, the individual vascular responses are orchestrated to ensure that blood flow supply matches myocardial oxygen demands at every time point. As shown later, some modalities of microcirculatory dysfunction consist in the loss of this orchestration of individual vascular responses.

### 3.3.1 Microvascular Resistance

Most of the vascular resistance of the coronary system is located at the level of the microcirculation. The pivotal work of Chilian et al. demonstrated that, under rest conditions, 75 % of coronary resistance is located in vessels with a diameter < 200 μm and 25 % of the coronary resistance is located in vessels < 100 μm [25]. The remaining resistance is in vessels larger than 200 μm, making the microcirculation almost solely responsible for the coronary intravascular resistance. Due to high resistance in these vessels, pressure declines gradually together with vessel diameter and can even reach pressures as low as 20–30 mmHg [6]. The mechanisms that alter microvascular resistance are described below.

### 3.3.2 Myogenic Response

Regulation of intravascular pressure at the level of the microcirculation is of key importance both in preventing myocardial ischemia and tissue damage due to edema [14]. The myogenic response, a key physiological mechanism addressing the control of intravascular pressure, is linked to the presence of stretching receptors located on the VSMC. These include voltage-dependent calcium channels [26, 27] whose density is inversely correlated to arteriolar diameter [28] and G proteins attached to the stretch-sensitive phospholipase C (PCL) [29] which stimulate cation channels via protein kinase C (PKC). Activation of the $K^{+ATP}$ channel causes VSMC relaxation, predominantly in the smallest vessels [30]. The $K^{+ATP}$ channel is activated by acidosis, ischemia, hypoxia, but also by, e.g., adenosine and prostacyclin [8]. Of note, the myogenic response occurs more often in the subepicardium compared to the ischemia-sensitive subendocardium [16], potentially as a mechanism to ensure transmural distribution of flow in shifting hemodynamic conditions.

### 3.3.3 Metabolic Response

A decrease in coronary oxygen leads directly to coronary vasodilatation through different pathways that include metabolites such as carbon dioxide ($CO_2$), reactive oxygen species (ROS) [31], and adenosine produced by degradation of adenine nucleotides (the latter envisaged by some investigators as a "back-up mechanism" when other vasodilatory mechanisms fail). The role of nitric oxygen (NO) in the metabolic response is uncertain. While it is true that NO levels increase with elevated metabolic activity [32], inhibition of NO did not influence vasodilatation in the microcirculation [33].

### 3.3.4 Mechanisms Regulated by the Endothelium

The endothelium is responsible for the production of vasodilatory and vasoconstrictor substances during several physiological and pathological conditions. In healthy vessels, an increase in coronary flow triggers endothelium-dependent vasodilatation [34], which occurs in the context of a release of vasoactive substances by endothelial cells including NO, endothelium-derived relaxing factor (EDHF), prostaglandins, antithrombin III, and tissue plasminogen activator [35]. These are released due to shear stress detected by the endothelial cell surface receptors. Shear stress on the vessel wall leads to activation of various endothelial pathways dependent on the initial shear stress. Laminar shear stress tends to induce an anti-inflammatory response and turbulent shear stress an inflammatory response [36, 37]. Interestingly, in several animal studies, it was found that depending on age, gender, presence of disease, and the usage of medication, different substances (e.g., prostaglandins) were responsible for the shear stress-mediated vasodilatory effect [38, 39].

Nitric oxide (NO) is produced by the endothelial NO synthase (eNOS) [40]. The production and function of NO is influenced by numerous factors, including pulsatile flow, shear stress, thrombin, adenosine diphosphate, histamine, or bradykinin [41]. The main effect of NO is VSMC relaxation, an effect mediated by a decrease in intracellular calcium [42]. Also with the resulting vasodilatory effect, NO has several relevant physiological effects on the biology of the vascular wall, including an anti-inflammatory effect that protects the endothelium against adhesion and infiltration of leukocytes [43], an inhibitory effect on the differentiation of monocytes to macrophages, which is an anti-atherosclerotic process [44]. NO counteracts the actions of the vasoconstrictors endothelin-1 (ET-1) and angiotensin II [45].

Endothelial-dependent hyperpolarizing factor (EDHF) is a vasodilator that acts independently of NO. EDHF causes hyperpolarization of VSMC in reaction to opening of calcium activated $K^+$ channels [46] leading to vasodilatation. In the presence of atherosclerosis, EDHF might compensate for other vasodilators (e.g., NO, in case of impaired

bioavailability) when they are unable to influence the vasomotor tone [47–49]. Hyperpolarization of the endothelial can be affected by multiple other substances, e.g., anandamide, C-natriuretic peptide, potassium ions, epoxyeicosatrienoic acid (EET), NO, and $H_2O_2$. Furthermore, $H_2O_2$ stimulates smooth muscle proliferation, endothelial cell adhesion, molecule expression, and thrombosis, whereas NO, EDHF, and EET are antithrombotic, preventing VSMC and suppressing endothelial activation [2].

The vascular endothelium also regulates a number of vasoconstriction factors, including thromboxane A2, prostaglandin, angiotensin II, and ET-1. The most potent vasoconstrictor of those mentioned is ET-1, which is produced by the endothelium; potentiates the effect of other vasoactive substances such as angiotensin II, norepinephrine, and serotonin; and has other relevant biological effects such as stimulation of leukocyte adhesion and recruitment, prothrombotic processes, and VSMC migration [45, 50].

### 3.3.5 Adrenergic Response

Adrenergic innervation of the different components of the microcirculation is very heterogeneous. The coronary vessels contain alpha-adrenergic receptors, which cause vasoconstriction and are invoked during exercise and counteracted by metabolic vasodilatation. Norepinephrine causes vasoconstriction in arterioles with a diameter > 100 μm and vasodilatation in arterioles with a diameter < 100 μm [51, 52]. It is thought that when the larger arterioles reduce in size, the pressure decreases which leads to vasodilatation in the smaller arterioles. Hypoperfusion causes alpha-adrenergic vasoconstriction and adenosine receptor blockade and also modulates adrenergic vasoconstriction. Stimulation of the beta-adrenergic receptors leads to vasodilatation in the larger vessels of the coronary circulation where there is a small surplus of beta2-adrenergic receptors compared to beta1-adrenergic receptors. This surplus is more commonly present in the microcirculation [53].

In normal conditions, the net effect of adrenergic stimulation on coronary flow is modulated by concomitant vasodilatory mechanisms of non-neural origin. This explains why while the autonomic nervous system alone plays a small role in the regulation of the healthy coronary circulation [51, 52], its effects on coronary flow become more important in the presence of hypercholesterolemia, endothelial dysfunction, or upstream severe stenosis [54].

## 3.4 Mechanisms of Microvascular Dysfunction

It is important to highlight that each of the previously discussed microcirculatory mechanisms ensuring coronary flow supply and regulation may be affected leading to a particular mode of microcirculatory dysfunction (Table 3.1). Camici and Crea [55] elegantly developed a classification to distinguish between the multiple geneses of CMVD (Table 3.2). We will describe the processes leading to the different forms of CMVD in more detail below.

**Table 3.1** Pathogenic mechanisms that contribute to the different types of CMVD

| CMVD | Main pathogenetic mechanisms |
|---|---|
| Type 1 | Endothelial dysfunction, SMC dysfunction, vascular remodeling |
| Type 2 | Vascular remodeling, SMC dysfunction, extramural compression, luminal obstruction |
| Type 3 | Endothelial dysfunction, SMC dysfunction, luminal obstruction |
| Type 4 | Luminal obstruction, autonomic dysfunction |
| Type 5[a] | Luminal obstruction, autonomic dysfunction |

*CMVD* coronary microvascular dysfunction, *SMC* smooth muscle cell
[a]Additional category suggested by Herrmann et al. [18]

**Table 3.2** Modified clinical classification of coronary microvascular dysfunction

| CMVD | Definition |
|---|---|
| Type 1 | Primary, i.e., in the absence of structural heart disease |
| Type 2 | In the presence of cardiomyopathies (incl. LVH, HOCM, DCM, amyloidosis) |
| Type 3 | In the presence of obstructive CAD (incl. ACS) |
| Type 4 | After coronary interventions |
| Type 5[a] | After cardiac transplantations |
| **Modifiers** Type 1[a] | |
| Duration | Acute or chronic |
| Symptoms | Asymptomatic or symptomatic |
| Therapy | None, minimal, moderate, or maximal level |

*ACS* acute coronary syndrome, *CAD* coronary artery disease, *CMVD* coronary microvascular dysfunction, *DCM* dilated cardiomyopathy, *HOCM* hypertrophic cardiomyopathy
[a]Additional category suggested by Herrmann et al. [18]

### 3.4.1 Endothelium-Dependent Dysfunction

The main consequence of endothelial dysfunction for the functionality of the microcirculation relates to flow-mediated dilation of large arterioles in response to an increase in myocardial

blood requirements. Endothelial dysfunction leads to production of substances with a constrictive effect on the microcirculation such as thromboxane A2, endothelin, prostaglandin H2, and superoxide [56]. Metabolic-driven vasodilation of small arterioles leads to an increase in flow that, in presence of endothelial dysfunction, induces flow-mediated constriction of larger arterioles. Furthermore, there might be an increased inflammatory and anti-angiogenic response resulting in capillary rarefaction [56]. Microvascular spasm can be suspected when the intracoronary acetylcholine test leads to chest pain and ECG abnormalities without development of spasm in the large epicardial vessels [57]. A sufficient response to other vasodilators such as adenosine, dipyridamole, and papaverine implies that there is an impairment of the VSMC [58].

### 3.4.2 Smooth Muscle Cell Dysfunction

Several studies investigated the involvement of classical cardiovascular risk factors, such as aging [59], hypertension [60, 61], diabetes [62, 63], dyslipidemia [64, 65], and insulin resistance [66] in relation to CMVD. Most used adenosine as the vasodilatator stimulus, which acts via receptors on VSMC. Results showed abnormal vasodilatation and impaired coronary flow reserve (CFR) in patients with these risk factors.

Rho-kinase might play a role in SMC dysfunction by promoting VSMC proliferation or by their involvement in the effects of different vasoactive factors. Selective Rho-kinase inhibitors are used to treat patients with microvascular angina [67].

### 3.4.3 Structural Remodeling of the Microvasculature

Structural abnormalities in the microcirculation occur and may have prognostic implications in various clinical settings such as coronary artery disease, diabetes mellitus, hypertension, hypertrophic cardiomyopathy, and transplant cardiac allograft vasculopathy [55, 68–73].

In the context of coronary artery disease, there is evidence suggesting that the presence of epicardial stenoses has an influence on the functionality of subtended microcirculation. In experimental animal models, the creation of an epicardial stenosis is followed by remodeling of subtended arterioles, with increased wall thickness, decreased lumen diameter, interstitial, perivascular replacement fibrosis, and VSMC proliferation [74]. Two other factors that contribute to vascular changes are shear stress [75] and NO. NO inhibits SMC growth and intimal hyperplasia and is under-expressed in case of limited flow (severe stenosis) [76, 77] resulting in microcirculatory remodeling [78]. These structural changes have evident clinical implications, which we will discuss below.

Diabetes mellitus is linked to structural abnormalities of the coronary microcirculation such as decreased capillary density, reduced myocardial perfusion, and consequently apoptosis and necrosis of the cardiomyocytes. In turn this leads to replacement fibrosis and gradual diastolic and systolic dysfunction and ultimately can cause heart failure [79].

Hypertension might ultimately lead to similar coronary microvascular alterations. Arterioles of patients with hypertension show medial thickening with a normal intimal layer. Hypertensive thickening of the wall is associated with diastolic blood pressure, but not with systolic which is obviously due to myocardial contraction during systole [80].

Coronary flow is impaired in patients with idiopathic dilated cardiomyopathy (IDCM) with seemingly normal arteries at angiography. We know that IDCM leads to structural and functional changes in the coronary microcirculation including interstitial, perivascular fibrosis [81] and decreased capillary density with luminal narrowing [82]. Decreased capillary density was associated with lower coronary flow reserve (CFR) and higher microvascular resistance. In consequence, arterioles and capillaries lose their autoregulation properties which can be unmasked by decreased CFR [83–87]. In hypertrophic cardiomyopathy (HOCM), we see the same structural changes with VSMC dysfunction, atypical coronary endothelial cells and thickening of the intima and media of the vessel wall. This is combined with a decreased luminal cross-sectional area and results in an abnormal vasodilatory capacity [88, 89]. This creates a substrate of chronic myocardial ischemia leading to myocyte death and replacement fibrosis. These conditions lead to a substrate of chronic myocardial ischemia causing myocyte death and replacement fibrosis.

Finally, structural remodeling of the coronary microcirculation also occurs in patients with cardiac transplantation as part of cardiac allograft vasculopathy, which causes a decrease in capillary density (capillary rarefaction) and arteriolar obliteration [73]. Other studies in these patients showed the same pattern of microvascular remodeling with obstructive microvasculopathy due to medial thickening and partially endothelial disease [69]. With time, these structural changes develop and increase microvascular resistance and cardiovascular events.

### 3.4.4 Extravascular Compression and Intraluminal Plugging

In patients with ACS, unfortunately despite successful restoration of antegrade flow, reperfusion paradoxically induces myocardial injury and myocardial cell death [90]. This additional injury causes an increased final infarct size after PCI compared to infarct size without reperfusion injury [91]. The inability of blood to perfuse a previously ischemic region despite successful treatment of epicardial obstruction, typically in the context of acute coronary syndromes and primary PCI, is called no-reflow [92].

Endothelial dysfunction, capillary plugging due to neutrophils migration, inflammation, and the formation of microthrombi are all factors that cause no-reflow in the setting of

plaque rupture [93–95]. Microthrombi and atheromatous particles may obstruct small arterioles downstream after plaque ulceration or rupture [96]. Athero-thrombotic embolization may also result from mechanical disruption during PCI, with a variable degree of flow impairment that reaches its maximal expression in the no-reflow phenomenon. It is unclear whether preconditioning of the ischemic area prior to an acute ischemic event provides protection against no-reflow [97].

Luminal obstruction is not only caused by atherothrombotic embolization, however is probably closely related to the amount of microvascular spasm that occurs in conjunction with the release of cholesterol crystals and macrophages from the plaque. While vascular spasm is usually transient, the flow reduction that it causes due to the combination of vascular spasm and microemboli is sufficient to cause permanent myocardial damage [98].

It has been shown that the typical MRI pattern of no-reflow is related, at least in part, to intramyocardial hemorrhage [99], and is associated with reduced LV ejection fraction and adverse remodeling. Myocardial edema and intramyocardial hemorrhage in the acute and subacute phases of myocardial infarction cause compression of the microvasculature and increase the impedance of the microvascular bed [100].

Finally elevated LV diastolic filling and intramyocardial pressures, commonly found in situations like aortic stenosis and cardiomyopathies, may cause decreased subendocardial flow [101], capillary rarefaction [102], and exhaustion of the capacity of coronary autoregulation [103].

### 3.4.5 Neural Dysregulation

The coronary arteries are surrounded by sympathic, parasympathetic, and nonadrenergic/noncholinergic nerves that significantly affect the vascular tone of the coronary microcirculation. Some of the vasoactive neurohumoral factors are neurotransmitters/co-transmitters, circulatory hormones, thrombus-related substances, and constituents released from the vascular wall [8]. For instance, adrenergic stimulation can impair coronary flow supply in clinical situations in which its vasoconstrictive effects are not counterbalanced by normally existing vasodilation mechanisms that are attenuated or abolished by disease. This explains why hyperglycemia, insulin resistance, inflammation, and autonomic dysfunction have been involved in the causative mechanisms of impaired coronary vascular function. α-adrenergic microvascular vasoconstriction is found directly after PCI. In line with this finding, α-adrenergic antagonist increases the vasodilatory effect of adenosine and blood flow velocity [104]. Arteriolar remodeling downstream of an epicardial stenosis has been linked to hyperreactivity to neural stimulation [105]. Therefore, neural regulation plays an important role in the dilator capacity of the coronary microcirculation. Microcirculatory dysfunction has also been proposed to play an important role in Takotsubo cardiomyopathy, a syndrome strongly linked to adrenergic overstimulation resulting from emotional stress [106–111].

## 3.5 Clinical and Prognostic Implications of Coronary Microvascular Dysfunction

The treatment of ischemic heart disease is largely based on a paradigm that gives epicardial coronary stenoses a central role in the generation of myocardial ischemia. However, cumulative evidence suggests that this causative relationship represents a simplistic view of ischemic heart disease [112]. In this sense, microcirculatory dysfunction has been demonstrated as an important, and in some cases, the predominant cause of myocardial ischemia either in the presence or absence of obstructive epicardial lesions, and can be a major determinant of patient outcomes [18]. In the following paragraphs, we will describe in detail different clinical settings in which CMVD plays a key role in the pathophysiological mechanisms and may be determinant in the patient outcomes.

### 3.5.1 Microvascular Angina

Defined as typical angina with positive ischemia testing but normal coronary angiography, this syndrome has been controversial since its recognition more than four decades ago. However, it is increasingly recognized that some cardiac domains beyond the epicardial arteries are involved in the mechanisms of different forms of ischemic heart disease. Microvascular angina seems to have specific etiologies; however, it is not well understood yet. One of the proposed mechanisms is an autonomic dysfunction, result of parasympathetic impairment which would affect the endothelial function [113]. The involvement of the autonomic system in this syndrome is indirectly supported by the well-accepted role of CMVD in Takotsubo syndrome as result of catecholamine dysregulation [114]. However, normal plasmatic levels of catecholamines have been found in patients with suspected microvascular angina [115], and other studies have failed to demonstrate autonomic dysfunction [116]. Another proposed causative mechanism is an abnormal perception of angina-like chest pain. This hypothesis is supported by affective disorders frequently found in these patients, as well the observed relief of symptoms with imipramine and stimulators of the nervous system [117]. However, this hypothesis is controversial, not well documented, and may be as a result of bias. Systemic endothelial dysfunction as a primary underlying mechanism of microvascular angina has been proposed based on the vascular involvement at other organ levels observed in patients with this syndrome. A depressed CFR has been found in the left anterior descending artery (assessed with transthoracic Doppler) in patients with chronic migraine, suggesting a common pathophysiological pathway of this relation between microvascular dysfunction and central nervous system [118]. On the other hand, renal insufficiency has been shown to be associated with reduced coronary flow in patients with nonobstructive CAD [119]. Furthermore, microvascular abnormalities in the retina of diabetic patients

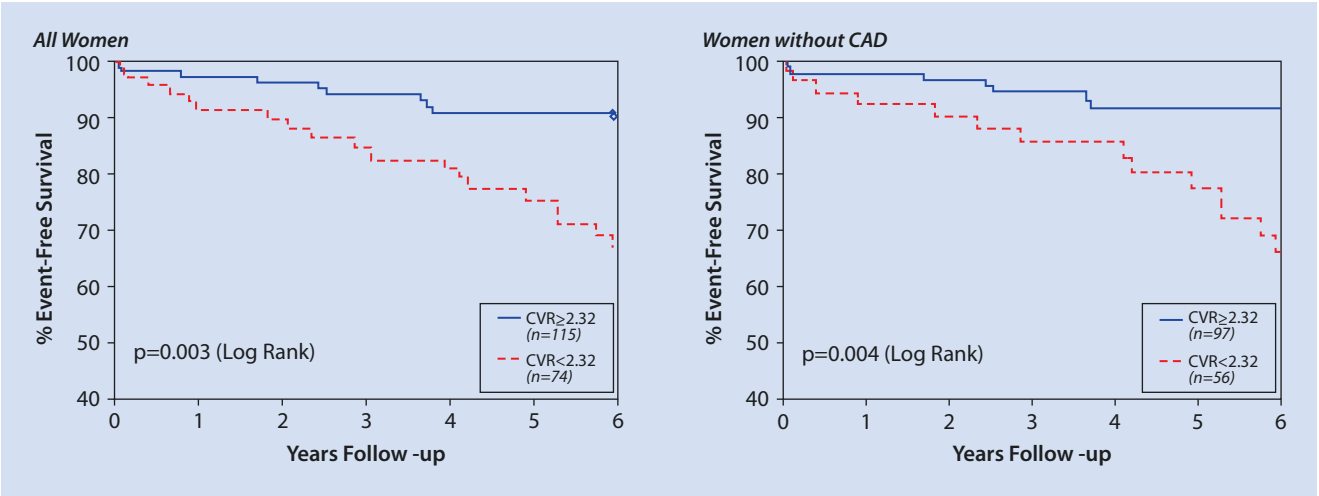


**Fig. 3.3** Coronary flow reserve and event-free survival. Coronary flow reserve (CFR) and event-free survival among all women (left) and those without CAD (right). Data represent unadjusted Kaplan-Meier curves for absence of death, nonfatal MI, nonfatal stroke, or hospitalization for CHF during follow-up. From Pepine et al. J Am Coll Cardiol. 2010 Jun 22;55(25):2825–32; with permission

have been correlated with a decreased CFR [120]. It appears that microvascular dysfunction may affect not only the heart but also other target organs in patients without obstructive CAD, which highlights the potential involvement of systemic endothelial dysfunction in the mechanism of microvascular angina. In fact, an impaired endothelium-mediated change in arterial tone of the fingertip vascular bed (assessed 5 min pre- and after brachial artery occlusion) has been found in patients with microvascular angina [121], which may be indicative of systemic endothelial dysfunction. Closely related to the previous hypothesis, chronic inflammation has been suggested to play a role in the pathogenesis of myocardial ischemia in this clinical subset. Microvascular dysfunction may also be linked to systemic inflammation in patients with high-risk coronary atherosclerosis [122]. A role for inflammation as modulator of microcirculatory function has also been proposed for patients with microvascular angina, with an inverse relationship between chronic levels of C-reactive protein and CFR, compared to healthy subjects [123].

Although it was initially thought that microvascular angina is associated with a good long-term prognosis, particularly in patients with normal epicardial coronary arteries and preserved ventricular function, current evidence implies that there is a worse prognosis in patients with concomitant conditions, including ischemia in noninvasive stress testing, persistent chest pain, diabetes, coronary atherosclerosis, or abnormal CFR [124, 125]. Several studies using noninvasive techniques (PET, CMR, SPECT, echocardiography) and intracoronary flow measurements (thermodilution and Doppler velocity) have consistently shown a strong correlation between CFR and prognosis of patients with microvascular angina. An abnormal CFR is an independent predictor of worse prognosis [126, 127, 128–131]. Women with long-term persistent angina after initial normal-appearing coronary angiography have an increased risk of developing coronary atherosclerosis and adverse outcomes at long-term follow-up. CFR, a valuable index to assess the state of microcirculation in the absence of obstructive CAD, correlated well with prognosis in women with suspected ischemia and cardiovascular risk factors; in particular, a CFR <2.32 has been associated with an increased risk of major adverse outcomes (death, myocardial infarction, stroke, and heart failure) in this population (Fig. 3.3) [132]. Beyond the impact on prognosis, microvascular angina notably affects the quality of life. Patients with this condition experience recurrent and disabling chest pain, requiring frequent medical assistance, being subjected to multiple and repetitive diagnostic tests [133, 134]. This, together with the poor response to traditional anti-ischemic medical treatment frequently observed in this syndrome [135], affects the emotional stability of patients and substantially raises health costs [136].

### 3.5.2 Role of Diabetes in CMVD

Chronic hyperglycemia plays a role in the development of cardiovascular disease. CMVD is more prevalent in patients with diabetes mellitus in whom a markedly reduced endothelial vasodilator function has been observed [62, 127, 137]. The abnormal CFR in this population may be as a consequence of disturbances at several coronary domains, including multivessel disease, diffuse coronary atherosclerosis, and CMVD. Multiple pathways commonly found in diabetic patients, namely, endothelial dysfunction as consequence of hyperglycemia, insulin resistance, and inflammation, as well as autonomic dysfunction, may contribute to CMVD. Moreover, CFR is a strong independent predictor of

cardiovascular outcomes in diabetic patients [138]. In this clinical setting, an abnormal CFR in the absence of obstructive CAD is associated with a high cardiac mortality rate, similar to that in patients with both diabetes and obstructive CAD; however, diabetes itself is not associated with excess cardiac mortality in presence of a normal CFR [139] (Fig. 3.3). This observation may have important prognostic implications as early identification of CMVD might lead to recognition of asymptomatic patients with increased risk of developing obstructive CAD. Early lifestyle modifications and optimization of medical treatment may avoid progression of CAD and cardiac outcomes [60, 64, 65, 139, 140].

### 3.5.3 CMVD in Acute Coronary Syndrome (ACS)

The status of the coronary microvasculature has prognostic implications in the pathophysiological mechanisms and outcomes of patients with ACS. In the STEMI subset, complete reperfusion of the subtended myocardial territory after opening an acute occluded coronary artery is not always achieved [71, 141]. This is immediately evident when slow flow or no-flow is observed and the ST segments remain elevated. CMVD is proposed as the mechanism to explain this phenomenon as result of high resistances in the small vessels. Microvascular obstruction secondary to microemboli of platelets from eroded coronary atherosclerotic plaques seems to be a determinant cause of CMVD in this subset [142]. In contrast to the classical autoregulation concept in which distal pressure drop caused by an epicardial stenosis is compensated by vasodilation of the coronary microvasculature, some studies have found signs of predominant microcirculatory vasoconstriction in ACS, supporting the argument that CMVD is involved in the development and maintenance of acute myocardial ischemia [143–147]. When myocardial perfusion is not restored despite opening the occluded artery, prognosis is significantly worse. Several invasive physiological techniques such as CFR, HMR (hyperemic microvascular resistance), and IMR (index of microcirculatory resistance) have been used to determine the role of coronary microvasculature in the outcomes of patients with ACS. Abnormal microvascular resistances, which are surrogated indicators of CMVD, have been associated with poor recovery of the left ventricular function, larger wall motion abnormalities, and a greater infarct size in STEMI patients [148, 149]. Studies using noninvasive methods indicate that the extension of the microvascular obstruction after an acute myocardial infarction is a strong prognostic marker of adverse cardiovascular outcomes [150–152]. Evaluated with cardiac magnetic resonance (CMR), a rate of microvascular obstruction of 54% was reported in patients with STEMI despite successful reperfusion, and the infarct size and grade of impairment of systolic function were largest in patients with microvascular obstruction [153]. CMR findings have been well correlated with histological studies [99].

### 3.5.4 CMVD in Stable CAD

CMVD may play a role in the symptomatic status and prognosis of patients with stable CAD. In some cases, CMVD may be the predominant cause of myocardial ischemia [18] and may explain the high prevalence of recurrent angina after PCI, which constitutes a major clinical problem. A study conducted in patients treated with PCI showed a higher prevalence of persistent angina 6–12 months after the index procedure in those with higher microcirculatory resistances and lower CFR than control subjects who remained asymptomatic [154]. Moreover, CMVD may be the cause of ischemia in vessels with FFR > 0.80, providing a partial explanation to the recurrent angina in patients with FFR-guided PCI [155].

Recent studies have that the combined assessment of intracoronary pressure and flow in patients with stable CAD can provide valuable prognostic information. Based on a retrospective analysis of a large cohort of patients with stable CAD investigated with FFR and Doppler-derived CFR, it has been shown that patients with abnormal CFR despite normal FFR have higher risk for MACE, while normal CFR despite abnormal FFR conveys equivalent cardiac outcomes compared with patients with normal FFR and CFR [156]. The discordance between FFR and CFR may originate from involvement of diffuse coronary atherosclerosis and CMVD in variable degrees [157]. In addition, a recent study has shown that in deferred-PCI patient group (FFR > 0.80), a worse long-term outcome (a composite of any death, myocardial infarction, and revascularization) occurred in the subgroup of patients with low CFR (<2) with high IMR (≥23U) [158].

### 3.5.5 CMVD in Hypertrophic Cardiomyopathy (HCM)

CMVD constitutes a substrate for myocardial ischemia in patients with HCM. Structural and morphological changes in the microcirculation have been postulated as an underlying mechanism for ischemia in this clinical setting [159]. The anatomical abnormalities consist of medial wall thickness and variable degrees of intimal thickening in the intramural coronary arterioles as a consequence of smooth muscle hypertrophy and collagen deposition, as well as reduced capillary density [160]. This remodeling causes functional abnormalities in the coronary microcirculation. Several studies with noninvasive techniques (PET and CMR) have shown a decrease in the hyperemic myocardial blood flow (hMBF) in patients with HCM compared with healthy subjects, but similar resting MBF, which reflects a reduction in the vasodilator response capacity [161–163]. An hMBF <1.1 ml/min $g^{-1}$ has been found the most powerful independent predictor of adverse outcomes, being associated with a 9.6-fold increase in age-adjusted relative risk of death [68]. Another proposed

mechanism contributing to microvascular dysfunction in patients is extravascular compression. A PET study in patients with HCM matched with healthy volunteers, found some surrogated markers of extravascular compression, such as left ventricular mass index and NT-proBNP, and was inversely correlated with hMBF, with a greater impact at the subendocardial myocardial layer [164]. In the absence of hemodynamically significant epicardial lesions, CMVD and microvascular remodeling may explain this inadequate increase in myocardial blood flow in response to a coronary vasodilator. The correlation between hMBF and HCM seems to be proportional to the left ventricle wall thickness, with a lower hMBF as the end-diastolic wall thickness increases, particularly in the endocardium [68, 163, 165]. However, it is important to note that patients with HCM have, in variable degrees, an increased systolic intramyocardial and left ventricle end-diastolic pressures, which may contribute to the myocardial perfusion defect. CMVD, chronic ischemia, and subsequent myocardial fibrosis may be important contributors to the natural history of HCM. CMR studies have shown a mismatch between MBF and myocardial fibrosis, the latter more important as the end-diastolic wall thickness increases [163, 166]. These abnormal structural and functional changes at different levels of the heart (coronary microcirculation, myocardium, and endocardium) contribute to adverse outcomes and life-threatening events in HCM patients such as ventricular arrhythmias, heart failure, and sudden death [167]. CMVD has been found to be an independent predictor of long-term systolic dysfunction in patients with HCM [168]. In light of these results, CMVD has been proposed as a potential target for early detection and treatment of high-risk HCM.

### 3.5.6 CMVD in Idiopathic Dilated Cardiomyopathy (IDCM)

By definition, IDCM is a cardiac muscle disease characterized by a depressed left ventricle ejection fraction and left ventricle dilatation without obstructive CAD in absence of a specific cause [169]. For this reason, it was previously thought that myocardial ischemia did not play a role in the natural history of this syndrome. Nonetheless, several studies have found evidence of chronic myocardial ischemia in patients with IDCM, even at early stages of the disease, and have consistently supported the theory that CMVD plays a key role in the pathophysiological mechanisms. The evidence is mainly derived from studies demonstrating myocardial blood flow abnormalities in patients with IDCM despite normal epicardial coronary arteries, which means a reduced capacity to increase the coronary blood flow, leading to oxygen demand–supply mismatch, chronic myocardial ischemia, and progression of disease [84–86, 170–172]. A significantly lower CFR, using intracoronary Doppler, has been found in patients with IDCM when compared with controls in all three major vascular territories [106]. In the same study, this reduced CFR was correlated with a depressed regional contractile reserve in the vascular territory of the left anterior descending evaluated with dobutamine echocardiography. Of note, extravascular mechanisms such as congestive heart failure and increased intramyocardial and left ventricle end-diastolic pressures may in part explain this reduction in CFR in IDCM [63, 84]. However, functional and structural changes in the microcirculation with areas of interstitial and perivascular fibrosis [173–175], as well as reduced capillary density [82], have been reported, which may explain the involvement of the microcirculation and the reduced hyperemic coronary flow. A reciprocal interaction between abnormal CFR and chronic myocardial ischemia would perpetuate a vicious circle, impairing the coronary microcirculation function and the left ventricle ejection fraction. Furthermore, it seems that the severity of microvascular dysfunction determines adverse cardiac outcomes in this population. A decreased CFR has been associated with worse prognosis (independent of the degree of left ventricle systolic dysfunction), being a predictor of sudden death and progression of heart failure [176–178]. Although the primary pathophysiological mechanisms involved in the development of IDCM are not well known there is strong evidence pointing towards the pivotal role of CMVD in disease progression and cardiovascular prognosis of IDCM patients.

### 3.5.7 CMVD in Takotsubo Cardiomyopathy (TTC)

TTC is a syndrome mimicking an acute myocardial infarction with severe left ventricle wall motion abnormalities, ECG repolarization changes and slight elevation of cardiac biomarkers, and the absence of obstructive CAD [179]. Several variants have been reported, depending of the extent and location of the wall motion abnormalities. The typical form consists of akinesis of the mid and distal segments of the left ventricle with hyperkinesis of the basal segments, also known as "apical ballooning syndrome," similar to the Japan octopus trap. The pathophysiological mechanisms are not yet clear, but it is believed that an emotional or physical stressor triggers an intense release of catecholamines, leading to a transient myocardial stunning. It has been hypothesized that CMVD plays a determinant role in the underlying mechanisms. A decreased coronary flow velocity reserve and a short diastolic deceleration time, measured with intracoronary Doppler, have been reported in patients with TTC [107]. These findings are supported by noninvasive studies, with assessment of coronary reserve by transthoracic Doppler, finding a reduced CFR in the acute phase of disease [180]. Other studies have documented indirect signs of CMVD on invasive coronary angiography, such as an abnormal TIMI frame count and abnormal TIMI myocardial perfusion grade [108, 181]. Furthermore, such abnormalities have not only been found in the myocardium subtended by the LAD but in the other major epicardial vessels, which suggests that CMVD may occur at multivessel level. Therefore, it seems that the coronary microvascular integrity is impaired, but what it is not yet clear if myocardial stunning is a consequence of metabolic disorder or CMVD.

## 3.6 Conclusion

Available evidence, accumulated over the previous decades, suggest that microcirculatory dysfunction is an important contributor to poor outcomes in multiple etiologies of heart disease. This constitutes a call for better methods to assess the state of the coronary microcirculation and to establish the mechanisms by which it is dysfunctional. Some factors have been consistently identified as markers of worse prognosis in patients with CMVD, such as persistent angina, abnormal CFR, and diabetes. The coronary microcirculation seems to play a key role in the development of CAD and is claiming more attention as a potential therapeutic target for the treatment of symptoms and prevention of cardiovascular outcomes.

## References

1. Teunissen PFA, de Waard GA, Hollander MR, Robbers LFHJ, Danad I, Biesbroek PS, et al. Doppler-derived intracoronary physiology indices predict the occurrence of microvascular injury and microvascular perfusion deficits after angiographically successful primary percutaneous coronary intervention. Circ Cardiovasc Interv. 2015;8(3), e001786.
2. Beyer AM, Gutterman DD. Regulation of the human coronary microcirculation. J Mol Cell Cardiol. 2012;52(4):814–21.
3. Feigl EO. Coronary physiology. Physiol Rev. 1983;63(1):1–205.
4. von Restorff W, Holtz J, Bassenge E. Exercise induced augmentation of myocardial oxygen extraction in spite of normal coronary dilatory capacity in dogs. Pflugers Arch. 1977;372(2):181–5.
5. Duncker DJ, Koller A, Merkus D, Canty Jr JM. Regulation of coronary blood flow in health and ischemic heart disease. Prog Cardiovasc Dis. 2015;57(5):409–22.
6. Schelbert HR. Anatomy and physiology of coronary blood flow. J Nucl Cardiol. 2010;17(4):545–54.
7. Eriksson S, Nilsson J, Sturesson C. Non-invasive imaging of microcirculation: a technology review. Med Devices Auckl NZ. 2014;7:445–52.
8. Komaru T, Kanatsuka H, Shirato K. Coronary microcirculation: physiology and pharmacology. Pharmacol Ther. 2000;86(3):217–61.
9. Beltrame JF, Crea F, Camici P. Advances in coronary microvascular dysfunction. Heart Lung Circ. 2009;18(1):19–27.
10. Bassingthwaighte JB, Yipintsoi T, Harvey RB. Microvasculature of the dog left ventricular myocardium. Microvasc Res. 1974;7(2):229–49.
11. Okun EM, Factor SM, Kirk ES. End-capillary loops in the heart: an explanation for discrete myocardial infarctions without border zones. Science. 1979;206(4418):565–7.
12. van Horssen P, van den Wijngaard JPHM, Brandt MJ, Hoefer IE, Spaan JAE, Siebes M. Perfusion territories subtended by penetrating coronary arteries increase in size and decrease in number toward the subendocardium. Am J Physiol Heart Circ Physiol. 2014;306(4):H496–504.
13. Hoffman JI. Autoregulation and heart rate. Circulation. 1990;82(5):1880–1.
14. Patel B, Fisher M. Therapeutic advances in myocardial microvascular resistance: unravelling the enigma. Pharmacol Ther. 2010;127(2):131–47.
15. Kuo L, Davis MJ, Chilian WM. Longitudinal gradients for endothelium-dependent and -independent vascular responses in the coronary microcirculation. Circulation. 1995;92(3):518–25.
16. Kuo L, Davis MJ, Chilian WM. Myogenic activity in isolated subepicardial and subendocardial coronary arterioles. Am J Physiol. 1988;255(6 Pt 2):H1558–62.
17. Kuo L, Davis MJ, Chilian WM. Endothelium-dependent, flow-induced dilation of isolated coronary arterioles. Am J Physiol. 1990;259(4 Pt 2):H1063–70.
18. Herrmann J, Kaski JC, Lerman A. Coronary microvascular dysfunction in the clinical setting: from mystery to reality. Eur Heart J. 2012;33(22):2771–83.
19. Jones CJ, Kuo L, Davis MJ, Chilian WM. Regulation of coronary blood flow: coordination of heterogeneous control mechanisms in vascular microdomains. Cardiovasc Res. 1995;29(5):585–96.
20. Kassab GS, Lin DH, Fung YC. Morphometry of pig coronary venous system. Am J Physiol. 1994;267(6 Pt 2):H2100–13.
21. Bosman J, Tangelder GJ, Oude Egbrink MG, Reneman RS, Slaaf DW. Capillary diameter changes during low perfusion pressure and reactive hyperemia in rabbit skeletal muscle. Am J Physiol. 1995;269(3 Pt 2):H1048–55.
22. Matsumoto T, Kajiya F. Coronary microcirculation: physiology and mechanics. Fluid Dyn Res. 2005;37(1–2):60.
23. Crea F, Camici PG, Bairey Merz CN. Coronary microvascular dysfunction: an update. Eur Heart J. 2014;35(17):1101–11.
24. Levy BI, Ambrosio G, Pries AR, Struijker-Boudier HA. Microcirculation in hypertension: a new target for treatment? Circulation. 2001;104(6):735–40.
25. Chilian WM, Eastham CL, Marcus ML. Microvascular distribution of coronary vascular resistance in beating left ventricle. Am J Physiol. 1986;251(4 Pt 2):H779–88.
26. Nelson MT, Patlak JB, Worley JF, Standen NB. Calcium channels, potassium channels, and voltage dependence of arterial smooth muscle tone. Am J Physiol. 1990;259(1 Pt 1):C3–18.
27. Davis MJ, Donovitz JA, Hood JD. Stretch-activated single-channel and whole cell currents in vascular smooth muscle cells. Am J Physiol. 1992;262(4 Pt 1):C1083–8.
28. Bowles DK, Hu Q, Laughlin MH, Sturek M. Heterogeneity of L-type calcium current density in coronary smooth muscle. Am J Physiol. 1997;273(4 Pt 2):H2083–9.
29. Park KS, Kim Y, Lee Y-H, Earm YE, Ho W-K. Mechanosensitive cation channels in arterial smooth muscle cells are activated by diacylglycerol and inhibited by phospholipase C inhibitor. Circ Res. 2003;93(6):557–64.
30. Sato K, Kanatsuka H, Sekiguchi N, Akai K, Wang Y, Sugimura A, et al. Effect of an ATP sensitive potassium channel opener, levcromakalim, on coronary arterial microvessels in the beating canine heart. Cardiovasc Res. 1994;28(12):1780–6.
31. Deussen A, Ohanyan V, Jannasch A, Yin L, Chilian W. Mechanisms of metabolic coronary flow regulation. J Mol Cell Cardiol. 2012;52(4):794–801.
32. Bernstein RD, Ochoa FY, Xu X, Forfia P, Shen W, Thompson CI, et al. Function and production of nitric oxide in the coronary circulation of the conscious dog during exercise. Circ Res. 1996;79(4):840–8.
33. Egashira K, Katsuda Y, Mohri M, Kuga T, Tagawa T, Kubota T, et al. Role of endothelium-derived nitric oxide in coronary vasodilatation induced by pacing tachycardia in humans. Circ Res. 1996;79(2):331–5.
34. Schindler TH, Nitzsche EU, Olschewski M, Brink I, Mix M, Prior J, et al. PET-measured responses of MBF to cold pressor testing correlate with indices of coronary vasomotion on quantitative coronary angiography. J Nucl Med Off Publ Soc Nucl Med. 2004;45(3):419–28.
35. Hearse DJ, Maxwell L, Saldanha C, Gavin JB. The myocardial vasculature during ischemia and reperfusion: a target for injury and protection. J Mol Cell Cardiol. 1993;25(7):759–800.
36. Traub O, Berk BC. Laminar shear stress: mechanisms by which endothelial cells transduce an atheroprotective force. Arterioscler Thromb Vasc Biol. 1998;18(5):677–85.
37. Canty JMJ, Schwartz JS. Nitric oxide mediates flow-dependent epicardial coronary vasodilation to changes in pulse frequency but not mean flow in conscious dogs. Circulation. 1994;89(1):375–84.
38. Koller A, Kaley G. Prostaglandins mediate arteriolar dilation to increased blood flow velocity in skeletal muscle microcirculation. Circ Res. 1990;67(2):529–34.
39. Huang A, Sun D, Carroll MA, Jiang H, Smith CJ, Connetta JA, et al. EDHF mediates flow-induced dilation in skeletal muscle arterioles of female eNOS-KO mice. Am J Physiol Heart Circ Physiol. 2001;280(6):H2462–9.

40. Palmer RM, Ashton DS, Moncada S. Vascular endothelial cells synthesize nitric oxide from L-arginine. Nature. 1988;333(6174): 664–6.
41. Moncada S, Palmer RM, Higgs EA. Nitric oxide: physiology, pathophysiology, and pharmacology. Pharmacol Rev. 1991;43(2):109–42.
42. Ignarro LJ, Cirino G, Casini A, Napoli C. Nitric oxide as a signaling molecule in the vascular system: an overview. J Cardiovasc Pharmacol. 1999;34(6):879–86.
43. Armstrong R. The physiological role and pharmacological potential of nitric oxide in neutrophil activation. Int Immunopharmacol. 2001;1(8):1501–12.
44. Lee RT, Libby P. The unstable atheroma. Arterioscler Thromb Vasc Biol. 1997;17(10):1859–67.
45. Verma S, Anderson TJ. Fundamentals of endothelial function for the clinical cardiologist. Circulation. 2002;105(5):546–9.
46. Miura H, Wachtel RE, Liu Y, Loberiza FRJ, Saito T, Miura M, et al. Flow-induced dilation of human coronary arterioles: important role of Ca(2+)-activated K(+) channels. Circulation. 2001; 103(15):1992–8.
47. Ohashi J, Sawada A, Nakajima S, Noda K, Takaki A, Shimokawa H. Mechanisms for enhanced endothelium-derived hyperpolarizing factor-mediated responses in microvessels in mice. Circ J Off J Jpn Circ Soc. 2012;76(7):1768–79.
48. Takaki A, Morikawa K, Tsutsui M, Murayama Y, Tekes E, Yamagishi H, et al. Crucial role of nitric oxide synthases system in endothelium-dependent hyperpolarization in mice. J Exp Med. 2008;205(9):2053–63.
49. Hellsten Y, Nyberg M, Jensen LG, Mortensen SP. Vasodilator interactions in skeletal muscle blood flow regulation. J Physiol. 2012;590(24):6297–305.
50. Yanagisawa M, Kurihara H, Kimura S, Tomobe Y, Kobayashi M, Mitsui Y, et al. A novel potent vasoconstrictor peptide produced by vascular endothelial cells. Nature. 1988;332(6163):411–5.
51. Griggs DMJ, Chilian WM, Boatwright RB, Shoji T, Williams DO. Evidence against significant resting alpha-adrenergic coronary vasoconstrictor tone. Fed Proc. 1984;43(14):2873–7.
52. Chilian WM, Boatwright RB, Shoji T, Griggs DMJ. Evidence against significant resting sympathetic coronary vasoconstrictor tone in the conscious dog. Circ Res. 1981;49(4):866–76.
53. Muller JM, Davis MJ, Chilian WM. Integrated regulation of pressure and flow in the coronary microcirculation. Cardiovasc Res. 1996;32(4):668–78.
54. DeFily DV, Patterson JL, Chilian WM. Endogenous adenosine modulates alpha 2- but not alpha 1-adrenergic constriction of coronary arterioles. Am J Physiol. 1995;268(6 Pt 2):H2487–94.
55. Camici PG, Crea F. Coronary microvascular dysfunction. N Engl J Med. 2007;356(8):830–40.
56. Pries AR, Reglin B. Coronary microcirculatory pathophysiology: can we afford it to remain a black box? Eur Heart J. 2016;38(7):478-488.
57. Ong P, Athanasiadis A, Borgulya G, Mahrholdt H, Kaski JC, Sechtem U. High prevalence of a pathological response to acetylcholine testing in patients with stable angina pectoris and unobstructed coronary arteries. The ACOVA Study (Abnormal COronary VAsomotion in patients with stable angina and unobstructed coronary arteries). J Am Coll Cardiol. 2012;59(7):655–62.
58. Lanza GA, Crea F. Primary coronary microvascular dysfunction: clinical presentation, pathophysiology, and management. Circulation. 2010;121(21):2317–25.
59. Moreau P, d'Uscio LV, Luscher TF. Structure and reactivity of small arteries in aging. Cardiovasc Res. 1998;37(1):247–53.
60. Antony I, Nitenberg A, Foult J-M, Aptecar E. Coronary vasodilator reserve in untreated and treated hypertensive patients with and without left ventricular hypertrophy. J Am Coll Cardiol. 1993;22(2): 514–20.
61. Rizzoni D, Palombo C, Porteri E, Muiesan ML, Kozàkovà M, La Canna G, et al. Relationships between coronary flow vasodilator capacity and small artery remodelling in hypertensive patients. J Hypertens. 2003;21(3):625–31.
62. Nahser PJJ, Brown RE, Oskarsson H, Winniford MD, Rossen JD. Maximal coronary flow reserve and metabolic coronary vasodilation in patients with diabetes mellitus. Circulation. 1995;91(3):635–40.
63. Nitenberg. Am J Cardiol. 1985;55(6):748–54.
64. Dayanikli F, Grambow D, Muzik O, Mosca L, Rubenfire M, Schwaiger M. Early detection of abnormal coronary flow reserve in asymptomatic men at high risk for coronary artery disease using positron emission tomography. Circulation. 1994;90(2):808–17.
65. Kaufmann PA, Gnecchi-Ruscone T, Schafers KP, Luscher TF, Camici PG. Low density lipoprotein cholesterol and coronary microvascular dysfunction in hypercholesterolemia. J Am Coll Cardiol. 2000;36(1):103–9.
66. Dagres N, Saller B, Haude M, Husing J, von Birgelen C, Schmermund A, et al. Insulin sensitivity and coronary vasoreactivity: insulin sensitivity relates to adenosine-stimulated coronary flow response in human subjects. Clin Endocrinol (Oxf). 2004;61(6):724–31.
67. Satoh K, Fukumoto Y, Shimokawa H. Rho-kinase: important new therapeutic target in cardiovascular diseases. Am J Physiol Heart Circ Physiol. 2011;301(2):H287–96.
68. Cecchi F, Olivotto I, Gistri R, Lorenzoni R, Chiriatti G, Camici PG. Coronary microvascular dysfunction and prognosis in hypertrophic cardiomyopathy. N Engl J Med. 2003;349(11):1027–35.
69. Hiemann NE, Wellnhofer E, Knosalla C, Lehmkuhl HB, Stein J, Hetzer R, et al. Prognostic impact of microvasculopathy on survival after heart transplantation: evidence from 9713 endomyocardial biopsies. Circulation. 2007;116(11):1274–82.
70. Chilian WM, et al. Coronary microcirculation in health and disease summary of an NHLBI workshop. Circulation. 1997;95(2):522–8.
71. Lerman A, Holmes DR, Herrmann J, Gersh BJ. Microcirculatory dysfunction in ST-elevation myocardial infarction: cause, consequence, or both? Eur Heart J. 2007;28(7):788–97.
72. Nemes A, Forster T, Geleijnse ML, Kutyifa V, Neu K, Soliman OII, et al. The additional prognostic power of diabetes mellitus on coronary flow reserve in patients with suspected coronary artery disease. Diabetes Res Clin Pract. 2007;78(1):126–31.
73. Escaned J, Flores A, Garcia-Pavia P, Segovia J, Jimenez J, Aragoncillo P, et al. Assessment of microcirculatory remodeling with intracoronary flow velocity and pressure measurements: validation with endomyocardial sampling in cardiac allografts. Circulation. 2009;120(16):1561–8.
74. Hong H. Remodeling of small intramyocardial coronary arteries distal to a severe epicardial coronary artery stenosis. Arterioscler Thromb Vasc Biol. 2002;22(12):2059–65.
75. Langille BL, Bendeck MP, Keeley FW. Adaptations of carotid arteries of young and mature rabbits to reduced carotid blood flow. Am J Physiol. 1989;256(4 Pt 2):H931–9.
76. Miller VM, Vanhoutte PM. Enhanced release of endothelium-derived factor(s) by chronic increases in blood flow. Am J Physiol. 1988;255(3 Pt 2):H446–51.
77. Loscalzo J. Nitric oxide and vascular disease. N Engl J Med. 1995;333(4):251–3.
78. Ito A, Egashira K, Kadokami T, Fukumoto Y, Takayanagi T, Nakaike R, et al. Chronic inhibition of endothelium-derived nitric oxide synthesis causes coronary microvascular structural changes and hyperreactivity to serotonin in pigs. Circulation. 1995;92(9):2636–44.
79. Yoon Y, Uchida S, Masuo O, Cejna M, Park J-S, Gwon H, et al. Progressive attenuation of myocardial vascular endothelial growth factor expression is a seminal event in diabetic cardiomyopathy: restoration of microvascular homeostasis and recovery of cardiac function in diabetic cardiomyopathy after replenishment of local vascular endothelial growth factor. Circulation. 2005;111(16):2073–85.
80. Jenkins JT, Boyle JJ, McKay IC, Richens D, McPhaden AR, Lindop GB. Vascular remodelling in intramyocardial resistance vessels in hypertensive human cardiac transplant recipients. Heart Br Card Soc. 1997;77(4):353–6.
81. O'Gara PT, Bonow RO, Maron BJ, Damske BA, Van Lingen A, Bacharach SL, et al. Myocardial perfusion abnormalities in patients

with hypertrophic cardiomyopathy: assessment with thallium-201 emission computed tomography. Circulation. 1987;76(6):1214–23.
82. Tsagalou EP, Anastasiou-Nana M, Agapitos E, Gika A, Drakos SG, Terrovitis JV, et al. Depressed coronary flow reserve is associated with decreased myocardial capillary density in patients with heart failure due to idiopathic dilated cardiomyopathy. J Am Coll Cardiol. 2008;52(17):1391–8.
83. Neglia D, Parodi O, Gallopin M, Sambuceti G, Giorgetti A, Pratali L, et al. Myocardial blood flow response to pacing tachycardia and to dipyridamole infusion in patients with dilated cardiomyopathy without overt heart failure. A quantitative assessment by positron emission tomography. Circulation. 1995;92(4):796–804.
84. Canetti M, Akhter MW, Lerman A, Karaalp IS, Zell JA, Singh H, et al. Evaluation of myocardial blood flow reserve in patients with chronic congestive heart failure due to idiopathic dilated cardiomyopathy. Am J Cardiol. 2003;92(10):1246–9.
85. van den Heuvel AF, van Veldhuisen DJ, van der Wall EE, Blanksma PK, Siebelink H-MJ, Vaalburg WM, et al. Regional myocardial blood flow reserve impairment and metabolic changes suggesting myocardial ischemia in patients with idiopathic dilated cardiomyopathy. J Am Coll Cardiol. 2000;35(1):19–28.
86. Prasad A, Higano ST, Al Suwaidi J, Holmes DRJ, Mathew V, Pumper G, et al. Abnormal coronary microvascular endothelial function in humans with asymptomatic left ventricular dysfunction. Am Heart J. 2003;146(3):549–54.
87. Skalidis EI, Parthenakis FI, Patrianakos AP, Hamilos MI, Vardas PE. Regional coronary flow and contractile reserve in patients with idiopathic dilated cardiomyopathy. J Am Coll Cardiol. 2004;44(10):2027–32.
88. Krams R, Kofflard MJ, Duncker DJ, von Birgelen C, Carlier S, Kliffen M, et al. Decreased coronary flow reserve in hypertrophic cardiomyopathy is related to remodeling of the coronary microcirculation. Circulation. 1998;97:230–3.
89. Takemura G, Takatsu Y, Fujiwara H. Luminal narrowing of coronary capillaries in human hypertrophic hearts: an ultrastructural morphometrical study using endomyocardial biopsy specimens. Heart Br Card Soc. 1998;79(1):78–85.
90. Piper HM, Garcia-Dorado D, Ovize M. A fresh look at reperfusion injury. Cardiovasc Res. 1998;38(2):291–300.
91. Hearse DJ, Humphrey SM, Chain EB. Abrupt reoxygenation of the anoxic potassium-arrested perfused rat heart: a study of myocardial enzyme release. J Mol Cell Cardiol. 1973;5(4):395–407.
92. Kloner RA, Ganote CE, Jennings RB. The "no-reflow" phenomenon after temporary coronary occlusion in the dog. J Clin Invest. 1974;54(6):1496–508.
93. Falk E. Unstable angina with fatal outcome: dynamic coronary thrombosis leading to infarction and/or sudden death. Autopsy evidence of recurrent mural thrombosis with peripheral embolization culminating in total vascular occlusion. Circulation. 1985;71(4):699–708.
94. Saber RS, Edwards WD, Bailey KR, McGovern TW, Schwartz RS, Holmes DRJ. Coronary embolization after balloon angioplasty or thrombolytic therapy: an autopsy study of 32 cases. J Am Coll Cardiol. 1993;22(5):1283–8.
95. Sato H, Iida H, Tanaka A, Tanaka H, Shimodouzono S, Uchida E, et al. The decrease of plaque volume during percutaneous coronary intervention has a negative impact on coronary flow in acute myocardial infarction: A major role of percutaneous coronary intervention-induced embolization. J Am Coll Cardiol. 2004;44(2):300–4.
96. Kotani J, Nanto S, Mintz GS, Kitakaze M, Ohara T, Morozumi T, et al. Plaque gruel of atheromatous coronary lesion may contribute to the no-reflow phenomenon in patients with acute coronary syndrome. Circulation. 2002;106(13):1672–7.
97. Iwakura K, Ito H, Kawano S, Shintani Y, Yamamoto K, Kato A, et al. Predictive factors for development of the no-reflow phenomenon in patients with reperfused anterior wall acute myocardial infarction. J Am Coll Cardiol. 2001;38(2):472–7.
98. Tanaka A, Kawarabayashi T, Nishibori Y, Sano T, Nishida Y, Fukuda D, et al. No-reflow phenomenon and lesion morphology in patients with acute myocardial infarction. Circulation. 2002;105(18):2148–52.
99. Robbers LFHJ, Eerenberg ES, Teunissen PFA, Jansen MF, Hollander MR, Horrevoets AJG, et al. Magnetic resonance imaging-defined areas of microvascular obstruction after acute myocardial infarction represent microvascular destruction and haemorrhage. Eur Heart J. 2013;34(30):2346–53.
100. Manciet LH, Poole DC, McDonagh PF, Copeland JG, Mathieu-Costello O. Microvascular compression during myocardial ischemia: mechanistic basis for no-reflow phenomenon. Am J Physiol. 1994;266(4 Pt 2):H1541–50.
101. Dunn RB, Griggs DMJ. Ventricular filling pressure as a determinant of coronary blood flow during ischemia. Am J Physiol. 1983;244(3):H429–36.
102. Breisch EA, Houser SR, Carey RA, Spann JF, Bove AA. Myocardial blood flow and capillary density in chronic pressure overload of the feline left ventricle. Cardiovasc Res. 1980;14(8):469–75.
103. Rajappan K, Rimoldi OE, Dutka DP, Ariff B, Pennell DJ, Sheridan DJ, et al. Mechanisms of coronary microcirculatory dysfunction in patients with aortic stenosis and angiographically normal coronary arteries. Circulation. 2002;105(4):470–6.
104. Gregorini L, Marco J, Farah B, Bernies M, Palombo C, Kozakova M, et al. Effects of selective alpha1- and alpha2-adrenergic blockade on coronary flow reserve after coronary stenting. Circulation. 2002;106(23):2901–7.
105. Sorop O, Merkus D, de Beer VJ, Houweling B, Pistea A, McFalls EO, et al. Functional and structural adaptations of coronary microvessels distal to a chronic coronary artery stenosis. Circ Res. 2008;102(7):795–803.
106. Ako J, Takenaka K, Uno K, Nakamura F, Shoji T, Iijima K, et al. Reversible left ventricular systolic dysfunction--reversibility of coronary microvascular abnormality. Jpn Heart J. 2001;42(3):355–63.
107. Kume T, Akasaka T, Kawamoto T, Yoshitani H, Watanabe N, Neishi Y, et al. Assessment of coronary microcirculation in patients with takotsubo-like left ventricular dysfunction. Circ J Off J Jpn Circ Soc. 2005;69(8):934–9.
108. Elesber A, Lerman A, Bybee KA, Murphy JG, Barsness G, Singh M, et al. Myocardial perfusion in apical ballooning syndrome correlate of myocardial injury. Am Heart J. 2006;152(3):469.e9–13.
109. Rigo F, Sicari R, Citro R, Ossena G, Buja P, Picano E. Diffuse, marked, reversible impairment in coronary microcirculation in stress cardiomyopathy: a Doppler transthoracic echo study. Ann Med. 2009;41(6):462–70.
110. Galiuto L, Garramone B, Scarà A, Rebuzzi AG, Crea F, La Torre G, et al. The extent of microvascular damage during myocardial contrast echocardiography is superior to other known indexes of post-infarct reperfusion in predicting left ventricular remodeling. J Am Coll Cardiol. 2008;51(5):552–9.
111. Martin EA, Prasad A, Rihal CS, Lerman LO, Lerman A. Endothelial function and vascular response to mental stress are impaired in patients with apical ballooning syndrome. J Am Coll Cardiol. 2010;56(22):1840–6.
112. Marzilli M, Merz CNB, Boden WE, Bonow RO, Capozza PG, Chilian WM, et al. Obstructive coronary atherosclerosis and ischemic heart disease: an elusive link! J Am Coll Cardiol. 2012;60(11):951–6.
113. Cemin R, Erlicher A, Fattor B, Pitscheider W, Cevese A. Reduced coronary flow reserve and parasympathetic dysfunction in patients with cardiovascular syndrome X. Coron Artery Dis. 2008;19(1):1–7.
114. Wittstein IS, Thiemann DR, Lima JAC, Baughman KL, Schulman SP, Gerstenblith G, et al. Neurohumoral features of myocardial stunning due to sudden emotional stress. N Engl J Med. 2005;352(6):539–48.
115. Rosen SD, Boyd H, Rhodes CG, Kaski JC, Camici PG. Myocardial beta-adrenoceptor density and plasma catecholamines in syndrome X. Am J Cardiol. 1996;78(1):37–42.

116. Frobert O, Molgaard H, Botker HE, Bagger JP. Autonomic balance in patients with angina and a normal coronary angiogram. Eur Heart J. 1995;16(10):1356–60.
117. Di Franco A, Lanza GA, Di Monaco A, Sestito A, Lamendola P, Nerla R, et al. Coronary microvascular function and cortical pain processing in patients with silent positive exercise testing and normal coronary arteries. Am J Cardiol. 2012;109(12):1705–10.
118. Aslan G, Sade LE, Yetis B, Bozbas H, Eroglu S, Pirat B, et al. Flow in the left anterior descending coronary artery in patients with migraine headache. Am J Cardiol. 2013;112(10):1540–4.
119. Chade AR, Brosh D, Higano ST, Lennon RJ, Lerman LO, Lerman A. Mild renal insufficiency is associated with reduced coronary flow in patients with non-obstructive coronary artery disease. Kidney Int. 2006;69(2):266–71.
120. Sundell J. et al. Diabetologia. 2004;47(4):725–31.
121. Tondi P, Santoliquido A, Di Giorgio A, Sestito A, Sgueglia GA, Flore R, et al. Endothelial dysfunction as assessed by flow-mediated dilation in patients with cardiac syndrome X: role of inflammation. Eur Rev Med Pharmacol Sci. 2011;15(9):1074–7.
122. Libby P, Nathan DM, Abraham K, Brunzell JD, Fradkin JE, Haffner SM, et al. Report of the National Heart, Lung, and Blood Institute-National Institute of Diabetes and Digestive and Kidney Diseases Working Group on Cardiovascular Complications of Type 1 Diabetes Mellitus. Circulation. 2005;111(25):3489–93.
123. Recio-Mayoral A, Rimoldi OE, Camici PG, Kaski JC. Inflammation and microvascular dysfunction in cardiac syndrome X patients without conventional risk factors for coronary artery disease. JACC Cardiovasc Imaging. 2013;6(6):660–7.
124. Johnson BD, Shaw LJ, Pepine CJ, Reis SE, Kelsey SF, Sopko G, et al. Persistent chest pain predicts cardiovascular events in women without obstructive coronary artery disease: results from the NIH-NHLBI-sponsored Women's Ischaemia Syndrome Evaluation (WISE) study. Eur Heart J. 2006;27(12):1408–15.
125. Sicari R, Palinkas A, Pasanisi EG, Venneri L, Picano E. Long-term survival of patients with chest pain syndrome and angiographically normal or near-normal coronary arteries: the additional prognostic value of dipyridamole echocardiography test (DET). Eur Heart J. 2005;26(20):2136–41.
126. Russo G, Di Franco A, Lamendola P, Tarzia P, Nerla R, Stazi A, et al. Lack of effect of nitrates on exercise stress test results in patients with microvascular angina. Cardiovasc Drugs Ther Spons Int Soc Cardiovasc Pharmacother. 2013;27(3):229–34.
127. Di Carli MF, Janisse J, Grunberger G, Ager J. Role of chronic hyperglycemia in the pathogenesis of coronary microvascular dysfunction in diabetes. J Am Coll Cardiol. 2003;41(8):1387–93.
128. Britten MB. Coron Artery Dis. 2004;15(5):259–64.
129. Marks DS. J Clin Hypertens (Greenwich). 2004;6(6):304–9.
130. Sicari R. Am J Cardiol. 2009;103(5):626–31.
131. Herzog BA. Am Coll Cardiol. 2009;54(2):150–6.
132. Pepine CJ, Anderson RD, Sharaf BL, Reis SE, Smith KM, Handberg EM, et al. Coronary microvascular reactivity to adenosine predicts adverse outcome in women evaluated for suspected ischemia. J Am Coll Cardiol. 2010;55(25):2825–32.
133. Vermeltfoort IA. Neth Heart J. 2012;20(9):365–71.
134. Romeo F. Am J Cardiol. 1993;71(8):669–73.
135. Russo G. Cardiovasc Drugs Ther. 2013;27(3):229–34.
136. Shaw LJ. Circulation. 2006;114(9):894–904.
137. Prior JO, Quinones MJ, Hernandez-Pampaloni M, Facta AD, Schindler TH, Sayre JW, et al. Coronary circulatory dysfunction in insulin resistance, impaired glucose tolerance, and type 2 diabetes mellitus. Circulation. 2005;111(18):2291–8.
138. Echavarria-Pinto M, van de Hoef TP, Serruys PW, Piek JJ, Escaned J. Facing the complexity of ischaemic heart disease with intracoronary pressure and flow measurements: beyond fractional flow reserve interrogation of the coronary circulation. Curr Opin Cardiol. 2014;29(6):564–70.
139. Murthy VL, Naya M, Foster CR, Gaber M, Hainer J, Klein J, et al. Association between coronary vascular dysfunction and cardiac mortality in patients with and without diabetes mellitus. Circulation. 2012;126(15):1858–68.
140. Camici PG, Rimoldi OE. The clinical value of myocardial blood flow measurement. J Nucl Med Off Publ Soc Nucl Med. 2009;50(7):1076–87.
141. Sorajja P, Gersh BJ, Costantini C, McLaughlin MG, Zimetbaum P, Cox DA, et al. Combined prognostic utility of ST-segment recovery and myocardial blush after primary percutaneous coronary intervention in acute myocardial infarction. Eur Heart J. 2005;26(7):667–74.
142. Perazzolo Marra M, Lima JAC, Iliceto S. MRI in acute myocardial infarction. Eur Heart J. 2011;32(3):284–93.
143. Marzilli M, Sambuceti G, Fedele S, L'Abbate A. Coronary microcirculatory vasoconstriction during ischemia in patients with unstable anging. J Am Coll Cardiol. 2000;35(2):327–34.
144. Gould KL, Lipscomb K, Calvert C. Compensatory changes of the distal coronary vascular bed during progressive coronary constriction. Circulation. 1975;51(6):1085–94.
145. Guyton RA, McClenathan JH, Michaelis LL. Evolution of regional ischemia distal to a proximal coronary stenosis: self-propagation of ischemia. Am J Cardiol. 1977;40(3):381–92.
146. Gorman MW, Sparks HVJ. Progressive coronary vasoconstriction during relative ischemia in canine myocardium. Circ Res. 1982;51(4):411–20.
147. Sambuceti G, Marzilli M, Marraccini P, Schneider-Eicke J, Gliozheni E, Parodi O, et al. Coronary vasoconstriction during myocardial ischemia induced by rises in metabolic demand in patients with coronary artery disease. Circulation. 1997;95(12):2652–9.
148. Fearon WF, Shah M, Ng M, Brinton T, Wilson A, Tremmel JA, et al. Predictive value of the index of microcirculatory resistance in patients with ST-segment elevation myocardial infarction. J Am Coll Cardiol. 2008;51(5):560–5.
149. Lim H-S, Yoon M-H, Tahk S-J, Yang H-M, Choi B-J, Choi S-Y, et al. Usefulness of the index of microcirculatory resistance for invasively assessing myocardial viability immediately after primary angioplasty for anterior myocardial infarction. Eur Heart J. 2009;30(23):2854–60.
150. Bolognese L, Carrabba N, Parodi G, Santoro GM, Buonamici P, Cerisano G, et al. Impact of microvascular dysfunction on left ventricular remodeling and long-term clinical outcome after primary coronary angioplasty for acute myocardial infarction. Circulation. 2004;109(9):1121–6.
151. de Waha S, Desch S, Eitel I, Fuernau G, Lurz P, Leuschner A, et al. Relationship and prognostic value of microvascular obstruction and infarct size in ST-elevation myocardial infarction as visualized by magnetic resonance imaging. Clin Res Cardiol. 2012;101(6):487–95.
152. Wu KC, Zerhouni EA, Judd RM, Lugo-Olivieri CH, Barouch LA, Schulman SP, et al. Prognostic significance of microvascular obstruction by magnetic resonance imaging in patients with acute myocardial infarction. Circulation. 1998;97(8):765–72.
153. Bekkers SCAM, Smulders MW, Passos VL, Leiner T, Waltenberger J, Gorgels APM, et al. Clinical implications of microvascular obstruction and intramyocardial haemorrhage in acute myocardial infarction using cardiovascular magnetic resonance imaging. Eur Radiol. 2010;20(11):2572–8.
154. Li Y, Yang D, Lu L, Wu D, Yao J, Hu X, et al. Thermodilutional confirmation of coronary microvascular dysfunction in patients with recurrent angina after successful percutaneous coronary intervention. Can J Cardiol. 2015;31(8):989–97.
155. Tonino PAL, De Bruyne B, Pijls NHJ, Siebert U, Ikeno F, van't Veer M. Fractional flow reserve versus angiography for guiding percutaneous coronary intervention. N Engl J Med. 2009;360(3):213–24.
156. van de Hoef TP, van Lavieren MA, Damman P, Delewi R, Piek MA, Chamuleau SAJ, et al. Physiological basis and long-term clinical outcome of discordance between fractional flow reserve and coronary flow velocity reserve in coronary stenoses of intermediate severity. Circ Cardiovasc Interv. 2014;7(3):301–11.

157. Echavarria-Pinto M, Escaned J, Macias E, Medina M, Gonzalo N, Petraco R, et al. Disturbed coronary hemodynamics in vessels with intermediate stenoses evaluated with fractional flow reserve: a combined analysis of epicardial and microcirculatory involvement in ischemic heart disease. Circulation. 2013;128(24):2557–66.
158. Lee JM, Jung J-H, Hwang D, Park J, Fan Y, Na S-H, et al. Coronary flow reserve and microcirculatory resistance in patients with intermediate coronary stenosis. J Am Coll Cardiol. 2016;67(10):1158–69.
159. Camici PG, Olivotto I, Rimoldi OE. The coronary circulation and blood flow in left ventricular hypertrophy. J Mol Cell Cardiol. 2012;52(4):857–64.
160. Camici PG, d'Amati G, Rimoldi O. Coronary microvascular dysfunction: mechanisms and functional assessment. Nat Rev Cardiol. 2014;12(1):48–62.
161. Camici P, Chiriatti G, Lorenzoni R, Bellina RC, Gistri R, Italiani G, et al. Coronary vasodilation is impaired in both hypertrophied and nonhypertrophied myocardium of patients with hypertrophic cardiomyopathy: a study with nitrogen-13 ammonia and positron emission tomography. J Am Coll Cardiol. 1991;17(4):879–86.
162. Choudhury L, Elliott P, Rimoldi O, Ryan M, Lammertsma AA, Boyd H, et al. Transmural myocardial blood flow distribution in hypertrophic cardiomyopathy and effect of treatment. Basic Res Cardiol. 1999;94(1):49–59.
163. Petersen SE, Jerosch-Herold M, Hudsmith LE, Robson MD, Francis JM, Doll HA, et al. Evidence for microvascular dysfunction in hypertrophic cardiomyopathy: new insights from multiparametric magnetic resonance imaging. Circulation. 2007;115(18):2418–25.
164. Knaapen P, Germans T, Camici PG, Rimoldi OE, ten Cate FJ, ten Berg JM, et al. Determinants of coronary microvascular dysfunction in symptomatic hypertrophic cardiomyopathy. Am J Physiol Heart Circ Physiol. 2008;294(2):H986–93.
165. Ismail TF, Hsu L-Y, Greve AM, Goncalves C, Jabbour A, Gulati A, et al. Coronary microvascular ischemia in hypertrophic cardiomyopathy - a pixel-wise quantitative cardiovascular magnetic resonance perfusion study. J Cardiovasc Magn Reson Off J Soc Cardiovasc Magn Reson. 2014;16:49.
166. Moon JC, Mogensen J, Elliott PM, Smith GC, Elkington AG, Prasad SK, et al. Myocardial late gadolinium enhancement cardiovascular magnetic resonance in hypertrophic cardiomyopathy caused by mutations in troponin I. Heart Br Card Soc. 2005;91(8):1036–40.
167. Basso C, Thiene G, Corrado D, Buja G, Melacini P, Nava A. Hypertrophic cardiomyopathy and sudden death in the young: pathologic evidence of myocardial ischemia. Hum Pathol. 2000;31(8):988–98.
168. Olivotto I, Cecchi F, Gistri R, Lorenzoni R, Chiriatti G, Girolami F, et al. Relevance of coronary microvascular flow impairment to long-term remodeling and systolic dysfunction in hypertrophic cardiomyopathy. J Am Coll Cardiol. 2006;47(5):1043–8.
169. Maron BJ, Towbin JA, Thiene G, Antzelevitch C, Corrado D, Arnett D, et al. Contemporary definitions and classification of the cardiomyopathies: an American Heart Association Scientific Statement from the Council on Clinical Cardiology, Heart Failure and Transplantation Committee; Quality of Care and Outcomes Research and Functional Genomics and Translational Biology Interdisciplinary Working Groups; and Council on Epidemiology and Prevention. Circulation. 2006;113(14):1807–16.
170. Treasure CB, Vita JA, Cox DA, Fish RD, Gordon JB, Mudge GH, et al. Endothelium-dependent dilation of the coronary microvasculature is impaired in dilated cardiomyopathy. Circulation. 1990;81(3):772–9.
171. Weismuller S, Czernin J, Sun KT, Fung C, Phelps ME, Schelbert HR. Coronary vasodilatory capacity is impaired in patients with dilated cardiomyopathy. Am J Card Imaging. 1996;10(3):154–62.
172. Inoue T, Sakai Y, Morooka S, Hayashi T, Takayanagi K, Yamanaka T, et al. Coronary flow reserve in patients with dilated cardiomyopathy. Am Heart J. 1993;125(1):93–8.
173. Dec GW, Fuster V. Idiopathic dilated cardiomyopathy. N Engl J Med. 1994;331(23):1564–75.
174. Parodi O, De Maria R, Oltrona L, Testa R, Sambuceti G, Roghi A, et al. Myocardial blood flow distribution in patients with ischemic heart disease or dilated cardiomyopathy undergoing heart transplantation. Circulation. 1993;88(2):509–22.
175. Lehrke S, Lossnitzer D, Schob M, Steen H, Merten C, Kemmling H, et al. Use of cardiovascular magnetic resonance for risk stratification in chronic heart failure: prognostic value of late gadolinium enhancement in patients with non-ischaemic dilated cardiomyopathy. Heart Br Card Soc. 2011;97(9):727–32.
176. Neglia D, Michelassi C, Trivieri MG, Sambuceti G, Giorgetti A, Pratali L, et al. Prognostic role of myocardial blood flow impairment in idiopathic left ventricular dysfunction. Circulation. 2002;105(2):186–93.
177. Koutalas E, Kanoupakis E, Vardas P. Sudden cardiac death in non-ischemic dilated cardiomyopathy: a critical appraisal of existing and potential risk stratification tools. Int J Cardiol. 2013;167(2):335–41.
178. Rigo F. The prognostic impact of coronary flow-reserve assessed by Doppler echocardiography in non-ischaemic dilated cardiomyopathy. Eur Heart J. 2006;27(11):1319–23.
179. Sharkey SW, Windenburg DC, Lesser JR, Maron MS, Hauser RG, Lesser JN, et al. Natural history and expansive clinical profile of stress (tako-tsubo) cardiomyopathy. J Am Coll Cardiol. 2010;55(4):333–41.
180. Meimoun P, Malaquin D, Benali T, Boulanger J, Zemir H, Tribouilloy C. Transient impairment of coronary flow reserve in tako-tsubo cardiomyopathy is related to left ventricular systolic parameters. Eur J Echocardiogr J Work Group Echocardiogr Eur Soc Cardiol. 2009;10(2):265–70.
181. Bybee KA, Prasad A, Barsness GW, Lerman A, Jaffe AS, Murphy JG, et al. Clinical characteristics and thrombolysis in myocardial infarction frame counts in women with transient left ventricular apical ballooning syndrome. Am J Cardiol. 2004;94(3):343–6.

# Remodeling of Epicardial Coronary Vessels

*Nieves Gonzalo, Vera Rodriguez, Christopher J. Broyd, Pilar Jimenez-Quevedo, and Javier Escaned*




J. Escaned, J. Davies (eds.), *Physiological Assessment of Coronary Stenoses and the Microcirculation*,
DOI 10.1007/978-1-4471-5245-3_4

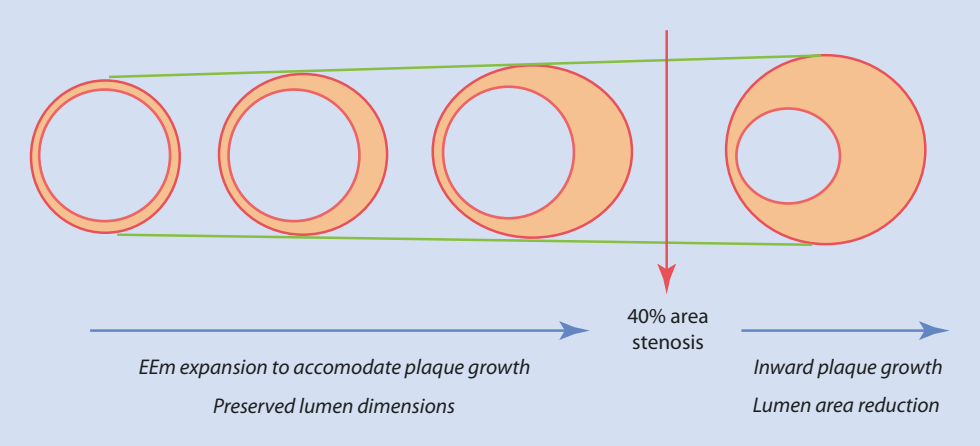


**Fig. 4.1** Schematic representation of the positive remodeling phenomenon. In human coronary arteries, the external elastic membrane (represented by the *red line*) expands to accommodate plaque growth and preserve lumen size. Plaque burden compromises lumen size only when 40 % or greater cross-sectional luminal narrowing is observed

## 4.1 Introduction

Coronary angiography is the main instrument used to evaluate the presence of stenoses caused by coronary atherosclerosis. An angiogram is a luminogram delineating the shape of the contrast-filled lumen, but it does not supply information about the vessel wall. It has long been recognized that segments with an angiographically "normal" appearance (i.e., without stenosis) may have atheroma when evaluated with more detailed pathology-based tools.

This discordance between angiography and pathology was explained by the remodeling phenomenon first described by Glagov in 1987. This author evaluated histological sections of left main coronary arteries and concluded that human coronary arteries enlarge in relation to plaque formation and that the increase in plaque burden compromises lumen size only when 40 % or greater cross-sectional luminal narrowing is observed [1, 2]. Thus, luminogram-based techniques (such as angiography) will not be able to detect the presence of coronary atherosclerosis until the disease is in at a relatively advanced stage (Fig. 4.1).

## 4.2 Techniques to Evaluate Coronary Remodeling

The compensatory vessel enlargement described above has since been confirmed in vivo with the introduction of intracoronary imaging techniques such as intravascular ultrasound (IVUS) [3–5]. IVUS allows the measurement of the cross-sectional vessel area (defined as the area limited by the external elastic membrane (EEM-CSA)). A remodeling index can be calculated as the ratio between the EEM-CSA at the lesion and the EEM-CSA at a reference point (defined as the most normal cross section located within 10 mm around the lesion, before any significant side branch). A recent IVUS study by Inaba et al. reproduced Glagov's observations in the left main stem in vivo confirming the increase in vessel area in proportion to the increase in plaque area and an absence of lumen area reduction until the plaque burden is greater than 40 % [6]. IVUS has therefore allowed evaluation of vessel remodeling in live living patients providing unique insights into information about the clinical implications of this phenomenon. Optical coherence tomography (OCT), another intracoronary imaging technique available in the cath lab, is more limited in this area because its lower penetration precludes the visualization of the EEM in vessels with plaque, especially if this is lipid-rich plaque. In the last years, multislice computed tomography (MSCT) has emerged as an alternative clinical tool to noninvasively evaluate the presence of coronary arterial remodeling [7–9].

## 4.3 Definitions

Positive, outward, or compensatory remodeling is defined as circumferential vessel enlargement in response to plaque growth. Negative, inward, or constrictive remodeling is defined as a decrease in vessel size in response to plaque development reflecting a failure of the vessel capacity to accommodate plaque growth. These two phenomena have been associated with different clinical scenarios and risk factors that will be further discussed in this chapter.

The American College of Cardiology Expert Consensus Document for IVUS interpretation states that when the lesion EEM area is greater than the reference EEM area, positive remodeling has taken place, and the remodeling index will be >1.0. If the lesion EEM area is smaller than the reference EEM area, negative remodeling has occurred, and the index will be <1.0 [10] (Fig. 4.2). However, different IVUS studies have used different cutoff points to define remodeling, and this may explain some contradictory results [11]. Further differences can be explained by the choice of reference segment for index calculation (distal, proximal, or mean) or the lack of a reliable healthy reference segment in many cases. Only serial IVUS examinations performed at different time points in the same subject can provide direct evidence of vessel remodeling avoiding the need for a reference segment that is often not available in patients with diffuse coronary disease [12, 13].

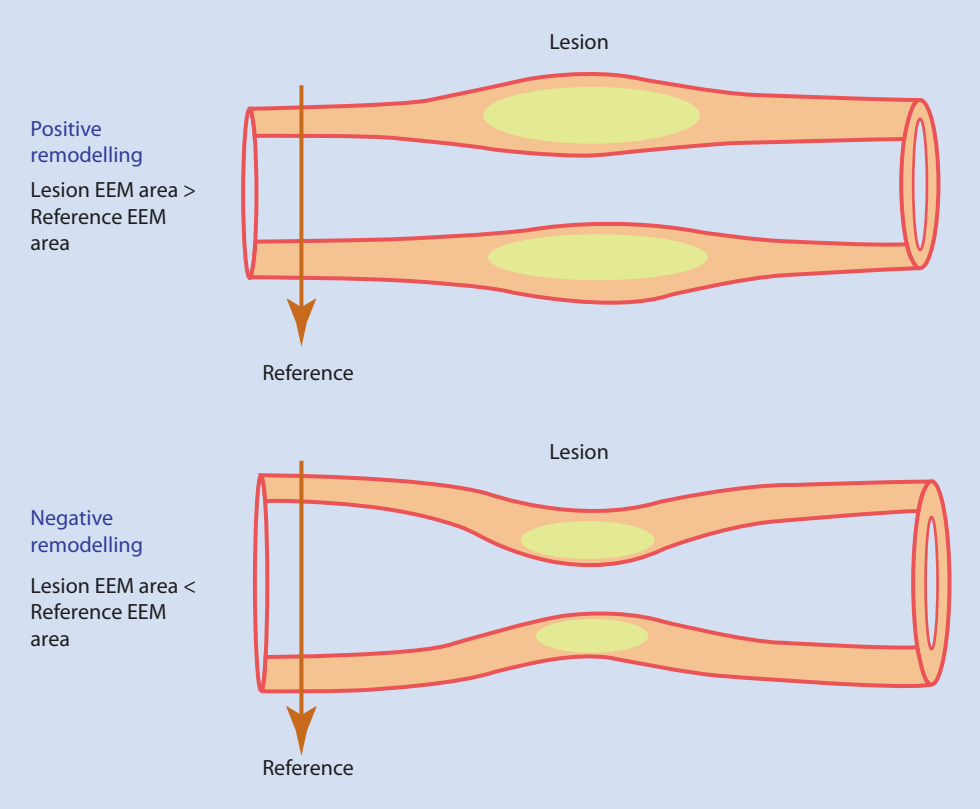


**Fig. 4.2** Graphic representation of positive and negative remodeling. Positive, outward, or compensatory remodeling is defined as circumferential vessel enlargement in response to plaque growth (the lesion external elastic membrane (EEM) area will be greater than the reference EEM area). Negative, inward, or constrictive remodeling is defined as a decrease in vessel size in response to plaque development (the lesion EEM will be smaller than the reference EEM area)

## 4.4 Physiopathology of Vessel Remodeling

In normal arteries, remodeling is a physiological response to changes in flow and shear stress conditions. The major stimuli for the initiation of vessel remodeling are these changes in hemodynamic parameters along with inflammation (induced by hemodynamic parameters or factors such as dyslipidemia). These stimuli induce the production of humoral factors (including cytokines and vasoactive agents such as nitric oxide) that through different biochemical pathways induce and promote changes in vessel structure in order to adapt to the new conditions. In this regard, a key role is played by the modification of the extracellular matrix by metalloproteinases (MMPs). Both experimental and human data suggest that this enzyme is involved in the degradation of components of the matrix leading to positive remodeling [14–16]. MMP activity can be induced by nitric oxide (NO) whose production is increased in the endothelium in high-flow conditions [17]. Additionally, NO is able to inhibit proliferation and induce apoptosis of smooth muscle cells, both of which contribute to outward remodeling. MMPs are produced by inflammatory cells (monocytes and macrophages) that can be recruited in the plaque by cell adhesion molecules (such as ICAM-1 and VCAM) which are themselves responsive to shear stress [18]. Other factors such as hypercholesterolemia can increase inflammatory cell infiltration in atherosclerotic plaques contributing to augmented MMP production and outward remodeling [19, 20].

Among the hemodynamic stimuli involved in remodeling, shear stress (SS), defined as the dragging frictional force exerted by blood in the arterial wall, seems to be the most relevant. In a serial intracoronary study performed in vivo, Stone et al. demonstrated that positive remodeling occurred both in segments with low SS and segments with moderate to high SS; however, in those segments with a low SS, there was associated plaque progression. They therefore suggested that positive remodeling in low SS segments is a compensatory phenomenon to accommodate atherosclerotic plaques, while in segments with moderate to high SS, it is a physiologic response to achieve normal SS values. They also found negative remodeling in 44 % of low SS segments, while this type of remodeling was very infrequent in segments with moderate to high SS [21].

Recently, a noninvasive approach using computational flow dynamics derived from coronary computed tomography angiography has also shown an association of low SS with excessive expansive remodeling [22].

Regarding constrictive remodeling, impairment of NO production due to endothelial dysfunction and genetically induced alterations in pathways that regulate the production of several cytokines (such as IL18 and macrophage migration inhibitory factor) have been proposed [17]. In addition, low-flow states may induce the production of factors that increase smooth muscle cell proliferation and collagen deposition, such as platelet-derived growth factor and transforming growth factor-β, further contributing to negative remodeling [23, 24].

## 4.5 Relation Between Risk Factors and Remodeling

As highlighted above dyslipidemia has been associated with positive remodeling through an increase in inflammation and MMP production within the plaque. It is also a pathogenic feature in coronary aneurysm formation which represents an extreme form of expansive vascular remodeling [24–26]. However, the literature shows there are conflicting results and reports in the literature regarding the relationship between dyslipidemia and vessel remodeling. A serial IVUS study by von Birgelen et al. failed to demonstrate a difference in vessel size according to LDL cholesterol levels [27], while two studies have reported that LDL levels can be a predictor of negative remodeling especially in diabetic patients [28, 29]. Alternatively, higher levels of HDL have been linked to positive remodeling in an autopsy study [30].

The evidence is also conflicting regarding the process of remodeling in relation to hypercholesterolemia therapy. Hamasaki et al. reported that cholesterol-lowering treatment is associated with an improvement in coronary lumen area caused by expansive vessel remodeling [31], whereas on the contrary serial IVUS data from the Reversal of Atherosclerosis with Aggressive Lipid Lowering Therapy (REVERSAL) trial showed constrictive vessel remodeling during statin treatment [32].

Constrictive remodeling is more frequent in patients with diabetes, especially those who are insulin dependent [33–36]. Jiménez-Quevedo et al. performed IVUS examination in 131 lesions in 80 diabetic patients and found a high prevalence of negative remodeling (up to 72 %) demonstrating that this type of vessel response was the main contributor to new stenosis formation and diffuse disease in this population [37]. Even in angiographically normal segments, diabetic patients have been shown to have smaller vessel areas despite a similar plaque burden as compared to nondiabetic patients [38]. Negative remodeling has also been associated with smoking, hypertension, and the long-term use of perindopril [39].

Among metabolic factors, higher homocysteine levels have been associated with positive remodeling [40], while adiponectin levels are increased in patients with negative remodeling [41].

## 4.6 Type of Remodeling and Underlying Plaque Composition

Histopathological and in vivo studies using intracoronary imaging techniques have demonstrated differences in underlying plaque composition depending on the type of remodeling present. Plaques with expansive remodeling are generally characterized by the presence of a high lipid content and inflammation [42, 43] (Fig. 4.3). Using IVUS radiofrequency (RF) analysis, Fujii et al. showed a linear relation between expansive remodeling and fibrofatty plaque area [43]. With the same technique, Rodriguez-Granillo et al. found a positive correlation between lipid core and remodeling index. Additionally, in this study all of the positively remodeled lesions were lipid-rich plaques, fibroatheromas, or thin-cap fibroatheromas (TCFA), the plaque type described as the most prone to rupture [39].

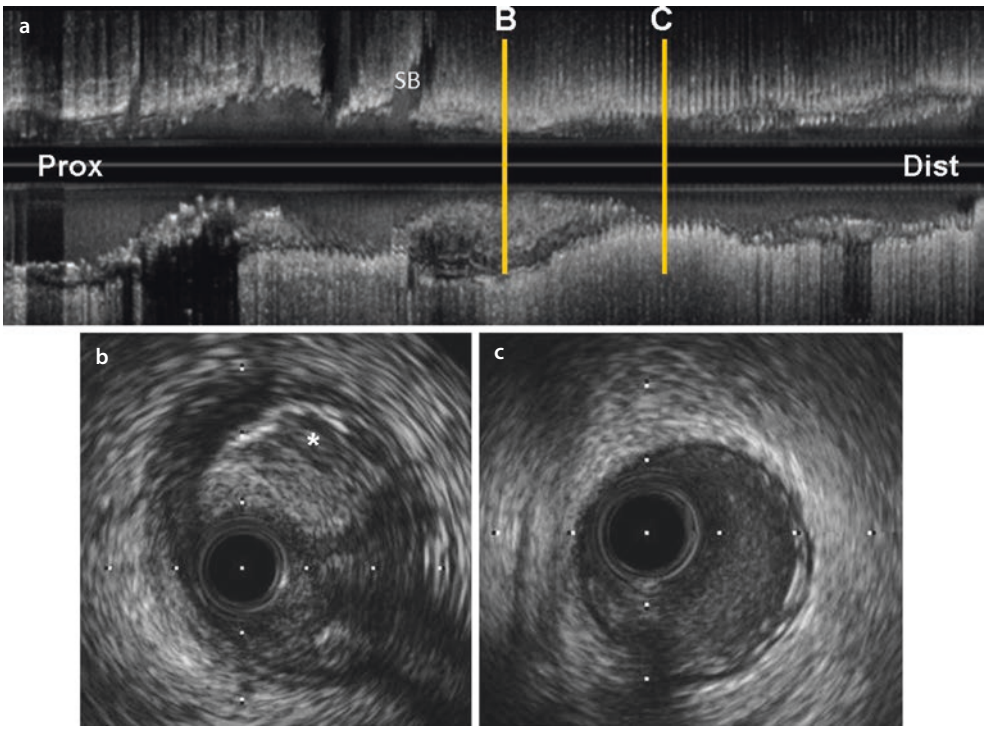


**Fig. 4.3** Positive remodeling. Example of a lesion with positive remodeling assessed by intravascular ultrasound (IVUS). **a** Longitudinal IVUS view showing an eccentric atherosclerotic plaque in the mid-segment of the artery, distal to a small side branch (*SB*). **b** IVUS cross section from the lesion showing a high plaque burden with a heterogeneous plaque composition (* indicates a hypoechogenic area suggestive of lipid content). **c** IVUS cross section at the distal reference. The external elastic membrane (EEM) area at the lesion site is greater than the reference EEM area. *Prox* proximal, *Dist* distal

Kume et al. evaluated the relationship between remodeling and plaque composition by OCT in ex vivo human coronary arteries. The authors found a higher percentage of lipid-rich plaques in patients with expansive remodeling (94 %) than in patients with constrictive remodeling (88 %). Similar results were found in an in vivo study that imaged coronary segments with IVUS and OCT where expansive remodeling was associated with a higher proportion of lipid-rich plaques, thinner fibrous caps with a higher macrophage density, and the presence of TCFA morphology [44, 45].

In contrast, negative remodeling has been associated with a stable fibrotic plaque morphology frequently located in proximal and ostial segments of the coronaries [3, 46–49] (Fig. 4.4). In a study using RF-IVUS, Rodriguez-Granillo et al. reported that lesions that had undergone negative remodeling displayed a stable phenotype, with 64 % having pathological intimal thickening, 29 % being fibrocalcific lesions, and only 7 % displaying fibroatheromatous characteristics. In pathology studies, erosion and chronic occlusions frequently demonstrate constrictive remodeling, while intra-plaque hemorrhage is usually associated with positive remodeling [42]. Negative remodeling is also frequent in the ostium of side branches and main branches in bifurcations even in lesions with low small plaque burdens, contributing to vessel narrowing in these segments [50]. Interestingly, negative remodeling seems to be a frequent finding in sites of vasospasm in patients with variant angina [51].

## 4.7 Vessel Remodeling, Plaque Vulnerability, and Acute Coronary Syndromes

Histopathological and intracoronary imaging studies have demonstrated that expansive remodeling is associated with many features related to plaque vulnerability such as high lipid content, macrophage infiltration, thinner fibrous caps, and lower collagen and smooth muscle cell content [42]. Furthermore, biomechanic studies suggest that lesions with expansive remodeling may be more mechanically unstable [52, 53].

These observations correlate with data that demonstrates a relationship between clinical presentation and remodeling type. Several studies using IVUS or MSCT have identified expansive remodeling as the most frequent pattern in acute coronary syndromes, while constrictive remodeling is more frequently observed in stable angina [8, 38, 54–60]. However, Hassani et al. reported that calcified and negatively remodeled plaques were frequently observed in elderly patients with myocardial infarction suggesting potential differences in the physiopathology and pathophysiology of acute coronary syndromes in octogenarians [61].

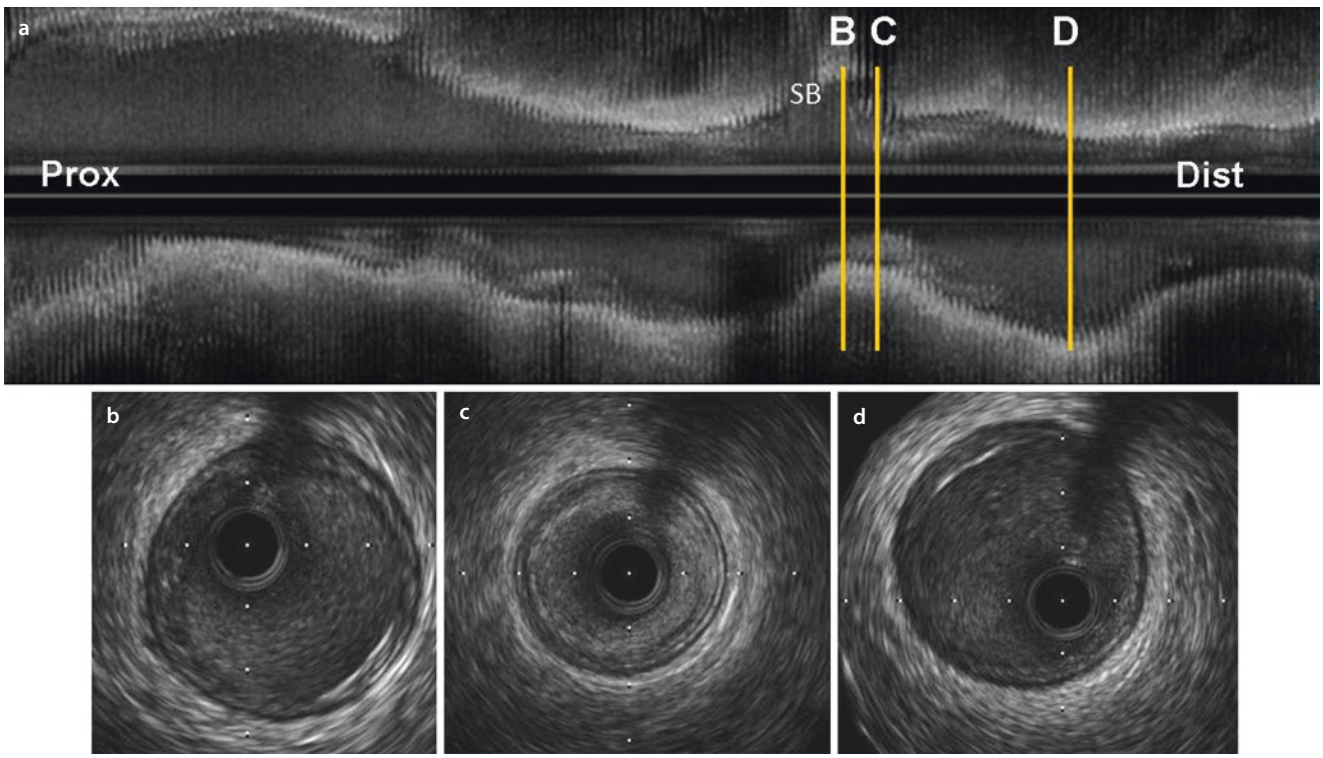


**Fig. 4.4** Negative remodeling. Example of a lesion with negative remodeling assessed by intravascular ultrasound (IVUS). **a** Longitudinal IVUS view showing a plaque distal to a side branch (*SB*). **b** IVUS cross section at the proximal reference. **c** IVUS cross section at the lesion showing a fibrotic concentric plaque. **d** IVUS cross section at the distal reference. The external elastic membrane (EEM) area at the lesion site is smaller than the reference EEM area. *Prox* proximal, *Dist* distal

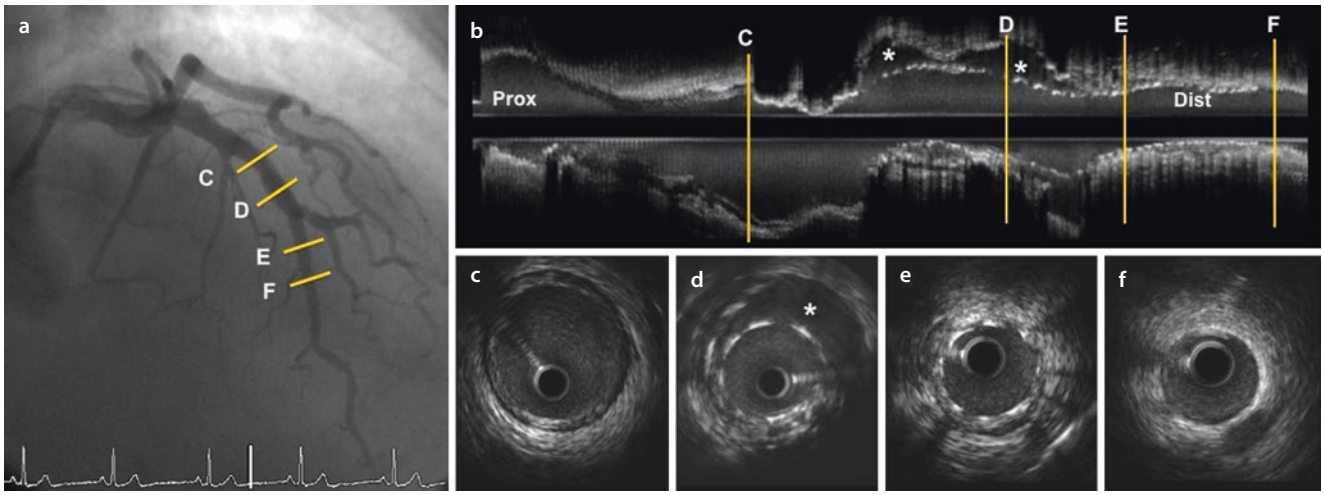


**Fig. 4.5** Positive remodeling after stenting. The figure shows an example of positive remodeling after drug-eluting stent implantation leading to late-acquired malapposition. **a** Angiographic image showing the region stented in the left anterior descending artery. **b** Longitudinal intravascular ultrasound (IVUS) view. Areas of stent malapposition can be observed (indicated by *). **c** Proximal reference. **d** IVUS cross section showing severe stent malapposition (indicated by *) caused by positive vessel remodeling with external elastic membrane (EEM) enlargement. **e** Distal segment of the stent showing good apposition. **f** Distal reference. The EEM area at the malapposition site is larger than the EEM area at the references

## 4.8 Vessel Remodeling After Percutaneous Coronary Interventions

Vascular remodeling plays an important role in the process of restenosis. In balloon angioplasty, late negative remodeling is the primary mechanism leading to restenosis [62]. Mintz et al. demonstrated, in a serial IVUS study, that 73 % of luminal loss between post-intervention and follow-up was attributable to a decrease in the EEM area and only 23 % was caused by neointimal area growth [63]. Intracoronary brachytherapy inhibited restenosis after balloon angioplasty mainly by inhibiting this negative remodeling.

Pre-interventional remodeling can have an influence in the outcome of interventional therapy. Dangas et al. evaluated 777 lesions treated with balloon angioplasty and showed that target lesion revascularization (TLR) was higher in lesions with positive remodeling compared to lesions with negative remodeling (31 % vs. 20 %, $p = 0.007$) [5]. Similar results have been described in patients treated with bare metal stents. Okura et al. reported a higher rate of TVR at 9 months in patients treated with BMS that showed pre-procedural positive remodeling (22.0 % vs. 4.1 %, $p = 0.01$). Furthermore, expansive remodeling pre-intervention has been recognized as a predictor of diffuse in-stent restenosis [64]. Regarding immediate results following immediately post-intervention, a higher acute luminal gain has been noted with direct stent implantation in lesions that display significant positive remodeling [65]. Mehran et al. described a higher increase in CK-MB post-procedurally in patients with marked expansive remodeling, suggesting an association between positive remodeling and distal embolization [66]. This correlates with several studies that show plaques with features of vulnerability (among them positive remodeling) to be more frequently associated with the no-reflow phenomenon [67].

In the drug-eluting stent era, vascular remodeling plays an important role in the long-term outcomes. Similar to those results seen with bare metal stents, the presence of positive remodeling pre-intervention correlates with significantly higher neointimal hyperplasia [68]. Late stent malapposition has been recognized as a predictor of stent thrombosis and can be caused by expansive vessel remodeling at the stent site [69] (Fig. 4.5). This local expansion may be induced by prolonged inflammation and a hypersensitivity in the vessel wall provoked by the drug-eluting polymer [70, 71]. OCT examinations after first-generation DES implantation very frequently show the presence of invaginations in the lumen between struts, a feature commonly associated with positive remodeling. These findings are now considered very rare with the newer generations of drug-eluting stents [72].

## 4.9 Vessel Remodeling in Transplant Graft Vasculopathy

Vascular remodeling plays a key role in the development of transplant graft vasculopathy. Vessel enlargement as a compensatory mechanism for plaque growth is impaired in epicardial vessels of cardiac allografts [73]. Thus, lower amounts of intimal growth (of only 20 % of vessel cross-sectional area) can compromise the vessel lumen size [74]. Several IVUS studies have demonstrated that coronary artery narrowing in transplanted patients is mainly caused by negative remodeling [75–77]. However, one study with a 5-year IVUS follow-up described a biphasic response with early lumen loss primarily caused by intimal thickening and late lumen loss caused by EEM area constriction [78]. Plaque shape can influence vessel remodeling in graft

vasculopathy where it has been shown that eccentric plaques have a higher remodeling index, most likely due to an increased coronary compliance [79].

## 4.10 Conclusions

Coronary remodeling is a major determinant in the clinical impact of coronary atherosclerosis. While initially vessel enlargement in response to plaque growth can be compensatory allowing lumen size to be maintained, this expansive remodeling is associated with several features of plaque vulnerability and ultimately may be a key process in culprit lesion development in acute coronary syndromes. Further research is needed to understand this complex phenomenon and its relationship with coronary atherosclerotic clinical manifestations.

## References

1. Glagov S, Weisenberg E, Zarins CK, Stankunavicius R, Kolettis GJ. Compensatory enlargement of human atherosclerotic coronary arteries. N Engl J Med. 1987;316:1371–5.
2. Sipahi I, Tuzcu EM, Schoenhagen P, Nicholls SJ, Chen MS, Crowe T, Loyd AB, Kapadia S, Nissen SE. Paradoxical increase in lumen size during progression of coronary atherosclerosis: observations from the REVERSAL trial. Atherosclerosis. 2006;189:229–35.
3. Hermiller JB, Tenaglia AN, Kisslo KB, Phillips HR, Bashore TM, Stack RS, Davidson CJ. In vivo validation of compensatory enlargement of atherosclerotic coronary arteries. Am J Cardiol. 1993;71:665–8.
4. Mintz GS, Kent KM, Pichard AD, Satler LF, Popma JJ, Leon MB. Contribution of inadequate arterial remodeling to the development of focal coronary artery stenoses. An intravascular ultrasound study. Circulation. 1997;95:1791–8.
5. Dangas G, Mintz GS, Mehran R, Lansky AJ, Kornowski R, Pichard AD, Satler LF, Kent KM, Stone GW, Leon MB. Preintervention arterial remodeling as an independent predictor of target-lesion revascularization after nonstent coronary intervention: an analysis of 777 lesions with intravascular ultrasound imaging. Circulation. 1999;99:3149–54.
6. Inaba S, Mintz GS, Shimizu T, Weisz G, Mehran R, Marso SP, Xu K, de Bruyne B, Serruys PW, Stone GW, Maehara A. Compensatory enlargement of the left main coronary artery: insights from the PROSPECT study. Coron Artery Dis. 2014;25:98–103.
7. Hernando L, Corros C, Gonzalo N, Hernandez-Antolin R, Banuelos C, Jimenez-Quevedo P, Bernardo E, Fernandez-Ortiz A, Escaned J, Macaya C, Alfonso F. Morphological characteristics of culprit coronary lesions according to clinical presentation: insights from a multimodality imaging approach. Int J Cardiovasc Imaging. 2013;29:13–21.
8. Tanaka M, Tomiyasu K, Fukui M, Akabame S, Kobayashi-Takenaka Y, Nakano K, Kadono M, Hasegawa G, Oda Y, Nakamura N. Evaluation of characteristics and degree of remodeling in coronary atherosclerotic lesions by 64-detector multislice computed tomography (MSCT). Atherosclerosis. 2009;203:436–41.
9. Kashiwagi M, Tanaka A, Kitabata H, Tsujioka H, Kataiwa H, Komukai K, Tanimoto T, Takemoto K, Takarada S, Kubo T, Hirata K, Nakamura N, Mizukoshi M, Imanishi T, Akasaka T. Feasibility of noninvasive assessment of thin-cap fibroatheroma by multidetector computed tomography. JACC Cardiovasc Imaging. 2009;2:1412–9.
10. Mintz GS, Nissen SE, Anderson WD, Bailey SR, Erbel R, Fitzgerald PJ, Pinto FJ, Rosenfield K, Siegel RJ, Tuzcu EM, Yock PG. American College of Cardiology Clinical Expert Consensus Document on Standards for Acquisition, Measurement and Reporting of Intravascular Ultrasound Studies (IVUS). A report of the American College of Cardiology Task Force on Clinical Expert Consensus Documents. J Am Coll Cardiol. 2001;37:1478–92.
11. Hibi K, Ward MR, Honda Y, Suzuki T, Jeremias A, Okura H, Hassan AH, Maehara A, Yeung AC, Pasterkamp G, Fitzgerald PJ, Yock PG. Impact of different definitions on the interpretation of coronary remodeling determined by intravascular ultrasound. Catheter Cardiovasc Interv. 2005;65:233–9.
12. Sipahi I, Tuzcu EM, Schoenhagen P, Nicholls SJ, Crowe T, Kapadia S, Nissen SE. Static and serial assessments of coronary arterial remodeling are discordant: an intravascular ultrasound analysis from the Reversal of Atherosclerosis with Aggressive Lipid Lowering (REVERSAL) trial. Am Heart J. 2006;152:544–50.
13. Jensen LO, Thayssen P, Mintz GS, Maeng M, Junker A, Galloe A, Christiansen EH, Hoffmann SK, Pedersen KE, Hansen HS, Hansen KN. Intravascular ultrasound assessment of remodelling and reference segment plaque burden in type-2 diabetic patients. Eur Heart J. 2007;28:1759–64.
14. Ye S, Humphries S, Henney A. Matrix metalloproteinases: implication in vascular matrix remodelling during atherogenesis. Clin Sci (Lond). 1998;94:103–10.
15. Schoenhagen P, Vince DG, Ziada KM, Kapadia SR, Lauer MA, Crowe TD, Nissen SE, Tuzcu EM. Relation of matrix-metalloproteinase 3 found in coronary lesion samples retrieved by directional coronary atherectomy to intravascular ultrasound observations on coronary remodeling. Am J Cardiol. 2002;89:1354–9.
16. Bassiouny HS, Song RH, Hong XF, Singh A, Kocharyan H, Glagov S. Flow regulation of 72-kD collagenase IV (MMP-2) after experimental arterial injury. Circulation. 1998;98:157–63.
17. Tronc F, Mallat Z, Lehoux S, Wassef M, Esposito B, Tedgui A. Role of matrix metalloproteinases in blood flow-induced arterial enlargement: interaction with NO. Arterioscler Thromb Vasc Biol. 2000;20:E120–6.
18. Walpola PL, Gotlieb AI, Cybulsky MI, Langille BL. Expression of ICAM-1 and VCAM-1 and monocyte adherence in arteries exposed to altered shear stress. Arterioscler Thromb Vasc Biol. 1995;15:2–10.
19. Aikawa M, Rabkin E, Okada Y, Voglic SJ, Clinton SK, Brinckerhoff CE, Sukhova GK, Libby P. Lipid lowering by diet reduces matrix metalloproteinase activity and increases collagen content of rabbit atheroma: a potential mechanism of lesion stabilization. Circulation. 1998;97:2433–44.
20. Tauth J, Pinnow E, Sullebarger JT, Basta L, Gursoy S, Lindsay Jr J, Matar F. Predictors of coronary arterial remodeling patterns in patients with myocardial ischemia. Am J Cardiol. 1997;80:1352–5.
21. Stone PH, Coskun AU, Kinlay S, Popma JJ, Sonka M, Wahle A, Yeghiazarians Y, Maynard C, Kuntz RE, Feldman CL. Regions of low endothelial shear stress are the sites where coronary plaque progresses and vascular remodelling occurs in humans: an in vivo serial study. Eur Heart J. 2007;28:705–10.
22. Katranas SA, Kelekis AL, Antoniadis AP, Chatzizisis YS, Giannoglou GD. Association of remodeling with endothelial shear stress, plaque elasticity, and volume in coronary arteries: a pilot coronary computed tomography angiography study. Angiology. 2014;65:413–9.
23. Mondy JS, Lindner V, Miyashiro JK, Berk BC, Dean RH, Geary RL. Platelet-derived growth factor ligand and receptor expression in response to altered blood flow in vivo. Circ Res. 1997;81:320–7.
24. Ward MR, Pasterkamp G, Yeung AC, Borst C. Arterial remodeling. Mechanisms and clinical implications. Circulation. 2000;102:1186–91.
25. Sudhir K, Ports TA, Amidon TM, Goldberger JJ, Bhushan V, Kane JP, Yock P, Malloy MJ. Increased prevalence of coronary ectasia in heterozygous familial hypercholesterolemia. Circulation. 1995;91:1375–80.
26. Antoniadis AP, Chatzizisis YS, Giannoglou GD. Pathogenetic mechanisms of coronary ectasia. Int J Cardiol. 2008;130:335–43.
27. von Birgelen C, Hartmann M, Mintz GS, Baumgart D, Schmermund A, Erbel R. Relation between progression and regression of atherosclerotic left main coronary artery disease and serum cholesterol levels as assessed with serial long-term (> or =12 months) follow-up intravascular ultrasound. Circulation. 2003;108:2757–62.

28. Jimenez-Quevedo P, Sabate M, Angiolillo D, Alfonso F, Hernandez-Antolin R, Banuelos C, Bernardo E, Ramirez C, Moreno R, Fernandez C, Escaned J, Macaya C. LDL-cholesterol predicts negative coronary artery remodelling in diabetic patients: an intravascular ultrasound study. Eur Heart J. 2005;26:2307–12.
29. Yoneyama S, Arakawa K, Yonemura A, Isoda K, Nakamura H, Ohsuzu F. Oxidized low-density lipoprotein and high-density lipoprotein cholesterol modulate coronary arterial remodeling: an intravascular ultrasound study. Clin Cardiol. 2003;26:31–5.
30. Taylor AJ, Burke AP, Farb A, Yousefi P, Malcom GT, Smialek J, Virmani R. Arterial remodeling in the left coronary system: the role of high-density lipoprotein cholesterol. J Am Coll Cardiol. 1999;34:760–7.
31. Hamasaki S, Higano ST, Suwaidi JA, Nishimura RA, Miyauchi K, Holmes Jr DR, Lerman A. Cholesterol-lowering treatment is associated with improvement in coronary vascular remodeling and endothelial function in patients with normal or mildly diseased coronary arteries. Arterioscler Thromb Vasc Biol. 2000;20:737–43.
32. Schoenhagen P, Tuzcu EM, Apperson-Hansen C, Wang C, Wolski K, Lin S, Sipahi I, Nicholls SJ, Magyar WA, Loyd A, Churchill T, Crowe T, Nissen SE. Determinants of arterial wall remodeling during lipid-lowering therapy: serial intravascular ultrasound observations from the Reversal of Atherosclerosis with Aggressive Lipid Lowering Therapy (REVERSAL) trial. Circulation. 2006;113:2826–34.
33. Nicholls SJ, Tuzcu EM, Kalidindi S, Wolski K, Moon KW, Sipahi I, Schoenhagen P, Nissen SE. Effect of diabetes on progression of coronary atherosclerosis and arterial remodeling: a pooled analysis of 5 intravascular ultrasound trials. J Am Coll Cardiol. 2008;52:255–62.
34. Schukro C, Syeda B, Yahya N, Gessl A, Holy EW, Pichler P, Derntl M, Glogar D. Volumetric intravascular ultrasound imaging to illustrate the extent of coronary plaque burden in type 2 diabetic patients. J Diabetes Complications. 2007;21:381–6.
35. Kornowski R, Mintz GS, Lansky AJ, Hong MK, Kent KM, Pichard AD, Satler LF, Popma JJ, Bucher TA, Leon MB. Paradoxic decreases in atherosclerotic plaque mass in insulin-treated diabetic patients. Am J Cardiol. 1998;81:1298–304.
36. Vavuranakis M, Stefanadis C, Toutouzas K, Pitsavos C, Spanos V, Toutouzas P. Impaired compensatory coronary artery enlargement in atherosclerosis contributes to the development of coronary artery stenosis in diabetic patients. An in vivo intravascular ultrasound study. Eur Heart J. 1997;18:1090–4.
37. Jimenez-Quevedo P, Suzuki N, Corros C, Ferrer C, Angiolillo DJ, Alfonso F, Hernandez-Antolin R, Banuelos C, Escaned J, Fernandez C, Costa M, Macaya C, Bass T, Sabate M. Vessel shrinkage as a sign of atherosclerosis progression in type 2 diabetes: a serial intravascular ultrasound analysis. Diabetes. 2009;58:209–14.
38. Nakamura M, Nishikawa H, Mukai S, Setsuda M, Nakajima K, Tamada H, Suzuki H, Ohnishi T, Kakuta Y, Nakano T, Yeung AC. Impact of coronary artery remodeling on clinical presentation of coronary artery disease: an intravascular ultrasound study. J Am Coll Cardiol. 2001;37:63–9.
39. Rodriguez-Granillo GA, Serruys PW, Garcia-Garcia HM, Aoki J, Valgimigli M, van Mieghem CA, McFadden E, de Jaegere PP, de Feyter P. Coronary artery remodelling is related to plaque composition. Heart. 2006;92:388–91.
40. Hong MK, Park SW, Lee CW, Choi SW, Song JM, Kang DH, Song JK, Kim JJ, Park SJ. Elevated homocysteine levels might be associated with coronary artery remodeling in patients with stable angina: an intravascular ultrasound study. Clin Cardiol. 2002;25:225–9.
41. Iwata A, Miura S, Mori K, Kawamura A, Nishikawa H, Saku K. Associations between metabolic factors and coronary plaque growth or arterial remodeling as assessed by intravascular ultrasound in patients with stable angina. Hypertens Res. 2008;31:1879–86.
42. Burke AP, Kolodgie FD, Farb A, Weber D, Virmani R. Morphological predictors of arterial remodeling in coronary atherosclerosis. Circulation. 2002;105:297–303.
43. Fujii K, Carlier SG, Mintz GS, Wijns W, Colombo A, Bose D, Erbel R, de Ribamar Costa Jr J, Kimura M, Sano K, Costa RA, Lui J, Stone GW, Moses JW, Leon MB. Association of plaque characterization by intravascular ultrasound virtual histology and arterial remodeling. Am J Cardiol. 2005;96:1476–83.
44. Kume T, Okura H, Kawamoto T, Akasaka T, Toyota E, Watanabe N, Neishi Y, Sukmawan R, Sadahira Y, Yoshida K. Relationship between coronary remodeling and plaque characterization in patients without clinical evidence of coronary artery disease. Atherosclerosis. 2008;197:799–805.
45. Garcia-Garcia HM, Goedhart D, Schuurbiers JC, Kukreja N, Tanimoto S, Daemen J, Morel MA, Bressers M, van Es GA, Wentzel JJ, Gijsen F, van der Steen AF, Serruys PW. Virtual histology and remodelling index allow in vivo identification of allegedly high-risk coronary plaques in patients with acute coronary syndromes: a three vessel intravascular ultrasound radiofrequency data analysis. EuroIntervention. 2006;2:338–44.
46. Kim SW, Mintz GS, Ohlmann P, Hassani SE, Michalek A, Escolar E, Bui AB, Pichard AD, Satler LF, Kent KM, Suddath WO, Waksman R, Weissman NJ. Comparative intravascular ultrasound analysis of ostial disease in the left main versus the right coronary artery. J Invasive Cardiol. 2007;19:377–80.
47. Takeuchi H, Morino Y, Matsukage T, Masuda N, Kawamura Y, Kasai S, Hashida T, Fujibayashi D, Tanabe T, Ikari Y. Impact of vascular remodeling on the coronary plaque compositions: an investigation with in vivo tissue characterization using integrated backscatter-intravascular ultrasound. Atherosclerosis. 2009;202:476–82.
48. Sabate M, Kay IP, de Feyter PJ, van Domburg RT, Deshpande NV, Ligthart JM, Gijzel AL, Wardeh AJ, Boersma E, Serruys PW. Remodeling of atherosclerotic coronary arteries varies in relation to location and composition of plaque. Am J Cardiol. 1999;84:135–40.
49. Higashikuni Y, Tanabe K, Yamamoto H, Aoki J, Nakazawa G, Onuma Y, Otsuki S, Yagishita A, Yachi S, Nakajima H, Hara K. Relationship between coronary artery remodeling and plaque composition in culprit lesions: an intravascular ultrasound radiofrequency analysis. Circ J. 2007;71:654–60.
50. Costa RA, Feres F, Staico R, Abizaid A, Costa Jr JR, Siqueira D, Tanajura LF, Damiani LP, Sousa A, Sousa JE, Colombo A. Vessel remodeling and plaque distribution in side branch of complex coronary bifurcation lesions: a grayscale intravascular ultrasound study. Int J Cardiovasc Imaging. 2013;29:1657–66.
51. Hong MK, Park SW, Lee CW, Ko JY, Kang DH, Song JK, Kim JJ, Mintz GS, Park SJ. Intravascular ultrasound findings of negative arterial remodeling at sites of focal coronary spasm in patients with vasospastic angina. Am Heart J. 2000;140:395–401.
52. Ohayon J, Finet G, Gharib AM, Herzka DA, Tracqui P, Heroux J, Rioufol G, Kotys MS, Elagha A, Pettigrew RI. Necrotic core thickness and positive arterial remodeling index: emergent biomechanical factors for evaluating the risk of plaque rupture. Am J Physiol Heart Circ Physiol. 2008;295:H717–27.
53. Richardson PD, Davies MJ, Born GV. Influence of plaque configuration and stress distribution on fissuring of coronary atherosclerotic plaques. Lancet. 1989;2:941–4.
54. Schoenhagen P, Ziada KM, Kapadia SR, Crowe TD, Nissen SE, Tuzcu EM. Extent and direction of arterial remodeling in stable versus unstable coronary syndromes : an intravascular ultrasound study. Circulation. 2000;101:598–603.
55. Kaji S, Akasaka T, Hozumi T, Takagi T, Kawamoto T, Ueda Y, Yoshida K. Compensatory enlargement of the coronary artery in acute myocardial infarction. Am J Cardiol. 2000;85:1139–41. A1139.
56. Kotani J, Mintz GS, Castagna MT, Pinnow E, Berzingi CO, Bui AB, Pichard AD, Satler LF, Suddath WO, Waksman R, Laird Jr JR, Kent KM, Weissman NJ. Intravascular ultrasound analysis of infarct-related and non-infarct-related arteries in patients who presented with an acute myocardial infarction. Circulation. 2003;107:2889–93.
57. Hong YJ, Jeong MH, Choi YH, Ko JS, Lee MG, Kang WY, Lee SE, Kim SH, Park KH, Sim DS, Yoon NS, Youn HJ, Kim KH, Park HW, Kim JH, Ahn Y, Cho JG, Park JC, Kang JC. Positive remodeling is associated with more plaque vulnerability and higher frequency of plaque prolapse accompanied with post-procedural cardiac enzyme elevation

compared with intermediate/negative remodeling in patients with acute myocardial infarction. J Cardiol. 2009;53:278–87.
58. Imazeki T, Sato Y, Inoue F, Anazawa T, Tani S, Matsumoto N, Takayama T, Uchiyama T, Saito S. Evaluation of coronary artery remodeling in patients with acute coronary syndrome and stable angina by multislice computed tomography. Circ J. 2004;68:1045–50.
59. Motoyama S, Kondo T, Sarai M, Sugiura A, Harigaya H, Sato T, Inoue K, Okumura M, Ishii J, Anno H, Virmani R, Ozaki Y, Hishida H, Narula J. Multislice computed tomographic characteristics of coronary lesions in acute coronary syndromes. J Am Coll Cardiol. 2007;50:319–26.
60. Smits PC, Pasterkamp G, van Ufford MA Q, Eefting FD, Stella PR, de Jaegere PP, Borst C. Coronary artery disease: arterial remodelling and clinical presentation. Heart. 1999;82:461–4.
61. Hassani SE, Mintz GS, Fong HS, Kim SW, Xue Z, Pichard AD, Satler LF, Kent KM, Suddath WO, Waksman R, Weissman NJ. Negative remodeling and calcified plaque in octogenarians with acute myocardial infarction: an intravascular ultrasound analysis. J Am Coll Cardiol. 2006;47:2413–9.
62. Lafont A, Guzman LA, Whitlow PL, Goormastic M, Cornhill JF, Chisolm GM. Restenosis after experimental angioplasty. Intimal, medial, and adventitial changes associated with constrictive remodeling. Circ Res. 1995;76:996–1002.
63. Mintz GS, Popma JJ, Pichard AD, Kent KM, Satler LF, Wong C, Hong MK, Kovach JA, Leon MB. Arterial remodeling after coronary angioplasty: a serial intravascular ultrasound study. Circulation. 1996;94:35–43.
64. Sahara M, Kirigaya H, Oikawa Y, Yajima J, Ogasawara K, Satoh H, Nagashima K, Hara H, Nakatsu Y, Aizawa T. Arterial remodeling patterns before intervention predict diffuse in-stent restenosis: an intravascular ultrasound study. J Am Coll Cardiol. 2003;42:1731–8.
65. Finet G, Weissman NJ, Mintz GS, Satler LF, Kent KM, Laird JR, Adelmann GA, Ajani AE, Castagna MT, Rioufol G, Pichard AD. Mechanism of lumen enlargement with direct stenting versus predilatation stenting: influence of remodelling and plaque characteristics assessed by volumetric intracoronary ultrasound. Heart. 2003;89:84–90.
66. Mehran R, Dangas G, Mintz GS, Lansky AJ, Pichard AD, Satler LF, Kent KM, Stone GW, Leon MB. Atherosclerotic plaque burden and CK-MB enzyme elevation after coronary interventions : intravascular ultrasound study of 2256 patients. Circulation. 2000;101:604–10.
67. Jang JS, Jin HY, Seo JS, Yang TH, Kim DK, Park YA, Cho KI, Park YH, Kim DS. Meta-analysis of plaque composition by intravascular ultrasound and its relation to distal embolization after percutaneous coronary intervention. Am J Cardiol. 2013;111:968–72.
68. Kang WC, Oh KJ, Han SH, Ahn TH, Chung WJ, Shin MS, Koh KK, Choi IS, Shin EK. Effect of preinterventional arterial remodeling on intimal hyperplasia after implantation of a polymer-based paclitaxel-eluting stent: angiographic and IVUS study. Int J Cardiol. 2007;123:50–4.
69. Hassan AK, Bergheanu SC, Stijnen T, van der Hoeven BL, Snoep JD, Plevier JW, Schalij MJ, Wouter Jukema J. Late stent malapposition risk is higher after drug-eluting stent compared with bare-metal stent implantation and associates with late stent thrombosis. Eur Heart J. 2010;31:1172–80.
70. Virmani R, Guagliumi G, Farb A, Musumeci G, Grieco N, Motta T, Mihalcsik L, Tespili M, Valsecchi O, Kolodgie FD. Localized hypersensitivity and late coronary thrombosis secondary to a sirolimus-eluting stent: should we be cautious? Circulation. 2004;109:701–5.
71. Jimenez-Quevedo P, Sabate M, Angiolillo DJ, Costa MA, Alfonso F, Gomez-Hospital JA, Hernandez-Antolin R, Banuelos C, Goicolea J, Fernandez-Aviles F, Bass T, Escaned J, Moreno R, Fernandez C, Macaya C. Vascular effects of sirolimus-eluting versus bare-metal stents in diabetic patients: three-dimensional ultrasound results of the Diabetes and Sirolimus-Eluting Stent (DIABETES) Trial. J Am Coll Cardiol. 2006;47:2172–9.
72. Radu MD, Raber L, Kalesan B, Muramatsu T, Kelbaek H, Heo J, Jorgensen E, Helqvist S, Farooq V, Brugaletta S, Garcia-Garcia HM, Juni P, Saunamaki K, Windecker S, Serruys PW. Coronary evaginations are associated with positive vessel remodelling and are nearly absent following implantation of newer-generation drug-eluting stents: an optical coherence tomography and intravascular ultrasound study. Eur Heart J. 2014;35:795–807.
73. Lim TT, Liang DH, Botas J, Schroeder JS, Oesterle SN, Yeung AC. Role of compensatory enlargement and shrinkage in transplant coronary artery disease. Serial intravascular ultrasound study. Circulation. 1997;95:855–9.
74. Li HY, Tanaka K, Oeser B, Wertman B, Kobashigawa JA, Tobis JM. Compensatory enlargement in transplant coronary artery disease: an intravascular ultrasound study. Chin Med J (Engl). 2006;119:564–9.
75. Li H, Tanaka K, Oeser B, Kobashigawa JA, Tobis JM. Vascular remodelling after cardiac transplantation: a 3-year serial intravascular ultrasound study. Eur Heart J. 2006;27:1671–7.
76. Li H, Tanaka K, Chhabra A, Oeser B, Kobashigawa JA, Tobis JM. Vascular remodeling 1 year after cardiac transplantation. J Heart Lung Transplant. 2007;26:56–62.
77. Fearon WF, Potena L, Hirohata A, Sakurai R, Yamasaki M, Luikart H, Lee J, Vana ML, Cooke JP, Mocarski ES, Yeung AC, Valantine HA. Changes in coronary arterial dimensions early after cardiac transplantation. Transplantation. 2007;83:700–5.
78. Tsutsui H, Ziada KM, Schoenhagen P, Iyisoy A, Magyar WA, Crowe TD, Klingensmith JD, Vince DG, Rincon G, Hobbs RE, Yamagishi M, Nissen SE, Tuzcu EM. Lumen loss in transplant coronary artery disease is a biphasic process involving early intimal thickening and late constrictive remodeling: results from a 5-year serial intravascular ultrasound study. Circulation. 2001;104:653–7.
79. Schwarzacher SP, Uren NG, Ward MR, Schwarzkopf A, Giannetti N, Hunt S, Fitzgerald PJ, Oesterle SN, Yeung AC. Determinants of coronary remodeling in transplant coronary disease: a simultaneous intravascular ultrasound and Doppler flow study. Circulation. 2000;101:1384–9.

# Collateral Circulation

## Remodeling of the Coronary Circulation: Arteriogenesis, Angiogenesis, and Vasculogenesis

*Christian Seiler*




J. Escaned, J. Davies (eds.), *Physiological Assessment of Coronary Stenoses and the Microcirculation*,
DOI 10.1007/978-1-4471-5245-3_5

## 5.1 Introduction

Cardiovascular disease is the leading cause of death in industrialized countries and may become the most important reason for mortality worldwide [1]. In the vast majority thereof, death is the consequence of cerebral or myocardial infarction, both of which are characterized by acute vessel occlusion in the context of atherosclerosis [2]. In this situation, outcome depends critically upon the extent of infarcted tissue [3]. Myocardial infarct size is reflected by the degree of ECG ST-segment elevation during the acute phase [4] and is directly determined by the duration of coronary occlusion, the ischemic area at risk for infarct, the lack of collateral supply to the jeopardized region, the absence of preconditioning ischemic episodes prior to, and the level of myocardial oxygen consumption during the acute coronary event [5].

Remodeling of the coronary circulation describes the structural transformation of the coronary arterial tree with its native vascular branches and anastomoses in response to permanently altering flow conditions. This process occurring within 10–14 days following the altered physical condition is called arteriogenesis in a general sense [6, 7], which describes both structural vascular enlargement and shrinkage of any part of the coronary arterial circulation. More specifically, "arteriogenesis" is employed to designate physically induced structural growth of coronary arterial and arteriolar anastomoses, i.e., collateral pathways (Fig. 5.1; "collateral vessel growth") [8–10]. In comparison, the terms angiogenesis and vasculogenesis employed in the context of collateral development are not related to physical, but biochemical/molecular, (patho-)physiologic, and embryologic influences. Vasculogenesis occurs during embryologic development of the circulatory system and is defined as the de novo formation of blood vessels from endothelial precursor cells, which migrate and differentiate in response to local signals [11, 12]. New vessels can subsequently develop from the preexisting plexus by sprouting and intussusception. This formation of new vessels has been called angiogenesis (Fig. 5.1) [10, 13]. Angiogenesis as opposed to vasculogenesis is not restricted to the developing organism, but occurs physiologically in tissue repair or during the female

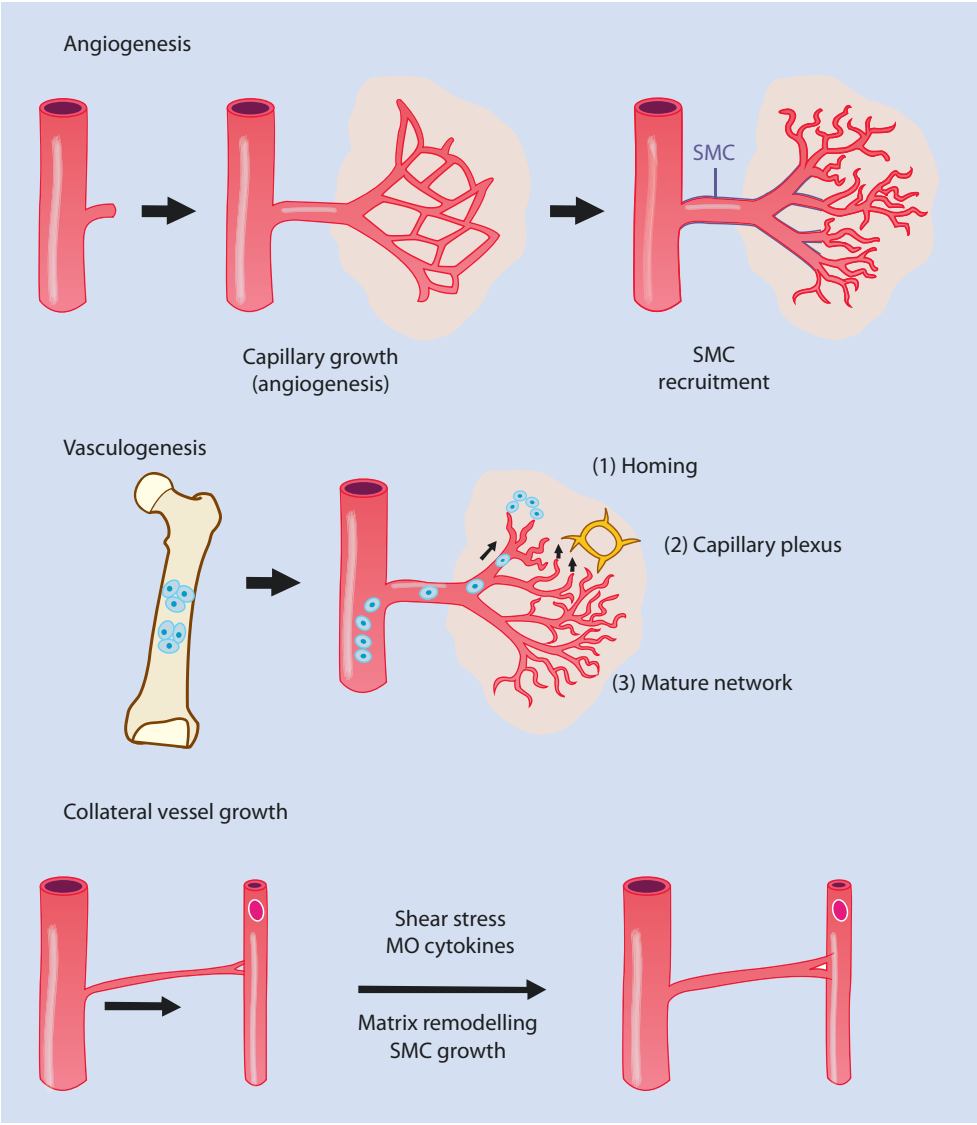


**Fig. 5.1** Schematic illustration of the development of vascular systems. See text for details. Abbreviations: *MO* monocytic cytokines, *SMC* smooth muscle cell [40]

reproductive cycle and pathophysiologically in response to ischemia [13].

In the above context, this chapter reviews the physiologic/physical principles governing coronary arteriogenesis, the clinical relevance of the coronary collateral circulation, its assessment, and influence on invasive hemodynamic coronary stenosis measurement.

## 5.2 Physiologic Principles Relevant to Coronary Arteriogenesis

The basic physiologic and physical principles operative in the coronary circulation in general also apply to its anastomoses, i.e., the collateral arteries and arterioles [14]. Oxygen is the main nutrient for the myocardium, whose demand is determined by ventricular wall stress, heart rate, and myocardial contractility [4]. Oxygen extraction from hemoglobin is close to maximal in myocardial tissue under normal metabolic conditions, and therefore, changes in oxygen demand are regulated by altering rates of coronary blood flow ($Q$ in ml/min). According to Ohm's law, the perfusion pressure drop ($\Delta P$ in mmHg) along increasingly smaller tubes can be described as the product of the vascular resistance ($R$ in dyn s $cm^{-5}$) to flow and the flow rate $Q$: $\Delta P = R \bullet Q$. In the coronary circulation, $\Delta P$ is the difference between mean aortic perfusion pressure ($P_{ao}$, mmHg) and mean central venous pressure (CVP, mmHg). In the normal coronary circulation, $R$ is mainly due to viscous friction between the blood and the endothelium covering the wall of small vessels; this can be appreciated by the fact that the pressure drop in a normal *epicardial* coronary tree is equal to a mere 5 mmHg. Based on Ohm's law, pressure drop along the vascular path is further described by Hagen-Poiseuille's law, which specifies the components of vascular geometry contributing to its resistance against flow ($R = 8\eta l/\pi r^4$; with l being vascular segment length and r being the internal vessel radius, η is the blood viscosity). The balance between two energy-consuming factors related to the transport of blood, i.e., the "cost" of pumping the blood through the circulation as opposed to the "cost" of building and maintaining the circulation, defines the term "minimum energy dissipation," the principle of which is compatible with the structural design of the entire coronary artery tree including its anastomoses [15]. According to the law of minimum viscous energy loss, the cross-sectional area of a coronary artery at any point in the arterial tree is proportional to the flow rate $Q^{2/3}$ at this site [15]. Thus, a permanent increase in coronary flow as induced, e.g., by an arteriovenous shunt between the left anterior descending artery and the right ventricle (Fig. 5.2), stimulates coronary caliber enlargement or remodeling (arteriogenesis) of the native left anterior descending (LAD) artery as well as the collateral artery supplying the functional LAD occlusion at the site of the fistula (Fig. 5.2). Using various measurement techniques, normal myocardial perfusion under resting conditions has been documented to be close to 1 ml/min/g of tissue [16]. Thus numerically (unity between flow rate and regional mass in grams), $Q$ in Ohm's or Hagen-Poiseuille's law can be replaced by regional myocardial mass ($M$, supplied by blood at any point of interest in the coronary tree), which is equal to the ischemic area at risk (AR) for myocardial infarction. AR and M can also be defined angiographically in terms of summed coronary artery branch lengths distal to any point in the coronary tree relative to the entire coronary artery tree length [17]. This definition of AR establishes the relation between collateral vessels and AR.

In the presence of a hemodynamically relevant coronary artery stenosis, perfusion pressure distal to the narrowed segment is reduced mainly due to turbulent energy losses. Autoregulation maintains basal flow distal to the stenosis by microvascular vasodilation up to a critical reduction in the vessel lumen area, beyond which resting coronary blood flow is also reduced [18]. Concurrently, the pressure drop across the stenosis leads to a pressure gradient along preexisting collateral vessels connecting to the normal vessel. In turn, they are recruited by flow augmentation from the donor artery across the collateral network to the stenotic recipient coronary artery. Heightened flow velocity leads to a proportional increase in fluid shear stress, whereas the increased intravascular pressure leads to a proportional increase in circumferential wall stress [19]. With a prolonged stimulus, the collateral vessels (arteries and arterioles) react by increasing the lumen diameter (and also length; arteriogenesis) to normalize fluid shear stress and by increasing the wall thickness to normalize circumferential wall [20].

## 5.3 Clinical Relevance of the Coronary Collateral Circulation

The thus provided net increase in coronary collateral bulk flow to the vascular area at risk for infarction varies considerably depending on the existence and extent of preexistent anastomoses, on the severity of the upstream atherosclerotic obstruction, and on other environmental and also genetic factors (Fig. 5.3) [21–23]. Blood flow can increase maximally 10–20-fold by arteriogenesis, but only 1.5–1.7-fold by angiogenesis, i.e., the process referring to sprouting of new, minute, high-resistance, low-flow capillaries (see also Fig. 5.1) [24]. To generate the same lumen area as the artery by angiogenesis would essentially mean replacing the organ with capillaries [20]. Thus, arteriogenesis has the capacity to compensate for an occluded artery, whereas angiogenesis does not [25]. Even though mature collaterals are able to deliver bulk flow to jeopardized tissue, collateral remodeling stops short of completely reconstituting the function of an occluded artery [24, 26]. Primarily responsible for this circumstance is the premature normalization of the dominant driving force for continued outward remodeling – fluid shear stress. Even a small increase in luminal diameter leads to a much larger fall in fluid shear stress, consequence of fluid shear stress being inversely related to the third power of the vessel radius. Normal maximal blood flow is, therefore, not achievable even in healthy collateral-dependent tissues [7].

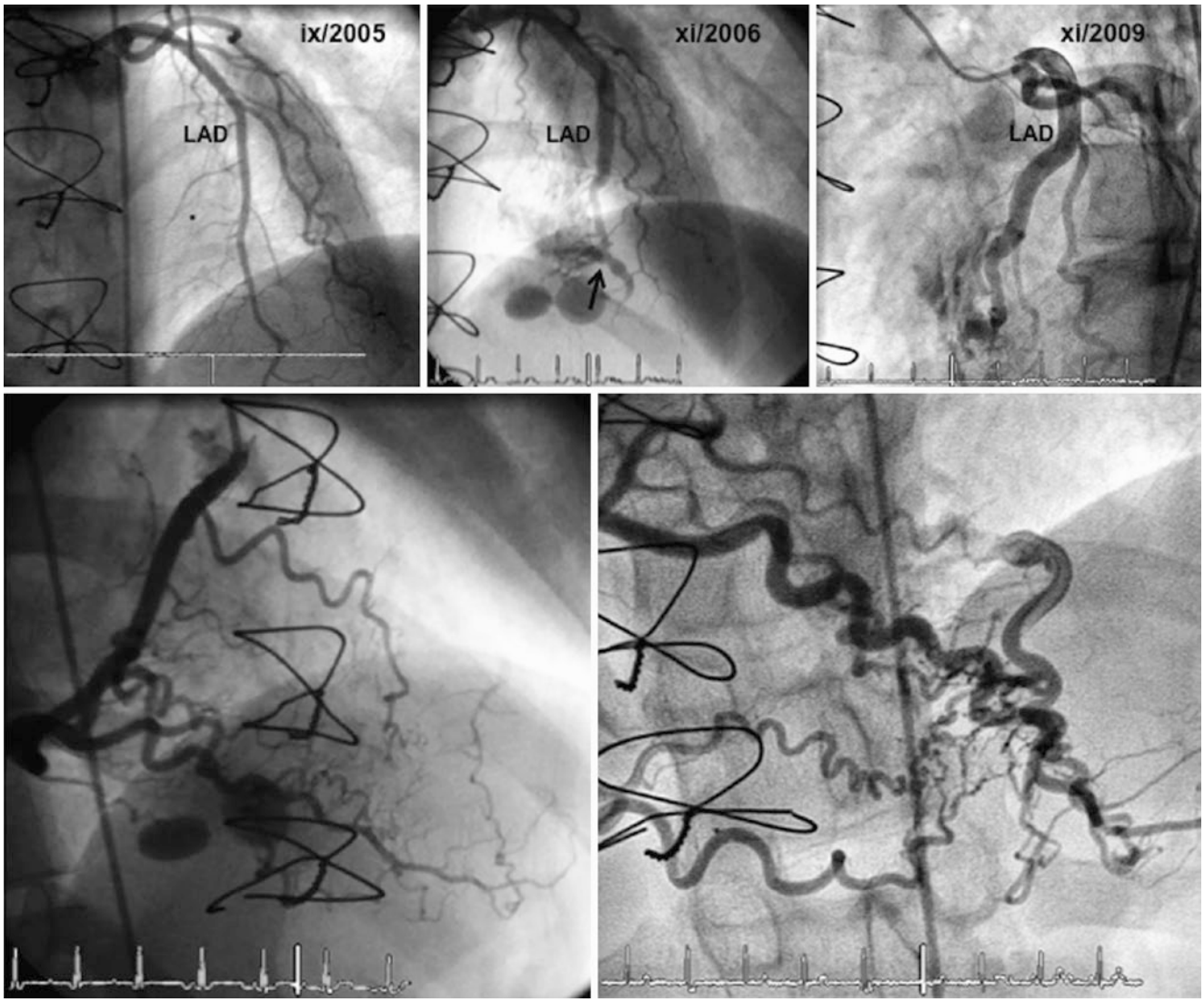


**Fig. 5.2** Upper panels: Left coronary angiogram of a female heart transplant patient with iatrogenic fistula between the left anterior descending (*LAD*) coronary artery and the right ventricle in the course of myocardial biopsy (2005: normal left coronary angiogram; anteroposterior cranial view; 2006: fistula →). In 2006, the LAD distal to the fistula is occluded with regard to antegrade flow. By 2009, the size of the LAD has much increased (*upper right panel*). *Lower panels*: Right coronary angiogram of the same patient. Between 2006 (*left lower panel*) and 2009 (*right lower panel*), the collateral vessels between the right coronary artery and the left anterior descending artery have become considerably larger; entire retrograde filling of the LAD to the site of occlusion/fistula [27]

Conversely, a complete functional reconstitution is achieved when fluid shear stress is artificially increased (see also Fig. 5.2) [24, 26, 27]. Notwithstanding these pathogenetic limitations, coronary arteriogenesis salvages myocardium at risk for infarction and, thus, has a beneficial effect on survival (Fig. 5.3) [28, 29].

The clinical relevance of the coronary collateral circulation relates to the beneficial effect of well-developed collaterals in preserving viability and function of dependent myocardium in the context of the acute and chronic manifestations of CAD. The partly contradictory results regarding the protective effect of coronary collaterals are chiefly related to the collateral circulation being both a marker of CAD severity and a predictor of future cardiac events [29]. In other words, the positive correlation between the angiographic presence of coronary collaterals and an unfavorable prognosis in patients with ischemic heart disease is confounded by the extent of CAD severity (explaining both) [30]. Therefore, an investigation aimed at the prognostic impact of collaterals has to correct for the severity of the underling coronary disease. A major determinant of long-term survival in coronary artery disease is LV ejection fraction, the preservation of which is associated with the coronary collateral circulation both in acute and chronic CAD [31]. With acute ischemia, the outcome is critically dependent on the extent of myocardial infarction, which increases with coronary artery occlusion time and with the area at risk for infarction, but decreases with increasing collateral supply [3, 5]. Therefore, the beneficial effect of better and timely developed collaterals is self-evident in acute coronary syndrome [3]. Moreover, not only

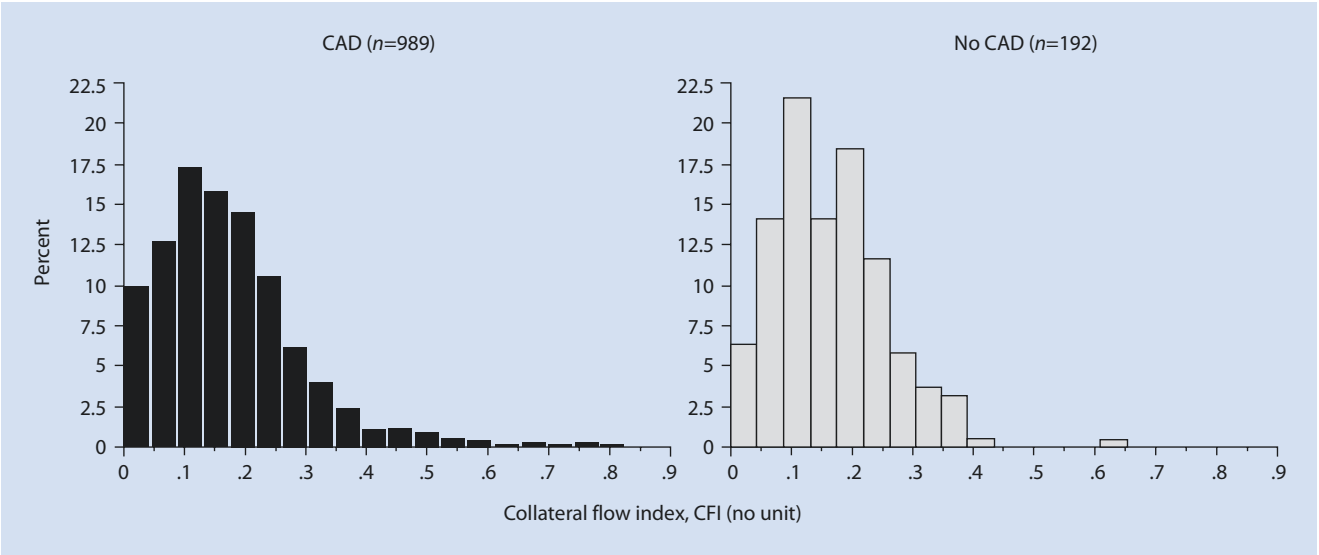


**Fig. 5.3** Frequency distribution (in percent; vertical axis) in quantitative coronary collateral function expressed as collateral flow index (CFI, horizontal axis; i.e., the ratio of coronary occlusive pressure to aortic pressure both subtracted by central venous pressure) among patients with and without coronary artery disease (*CAD*)

is the recovery of left ventricular function after reperfused acute myocardial infarction determined by the extent of collateral supply, but it is also less dependent on time to reperfusion in patients with sufficient collaterals [32]. Furthermore, in patients with acute myocardial infarction, poor collaterals are related to the early occurrence of cardiogenic shock, which portends a particularly high mortality [33]. In the context of the arrhythmogenic potential of myocardial ischemia, a clinical study has shown a protective effect of the collateral circulation on ischemia-induced QT prolongation, while experimental studies primarily investigated the susceptibility to ventricular fibrillation in acute coronary occlusion [34].

With chronic ischemia, a (further) decline in LV function results from hibernating and stunned myocardium [35]. Here, the not infrequently encountered case of completely normal ventricular function in the presence of a CTO exemplifies the protective effect of the coronary collateral network [36, 37]. Furthermore, it has been shown that regional LV function is directly related to the amount of collateral flow during both acute and chronic coronary occlusions [31]. Concerning postinfarction sequelae, the relevant protective role of collaterals has been shown to result in a reduction of postinfarct ventricular dilatation and less ventricular aneurysm formation [3].

Regarding the impact of the coronary collateral circulation on mortality, the majority of studies have relied on angiographic assessment. A recent meta-analysis included 12 angiographic studies, as well as a large study with quantitatively determined collateral assessment [28]. The pooled study population consisted of more than 6500 patients with stable CAD or subacute and acute myocardial infarction. With high versus low coronary collateral circulation, a significant 36 % reduced mortality was demonstrated (Fig. 5.4) [28]. Similarly, the latest follow-up (mean 7.3 ± 4.3 years) of a large prospective cohort with chronic stable CAD and quantitatively assessed collateral function again showed a reduction in all-cause mortality and, specifically, relevant and significant reductions in cardiac mortality and major adverse cardiac events with a well-functioning coronary collateral circulation [29].

## 5.4 Assessment of Coronary Collateral Structure and Function

### Coronary Occlusion Model

Accurate assessment of the coronary collateral circulation requires (transient) coronary occlusion, regardless of the employed method [38]. In the presence of coronary stenosis, the contribution of normal antegrade blood flow cannot be discerned from the recruited blood flow via the anastomotic pathways. In the absence of a coronary stenosis, there is probably no measurable net blood flow across nonrecruited preformed collaterals. Noninvasive techniques, such as positron emission tomography perfusion imaging, are, therefore, limited to the remodeled collateral circulation supplying chronic total coronary occlusions [39]. With regard to invasive techniques, qualitative and quantitative methods can be differentiated. Assessment of electrocardiographic signs during coronary occlusion can further characterize the function of coronary collaterals [14]. Quantitative functional measures of hemodynamic coronary stenosis severity, in particular fractional flow reserve (FFR), can be employed for *intraindividual* assessment of relative collateral function changes as long as the stenotic lesion is left untouched and given that coronary microcirculatory resistance to flow is constant and minimal. This is not an exemption to but a consequence of

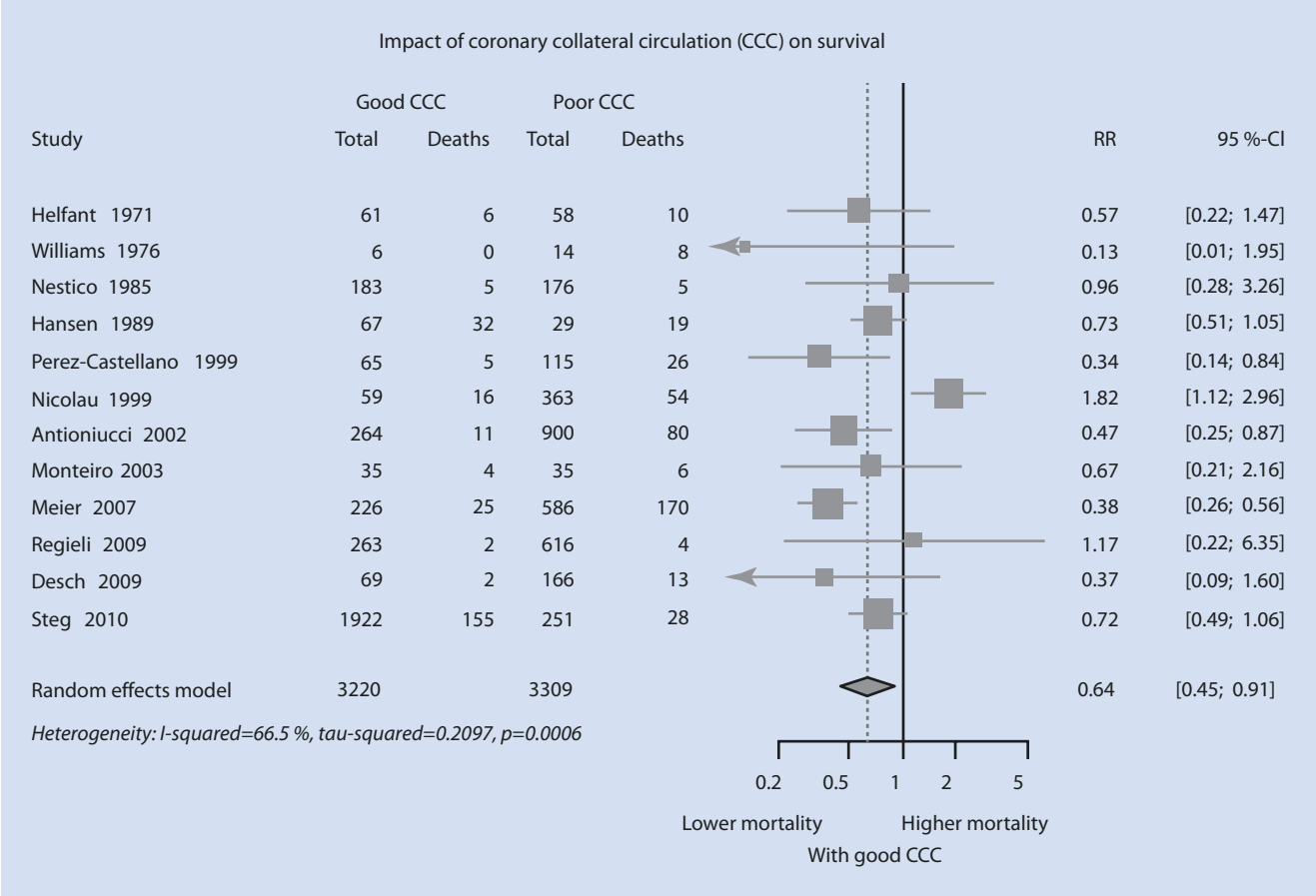


**Fig. 5.4** Forrest plot of the impact of a well-developed coronary collateral circulation ("*good CCC*") on overall survival in patients with coronary artery disease from 12 different studies [28]

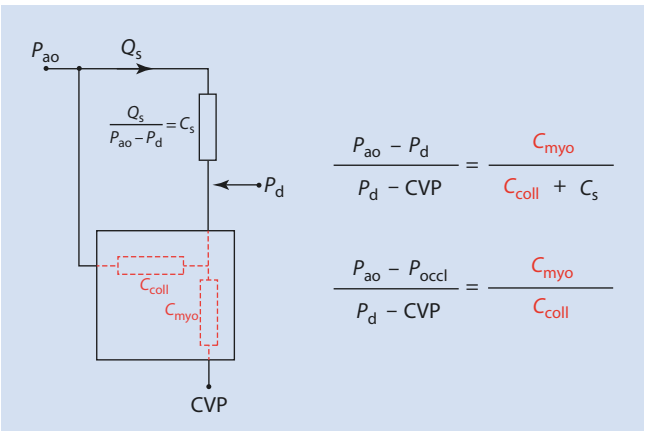


**Fig. 5.5** Schematic of an electrical analogue model of the coronary circulation with its perfusion pressure source (mean aortic pressure, $P_{ao}$), one bifurcation, whereby one branch is obstructed by a stenotic lesion (flow conductance in the stenotic branch, $C_s$), and the other branch is connected to the stenotic branch via an anastomosis (collateral flow conductance, $C_{coll}$). $C_s$ is calculated by Ohm's law on the basis of flow in ($Q_s$) and pressure drop across the stenotic vessel. The composite of collateral and downstream myocardial conductance ($C_{myo}$) is indicated by the square. Pressure values directly obtainable aside from $P_{ao}$ are distal coronary pressure ($P_d$) and central venous pressure (*CVP*) [40]

the above condition of coronary occlusion for identifiable collateral measurement. Myocardial mass perfusion or myocardial conductance results from both the contributions of coronary flow via the native patent coronary artery and of flow coming from adjacent native coronary arteries via anastomoses (collateral flow) (Fig. 5.5) [40].

## Angiographic Collateral Assessment

For proper angiographic assessment, occlusion of the collateral-receiving artery either spontaneously, or by balloon inflation, is mandatory (Fig. 5.6), even when some angiographic contrast filling of collaterals may be spontaneously present [14]. Furthermore, proper assessment by the angiographic method usually requires a double intubation technique to allow injection of contrast agent in the presumable (ipsi- and/or contralateral) donor artery and placement of an occluding balloon in the recipient artery (Fig. 5.6). However, in clinical practice and even in clinical studies, balloon occlusion is rarely performed, when occlusion is not spontaneously present, which lowers the sensitivity of the already blunt method. With the originally described angiographic score according to Rentrop et al. [41, 42], absent contrast filling of collateral connections or up to the side branch of the recipient artery denotes insufficient collaterals

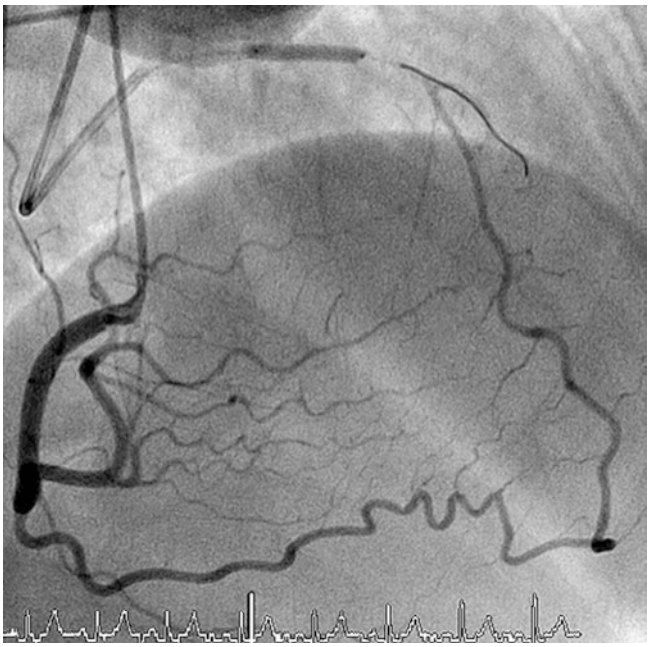

**Fig. 5.6** Right coronary artery (RCA) angiogram with double-intubation technique in a patient with recanalized chronic total occlusion of the proximal left anterior descending coronary artery. During RCA contrast injection, the recanalized LAD occlusion is re-obstructed by an angioplasty balloon (opaque markers). The LAD is filled entirely via a large branch collateral artery

(score of 0 and 1, respectively), while contrast filling of the epicardial main branch of the recipient artery, either partial (score of 2) or complete (score of 3), indicates sufficient collaterals. Although the Rentrop score shows (albeit moderate) correlation with functional collateral measures, it has relevant shortcomings [40]. A major limitation is the inability of the Rentrop score to adequately assess the functional significance, i.e., the protective effect, especially of recruitable but not spontaneously visible collateral vessels [43]. Instead of angiographic grading, assessment of collaterals by the semiquantitative washout collaterometry relies on the time to clearance of contrast medium trapped by balloon occlusion [44]. It correlates well with invasively determined collateral function and distinguishes accurately between sufficient and insufficient collaterals [44].

## Quantitative Collateral Function Assessment

Invasively determined, quantitative measures of collateral function rely on the determination of distal coronary pressure or flow velocity signals [45]. To this purpose, a coronary guide wire, equipped with a pressure and/or Doppler sensor near its tip, is positioned distally in the coronary artery of interest. Temporary blockage of the normal antegrade flow is thereafter performed either during therapeutic coronary angioplasty, or diagnostic balloon occlusion at low inflation pressure, the acute and long-term safety of which has been confirmed [46]. Mean distal coronary occlusive pressure ($P_{occl}$) is then set in relation to the temporal mean of aortic pressure ($P_{ao}$) measured via the angioplasty guide catheter, both subtracted by the back pressure, represented by central venous pressure (CVP), to calculate pressure-derived collateral flow index (CFI, Fig. 5.7) [45]. Similarly, distal flow velocity during coronary occlusion is compared against resting flow velocity when normal antegrade flow has been restored, to derive velocity-derived CFI [45]. Pressure signals can be reliably obtained and are robust to influences such as vessel anatomy, whereas Doppler signals are prone to wall-motion artifacts,

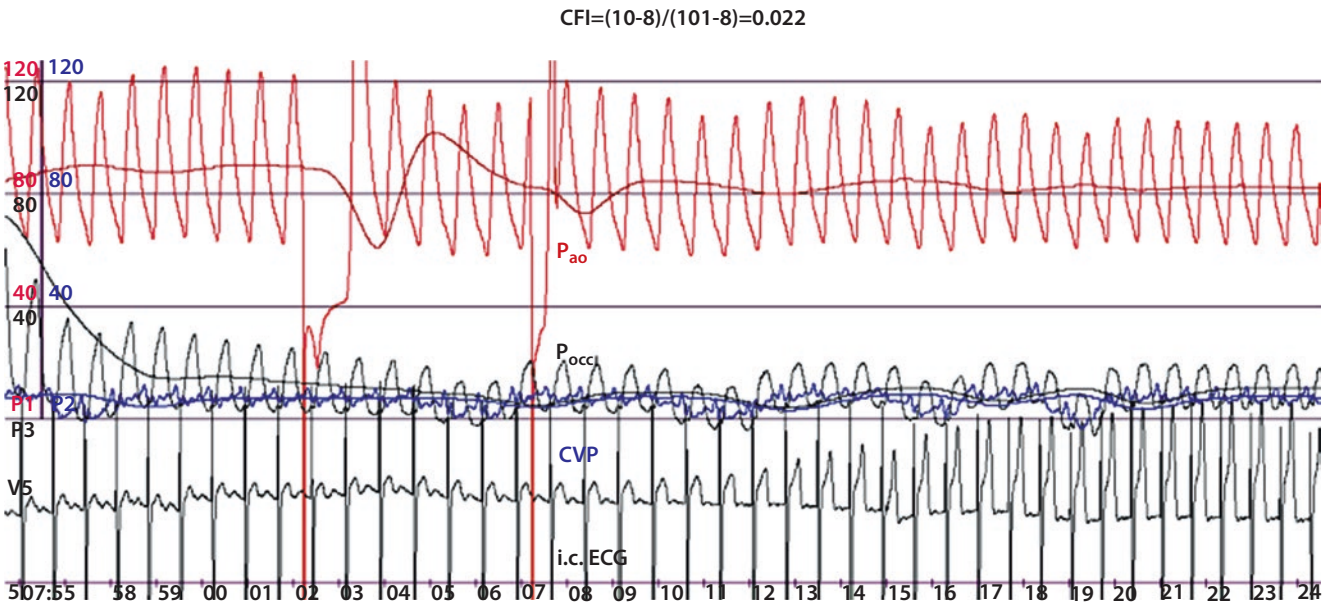


**Fig. 5.7** Quantitative measurement of coronary collateral function. Simultaneous recordings of phasic and mean aortic ($P_{ao}$ for mean pressure in *red*), distal coronary occlusive pressure ($P_{occl}$ in *black*), and central venous pressure (CVP in *blue*), as well as an intracoronary ECG lead. Collateral flow index (CFI; mmHg/mmHg) is calculated as ($P_{occl}$-CVP)/($P_{ao}$-CVP). Pressures are shown at the beginning of the 1-min coronary balloon (time scale in seconds) with the decrease in $P_{occl}$ at the *left side* and with the increasing ECG ST elevations starting at second 08. $P_{occl}$ is only very slightly above CVP, thus, CFI is close to zero, and therefore, the ECG ST segment markedly elevated

and registration of optimal signals is often not achievable [14, 45]. Pressure-derived CFI has been shown to correlate closely to myocardial perfusion during balloon occlusion as assessed by perfusion imaging and quantitative myocardial contrast echocardiography (MCE) [47, 48]. The limitation that is beyond a critical level of LV filling pressure >27 mmHg, $P_{occl}$ is determined solely by this transmural force and no longer by collateral driving pressure (waterfall mechanism), applies in acute myocardial infarction [49]. Currently, pressure-derived CFI measurement is the gold standard for collateral assessment. In a strict sense, sufficient collaterals have been defined as those preventing signs of myocardial ischemia in the very sensitive intracoronary ECG during coronary (balloon) occlusion [50, 51]. In this context, a pressure-derived CFI ≥ 0.217 best detects sufficient collateral supply [52]. In other words, a collateral supply amounting to more than 22 % of normal antegrade flow during epicardial coronary patency is sufficient to prevent myocardial ischemia under resting conditions, a finding supported by a study performed with single photon emission tomography among patients with acute myocardial infarction before revascularization [53].

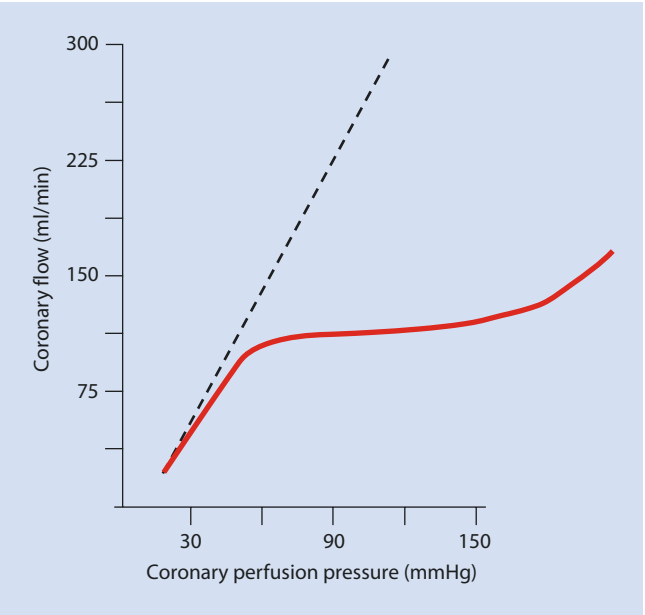


**Fig. 5.8** Schematic illustration of autoregulation of coronary blood flow, which is constant at around 1 ml/min over a wide range of perfusion pressures (*red line*). During the state of maximum microcirculatory vasodilation (*broken line*), i.e., minimum resistance, coronary flow varies directly with varying perfusion pressures

## 5.5 Influence of Coronary Collateral Function on Hemodynamic Stenosis Measurement Using Fractional Flow Reserve

The abovementioned principle of coronary flow autoregulation is tightly related to the role of the microcirculatory resistance, and it is defined as the maintenance of resting myocardial perfusion (1 ml/min/g) under perfusion pressure challenges over a wide range of 50–150 mmHg (Fig. 5.8) [18, 54]. Autoregulation of coronary flow can be entirely inhibited by inducing constant minimal microcirculatory resistance during maximal myocardial hyperemia. This is achieved in response to a brief and systematically applied episode of maximal ischemia, by physical exercise, cold pressor test, and various pharmacological substances such as acetylcholine, adenosine, dipyridamole, dobutamine, and papaverine. During inactivation of the coronary microcirculatory vasomotor function, coronary flow or perfusion changes are directly reflected by coronary perfusion pressure changes (Fig. 5.8) [18]. Accordingly, Ohm's physical law ($\Delta P = R \bullet Q$; see above) is practically applied to the coronary circulation. Indeed, it is the basis of nearly all clinical coronary invasive measurements for the assessment of the hemodynamic severity of stenotic lesion(s). This is the case despite several theoretical shortcomings of Ohm's law in the presence of a fluid such as blood instead of water; that is, the viscosity of water remains constant despite augmenting shear rate at the inner vascular surface while blood viscosity increases. This non-Newtonian behavior of blood has an overproportional influence of flow increase on endothelial activation and on microvascular resistance.

Currently, the pressure-derived, hyperemic ratio of mean coronary pressure distal to the stenosis ($P_d$) divided by mean aortic pressure ($P_{ao}$) during adenosine infusion at 140 µg/kg/min (fractional flow reserve, FFR) is regarded standard for the invasive coronary stenosis severity assessment (Fig. 5.9) [55, 56]. It is based on the above-described theoretical framework involving Ohm's law and the need for maximal hyperemia for inhibition of coronary autoregulation. FFR measurement of intermediate coronary stenoses is recommended by guidelines when demonstration of ischemia by noninvasive testing is unavailable [57]. Notwithstanding, visual angiographic stenosis assessment of percent diameter reduction as the decisional basis for or against revascularization continues to be the far predominant method [58]. Technically and in the context of the robust coronary pressure recordings, $P_d$ and simultaneous $P_{ao}$ are simple to acquire, and the induction of hyperemia using intravenous adenosine is safe. It is likely that the low acceptance rate of FFR in clinical routine is rather related to the small effort required in addition to angiography than to its theoretical shortcomings, which are now outlined.

In two of the studies importantly contributing to the mentioned guideline recommendation [57], FFR is defined as "maximal blood flow in a stenotic artery to normal maximal flow" [59], and an FFR ≤ 0.80 is described as "a drop in maximal blood flow of 20 % or more caused by stenosis", respectively [60]. The two FFR definitions are consistent, and they both point to the relevant variables "blood

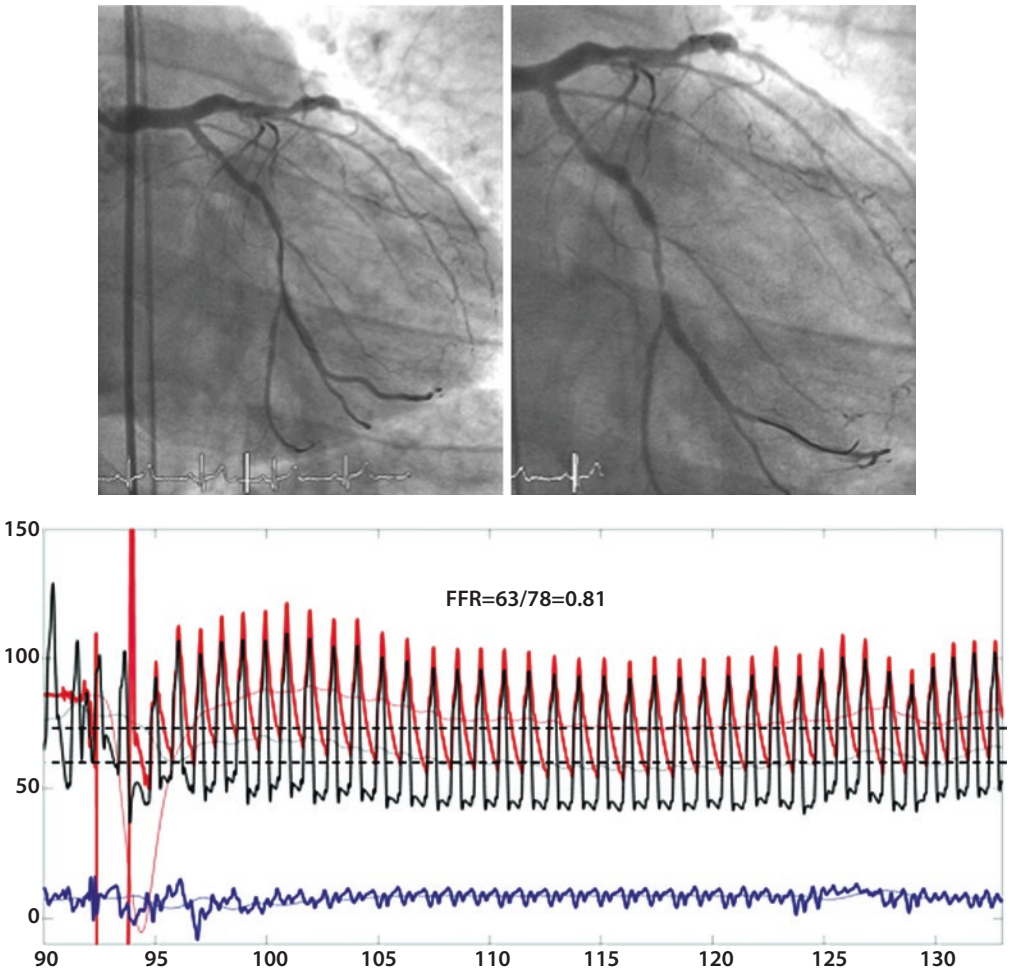


**Fig. 5.9** Angiogram of the left coronary artery with serial stenoses of the left circumflex artery (*upper panels*). The pressure sensor wire (location of the sensor at the junction between the light and the opaque part of the wire) is first positioned proximal to the tightest stenosis (*left upper panel*), and then distal to it (*right upper panel*). The pressure tracings (*lower panel*) are recorded with the pressure sensor distal to the stenoses (wire tip in the marginal branch). The following phasic and mean pressures are recorded simultaneously: Aortic pressure, $P_{ao}$ (mean) in red, coronary pressure distal to the stenoses in *black* ($P_d$), central venous pressure in *blue* (CVP). Fractional flow reserve (*FFR*) is taken as the steady state minimum ratio of $P_d/P_{ao}$ (*broken lines*) over several cardiac cycles

flow," "maximal blood flow," and "stenosis." According to Ohm's law, coronary pressure $P_d$ can be taken for flow Q only under the necessary condition of a constant and minimal microcirculatory resistance $R$: $\Delta P = R \times Q$. It is debatable whether $R$ is constant and minimal using standard hyperemia induction with intravenous adenosine. Therefore, the term "flow" and the adjective "maximal" are subject to error.

The case shown in Fig. 5.10 of a balloon-occluded ostial stenosis of the right coronary artery with simultaneously obtained FFR = 0.83 indicates that also the term "stenosis" in the above description of FFR is a misnomer (Fig. 5.10). FFR in the situation of a total coronary occlusion would be expected below the "ischemic" detection threshold of 0.80, and it is only the angiographically depicted collateral supply from the left circumflex coronary artery, which can explain a "compensation" of a low FFR caused by the *occlusion*. Indeed, FFR as recorded in the catheterization laboratory for stenosis assessment is not a stenosis-specific but a *myocardial* hemodynamic parameter:

$FFR = FFR_S + CFI$ [55], where $FFR_S$ is the stenosis-specific FFR and CFI (collateral flow index) is the above-outlined parameter of collateral function as determined during a 1-min coronary balloon occlusion [45]. The formerly cited description of FFR [59] implies that the contribution of functional anastomoses between the coronary territories (collateral circulation) is negligible. The case shown in Fig. 5.10 contradicts the assumption of nonfunctional anastomoses. Furthermore, immediately postocclusive hyperemia would be different from adenosine-induced hyperemia depending on the function of collaterals to the occluded vessel. Figure 5.11 depicts a case without functional collaterals showing a lower postischemic than adenosine-induced hyperemic FFR (Fig. 5.11). The difference in FFR between the two types of hyperemia induction is directly related to CFI as obtained during a systematic 1-min proximal coronary balloon occlusion (Fig. 5.12). The direct and stenosis-mitigating influence of CFI on FFR leave it open whether the survival benefit of patients deferred for PCI on the

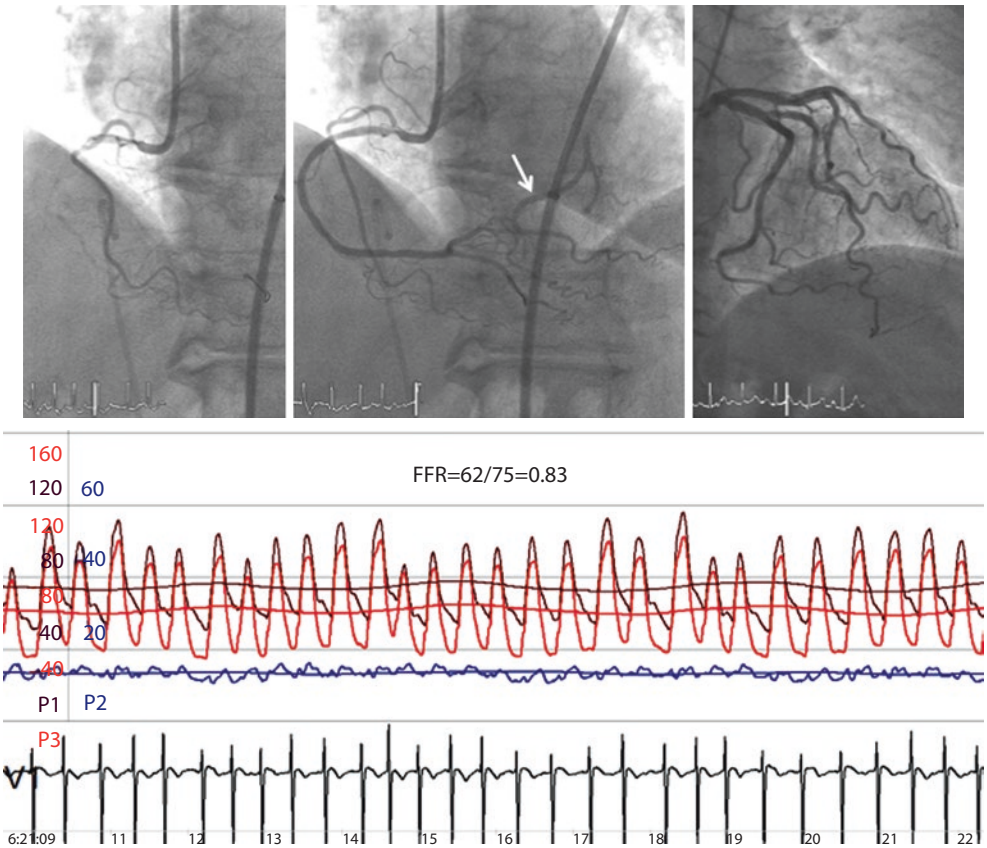


**Fig. 5.10** Coronary angiograms of the balloon-occluded right coronary artery (RCA, *left upper panel*) of the patent RCA with an ostial stenosis (*mid upper panel*) and showing part of the distal left circumflex coronary artery (*arrow*); the upper right panel depicts a left coronary angiogram with an identical trace of the distal left circumflex artery as shown in the mid upper panel. The pressure and ECG tracings are recorded during ostial RCA balloon occlusion: mean ($P_{ao}$) and phasic aortic pressure in *black*, mean ($P_{occl}$) and phasic coronary occlusive pressure in *red*, central venous pressure (CVP) in *blue*, intracoronary ECG in *black*. FFR: fractional flow reserve as $P_{occl}/P_{ao}$

basis of FFR > 0.80 (FAME1 trial [59]) is due to the insignificance of the untouched stenosis or to the protective effect of the collateral circulation [28]. This uncertainty does, however, not contradict the recommendation of FFR measurement as invasive ischemia test in the absence of noninvasive testing. Its purpose is sorting out the coronary stenosis in which *no* PCI has to be performed. Conversely, in hemodynamically relevant stenosis (FFR ≤ 0.80) PCI should be proven superior to medical therapy among patients with chronic CAD. This was the aim of the a cited FAME2 study [60]; its only positive finding of a 4.0 % rate during 2 years in urgent revascularization in the PCI group vs. 16.3 % in the medical group ($p < 0.0001$) cannot be interpreted as PCI efficiency, but as self-fulfilling prophecy keeping in mind that the study was designed open label and the FFR threshold for ischemia ≤0.80 was well accepted beforehand. In this setting, the physician of a patient in the medical group with chest discomfort was overly motivated for urgent referral for PCI. In other words, there was a bias by study design in favor of urgent revascularization in the medical group by omitting PCI at study inclusion.

## 5.6 Conclusions

Remodeling or arteriogenesis of the coronary circulation describes the structural transformation of the coronary arterial tree with its native vascular branches and anastomoses in response to permanently altering flow conditions. Vasculogenesis occurs during embryologic development of the circulatory system and is the de novo formation of blood vessels from endothelial precursor cells, which migrate and differentiate in response to local signals. New vessels can subsequently develop from the preexisting plexus by sprouting and intussusception. This formation of new vessels is defined as angiogenesis. The basic physiologic and physical principles operative in the coronary circulation in general also apply to its anastomoses, i.e., the collateral arteries and arterioles. A well-developed coronary collateral circulation is beneficial by reducing all-cause mortality. The coronary collateral circulation is functionally assessed by collateral flow index (CFI) measurement, i.e., the ratio of simultaneously obtained mean coronary occlusive and mean aortic pressure both subtracted by central venous pressure. CFI directly interferes with the hemodynamic relevance of a coronary stenosis by mitigating its significance.

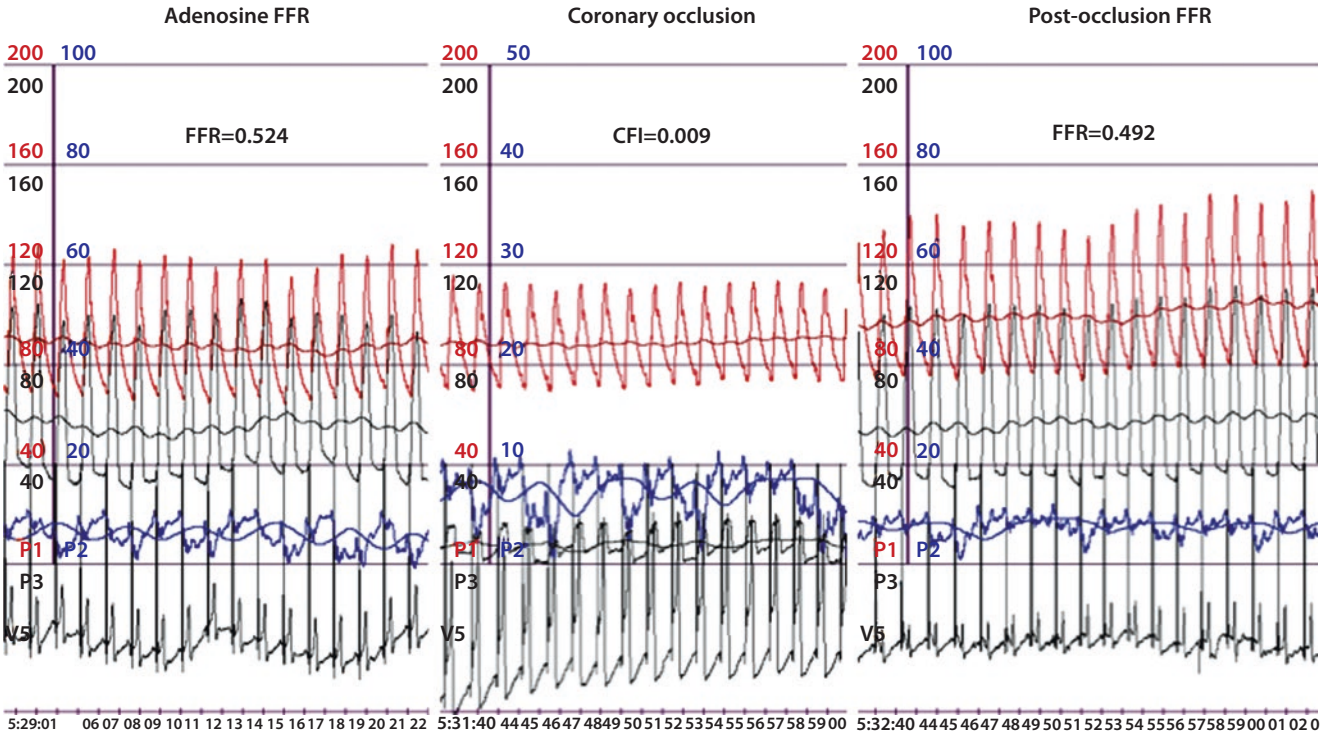


**Fig. 5.11** Simultaneous recordings of phasic and mean aortic ($P_{ao}$ for mean pressure in *red*), distal coronary ($P_d$ for mean pressure in *black*), occlusive coronary ($P_{occl}$ in *black*), and central venous pressure (CVP in *blue*), as well as an intracoronary ECG lead during different states of myocardial hyperemia (*left* and *right panel*) and during myocardial ischemia in the context of coronary balloon occlusion (*middle panel*). Abbreviations: *CFI* collateral flow index, *FFR* fractional flow reserve. During coronary occlusion, marked ECG ST-segment elevations are visible

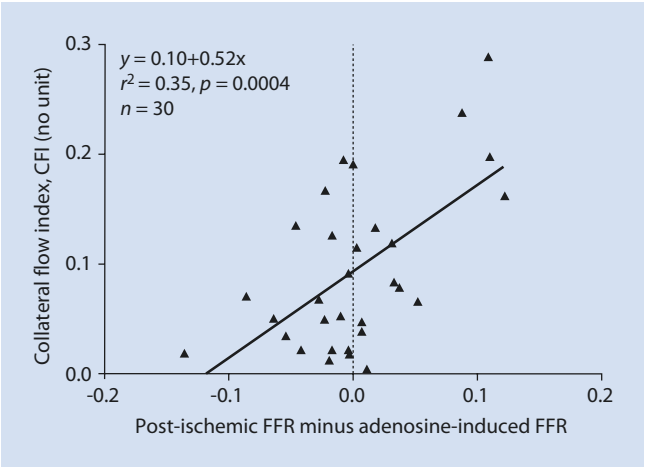


**Fig. 5.12** Relation between the fractional flow reserve (*FFR*) difference (postischemic minus adenosine-induced FFR, *x*-axis) and collateral flow index as obtained in the same vessel (*y*-axis)

## References

1. WHO. Global status report on noncommunicable diseases 2010. Geneva: World Health Organization; 2011.
2. WHO. Global atlas on cardiovascular disease prevention and control. Geneva: World Health Organization; 2011.
3. Habib GB, Heibig J, Forman SA, Brown BG, Roberts R, Terrin ML, Bolli R. Influence of coronary collateral vessels on myocardial infarct size in humans. Results of phase i thrombolysis in myocardial infarction (timi) trial. The timi investigators. Circulation. 1991;83:739–46.
4. Maroko PR, Kjekshus JK, Sobel BE, Watanabe T, Covell JW, Ross JJ, Braunwald E. Factors influencing infarct size following experimental coronary artery occlusions. Circulation. 1971;43:67–82.
5. Reimer KA, Ideker RE, Jennings RB. Effect of coronary occlusion site on ischaemic bed size and collateral blood flow in dogs. Cardiovasc Res. 1981;15:668–74.
6. Brownlee RD, Langille BL. Arterial adaptions to altered blood flow. Can J Physiol Pharmacol. 1991;69:978–83.
7. Hoefer IE, van Royen N, Buschmann IR, Piek JJ, Schaper W. Time course of arteriogenesis following femoral artery occlusion in the rabbit. Cardiovasc Res. 2001;49:609–17.

8. Ito WD, Arras M, Winkler B, Scholz D, Htun P, Schaper W. Angiogenesis but not collateral growth is associated with ischemia after femoral artery occlusion. Am J Physiol. 1997;273:H1255–65.
9. Arras M, Wulf DI, Scholz D, Winkler B, Schaper J, Schaper W. Monocyte activation in angiogenesis and collateral growth in the rabbit hindlimb. J Clin Invest. 1998;101:40–50.
10. Faber JE, Chilian WM, Deindl E, van Royen N, Simons M. A brief etymology of the collateral circulation. Arterioscler Thromb Vasc Biol. 2014;34:1854–9.
11. Reiner L, Molnar J, Jimenez F, Freudenthal R. Interarterial coronary anastomoses in neonates. Arch Pathol. 1961;71:103–12.
12. Fischer C, Schneider M, Carmeliet P. Principles and therapeutic implications of angiogenesis, vasculogenesis and arteriogenesis. Handb Exp Pharmacol. 2006;176:157–212.
13. Risau W. Mechanisms of angiogenesis. Nature. 1997;386:671–4.
14. Seiler C. Assessment and impact of the human coronary collateral circulation on myocardial ischemia and outcome. Circ Cardiovasc Interv. 2013;6:719–28.
15. Seiler C, Kirkeeide RL, Gould KL. Basic structure-function relations of the epicardial coronary vascular tree. Basis of quantitative coronary arteriography for diffuse coronary artery disease. Circulation. 1992;85:1987–2003.
16. Bergmann SR, Herrero P, Markham J, Weinheimer CJ, Walsh MN. Noninvasive quantitation of myocardial blood flow in human subjects with oxygen-15-labeled water and positron emission tomography. J Am Coll Cardiol. 1989;14:639–52.
17. Seiler C, Kirkeeide RL, Gould KL. Measurement from arteriograms of regional myocardial bed size distal to any point in the coronary vascular tree for assessing anatomic area at risk. J Am Coll Cardiol. 1993;21:783–97.
18. Westerhof N, Boer C, Lamberts RR, Sipkema P. Cross-talk between cardiac muscle and coronary vasculature. Physiol Rev. 2006;86:1263–308.
19. Schaper W, Ito WD. Molecular mechanisms of coronary collateral vessel growth. Circ Res. 1996;79:911–9.
20. Schaper W, Scholz D. Factors regulating arteriogenesis. Arterioscler Thromb Vasc Biol. 2003;23:1143–51.
21. Pohl T, Seiler C, Billinger M, Herren E, Wustmann K, Mehta H, Windecker S, Eberli FR, Meier B. Frequency distribution of collateral flow and factors influencing collateral channel development. Functional collateral channel measurement in 450 patients with coronary artery disease. J Am Coll Cardiol. 2001;38:1872–8.
22. Kinnaird T, Stabile E, Zbinden S, Burnett MS, Epstein SE. Cardiovascular risk factors impair native collateral development and may impair efficacy of therapeutic interventions. Cardiovasc Res. 2008;78:257–64.
23. Chalothorn D, Faber JE. Formation and maturation of the native cerebral collateral circulation. J Mol Cell Cardiol. 2010;49:251–9.
24. Eitenmuller I, Volger O, Kluge A, Troidl K, Barancik M, Cai WJ, Heil M, Pipp F, Fischer S, Horrevoets AJ, Schmitz-Rixen T, Schaper W. The range of adaptation by collateral vessels after femoral artery occlusion. Circ Res. 2006;99:656–62.
25. Scholz D, Ziegelhoeffer T, Helisch A, Wagner S, Friedrich C, Podzuweit T, Schaper W. Contribution of arteriogenesis and angiogenesis to postocclusive hindlimb perfusion in mice. J Mol Cell Cardiol. 2002;34:775–87.
26. Heil M, Schaper W. Influence of mechanical, cellular, and molecular factors on collateral artery growth (arteriogenesis). Circ Res. 2004;95:449–58.
27. Vogel R, Traupe T, Steiger VS, Seiler C. Physical coronary arteriogenesis: a human "model" of collateral growth promotion. Trends Cardiovasc Med. 2010;20:129–33.
28. Meier P, Hemingway H, Lansky AJ, Knapp G, Pitt B, Seiler C. The impact of the coronary collateral circulation on mortality: a meta-analysis. Eur Heart J. 2012;33:614–21.
29. Seiler C, Engler R, Berner L, Stoller M, Meier P, Steck H, Traupe T. Prognostic relevance of coronary collateral function: confounded or causal relationship? Heart. 2013;99:1408–14.
30. Koerselman J, de Jaegere PP, Verhaar MC, Grobbee DE, van der Graaf Y. Prognostic significance of coronary collaterals in patients with coronary heart disease having percutaneous transluminal coronary angioplasty. Am J Cardiol. 2005;96:390–4.
31. Seiler C, Pohl T, Lipp E, Hutter D, Meier B. Regional left ventricular function during transient coronary occlusion: relation with coronary collateral flow. Heart. 2002;88:35–42.
32. Lee CW, Park SW, Cho GY, Hong MK, Kim JJ, Kang DH, Song JK, Lee HJ, Park SJ. Pressure-derived fractional collateral blood flow: a primary determinant of left ventricular recovery after reperfused acute myocardial infarction. J Am Coll Cardiol. 2000;35:949–55.
33. Waldecker B, Waas W, Haberbosch W, Voss R, Wiecha J, Tillmanns H. Prevalence and significance of coronary collateral circulation in patients with acute myocardial infarct. Z Kardiol. 2002;91:243–8.
34. Meier P, Gloekler S, de Marchi SF, Zbinden R, Delacretaz E, Seiler C. An indicator of sudden cardiac death during brief coronary occlusion: Electrocardiogram qt time and the role of collaterals. Eur Heart J. 2010;31:1197–204.
35. Chareonthaitawee P, Gersh BJ, Araoz PA, Gibbons RJ. Revascularization in severe left ventricular dysfunction: the role of viability testing. J Am Coll Cardiol. 2005;46:567–74.
36. Choi JH, Chang SA, Choi JO, Song YB, Hahn JY, Choi SH, Lee SC, Lee SH, Oh JK, Choe Y, Gwon HC. Frequency of myocardial infarction and its relationship to angiographic collateral flow in territories supplied by chronically occluded coronary arteries. Circulation. 2013;127:703–9.
37. Werner GS, Ferrari M, Betge S, Gastmann O, Richartz BM, Figulla HR. Collateral function in chronic total coronary occlusions is related to regional myocardial function and duration of occlusion. Circulation. 2001;104:2784–90.
38. Traupe T, Gloekler S, de Marchi SF, Werner GS, Seiler C. Assessment of the human coronary collateral circulation. Circulation. 2010;122:1210–20.
39. Demer LL, Gould KL, Goldstein RA, Kirkeeide RL. Noninvasive assessment of coronary collaterals in man by pet perfusion imaging. J Nucl Med. 1990;31:259–70.
40. Seiler C. Collateral circulation of the heart. London: Springer; 2009.
41. Rentrop K, Cohen M, Blanke H, Phillips R. Changes in collateral channel filling immediately after controlled coronary artery occlusion by an angioplasty balloon in human subjects. J Am Coll Cardiol. 1985;5:587–92.
42. Rentrop K, Thornton J, Feit F, Van Buskirk M. Determinants and protective potential of coronary arterial collaterals as assessed by an angioplasty model. Am J Cardiol. 1988;61:677–84.
43. Piek JJ, van Liebergen RA, Koch KT, Peters RJ, David GK. Clinical, angiographic and hemodynamic predictors of recruitable collateral flow assessed during balloon angioplasty coronary occlusion. J Am Coll Cardiol. 1997;29:275–82.
44. Seiler C, Billinger M, Fleisch M, Meier B. Washout collaterometry: a new method of assessing collaterals using angiographic contrast clearance during coronary occlusion. Heart. 2001;86:540–6.
45. Seiler C, Fleisch M, Garachemani A, Meier B. Coronary collateral quantitation in patients with coronary artery disease using intravascular flow velocity or pressure measurements. J Am Coll Cardiol. 1998;32:1272–9.
46. Gloekler S, Traupe T, Meier P, Steck H, de Marchi SF, Seiler C. Safety of diagnostic balloon occlusion in normal coronary arteries. Am J Cardiol. 2010;105:1716–22.
47. Matsuo H, Watanabe S, Kadosaki T, Yamaki T, Tanaka S, Miyata S, Segawa T, Matsuno Y, Tomita M, Fujiwara H. Validation of collateral fractional flow reserve by myocardial perfusion imaging. Circulation. 2002;105:1060–5.
48. Vogel R, Zbinden R, Indermuhle A, Windecker S, Meier B, Seiler C. Collateral-flow measurements in humans by myocardial contrast echocardiography: validation of coronary pressure-derived collateral-flow assessment. Eur Heart J. 2006;27:157–65.

49. de Marchi S, Oswald P, Windecker S, Meier B, Seiler C. Reciprocal relationship between left ventricular filling pressure and the recruitable human coronary collateral circulation. Eur Heart J. 2005;26:558–66.
50. Friedman P, Shook T, Kirshenbaum J, Selwyn A, Ganz P. Value of the intracoronary electrocardiogram to monitor myocardial ischemia during percutaneous transluminal coronary angioplasty. Circulation. 1986;74:330–9.
51. de Marchi S, Meier P, Oswald P, Seiler C. Variable ECG signs of ischemia during controlled occlusion of the left and right coronary artery in humans. Am J Physiol. 2006;291:H351–6.
52. de Marchi SF, Streuli S, Haefeli P, Gloekler S, Traupe T, Warncke C, Rimoldi SF, Stortecky S, Steck H, Seiler C. Determinants of prognostically relevant intracoronary electrocardiogram ST-segment shift during coronary balloon occlusion. Am J Cardiol. 2012;110:1234–9.
53. Christian T, Berger PB OCM, Hodge DO, Gibbons RJ. Threshold values for preserved viability with a noninvasive measurement of collateral blood flow during acute myocardial infarction treated by direct coronary angioplasty. 1999;100(24):2392–5.
54. de Marchi SF, Gloekler S, Rimoldi SF, Rölli P, Steck H, Seiler C. Microvascular response to metabolic and pressure challenge in the human coronary circulation. Am J Physiol Heart Circ Physiol. 2011;301:H434–41.
55. Pijls NHJ, van Son JAM, Kirkeeide RL, de Bruyne B, Gould KL. Experimental basis of determining maximum coronary, myocardial, and collateral blood flow by pressure measurements for assessing functional stenosis severity before and after percutaneous coronary angioplasty. Circulation. 1993;86:1354–67.
56. Kern MJ, Lerman A, Bech JW, De Bruyne B, Eeckhout E, Fearon WF, Higano ST, Lim MJ, Meuwissen M, Piek JJ, Pijls NH, Siebes M, Spaan JA; CoCC AHACoDaICC. Physiological assessment of coronary artery disease in the cardiac catheterization laboratory: a scientific statement from the american heart association committee on diagnostic and interventional cardiac catheterization, council on clinical cardiology. Circulation. 2006;114:1321–41.
57. Windecker S, Kolh P, Alfonso F, Collet JP, Cremer J, Falk V, Filippatos G, Hamm C, Head SJ, Jüni P, Kappetein AP, Kastrati A, Knuuti J, Landmesser U, Laufer G, Neumann FJ, Richter DJ, Schauerte P, Sousa UM, Stefanini GG, Taggart DP, Torracca L, Valgimigli M, Wijns W, Witkowski A. 2014 ESC/EACTS guidelines on myocardial revascularization: the task force on myocardial revascularization of the European Society of Cardiology (ESC) and the European Association for Cardio-Thoracic Surgery (EACTS) developed with the special contribution of the European Association of Percutaneous Cardiovascular Interventions (EAPCI). Eur Heart J. 2014;35:2541–619.
58. Toth GG, Toth B, Johnson NP, De Vroey F, Di Serafino L, Pyxaras S, Rusinaru D, Di Gioia G, Pellicano M, Barbato E, Van Mieghem C, Heyndrickx GR, De Bruyne B, Wijns W. Revascularization decisions in patients with stable angina and intermediate lesions: results of the international survey on interventional strategy. Circ Cardiovasc Interv. 2014;7:751–9.
59. Tonino PA, De Bruyne B, Pijls NH, Siebert U, Ikeno F, van't Veer M, Klauss V, Manoharan G, Engstrøm T, Oldroyd KG, Ver Lee PN, MacCarthy PA, Fearon WF; Investigators FS. Fractional flow reserve versus angiography for guiding percutaneous coronary intervention. N Engl J Med. 2009;360:213–24.
60. De Bruyne B, Fearon WF, Pijls NH, Barbato E, Tonino P, Piroth Z, Jagic N, Mobius-Winckler S, Rioufol G, Witt N, Kala P, MacCarthy P, Engström T, Oldroyd K, Mavromatis K, Manoharan G, Verlee P, Frobert O, Curzen N, Johnson JB, Limacher A, Nüesch E, Jüni P; Investigators FT. Fractional flow reserve-guided PCI for stable coronary artery disease. N Engl J Med. 2014;371:1208–17.

# The Epicardial Vessels and the Coronary Microcirculation in Different Pathologies

Contents

# The Effect of Cardiovascular Risk Factors on the Coronary Circulation

## Effects of Cardiovascular Risk Factors on Coronary Circulation: Hypertension, Diabetes, Dyslipidemia

*Luis Felipe Valenzuela-García, Yasushi Matsuzawa, and Amir Lerman*




J. Escaned, J. Davies (eds.), *Physiological Assessment of Coronary Stenoses and the Microcirculation*,
DOI 10.1007/978-1-4471-5245-3_6

## 6.1 Abbreviations

| | |
|---|---|
| ADMA | Asymmetric dimethylarginine |
| Ach | Acetylcholine |
| CAD | Coronary artery disease |
| CBF | Coronary blood flow |
| CFR | Coronary flow reserve |
| CHD | Coronary heart disease |
| CMD | Coronary microvascular dysfunction |
| CV | Cardiovascular |
| CVRF | Cardiovascular risk factors |
| ED | Endothelial dysfunction |
| EDCF | Endothelium-derived contracting factor |
| EDRF | Endothelium-derived relaxing factor |
| EF | Endothelial function |
| eNOS | Endothelial nitric oxide synthase |
| FMD | Flow-mediated vasodilation |
| LVH | Left ventricular hypertrophy |
| MBF | Myocardial blood flow |
| NO | Nitric oxide |
| RH-PAT | Reactive hyperemia-peripheral artery tonometry |
| ROS | Reactive oxygen species |



## 6.2 From Traditional Risk Factors to a More Personalized Medicine

The atherosclerotic plaque and its limitation to normal coronary blood flow (CBF) constitute the more evident effect of traditional cardiovascular risk factors (CVRF) on the endothelium of epicardial coronary arteries. However, at an early stage, CVRF may cause coronary microvascular dysfunction (CMD) prior to any plaque development through both an endothelial-dependent and endothelial-independent mechanism. Clinical studies have shown that in patients without known risk factors for coronary artery disease (CAD), intracoronary infusion of acetylcholine (Ach, an endothelium-dependent vascular relaxant) vasodilate normal epicardial and coronary microvascular arteries, while in patients with traditional and nontraditional CVRF, the same agent failed to dilate and even mediated vasoconstriction (reflecting the effect of muscarinic vascular smooth muscle contraction), even in the absence of angiographically detectable atherosclerotic lesions [1]. This paradoxical effect is the result of endothelial dysfunction (ED). Since endothelium flow-related regulation is present in small resistance arterioles up to 100–200 μ [2, 3], coronary microvascular ED can be assessed after intracoronary infusion of Ach, by measuring the epicardial vessel diameter and velocity through a Doppler wire to calculate CBF [4]. Moreover, there is evidence of a longitudinal gradient for endothelium-dependent and endothelium-independent vascular responses in the coronary microcirculation [2, 3]. Adenosine increases blood flow in the coronary microcirculation, mostly by non-endothelial-dependent mechanisms predominant in arterioles less than 100 μm [3, 5], via receptors on microvascular smooth muscle cells that modulate intracellular calcium [6]. Therefore, when the vasodilator stimulus is through intracoronary adenosine (bolus or infusion), an essentially endothelial-independent coronary flow reserve (CFR) can be quantified measuring velocity through a Doppler wire [4]. Remarkably, the intravenous infusion of adenosine as used in less invasive methods to assess CFR is unable to localize the relative contribution of ED to the CMD since it mediates an increase in myocardial oxygen demand (significantly decreasing arterial pressure and increasing heart rate) [7] and therefore increases CBF flow by both endothelium-dependent and non-endothelium-dependent mechanisms. During the last decade, most of the evidence on the effect of CVRF over the coronary microcirculation comes from studies performed with less invasive methods using intravenous adenosine infusion. To minimize confussion we will include these studies under the title "non-endothelium-dependent coronary microvascular dysfunction." However, at present, the most definite evaluation of the coronary microcirculation remains invasive in nature [3] allowing us to precisely address the contribution of endothelial-dependent and endothelial-independent mechanisms on CMD. This is an important concept since in acccordance to previous reports, there is conflicting evidence of the predictive value of CFR for CV events; however, the predictive value of epicardial and microvascular ED in predicting major CV events is well established [8–10].

Endothelial dysfunction (ED) is a predominantly functional first manifestation of atherosclerosis, but it is also important in the pathogenesis of atherosclerosis because it contributes to the initiation and evolution of prothrombotic, proinflammatory and proliferative states. ED is associated with unfavorable physiological vascular changes such as vasomotor tone alterations, thrombotic dysfunctions, smooth muscle cell proliferation and migration, as well as leukocyte adhesion [11]. Its development precedes vascular morphological changes and occurrence of atherosclerotic complications [12]. Most traditional CVRFs have the potential to initiate endothelial cell injury and abnormal repair causing ED [13]. However, many individuals with coronary heart disease (CHD) have only one, if any of the classic CVRFs which taken together are thought to account for only 50 % of CHD [14], indicating the existence of nontraditional risk factors for atherosclerosis. Moreover, there is a notable interindividual heterogeneity in response to CVRFs, also affecting cardiovascular drug efficacy. For example, considerable residual risk persists among patients treated with even maximal dose of statins. Approximately 22 % of patients acute coronary syndrome (ACS) and 9 % of patients with stable CHD proceeded to second cardiovascular events during 2-year and 5-year of follow-up period, respectively [15, 16]. Thus, the current non-individualized patient-specific approach may have limitations derived from the insufficiency of CVRF to accurately identify individual risk or etiologic causes of atherosclerosis.

Invasive assessment of coronary endothelial function by catheterization is considered the reference standard for evaluating coronary microvascular dysfunction (CMD) [4], but

its invasive nature precludes its widespread use in the population. Based on the systemic nature of ED [17], basically two peripheral noninvasive techniques, brachial artery flow-mediated vasodilation (FMD) and reactive hyperemia-peripheral arterial tonometry (RH-PAT), have been developed, and both are based on the same principle of reactive hyperemia. There is conflicting evidence about the relationship between endothelial function (EF) in the coronary and brachial arteries [18, 19], and considering the different physiological role of conduit and resistance arteries, important differences should be considered. Whereas reduced NO activity in response to stimuli plays a central role in the pathophysiology of ED in the conduit arteries, NO in the microcirculation may primarily modulate tissue metabolism. Since metabolic and other factors are becoming increasingly important in the regulation of microvascular function, pharmacologic tests inducing NO release might not reflect the full physiologic adaption of microvascular EF in response to exercise or ischemia. Furthermore, brachial FMD is particularly sensitive to being impaired by traditional risk factors (e.g., age, hypertension), whereas fingertip RH-PAT index (RHI) that reflects smaller vessels is more sensitive to metabolic risk factors, especially body mass index and diabetes mellitus. Micro- and macrovascular dysfunction could also reflect different stages of vascular disease as conduit artery ED may be more important in patients with existing atherosclerosis and microvascular dysfunction may be an earlier indicator of risk. The fact that micro- and macrovascular EF only show a moderate correlation with each other should raise caution against the extrapolation of findings in one circulation level to the other and argue for the integration of the methods [20].

In summary, direct assessment of vascular injury by measuring EF rather than risk factor estimation could be a reliable method to identify the functional significance of CVRF in a more personalized approach to individual patient risk. Moreover, ED may be regarded as an integrated index of all atherogenic and atheroprotective factors present in an individual, including unknown factors and genetic predisposition [21]. Thus, it can be a potentially useful clinical strategy to consider EF in the assessment of atherosclerosis and the vulnerability of the patients not only to prevent atherosclerotic complications but also to determine the efficacy of current ongoing and future therapeutic options. Targeting and treating ED would be treating atherosclerosis itself.

## 6.3 Molecular Basis of Endothelial Dysfunction in Vascular Disease

Endothelial dysfunction (ED) results essentially from a loss of nitric oxide (NO) activity that may be secondary to inability of the endothelium to generate adequate amounts of bioactive NO or an increase in the degradation of NO. The most relevant physiological effects of NO on the vascular wall are summarized in Table 6.1. The earliest detectable manifestation of atherosclerosis is a decrease in the bioavailability of NO in response to physiological, pharmacologic, or hemodynamic stimuli [22]. The result is an impairment of NO-mediated vasodilation but also an impairment of its anti-inflammatory and anticoagulant properties [23–26].

**Table 6.1** Nitric oxide vascular functions

| |
|---|
| Regulating vascular tone |
| Relaxing vascular smooth muscle cells |
| Inhibiting endothelin-1 production |
| Anti-inflammatory atheroprotective |
| Inhibiting LDL oxidation and lipid entry into the arterial intima |
| Inhibiting leukocyte adhesion |
| Inhibiting smooth cells proliferation |
| Antithrombotic |
| Inhibiting platelet adhesion |
| Inhibiting platelet aggregation |
| Adaptive remodeling to chronic changes in flow |
| Angiogenesis |
| Reparative (activation of endothelial progenitor cells) |

A decrease in the bioavailability of NO is largely considered to be the central mechanism for ED, even though other endothelium-derived relaxing (EDRF) or contracting factors (EDCF) may be also involved. Classically, the term EDRF referred mainly to NO; however, it has been recognized that there are several types of EDRFs, including NO, PGI2, and the endothelium-derived hyperpolarizing factor (EDHF). Each EDRF induces the relaxation of proximal vascular smooth muscle cells through its own pathway [27] (Fig. 6.1).

Nitric oxide is produced by three isoforms of NO synthase, and one of them is located in the endothelium: endothelial nitric oxide synthase (eNOS). All NOS utilize L-arginine and molecular oxygen as substrates and require cofactors: reduced nicotinamide adenine dinucleotide phosphate (NADPH), flavin adenine dinucleotide (FAD), flavin mononucleotide (FMN), and (6*R*-) 5,6,7,8-tetrahydrobiopterin ($BH_4$). All NOS bind calmodulin and contain hem [28].

The most well-recognized mechanism of NO for vasorelaxation is the activation of soluble guanylyl cyclase (sGC) in smooth muscle cells. Activated sGC catalyses the conversion of guanosine triphosphate (GTP) to cyclic guanosine monophosphate (cGMP). cGMP directly and indirectly modulates numerous targets, including protein kinases such as protein kinase G (PKG) which is the primary downstream target of cGMP in smooth muscle cells. PKG activates the myosin light-chain phosphatase (MLCP), which dephosphorylates smooth muscle myosin, resulting in vasorelaxation [29].

Cardiovascular risk factors are associated with an increased production of reactive oxygen species (ROS) a phenomenon called oxidative stress, mainly through NADPH oxidases upregulation and uncoupled eNOS (Fig. 6.2) [28].

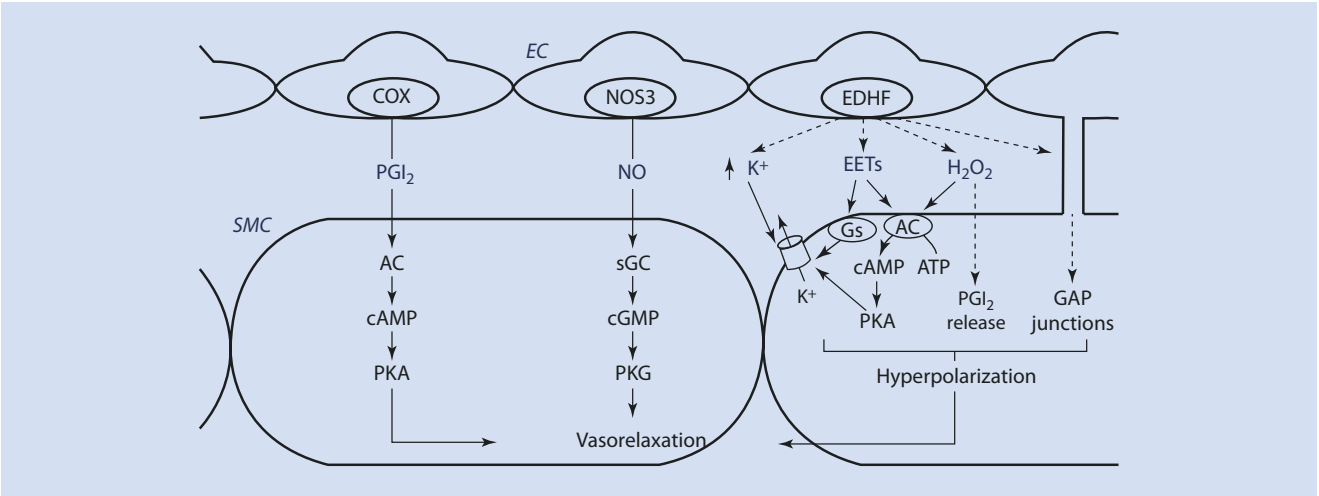


**Fig. 6.1** Small resistance arteries induce vasorelaxation via multiple vasorelaxing pathways including NOS, COX, and EDHF pathways in the normotensive condition. COX in endothelial cells produces PGI2. PGI2 can cross the membrane of endothelial cells and binds IP receptor on the plasma membrane of smooth muscle cells, which induces the activation of the adenylyl cyclase (AC)/cyclic adenosine monophosphate (cAMP)/protein kinase A (PKA) signal transduction pathway. Activated PKA phosphorylates target proteins, resulting in vasorelaxation. eNOS produces NO in response to several stimuli such as shear stress, hypoxia, and vasoactive neurotransmitters. NO activates soluble guanylyl cyclase (sGC) in smooth muscle cells. Activated sGC catalyzes the conversion of guanosine triphosphate (GTP) to cyclic guanosine monophosphate (cGMP). cGMP directly and indirectly modulates numerous targets, including protein kinases such as protein kinase G (PKG), resulting in vasorelaxation. Intercellular K+ ion, EETs, hydrogen peroxide ($H_2O_2$), and gap junctions, proposed candidates of EDHF, induce various K+ channel activation by complex mechanisms to facilitate hyperpolarization of the underlying smooth muscle cells, which results in vasorelaxation [27]

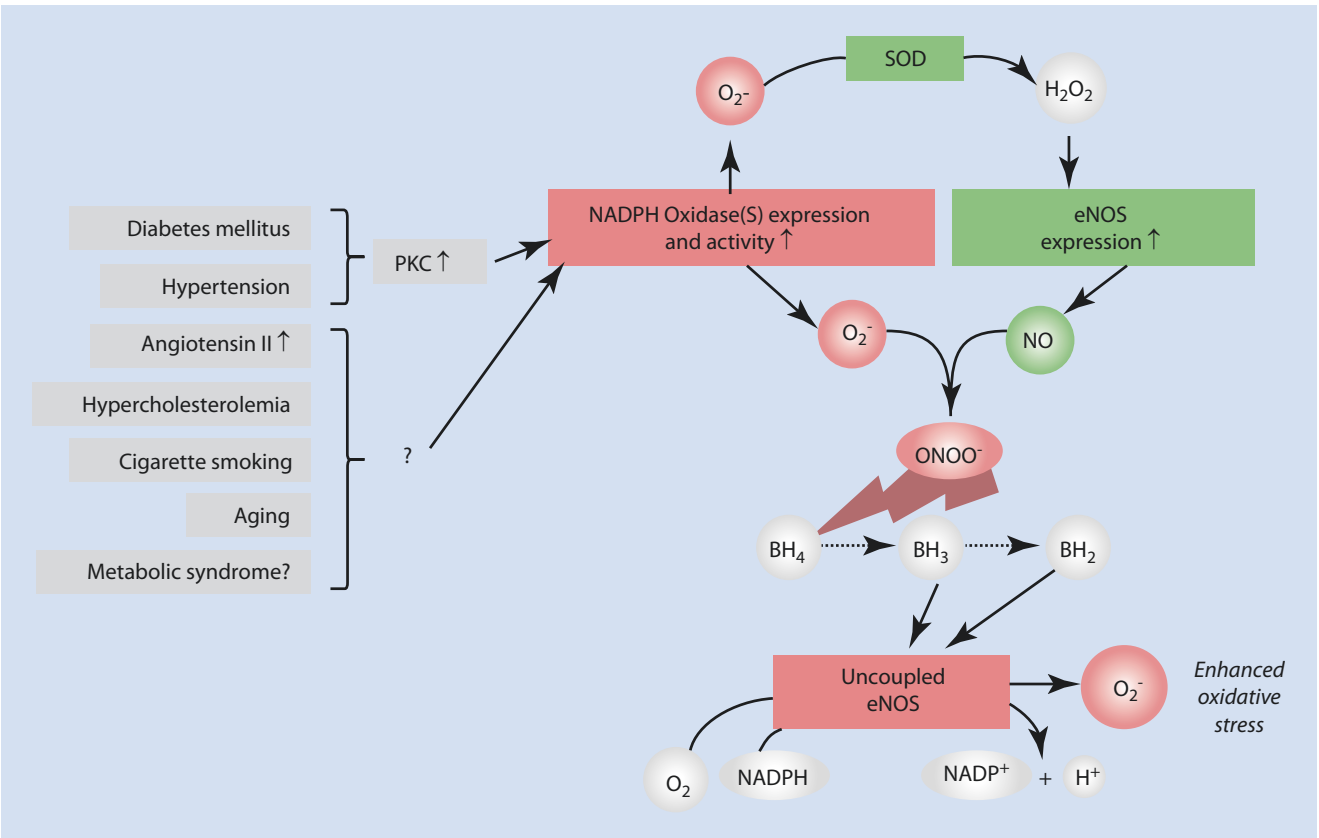


**Fig. 6.2** NADPH oxidases upregulations and eNOS overexpression are common in vascular disease. $H_2O_2$, the dismutation product of $O_2^-$, can increase eNOS expression via transcriptional and post-transcriptional mechanisms (SOD, superoxide dismutase). In addition, protein kinase C inhibitors reduce e NOS expression levels in vascular disease. The products of NADPH oxidases and eNOS, $O_2$, and NO rapidly recombine to form peroxynitrite ($ONOO^-$). This can oxidize the essential cofactor of eNOS tetrahydrobiopterin (BH4) to trihydrobiopterin radical ($BH_3$) which disproportionate to the quinonoid 6,7-[8H]-H2-biopterin (BH2). This sequence cause "eNOS uncoupling" [28]

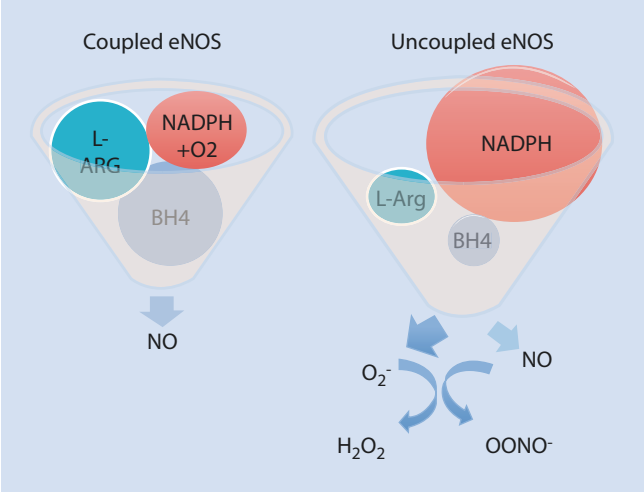


**Fig. 6.3** Nitric oxide (NO) is produced from L-arginine and molecular oxygen ($O_2$) by endothelial nitric oxide synthase (eNOS) in a "coupled" process involving tetrahydrobiopterin ($BH_4$) and nicotinamide adenine dinucleotide phosphate (NADPH). When "uncoupling" of NO production exists due to a reduction in the receptor-mediated intracellular availability of L-arginine (by oxidized LDL), an increased redox imbalance (due to increased NADH/NADPH), and/or decreased availability of $BH_4$ (due to oxidation), the result is a transference of electrons to $O_2$ to form superoxide ($O_2^-$). Superoxide in turn reacts with and consumes NO, forming the oxidant species peroxynitrite ($OONO^-$) and hydrogen peroxide

However, there are other potentially implicated enzyme systems such as xanthine oxidase and enzymes of the mitochondrial respiratory chain. Oxidative stress contributes to ED by activating protein kinase C (PKC), polyol, hexosamine, and NF kappa B pathways, as well as increasing asymmetric dimethylarginine ADMA and advanced glycation end products [30].

The NADPH oxidases are expressed in the three layers of vascular wall: endothelial and smooth muscle cells, as well as in the adventitia. In the presence of CVRF and many types of vascular disease, NADPH oxidases are upregulated in the vascular wall and generate superoxide ($O_2^-$). In experimental diabetes mellitus and angiotensin II-induced hypertension, this has been shown to be mediated by PKC [31]. Expression of eNOS is also increased in vascular disease. The dismutation product of $O_2^-$ (hydrogen peroxide, $H_2O2$) and PKC activation can both increase eNOS expression [32]. Oxidative stress will increase degradation of NO by its reaction with superoxide, but it may also convert eNOS from an NO-producing enzyme to a dysfunctional enzyme that generates superoxide. This process has been referred to as NOS uncoupling (Fig. 6.3). The enhanced endothelial NOS expression aggravates the situation. Mechanisms implicated in eNOS uncoupling include oxidation of the critical NOS cofactor $BH_4$, depletion of L-arginine, accumulation of endogenous methylarginines, and S-glutathionylation of eNOS. The products of NADPH oxidases and eNOS ($O_2^-$ and NO) rapidly recombine to form peroxynitrite ($OONO^-$) which oxidize the essential cofactor of endothelial NOS tetrahydrobiopterin ($BH_4$) to trihydrobiopterin ($BH_3$) [33] which disproportionate to the quinonoid ($BH_2$). The oxidation of $BH_4$ to biologically inactive products such as the $BH_3$ radical or $BH_2$ also reduces the affinity of the substrate L-arginine to NO, and eNOS catalyses the uncoupled reduction in O2, leading to the production of $O_2^-$, $H_2O_2$, and peroxynitrite which may result in cellular oxidative injury.

The conventional risk factors for atherosclerosis, hypertension, diabetes mellitus, and hypercholesterolemia are all associated with excess ROS. As a result, NO bioavailability is reduced and NO-mediated vasodilation is impaired. This is the situation where EDHF may play a more prominent role in agonist-induced vasodilation. Hyperpolarization of vascular smooth muscle cells may cause vasorelaxation by decreasing the opening of voltage-gated $Ca^{2+}$ channels to reduce $Ca^{2+}$ influx which results in vascular relaxation [34]. In conditions of enhanced oxidative stress where NO levels are reduced, EDHF can compensate for loss of NO-mediated vasodilation [35, 36]. There is evidence to suggest the existence of more than one EDHF within a single vessel; candidates proposed as EDHFs include $H_2O_2$, $K^+$ ion, gap junctions, and epoxyeicosatrienoic acids which are metabolites of arachidonic acid produced by the epoxygenase pathway [37].

## 6.4 Arterial Hypertension

### 6.4.1 Non-endothelium-Dependent Coronary Microvascular Dysfunction

The blunting of CFR in hypertension is associated with left ventricular hypertrophy (LVH) [38]. Impairment of CFR is transmural and correlates with systolic blood pressure. Under resting conditions subendocardial myocardial blood flow (MBF) is higher than subepicardial MBF. Consequently, CFR is lower in the subendocardium as a result of a higher baseline MBF. However, during pharmacologic stress and exercise, the coronary resistance decreases. The expected MBF increase in patients is severely impaired across the myocardium due to higher extravascular compression as compared to age- and sex-matched normal volunteers [39]. Remarkably, this transmural impairment is different to the subendocardial selective one observed in patients with aortic stenosis [38, 40].

A combination of different mechanisms contribute to the impairment of endothelial-independent CMD (CFR) in long-standing hypertension with LVH, including the increased volume of cardiomyocytes, perimyocytic fibrosis resulting in a relative rarefaction of capillaries [41], sympathetically mediated vasoconstriction [42], and arteriolar remodeling with increased wall/lumen ratio and perivascular fibrosis [43, 44].

The observed impairment of CFR and increased coronary vascular resistance in systemic hypertension could result not only from changes in the structure of coronary resistance vessels both intrinsic and secondary to the increased blood

pressure [45] but also from the effects of a "relative" and "functional" capillary rarefaction [41]. The decrease of the cross-sectional area of the resistance arterioles is paralleled by a chronic constriction to compensate the elevated perfusion pressure, which in turn leads to a dysfunctional microcirculation less responsive to vasodilator stimuli. This is somewhat different to what occurs in aortic stenosis wherein left ventricular outflow obstruction in subcoronary position protects the coronary vessels from increased pressure. It prevents arterial wall thickening, rendering subendocardial vessels more deformable and sensitive to the increased intracavitary pressure. Furthermore, if capillary density is estimated as capillary number per unit area, the density is decreased proportionally to the increase of the volume of the myocytes, and therefore, there is "relative" rarefaction rather than decrease of absolute number of capillaries. In addition, anatomically existing but underperfused vessels can cause a "functional" rarefaction.



### 6.4.2 Endothelial-Dependent Coronary Microvascular Dysfunction

Forearm circulation [46–48] and CBF [49] in response to the intra-arterial injection of ACh are reduced in patients with hypertension. Such impaired endothelium-dependent vasorelaxation has also been observed in numerous studies using hypertensive animal models. It is not clear if ED is the cause [50] or a consequence [51, 52], but there is evidence of its role in the functional abnormalities of epicardial coronary arteries [53–56] and resistance vessels [57] observed in hypertensive patients. Remarkably, arterial hypertension without established LVH has no apparent effect upon systemic ACh-induced increases in CBF in the intact human coronary circulation [56]. At this stage, ED can be confined to epicardial coronary arteries.

Small resistance arteries induce vasorelaxation via multiple vasorelaxing pathways including NOS, COX, and EDHF pathways in the normotensive condition. The contribution of EDHF-mediated relaxation appears significantly greater in small resistance vessels than in large conduit vessels [58, 59] and when the eNOS pathway is absent [36]. However, the NOS-dependent component becomes the primary EDRF pathway in small arteries in the hypertensive condition, in which NOS utilizes both NOS-derived NO/cGMP and NOS-dependent H2O2 to promote vasorelaxation, while other EDRFs are diminished [27].

### 6.4.3 Effect on Epicardial Conductance Vessel

As long as hypertension has not already induced LVH and thereby affected endothelium-independent CFR and endothelium-dependent CBF, coronary ED in hypertensive patients is confined to the large epicardial vessels, which are continuously exposed to high pulsatile pressure and shear stress [60–62]. In those patients, ED can be detected through FMD of the brachial artery [46], even when hypertensive vascular disease rarely develops in the large vessels of the human forearm circulation, as opposed to the large arteries of the cerebral and limb circulation which are common targets of hypertension.

Systemic hypertension may presumably have a role on wall shear stress (WSS) and pressure drop through a coronary stenosis (plaque stress) that may result in coronary plaque rupture. Accordingly, systolic blood pressure predicts cardiovascular ischemic events [63]. It is well known that WSS is atherogenic by attenuating the expression of genes that may protect against atherosclerosis, including forms of the enzymes superoxide dismutase and eNOS with its dependent atheroprotection. However, evidence suggests that WSS represents a negligible load on the developed plaque when compared with pressure. It seems that pressure distribution across the stenosis is more important for plaque vulnerability and rupture. Any increase in systemic pressure over a coronary stenosis will increase the pressure drop through the stenosis (plaque stress) becoming an important mechanical trigger for plaque rupture [64].

### 6.4.4 Reversibility with Pharmacologic Intervention

An adequate control of hypertension is expected to induce a parallel improvement in CFR and CBF through regression of LVH. Concomitantly but even before this happens, a significant improvement of peripheral and coronary ED can be achieved with the use of specific drugs (Table 6.2).

#### Renin-Angiotensin-Aldosterone System (RAAS) Inhibitors

In addition to lowering blood pressure, angiotensin-converting enzyme inhibitors (ACEIs) and angiotensin-receptor blockers (ARBs) possess direct cardiovascular protective effects. ACEIs improve EF by reducing the production of angiotensin II [65, 66]. Similarly, the mechanisms by which ARBs improve EF are based on their ability to inhibit angiotensin II receptors [66]. Although studies on the effects of ACEIs and ARBs on ED have yielded conflicting results, two meta-analyses of randomized controlled trials demonstrated that each of ACEIs and ARBs improved peripheral EF and are superior to other antihypertensive drugs including calcium channel blockers and β-blockers and there was no significant difference between ACEIs and ARBs effect on EF [67, 68].

Aliskiren is a non-peptide renin inhibitor, which blocks RAAS at the first and rate-limiting step, therefore reducing the circulating levels of angiotensin II (at least theoretically) more effectively than ACEIs and ARBs. A recent study reported that the addition of aliskiren had beneficial effect on EF [69]. However, another study demonstrated that renin inhibition with aliskiren did not improve EF which is in accordance to

**Table 6.2** Reversibility of ED with pharmacological intervention

| | QE | RCT | Meta-An | Evidence of benefit |
|---|---|---|---|---|
| **Hypertension** | | | | |
| ACEi/ARB | | | ++ | Robust |
| Aliskiren | + | | | Insufficient |
| CCB | + (Lacidipine) | + (Nifedipine)<br>– (Amlodipine) | | Conflicting |
| Beta-blockers | + (Carvedilol) | + (Carvedilol) | | Consistent |
| **Dyslipidemia** | | | | |
| Statins | | + | + | Robust |
| L-Arginine | + | | | Insufficient |
| CETPi | | | – | Deleterious |
| Lp-$PLA_2$ | | | | Insufficient |
| Omega-3 | | + | + | Robust |
| **Diabetes mellitus** | | | | |
| Insulin | +/– | | | Insufficient |
| Metformin | | +/– | | Conflicting |
| Sulfonylureas | | + (Gliclazide)<br>– (Glibenclamide) | | Conflicting |
| Thiazolides | | +/– | | Conflicting |
| α-Glucosidase | | +/– | | Conflicting |
| GLP1-agonist | + | + | | Consistent |
| DPP4 | + | + | | Consistent |

*ED* endothelial dysfunction, *QE* quasi-experimental study, *RCT* randomized clinical trial, *Meta-A* meta-analyses, + beneficial effect, – not useful or deleterious effect, *ACEi* angiotensin-converting enzyme inhibitors, *ARB* angiotensin-receptor blockers, *CCB* calcium channel blockers, *CETPi* cholesterol ester transfer protein inhibitors, *Lp-$PLA_2$* lipoprotein-associated phospholipase $A_2$ inhibitors, *GLP1* glucagon-like peptide-1, *DDP4* dipeptidyl peptidase 4 inhibitor. See text for references

the negative clinical trial using the drug [70–72]. Therefore, evidence on the effect of aliskiren on EF in human is scarce, and the results are conflicting. Also, clinical efficacy of aliskiren on cardiovascular outcomes is still not clear. Ongoing clinical trials series, evaluating the effects of aliskiren on cardiovascular outcomes, will identify the role of direct renin inhibition as an alternative treatment for hypertension and other atherosclerotic diseases.

## Calcium Channel Blockers

Certain dihydropyridine-type calcium channel blockers (CCB) have been shown to modify EF by enhancing eNOS activity resulting in increased NO production [73]. Although not randomized, one study showed that lacidipine improved peripheral EF as assessed by intra-brachial infusion of ACh and bradykinin, in hypertensive subjects [74]. The Evaluation of Nifedipine and Cerivastatin on Recovery of Coronary Endothelial Function (ENCORE) I and II trials showed that long-acting nifedipine consistently improved coronary EF for up to 2 years in patients with stable CHD [75, 76]. On the other hand, in a randomized double-blind study of apparently healthy young adults with a strong family history of premature of CAD but no other identifiable CVRF, although amlodipine significantly improved peripheral EF, its improvement did not significantly differ from placebo group [77]. To date no meta-analyses on the effects of CCB on EF have been reported. Further studies are needed to clarify these relationships.

## β-Blockers

The third-generation β-blockers nebivolol and carvedilol may improve EF. Nebivolol causes vasodilation primarily through the release of endothelium-derived NO [78]. Interestingly, intra-arterial infusion of nebivolol in the forearm of healthy subjects is associated with an increase in forearm blood flow, which can be prevented by NO synthesis inhibition [79, 80]. It is thought to be mediated through β3 receptor activation and by interaction with estrogen receptors [81]. Carvedilol, a nonselective β-blocker with

additional α1 adrenoceptor antagonist activity, also has been shown to elevate antioxidant effect and improve ED [82]. In a recent randomized study of patients with hypertension and diabetes mellitus, compared with metoprolol, carvedilol was able to improve EF as assessed by FMD [83].

## 6.5 Dyslipidemia

### 6.5.1 Non-endothelium-Dependent Coronary Microvascular Dysfunction



Using positron emission tomography (PET) myocardial blood flow measurement in response to intravenous adenosine, a reduction in CFR (presumably by both endothelium- and non-endothelium-dependent mechanisms) has been documented in hypercholesterolemic asymptomatic subjects with normal coronary arteries [84, 85].

### 6.5.2 Endothelial-Dependent Coronary Microvascular Dysfunction

Patients with coronary atherosclerosis and normal cholesterol levels may show reductions in epicardial artery cross-sectional areas and impairment of papaverine-induced increases in CBF. In contrast, patients with high cholesterol level exhibit a selective impairment of their coronary microvasculature to relax in response to ACh [1, 56] which is directly related to the total serum cholesterol level and may respond to therapy [86]. Several mechanisms of low-density lipoprotein (LDL)-associated vascular dysfunction have been reported. Reduced endothelial NO bioactivity has been demonstrated in hypercholesterolemic animals [87] and humans [56]. The oxidized form of LDL is markedly more effective than native LDL cholesterol in causing ED [88, 89] by reducing NO synthesis through an interference with the receptor-mediated intracellular availability of L-arginine [87]. Oxidized LDL cholesterol, per se, has been shown to cause ED in vitro [88] and to decrease endothelium-dependent vasodilation in ex vivo experiments [89]. Interestingly, very early in the process of atherosclerosis during hypercholesterolemia in humans, endothelium-dependent responses are impaired first by a depressed receptor-mediated initiation of the production and/or release of EDRF, whereas flow-dependent dilation, which is strictly endothelium dependent but bypasses receptor-mediated mechanisms, is well preserved [1]. In addition, LDL cholesterol has been shown to increase vascular production of superoxide anion [90, 91] which can inactivate NO rapidly [92].

### 6.5.3 Effect on Epicardial Conductance Vessels

Extracellular lipid accumulation is a first step in atheroma formation. This process is considered to be associated with a chronic inflammatory process [22] closely related to alterations in lipid metabolism, since inflammatory cells are never seen in the intima in the absence of lipid [93]. Permeability of endothelium, which can be regarded as a parameter of endothelial function favours LDL increases at sites of lesion predilection. They accumulate in the intima, bind to proteoglycan, and tend to coalesce into aggregates. Lipoprotein particles bound to proteoglycan have increased susceptibility to oxidative stress. Later, intracellular lipid accumulation results in foam cell formation. Up to this point, the atheroma lesion consists primarily of lipid-engorged macrophages. Complex features such as fibrosis, thrombosis, and calcification are not present at this time, and evidence suggests that such lesions can regress, at least to some extent. A large lipid pool is an important microanatomic feature of the so-called vulnerable atherosclerotic plaque. From a strictly biomechanical viewpoint, a large lipid pool can serve to concentrate biomechanical forces on the shoulder regions of plaques, which are common sites of rupture of the fibrous cap [94]. The coronary segments with ED in patients with minimal coronary atherosclerosis are associated with plaque characteristics that are typical of vulnerable plaques such as large lipid core [95, 96] and macrophages accumulation [97] even prior to the development of any visible lesion.

### 6.5.4 Reversibility with Pharmacologic Intervention

ED has been demonstrated to be reversible after dietary correction of hypercholesterolemia [98] and a number of other cholesterol-lowering strategies and specific drugs. However, not all the findings are consistent, suggesting that ED is a complex condition that may require a multifactorial strategy to achieve the best cardiovascular outcome.

#### Statins

A number of randomized, placebo-controlled studies have shown beneficial effects of statins on ED in type 2 diabetes (T2D) subjects [99, 100]. However there is conflicting evidence [101, 102]. Improvement in EF occurred within days of treatment, prior to any plasma lipid changes, and was correlated with a reduction in oxidative stress, inflammation, and endothelial cell activation [103]. Statins reduce cardiovascular events beyond their cholesterol-lowering effects and play an important role in the primary and secondary prevention in high-risk individuals [104, 105]. The beneficial effect of statins on coronary and peripheral EF is attributed partly to their anti-inflammatory and antioxidant properties [105]. A recent meta-analysis of 46 randomized clinical trials concluded that statin therapy is associated with a significant improvement in both coronary and peripheral EF [106]. However, not all studies proved the beneficial effect of statins on EF [107], and noteworthy, considerable residual risk persists among statin-treated patients.

### L-Arginine

Microvascular ED of patients with hypercholesterolemia has been demonstrated to be reversible by L-arginine [108]. Also, the administration of L-arginine normalizes CBF responses to ACh in vivo in humans with hypercholesterolemia but has no effect in patients with atherosclerosis and normal levels of cholesterol. However, there is conflictive evidence on the subject. Although the proposed mechanism would be an interference of lipoproteins with the receptor-mediated intracellular availability of L-arginine, we have shown that its effect is not always related with cholesterol levels [109].

### Cholesterol Ester Transfer Protein (CETP) Inhibitors

CETP is a plasma protein that facilitates the transport of cholesteryl esters from high-density lipoprotein (HDL) to Apo B-containing lipoproteins and may increase HDL cholesterol, by inhibition of this transport between LDL and HDL particles. However, an unexpected increase in cardiovascular events and mortality was observed in patients treated with Torcetrapib in the ILLUMINATE trial [110]. It was suggested that the sustained and marked impairment of EF might at least in part explain the results [111]. Dalcetrapib did not improve EF either in the Dal-VESSEL study [112], and subsequently the phase III outcome trial for dalcetrapib, dal-OUTCOMES trial, was prematurely terminated due to lack of efficacy on major cardiovascular outcomes [113]. Two other highly potent CETP inhibitors, anacetrapib and evacetrapib, may be promising new options [114], but the impact of both of them on EF has not been investigated yet.

### Omega-3 Fatty Acids

A number of randomized clinical trials have been designed specifically to provide a controlled evaluation of the effects of omega-3 fatty acids on cardiovascular events. Although conflicting findings have been found on this issue [115], large-scale prospective studies and meta-analyses have demonstrated that intake of omega-3 fatty acids has a beneficial impact on cardiovascular outcomes [116–118]. Furthermore a recent meta-analysis of randomized controlled trials suggested that supplementation of omega-3 fatty acids may improve EF [119]. Although the mechanism underlying this protective effect has not been identified, reduced production of inflammatory cytokines might partly contribute [120, 121].

### Lipoprotein-Associated Phospholipase A2 (Lp-PLA2) Inhibitors

Lp-$PLA_2$ is highly expressed in atherosclerotic lesions, in particular vulnerable plaques [122–124], and has been shown to increase inflammation through producing arachidonic acid precursors from membrane glycerophospholipids, suggesting that this enzyme might be a potential therapeutic target [125]. Accordingly LP-PLA2 has been shown to be independently associated with coronary artery ED [126, 127], with conflictive evidence though [128]. To date, evidence of the impact of darapladib (a selective oral inhibitor of Lp-$PLA_2$) on EF is lacking, and clinical trials so far have been negative to improve outcomes [129, 130].

### PCSK9 Inhibitors

The discovery of proprotein convertase subtilisin kexin 9 (PCSK9) has considerably changed the therapeutic options in the field of lipid management. PCSK9 reduces LDL receptor recycling, leading to a decrease of LDL cholesterol (LDL-C) receptors on the surface of hepatocytes and a subsequent increase of circulating LDL-C levels. Monoclonal antibodies that inhibit PCSK9 have emerged as a new class of drugs that very effectively lower LDL cholesterol levels. Both the ODYSSEY LONG TERM trial (evolocumab) [131] and OSLER trials (alirocumab) [132] have shown an approximately 50 % reductions in composite cardiovascular events at 12 to 18 months. Although post hoc analyses, exploratory and based on a relatively small number of events, these results are consistent with a large reduction in LDL cholesterol levels (up to 60 %) without an excess of adverse effects. The Further Cardiovascular Outcomes Research with PCSK9 Inhibition in Subjects with Elevated Risk (FOURIER) study (NCT01764633) is an ongoing trial that is intended to provide a definitive assessment of the cardiovascular benefit of evolocumab. Although in human endothelial cells, oxidized LDL-induced apoptosis was associated with increased expression of PCSK9 [133], no studies so far have reported the effect of PCSK9 on peripheral and/or coronary EF. To date, some experimental studies reported that PCSK9 is associated with inflammation [134], oxidative stress, and ED [135].

## 6.6 Diabetes Mellitus

### 6.6.1 Non-endothelium-Dependent Coronary Microvascular Dysfunction

An impaired CFR in response to adenosine has been demonstrated through intracoronary Doppler and intracoronary infusion of adenosine or papaverine in diabetes mellitus (DM) patients with angiographically normal coronary arteries [136, 137]. Also, using PET myocardial blood flow measurement in response to intravenous dipyridamole or adenosine, a similar reduction in CFR, presumably by both endothelium- and non-endothelium-dependent mechanisms, has been demonstrated in subjects with both type 1 and type 2 DM. These results suggest a key role of chronic hyperglycemia in the pathogenesis of vascular dysfunction in DM [138, 139].

### 6.6.2 Endothelial-Dependent Coronary Microvascular Dysfunction

Chronic hyperglycemia is associated with ED [139, 140]. The underlying pathogenic mechanisms in type 2 diabetes mellitus (T2DM) probably involve uncoupling of eNOS activity,

uncoupling of mitochondrial oxidative phosphorylation, and activation of vascular NADPH oxidase [141, 142]. The main factors that combine to cause these biochemical disturbances are insulin resistance, oxidative stress, dyslipidemia, and inflammation [143]. Other clinical factors contributing either individually or synergistically to ED of DM patients include hypertension [144], visceral obesity [145], postprandial hyperlipidemia [146], fasting and postprandial hyperglycemia [147], and elevated levels of asymmetric dimethylarginine ADMA [147].

Insulin resistance (IR) has been proposed as one of the main mechanisms for myocardial ischemia according to previous evidence suggesting a reciprocal relationship between IR and endothelial function [148–151]. Experimental investigation in animal models [152, 153] and human cross-sectional studies performing indirect measurements of ED [154–156] strongly support this relationship, although conflicting evidence exists [157]. Moreover, interventions aiming at improving insulin sensitivity have been shown to improve EF and decrease myocardial ischemia in patients without obstructive atherosclerosis [158]. There is evidence of microcirculatory dysfunction in type 2 diabetes mellitus (T2DM) [159] and impaired glucose tolerance and IR as measured by PET. However, a direct assessment of the interaction of IR on coronary epicardial and microvascular ED in humans has not been reported. The role of IR on early coronary atherosclerosis and ischemic symptoms in patients without obstructive CAD needs further investigation due to the high prevalence of this association in patients with chest pain. We could hypothesize that a progressive increase in severity of IR along disorders of the glucose metabolism is associated with a higher prevalence of microvascular ED, but this is an area needing further research, as well as the interaction between IR and age on coronary microvascular ED.

### 6.6.3 Effect on Epicardial Conductance Vessels

Traditional CVRFs are present in diabetes mellitus; however, it does not completely account for the increased risk observed in these patients. ED and abnormalities in lipid metabolism are common mechanisms, but there is evidence of several others like perturbations in the proteo-fibrinolytic system and platelet biology as well as an increased systemic inflammation yielding plaques with characteristics of high risk of rupture and thrombosis [160, 161].

### 6.6.4 Reversibility with Pharmacologic Intervention

Intensive glycemic control reduces the progression of coronary disease [162, 163] including manifestation and progression of nephropathy, end-stage renal disease, and retinopathy. However, the benefit of achieving an optimal HbA1C level to minimize or reverse the manifestation and progression of CMD in T2DM patients has not been reported. Previous evidence on the subject is scarce and limited [164–168]. Two small-randomized trials evaluating different therapeutic strategies over peripheral ED did not find any relationship between glycemic control and ED [164, 165]. However, CMD was not evaluated in these studies, and the current glycemic target of Hb1C < 7 % was not necessarily achieved [169]. Two studies that addressed the association between HbA1c levels and CFR as evaluated with Doppler echocardiography [166, 167] found no differences between T2DM patients with a good vs. poor glycemic control, but one [167] reported an improvement of CFR after 6 months in those patients who achieved HbA1C < 7 %. In DM patients with chest pain and normal coronary angiogram [168], an optimal glycemic control did not reduce the incidence of epicardial coronary artery spasm. In accordance with these results, previous studies have emphasized the importance of acute glycemic fluctuations from peaks to nadir as a cause of excessive protein glycation, activations of oxidative stress [170, 171], and ED in DM patients [172] even with an optimal glycemic control based on HbA1c levels.

#### Insulin Therapy

The role of insulin therapy on ED in T2DM is still controversial. One reason would be a failure to separate the effects of insulin from those of proinsulin, which is pro-atherogenic. Although the addition of isophane insulin glargine improved forearm vascular reactivity in patients treated with metformin alone [173], insulin may worsen ED in subjects with impaired sensitivity of the phosphatidylinositol 3-kinase-dependent pathways [174, 175]. The controversy concerning the atherogenic effects of insulin may reflect differences in the way in which the two pathways (phosphatidylinositol kinase (PI-3K) pathway and mitogen-activated protein kinase (MAPK) pathway are affected by insulin in the healthy and insulin-resistant endothelium [176, 177].

#### Metformin

Metformin improves insulin sensitivity and glucose homeostasis and is demonstrated to activate 5′ adenosine monophosphate-activated protein kinase (AMPK) in tissues [177]. AMPK system controls systemic energy balance and metabolism and may be partly responsible for the health benefit of exercise. Several studies in different patient groups, including patients with type 1 diabetes, have demonstrated that administration of metformin improves EF [178–182] although a few showed no significant beneficial effect [183, 184].

#### Sulfonylureas

Although sulfonylureas may elevate the risk of cardiovascular disease in patients with T2DM [185], there is insufficient evidence from randomized controlled trials to determine its clinical efficacy on cardiovascular outcomes [186]. Through stimulating insulin secretion, sulfonylureas are believed to favor the development of hypoglycemia and weight gain,

accelerate beta-cell apoptosis and beta-cell exhaustion, and impair EF, thereby increasing the risk for ischemic complications. Several studies have reported negative effects of glibenclamide on EF, although a few showed improved EF, e.g., gliclazide has antioxidant properties that might prevent ED [177, 187, 188]. In summary, to date there is no robust clinical evidence, and there might be differences among sulfonylureas regarding their effects on EF.

### Thiazolidinediones

The peroxisome proliferator-activated receptors γ, to which thiazolidinediones bind, are expressed in adipose tissue, pancreatic β-cells, endothelium, and macrophages [189] Thiazolidinediones activate eNOS [190] and might also have antioxidant properties thereby increasing NO bioavailability [191]. The beneficial effects of thiazolidinediones on endothelium have been reported by several [184, 192–195] but not all clinical studies [196]. It is reported that rosiglitazone can reduce intracellular levels of the enzyme involved in tetrahydrobiopterin synthesis and inhibit cytokine-induced NO synthesis [197]. Thus, its effect on NO bioavailability and NO synthase function remains to be fully explored, and the independent effect of these drugs on EF remains unsolved. Accordingly, there is conflictive evidence on the clinical benefit of these agents to improve cardiovascular outcomes [198–202].

### α-Glucosidase Inhibitors

Repeated postprandial hyperglycemia might have an important role in the development of atherosclerosis by suppressing vascular EF [203]. α-Glucosidase inhibitors delay digestion of complex carbohydrates in the upper small bowel and subsequently retard absorption of glucose and "blunt" postprandial hyperglycemia by inhibiting α-glucosidases in the brush border of the small intestine. Unlike some other blood glucose-lowering agents, no adverse signals of potential cardiovascular risk have emerged in relation to α-glucosidase inhibitor use. On the contrary, significant beneficial cardiovascular outcome results have been reported by the landmark Study to Prevent Non-Insulin-Dependent Diabetes Mellitus (STOP-NIDDM) trial [204]. However, other large randomized clinical trials failed to show beneficial effect of α-glucosidase inhibitors on cardiovascular outcomes [205, 206]. In agreement with these results from clinical trials, the reported effect of α-glucosidase inhibitors on EF is also conflicting [207–210]. Thus, the effect of the drug on endothelial function may parallel the effect on CV events, underscoring the role of endothelial function as a therapeutic target.

### Incretins Glucagon-Like Peptide-1 (GLP-1) and Dipeptidyl Peptidase 4 Inhibitor (DPP4-I)

In addition to the well-characterized actions of glucagon-like peptide-1 (GLP-1) on glycemic controls, GLP-1 acts on endothelium as well as cardiac and vascular myocytes, which express a functional GLP-1 receptor. GLP-1 receptor-dependent and GLP-1 receptor-independent pathways have been proposed for the beneficial cardiovascular effects of GLP-1 [211]. Dipeptidyl peptidase 4 inhibitor (DPP4-I) maintains the plasma level of active GLP-1 and increases NO production with increased eNOS phosphorylation [212]. In recent years, incretin mimetics GLP-1 receptor agonists and DPP4-Is have received particular attention for their potential to positively impact cardiovascular outcomes. Although an increasing body of literature from preclinical and early phase clinical studies has indicated that both GLP-1 receptor agonists and DPP4-Is may exert glucose-independent beneficial effects on cardiovascular outcomes [213], the results from ongoing large-scale trials might provide valuable new insights about the impact of these incretin-based therapies on cardiovascular outcomes. Several clinical studies reported that EF was improved by GLP-1 and DPP4-I [214–218] although their effect remains controversial, because most of these were non-randomized trials and included a small number of patients. Large-scale randomized studies are needed to further clarify the impact of GLP-1 and DPP4-I on EF.

## 6.7 Conclusions and Future Directions

CMD is the result of anatomic and functional changes occurring when traditional, novel, and yet unknown CVRFs are present in an individual. ED is a predominantly functional and reversible first manifestation of atherosclerosis that precedes vascular morphological changes and occurrence of cardiovascular events. Therefore, in addition to the current strategy to control traditional CVRF, we need to focus on the effect on ED as a therapeutic target. Efforts should be done to identify appropriate targets to attenuate and reverse the initial steps of the process and the complications of atherosclerosis. An effort should be made to strengthen ED as an endpoint of clinical studies. The role of the assessment of endothelial function in clinical practice continues to emerge. Prospective randomized studies in this area are needed to answer the question of whether endothelial function-guided therapies will provide benefits in improving outcomes in patients with risk factors and in patients with established CV conditions. Such further studies may usher us into a new era of individualized medicine in cardiology.

## References

1. Zeiher AM, Drexler H, Wollschlager H, Just H. Modulation of coronary vasomotor tone in humans. Progressive endothelial dysfunction with different early stages of coronary atherosclerosis. Circulation. 1991;83(2):391–401.
2. Kuo L, Davis MJ, Chilian WM. Longitudinal gradients for endothelium-dependent and -independent vascular responses in the coronary microcirculation. Circulation. 1995;92(3):518–25.
3. Herrmann J, Kaski JC, Lerman A. Coronary microvascular dysfunction in the clinical setting: from mystery to reality. Eur Heart J. 2012;33(22):2771–82b. doi:10.1093/eurheartj/ehs246.

4. Hasdai D, Cannan CR, Mathew V, Holmes Jr DR, Lerman A. Evaluation of patients with minimally obstructive coronary artery disease and angina. Int J Cardiol. 1996;53(3):203–8.
5. Rembert JC, Boyd LM, Watkinson WP, Greenfield Jr JC. Effect of adenosine on transmural myocardial blood flow distribution in the awake dog. Am J Physiol. 1980;239(1):H7–13.
6. Tune JD, Gorman MW, Feigl EO. Matching coronary blood flow to myocardial oxygen consumption. J Appl Physiol. 2004;97(1):404–15. doi:10.1152/japplphysiol.01345.2003.
7. Wilson RF, Wyche K, Christensen BV, Zimmer S, Laxson DD. Effects of adenosine on human coronary arterial circulation. Circulation. 1990;82(5):1595–606.
8. Schachinger V, Britten MB, Zeiher AM. Prognostic impact of coronary vasodilator dysfunction on adverse long-term outcome of coronary heart disease. Circulation. 2000;101(16):1899–906.
9. Halcox JP, Schenke WH, Zalos G, Mincemoyer R, Prasad A, Waclawiw MA, Nour KR, Quyyumi AA. Prognostic value of coronary vascular endothelial dysfunction. Circulation. 2002;106(6):653–8.
10. Targonski PV, Bonetti PO, Pumper GM, Higano ST, Holmes Jr DR, Lerman A. Coronary endothelial dysfunction is associated with an increased risk of cerebrovascular events. Circulation. 2003;107(22):2805–9. doi:10.1161/01.CIR.0000072765.93106.EE.
11. Kinlay S, Libby P, Ganz P. Endothelial function and coronary artery disease. Curr Opin Lipidol. 2001;12(4):383–9.
12. Gossl M, Yoon MH, Choi BJ, Rihal C, Tilford JM, Reriani M, Gulati R, Sandhu G, Eeckhout E, Lennon R, Lerman LO, Lerman A. Accelerated coronary plaque progression and endothelial dysfunction: serial volumetric evaluation by IVUS. JACC Cardiovasc Imaging. 2014;7(1):103–4. doi:10.1016/j.jcmg.2013.05.020.
13. Hamburg NM, Keyes MJ, Larson MG, Vasan RS, Schnabel R, Pryde MM, Mitchell GF, Sheffy J, Vita JA, Benjamin EJ. Cross-sectional relations of digital vascular function to cardiovascular risk factors in the Framingham Heart Study. Circulation. 2008;117(19):2467–74. doi:10.1161/CIRCULATIONAHA.107.748574.
14. Khot UN, Khot MB, Bajzer CT, Sapp SK, Ohman EM, Brener SJ, Ellis SG, Lincoff AM, Topol EJ. Prevalence of conventional risk factors in patients with coronary heart disease. JAMA. 2003;290(7):898–904. doi:10.1001/jama.290.7.898.
15. Cannon CP, Braunwald E, McCabe CH, Rader DJ, Rouleau JL, Belder R, Joyal SV, Hill KA, Pfeffer MA, Skene AM. Intensive versus moderate lipid lowering with statins after acute coronary syndromes. N Engl J Med. 2004;350(15):1495–504. doi:10.1056/NEJMoa040583.
16. LaRosa JC, Grundy SM, Waters DD, Shear C, Barter P, Fruchart JC, Gotto AM, Greten H, Kastelein JJ, Shepherd J, Wenger NK. Intensive lipid lowering with atorvastatin in patients with stable coronary disease. N Engl J Med. 2005;352(14):1425–35. doi:10.1056/NEJMoa050461.
17. Anderson TJ, Gerhard MD, Meredith IT, Charbonneau F, Delagrange D, Creager MA, Selwyn AP, Ganz P. Systemic nature of endothelial dysfunction in atherosclerosis. Am J Cardiol. 1995;75(6):71B–4.
18. Teragawa H, Ueda K, Matsuda K, Kimura M, Higashi Y, Oshima T, Yoshizumi M, Chayama K. Relationship between endothelial function in the coronary and brachial arteries. Clin Cardiol. 2005;28(10):460–6.
19. Hamburg NM, Palmisano J, Larson MG, Sullfutuire LM, Lehman BT, Vasan RS, Levy D, Mitchell GF, Vita JA, Benjamin EJ. Relation of brachial and digital measures of vascular function in the community: the Framingham heart study. Hypertension. 2011;57(3):390–6. doi:10.1161/HYPERTENSIONAHA.110.160812.
20. Flammer AJ, Anderson T, Celermajer DS, Creager MA, Deanfield J, Ganz P, Hamburg NM, Luscher TF, Shechter M, Taddei S, Vita JA, Lerman A. The assessment of endothelial function: from research into clinical practice. Circulation. 2012;126(6):753–67. doi:10.1161/CIRCULATIONAHA.112.093245.
21. Bonetti PO, Lerman LO, Lerman A. Endothelial dysfunction: a marker of atherosclerotic risk. Arterioscler Thromb Vasc Biol. 2003;23(2):168–75.
22. Ross R. Atherosclerosis – an inflammatory disease. N Engl J Med. 1999;340(2):115–26. doi:10.1056/NEJM199901143400207.
23. Rudic RD, Shesely EG, Maeda N, Smithies O, Segal SS, Sessa WC. Direct evidence for the importance of endothelium-derived nitric oxide in vascular remodeling. J Clin Invest. 1998;101(4):731–6. doi:10.1172/JCI1699.
24. Forstermann U. Oxidative stress in vascular disease: causes, defense mechanisms and potential therapies. Nat Clin Pract Cardiovasc Med. 2008;5(6):338–49. doi:10.1038/ncpcardio1211.
25. Murohara T, Asahara T, Silver M, Bauters C, Masuda H, Kalka C, Kearney M, Chen D, Symes JF, Fishman MC, Huang PL, Isner JM. Nitric oxide synthase modulates angiogenesis in response to tissue ischemia. J Clin Invest. 1998;101(11):2567–78. doi:10.1172/JCI1560.
26. Landmesser U, Engberding N, Bahlmann FH, Schaefer A, Wiencke A, Heineke A, Spiekermann S, Hilfiker-Kleiner D, Templin C, Kotlarz D, Mueller M, Fuchs M, Hornig B, Haller H, Drexler H. Statin-induced improvement of endothelial progenitor cell mobilization, myocardial neovascularization, left ventricular function, and survival after experimental myocardial infarction requires endothelial nitric oxide synthase. Circulation. 2004;110(14):1933–9. doi:10.1161/01.CIR.0000143232.67642.7A.
27. Kang KT. Endothelium-derived relaxing factors of small resistance arteries in hypertension. Toxicol Res. 2014;30(3):141–8. doi:10.5487/TR.2014.30.3.141.
28. Forstermann U, Sessa WC. Nitric oxide synthases: regulation and function. Eur Heart J. 2012;33(7):829–37, 837a–7d. doi:10.1093/eurheartj/ehr304.
29. Dudzinski DM, Igarashi J, Greif D, Michel T. The regulation and pharmacology of endothelial nitric oxide synthase. Annu Rev Pharmacol Toxicol. 2006;46:235–76. doi:10.1146/annurev.pharmtox.44.101802.121844.
30. Woodman RJ, Chew GT, Watts GF. Mechanisms, significance and treatment of vascular dysfunction in type 2 diabetes mellitus: focus on lipid-regulating therapy. Drugs. 2005;65(1):31–74.
31. Drummond GR, Cai H, Davis ME, Ramasamy S, Harrison DG. Transcriptional and posttranscriptional regulation of endothelial nitric oxide synthase expression by hydrogen peroxide. Circ Res. 2000;86(3):347–54.
32. Li H, Oehrlein SA, Wallerath T, Ihrig-Biedert I, Wohlfart P, Ulshofer T, Jessen T, Herget T, Forstermann U, Kleinert H. Activation of protein kinase C alpha and/or epsilon enhances transcription of the human endothelial nitric oxide synthase gene. Mol Pharmacol. 1998;53(4):630–7.
33. Bec N, Gorren AFC, Mayer B, Schmidt PP, Andersson KK, Lange R. The role of tetrahydrobiopterin in the activation of oxygen by nitric-oxide synthase. J Inorg Biochem. 2000;81(3):207–11.
34. Jackson WF. Ion channels and vascular tone. Hypertension. 2000;35(1 Pt 2):173–8.
35. Liu Y, Gutterman DD. Vascular control in humans: focus on the coronary microcirculation. Basic Res Cardiol. 2009;104(3):211–27. doi:10.1007/s00395-009-0775-y.
36. Huang A, Sun D, Smith CJ, Connetta JA, Shesely EG, Koller A, Kaley G. In eNOS knockout mice skeletal muscle arteriolar dilation to acetylcholine is mediated by EDHF. Am J Physiol Heart Circ Physiol. 2000;278(3):H762–8.
37. Vanhoutte PM. Endothelium-dependent hyperpolarizations: the history. Pharmacol Res. 2004;49(6):503–8. doi:10.1016/j.phrs.2003.11.015.
38. Hamasaki S, Al Suwaidi J, Higano ST, Miyauchi K, Holmes Jr DR, Lerman A. Attenuated coronary flow reserve and vascular remodeling in patients with hypertension and left ventricular hypertrophy. J Am Coll Cardiol. 2000;35(6):1654–60.
39. Rimoldi O, Rosen SD, Camici PG. The blunting of coronary flow reserve in hypertension with left ventricular hypertrophy is transmural and correlates with systolic blood pressure. J Hypertens. 2014;32(12):2465–71. doi:10.1097/HJH.0000000000000338; discussion 2471.
40. Rajappan K, Rimoldi OE, Dutka DP, Ariff B, Pennell DJ, Sheridan DJ, Camici PG. Mechanisms of coronary microcirculatory dysfunction in patients with aortic stenosis and angiographically normal coronary arteries. Circulation. 2002;105(4):470–6.

41. Feihl F, Liaudet L, Waeber B, Levy BI. Hypertension: a disease of the microcirculation? Hypertension. 2006;48(6):1012–7. doi:10.1161/01.HYP.0000249510.20326.72.
42. Heusch G, Baumgart D, Camici P, Chilian W, Gregorini L, Hess O, Indolfi C, Rimoldi O. alpha-adrenergic coronary vasoconstriction and myocardial ischemia in humans. Circulation. 2000;101(6):689–94.
43. Feihl F, Liaudet L, Levy BI, Waeber B. Hypertension and microvascular remodelling. Cardiovasc Res. 2008;78(2):274–85. doi:10.1093/cvr/cvn022.
44. Schwartzkopff B, Frenzel H, Dieckerhoff J, Betz P, Flasshove M, Schulte HD, Mundhenke M, Motz W, Strauer BE. Morphometric investigation of human myocardium in arterial hypertension and valvular aortic stenosis. Eur Heart J. 1992;13 Suppl D:17–23.
45. Tice FD, Peterson JW, Orsinelli DA, Binkley PF, Cody RJ, Guthrie R, Pearson AC. Vascular hypertrophy is an early finding in essential hypertension and is related to arterial pressure waveform contour. Am Heart J. 1996;132(3):621–7.
46. Linder L, Kiowski W, Buhler FR, Luscher TF. Indirect evidence for release of endothelium-derived relaxing factor in human forearm circulation in vivo. Blunted response in essential hypertension. Circulation. 1990;81(6):1762–7.
47. Taddei S, Virdis A, Mattei P, Ghiadoni L, Fasolo CB, Sudano I, Salvetti A. Hypertension causes premature aging of endothelial function in humans. Hypertension. 1997;29(3):736–43.
48. Panza JA, Quyyumi AA, Brush Jr JE, Epstein SE. Abnormal endothelium-dependent vascular relaxation in patients with essential hypertension. N Engl J Med. 1990;323(1):22–7. doi:10.1056/NEJM199007053230105.
49. Treasure CB, Klein JL, Vita JA, Manoukian SV, Renwick GH, Selwyn AP, Ganz P, Alexander RW. Hypertension and left ventricular hypertrophy are associated with impaired endothelium-mediated relaxation in human coronary resistance vessels. Circulation. 1993;87(1):86–93.
50. Taddei S, Virdis A, Mattei P, Arzilli F, Salvetti A. Endothelium-dependent forearm vasodilation is reduced in normotensive subjects with familial history of hypertension. J Cardiovasc Pharmacol. 1992;20 Suppl 12:S193–5.
51. Hongo K, Nakagomi T, Kassell NF, Sasaki T, Lehman M, Vollmer DG, Tsukahara T, Ogawa H, Torner J. Effects of aging and hypertension on endothelium-dependent vascular relaxation in rat carotid artery. Stroke. 1988;19(7):892–7.
52. Takase H, Moreau P, Kung CF, Nava E, Luscher TF. Antihypertensive therapy prevents endothelial dysfunction in chronic nitric oxide deficiency. Effect of verapamil and trandolapril. Hypertension. 1996;27(1):25–31.
53. Bossaller C, Habib GB, Yamamoto H, Williams C, Wells S, Henry PD. Impaired muscarinic endothelium-dependent relaxation and cyclic guanosine 5′-monophosphate formation in atherosclerotic human coronary artery and rabbit aorta. J Clin Invest. 1987;79(1):170–4. doi:10.1172/JCI112779.
54. Forstermann U, Mugge A, Alheid U, Haverich A, Frolich JC. Selective attenuation of endothelium-mediated vasodilation in atherosclerotic human coronary arteries. Circ Res. 1988;62(2):185–90.
55. Ludmer PL, Selwyn AP, Shook TL, Wayne RR, Mudge GH, Alexander RW, Ganz P. Paradoxical vasoconstriction induced by acetylcholine in atherosclerotic coronary arteries. N Engl J Med. 1986;315(17):1046–51. doi:10.1056/NEJM198610233151702.
56. Zeiher AM, Drexler H, Saurbier B, Just H. Endothelium-mediated coronary blood flow modulation in humans. Effects of age, atherosclerosis, hypercholesterolemia, and hypertension. J Clin Invest. 1993;92(2):652–62. doi:10.1172/JCI116634.
57. Vallance P, Collier J, Moncada S. Effects of endothelium-derived nitric oxide on peripheral arteriolar tone in man. Lancet. 1989;2(8670):997–1000.
58. Feletou M, Vanhoutte PM. Endothelium-derived hyperpolarizing factor: where are we now? Arterioscler Thromb Vasc Biol. 2006;26(6):1215–25. doi:10.1161/01.ATV.0000217611.81085.c5.
59. Tomioka H, Hattori Y, Fukao M, Sato A, Liu M, Sakuma I, Kitabatake A, Kanno M. Relaxation in different-sized rat blood vessels mediated by endothelium-derived hyperpolarizing factor: importance of processes mediating precontractions. J Vasc Res. 1999;36(4):311–20. doi:25659.
60. Treasure CB, Manoukian SV, Klein JL, Vita JA, Nabel EG, Renwick GH, Selwyn AP, Alexander RW, Ganz P. Epicardial coronary artery responses to acetylcholine are impaired in hypertensive patients. Circ Res. 1992;71(4):776–81.
61. Dzau VJ, Safar ME. Large conduit arteries in hypertension: role of the vascular renin-angiotensin system. Circulation. 1988;77(5):947–54.
62. Zeiher AM, Drexler H. Coronary hemodynamic determinants of epicardial artery vasomotor responses during sympathetic stimulation in humans. Basic Res Cardiol. 1991;86 Suppl 2:203–13.
63. Rodriguez CJ, Swett K, Agarwal SK, Folsom AR, Fox ER, Loehr LR, Ni H, Rosamond WD, Chang PP. Systolic blood pressure levels among adults with hypertension and incident cardiovascular events: the atherosclerosis risk in communities study. JAMA Intern Med. 2014;174(8):1252–61. doi:10.1001/jamainternmed.2014.2482.
64. Li ZY, Taviani V, Tang T, Sadat U, Young V, Patterson A, Graves M, Gillard JH. The mechanical triggers of plaque rupture: shear stress vs pressure gradient. Br J Radiol. 2009;82(Spec No 1):S39–45. doi:10.1259/bjr/15036781.
65. Alreja G, Joseph J. Renin and cardiovascular disease: worn-out path, or new direction. World J Cardiol. 2011;3(3):72–83. doi:10.4330/wjc.v3.i3.72.
66. Watanabe T, Barker TA, Berk BC. Angiotensin II and the endothelium: diverse signals and effects. Hypertension. 2005;45(2):163–9. doi:10.1161/01.HYP.0000153321.13792.b9.
67. Shahin Y, Khan JA, Samuel N, Chetter I. Angiotensin converting enzyme inhibitors effect on endothelial dysfunction: a meta-analysis of randomised controlled trials. Atherosclerosis. 2011;216(1):7–16. doi:10.1016/j.atherosclerosis.2011.02.044.
68. Li S, Wu Y, Yu G, Xia Q, Xu YW. Angiotensin II receptor blockers improve peripheral endothelial function: a meta-analysis of randomized controlled trials. PLoS One. 2014;9(3). doi:ARTN e90217. 10.1371/journal.pone.0090217.
69. Bonadei I, Vizzardi E, D'Aloia A, Sciatti E, Raddino R, Metra M. Role of aliskiren on arterial stiffness and endothelial function in patients with primary hypertension. J Clin Hypertens. 2014;16(3):202–6. doi:10.1111/jch.12262.
70. Flammer AJ, Gossl M, Li J, Reriani M, Shonyo S, Loeffler D, Herrmann J, Lerman LO, Lerman A. Renin inhibition with aliskiren lowers circulating endothelial progenitor cells in patients with early atherosclerosis. J Hypertens. 2013;31(3):632–5. doi:10.1097/HJH.0b013e32835c6d2d.
71. Schroten NF, Damman K, Hemmelder MH, Voors AA, Navis G, Gaillard CA, van Veldhuisen DJ, Van Gilst WH, Hillege HL. Effect of additive renin inhibition with aliskiren on renal blood flow in patients with Chronic Heart Failure and Renal Dysfunction (Additive Renin Inhibition with Aliskiren on renal blood flow and Neurohormonal Activation in patients with Chronic Heart Failure and Renal Dysfunction). Am Heart J. 2015;169(5):693–701. doi:10.1016/j.ahj.2014.12.016, e693.
72. Gheorghiade M, Bohm M, Greene SJ, Fonarow GC, Lewis EF, Zannad F, Solomon SD, Baschiera F, Botha J, Hua TA, Gimpelewicz CR, Jaumont X, Lesogor A, Maggioni AP, Investigators A, Coordinators. Effect of aliskiren on postdischarge mortality and heart failure readmissions among patients hospitalized for heart failure: the ASTRONAUT randomized trial. JAMA. 2013;309(11):1125–35. doi:10.1001/jama.2013.1954.
73. Tang EH, Vanhoutte PM. Endothelial dysfunction: a strategic target in the treatment of hypertension? Pflugers Arch. 2010;459(6):995–1004. doi:10.1007/s00424-010-0786-4.
74. Taddei S, Virdis A, Ghiadoni L, Uleri S, Magagna A, Salvetti A. Lacidipine restores endothelium-dependent vasodilation in essential hypertensive patients. Hypertension. 1997;30(6):1606–12.
75. Investigators E. Effect of nifedipine and cerivastatin on coronary endothelial function in patients with coronary artery disease: the ENCORE I Study (Evaluation of Nifedipine and Cerivastatin On Recovery of coronary Endothelial function). Circulation. 2003;107(3):422–8.

76. Luscher TF, Pieper M, Tendera M, Vrolix M, Rutsch W, van den Branden F, Gil R, Bischoff KO, Haude M, Fischer D, Meinertz T, Munzel T. A randomized placebo-controlled study on the effect of nifedipine on coronary endothelial function and plaque formation in patients with coronary artery disease: the ENCORE II study. Eur Heart J. 2009;30(13):1590–7. doi:10.1093/eurheartj/ehp151.
77. Clarkson P, Mullen MJ, Donald AE, Powe AJ, Thomson H, Thorne SA, Bull T, Deanfield JE. The effect of amlodipine on endothelial function in young adults with a strong family history of premature coronary artery disease: a randomised double blind study. Atherosclerosis. 2001;154(1):171–7.
78. Gao YS, Nagao T, Bond RA, Janssens WJ, Vanhoutte PM. Nebivolol induces endothelium-dependent relaxations of canine coronary arteries. J Cardiovasc Pharmacol. 1991;17(6):964–9.
79. Cockcroft JR, Chowienczyk PJ, Brett SE, Chen CP, Dupont AG, Van Nueten L, Wooding SJ, Ritter JM. Nebivolol vasodilates human forearm vasculature: evidence for an L-arginine/NO-dependent mechanism. J Pharmacol Exp Ther. 1995;274(3):1067–71.
80. Prisant LM. Nebivolol: pharmacologic profile of an ultraselective, vasodilatory beta1-blocker. J Clin Pharmacol. 2008;48(2):225–39. doi:10.1177/0091270007310378.
81. Broeders MA, Doevendans PA, Bekkers BC, Bronsaer R, van Gorsel E, Heemskerk JW, Egbrink MG, van Breda E, Reneman RS, van Der Zee R. Nebivolol: a third-generation beta-blocker that augments vascular nitric oxide release: endothelial beta(2)-adrenergic receptor-mediated nitric oxide production. Circulation. 2000;102(6):677–84.
82. Feuerstein GZ, Ruffolo Jr RR. Carvedilol, a novel multiple action antihypertensive agent with antioxidant activity and the potential for myocardial and vascular protection. Eur Heart J. 1995;16 Suppl F:38–42.
83. Bank AJ, Kelly AS, Thelen AM, Kaiser DR, Gonzalez-Campoy JM. Effects of carvedilol versus metoprolol on endothelial function and oxidative stress in patients with type 2 diabetes mellitus. Am J Hypertens. 2007;20(7):777–83. doi:10.1016/j.amjhyper.2007.01.019.
84. Kaufmann PA, Gnecchi-Ruscone T, Schafers KP, Luscher TF, Camici PG. Low density lipoprotein cholesterol and coronary microvascular dysfunction in hypercholesterolemia. J Am Coll Cardiol. 2000;36(1):103–9.
85. Dayanikli F, Grambow D, Muzik O, Mosca L, Rubenfire M, Schwaiger M. Early detection of abnormal coronary flow reserve in asymptomatic men at high risk for coronary artery disease using positron emission tomography. Circulation. 1994;90(2):808–17.
86. Hamasaki S, Higano ST, Suwaidi JA, Nishimura RA, Miyauchi K, Holmes Jr DR, Lerman A. Cholesterol-lowering treatment is associated with improvement in coronary vascular remodeling and endothelial function in patients with normal or mildly diseased coronary arteries. Arterioscler Thromb Vasc Biol. 2000;20(3):737–43.
87. Tanner FC, Noll G, Boulanger CM, Luscher TF. Oxidized low density lipoproteins inhibit relaxations of porcine coronary arteries. Role of scavenger receptor and endothelium-derived nitric oxide. Circulation. 1991;83(6):2012–20.
88. Simon BC, Cunningham LD, Cohen RA. Oxidized low density lipoproteins cause contraction and inhibit endothelium-dependent relaxation in the pig coronary artery. J Clin Invest. 1990;86(1):75–9. doi:10.1172/JCI114718.
89. Hein TW, Kuo L. LDLs impair vasomotor function of the coronary microcirculation: role of superoxide anions. Circ Res. 1998;83(4):404–14.
90. Ohara Y, Peterson TE, Harrison DG. Hypercholesterolemia increases endothelial superoxide anion production. J Clin Invest. 1993;91(6):2546–51. doi:10.1172/JCI116491.
91. Pritchard Jr KA, Groszek L, Smalley DM, Sessa WC, Wu M, Villalon P, Wolin MS, Stemerman MB. Native low-density lipoprotein increases endothelial cell nitric oxide synthase generation of superoxide anion. Circ Res. 1995;77(3):510–8.
92. Rubanyi GM, Vanhoutte PM. Superoxide anions and hyperoxia inactivate endothelium-derived relaxing factor. Am J Physiol. 1986;250(5 Pt 2):H822–7.
93. Nakashima Y, Plump AS, Raines EW, Breslow JL, Ross R. ApoE-deficient mice develop lesions of all phases of atherosclerosis throughout the arterial tree. Arterioscler Thromb. 1994;14(1):133–40.
94. Libby P. The vascular biology of atherosclerosis. In: Bonow R, Mann D, Zipes D, Libby P, editors. Braunwald's heart disease: a textbook of cardiovascular medicine. 9th ed. Elsevier Science. Philadelphia. 2007; p. 900–4.
95. Lavi S, Bae JH, Rihal CS, Prasad A, Barsness GW, Lennon RJ, Holmes Jr DR, Lerman A. Segmental coronary endothelial dysfunction in patients with minimal atherosclerosis is associated with necrotic core plaques. Heart. 2009;95(18):1525–30. doi:10.1136/hrt.2009.166017.
96. Choi BJ, Prasad A, Gulati R, Best PJ, Lennon RJ, Barsness GW, Lerman LO, Lerman A. Coronary endothelial dysfunction in patients with early coronary artery disease is associated with the increase in intravascular lipid core plaque. Eur Heart J. 2013;34(27):2047–54. doi:10.1093/eurheartj/eht132.
97. Choi BJ, Matsuo Y, Aoki T, Kwon TG, Prasad A, Gulati R, Lennon RJ, Lerman LO, Lerman A. Coronary endothelial dysfunction is associated with inflammation and vasa vasorum proliferation in patients with early atherosclerosis. Arterioscler Thromb Vasc Biol. 2014;34(11):2473–7. doi:10.1161/ATVBAHA.114.304445.
98. Czernin J, Barnard RJ, Sun KT, Krivokapich J, Nitzsche E, Dorsey D, Phelps ME, Schelbert HR. Effect of short-term cardiovascular conditioning and low-fat diet on myocardial blood flow and flow reserve. Circulation. 1995;92(2):197–204.
99. Dalla Nora E, Passaro A, Zamboni PF, Calzoni F, Fellin R, Solini A. Atorvastatin improves metabolic control and endothelial function in type 2 diabetic patients: a placebo-controlled study. J Endocrinol Invest. 2003;26(1):73–8.
100. Adel A, Abdel-Salam Z, Nammas W. Low-dose statin therapy improves endothelial function in type 2 diabetic patients with normal serum total cholesterol: a randomized placebo-controlled study. J Clin Hypertens. 2010;12(10):820–5. doi:10.1111/j.1751-7176.2010.00367.x.
101. Balletshofer BM, Goebbel S, Rittig K, Enderle M, Schmolzer I, Wascher TC, Ferenc Pap A, Westermeier T, Petzinna D, Matthaei S, Haring HU. Intense cholesterol lowering therapy with a HMG-CoA reductase inhibitor does not improve nitric oxide dependent endothelial function in type-2-diabetes--a multicenter, randomised, double-blind, three-arm placebo-controlled clinical trial. Exp Clin Endocrinol Diabetes. 2005;113(6):324–30. doi:10.1055/s-2005-865642.
102. van Venrooij FV, van de Ree MA, Bots ML, Stolk RP, Huisman MV, Banga JD, Group DS. Aggressive lipid lowering does not improve endothelial function in type 2 diabetes: the Diabetes Atorvastatin Lipid Intervention (DALI) Study: a randomized, double-blind, placebo-controlled trial. Diabetes Care. 2002;25(7):1211–6.
103. Ceriello A, Assaloni R, Da Ros R, Maier A, Piconi L, Quagliaro L, Esposito K, Giugliano D. Effect of atorvastatin and irbesartan, alone and in combination, on postprandial endothelial dysfunction, oxidative stress, and inflammation in type 2 diabetic patients. Circulation. 2005;111(19):2518–24. doi:10.1161/01.CIR.0000165070.46111.9F.
104. Smith Jr SC, Benjamin EJ, Bonow RO, Braun LT, Creager MA, Franklin BA, Gibbons RJ, Grundy SM, Hiratzka LF, Jones DW, Lloyd-Jones DM, Minissian M, Mosca L, Peterson ED, Sacco RL, Spertus J, Stein JH, Taubert KA, World Heart F, the Preventive Cardiovascular Nurses A. AHA/ACCF Secondary Prevention and Risk Reduction Therapy for Patients with Coronary and other Atherosclerotic Vascular Disease: 2011 update: a guideline from the American Heart Association and American College of Cardiology Foundation. Circulation. 2011;124(22):2458–73. doi:10.1161/CIR.0b013e318235eb4d.
105. Bonetti PO, Lerman LO, Napoli C, Lerman A. Statin effects beyond lipid lowering – are they clinically relevant? Eur Heart J. 2003;24(3):225–48.
106. Reriani MK, Dunlay SM, Gupta B, West CP, Rihal CS, Lerman LO, Lerman A. Effects of statins on coronary and peripheral endothelial function in humans: a systematic review and meta-analysis of randomized controlled trials. Eur J Cardiovasc Prev Rehabil. 2011;18(5):704–16. doi:10.1177/1741826711398430.
107. Vita JA, Yeung AC, Winniford M, Hodgson JM, Treasure CB, Klein JL, Werns S, Kern M, Plotkin D, Shih WJ, Mitchel Y, Ganz P. Effect of

cholesterol-lowering therapy on coronary endothelial vasomotor function in patients with coronary artery disease. Circulation. 2000;102(8):846–51.
108. Drexler H, Zeiher AM, Meinzer K, Just H. Correction of endothelial dysfunction in coronary microcirculation of hypercholesterolaemic patients by L-arginine. Lancet. 1991;338(8782–8783):1546–50.
109. Lerman A, Burnett Jr JC, Higano ST, McKinley LJ, Holmes Jr DR. Long-term L-arginine supplementation improves small-vessel coronary endothelial function in humans. Circulation. 1998;97(21):2123–8.
110. Barter PJ, Caulfield M, Eriksson M, Grundy SM, Kastelein JJ, Komajda M, Lopez-Sendon J, Mosca L, Tardif JC, Waters DD, Shear CL, Revkin JH, Buhr KA, Fisher MR, Tall AR, Brewer B, Investigators I. Effects of torcetrapib in patients at high risk for coronary events. N Engl J Med. 2007;357(21):2109–22. doi:10.1056/NEJMoa0706628.
111. Simic B, Hermann M, Shaw SG, Bigler L, Stalder U, Dorries C, Besler C, Luscher TF, Ruschitzka F. Torcetrapib impairs endothelial function in hypertension. Eur Heart J. 2012;33(13):1615–24. doi:10.1093/eurheartj/ehr348.
112. Luscher TF, Taddei S, Kaski JC, Jukema JW, Kallend D, Munzel T, Kastelein JJ, Deanfield JE, Dal VI. Vascular effects and safety of dalcetrapib in patients with or at risk of coronary heart disease: the dal-VESSEL randomized clinical trial. Eur Heart J. 2012;33(7):857–65. doi:10.1093/eurheartj/ehs019.
113. Schwartz GG, Olsson AG, Abt M, Ballantyne CM, Barter PJ, Brumm J, Chaitman BR, Holme IM, Kallend D, Leiter LA, Leitersdorf E, McMurray JJ, Mundl H, Nicholls SJ, Shah PK, Tardif JC, Wright RS, Dal OI. Effects of dalcetrapib in patients with a recent acute coronary syndrome. N Engl J Med. 2012;367(22):2089–99. doi:10.1056/NEJMoa1206797.
114. Cannon CP, Shah S, Dansky HM, Davidson M, Brinton EA, Gotto AM, Stepanavage M, Liu SX, Gibbons P, Ashraf TB, Zafarino J, Mitchel Y, Barter P, Determining the E, Tolerability I. Safety of anacetrapib in patients with or at high risk for coronary heart disease. N Engl J Med. 2010;363(25):2406–15. doi:10.1056/NEJMoa1009744.
115. Hooper L, Thompson RL, Harrison RA, Summerbell CD, Moore H, Worthington HV, Durrington PN, Ness AR, Capps NE, Davey Smith G, Riemersma RA, Ebrahim SB. Omega 3 fatty acids for prevention and treatment of cardiovascular disease. Cochrane Database Syst Rev. 2004;4, CD003177. doi:10.1002/14651858.CD003177.pub2.
116. Hu FB, Bronner L, Willett WC, Stampfer MJ, Rexrode KM, Albert CM, Hunter D, Manson JE. Fish and omega-3 fatty acid intake and risk of coronary heart disease in women. JAMA. 2002;287(14):1815–21.
117. He K, Song Y, Daviglus ML, Liu K, Van Horn L, Dyer AR, Greenland P. Accumulated evidence on fish consumption and coronary heart disease mortality: a meta-analysis of cohort studies. Circulation. 2004;109(22):2705–11. doi:10.1161/01.CIR.0000132503.19410.6B.
118. Casula M, Soranna D, Catapano AL, Corrao G. Long-term effect of high dose omega-3 fatty acid supplementation for secondary prevention of cardiovascular outcomes: a meta-analysis of randomized, placebo controlled trials [corrected]. Atheroscler Suppl. 2013;14(2):243–51. doi:10.1016/S1567-5688(13)70005-9.
119. Wang Q, Liang X, Wang L, Lu X, Huang J, Cao J, Li H, Gu D. Effect of omega-3 fatty acids supplementation on endothelial function: a meta-analysis of randomized controlled trials. Atherosclerosis. 2012;221(2):536–43. doi:10.1016/j.atherosclerosis.2012.01.006.
120. He K, Liu K, Daviglus ML, Jenny NS, Mayer-Davis E, Jiang R, Steffen L, Siscovick D, Tsai M, Herrington D. Associations of dietary long-chain n-3 polyunsaturated fatty acids and fish with biomarkers of inflammation and endothelial activation (from the Multi-Ethnic Study of Atherosclerosis [MESA]). Am J Cardiol. 2009;103(9):1238–43. doi:10.1016/j.amjcard.2009.01.016.
121. Egert S, Stehle P. Impact of n-3 fatty acids on endothelial function: results from human interventions studies. Curr Opin Clin Nutr Metab Care. 2011;14(2):121–31. doi:10.1097/MCO.0b013e3283439622.
122. Finn AV, Nakano M, Narula J, Kolodgie FD, Virmani R. Concept of vulnerable/unstable plaque. Arterioscler Thromb Vasc Biol. 2010;30(7):1282–92. doi:10.1161/ATVBAHA.108.179739.
123. Hakkinen T, Luoma JS, Hiltunen MO, Macphee CH, Milliner KJ, Patel L, Rice SQ, Tew DG, Karkola K, Yla-Herttuala S. Lipoprotein-associated phospholipase A(2), platelet-activating factor acetylhydrolase, is expressed by macrophages in human and rabbit atherosclerotic lesions. Arterioscler Thromb Vasc Biol. 1999;19(12):2909–17.
124. Kolodgie FD, Burke AP, Skorija KS, Ladich E, Kutys R, Makuria AT, Virmani R. Lipoprotein-associated phospholipase A2 protein expression in the natural progression of human coronary atherosclerosis. Arterioscler Thromb Vasc Biol. 2006;26(11):2523–9. doi:10.1161/01.ATV.0000244681.72738.bc.
125. Schaloske RH, Dennis EA. The phospholipase A2 superfamily and its group numbering system. Biochim Biophys Acta. 2006;1761(11):1246–59. doi:10.1016/j.bbalip.2006.07.011.
126. Lavi S, McConnell JP, Rihal CS, Prasad A, Mathew V, Lerman LO, Lerman A. Local production of lipoprotein-associated phospholipase A2 and lysophosphatidylcholine in the coronary circulation: association with early coronary atherosclerosis and endothelial dysfunction in humans. Circulation. 2007;115(21):2715–21. doi:10.1161/CIRCULATIONAHA.106.671420.
127. Yang EH, McConnell JP, Lennon RJ, Barsness GW, Pumper G, Hartman SJ, Rihal CS, Lerman LO, Lerman A. Lipoprotein-associated phospholipase A2 is an independent marker for coronary endothelial dysfunction in humans. Arterioscler Thromb Vasc Biol. 2006;26(1):106–11. doi:10.1161/01.ATV.0000191655.87296.ab.
128. Garg PK, McClelland RL, Jenny NS, Criqui M, Liu K, Polak JF, Jorgensen NW, Cushman M. Association of lipoprotein-associated phospholipase A(2) and endothelial function in the Multi-Ethnic Study of Atherosclerosis (MESA). Vasc Med. 2011;16(4):247–52. doi:10.1177/1358863X11411360.
129. Investigators S, White HD, Held C, Stewart R, Tarka E, Brown R, Davies RY, Budaj A, Harrington RA, Steg PG, Ardissino D, Armstrong PW, Avezum A, Aylward PE, Bryce A, Chen H, Chen MF, Corbalan R, Dalby AJ, Danchin N, De Winter RJ, Denchev S, Diaz R, Elisaf M, Flather MD, Goudev AR, Granger CB, Grinfeld L, Hochman JS, Husted S, Kim HS, Koenig W, Linhart A, Lonn E, Lopez-Sendon J, Manolis AJ, Mohler 3rd ER, Nicolau JC, Pais P, Parkhomenko A, Pedersen TR, Pella D, Ramos-Corrales MA, Ruda M, Sereg M, Siddique S, Sinnaeve P, Smith P, Sritara P, Swart HP, Sy RG, Teramoto T, Tse HF, Watson D, Weaver WD, Weiss R, Viigimaa M, Vinereanu D, Zhu J, Cannon CP, Wallentin L. Darapladib for preventing ischemic events in stable coronary heart disease. N Engl J Med. 2014;370(18):1702–11. doi:10.1056/NEJMoa1315878.
130. O'Donoghue ML, Braunwald E, White HD, Lukas MA, Tarka E, Steg PG, Hochman JS, Bode C, Maggioni AP, Im K, Shannon JB, Davies RY, Murphy SA, Crugnale SE, Wiviott SD, Bonaca MP, Watson DF, Weaver WD, Serruys PW, Cannon CP, Investigators S-T, Steen DL. Effect of darapladib on major coronary events after an acute coronary syndrome: the SOLID-TIMI 52 randomized clinical trial. Jama. 2014;312(10):1006–15. doi:10.1001/jama.2014.11061.
131. Robinson JG, Farnier M, Krempf M, Bergeron J, Luc G, Averna M, Stroes ES, Langslet G, Raal FJ, El Shahawy M, Koren MJ, Lepor NE, Lorenzato C, Pordy R, Chaudhari U, Kastelein JJ, Investigators OLT. Efficacy and safety of alirocumab in reducing lipids and cardiovascular events. N Engl J Med. 2015;372(16):1489–99. doi:10.1056/NEJMoa1501031.
132. Sabatine MS, Giugliano RP, Wiviott SD, Raal FJ, Blom DJ, Robinson J, Ballantyne CM, Somaratne R, Legg J, Wasserman SM, Scott R, Koren MJ, Stein EA, Open-Label Study of Long-Term Evaluation against LDLCI. Efficacy and safety of evolocumab in reducing lipids and cardiovascular events. N Engl J Med. 2015;372(16):1500–9. doi:10.1056/NEJMoa1500858.
133. Wu CY, Tang ZH, Jiang L, Li XF, Jiang ZS, Liu LS. PCSK9 siRNA inhibits HUVEC apoptosis induced by ox-LDL via Bcl/Bax-caspase9-caspase3 pathway. Mol Cell Biochem. 2012;359(1–2):347–58. doi:10.1007/s11010-011-1028-6.
134. Feingold KR, Moser AH, Shigenaga JK, Patzek SM, Grunfeld C. Inflammation stimulates the expression of PCSK9. Biochem Biophys Res Commun. 2008;374(2):341–4. doi:10.1016/j.bbrc.2008.07.023.
135. Urban D, Poss J, Bohm M, Laufs U. Targeting the proprotein convertase subtilisin/kexin type 9 for the treatment of dyslipidemia and atherosclerosis. J Am Coll Cardiol. 2013;62(16):1401–8. doi:10.1016/j.jacc.2013.07.056.

136. Nitenberg A, Valensi P, Sachs R, Dali M, Aptecar E, Attali JR. Impairment of coronary vascular reserve and ACh-induced coronary vasodilation in diabetic patients with angiographically normal coronary arteries and normal left ventricular systolic function. Diabetes. 1993;42(7):1017–25.
137. Nahser Jr PJ, Brown RE, Oskarsson H, Winniford MD, Rossen JD. Maximal coronary flow reserve and metabolic coronary vasodilation in patients with diabetes mellitus. Circulation. 1995;91(3):635–40.
138. Pitkanen OP, Nuutila P, Raitakari OT, Ronnemaa T, Koskinen PJ, Iida H, Lehtimaki TJ, Laine HK, Takala T, Viikari JS, Knuuti J. Coronary flow reserve is reduced in young men with IDDM. Diabetes. 1998;47(2):248–54.
139. Di Carli MF, Janisse J, Grunberger G, Ager J. Role of chronic hyperglycemia in the pathogenesis of coronary microvascular dysfunction in diabetes. J Am Coll Cardiol. 2003;41(8):1387–93.
140. Hamilton SJ, Watts GF. Endothelial dysfunction in diabetes: pathogenesis, significance, and treatment. Rev Diabet Stud. 2013;10(2–3):133–56. doi:10.1900/RDS.2013.10.133.
141. Tabit CE, Chung WB, Hamburg NM, Vita JA. Endothelial dysfunction in diabetes mellitus: molecular mechanisms and clinical implications. Rev Endocr Metab Disord. 2010;11(1):61–74. doi:10.1007/s11154-010-9134-4.
142. Chew GT, Watts GF. Coenzyme Q10 and diabetic endotheliopathy: oxidative stress and the 'recoupling hypothesis'. QJM. 2004;97(8):537–48. doi:10.1093/qjmed/hch089.
143. Dandona P, Aljada A, Chaudhuri A, Mohanty P. Endothelial dysfunction, inflammation and diabetes. Rev Endocr Metab Disord. 2004;5(3):189–97. doi:10.1023/B:REMD.0000032407.88070.0a.
144. Dandona P, Chaudhuri A, Aljada A. Endothelial dysfunction and hypertension in diabetes mellitus. Med Clin North Am. 2004;88(4):911–31. doi:10.1016/j.mcna.2004.04.006, x–xi.
145. Arcaro G, Zamboni M, Rossi L, Turcato E, Covi G, Armellini F, Bosello O, Lechi A. Body fat distribution predicts the degree of endothelial dysfunction in uncomplicated obesity. Int J Obes Relat Metab Disord. 1999;23(9):936–42.
146. Nappo F, Esposito K, Cioffi M, Giugliano G, Molinari AM, Paolisso G, Marfella R, Giugliano D. Postprandial endothelial activation in healthy subjects and in type 2 diabetic patients: role of fat and carbohydrate meals. J Am Coll Cardiol. 2002;39(7):1145–50.
147. Shige H, Ishikawa T, Suzukawa M, Ito T, Nakajima K, Higashi K, Ayaori M, Tabata S, Ohsuzu F, Nakamura H. Endothelium-dependent flow-mediated vasodilation in the postprandial state in type 2 diabetes mellitus. Am J Cardiol. 1999;84(10):1272–4, A1279.
148. Steinberg HO, Brechtel G, Johnson A, Fineberg N, Baron AD. Insulin-mediated skeletal muscle vasodilation is nitric oxide dependent. A novel action of insulin to increase nitric oxide release. J Clin Invest. 1994;94(3):1172–9. doi:10.1172/JCI117433.
149. Kim JA, Montagnani M, Koh KK, Quon MJ. Reciprocal relationships between insulin resistance and endothelial dysfunction: molecular and pathophysiological mechanisms. Circulation. 2006;113(15):1888–904. doi:10.1161/CIRCULATIONAHA.105.563213.
150. Cersosimo E, DeFronzo RA. Insulin resistance and endothelial dysfunction: the road map to cardiovascular diseases. Diabetes Metab Res Rev. 2006;22(6):423–36. doi:10.1002/dmrr.634.
151. Lteif A, Vaishnava P, Baron AD, Mather KJ. Endothelin limits insulin action in obese/insulin-resistant humans. Diabetes. 2007;56(3):728–34. doi:10.2337/db06-1406.
152. Duncan ER, Walker SJ, Ezzat VA, Wheatcroft SB, Li JM, Shah AM, Kearney MT. Accelerated endothelial dysfunction in mild prediabetic insulin resistance: the early role of reactive oxygen species. Am J Physiol Endocrinol Metab. 2007;293(5):E1311–9. doi:10.1152/ajpendo.00299.2007.
153. Kearney MT, Duncan ER, Kahn M, Wheatcroft SB. Insulin resistance and endothelial cell dysfunction: studies in mammalian models. Exp Physiol. 2008;93(1):158–63. doi:10.1113/expphysiol.2007.039172.
154. Steinberg HO, Chaker H, Leaming R, Johnson A, Brechtel G, Baron AD. Obesity/insulin resistance is associated with endothelial dysfunction. Implications for the syndrome of insulin resistance. J Clin Invest. 1996;97(11):2601–10. doi:10.1172/JCI118709.
155. Han KA, Patel Y, Lteif AA, Chisholm R, Mather KJ. Contributions of dysglycaemia, obesity, and insulin resistance to impaired endothelium-dependent vasodilation in humans. Diabetes Metab Res Rev. 2011;27(4):354–61. doi:10.1002/dmrr.1183.
156. Muniyappa R, Sowers JR. Role of insulin resistance in endothelial dysfunction. Rev Endocr Metab Disord. 2013;14(1):5–12. doi:10.1007/s11154-012-9229-1.
157. Cavallo Perin P, Pacini G, Giunti S, Comune M, Conte MR, Cassader M, Pagano G. Microvascular angina (cardiological syndrome X) per se is not associated with hyperinsulinaemia or insulin resistance. Eur J Clin Invest. 2000;30(6):481–6.
158. Jadhav S, Ferrell W, Greer IA, Petrie JR, Cobbe SM, Sattar N. Effects of metformin on microvascular function and exercise tolerance in women with angina and normal coronary arteries: a randomized, double-blind, placebo-controlled study. J Am Coll Cardiol. 2006;48(5):956–63. doi:10.1016/j.jacc.2006.04.088.
159. Prior JO, Quinones MJ, Hernandez-Pampaloni M, Facta AD, Schindler TH, Sayre JW, Hsueh WA, Schelbert HR. Coronary circulatory dysfunction in insulin resistance, impaired glucose tolerance, and type 2 diabetes mellitus. Circulation. 2005;111(18):2291–8. doi:10.1161/01.CIR.0000164232.62768.51.
160. Mathewkutty S, McGuire DK. Platelet perturbations in diabetes: implications for cardiovascular disease risk and treatment. Expert Rev Cardiovasc Ther. 2009;7(5):541–9. doi:10.1586/erc.09.30.
161. Libby P, Plutzky J. Inflammation in diabetes mellitus: role of peroxisome proliferator-activated receptor-alpha and peroxisome proliferator-activated receptor-gamma agonists. Am J Cardiol. 2007;99(4A):27B–40. doi:10.1016/j.amjcard.2006.11.004.
162. Standards of medical care in diabetes--2010. Diabet Care. 2010;33 Suppl 1:S11–61. doi:10.2337/dc10-S011.
163. Intensive blood-glucose control with sulphonylureas or insulin compared with conventional treatment and risk of complications in patients with type 2 diabetes (UKPDS 33). UK Prospective Diabetes Study (UKPDS) Group. Lancet. 1998;352(9131):837–53.
164. Maiorana A, O'Driscoll G, Cheetham C, Dembo L, Stanton K, Goodman C, Taylor R, Green D. The effect of combined aerobic and resistance exercise training on vascular function in type 2 diabetes. J Am Coll Cardiol. 2001;38(3):860–6.
165. Reboussin DM, Goff Jr DC, Lipkin EW, Herrington DM, Summerson J, Steffes M, Crouse 3rd RJ, Jovanovic L, Feinglos MN, Probstfield JL, Banerji MA, Pettitt DJ, Williamson J. The combination oral and nutritional treatment of late-onset diabetes mellitus (CONTROL DM) trial results. Diabet Med. 2004;21(10):1082–9. doi:10.1111/j.1464-5491.2004.01289.x.
166. Cortigiani L, Rigo F, Gherardi S, Sicari R, Galderisi M, Bovenzi F, Picano E. Additional prognostic value of coronary flow reserve in diabetic and nondiabetic patients with negative dipyridamole stress echocardiography by wall motion criteria. J Am Coll Cardiol. 2007;50(14):1354–61. doi:10.1016/j.jacc.2007.06.027.
167. Erdogan D, Akcay S, Yucel H, Ersoy IH, Icli A, Kutlucan A, Arslan A, Yener M, Ozaydin M, Tamer MN. The effects of good glycaemic control on left ventricular and coronary endothelial functions in patients with poorly controlled Type 2 diabetes mellitus. Clin Endocrinol (Oxf). 2014. doi:10.1111/cen.12520.
168. Li YJ, Hyun MH, Rha SW, Chen KY, Jin Z, Dang Q, Park CM, Lee JE, Park JY, Choi CU, Na JO, Lim HE, Kim JW, Kim EJ, Park CG, Seo HS, Oh DJ. Diabetes mellitus is not a risk factor for coronary artery spasm as assessed by an intracoronary acetylcholine provocation test: angiographic and clinical characteristics of 986 patients. J Invasive Cardiol. 2014;26(6):234–9.
169. Ryden L, Grant PJ, Anker SD, Berne C, Cosentino F, Danchin N, Deaton C, Escaned J, Hammes HP, Huikuri H, Marre M, Marx N, Mellbin L, Ostergren J, Patrono C, Seferovic P, Sousa Uva M, Taskinen MR, Tendera M, Tuomilehto J, Valensi P, Zamorano JL. ESC guidelines on diabetes, pre-diabetes and diseases of the cardiovascular system

developed in cooperation with the EASD. Kardiol Pol. 2013;71 Suppl 11:S319–94. doi:10.5603/KP.2013.0289.
170. Monnier L, Mas E, Ginet C, Michel F, Villon L, Cristol JP, Colette C. Activation of oxidative stress by acute glucose fluctuations compared with sustained chronic hyperglycemia in patients with type 2 diabetes. JAMA. 2006;295(14):1681–7. doi:10.1001/jama.295.14.1681.
171. Ceriello A, Esposito K, Piconi L, Ihnat MA, Thorpe JE, Testa R, Boemi M, Giugliano D. Oscillating glucose is more deleterious to endothelial function and oxidative stress than mean glucose in normal and type 2 diabetic patients. Diabetes. 2008;57(5):1349–54. doi:10.2337/db08-0063.
172. Torimoto K, Okada Y, Mori H, Tanaka Y. Relationship between fluctuations in glucose levels measured by continuous glucose monitoring and vascular endothelial dysfunction in type 2 diabetes mellitus. Cardiovasc Diabetol. 2013;12:1. doi:10.1186/1475-2840-12-1.
173. Vehkavaara S, Yki-Jarvinen H. 3.5 years of insulin therapy with insulin glargine improves in vivo endothelial function in type 2 diabetes. Arterioscler Thromb Vasc Biol. 2004;24(2):325–30. doi:10.1161/01.ATV.0000113817.48983.c5.
174. Antoniades C, Tousoulis D, Marinou K, Papageorgiou N, Bosinakou E, Tsioufis C, Stefanadi E, Latsios G, Tentolouris C, Siasos G, Stefanadis C. Effects of insulin dependence on inflammatory process, thrombotic mechanisms and endothelial function, in patients with type 2 diabetes mellitus and coronary atherosclerosis. Clin Cardiol. 2007;30(6):295–300. doi:10.1002/clc.20101.
175. Potenza MA, Gagliardi S, Nacci C, Carratu MR, Montagnani M. Endothelial dysfunction in diabetes: from mechanisms to therapeutic targets. Curr Med Chem. 2009;16(1):94–112.
176. Rask-Madsen C, King GL. Mechanisms of Disease: endothelial dysfunction in insulin resistance and diabetes. Nat Clin Pract Endocrinol Metab. 2007;3(1):46–56. doi:10.1038/ncpendmet0366.
177. Nathanson D, Nystrom T. Hypoglycemic pharmacological treatment of type 2 diabetes: targeting the endothelium. Mol Cell Endocrinol. 2009;297(1–2):112–26. doi:10.1016/j.mce.2008.11.016.
178. Mather KJ, Verma S, Anderson TJ. Improved endothelial function with metformin in type 2 diabetes mellitus. J Am Coll Cardiol. 2001;37(5):1344–50.
179. Pitocco D, Zaccardi F, Tarzia P, Milo M, Scavone G, Rizzo P, Pagliaccia F, Nerla R, Di Franco A, Manto A, Rocca B, Lanza GA, Crea F, Ghirlanda G. Metformin improves endothelial function in type 1 diabetic subjects: a pilot, placebo-controlled randomized study. Diabetes Obes Metab. 2013;15(5):427–31. doi:10.1111/dom.12041.
180. Jensterle M, Sebestjen M, Janez A, Prezelj J, Kocjan T, Keber I, Pfeifer M. Improvement of endothelial function with metformin and rosiglitazone treatment in women with polycystic ovary syndrome. Eur J Endocrinol. 2008;159(4):399–406. doi:10.1530/EJE-08-0507.
181. Vitale C, Mercuro G, Cornoldi A, Fini M, Volterrani M, Rosano GM. Metformin improves endothelial function in patients with metabolic syndrome. J Intern Med. 2005;258(3):250–6. doi:10.1111/j.1365-2796.2005.01531.x.
182. de Aguiar LG, Bahia LR, Villela N, Laflor C, Sicuro F, Wiernsperger N, Bottino D, Bouskela E. Metformin improves endothelial vascular reactivity in first-degree relatives of type 2 diabetic patients with metabolic syndrome and normal glucose tolerance. Diabetes Care. 2006;29(5):1083–9. doi:10.2337/diacare.2951083.
183. Kelly AS, Bergenstal RM, Gonzalez-Campoy JM, Katz H, Bank AJ. Effects of exenatide vs. metformin on endothelial function in obese patients with pre-diabetes: a randomized trial. Cardiovasc Diabetol. 2012;11:64. doi:10.1186/1475-2840-11-64.
184. Natali A, Baldeweg S, Toschi E, Capaldo B, Barbaro D, Gastaldelli A, Yudkin JS, Ferrannini E. Vascular effects of improving metabolic control with metformin or rosiglitazone in type 2 diabetes. Diabetes Care. 2004;27(6):1349–57.
185. Phung OJ, Schwartzman E, Allen RW, Engel SS, Rajpathak SN. Sulphonylureas and risk of cardiovascular disease: systematic review and meta-analysis. Diabet Med. 2013;30(10):1160–71. doi:10.1111/dme.12232.
186. Hemmingsen B, Schroll JB, Lund SS, Wetterslev J, Gluud C, Vaag A, Sonne DP, Lundstrom LH, Almdal T. Sulphonylurea monotherapy for patients with type 2 diabetes mellitus. Cochrane Database Syst Rev. 2013;4, CD009008. doi:10.1002/14651858.CD009008.pub2.
187. Rakel A, Renier G, Roussin A, Buithieu J, Mamputu JC, Serri O. Beneficial effects of gliclazide modified release compared with glibenclamide on endothelial activation and low-grade inflammation in patients with type 2 diabetes. Diabetes Obes Metab. 2007;9(1):127–9. doi:10.1111/j.1463-1326.2006.00571.x.
188. Riveline JP, Danchin N, Ledru F, Varroud-Vial M, Charpentier G. Sulfonylureas and cardiovascular effects: from experimental data to clinical use. Available data in humans and clinical applications. Diabetes Metab. 2003;29(3):207–22.
189. Yki-Jarvinen H. Thiazolidinediones. N Engl J Med. 2004;351(11):1106–18. doi:10.1056/NEJMra041001.
190. Ryan MJ, Didion SP, Mathur S, Faraci FM, Sigmund CD. PPAR(gamma) agonist rosiglitazone improves vascular function and lowers blood pressure in hypertensive transgenic mice. Hypertension. 2004;43(3):661–6. doi:10.1161/01.HYP.0000116303.71408.c2.
191. Hwang J, Kleinhenz DJ, Lassegue B, Griendling KK, Dikalov S, Hart CM. Peroxisome proliferator-activated receptor-gamma ligands regulate endothelial membrane superoxide production. Am J Physiol Cell Physiol. 2005;288(4):C899–905. doi:10.1152/ajpcell.00474.2004.
192. Calnek DS, Mazzella L, Roser S, Roman J, Hart CM. Peroxisome proliferator-activated receptor gamma ligands increase release of nitric oxide from endothelial cells. Arterioscler Thromb Vasc Biol. 2003;23(1):52–7.
193. Pistrosch F, Passauer J, Fischer S, Fuecker K, Hanefeld M, Gross P. In type 2 diabetes, rosiglitazone therapy for insulin resistance ameliorates endothelial dysfunction independent of glucose control. Diabetes Care. 2004;27(2):484–90.
194. Martens FM, Visseren FL, de Koning EJ, Rabelink TJ. Short-term pioglitazone treatment improves vascular function irrespective of metabolic changes in patients with type 2 diabetes. J Cardiovasc Pharmacol. 2005;46(6):773–8.
195. Campia U, Matuskey LA, Panza JA. Peroxisome proliferator-activated receptor-gamma activation with pioglitazone improves endothelium-dependent dilation in nondiabetic patients with major cardiovascular risk factors. Circulation. 2006;113(6):867–75. doi:10.1161/CIRCULATIONAHA.105.549618.
196. Sidhu JS, Cowan D, Kaski JC. Effects of rosiglitazone on endothelial function in men with coronary artery disease without diabetes mellitus. Am J Cardiol. 2004;94(2):151–6. doi:10.1016/j.amjcard.2004.03.051.
197. Linscheid P, Keller U, Blau N, Schaer DJ, Muller B. Diminished production of nitric oxide synthase cofactor tetrahydrobiopterin by rosiglitazone in adipocytes. Biochem Pharmacol. 2003;65(4):593–8.
198. Lincoff AM, Wolski K, Nicholls SJ, Nissen SE. Pioglitazone and risk of cardiovascular events in patients with type 2 diabetes mellitus: a meta-analysis of randomized trials. JAMA. 2007;298(10):1180–8. doi:10.1001/jama.298.10.1180.
199. Nissen SE, Wolski K. Effect of rosiglitazone on the risk of myocardial infarction and death from cardiovascular causes. N Engl J Med. 2007;356(24):2457–71. doi:10.1056/NEJMoa072761.
200. Home PD, Pocock SJ, Beck-Nielsen H, Curtis PS, Gomis R, Hanefeld M, Jones NP, Komajda M, McMurray JJ, Team RS. Rosiglitazone evaluated for cardiovascular outcomes in oral agent combination therapy for type 2 diabetes (RECORD): a multicentre, randomised, open-label trial. Lancet. 2009;373(9681):2125–35. doi:10.1016/S0140-6736(09)60953-3.
201. Singh S, Loke YK, Furberg CD. Long-term risk of cardiovascular events with rosiglitazone: a meta-analysis. JAMA. 2007;298(10):1189–95. doi:10.1001/jama.298.10.1189.
202. Dormandy JA, Charbonnel B, Eckland DJ, Erdmann E, Massi-Benedetti M, Moules IK, Skene AM, Tan MH, Lefebvre PJ, Murray GD, Standl E, Wilcox RG, Wilhelmsen L, Betteridge J, Birkeland K, Golay A,

Heine RJ, Koranyi L, Laakso M, Mokan M, Norkus A, Pirags V, Podar T, Scheen A, Scherbaum W, Schernthaner G, Schmitz O, Skrha J, Smith U, Taton J, Investigators PR. Secondary prevention of macrovascular events in patients with type 2 diabetes in the PROactive Study (PROspective pioglitAzone Clinical Trial In macroVascular Events): a randomised controlled trial. Lancet. 2005;366(9493):1279–89. doi:10.1016/S0140-6736(05)67528-9.

203. Standl E, Schnell O, Ceriello A. Postprandial hyperglycemia and glycemic variability: should we care? Diabetes Care. 2011;34 Suppl 2:S120–7. doi:10.2337/dc11-s206.
204. Chiasson JL, Josse RG, Gomis R, Hanefeld M, Karasik A, Laakso M, Group S-NTR. Acarbose for prevention of type 2 diabetes mellitus: the STOP-NIDDM randomised trial. Lancet. 2002;359(9323):2072–7. doi:10.1016/S0140-6736(02)08905-5.
205. Raz I, Wilson PW, Strojek K, Kowalska I, Bozikov V, Gitt AK, Jermendy G, Campaigne BN, Kerr L, Milicevic Z, Jacober SJ. Effects of prandial versus fasting glycemia on cardiovascular outcomes in type 2 diabetes: the HEART2D trial. Diabetes Care. 2009;32(3):381–6. doi:10.2337/dc08-1671.
206. Group NS, Holman RR, Haffner SM, McMurray JJ, Bethel MA, Holzhauer B, Hua TA, Belenkov Y, Boolell M, Buse JB, Buckley BM, Chacra AR, Chiang FT, Charbonnel B, Chow CC, Davies MJ, Deedwania P, Diem P, Einhorn D, Fonseca V, Fulcher GR, Gaciong Z, Gaztambide S, Giles T, Horton E, Ilkova H, Jenssen T, Kahn SE, Krum H, Laakso M, Leiter LA, Levitt NS, Mareev V, Martinez F, Masson C, Mazzone T, Meaney E, Nesto R, Pan C, Prager R, Raptis SA, Rutten GE, Sandstroem H, Schaper F, Scheen A, Schmitz O, Sinay I, Soska V, Stender S, Tamas G, Tognoni G, Tuomilehto J, Villamil AS, Vozar J, Califf RM. Effect of nateglinide on the incidence of diabetes and cardiovascular events. N Engl J Med. 2010;362(16):1463–76. doi:10.1056/NEJMoa1001122.
207. Shimabukuro M, Higa N, Chinen I, Yamakawa K, Takasu N. Effects of a single administration of acarbose on postprandial glucose excursion and endothelial dysfunction in type 2 diabetic patients: a randomized crossover study. J Clin Endocrinol Metab. 2006;91(3):837–42. doi:10.1210/jc.2005-1566.
208. Wascher TC, Schmoelzer I, Wiegratz A, Stuehlinger M, Mueller-Wieland D, Kotzka J, Enderle M. Reduction of postchallenge hyperglycaemia prevents acute endothelial dysfunction in subjects with impaired glucose tolerance. Eur J Clin Invest. 2005;35(9):551–7. doi:10.1111/j.1365-2362.2005.01550.x.
209. Pistrosch F, Schaper F, Passauer J, Koehler C, Bornstein SR, Hanefeld M. Effects of the alpha glucosidase inhibitor acarbose on endothelial function after a mixed meal in newly diagnosed type 2 diabetes. Hormone Metabol Res. 2009;41(2):104–8. doi:10.1055/s-0028-1103276.
210. Ayaori M, Iwakami N, Uto-Kondo H, Sato H, Sasaki M, Komatsu T, Iizuka M, Takiguchi S, Yakushiji E, Nakaya K, Yogo M, Ogura M, Takase B, Murakami T, Ikewaki K. Dipeptidyl peptidase-4 inhibitors attenuate endothelial function as evaluated by flow-mediated vasodilatation in type 2 diabetic patients. J Am Heart Assoc. 2013;2(1), e003277. doi:10.1161/JAHA.112.003277.
211. Ban K, Noyan-Ashraf MH, Hoefer J, Bolz SS, Drucker DJ, Husain M. Cardioprotective and vasodilatory actions of glucagon-like peptide 1 receptor are mediated through both glucagon-like peptide 1 receptor-dependent and -independent pathways. Circulation. 2008;117(18):2340–50. doi:10.1161/CIRCULATIONAHA.107.739938.
212. Matsubara J, Sugiyama S, Sugamura K, Nakamura T, Fujiwara Y, Akiyama E, Kurokawa H, Nozaki T, Ohba K, Konishi M, Maeda H, Izumiya Y, Kaikita K, Sumida H, Jinnouchi H, Matsui K, Kim-Mitsuyama S, Takeya M, Ogawa H. A dipeptidyl peptidase-4 inhibitor, des-fluorositagliptin, improves endothelial function and reduces atherosclerotic lesion formation in apolipoprotein E-deficient mice. J Am Coll Cardiol. 2012;59(3):265–76. doi:10.1016/j.jacc.2011.07.053.
213. Advani A, Bugyei-Twum A, Connelly KA. Cardiovascular effects of incretins in diabetes. Canadian J Diabet. 2013;37(5):309–14. doi:10.1016/j.jcjd.2013.06.010.
214. Tesauro M, Schinzari F, Adamo A, Rovella V, Martini F, Mores N, Barini A, Pitocco D, Ghirlanda G, Lauro D, Campia U, Cardillo C. Effects of GLP-1 on forearm vasodilator function and glucose disposal during hyperinsulinemia in the metabolic syndrome. Diabetes Care. 2013;36(3):683–9. doi:10.2337/dc12-0763.
215. Nystrom T, Gutniak MK, Zhang Q, Zhang F, Holst JJ, Ahren B, Sjoholm A. Effects of glucagon-like peptide-1 on endothelial function in type 2 diabetes patients with stable coronary artery disease. Am J Physiol Endocrinol Metab. 2004;287(6):E1209–15. doi:10.1152/ajpendo.00237.2004.
216. Kubota Y, Miyamoto M, Takagi G, Ikeda T, Kirinoki-Ichikawa S, Tanaka K, Mizuno K. The dipeptidyl peptidase-4 inhibitor sitagliptin improves vascular endothelial function in type 2 diabetes. J Korean Med Sci. 2012;27(11):1364–70. doi:10.3346/jkms.2012.27.11.1364.
217. van Poppel PC, Netea MG, Smits P, Tack CJ. Vildagliptin improves endothelium-dependent vasodilatation in type 2 diabetes. Diabetes Care. 2011;34(9):2072–7. doi:10.2337/dc10-2421.
218. Matsubara J, Sugiyama S, Akiyama E, Iwashita S, Kurokawa H, Ohba K, Maeda H, Fujisue K, Yamamoto E, Kaikita K, Hokimoto S, Jinnouchi H, Ogawa H. Dipeptidyl peptidase-4 inhibitor, sitagliptin, improves endothelial dysfunction in association with its anti-inflammatory effects in patients with coronary artery disease and uncontrolled diabetes. Circ J. 2013;77(5):1337–44.

# The Coronary Circulation in Acute Coronary Syndromes

*Murat Sezer, Mauro Echavarria Pinto, Nicola Ryan, and Sabahattin Umman*




J. Escaned, J. Davies (eds.), *Physiological Assessment of Coronary Stenoses and the Microcirculation*,
DOI 10.1007/978-1-4471-5245-3_7

## 7.1 Introduction

Acute coronary syndromes constitute one of the most serious presentations of ischemic heart disease, accounting for a significant proportion of patients investigated and treated in the catheterization laboratory. When assessing both coronary stenoses and the microcirculation in the context of acute coronary syndromes (ACS), it is important to bear in mind that both ST elevation myocardial infarction (STEMI) and non-ST-elevation myocardial infarction (NSTE-ACS) are associated with distinct modifications in coronary physiology and that therefore the principles applied to their assessment in chronic stable angina may not hold true. In this chapter we discuss the pathophysiology of the microvasculature during ACS followed by a review of the benefits and limitations of physiological assessment of both epicardial stenosis and the microvasculature during ACS.



## 7.2 The Coronary Microvasculature in Acute Coronary Syndromes

### 7.2.1 ST Elevation MI (STEMI)

STEMI includes a wide variety of pathological substrates as documented by both autopsy series and intracoronary imaging studies [1, 2]. Autopsy studies and clinical studies have demonstrated that plaque rupture and superimposed thrombosis account for the majority of the cases presenting with ACS, although plaque erosion is also a frequent substrate (up to one-third of the patients) [3–6].

During STEMI, acute occlusion of an epicardial coronary artery, due to a thrombotic reaction developing in response to both plaque rupture and erosion, initiates a chain of events (ischemia and subsequent reperfusion) that eventually results in loss of viability of cardiomyocytes in the subtended myocardial territory. In parallel, changes emerge in the architectural structure of the coronary microcirculation. Timely complete and sustained reperfusion of the myocardial area at risk is the most critical step for salvaging ischemic myocardium.

Primary percutaneous coronary intervention (PPCI) is widely accepted as the most effective treatment. However, complete restoration of epicardial patency does not necessarily translate into adequate reperfusion in the microcirculation. The incidence of severe microvascular injury/obstruction post-PPCI is reported at 5–50 % depending on the method used for detection [7]. Clinically, the presence and extent of microvascular injury MVI is strongly related with impaired myocardial salvage, reduced ejection fraction, long-term adverse left ventricular remodeling, and adverse outcome [8].

Microvascular injury first develops in the infarct core and evolves spatially and temporally over time. Reopening of infarct-related artery (IRA) does not immediately terminate progressive myocardial damage in the area at risk. Consistently, the size of MVI zone has been shown to increase up to 48 h after reperfusion. Myocardial blood flow in certain MVI areas is hyperemic during the first minutes of reperfusion, but regional blood flow in the at-risk area rapidly and progressively declines and reaches a plateau within 2–8 h after reperfusion resulting in nearly threefold increase in anatomic MVI (no-reflow) zone [9].

Potential mechanisms underlying microvascular impairment and thereby myocardial malperfusion after complete restoration of epicardial blood flow by PPCI are likely to be multifactorial. After reperfusion, both intraluminal obstruction and extravascular compressive forces (mainly generated by the surrounding edematous and hemorrhagic myocardial compartment) appear to be involved in the development of microvascular impairment. Mechanisms can be classified under two general headings as intraluminal obstruction or extravascular compression (Fig. 7.1). In general, intraluminal obstructive and extravascular compressive pathologies are interconnected in the development of PPCI microvascular impairment. In the following sections, we will review the pathophysiology of microvascular impairment.

#### Role of Atherothrombotic Embolization

Atherothrombotic embolization from a culprit STEMI lesion is considered one of the leading mechanisms contributing to the occurrence of microvascular dysfunction after PPCI. Embolized particles during PPCI can cause mechanical obstruction due to their mass effect and can also activate pathways that trigger in situ coagulation and inflammatory responses in the downstream microcirculation. Atherothrombotic embolization is associated with reduced coronary flow [10], larger infarct size, and more extensive microvascular damage [11, 12].

#### Role of Circulating Blood Cells: Leucocyte, Leucocyte/Platelet Plugging and Red-Cell Aggregates

Leucocyte and platelet plugging and red-cell aggregation also contribute to intraluminal microvascular obstruction. Neutrophils worsen microvascular reperfusion by adhering to the endothelium with platelets and releasing cytokines or other factors that reduce microvascular blood flow. Significant relationships have been shown between MVO and total white blood cell count [13] and neutrophil [14] and monocyte [15] counts.

#### Role of Humoral Factors (In Situ Thrombosis) in MVI

A potential contributor to MVI may be in situ (de novo) thrombosis. In the ischemic period, hypoxic injury of the microvascular endothelium can provoke a procoagulant milieu and de novo fibrin formation at the microvascular level. Additionally, reperfusion significantly impairs t-PA release from the endothelium [16], which may further facilitate in situ thrombosis in the region where hypoxic endothelial injury occurred. Fibrinogen can also contribute to impeding flow via facilitating red blood cell aggregation and mediating the inflammatory process in the related microcirculatory region (Fig. 7.2). In favor of this hypothesis, lyses of microvascular thrombus by intracoronary

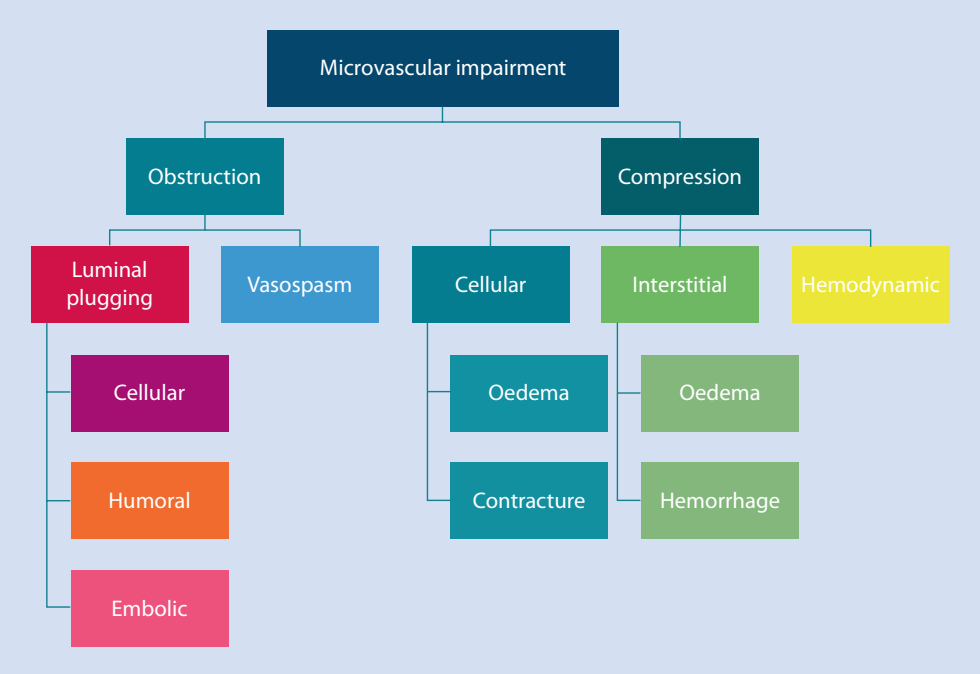


**Fig. 7.1** Potential mechanisms underlying obstruction and external compression of the microcirculation developing after PPCI

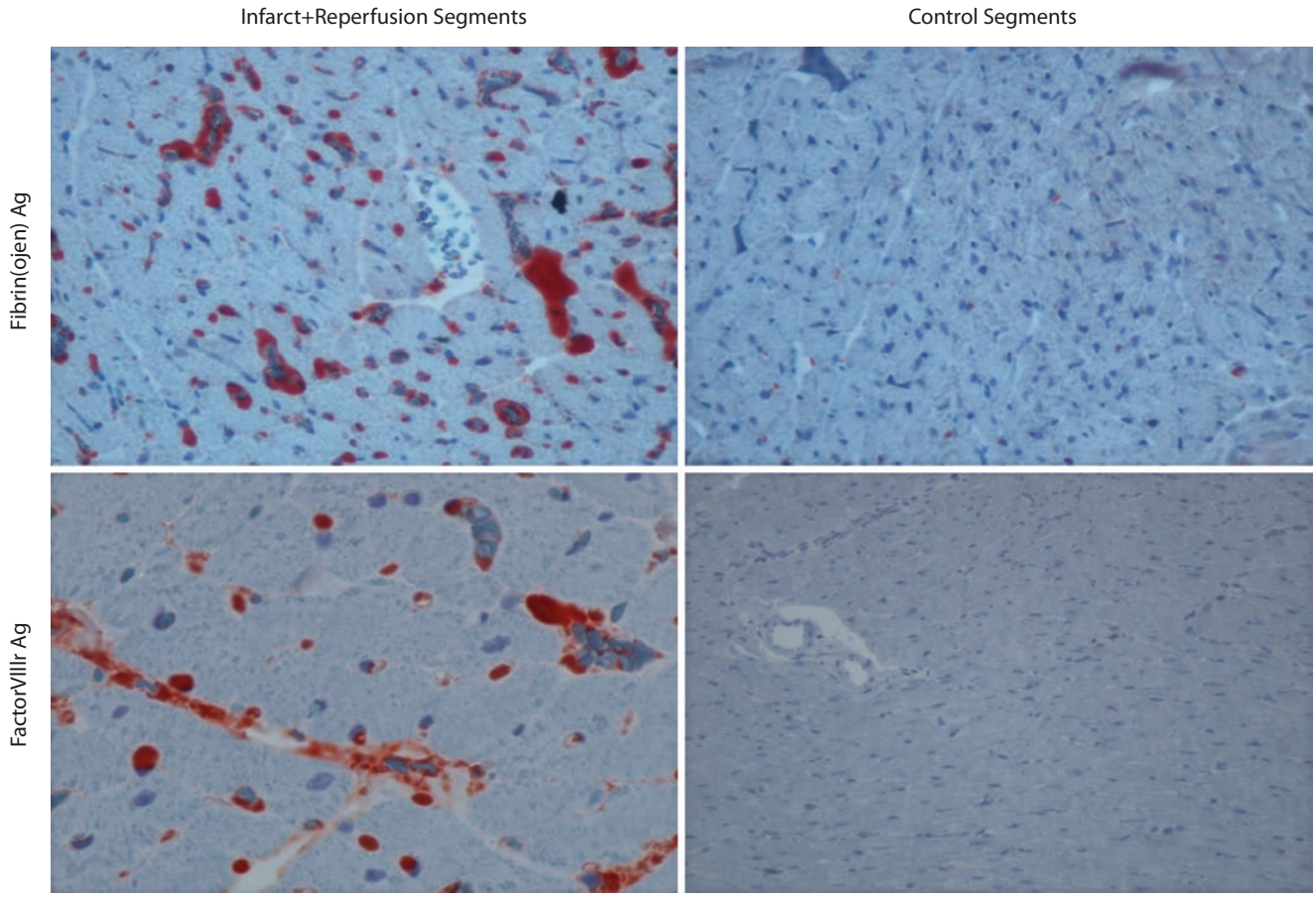


**Fig. 7.2** In situ thrombosis shown in ischemia/reperfusion model (Wistar rat's heart). Immunohistochemical staining performed for fibrin and fibrinogen (*first row*) and for platelets (*second row*). Ischemic/reperfused segments shown in the *first column* and control segments shown in the *second column*

streptokinase given immediately after PPCI resulted in significant reduction in coronary microvascular resistance and improvement in CFR [17].

## Extravascular Compression of Microcirculation

External compression of the capillary bed by myocardial edema and/or hemorrhage in the surrounding myocardium after reperfusion may lead to an increase in microvascular resistance, which eventually reduces myocardial perfusion. Post-reperfusion myocardial edema and intramyocardial hemorrhage (IMH) are both partly the cause and consequence of the microvascular injury developing after reperfusion (Fig. 7.3). The capillary bed is the most vulnerable segment for the collapse in the coronary vascular network. External compression generated by intramyocardial edema and hemorrhage causes capillaries to shrink in diameter, leading to logarithmic increase in resistance and a decrease in myocardial blood flow. Therefore, in addition to intraluminal obstruction, an important mechanism responsible for microvascular impairment after PPCI is the decreased cross-sectional microvascular area or collapse caused by external compression caused by surrounding edema and intramyocardial hemorrhage.

Hypoxia-induced disruption in endothelial barrier facilitates extravasation of blood cells upon reperfusion. Therefore, intramyocardial hemorrhage (IMH) and loss of vascular integrity are closely linked. The presence of IMH is associated with larger infarcts, and it has been repeatedly shown that patients with IMH on T2W imaging have CMR-defined MVO. Recent histological assessment explained this strong interrelationship shown between CMR-defined areas of MVO and IMH [18].

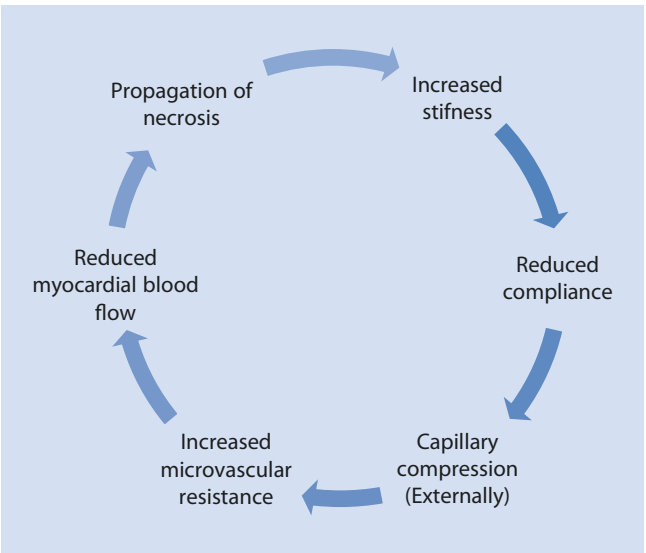


**Fig. 7.3** Interrelationship between external compression caused by myocardial edema/intramyocardial hemorrhage and microvascular impairment

Another factor that may cause microvascular obstruction by external compression is myocardial edema. Myocardial edema occurs immediately after epicardial occlusion and abruptly expands during the first minute of reperfusion. The volume of edema seems to reach its peak value on day 3 after reperfusion [19] remains unchanged over the first weeks after the acute event and decreases thereafter [20]. Tissue edema (interstitial or cellular) might substantially contribute to increase in coronary microvascular resistance by compressing the microvascular bed externally

Finally, in STEMI increased diastolic filling pressures on top of increased muscle stiffness due to cellular and interstitial edema contribute to a decrease in intramyocardial vascular capacitance and limit coronary flow in late diastole. Therefore, transmitted increased intracavitary pressure can also contribute to external compression of microcirculation particularly in the subendocardial region, which eventually results in increase microvascular resistance and reduced myocardial perfusion.

### 7.2.2 Non-ST-Elevation MI (NSTEMI)

Few studies have assessed the incidence, correlates, and/or impact of MVO in non-ST-elevation myocardial infarction (NSTEMI). In patients with NSTEMI undergoing early PCI, the frequency of MVO detected by CMR varied from 14 to 30 % [21–23]. The exact reason for the different prevalence of MVO in NSTEMI is unknown; however, it may be related to the heterogeneity of clinical presentation. Similar to STEMI, the presence of MVO in CMR is associated with infarct size in patients with NSTEMI undergoing PCI [22]. At present, it is not clear whether the pathogenesis of MVO is similar in NSTEMI and STEMI patients undergoing PCI. However, the presence of a similar fragile atherothrombotic substrate in culprit vessels in NSTEMI supports distal embolization and microvascular plugging as the leading mechanism for microvascular injury.

## 7.3 Physiological Assessment of Coronary Stenoses in ACS

### 7.3.1 Assessment of the Culprit-Vessel Stenosis

In the culprit vessel of ACS, the early post-STEMI phase is characterized by coronary vasospasm, microvascular platelet plugging, endothelial dysfunction, thrombus embolization, vascular stunning, and intramyocardial hemorrhage [24]. These dynamic changes in the infarcting myocardial bed are associated with an evolving microvascular hyperemic response, hyperemic flow, trans-stenotic pressure gradients, and as a consequence FFR values [25]. Therefore, not only

will the distant myocardial mass not respond appropriately to the hyperemic stimuli, but also the anatomical consequences of the culprit plaque can change as a result of shifting plaque geometry. Hence, the use of FFR in the culprit vessel during the hyperacute phase of STEMI is not recommended [26].

Nuclear imaging studies have observed that as early as 6 days post-infarction, FFR can reliably outline post-STEMI inducible ischemia [27, 28]. However, it is important to note that after STEMI, the mass of viable myocardium decreases in the perfused territory; therefore, for a given stenosis, hyperemic flow and trans-stenotic gradient will decrease, thus increasing the FFR [27]. This implies that the hemodynamic consequences of the culprit stenosis decrease after STEMI because the flow demand of the supplied myocardium has decreased [27]. Interestingly and in spite of this reduction in viable myocardium, a study performed in chronically infarcted territories (3.7 and 6.3 months after STEMI) observed that most culprit stenoses will still be hemodynamically significant (FFR: 0.60 ± 0.14, range 0.26–0.77) for the perfused viable mass within the infarction [29]. Finally, the FFR cutoff established for non-infarcted territories (0.75) appears dependable in infarct areas [30].

### 7.3.2 Non-culprit Stenoses in ACS: Can They Be Assessed Physiologically?

The clinical benefit of restoring patency in the culprit vessel in patients admitted for ST-segment myocardial infarction (STEMI) is well established; however, a sizable proportion of patients with ACS have bystander multivessel disease (MVD) [31]. The treatment strategy for non-culprit MVD is not well established; however, the evidence supporting the role of invasive coronary physiology indices to guide treatment of non-culprit MVD is growing. Contemporary trial such as pexelizumab in conjunction with angioplasty in acute myocardial infarction (APEX-AMI) [32] and preventative angioplasty in acute myocardial infarction (PRAMI) trial [33] have estimated the prevalence of non-culprit stenosis at 41 % and 54 %, respectively, in patients admitted for STEMI. Likewise, 30–59 % of patients admitted with NSTE-ACS have MVD [34, 35]. Occlusion of the infarct-related artery may precipitate myocardial ischemia in distant myocardial beds supplied by non-culprit stenosis, due to compensatory hyperkinesis or from a sudden lack of collateral support. This means the functional relevance of non-culprit stenosis may be difficult to determine.

Fractional flow reserve (FFR) has become the standard method to assess the physiological significance of epicardial stenoses [36]. However, the use of FFR in the setting of ACS has theoretical limitations. FFR is dependent on the ability to achieve maximal coronary flow, where resistance is minimal and constant, and blood flow is thus proportional to driving pressure. Therefore, FFR requires the achievement of maximal hyperemia to accurately characterize the ischemic potential of the epicardial stenosis. During ACS, there are several factors that might theoretically impair the hyperemic response in both culprit and non-culprit territories, and thus the achievement of maximal hyperemia, which could ultimately lead to higher FFR values [37]. Transitory microcirculatory dysfunction in non-culprit territories has been described [38], and local neurohumoral reflexes [39], vasoconstriction, and elevated LV-end diastolic pressure [40] have been proposed as underlying mechanisms. Proof-of-concept studies have suggested that FFR might underestimate stenosis severity in NSTE-ACS compared to hyperemic stenosis resistance [41, 42], which is a more specific index of epicardial stenosis severity [43].

Several studies have investigated the reliability of FFR in assessing the functional significance of non-culprit stenoses (Table 7.1) [41, 44–46]. A large study including 101 patients with ACS (75 with STEMI and 26 with NSTE-ACS) measured FFR acutely and 35 ± 4 days post-event in non-culprit vessels [44]. Notably, there was no significant difference between the acute FFR value and follow-up in patients with STEMI (0.78 ± 0.10 vs. 0.76 ± 0.10, $p$ = NS) or non-ST-segment elevation infarction (NSTEMI) (0.77 ± 0.10 vs. 0.77 ± 0.20, $p$ = NS). Importantly, in only two stenoses did an initial FFR >0.80 subsequently decreased to <0.75. 328 (32.6 %) of the patients included in FAME had NSTE-ACS [47]. In these, the use of FFR to guide PCI resulted in similar risk reduction in major adverse cardiac events (MACE) and its components, compared to patients with stable symptoms (absolute risk reduction of 5.1 % vs. 3.7 %, respectively, $p$ = 0.92) [47]. The FAMOUS-NSTEMI [48] trial (FFR vs. angiography in guiding management to optimize outcomes in NSTEMI), a prospective, multicentre, parallel group, 1:1 randomized, controlled trial that included 350 NSTEMI patients with ≥1 coronary stenosis with ≥30 % of the lumen diameter assessed visually, addressed whether routine FFR measurements in NSTEMI are feasible and safe, by comparing the management and outcomes of conventional angiography guidance ($n$ = 174) with FFR guidance ($n$ = 176). The primary endpoint, the proportion of patients treated with medical therapy, was significantly higher in the FFR-guided group [23 (13.2 %) vs. 40 (22.7 %), difference 9.5 % (95 % CI: 1.4 %, 17.7 %), $p$ = 0.022]. As secondary endpoints, the FFR-guided approach (1) resulted in changes in stenosis classification and patient management in one-fifth of patients and (2) reduced revascularization at the index procedure. Notably, revascularization remained lower in the FFR-guided group [79.0 vs. 86.8 %, difference 7.8 % (20.2 %, 15.8 %), $P$ = 0.054] at 12 months. These figures are in line with findings from a recent French FFR registry data [49] (Figs. 7.4 and 7.5).

Despite the theoretical limitations of FFR during ACS, available data supports its use as a tool to guide revascularization in bystander MVD. Deferral of revascularization based on FFR seems both cost effective and safe in this complex clinical scenario.

**Table 7.1** Diagnostic accuracy of fractional flow reserve (FFR) in acute coronary syndromes

| First author | Year | Design | Index | Study outline, objective | Clinical setting | *N*, total | *N*, ACS subset | Main findings |
|---|---|---|---|---|---|---|---|---|
| *Reliability of FFR culprit vessels* | | | | | | | | |
| De Bruyne [27] | 2001 | Diagnostic, analytical | FFR | A prior-defined comparison of FFR 0.75 cut-off against SPECT in post-MI patients | Culprit vessels of MI ≥6 days | 57 | 57 | Ss, 82 %; Sp, 87 %; Acc, 85 %; optimal FFR cut-off, 0.78 |
| Usui [33] | 2003 | Diagnostic, descriptive | FFR | FFR vs. SPECT in stable and post-MI patients | Culprit vessels <3 months | 167 | 74 | Post-MI patients: Ss, 79 %; Sp, 74 %; optimal FFR cut-off, 0.76 |
| Samady [28] | 2006 | Diagnostic, descriptive | FFR | FFR vs. SPECT and contrast Echo in post-MI patients | Culprit vessels of MI <6 days | 48 | 48 | Either SPECT or Echo: Ss, 88 %; Sp, 93 %; Acc, 91 %; optimal FFR cut-off, 0.78 |
| *Reliability of FFR in non-culprit vessels* | | | | | | | | |
| Ntalianis [44] | 2010 | Cohort | FFR | FFR measured acutely and after 35 ± 4 days in non-culprit arteries post-ACS | NSTEMI, STEMI | 101 | 101 | No significant change in FFR, both acute and follow-up: 0.77 ± 0.13, $p$ = NS |
| Wood [17] | 2013 | Cohort | FFR | FFR measured acutely and after 42 ± 10 days in non-culprit arteries post-STEMI | STEMI | 47 | 47 | Significant, albeit modest, change in FFR: from 0.84 ± 0.08 to 0.82 ± 0.08, $p$ = 0.025 |
| Niccoli [13] | 2014 | Transversal, analytical | FFR/HSR | FFR vs. HSR comparison in NSTEMI vs. stable patients | NSTEMI, stable | 30 | 15 | FFR and HSR discordance more frequent in NSTEMI: 85.7 % vs. 39.1 %, $p$ = 0.04 |
| Indolfi [46] | 2015 | Transversal, analytical | iFR/FFR | iFR vs. FFR comparison in ACS vs. stable patients | UA, NSTEMI, STEMI, stable | 82 | 53 | The diagnostic accuracy of iFR in ACS was not inferior to stable patients: 79.5 % in ACS vs. 84.4 % in S, $p$ = 0.497 |

*FFR* fractional flow reserve, *iFR* instantaneous wave free ratio, *HSR* hyperemic stenosis resistance index, *SPECT* myocardial scintigraphy, *Echo* echocardiography, *ACS* acute coronary syndromes, *MI* myocardial infarction, *STEMI* ST-elevation myocardial infarction, *NSTEMI* non-ST-elevation myocardial infarction, *UA* unstable angina, *SS* sensitivity, *Sp* specificity, *Acc* accuracy

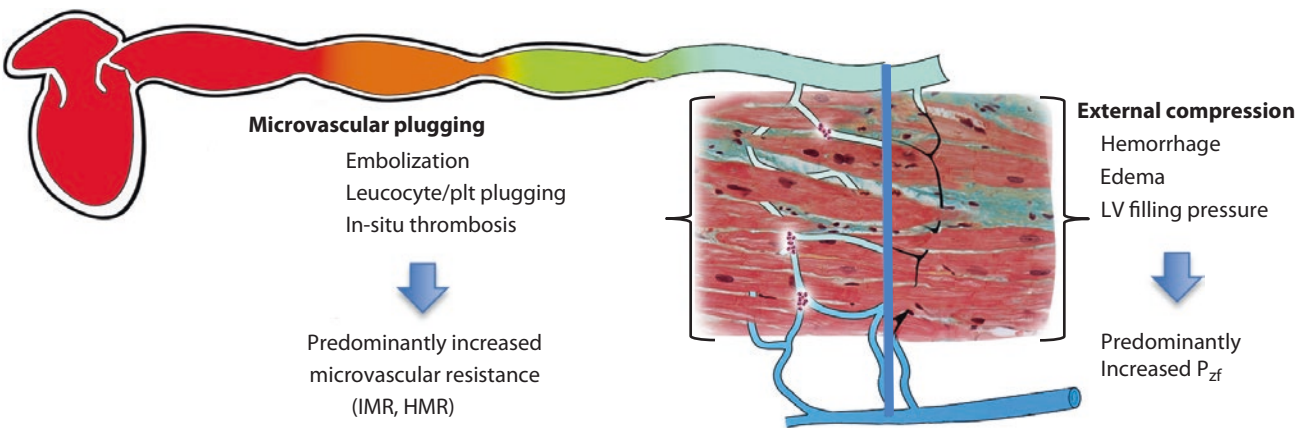


**Fig. 7.4** Principle mechanisms behind microvascular impairment and invasive indices used in diagnosis

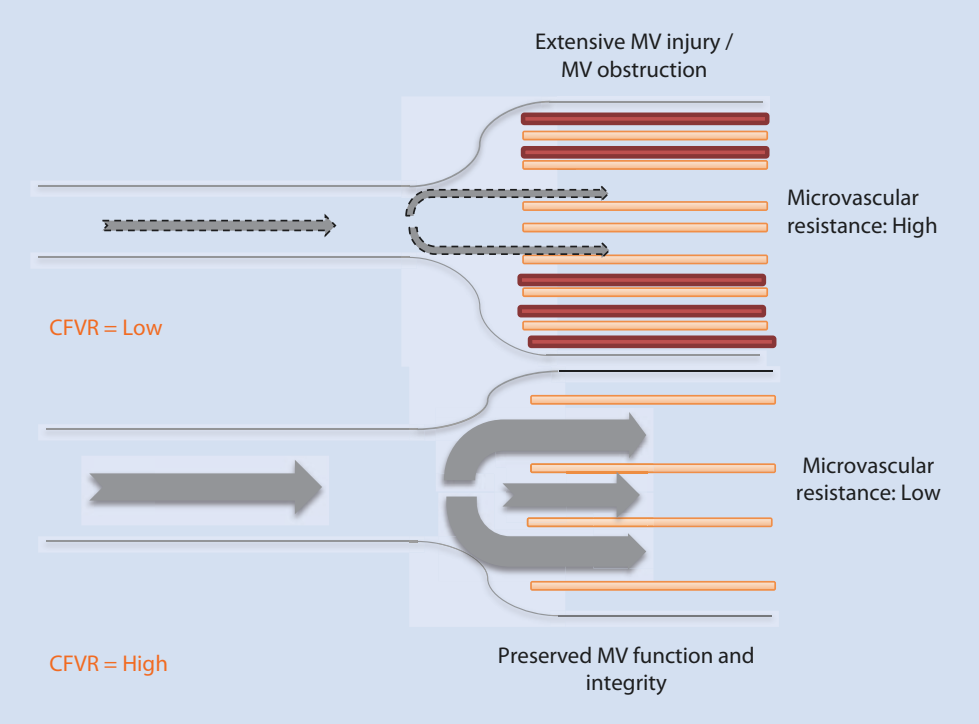


**Fig. 7.5** After primary PCI, presence of extensive injury in the distal microvascular bed supplied by reopened epicardial artery results in decreased myocardial blood flow which leads to decreased coronary flow velocity reserve (CFVR) and increased microvascular resistance (A = high microvascular resistance and abnormal CFR). If distal microcirculatory integrity was preserved, myocardial blood flow would largely be maintained due to normal microvascular resistance (B = low microvascular resistance and normal CFR)

## 7.4 Invasive Assessment of the Microcirculation in STEMI

Despite achieving optimal epicardial reperfusion as assessed by angiography, microvascular obstruction (MVO) can be detected on cardiac magnetic resonance imaging (CMR) in approximately 40 % of patients undergoing primary PCI (PPCI). The presence and extent of MVO after PPCI are associated with impaired myocardial salvage [50], impaired LV function [51], and worse outcome [52] in both short- and long-term follow-up. Therefore, assessment of the microvascular status at the time of PPCI has enormous prognostic value. Although there is no proven therapy to limit microvascular injury post-PPCI, in order to be able to intervene in this ongoing and progressive process, microvascular functional and structural status should be assessed immediately post-PPCI. In this section we focus on the invasive assessment of the microcirculation post-PPCI using both angiographic tools Niccoli and wire-based techniques

### 7.4.1 Angiographic Assessment of the Microcirculatory Status Post-PPCI

Thrombolysis in myocardial infarction (TIMI) frame count (TFC) and myocardial blush grade (MBG) assessment were introduced for the indirect assessment of microvascular status after PPCI. TFC has been shown to reflect epicardial blood flow velocity and is linked to prognosis; however, it does not correlate well with intracoronary Doppler parameters indicating microvascular injury after PPCI [53]. The MBG is scored on a scale of 0–3, with a MBG 0–1 indicating microvascular obstruction [54]. However, MBG only indirectly reflects microvascular status with substantial underestimation of microvascular obstruction compared to cardiac magnetic resonance (CMR) imaging in patients undergoing PPCI [55]. Given recent studies showing that angiographic methods do not accurately predict microvascular obstruction on CMR [56–58], their utility in predicting microvascular injury post-PPCI is limited.

### 7.4.2 Wire-Based Assessment of the Microcirculatory Status Post-PPCI

To date, there is no widely accepted and fully validated method to accurately and directly identify microvascular injury post-PCI in the catheterization laboratory. However, the presence of microvascular injury can be detected by intracoronary measurement of pressure and flow following PPCI. Direct invasive assessment combining coronary flow and pressure by using sensor-tipped guide wires appears to be the most sensitive and accurate approach to assesses microvascular status after primary PCI.

#### Intracoronary Doppler-Derived Coronary Flow Velocity Reserve (CFVR) and Doppler Flow Velocity Patterns in the Assessment of Post-PPCI Microcirculatory Status

Post-PPCI, characteristic coronary blood flow velocity patterns associated with MVI are "systolic flow reversal," "rapid deceleration of diastolic flow," and a "reduced coronary flow

velocity reserve (CFVR)" [59–62]. The extent of MVO on CMR is shown to correlate with CFVR, diastolic deceleration time, and diastolic/systolic velocity ratio acquired 4–8 days post-PPCI [63]. Furthermore, patients without MVO on CMR did not show systolic flow reversal pattern in intracoronary Doppler envelopes [64].

Several studies have indicated that CFVR assessed in the infarct-related artery post-PPCI is the most valuable prognostic marker of recovery of left ventricular function after STEMI [65–67]. The CFVR measured in the infarct-related artery (IRA) is related with extent of MVO in CMR [64]. Decreased reference vessel CFVR (<2.1) after PPCI for acute anterior wall STEMI was recently shown to be associated with significantly increased long-term cardiac mortality [38].

The presence of MVO in CMR [63] and myocardial contrast echocardiography [60, 61] is associated with shortening of diastolic deceleration time, appearance of systolic flow reversal, and disappearance of systolic antegrade flow in intracoronary Doppler measurement immediately post-PPCI resulting in systolic flow reversal. Clinically, rapid deceleration time of diastolic flow measured in reopened IRA (<600 ms) is associated with lack of recovery in ventricular regional function, poor long-term ejection fraction, and larger infarct size [68, 69].

However, CFVR has two well-recognized limitations that may affect its reproducibility: (1) its inability to distinguish between relative epicardial and microvascular contribution to total coronary resistance [70] and (2) its dependence upon hemodynamic factors [64]. To overcome these limitations, another parameter "microvascular resistance," which is specific to the microcirculation and less affected by hemodynamic conditions [64], was introduced.

## Microvascular Resistance Indices in the Assessment of Post-PPCI Microcirculatory Status

Coronary microvascular resistance constitutes an interesting alternative to CFVR in the assessment of the coronary microcirculation after PPCI. Measurements of microcirculatory resistance can be thermodilution based (index of microvascular resistance = IMR) or Doppler based (hyperemic microvascular resistance = HMR). Regardless of the method used, microvascular resistance (IMR or HMR) is a particularly valuable measurement in determining increased coronary microvascular resistance.

The background and methods of measuring IMR are described elsewhere in this book. Importantly, IMR is not affected by the presence of moderate to severe epicardial stenoses, therefore specifically measures microcirculatory resistance. In the presence of severe stenosis (FFR < 0.60), the possible contribution of collaterals (coronary wedge pressure) can be accounted for and IMR value adjusted [71]. Additionally, as IMR is measured at maximal hyperemia, it is not influenced by hemodynamic conditions. Post-PPCI IMR provides a specific, quantitative, and independent (in the absence of additional hemodynamically severe stenosis in the IRA) evaluation of the microvasculature subtended by the IRA.

IMR measured immediately post-PPCI is strongly associated with MVO, infarct volume, and LV function assessed by CMR [72]. IMR values and shape of thermodilution curves also correlate with infarct size by CMR [18, 72, 73]. IMR in the reopened IRA is predictive of LV function and LV functional recovery as assessed by echocardiographic wall motion score index at 3-month and 6-month follow-up [74, 75] and by CMR at 3-month follow-up [75]. Myocardial viability measured by fluorodeoxyglucose PET at 6-month follow-up has been demonstrated to correlate with IMR [75]. In addition to predicting myocardial salvage, post-PPCI IMR is a powerful predictor of several infarct characteristics as assessed by CMR, including infarct size, microvascular obstruction, and intramyocardial hemorrhage [18]. Additionally, IMR measured 48 h after primary PCI also predicts recovery in infarct size [76]. In particular, elevated IMR (>40) measured at the time of PPCI predicts poor long-term outcomes [74].

Although there is no widely accepted/well-established cutoff value for IMR after PPCI, the suggested values in predicting MVO are 35 units [72], LV remodeling 33 units [74], and long-term mortality 40 units [74]. These cutoff values may identify high-risk patients immediately after PPCI in whom adjunctive pharmacological therapies can be considered.

The background and methods of measuring HMR are described elsewhere in this book. Measurement of distal pressure and flow velocity after reperfusion may provide important information on the state of coronary microvasculature. Regardless of the etiology of microvascular impairment, increased HMR values measured in the IRA after reperfusion represent microcirculatory damage. The ability of HMR to detect increased microvascular resistance due to the loss of capillaries and arterioles in the chronically infarcted heart has been shown [77].

In STEMI, HMR measured immediately after PPCI is predictive of both enzymatic infarct size and infarct size as defined by CMR [78]. Furthermore, it can distinguish between non-transmural and transmural MI, which has prognostic importance [78]. HMR immediately after reperfusion also predicts long-term left ventricular remodeling [79] which occurs approximately 20–35 % of patients despite complete and sustained flow in the IRA [79, 80]. It has been shown that HMR measured after PPCI predicts occurrence of CMR-defined microvascular injury, early phase and final infarct sizes, and PET-derived myocardial blood impairment [81]. This study suggests a cutoff value of 2.5 mmHg/cm per second for predicting the occurrence of CMR-defined microvascular injury [81]. Suggested cutoff points for HMR in predicting infarct transmurality (3.25 mmHg/cm per second) [78], left ventricular remodeling (2.96 mmHg/cm per second) [82], and extensive microvascular injury (2.5 mmHg/cm per second) [81] may help us to identify high-risk patients in the catheterization laboratory immediately post-PPCI.

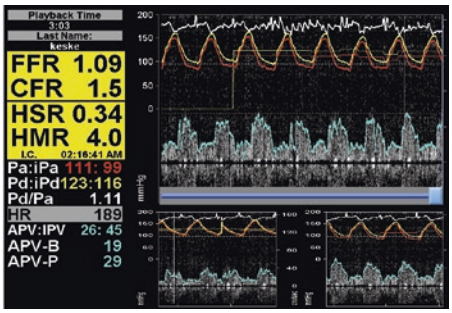


Immediately after PPCI
(HMR= 4 mmHg.cm$^{-1}$.second)

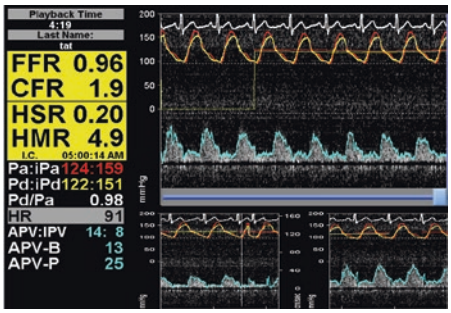


15 min. after PPCI
(HMR= 4.9 mmHg.cm$^{-1}$.second)

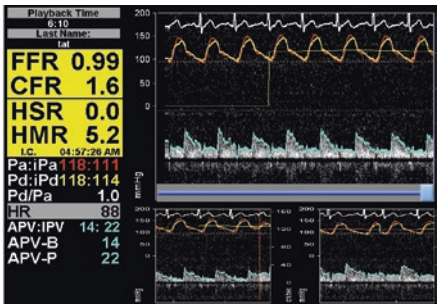


30 min after PPCI
(HMR= 5.2 mmHg.cm$^{-1}$.second)

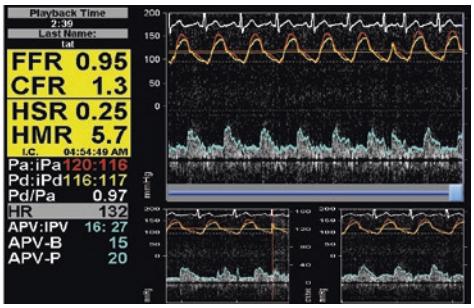


60 min after PPCI
(HMR= 5.7 mmHg.cm$^{-1}$.second)

**Fig. 7.6** An example of dynamic changes (progressive deterioration) in microvascular perfusion after successful PPCI as evidenced by progressive increase observed in hyperemic microvascular resistance (HMR) within an hour of PPCI. In this patient, following successful PPCI for acute anterior myocardial infarction, HMR was measured at four different time points (immediately after PPCI and 15, 30, and 60 min after PPCI). Progressive deterioration in myocardial blood flow and progressive increase in HMR (from 4 to 5.7 mmHg.cm$^{-1}$.second at 60 min) are seen in intracoronary pressure/Doppler tracings

Like IMR, HMR performed immediately after PPCI can identify patients with severe microvascular injury in the catheterization laboratory. Given its simplicity, its high reproducibility of the measurement, and its predictive power, measuring HMR immediately after primary PCI may make microvascular injury a viable target for therapeutic interventions.

After reestablishing epicardial patency, the progressive/ongoing nature of microvascular injury in the reperfused territory complicates the timing of measurement of microvascular resistance. It is known that myocardial blood flow in areas of MVO is hyperemic during the first minutes of reperfusion but progressively decreases within 2–3 h, resulting in a two-fold increase in zone of microvascular injury [83] (Fig. 7.6). Therefore, single Doppler flow velocity and/or microvascular resistance measurements performed immediately after PPCI may underestimate the degree of microvascular injury/obstruction subsequently present as assessed by CMR.

## Microvascular Capacitance in the Assessment of Post-PPCI Microcirculatory Status

The background and methods of measuring zero flow pressure ($P_{zf}$) in the coronary circulation are described elsewhere in this book. As $P_{zf}$ provides information on the effects of intraventricular and interstitial myocardial pressure (external forces) on coronary microvasculature, $P_{zf}$ measured after PPCI is associated mainly with microvascular impairment due to external microcirculatory compression [40].

$P_{zf}$ increases in patients with reperfused anterior myocardial infarction with no reflow when compared to the normal reflow group [84]. Importantly, the relationship between $P_{zf}$ and the development of MVI [17] is supported by studies reporting relationships between $P_{zf}$ measured after PPCI and viable myocardium assessed by CMR or PET [82, 85]. Intramyocardial hemorrhage and/or edema occurring in reperfused STEMI can contribute to an increase in microvascular resistance with a variable extent by generating an external compressive force on the microcirculation. The strong correlation shown between HMR and $P_{zf}$ supports this hypothesis [81].

Although it may provide additional and valuable information about the microvascular status after PPCI, at present, the clinical applicability $P_{zf}$ in the setting of acute STEMI is hampered by the difficulties associated with acquiring high-quality, artifact-free Doppler tracings that are required to generate pressure-velocity loops suitable for analysis.

## 7.5 Conclusion

Although acute coronary syndrome represents a different physiological state to stable coronary disease, many of the principles applied in stable CAD can be translated to ACS. The use of FFR is both safe and effective in evaluating bystander lesions in ACS, and its use appears beneficial. Although there are no specific targeted therapies for the treatment of MVO post-ACS, it is readily identified with intracoronary physiology at the time of PPCI. Given the poor prognosis in patients with MVO, early identification and optimization of medical therapy appear prudent.

## References


1. Kolodgie FD, Virmani R, Burke AP, Farb A, Weber DK, Kutys R, et al. Pathologic assessment of the vulnerable human coronary plaque. Heart. 2004;90(12):1385–91.
2. Narula J, Nakano M, Virmani R, Kolodgie FD, Petersen R, Newcomb R, et al. Histopathologic characteristics of atherosclerotic coronary disease and implications of the findings for the invasive and noninvasive detection of vulnerable plaques. J Am Coll Cardiol. 2013;61(10):1041–51.
3. Jia H, Abtahian F, Aguirre AD, Lee S, Chia S, Lowe H, et al. In vivo diagnosis of plaque erosion and calcified nodule in patients with acute coronary syndrome by intravascular optical coherence tomography. J Am Coll Cardiol. 2013;62(19):1748–58.
4. Cheruvu PK, Finn AV, Gardner C, Caplan J, Goldstein J, Stone GW, et al. Frequency and distribution of thin-cap fibroatheroma and ruptured plaques in human coronary arteries: a pathologic study. J Am Coll Cardiol. 2007;50(10):940–9.
5. Arbustini E, Dal Bello B, Morbini P, Burke AP, Bocciarelli M, Specchia G, et al. Plaque erosion is a major substrate for coronary thrombosis in acute myocardial infarction. Heart. 1999;82(3):269–72.
6. van der Wal AC, Becker AE, van der Loos CM, Das PK. Site of intimal rupture or erosion of thrombosed coronary atherosclerotic plaques is characterized by an inflammatory process irrespective of the dominant plaque morphology. Circulation. 1994;89(1):36–44.
7. Durante A, Camici PG. Novel insights into an "old" phenomenon: the no reflow. Int J Cardiol. 2015;187:273–80.
8. Niccoli G, Burzotta F, Galiuto L, Crea F. Myocardial no-reflow in humans. J Am Coll Cardiol. 2009;54(4):281–92.
9. Schwartz BG, Kloner RA. Coronary no reflow. Spec Issue Coron Blood Flow. 2012;52(4):873–82.
10. Okamura A, Ito H, Iwakura K, Kurotobi T, Koyama Y, Date M, et al. Clinical implications of distal embolization during coronary interventional procedures in patients with acute myocardial infarction: quantitative study with Doppler guidewire. JACC Cardiovasc Interv. 2008;1(3):268–76.
11. Napodano M, Peluso D, Marra MP, Frigo AC, Tarantini G, Buja P, et al. Time-dependent detrimental effects of distal embolization on myocardium and microvasculature during primary percutaneous coronary intervention. JACC Cardiovasc Interv. 2012;5(11):1170–7.
12. Skyschally A, Walter B, Heusch G. Coronary microembolization during early reperfusion: infarct extension, but protection by ischaemic postconditioning. Eur Heart J. 2013;34(42):3314–21.
13. Giampaolo Niccoli, Elena Falcioni, Nicola Cosentino, Francesco Fracassi, Marco Roberto, Alessandro Fabretti, et al. Impact of Accuracy of Fractional Flow Reserve to Reduction of Microvascular Resistance After Intracoronary Adenosine in Patients With Angina Pectoris or Non–ST-Segment Elevation Myocardial Infarction. DOI: http://dx.doi.org/10.1016/j.amjcard.2014.01.422.
14. Sezer M, Okcular I, Goren T, Oflaz H, Nisanci Y, Umman B, et al. Association of haematological indices with the degree of microvascular injury in patients with acute anterior wall myocardial infarction treated with primary percutaneous coronary intervention. Heart. 2007;93(3):313–8.
15. van der Laan AM, Hirsch A, Robbers LFHJ, Nijveldt R, Lommerse I, Delewi R, et al. A proinflammatory monocyte response is associated with myocardial injury and impaired functional outcome in patients with ST-segment elevation myocardial infarction. Am Heart J. 2012;163(1):57–65.e2.
16. Pedersen CM, Barnes G, Schmidt MR, Bøtker HE, Kharbanda RK, Newby DE, et al. Ischaemia–reperfusion injury impairs tissue plasminogen activator release in man. Eur Heart J. 2012;33(15):1920–7.
17. Sezer M, Oflaz H, Gören T, Okçular I, Umman B, Nişanci Y, et al. Intracoronary streptokinase after primary percutaneous coronary intervention. N Engl J Med. 2007;356(18):1823–34.
18. Robbers LF, Eerenberg ES, Teunissen PF, Jansen MF, Hollander MR et al. Magnetic resonance imaging-defined areas of microvascular obstruction after acute myocardial infarction represents microvascular destruction and haemorrhage. Eur Heart J. 2013;34:2346–53.
19. Carrick D, Haig C, Ahmed N, Rauhalammi S, Clerfond G, Carberry J, et al. Temporal evolution of myocardial hemorrhage and edema in patients after acute ST-segment elevation myocardial infarction: pathophysiological insights and clinical implications. J Am Heart Assoc Cardiovasc Cerebrovasc Dis. 2016;5(2), e002834.
20. Dall'Armellina E, Karia N, Lindsay AC, Karamitsos TD, Ferreira V, Robson MD, et al. Dynamic changes of edema and late gadolinium enhancement after acute myocardial infarction and their relationship to functional recovery and salvage index. Circ Cardiovasc Imaging. 2011;4(3):228–36.
21. Mewton N, Bonnefoy E, Revel D, Ovize M, Kirkorian G, Croisille P. Presence and extent of cardiac magnetic resonance microvascular obstruction in reperfused non-ST-elevated myocardial infarction and correlation with infarct size and myocardial enzyme release. Cardiology. 2009;113(1):50–8.
22. Guerra E, Hadamitzky M, Ndrepepa G, Bauer C, Ibrahim T, Ott I, et al. Microvascular obstruction in patients with non-ST-elevation myocardial infarction: a contrast-enhanced cardiac magnetic resonance study. Int J Cardiovasc Imaging. 2014;30(6):1087–95.
23. Van Assche LM, Bekkers SC, Senthilkumar A, Parker MA, Kim HW, Kim RJ. The prevalence of microvascular obstruction in acute myocardial infarction: importance of ST elevation, infarct size, transmurality and infarct age. J Cardiovasc Magn Reson. 2011;13(1):1–2.
24. Betgem RP, de Waard GA, Nijveldt R, Beek AM, Escaned J, van Royen N. Intramyocardial haemorrhage after acute myocardial infarction. Nat Rev Cardiol. 2015;12(3):156–67.
25. Tamita K, Akasaka T, Takagi T, Yamamuro A, Yamabe K, Katayama M, et al. Effects of microvascular dysfunction on myocardial fractional flow reserve after percutaneous coronary intervention in patients with acute myocardial infarction. Catheter Cardiovasc Interv. 2002;57(4):452–9.
26. Lotfi A, Jeremias A, Fearon WF, Feldman MD, Mehran R, Messenger JC, et al. Expert consensus statement on the use of fractional flow reserve, intravascular ultrasound, and optical coherence tomography. Catheter Cardiovasc Interv. 2014;83(4):509–18.
27. De Bruyne B, Pijls NHJ, Bartunek J, Kulecki K, Bech J-W, De Winter H, et al. Fractional flow reserve in patients with prior myocardial infarction. Circulation. 2001;104(2):157–62.
28. Samady H, Lepper W, Powers ER, Wei K, Ragosta M, Bishop GG, et al. Fractional flow reserve of infarct-related arteries identifies reversible defects on noninvasive myocardial perfusion imaging early after myocardial infarction. J Am Coll Cardiol. 2006;47(11):2187–93.
29. Beleslin B, Ostojic M, Djordjevic-Dikic A, Vukcevic V, Stojkovic S, Nedeljkovic M, et al. The value of fractional and coronary flow reserve in predicting myocardial recovery in patients with previous myocardial infarction. Eur Heart J. 2008;29(21):2617–24.
30. Marques KM, Knaapen P, Boellaard R, Westerhof N, Lammertsma AA, Visser CA, et al. Hyperaemic microvascular resistance is not increased in viable myocardium after chronic myocardial infarction. Eur Heart J. 2007;28(19):2320–5.
31. López-Palop R, Carrillo P, Frutos A, Castillo J, Cordero A, Toro M, et al. Usefulness of the fractional flow reserve derived by intracoronary pressure wire for evaluating angiographically intermediate lesions in acute coronary syndrome. Rev Esp Cardiol Engl Ed. 2010;63(06):686–94.
32. Toma M, Buller CE, Westerhout CM, Fu Y, O'Neill WW, Holmes DR, et al. Non-culprit coronary artery percutaneous coronary intervention during acute ST-segment elevation myocardial infarction: insights from the APEX-AMI trial. Eur Heart J. 2010;31(14):1701–7.
33. Yasuhiro Usui, Taishiro Chikamori, Hidefumi Yanagisawa, Takayuki Morishima, Satoshi Hida, Nobuhiro Tanaka, et al. Reliability of pressure-derived myocardial fractional flow reserve in assessing coronary artery stenosis in patients with previous myocardial infarction. DOI: http://dx.doi.org/10.1016/S0002-9149(03)00829-4.
34. Ragmin F, Fast Revascularisation During InStability in Coronary Artery Disease Investigators. Invasive compared with non-invasive

treatment in unstable coronary-artery disease: FRISC II prospective randomised multicentre study. Lancet. 1999;354(9180):708–15.
35. Effects of tissue plasminogen activator and a comparison of early invasive and conservative strategies in unstable angina and non-Q-wave myocardial infarction. Results of the TIMI IIIB Trial. Thrombolysis in Myocardial Ischemia. Circulation. 1994;89(4):1545–56.
36. Windecker S, Kolh P, Alfonso F, Collet J-P, Cremer J, Falk V, et al. 2014 ESC/EACTS Guidelines on myocardial revascularization. Zamorano, Jose Luis Achenbach, Stephan Baumgartner, Helmut Bax, Jeroen J. Bueno, Héctor Dean, Veronica Deaton, Christi Erol, Çetin Fagard, Robert Ferrari, Roberto Hasdai, David Hoes, Arno W. Kirchhof, Paulus Knuuti, Juhani Kolh, Philippe Lancellotti, Patrizio Linhart, Ales Nihoyannopoulos, Petros Piepoli, Massimo F. Ponikowski, Piotr Sirnes, Per Anton Tamargo, Juan Luis Tendera, Michal Torbicki, Adam Wijns, William Windecker, Stephan, Sousa Uva, Miguel, Achenbach, Stephan Pepper, John Anyanwu, Anelechi Badimon, Lina Bauersachs, Johann Baumbach, Andreas Beygui, Farzin Bonaros, Nikolaos De Carlo, Marco Deaton, Christi Dobrev, Dobromir Dunning, Joel Eeckhout, Eric Gielen, Stephan Hasdai, David Kirchhof, Paulus Luckraz, Heyman Mahrholdt, Heiko Montalescot, Gilles Paparella, Domenico Rastan, Ardawan J. Sanmartin, Marcelo Sergeant, Paul Silber, Sigmund Tamargo, Juan ten Berg, Jurrien Thiele, Holger van Geuns, Robert-Jan Wagner, Hans-Otto Wassmann, Sven Wendler, Olaf Zamorano, Jose Luis Weidinger, Franz Ibrahimov, Firdovsi Legrand, Victor Terzić, Ibrahim Postadzhiyan, Arman Skoric, Bosko Georgiou, Georgios M. Zelizko, Michael Junker, Anders Eha, Jaan Romppanen, Hannu Bonnet, Jean-Louis Aladashvili, Alexander Hambrecht, Rainer Becker, Dávid Gudnason, Thorarinn Segev, Amit Bugiardini, Raffaele Sakhov, Orazbek Mirrakhimov, Aibek Pereira, Bruno Felice, Herbert Trovik, Thor Dudek, Dariusz Pereira, Hélder Nedeljkovic, Milan A. Hudec, Martin Cequier, Angel Erlinge, David Roffi, Marco Kedev, Sasko Addad, Faouzi Yildirir, Aylin Davies, John, editor. Eur Heart J. 2014;35(37):2541–619.
37. Uren NG, Crake T, Lefroy DC, de Silva R, Davies GJ, Maseri A. Reduced coronary vasodilator function in infarcted and normal myocardium after myocardial infarction. N Engl J Med. 1994;331(4):222–7.
38. van de Hoef TP, Bax M, Meuwissen M, Damman P, Delewi R, de Winter RJ, et al. Impact of coronary microvascular function on long-term cardiac mortality in patients with acute ST-segment-elevation myocardial infarction. Circ Cardiovasc Interv. 2013;6(3):207–15.
39. Gregorini L, Marco J, Kozàkovà M, Palombo C, Anguissola GB, Marco I, et al. α-adrenergic blockade improves recovery of myocardial perfusion and function after coronary stenting in patients with acute myocardial infarction. Circulation. 1999;99(4):482–90.
40. Van Herck PL, Carlier SG, Claeys MJ, Haine SE, Gorissen P, Miljoen H, et al. Coronary microvascular dysfunction after myocardial infarction: increased coronary zero flow pressure both in the infarcted and in the remote myocardium is mainly related to left ventricular filling pressure. Heart. 2007;93(10):1231–7.
41. Niccoli G, Falcioni E, Cosentino N, Fracassi F, Roberto M, Fabretti A, et al. Impact of accuracy of fractional flow reserve to reduction of microvascular resistance after intracoronary adenosine in patients with angina pectoris or non–ST-segment elevation myocardial infarction. Am J Cardiol. 2014;113(9):1461–7.
42. Bax M, de Winter RJ, Koch KT, Schotborgh CE, Tijssen JGP, Piek JJ. Time course of microvascular resistance of the infarct and noninfarct coronary artery following an anterior wall acute myocardial infarction. Am J Cardiol. 2006;97(8):1131–6.
43. Meuwissen M. Hyperemic stenosis resistance index for evaluation of functional coronary lesion severity. Circulation. 2002;106(4):441–6.
44. Ntalianis A, Sels J-W, Davidavicius G, Tanaka N, Muller O, Trana C, et al. Fractional flow reserve for the assessment of nonculprit coronary artery stenoses in patients with acute myocardial infarction. JACC Cardiovasc Interv. 2010;3(12):1274–81.
45. Wood DA, Poulter RS, Boone R, Lim I, Bogale N, Starovoytov A, et al. TCT-628 stability of non culprit vessel fractional flow reserve in patients with st-segment elevation myocardial infarction. J Am Coll Cardiol. 2013;62(18_S1):B191.
46. Indolfi C, Mongiardo A, Spaccarotella C, Torella D, Caiazzo G, Polimeni A, et al. The instantaneous wave-free ratio (iFR) for evaluation of nonculprit lesions in patients with acute coronary syndrome and multivessel disease. Int J Cardiol. 2015;178:46–54.
47. Sels J-WEM, Tonino PAL, Siebert U, Fearon WF, Van't Veer M, De Bruyne B, et al. Fractional flow reserve in unstable angina and Non–ST-segment elevation myocardial infarction: experience from the FAME (Fractional flow reserve versus Angiography for Multivessel Evaluation) study. JACC Cardiovasc Interv. 2011;4(11):1183–9.
48. Layland J, Oldroyd KG, Curzen N, Sood A, Balachandran K, Das R, et al. Fractional flow reserve vs. angiography in guiding management to optimize outcomes in non-ST-segment elevation myocardial infarction: the British Heart Foundation FAMOUS-NSTEMI randomized trial. Eur Heart J. 2015;36(2):100–11.
49. Van Belle E, Rioufol G, Pouillot C, Cuisset T, Bougrini K, Teiger E, et al. Outcome impact of coronary revascularization strategy reclassification with fractional flow reserve at time of diagnostic angiography insights from a large French Multicenter Fractional Flow Reserve Registry. Circulation. 2014;129(2):173–85.
50. Limalanathan S, Eritsland J, Andersen GØ, Kløw N-E, Abdelnoor M, Hoffmann P. Myocardial salvage is reduced in primary pci-treated stemi patients with microvascular obstruction, demonstrated by early and late CMR. PLoS One. 2013;8(8):1–6.
51. Lombardo A, Niccoli G, Natale L, Bernardini A, Cosentino N, Bonomo L, et al. Impact of microvascular obstruction and infarct size on left ventricular remodeling in reperfused myocardial infarction: a contrast-enhanced cardiac magnetic resonance imaging study. Int J Cardiovasc Imaging. 2012;28(4):835–42.
52. de Waha S, Desch S, Eitel I, Fuernau G, Lurz P, Leuschner A, et al. Relationship and prognostic value of microvascular obstruction and infarct size in ST-elevation myocardial infarction as visualized by magnetic resonance imaging. Clin Res Cardiol. 2012;101(6):487–95.
53. Ohara Y, Hiasa Y, Takahashi T, Yamaguchi K, Ogura R, Ogata T, et al. Relation between the TIMI frame count and the degree of microvascular injury after primary coronary angioplasty in patients with acute anterior myocardial infarction. Heart. 2005;91(1):64–7.
54. van't Hof AWJ, Liem A, Suryapranata H, Hoorntje JCA, Boer M-J de, Zijlstra F, et al. Angiographic assessment of myocardial reperfusion in patients treated with primary angioplasty for acute myocardial infarction myocardial blush grade. Circulation. 1998;97(23):2302–6.
55. Vicente J, Mewton N, Croisille P, Staat P, Bonnefoy-Cudraz E, Ovize M, et al. Comparison of the angiographic myocardial blush grade with delayed-enhanced cardiac magnetic resonance for the assessment of microvascular obstruction in acute myocardial infarctions. Catheter Cardiovasc Interv. 2009;74(7):1000–7.
56. Wong DTL, Leung MCH, Richardson JD, Puri R, Bertaso AG, Williams K, et al. Cardiac magnetic resonance derived late microvascular obstruction assessment post ST-segment elevation myocardial infarction is the best predictor of left ventricular function: a comparison of angiographic and cardiac magnetic resonance derived measurements. Int J Cardiovasc Imaging. 2012;28(8):1971–81.
57. Nijveldt R, Beek AM, Hirsch A, Stoel MG, Hofman MBM, Umans VAWM, et al. Functional recovery after acute myocardial infarction: comparison between angiography, electrocardiography, and cardiovascular magnetic resonance measures of microvascular injury. J Am Coll Cardiol. 2008;52(3):181–9.
58. Husser O, Bodi V, Sanchis J, Nunez J, Lopez-Lereu MP, Monmeneu JV, et al. Predictors of cardiovascular magnetic resonance-derived microvascular obstruction on patient admission in STEMI. Int J Cardiol. 2013;166(1):77–84.
59. Iwakura K, Ito H, Takiuchi S, Taniyama Y, Nakatsuchi Y, Negoro S, et al. Alternation in the coronary blood flow velocity pattern in patients with No reflow and reperfused acute myocardial infarction. Circulation. 1996;94(6):1269–75.
60. Okamura A, Ito H, Iwakura K, Kawano S, Inoue K, Yamamoto K, et al. Usefulness of a new grading system based on coronary flow velocity pattern in predicting outcome in patients with acute myocardial

infarction having percutaneous coronary intervention. Am J Cardiol. 2005;96(7):927–32.
61. Montisci R, Chen L, Ruscazio M, Colonna P, Cadeddu C, Caiati C, et al. Non-invasive coronary flow reserve is correlated with microvascular integrity and myocardial viability after primary angioplasty in acute myocardial infarction. Heart. 2006;92(8):1113–8.
62. Nohtomi Y, Takeuchi M, Nagasawa K, Arimura K, Miyata K, Kuwata K, et al. Persistence of systolic coronary flow reversal predicts irreversible dysfunction after reperfused anterior myocardial infarction. Heart. 2003;89(4):382–8.
63. Hirsch A, Nijveldt R, Haeck JDE, Beek AM, Koch KT, Henriques JPS, et al. Relation between the assessment of microvascular injury by cardiovascular magnetic resonance and coronary Doppler flow velocity measurements in patients with acute anterior wall myocardial infarction. J Am Coll Cardiol. 2008;51(23):2230–8.
64. Ng MKC. Invasive assessment of the coronary microcirculation: superior reproducibility and less hemodynamic dependence of index of microcirculatory resistance compared with coronary flow reserve. Circulation. 2006;113(17):2054–61.
65. Takahashi T, Hiasa Y, Ohara Y, Miyazaki S, Ogura R, Miyajima H, et al. Usefulness of coronary flow reserve immediately after primary coronary angioplasty for acute myocardial infarction in predicting long-term adverse cardiac events. Am J Cardiol. 2007;100(5):806–11.
66. Teiger E, Garot J, Aptecar E, Bosio P, Woscoboinik J, Pernes JM, et al. Coronary blood flow reserve and wall motion recovery in patients undergoing angioplasty for myocardial infarction. Eur Heart J. 1999;20(4):285–92.
67. Wakatsuki T, Nakamura M, Tsunoda T, Toma H, Degawa T, Oki T, et al. Coronary flow velocity immediately after primary coronary stenting as a predictor of ventricular wall motion recovery in acute myocardial infarction. J Am Coll Cardiol. 2000;35(7):1835–41.
68. Kawamoto T, Yoshida K, Akasaka T, Hozumi T, Takagi T, Kaji S, et al. Can coronary blood flow velocity pattern after primary percutaneous transluminal coronary angiography predict recovery of regional left ventricular function in patients with acute myocardial infarction? Circulation. 1999;100(4):339–45.
69. Okcular I, Sezer M, Aslanger E, Cimen A, Umman B, Nisancı Y, et al. The accuracy of deceleration time of diastolic coronary flow measured by transthoracic echocardiography in predicting long-term left ventricular infarct size and function after reperfused myocardial infarction. Eur Heart J Cardiovasc Imaging. 2010;11(10):823–8.
70. Kern MJ. Coronary physiology revisited practical insights from the cardiac catheterization laboratory. Circulation. 2000;101(11):1344–51.
71. Aarnoudse W. Epicardial stenosis severity does not affect minimal microcirculatory resistance. Circulation. 2004;110(15):2137–42.
72. McGeoch R, Watkins S, Berry C, Steedman T, Davie A, Byrne J, et al. The index of microcirculatory resistance measured acutely predicts the extent and severity of myocardial infarction in patients with ST-segment elevation myocardial infarction. JACC Cardiovasc Interv. 2010;3(7):715–22.
73. Fukunaga M, Fujii K, Kawasaki D, Sawada H, Miki K, Tamaru H, et al. Thermodilution-derived coronary blood flow pattern immediately after coronary intervention as a predictor of microcirculatory damage and midterm clinical outcomes in patients with ST-segment-elevation myocardial infarction. Circ Cardiovasc Interv. 2014;7(2):149–55.
74. Fearon WF, Shah M, Ng M, Brinton T, Wilson A, Tremmel JA, et al. Predictive value of the index of microcirculatory resistance in patients with ST-segment elevation myocardial infarction. J Am Coll Cardiol. 2008;51(5):560–5.
75. Lim H-S, Yoon M-H, Tahk S-J, Yang H-M, Choi B-J, Choi S-Y, et al. Usefulness of the index of microcirculatory resistance for invasively assessing myocardial viability immediately after primary angioplasty for anterior myocardial infarction. Eur Heart J. 2009;30(23):2854–60.
76. Sezer M, Aslanger EK, Cimen AO, Yormaz E, Turkmen C, Umman B, et al. Concurrent microvascular and infarct remodeling after successful reperfusion of ST-elevation acute myocardial infarction. Circ Cardiovasc Interv. 2010;3(3):208–15.
77. Koudstaal S, Jansen of Lorkeers SJ, van Slochteren FJ, van der Spoel TIG, van de Hoef TP, Sluijter JP, et al. Assessment of coronary microvascular resistance in the chronic infarcted pig heart. J Cell Mol Med. 2013;17(9):1128–35.
78. Kitabata H, Imanishi T, Kubo T, Takarada S, Kashiwagi M, Matsumoto H, et al. Coronary microvascular resistance index immediately after primary percutaneous coronary intervention as a predictor of the transmural extent of infarction in patients with ST-segment elevation anterior acute myocardial infarction. JACC Cardiovasc Imaging. 2009;2(3):263–72.
79. Garot P, Pascal O, Simon M, Monin JL, Teiger E, Garot J, et al. Impact of microvascular integrity and local viability on left ventricular remodelling after reperfused acute myocardial infarction. Heart. 2003;89(4):393–7.
80. Bolognese L, Carrabba N, Parodi G, Santoro GM, Buonamici P, Cerisano G, et al. Impact of microvascular dysfunction on left ventricular remodeling and long-term clinical outcome after primary coronary angioplasty for acute myocardial infarction. Circulation. 2004;109(9):1121–6.
81. Teunissen PFA, de Waard GA, Hollander MR, Robbers LFHJ, Danad I, Biesbroek PS, et al. Doppler-derived intracoronary physiology indices predict the occurrence of microvascular injury and microvascular perfusion deficits after angiographically successful primary percutaneous coronary intervention. Circ Cardiovasc Interv. 2015;8(3), e001786.
82. Kitabata H, Kubo T, Ishibashi K, Komukai K, Tanimoto T, Ino Y, et al. Prognostic value of microvascular resistance index immediately after primary percutaneous coronary intervention on left ventricular remodeling in patients with reperfused anterior acute ST-segment elevation myocardial infarction. JACC Cardiovasc Interv. 2013;6(10):1046–54.
83. Reffelmann T, Kloner RA. Microvascular reperfusion injury: rapid expansion of anatomic no reflow during reperfusion in the rabbit. Am J Physiol Heart Circ Physiol. 2002;283(3):H1099–107.
84. Ito H, Terai K, Iwakura K, Kawase I, Fujii K. Hemodynamics of microvascular dysfunction in patients with anterior wall acute myocardial infarction. Am J Cardiol. 2004;94(2):209–12.
85. Shimada K, Sakanoue Y, Kobayashi Y, Ehara S, Hirose M, Nakamura Y, et al. Assessment of myocardial viability using coronary zero flow pressure after successful angioplasty in patients with acute anterior myocardial infarction. Heart. 2003;89(1):71–6.
86. Usui Y, Chikamori T, Yanagisawa H, Morishima T, Hida S, Tanaka N, Takazawa K, Yamashina A. Reliability of pressure-derived myocardial fractional flow reserve in assessing coronary artery stenosis in patients with previous myocardial infarction. Am J Cardiol. 2003;92(6):699–702. doi: http://dx.doi.org/10.1016/S0002-9149(03)00829-4.
87. Niccoli G, Falcioni E, Cosentino N, Fracassi F, Roberto M, Fabretti A, Panebianco M, Scalone G, Burzotta F, Trani C, Leone AM, Davies J, Crea F. Impact of accuracy of fractional flow reserve to reduction of microvascular resistance after intracoronary adenosine in patients with angina pectoris or non–ST-segment elevation myocardial infarction. Am J Cardiol. 2014;113(9):1461–7. doi: http://dx.doi.org/10.1016/j.amjcard.2014.01.422.

# Acute and Chronic Vascular Effects of Percutaneous Coronary Interventions

## Physiological Assessment of Coronary Stenoses and the Microcirculation

*Diego Arroyo, Serban Puricel, Mario Togni, and Stéphane Cook*




J. Escaned, J. Davies (eds.), *Physiological Assessment of Coronary Stenoses and the Microcirculation*,
DOI 10.1007/978-1-4471-5245-3_8

## 8.1 Introduction

Percutaneous coronary intervention whether simple balloon angioplasty or in the case of stent implantation is associated with a broad spectrum of acute and chronic, sometimes deleterious effect, which may impact clinical outcomes.

Balloon angioplasty induces an overexpansion of the atheromatous plaque with radial and longitudinal redistribution. In doing so, angioplasty provokes two direct complications. The first is the immediate elastic recoil of the distended artery, which may be as significant as 30 % depending on structural constraint and centripetal force. The second adverse effect is the rupture of the internal elastic membrane with cell penetration within the intima and subsequent neointimal hyperplasia.

Intracoronary prosthesis implantation whether stent or scaffold is associated with a different type of physical or pharmacological stress leading to chronic inflammation and two late consequences. One is neoatherogenesis: the development of a new plaque within the stent lumen, similar to that found in atherosclerosis. The other is a hypersensitivity reaction with a necrotizing vasculitis of the vessel wall, positive remodeling, and the risk of secondary thrombosis.

Stent implantation disturbs endothelial physiology and adaptation to increased workload such as exercise. There is an imbalance between the vasodilating and vasoconstricting endothelial properties resulting in endothelial dysfunction and paradoxical vasoconstriction in the segments adjacent to the stent or scaffold.

## 8.2 Vessel Recoil and Negative Remodeling

Vessel recoil is the immediate reduction in vessel lumen size post balloon dilatation due to the contraction of distended and/or ruptured coronary segments. The extent of recoil depends on plaque composition and generally follows a two-phase process. The immediate acute recoil is mostly seen in fibrous plaques. A negative or constrictive remodeling develops thereafter in the 6 months following balloon angioplasty. The first studies on angioplasty observed significant acute recoil (defined as a decrease in mean lumen diameter [MLD] of >0.3 mm or a residual stenosis >50 %) in as much as 30 –50 % of dilated segments [1–3]. This return to the original vessel size is not only due to "physiological" and mechanistic recoil. Other putative factors include dissection, spasm, and thrombus formation, but the first studies to have employed intravascular ultrasound (IVUS) for coronary assessment after angioplasty show that the effects are of little importance compared to constriction and negative remodeling. The scar tissue within the vessel wall may lead to late restenosis in as many as 30–50 % of segments treated with balloon angioplasty [4–8]. The factors as those explained in ▶ Chap. 7 play certainly the same role in negative remodeling found after balloon angioplasty.

As nicely demonstrated in the Serial Ultrasound Restenosis (SURE) study, there is a constrictive effect of the external elastic membrane (EEM) due to the scarring process. A total of 61 lesions were analyzed with IVUS prior to balloon angioplasty ($n = 35$) or directional atherectomy ($n = 26$) and then directly post procedure, at 24 h, 1 month, and 6 months. The initial EEM enlargement at 1 month was followed by constriction at 6 months [9]. The most significant predictive factors of restenosis after balloon angioplasty without stent implantation are residual plaque burden (calculated as residual plaque area/external elastic lamina area) and positive remodeling before plain old balloon angioplasty.

## 8.3 Neointimal Hyperplasia

Neointimal hyperplasia develops after arterial wall damage. This phenomenon is similar to that of plexogenic pulmonary angiopathy encountered in primary pulmonary hypertension as well as Eisenmenger reactions seen in congenital heart disease. The artery shows medial and intimal thickening; plexiform lesions develop at branch points probably as a result of shear stress and damage results in transmural destruction that is repaired by granulation tissue with further loss of elastic tissue. Our current understanding of this phenomenon involves cellular recruitment (monocytes, macrophage, and neutrophils), smooth muscle cell migration due to the rupture of the internal elastic membrane and collagen deposits. Cellular migration is, among other substances, due to cytosine excretion. The overstretching associated with either balloon angioplasty or bare-metal stent (BMS) implantation triggers neointimal proliferation [10–12]. Procedure-related factors inducing vessel wall overstretching will also stimulate neointimal hyperplasia. Other patient-related factors have been held responsible such as diabetes, renal insufficiency, and genetic predispositions. Cytotoxic drugs amongst which paclitaxel, sirolimus, everolimus, and biolimus, hinder cellular proliferation: a key to drug-eluting stent (DES) [13] mechanism and action.

Neointimal hyperplasia after stent implantation was thought to be a two-step phenomenon. The initial growth phase would likely last 6 months after which would follow a plateau phase named the "late quiescent period" [14–16]. We have since understood that coronary arteries were more complex and above all dynamic. On the long term, restenosis may either regress [15] or progress [17]. It is conceivable that the artery reacts dynamically to stent implantation alternating between phases of restenosis regression and renarrowing (restenosis expansion or neoatherogenesis) [18]. Overall, the original concept of restenosis as a time-related phenomenon observed after balloon angioplasty [19] has been substantially altered with the introduction and further developments in DES technology [20].

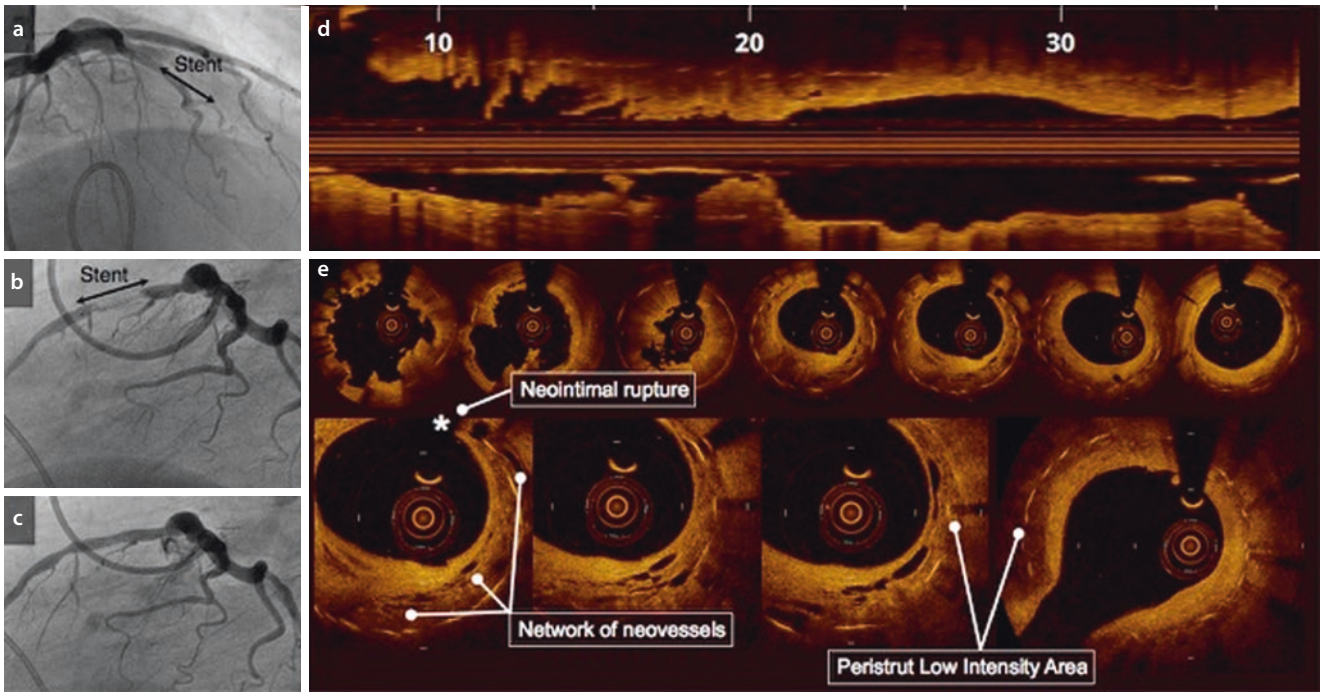


**Fig. 8.1** Representative illustration of patient suffering from very late-stent thrombosis due to neoatherosclerotic plaque disruption (*). Panel **a** depicts coronary angiograms before, Panel **b** during, and Panel **c** after PCI. Panel **d** represents the longitudinal OCT reconstruction and Panel **e** cross sections of OCT with abundant neovessels and peristrut low-intensity areas

## 8.4 Neoatherogenesis

In 2003, Farb and colleagues reported two necroptic cases of late-stent thrombosis due to rupture of lipid-rich plaque with extensive plaque prolapse within the lumen [21]. In 2007, Ramcharitar and colleagues presented two cases of late-occurring stent failure due to plaque rupture of an atherosclerosis process within neointimal hyperplasia after stent implantation [22]. The term neoatherogenesis was coined and used to define the atherosclerosis changes within the neointima inside the coronary artery stent. Several histologic [23], fluoroscopic [24], and intravascular imaging studies have demonstrated that stent-associated neoatherogenesis was different than native artery atherosclerosis and often associated with necrosis and hemorrhage within the plaque and plaque instability [25]. Neoatherogenesis has since been associated with late clinical events such as late-stent thrombosis in both BMS and DES, but it occurs earlier in DES than in BMS [23]. Figure 8.1 depicts a case of stent thrombosis in the mid-left anterior descending artery due to neoatherogenesis, 10 years after BMS implantation.

## 8.5 Hypersensitivity Reaction and Positive Remodeling

### 8.5.1 First-Generation Drug-Eluting Stents

Several cases of DES thrombosis, involving paclitaxel- (PES) and sirolimus-eluting stents (SES) many years after implantation, were reported by the end of 2003. Virmani et al. published a series of pivotal studies with necropsy and histological findings that shed light on the responsible mechanisms; they found granulomas and positive remodeling of the external elastic membrane with pathological scarring tissue and loss of stent strut endothelialization [26–28]. The pathological remodeling of the external elastic membrane associated with stent strut malapposition was confirmed in vivo in patients suffering from stent thrombosis [29]. The inflammatory reaction seen in many cases of DES thrombosis may be different depending on stent type but is usually due to late hypersensitivity to one of the stent components. Figure 8.2 depicts a case of stent thrombosis due to secondary malapposition due to hypersensitivity reaction and positive remodeling. This case illustrates the so-called "paragliding" or "cauliflower" phenomenon.

Efforts were thus made to create more biocompatible polymers such as that used in everolimus-eluting stents (EES) and, eventually, bioresorbable polymers seen in biolimus-eluting stents (BES). This led to a reduction in late-stent thrombosis and late adverse events overall. But the lactic acidification of the media from the polymer could impact vascular healing at the stent vicinity and promote a deleterious inflammatory reaction [30].

### 8.5.2 Bioresorbable Vascular Scaffolds

The unresolved problem of neointimal proliferation and very late-stent thrombosis from lingering polymers and vascular

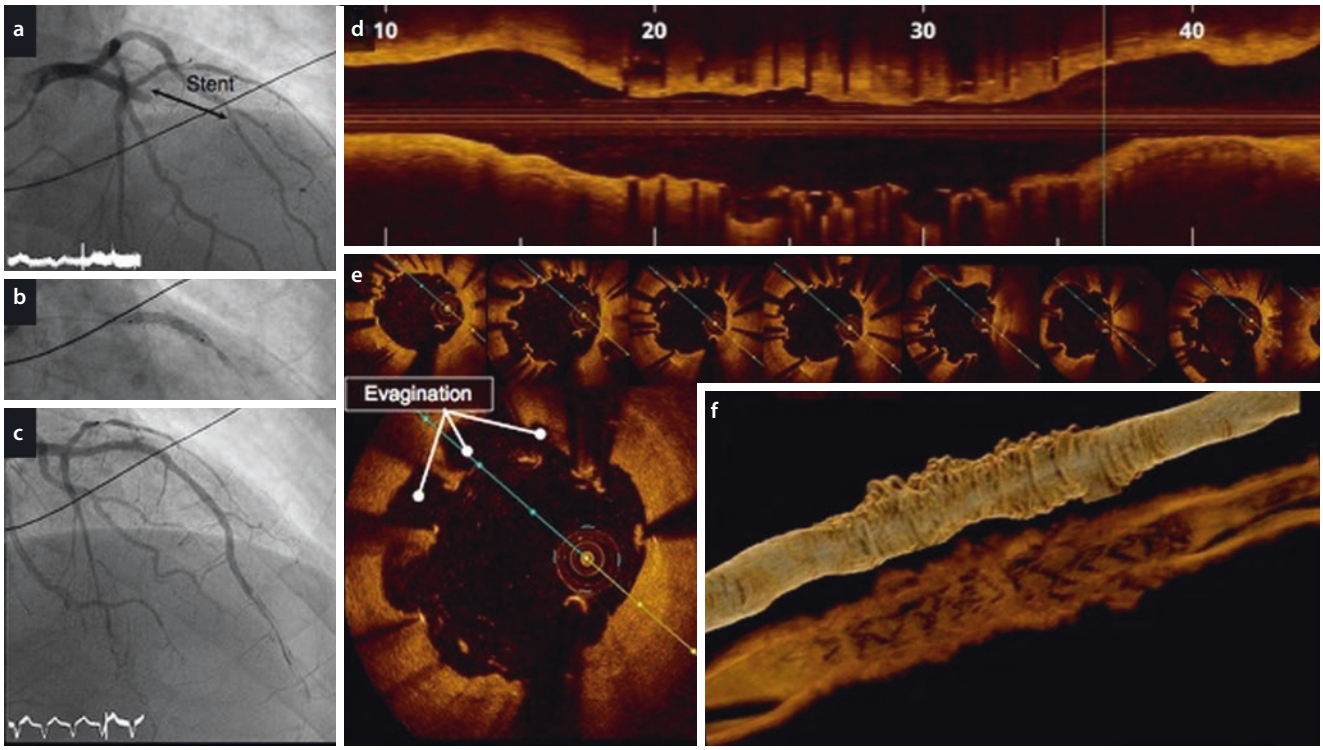


**Fig. 8.2** Representative illustration of patient suffering from very late-stent thrombosis due to hypersensitivity reaction 7 years after sirolimus-eluting stent implantation in left anterior descending coronary artery. Panel **a** depicts coronary angiograms before, Panel **b** during, and Panel **c** after PCI. Panel **d** represents the longitudinal OCT reconstruction and Panel **e** cross sections of OCT with the presence of evaginations (paragliding or cauliflower phenomenon). Panel **f** is 3-D rendering reconstructions highlighting these evaginations

scaffolds led to the development of new-generation completely resorbable stents. The *Absorb*™ (Abbott Vascular, Illinois, USA) was the first CE-approved bioresorbable vascular scaffold (BVS). It uses a poly-L-lactide polymer that undergoes a four-stage bioresorption through hydration, depolymerization, polymer fragmentation, and dissolution over 2 years via Krebs cycle [31]. Putative advantages over conventional DES included restoration of physiological processes, namely, vasomotion and remodeling, superior conformability, beneficial edge-vascular response, and suppression of late-stent malapposition [32]. Although recently published randomized trials have delivered promising results [33, 34], many case series and observational studies suggest an increase in scaffold thrombosis (ScT). In the GHOST-UE registry, ScT was 2 % at 6 months [35], 3 % at 6 months in the single-center AMC registry [36], and finally 2 % at 1 month in the BVS-EXAMINATION cohort [13]. In the latter propensity score-matched study, 290 patients with ST-elevation myocardial infarction had higher ScT at 1 month compared to DES or BMS (2.1 % for BVS; 0.3 % for DES and 1.0 % for BMS, $p = 0.06$ BVS vs DES).

Intravascular imaging with OCT has demonstrated that early ScT was mainly associated with unsatisfactory immediate angiographic results (geographical miss, incomplete stent expansion, malapposition) or insufficient double antiplatelet therapy. However, OCT analysis in late ScT showed strut discontinuity and fracture with strut recoil in the vessel lumen. Vessel wall analysis depicted evagination, neovascularization, and peristrut low-intensity areas (PLIA) [37]. The causes and consequences of PLIA remain uncertain in BVS; this phenomenon is also often observed in scaffolds that have not developed thrombosis. A recently published trial in 26 coronary swine segments treated with everolimus-eluting DES demonstrates a direct correlation between the degree of PLIA and peristrut inflammation at histology [38]. Peristrut low-intensity areas may also be an indicator of vascular edema due to the hydrolysis of polylactide. The association of PLIA and late ScT requires further investigation. Figure 8.3 depicts case of late ScT with OCT analysis.

## 8.6 Vasomotor Response and Functional Restoration

The normal endothelial function regulates vasomotor tone (via nitric oxide), the inhibition of vascular inflammation (e.g., prostaglandins), local thrombolysis, and fibrinolysis (via tissue plasminogen activator) [39]. Losing this regulation may

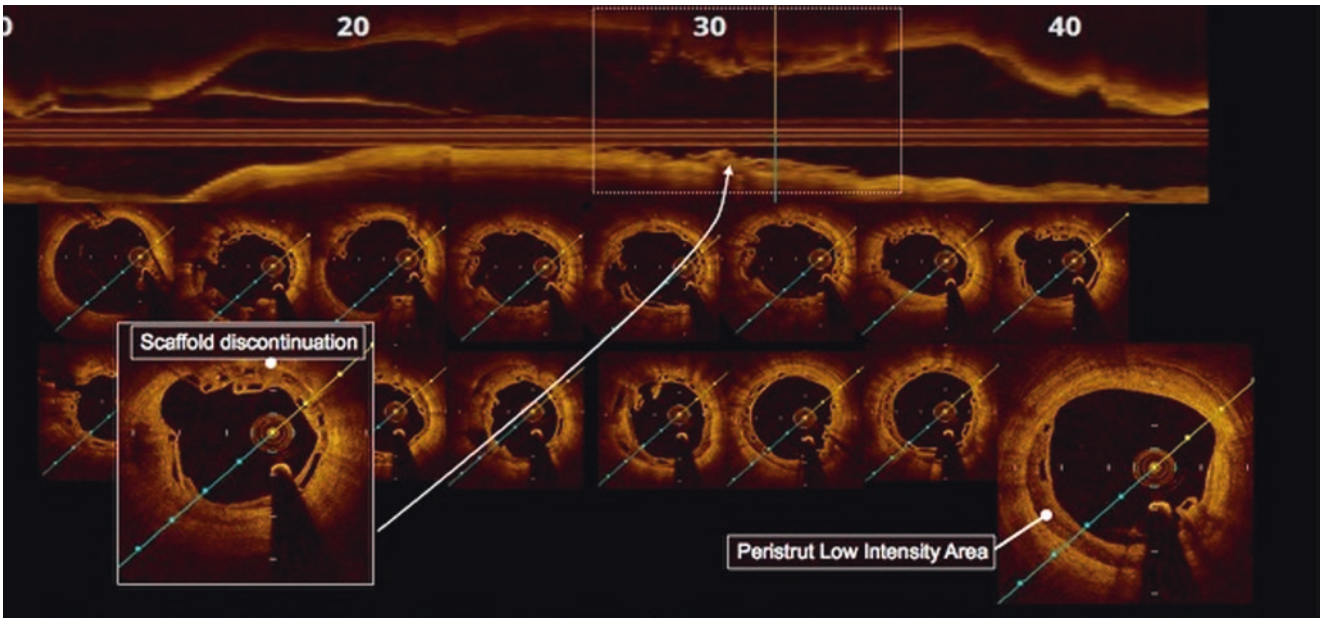


**Fig. 8.3** OCT example of thrombosis of one bioresorbable vascular scaffold almost 2 years after implantation. The longitudinal reconstruction depicts a relative small scaffold for the vessel (due to chronic recoil). The cross sections depict intense peristrut low-intensity areas with strut discontinuities

promote thrombosis resulting in adverse cardiovascular outcomes. Normal endothelium function and vasomotion generates vasodilation under exercise conditions, but this is impaired in coronary artery disease where exercise results in paradoxical vasoconstriction of the stenotic segment [40].

Endothelial dysfunction was first reported after BMS implantation [39] and was initially associated with mechanical injury of the vessel. However, it is also impaired after the implantation of first-generation SES and PES with paradoxical vasoconstriction of segments adjacent to the stent in response to reactivity testing (acetylcholine infusion, rapid atrial pacing, or supine bicycle exercise testing), while BMS demonstrated normal vasomotor function of the peristent segments [41–45] (Fig. 8.4). Among the mechanisms of endothelial dysfunction and vasomotion found after DES implantation are direct toxicity of the drug eluted, hypersensitivity to the stent polymer, delayed endothelial healing, and persistent inflammatory response [46].

It was hypothesized that later-generation DES with more biocompatible polymers and biodegradable polymers would limit endothelial dysfunction and preserve vasomotion. Results are conflicting, and a very recently published study comparing EES and BES, 16 months after implantation, showed exercise-induced endothelium-dependent paradoxical coronary vasoconstriction of the segments adjacent to the stent in both groups. Suggesting that endothelial dysfunction after DES implantation is not primarily caused by the durability of the polymer coating [47].

One of the presumed advantages of BVS would be restoration of vessel physiology after complete scaffold resorption. Preliminary data from the ABSORB Cohort A suggests that vasomotion after acetylcholine infusion may be preserved [48, 49]. Vasomotion at 3-year follow-up is one of the co-primary end points of the ABSORB II trial, the results of which should clarify the potential benefits of BVS implantation. Importantly, it has yet to be established whether or not abnormal vasomotor response results in adverse clinical events.

## 8.7 Conclusion

Percutaneous coronary interventions have been a major breakthrough in the history of medicine leading to ample successes. But a careful appraisal of the mechanisms behind the acute and chronic consequences is paramount to interpreting clinical data, understanding early and late adverse events, and imagining ways to decrease them. It is from the meticulous analysis of factors such as elastic recoil, neointimal hyperplasia, neoatherogenesis, hypersensitivity, and, more recently, vasomotor response that the devices have been continuously improving and with them adverse events decreasing. Technological innovations such as DES with biodegradable polymers and bioresorbable vascular scaffolds still continue to disturb vessel physiology and healing.


**Fig. 8.4** An example of exercise-induced vasoconstriction in a patient treated with biolimus-eluting coronary stent (S). **a** Baseline. Vasoconstriction at the peri-stent segments (*) can be observed after exercise at **b** 50 and **c** 100 watts and vanishes after nitroglycerin administration **d**.

## References


1. Nobuyoshi M, Kimura T, Nosaka H, Mioka S, Ueno K, Yokoi H, et al. Restenosis after successful percutaneous transluminal coronary angioplasty: serial angiographic follow-up of 229 patients. J Am Coll Cardiol. 1988;12(3):616–23.
2. Rodriguez AE, Santaera O, Larribau M, Fernandez M, Sarmiento R, Perez B, et al. Coronary stenting decreases restenosis in lesions with early loss in luminal diameter 24 hours after successful PTCA. Circulation. 1995;91(5):1397–402.
3. Rensing BJ, Hermans WR, Beatt KJ, Laarman GJ, Suryapranata H, van den Brand M, et al. Quantitative angiographic assessment of elastic recoil after percutaneous transluminal coronary angioplasty. Am J Cardiol. 1990;66(15):1039–44.
4. Corcos T, David PR, Val PG, Renkin J, Dangoisse V, Rapold HG, et al. Failure of diltiazem to prevent restenosis after percutaneous transluminal coronary angioplasty. Am Heart J. 1985;109(5 Pt 1):926–31.
5. Essed CE, Van den Brand M, Becker AE. Transluminal coronary angioplasty and early restenosis. Fibrocellular occlusion after wall laceration. Br Heart J. 1983;49(4):393–6.
6. Serruys PW, Luijten HE, Beatt KJ, Geuskens R, de Feyter PJ, van den Brand M, et al. Incidence of restenosis after successful coronary angioplasty: a time-related phenomenon. A quantitative angiographic study in 342 consecutive patients at 1, 2, 3, and 4 months. Circulation. 1988;77(2):361–71.
7. Thornton MA, Gruentzig AR, Hollman J, King 3rd SB, Douglas JS. Coumadin and aspirin in prevention of recurrence after transluminal coronary angioplasty: a randomized study. Circulation. 1984;69(4):721–7.
8. Reis GJ, Boucher TM, Sipperly ME, Silverman DI, McCabe CH, Baim DS, et al. Randomised trial of fish oil for prevention of restenosis after coronary angioplasty. Lancet. 1989;2(8656):177–81.
9. Kimura T, Kaburagi S, Tamura T, Yokoi H, Nakagawa Y, Yokoi H, et al. Remodeling of human coronary arteries undergoing coronary angioplasty or atherectomy. Circulation. 1997;96(2):475–83.
10. Danenberg HD, Fishbein I, Gao J, Monkkonen J, Reich R, Gati I, et al. Macrophage depletion by clodronate-containing liposomes reduces neointimal formation after balloon injury in rats and rabbits. Circulation. 2002;106(5):599–605.
11. Danenberg HD, Welt FG, Walker 3rd M, Seifert P, Toegel GS, Edelman ER. Systemic inflammation induced by lipopolysaccharide increases neointimal formation after balloon and stent injury in rabbits. Circulation. 2002;105(24):2917–22.
12. Serrano MC, Vavra AK, Jen M, Hogg ME, Murar J, Martinez J, et al. Poly(diol-co-citrate)s as novel elastomeric perivascular wraps for the reduction of neointimal hyperplasia. Macromol Biosci. 2011;11(5):700–9.
13. Brugaletta S, Gori T, Low AF, Tousek P, Pinar E, Gomez-Lara J, et al. Absorb bioresorbable vascular scaffold versus everolimus-eluting metallic stent in ST-segment elevation myocardial infarction: 1-year results of a propensity score matching comparison: the BVS-EXAMINATION Study (bioresorbable vascular scaffold-a clinical evaluation of everolimus eluting coronary stents in the treatment of patients with ST-segment elevation myocardial infarction). JACC Cardiovasc Interv. 2015;8(1 Pt B):189–97.
14. Schatz RA, Palmaz JC, Tio FO, Garcia F, Garcia O, Reuter SR. Balloon-expandable intracoronary stents in the adult dog. Circulation. 1987;76(2):450–7.

15. Kimura T, Yokoi H, Nakagawa Y, Tamura T, Kaburagi S, Sawada Y, et al. Three-year follow-up after implantation of metallic coronary-artery stents. N Engl J Med. 1996;334(9):561–6.
16. Komatsu R, Ueda M, Naruko T, Kojima A, Becker AE. Neointimal tissue response at sites of coronary stenting in humans: macroscopic, histological, and immunohistochemical analyses. Circulation. 1998;98(3):224–33.
17. Park SJ, Kang SJ, Virmani R, Nakano M, Ueda Y. In-stent neoatherosclerosis: a final common pathway of late stent failure. J Am Coll Cardiol. 2012;59(23):2051–7.
18. Kimura T, Abe K, Shizuta S, Odashiro K, Yoshida Y, Sakai K, et al. Long-term clinical and angiographic follow-up after coronary stent placement in native coronary arteries. Circulation. 2002;105(25):2986–91.
19. Nobuyoshi M, Kimura T, Ohishi H, Horiuchi H, Nosaka H, Hamasaki N, et al. Restenosis after percutaneous transluminal coronary angioplasty: pathologic observations in 20 patients. J Am Coll Cardiol. 1991;17(2):433–9.
20. Farb A, Kolodgie FD, Hwang JY, Burke AP, Tefera K, Weber DK, et al. Extracellular matrix changes in stented human coronary arteries. Circulation. 2004;110(8):940–7.
21. Farb A, Burke AP, Kolodgie FD, Virmani R. Pathological mechanisms of fatal late coronary stent thrombosis in humans. Circulation. 2003;108(14):1701–6.
22. Ramcharitar S, Garcia-Garcia HM, Nakazawa G, Kukreja N, Ligthart J, Virmani R, et al. Ultrasonic and pathological evidence of a neo-intimal plaque rupture in patients with bare metal stents. EuroIntervention J EuroPCR Collab Work Group Interv Cardiol Eur Soc Cardiol. 2007;3(2):290–1.
23. Nakazawa G, Vorpahl M, Finn AV, Narula J, Virmani R. One step forward and two steps back with drug-eluting-stents: from preventing restenosis to causing late thrombosis and nouveau atherosclerosis. J Am Coll Cardiol Img. 2009;2(5):625–8.
24. Yokoyama S, Takano M, Yamamoto M, Inami S, Sakai S, Okamatsu K, et al. Extended follow-up by serial angioscopic observation for bare-metal stents in native coronary arteries: from healing response to atherosclerotic transformation of neointima. Circ Cardiovasc Interv. 2009;2(3):205–12.
25. Takano M, Yamamoto M, Inami S, Murakami D, Ohba T, Seino Y, et al. Appearance of lipid-laden intima and neovascularization after implantation of bare-metal stents extended late-phase observation by intracoronary optical coherence tomography. J Am Coll Cardiol. 2009;55(1):26–32.
26. Virmani R, Guagliumi G, Farb A, Musumeci G, Grieco N, Motta T, et al. Localized hypersensitivity and late coronary thrombosis secondary to a sirolimus-eluting stent: should we be cautious? Circulation. 2004;109(6):701–5.
27. Nakazawa G, Finn AV, Vorpahl M, Ladich ER, Kolodgie FD, Virmani R. Coronary responses and differential mechanisms of late stent thrombosis attributed to first-generation sirolimus- and paclitaxel-eluting stents. J Am Coll Cardiol. 2011;57(4):390–8.
28. Joner M, Finn AV, Farb A, Mont EK, Kolodgie FD, Ladich E, et al. Pathology of drug-eluting stents in humans: delayed healing and late thrombotic risk. J Am Coll Cardiol. 2006;48(1):193–202.
29. Cook S, Wenaweser P, Togni M, Billinger M, Morger C, Seiler C, et al. Incomplete stent apposition and very late stent thrombosis after drug-eluting stent implantation. Circulation. 2007;115(18):2426–34.
30. Jukema JW, Ahmed TA, Verschuren JJ, Quax PH. Restenosis after PCI. Part 2: prevention and therapy. Nat Rev Cardiol. 2012;9(2):79–90.
31. Onuma Y, Serruys PW. Bioresorbable scaffold: the advent of a new era in percutaneous coronary and peripheral revascularization? Circulation. 2011;123(7):779–97.
32. Gogas BD, Farooq V, Onuma Y, Serruys PW. The ABSORB bioresorbable vascular scaffold: an evolution or revolution in interventional cardiology? Hellenic J Cardiol. 2012;53(4):301–9.
33. Serruys PW, Chevalier B, Dudek D, Cequier A, Carrie D, Iniguez A, et al. A bioresorbable everolimus-eluting scaffold versus a metallic everolimus-eluting stent for ischaemic heart disease caused by de-novo native coronary artery lesions (ABSORB II): an interim 1-year analysis of clinical and procedural secondary outcomes from a randomised controlled trial. Lancet. 2015;385(9962):43–54.
34. Puricel S, Arroyo D, Corpataux N, Baeriswyl G, Lehmann S, Kallinikou Z, et al. Comparison of everolimus- and biolimus-eluting coronary stents with everolimus-eluting bioresorbable vascular scaffolds. J Am Coll Cardiol. 2015;65(8):791–801.
35. Capodanno D, Gori T, Nef H, Latib A, Mehilli J, Lesiak M, et al. Percutaneous coronary intervention with everolimus-eluting bioresorbable vascular scaffolds in routine clinical practice: early and midterm outcomes from the European multicentre GHOST-EU registry. EuroIntervention J EuroPCR Collab Work Group Interv Cardiol Eur Soc Cardiol. 2015;10(10):1144–53.
36. Kraak RP, Hassell ME, Grundeken MJ, Koch KT, Henriques JP, Piek JJ, et al. Initial experience and clinical evaluation of the absorb bioresorbable vascular scaffold (BVS) in real-world practice: the AMC Single Centre Real World PCI Registry. EuroIntervention J EuroPCR Collab Work Group Interv Cardiol Eur Soc Cardiol. 2015;10(10):1160–8.
37. Cuculi F, Puricel S, Jamshidi P, Velntin J, Kallinikou Z, Toggweiler S, et al. Optical coherence tomography findings in bioresorbable vascular scaffolds thrombosis. Circ Cardiovasc Interv. 2015;8(10):e002518.
38. Tellez A, Afari ME, Buszman PP, Seifert P, Cheng Y, Milewski K, et al. Peristrut low-intensity areas in optical coherence tomography correlate with peri-strut inflammation and neointimal proliferation: an in-vivo correlation study in the familial hypercholesterolemic coronary swine model of in-stent restenosis. Coron Artery Dis. 2014;25(7):595–601.
39. Caramori PR, Lima VC, Seidelin PH, Newton GE, Parker JD, Adelman AG. Long-term endothelial dysfunction after coronary artery stenting. J Am Coll Cardiol. 1999;34(6):1675–9.
40. Gordon JB, Ganz P, Nabel EG, Fish RD, Zebede J, Mudge GH, et al. Atherosclerosis influences the vasomotor response of epicardial coronary arteries to exercise. J Clin Invest. 1989;83(6):1946–52.
41. Hofma SH, van der Giessen WJ, van Dalen BM, Lemos PA, McFadden EP, Sianos G, et al. Indication of long-term endothelial dysfunction after sirolimus-eluting stent implantation. Eur Heart J. 2006;27(2):166–70.
42. Togni M, Raber L, Cocchia R, Wenaweser P, Cook S, Windecker S, et al. Local vascular dysfunction after coronary paclitaxel-eluting stent implantation. Int J Cardiol. 2007;120(2):212–20.
43. Togni M, Windecker S, Cocchia R, Wenaweser P, Cook S, Billinger M, et al. Sirolimus-eluting stents associated with paradoxic coronary vasoconstriction. J Am Coll Cardiol. 2005;46(2):231–6.
44. Kim JW, Suh SY, Choi CU, Na JO, Kim EJ, Rha SW, et al. Six-month comparison of coronary endothelial dysfunction associated with sirolimus-eluting stent versus Paclitaxel-eluting stent. JACC Cardiovasc Interv. 2008;1(1):65–71.
45. Fuke S, Maekawa K, Kawamoto K, Saito H, Sato T, Hioka T, et al. Impaired endothelial vasomotor function after sirolimus-eluting stent implantation. Circ J Off J Jpn Circ Soc. 2007;71(2):220–5.
46. Hamilos MI, Ostojic M, Beleslin B, Sagic D, Mangovski L, Stojkovic S, et al. Differential effects of drug-eluting stents on local endothelium-dependent coronary vasomotion. J Am Coll Cardiol. 2008;51(22):2123–9.
47. Puricel S, Kallinikou Z, Espinola J, Arroyo D, Goy JJ, Stauffer JC, et al. Comparison of endothelium-dependent and -independent vasomotor response after abluminal biodegradable polymer biolimus-eluting stent and persistent polymer everolimus-eluting stent implantation (COMPARE-IT). Int J Cardiol. 2016;202:525–31.
48. Sarno G, Bruining N, Onuma Y, Garg S, Brugaletta S, De Winter S, et al. Morphological and functional evaluation of the bioresorption of the bioresorbable everolimus-eluting vascular scaffold using IVUS, echogenicity and vasomotion testing at two year follow-up: a patient level insight into the ABSORB a clinical trial. Int J Cardiovasc Imaging. 2012;28(1):51–8.
49. Brugaletta S, Heo JH, Garcia-Garcia HM, Farooq V, van Geuns RJ, de Bruyne B, et al. Endothelial-dependent vasomotion in a coronary segment treated by ABSORB everolimus-eluting bioresorbable vascular scaffold system is related to plaque composition at the time of bioresorption of the polymer: indirect finding of vascular reparative therapy? Eur Heart J. 2012;33(11):1325–33.

# The Coronary Circulation in Cardiomyopathies and Cardiac Allografts

## Effect of Specific Pathologies on Epicardial Vessels and the Microcirculation

*Christopher J. Broyd, Fernando Dominguez, and Pablo Garcia-Pavia*




J. Escaned, J. Davies (eds.), *Physiological Assessment of Coronary Stenoses and the Microcirculation*,
DOI 10.1007/978-1-4471-5245-3_9

## 9.1 Introduction

While all cardiomyopathies share the definition of a disease that primarily affects the structure of the myocardium, the resultant diseases are diverse. However, one unifying feature is that these structural abnormalities all impinge to greater or lesser extents on the microcirculation. Additionally, some have significant influential effects on the epicardial system as well. In fact, often the resultant morbidity and mortality of these diseases are severely influenced by the effect of coronary microvascular dysfunction (CMD).

As both noninvasive and invasive techniques are increasing in sophistication and can provide information on separated domains within the coronary tree, their application to cardiomyopathic processes provides an insight into the pathology of these diseases. However, perhaps more importantly, they also act as a supplementary diagnostic tool and may even confer some risk stratification options. As more specific treatment options emerge in a variety of these diseases that until now could only be managed supportively, identifying the disease processes early and instigating these therapies in a timely fashion can only be advantageous. Therefore, appreciation of the impact of these processes on the macro- and microcirculation is essential to appropriately manage these patients.

During this chapter, we consider how the coronary circulation is impacted by these conditions, dividing them broadly into primary and secondary causes, and discuss investigative options that target the epicardial and (particularly) the microcirculatory domains. Additionally, we go on to discuss the process of cardiac allograft vasculopathy, its impact on the coronary system, and recent insights in this field.

## 9.2 Primary Cardiomyopathies

### 9.2.1 Hypertrophic Cardiomyopathy

#### Background

Hypertrophic cardiomyopathy (HCM) is the most common genetic heart disease with a prevalence of around 1:500 with significant variability in its phenotype, pathophysiology, and clinical course. HCM is one of the commonest causes of sudden cardiac death in the young, and with the advent of ICD for SCD prevention, mortality and morbidity of this disease are dominated by heart failure. HCM is most commonly caused by mutation in a gene that codifies for proteins of the sarcomere resulting in a thickening of the heart muscle as well as significant myocardial disarray.

The presence of an abnormal microvascular function has been recognized clinically in HCM as the description of angina [1] or even the presence of frank myocardial infarction [2] in the absence of significant epicardial coronary disease. Formal documentation of relative myocardial ischemia using thallium scanning was first performed almost 35 years ago [3], and there now exists a substantial body of evidence, across a diverse array of modalities, to demonstrate this.

Experimental models and histology studies have demonstrated several potential etiological mechanisms most likely which synergistically interact to cause this relative myocardial ischemia. Additionally, it is now appreciated to not simply be a benign result of myocardial hypertrophy but is actively involved in disease progression, morbidity, and mortality. Its recognition and perhaps quantification are likely therefore to be an important facet in the future in the management of this condition and may ultimately play a role in risk stratification.

### 9.2.2 Evidence for Microvascular Dysfunction in HCM and Their Prognostic Insights

The most widespread investigative tool for the investigation of the microcirculation is the measurement of coronary flow reserve (CFR), which can be achieved through a number of modalities as outlined below. Many of those modalities allow not just a binary outcome measure but a semi- or absolute quantification of the microvascular burden.

### 9.2.3 Scintigraphy and Biochemistry

The earliest work in this field used thallium-201 and angiography to demonstrate the presence of ischemia but the absence of significant coronary disease. Further work using exercise scintigraphy in conjunction with invasive cardiac vein lactate sampling as a biochemical marker of myocardial ischemia has demonstrated the presence of reversible defects in a significant number of patients with HCM and that this corresponds to biochemical-confirmed myocardial ischemia [4]. Those patients with abnormal scans appear to more frequently suffer from chest pain despite unobstructed coronary arteries [3]. A similar invasive biochemical study used coronary sinus pH as a marker of myocardial ischemia and demonstrated it to be significantly low compared to controls during dipyridamole stress, often in conjunction with significant chest pain [5].

SPECT has also been used for prognostic purposes. A study showed that HCM patients with a positive thallium scan and no evidence of coronary disease had a higher incidence of VT or arrhythmias requiring pacemaker implantation [6]. A beneficial effect of verapamil in HCM was also being demonstrated with this modality with an increase in exercise tolerance and a decrease in exercise-induced defects occurred following its administration [7]. Finally, SPECT has been used for more global prognostication with a higher risk of cardiovascular death in HCM patients with abnormal imaging results [8].

While thallium scans can demonstrate the presence of inducible ischemia with dipyridamole stimulation, interestingly an unconnected proportion of patients appear to

have evidence of ischemia on ambulatory ECG monitoring during daily life [9]. Therefore, while many patients may have no evidence of myocardial ischemia with provocation, that does not mean they are entirely free of microvascular ischemia.

### 9.2.4 Echocardiography

Direct imaging of the LAD using transthoracic echocardiography is now a feasible mechanism for the assessment of coronary flow reserve [10]. Using echocardiography, control patients have lower resting peak diastolic flow rates compared to all HCM patients but similar hyperemic peaks amounting to a reduced CFR [11].

Further information can also be gleaned with this modality. Firstly, symptomatic patients with HCM have been noted to have a CFR lower than those who are asymptomatic [12]. Additionally, patients with HCM appear to have an inverse linear relationship between wall thickness and coronary flow reserve in the territory in question as assessed by echocardiographic imaging of the LAD or PDA [13]. CFR assessed through echocardiography has also been reported as a prognostic parameter in HCM. Using a cutoff value of 2, an abnormal CFR has been reported to infer a tenfold increased risk of significant future events [12].

Certain resting parameters have been noted to reflect microvascular dysfunction, mostly in the context of acute myocardial infarction [14, 15]. However, these parameters have also been noted in HCM patients, particularly systolic flow reversal, slow acceleration, and rapid diastolic deceleration time [16].

### 9.2.5 MRI

As with echocardiography, MRI has demonstrated that CFR is predominantly reduced in HCM due to a lower hyperemic flow rate. However, MRI is also able to quantify where this abnormality dominates; this is particularly in the endocardial layer and is in proportion to the magnitude of the hypertrophy [17] with a significant inverse relationship between wall thickness and hyperemic myocardial blood flow [17]. By combining MRI with PET studies, the reduction in hyperemic flow can be regionalized to areas adjacent to fibrosis [18] suggesting therefore that replacement fibrosis may be the result of ischemia and cell death.

MRI has also been used to demonstrate the presence of scarring in patients with minimal or no symptoms and predominantly occurs in hypertrophied regions [17], and its presence is often linked with a reduced contraction [19]. Two reports of explanted hearts of patients that had undergone recent MRI demonstrated that late gadolinium enhancement appeared to be related to the amount of collagen but not myocardial disarray as was regional wall motion [20, 21].

### 9.2.6 PET

Similar to echocardiographically determined CFR, PET has also demonstrated CFR to be lower in HCM patients who are symptomatic compared to asymptomatic [22]. Again, many studies using PET have demonstrated an abnormally low peak myocardial blood flow, which is the cause of the abnormally low CFR. Additionally, in those patients with an abnormal fractional shortening, a positive linear correlation was noted with dipyridamole myocardial blood flow [23] implying that this microvascular dysfunction is involved in the development of systolic impairment in HCM.

Importantly however, PET scanning has demonstrated that even in a non-hypertrophied free wall, microcirculatory abnormalities are appreciable despite the echocardiographic appearance of normality [22]. PET scanning reveals a markedly blunted response to dipyridamole in patients with HCM, and in turn this feature is a good predictor of adverse outcomes (clinical deterioration or death) [24] or a more rapid deterioration in systolic function over time [25].

The positive effect of verapamil therapy has been demonstrated with PET where subendocardial underperfusion improved in individuals randomized to therapy versus placebo [26]. Interestingly, there was no increase in overall myocardial blood flow, but rather redistribution appears to occur [27].

### 9.2.7 Myocardial Contrast Echocardiography

The only available data with this technique comes from a combined study with myocardial contrast echocardiography and PET scans that demonstrated relative myocardial blood flow and hyperemic myocardial blood flow to be influenced by LVEDP, outflow tract gradient, and LV mass index [28].

### 9.2.8 Invasive Catheterization Studies

The presence of an abnormal CFR in HCM has also been demonstrated invasively using a conventional Doppler-tipped flow wire. Additionally, coronary resistance ratio (the ratio of coronary resistance at rest and hyperemia where resistance = aortic pressure−end-diastolic pressure/velocity) was found to be reduced in HCM compared to controls [29].

### 9.2.9 Causes of Microvascular Dysfunction in HCM

Both animal experimental studies and work with pediatric and adult patients with hypertrophied hearts have provided insight into the potential mechanisms for microvascular dysfunction in HCM. While a number of pathological features are present in HCM, it is unlikely that a single mechanism is responsible for the significant microvascular abnormalities seen in this condition. Instead these mechanisms interact to greater or lesser extents in a synergistic fashion.

### 9.2.10 Relative Arteriolar Lumen Size

Many have suggested that the morphological abnormalities of the intramural coronary arteries are the primary substrate for microvascular dysfunction [30]. Insightful work from Kramset al. investigated both intracoronary physiology using a Doppler flow wire and biopsy or myectomy-obtained histology patterns in patients with HCM and controls. A relative reduction in the size of the arteriolar lumen was noted in patients with HCM compared to controls. Additionally, the coronary resistance ratio was linearly related to relative arteriolar lumen size [29], features confirmed by a second group in the same year using the inert chromatographic argon method to determine coronary resistance [31].

Necropsy studies have also demonstrated the presence of abnormal intramural microcirculatory vessels (arterioles) in the majority (80 %) of patients with hypertrophic cardiomyopathy with a narrowed lumen due to proliferation of the intima and medial smooth muscle cells and collagen [32, 33]. Because necropsy studies have an inherent bias toward higher-risk patients, studies with combined MRI and myectomy histology were undertaken and were able to demonstrate again a relationship between small intramural coronary arteriole dysplasia and scarring in HCM patients [34].

Interestingly, this abnormal arteriolar wall structure appears to be inherent to HCM left ventricular hypertrophy. While it is seen in left ventricular hypertrophy models in both guinea pigs [35–37] and rats [38–40], it has not been reproduced in ventricular biopsies taken from humans with LVH secondary to hypertension [41] or in pig models [42]. Additionally, autopsy specimens from patients with LVH secondary to aortic stenosis do not show intramyocardial arteriole wall thickening [43].

### 9.2.11 Decreased Density of Coronary Resistance Vessels in Hypertrophied Myocardium

In order for vessel density to be maintained, and to protect against relative ischemia, as muscle mass increases, perforating vessel number and size needs to increase in parallel. However, this does not appear to be the case in left ventricular hypertrophy – either in the form of HCM or from secondary causes with mass outstripping that of vessel number or size.

Both arteriolar [31] and capillary density [29] are reduced in HCM and accompany the resultant changes in coronary resistance. In animal models of LVH, changes in the vascular bed do not seem to parallel myocyte growth in left ventricular hypertrophy. In pig [42] and dog [44] models of left ventricular hypertrophy with demonstrably impaired CFR, anatomical studies have shown that hypertrophy causes a reduction in endomyocardial capillary density. Interestingly, a separate study has shown this phenomenon is less evident at 1 year suggesting there may be a lag, rather than absolute deficit, between LVH and new vessel growth [45].

A similar relative reduction in cardiac vessel growth during hypertrophy has also been demonstrated in rats by assessing cardiac cyclic GMP (cGMP) kinase levels (cGMP is a protein involved in the regulation of vascular smooth muscle tone) [46]. In humans, autopsy studies of patients with LVH due to aortic stenosis have shown a decrease in coronary capillary density in comparison to controls [47].

### 9.2.12 Increased Perivascular Compression Due to Changes in Myocardial Structure and a Greater Compressive Effect of Systole

In humans, there is a linear correlation between coronary resistance and left ventricular end-diastolic pressure (LVEDP) suggesting the importance of these external compressive forces [48]; however, the reduction in coronary reserve is proportionally greater than the increase in LVEDP reinforcing the multifactorial nature of this problem. In the guinea pig model, the effect of perivascular compression, as well as the increase in the compressive effect of systole, has been demonstrated to impact negatively on coronary flow reserve with LVH [49].

Certainly in adults with hypertrophy induced by aortic stenosis, PET scanning and pre- and post-aortic valve replacement have shown a strong correlation between CFR and the hemodynamic load on the left ventricle and hemodynamic severity of the valve stenosis. They did not find a relationship with left ventricular mass and go on to suggest microvascular dysfunction results predominantly from extravascular compressive mechanisms as well as changes in diastolic perfusion time [50].

### 9.2.13 Increased Muscle Mass

Despite these studies in aortic stenosis [50], without an outflow tract gradient, it is well accepted that the more muscle mass present, the higher the oxygen demands of the heart will be and the potential for microvascular dysfunction. On a macroscopic level, the size of the large coronary arteries increases with LVH, and after aortic valve replacement for aortic stenosis, the arteries return to normal [51]. However, studies in animals and humans have suggested that the increase in size is not proportional to the increase in cross-sectional muscle mass creating a relative imbalance in oxygen supply and demand [42, 43].

Certainly, a huge evidence base exists to demonstrate the prognostic effect of secondary left ventricular hypertrophy. For example, the Framington study showed that left ventricular mass measured by echocardiography was associated with cardiovascular events, cardiovascular deaths, and death from all cause independent of other cardiovascular risk factors [52–54]. For every increment of 50 g/m height in LV mass, the relative risk of cardiovascular disease was increased approximately 1.5-fold, effects that are independent from that of blood pres-

sure [55]. Additionally, this effect on the microvasculature is reversible and has been shown in many animal models [56–60] and in pharmacologically treated patients [61–65].

### 9.2.14 Increased Diffusion Distance from Capillary to Center of Hypertrophied Myocardial Cells

It has also been suggested that as the myocytes increase in size, there is an increased diffusion distance from the capillary to the center of the cell [66, 67]. Additionally, the pressure within the myocardial cells is increased [68], and these factors will impair oxygen transfer. However, these findings are not supported in all studies [69].

### 9.2.15 Endothelial Dysfunction



Structural changes in coronary vasculature may not fully account for the reduction in coronary reserve, and there may in fact be a change at the endothelial level as well. For example, coronary reserve has been shown to be reduced in hypertensive patients [70, 71] and animal models [72] prior to the development of LVH. Rats with LVH have been shown to have a reduced production of coronary nitric oxide synthase, another reflection of endothelial dysfunction [36]. Using explanted coronary arteries from a guinea pig model of LVH, Mcgoldrick et al. confirmed that coronary vessels from hypertrophied hearts have impaired relaxation to endothelial-dependent and independent agents [73].

Additionally, LVH also results in a greater propensity to anerobic metabolism due to an attenuated microvascular response to hyperemia [35, 74]. They are therefore more vulnerable to the effects of myocardial ischemia as they are unable to recover as well from such insults. For example, in dogs with LVH, occlusion of the circumflex artery resulted in a much larger area of infarction than controls [75].

However, the majority of these studies are conducted in models or patients with secondary LVH. Endothelial cells may therefore be responding to exogenous systemic pressure, and therefore extrapolating these conclusions to patients with HCM is done with extreme caution.

### 9.2.16 Non-atherosclerotic Epicardial Influence

Relative myocardial ischemia and worsening microvascular dysfunction may also be stimulated from non-atherosclerotic epicardial vessels due to significant myocardial bridging. Historical work examining angiograms from 36 children (mean age 7.1 years) demonstrated 28 % to have myocardial bridging which caused compression of the LAD for 50 % of diastole. In those patients with a myocardial bridge, chest pain, previous cardiac arrest, and ventricular tachycardia were more frequent [76]. A case report of a child who suffered sudden cardiac death confirmed the presence of both an intramurally directed LAD and a hemorrhagic acute septal myocardial infarction representing perhaps cause and effect [77].

### 9.2.17 The Influence of Outflow Tract Obstruction

Invasive work with aortic stenosis, in particular in patients undergoing transcatheter valve therapy, has shown clearly that the presence of an outflow tract obstruction has a marked detrimental effect on microvascular function over and above that of left ventricular hypertrophy [78]. Therefore, it is of no surprise that a similar feature exists in HCM. For example, oxygen consumption per 100 g in a series of 14 patients has been found to be equivalent to controls implying that metabolic demand is unchanged [31]. However, this feature is altered in the presence of an outflow tract obstruction where myocardial oxygen demand is increased [1].

Invasive studies using Doppler flow wires have shown an inverse relationship between peak outflow tract gradient and CFR [79]. Patients with an outflow tract obstruction (of >30 mmHg) tend to have higher resting peak coronary velocity but equivalent hyperemic velocities translating to lower coronary flow reserve than patients with hypertrophy but no gradient as seen using noninvasive Doppler [11]. Interestingly, surgical myectomy has been shown to improve myocardial dynamics with a reduction in myocardial lactate production [80].

### 9.2.18 Other Structural Changes Favoring Microvascular Dysfunction

There are also substantially higher levels of collagen and matrix connective tissue [81] with increased turnover rates [82], evidence of fibrosis [83], and myocyte disarray [84], all of which may contribute to microvascular dysfunction. Individual studies have suggested that the collagen and disarray are more likely in the mesocardium than endo- or epicardium.

A separate similar necropsy study of sudden death in HCM identified isolated or multiple septal scars in nearly two-thirds of patients implying that this relative ischemia from microvascular dysfunction may cause tissue infarction and be a factor involved in life-threatening arrhythmias [85].

### 9.2.19 Conclusion

The evidence for microvascular dysfunction in HCM is overwhelming and can be recognized clinically, prognostically, and through a variety of investigative modalities. While this was first appreciated 35 years ago, what is now more well appreciated is the role that microvascular dysfunction has in morbidity and mortality.

The cause of microvascular dysfunction is multifactorial and certainly involves microstructural abnormalities such as a decreased lumen-vessel ratio and a reduction in capillary and arteriole density. The demanding effect of left ventricular mass on oxygen necessities is also evident and is a significant cause of resultant scarring, arrhythmogenesis, and the progression to heart failure.

However, the information obtained, particularly from PET scanning, is very insightful, demonstrating that significant abnormalities exist in the microvasculature even in non-thickened myocardium. Therefore, it appears the microvasculature is not just a passive result from these mechanisms but an important feature of the disease, and in fact despite its name, one of the primary features of hypertrophic cardiomyopathy is a disorganized microstructure.

At present, there are options for both medical and device therapy in the treatment of these patients. Conventional risk stratification does not require a microvascular assessment. However, given its prognostic influence and its primary role in HCM, this may change in the future with the above investigative modalities providing both quantitative information and an ability to monitor therapy.

## 9.3 Dilated Cardiomyopathy (DCM)

DCM is characterized by reduced contractile function and dilation of the left or both ventricular chambers. In this regard, we will refer to idiopathic DCM, whose diagnosis requires exclusion of significant coronary artery disease (CAD), as well as heavy alcohol consumption or systemic diseases such as diabetes mellitus (DM), which can cause DCM by themselves. The classical pathogenic mechanisms in "idiopathic" DCM include genetic, viral, or autoimmune etiology. Up to 20–45 % of patients respond to treatment, but prognosis is still poor with a 20 % survival at 5 years [86]

Coronary microvascular dysfunction (CMD) in DCM is thought to be present from very early phases of the disease, and it is associated with an increased risk of sudden cardiac death and cardiac events [87].

It is thought that left ventricular dysfunction and structural alterations of the myocardium such as perivascular fibrosis lead to abnormalities in the myocardial blood flow (MBF) by extravascular mechanisms. For instance, by an increase in wall stress in advanced DCM that eventually would raise oxygen demand [88]. In this setting, vasodilator therapy with angiotensin-converting enzyme (ACE) inhibitors or the combination of isosorbide dinitrate and hydralazine can reduce ventricular preload and improve extravascular compression [89].

On the other hand, vascular abnormalities are present, with reduced capillary density and endothelial dysfunction. Consequently, MBF and CFR are impaired [90, 91], and together with the increased oxygen [89] demand due to the extravascular mechanisms, they contribute to continuous episodes of ischemia that will worsen left ventricular ejection fraction. Vasodilator therapy could have also a role in improving endothelial dysfunction and preventing microvascular remodeling [92, 93].

### 9.3.1 Arrhythmogenic Right Ventricular Cardiomyopathy (ARVC)

ARVC is a genetically determined heart muscle disease histologically characterized by fibro-fatty replacement of the right ventricular (RV) myocardium, with an estimated prevalence of 1:5000 in the general population. In early stages, structural changes may be confined to a specific region of the RV, including the inflow tract, outflow tract, and apex [94]. In a more advanced phase of the disease, these abnormalities can also affect the left ventricle, resulting in a DCM phenotype.

Regarding microcirculation in this population, there is very little information. Paul M et al. have shown a significantly reduced hyperemic MBF and increased coronary vascular resistance in a small cohort of patients with non-failing ARVC, compared to controls [95]. Other studies have been focused on the myocardial autonomic dysfunction in ARVC patients and its vascular consequences. As a result of increased norepinephrine release at the presynaptic cleft, a downregulation of β-adrenergic receptors occurs. Consequently, β-adrenoceptor-mediated vasodilatation is impaired in ARVC during increased sympathetic tone, while α-adrenoceptor vasoconstriction is preserved. Thus, maximal MBF is eventually reduced [96].

### 9.3.2 Left Ventricular Non-compaction (LVNC)

LVNC is a myocardial disorder, which is thought to occur due to an early cessation of compaction of trabecular meshwork during embryogenesis. This leads to a two-layered ventricular wall, with a thinner compact epicardial component and an inner prominently trabeculated layer. In the position statement of the European Society of Cardiology, LVNC is regarded as an unclassified cardiomyopathy because it is not clear whether it is a separate cardiomyopathy or merely a morphological trait shared by other entities. In addition, although it has been observed that a genetic basis may be present in LVNC, the relationship between genotype and phenotype is not clear [97].

Although information concerning CMD in LVNC is scarce in the literature, a study by Jenni et al. was specifically designed to address this issue [98]. MBF and CFR were quantified in 12 LVNC patients compared to 14 control subjects using positron emission tomography (PET) and (13) N-ammonia. CFR was significantly decreased in LVNC subjects compared to controls, but the perfusion defects were not only confined to the non-compacted segments as some morphologically unaffected regions showed abnormalities too. However, segments with wall motion abnormalities did show a greater impairment of CFR. Thus, CMD might be present in LVNC but does not seem to be related with LVNC phenotype.

### 9.3.3 Stress-Induced (Tako-Tsubo) Cardiomyopathy

Tako-tsubo cardiomyopathy or transient LV apical ballooning syndrome is defined by transient LV dysfunction, electrocardiographic changes that mimic acute myocardial infarction (MI), and release of myocardial enzymes in the absence of obstructive coronary artery disease. Its prevalence among clinically suspected acute coronary syndromes ranges between 1.2 and 2.0 %, and it was first described during the 1990s in Japan, where *tako-tsubo* is a pot with a narrow neck and a circular bottom used for trapping octopuses [99]. It is mainly seen in postmenopausal women and is usually associated with emotional or physical stress [100].

The underlying pathological mechanisms of this entity are still not completely understood, but multivessel coronary vasospasm, catecholamine-induced myocardial-stunning abnormalities, spontaneous coronary thrombus lysis, and CMD are some of the proposed etiologies. Some studies support the role of CMD in apical ballooning syndrome. For instance, it has been observed that the initially impaired CFR in these patients improves spontaneously 1 month after the acute phase, assessed by transthoracic Doppler. During the acute setting, contrast echocardiography evidences a clear perfusion defect in segments with wall motion abnormalities, but after intravenous adenosine, the coronary perfusion transiently recovers, and these regional wall motion abnormalities disappear. Hence, these findings prove that one of the pathogenic mechanisms might be reversible CMD [101]. Nonetheless, other studies have observed that CMD is present beyond the acute phase in more than 90 % of the patients, even when left ventricular function has normalized [102]. Along with these findings, a follow-up study by Martin et al. demonstrated an impaired endothelial response to acute mental stress in patients with a history of tako-tsubo syndrome [103].

The fact that stress-induced cardiomyopathy is mainly observed in postmenopausal women may be due to decreased estrogen concentrations, which lead to a reduction in nitric oxide bioavailability and eventually impair coronary microcirculation [104]. Moreover, when compared to patients with acute MI, plasma catecholamine levels have been proved to be higher in tako-tsubo cardiomyopathy, and they remain elevated at least 1 week after the acute phase [105].

### 9.3.4 Myocarditis and Inflammatory Cardiomyopathy

Some of the viruses responsible for myocarditis specifically infect endothelial cells, such as parvovirus B19 (PVB19) or herpesvirus type 6. PVB19 primarily infects erythroid progenitor cells in the bone marrow during childhood, and there is a very high prevalence of persistent and asymptomatic latent infections [106]. Myocarditis symptoms usually respond to reactivations, when chest pain is usually the main symptom as the primary erythrovirus receptor P and its coreceptors are present in endothelial cells, including the coronary arteries. Thus, angina-like symptoms have been related to endothelial dysfunction, and it has been observed that virus-positive patients have a lower increase in CBF after acetylcholine, compared to controls [107]. The mechanisms by which PVB19 causes endothelial damage are still not completely understood. However, studies have shown that endogenous release of PVB19-infected endothelial progenitor cells from the bone marrow may injure the endothelium during vascular repair. In this setting, IFN-β has proven to improve endothelial dysfunction by inhibiting viral transcription, although it does not clear the virus completely [108] (Fig. 9.1).

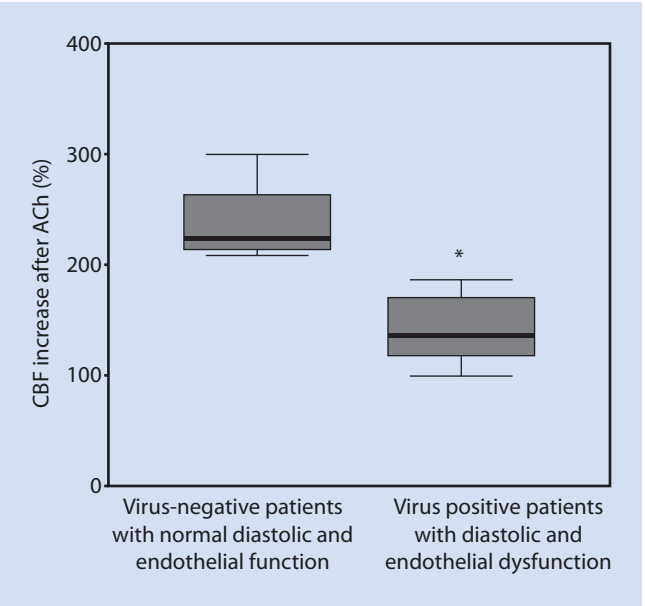


**Fig. 9.1** CBF changes after intracoronary ACh injection, measured by Doppler flow-wire technique. CBF increase of virus-positive patients with diastolic and endothelial dysfunction (n:11) was reduced compared with virus-negative patients with normal diastolic and endothelial function (n:7) (141:14 % vs 239:21 %, **P*:0.003) (Illustration from Ref. [107])

## 9.4 Secondary Cardiomyopathies

In this section, we will review how systemic diseases that involve the heart specifically impair microvascular function. The literature concerning this subject is scarce, so this chapter will focus on two main entities: Anderson-Fabry disease and amyloidosis.

### 9.4.1 Anderson-Fabry Disease (AFD)

AFD is a recessive X-linked lysosomal storage disorder due to a deficiency of alpha-galactosidase A, which results in storage of a glycosphingolipid called globotriaosylceramide

(Gb3) in different tissues. These include the kidney, central and peripheral nervous system, skin, and heart. Left ventricular hypertrophy is the most common cardiac abnormality associated with this disorder, and as it happens in HCM, patients can present with chest discomfort suggesting angina pectoris despite normal epicardial coronary arteries. Attending to these clinical characteristics, several studies have aimed to detect CMD in these patients. Elliot et al. observed that male patients with AFD had a significantly lower MBF and CFR compared to normal controls using PET [109]. All of these subjects had LV hypertrophy, and it has been suggested that angina could respond to lumen narrowing of intramyocardial arteries due to hypertrophy and hyperplasia of cardiomyocytes, as well as perivascular fibrosis [110]. However, a recent study showed that coronary microvascular function is impaired in AFD patients irrespective of LV hypertrophy and gender compared to controls. Thus, evidence of CMD could prematurely detect cardiac involvement in this population [111]. This would have direct clinical consequences because patients could eventually benefit from enzyme replacement therapy at an early stage of the disease, when there is evidence of a greater efficacy and better outcome [112].

As for the pathophysiological mechanisms that led to CMD when LV hypertrophy is not present, these could include endothelial dysfunction due to Gb3 storage that cardiac energetic metabolism, nitric oxide pathway dysregulation, or microvascular remodeling.

### 9.4.2 Cardiac Amyloidosis (CA)

CA responds to the extracellular deposition of a misfolded protein in the heart tissue, either in the context of a systemic disease or as a more localized form.

The most common amyloid fibrils that affect the heart are light chain and transthyretin proteins, which could result in LV hypertrophy and restrictive cardiomyopathy [113].

Amyloid deposits can be found in the interstitium between cardiac myocytes and also in perivascular regions and the medial layer of intramyocardial coronary vessels [114]. Thus, CMD is a potential complication of CA due to pathophysiological mechanisms seen in other entities, such as extrinsic compression of the microvasculature or impairment of endothelial function secondary to the presence of amyloid within the vessels. Following this hypothesis, Dorbala and colleagues described the coronary microvascular function in 21 CA patients without epicardial coronary artery disease, compared to ten subjects with hypertensive LV (Fig. 9.2) [115]. The CA group showed significantly decreased rest MBF, stress MBF and CFR compared to the LV hypertrophy group, as well as a higher minimal coronary vascular resistance. As both groups presented LV hypertrophy, this study reinforces the idea that increased LV mass is not solely responsible for CMD, and other pathophysiological mechanisms may be present. For instance, it is known that

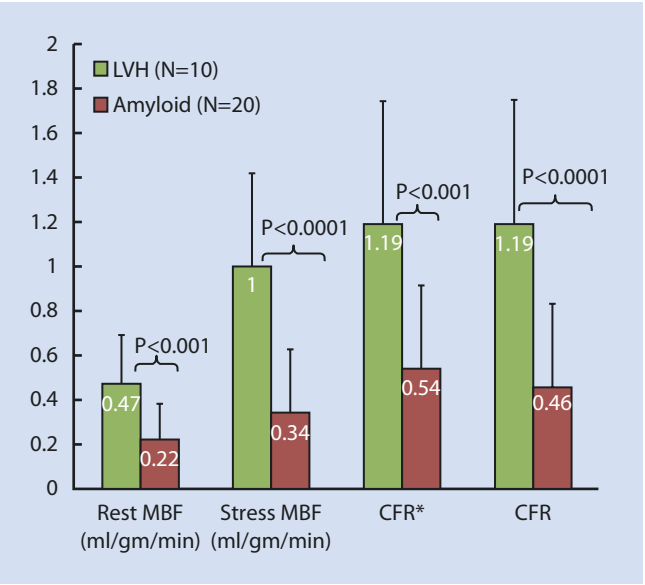


**Fig. 9.2** Mean rest and stress MBF as well as CFR per unit LV mass in the LVH and amyloid groups. The rest MBF was higher in the LVH group. Peak stress MBF, CFR (CFR unadjusted)*, and CFR values were significantly lower in the amyloid group than in the LVH group. *CFR* coronary flow reserve, *LV* Left ventricular, *LVH* left ventricular hypertrophy, *MBF* myocardial blood flow (Adapted from Ref. [115])

patients diagnosed with amyloidosis present autonomic disturbances, and autonomic denervation could potentially affect MBF and CFR as it has been previously seen in diabetic patients [116]. However, further studies are needed in order to address this issue.

## 9.5 Cardiac Allograft Vasculopathy

### 9.5.1 Introduction

Since 1982, more than 110,000 cardiac transplants have been performed worldwide with a current rate of approximately 5000 per year. Huge effort has been expended to combat what was initially the main postoperative issue of acute rejection. With modern transplant immunosuppression, the morbidity and mortality of this process have been dramatically reduced, and as a result, survival now exceeds a median of 10 years. However, this has led to the dominance of chronic rejection as a postoperative problem, one of the main causes for which is cardiac allograft vasculopathy (CAV).

CAV is a fibro-proliferative disorder causing accelerated coronary artery disease with progressive, diffuse, and circumferential intimal lesions that ultimately progress to occlude coronary blood flow. It shares many features similar to conventional atherosclerosis with increased cell adhesion molecular expression, leukocyte infiltration, similar cytokine profiles, aberrant extracellular and intracellular lipids, intimal smooth muscle cell migration, endothelial dysfunction, and abnormal apoptosis [117]. Its risk is progressive over

time with an incidence of 8 % at 1 year, 30 % at 5 years, and 50 % at 10 years [118].

CAV represents a major source of morbidity and mortality and is a significant cause of graft loss and death after the first year [119]. The resultant coronary occlusive disease leads to congestive heart failure, arrhythmias, myocardial infarction, and sudden death. Given the sensory properties of a denervated heart, unfortunately often the initial presentation of CAV is the latter scenario thus necessitating regular screening. Overall, CAV is estimated to be responsible for 10–15 % of cardiac deaths after transplantation. Therefore, the understanding of its pathophysiology and the application of potential therapies are foremost in current transplant medicine representing a significant target in these patients's management.

### 9.5.2 Pathogenesis of CAV



Allograft vasculopathy occurs to some extent in the majority of solid organ transplantations, but the exact mechanism in which CAV is induced still remains subject to some debate. Certainly, both donor and recipient cells are involved, but it is not clear which cells are active and passive in its development. There is also evidence for both immunological and non-immunological processes although the former probably dominate given the observation that only donor vessels (and not native arteries) develop arteriopathy despite exposure to the same circulatory risk factors [120].

Many investigators believe immune-mediated injury to the graft is the fundamental initiator of CAV. This is instigated by T-cells which produce a cytotoxic cellular response (causing the release of cytokines such as interleukin-2 and interferon-γ) as well as B-cell antibody production [121]. This occurs either directly (through direct recognition of donor MHC-peptide complexes by host T-cells) or indirectly (when MHC molecules or minor antigens are processed into peptides and presented to T-cells). Platelet activation also seems to play a significant role [122] along with endothelial and smooth muscle progenitor cells [123]. HLA matching is important, and the degree of mismatch corresponds with the severity of CAV [124].

Additionally, given that chronic rejection can occur when hearts are transplanted into syngeneic mice [125], it is evident that mechanisms other than those involving an alloantigenic process are also involved in the pathogenesis of CAV. Evidence exists for a potential role for antigenic recognition of cardiac myosin [126], vimentin [127], or collagen V [128]. Infective complications are important, particularly that of cytomegalovirus which seems to promote chronic vascular rejection of most solid organs and is associated with a 28 % rate of obstructive CAV 5 years after heart transplantation [129]. Additionally, it is noted that *Chlamydia pneumoniae* IgG titres correspond to the severity of allograft atherosclerosis after transplantation [130].

Other donor factors also appear to play an influencing part in this process. For example, it is possible that the presence of "explosive" brain death induces an expression of inflammatory mediators in peripheral organs eventually making them more susceptible to MHC-driven processes. This has been seen in both animal models [131] and with IVUS in human transplant recipients [132]. Conventional cardiac risk factors in the donor, such as smoking and hypertension, and a history of coronary disease are risk factors [133] as is the ischemic time at procurement [134].

Of note the development of CAV does not seem to relate to the number or severity of cellular rejection episodes [135], and adequate immunosuppression, sufficient to prevent acute allograft failure due to rejection, does not alter the course of CAV [136]. However, particular regimens such as those involving cyclosporine and tacrolimus increase the risk of chronic renal disease, hyperlipidemia, and hypertension which may exacerbate CAV [133].

Cardiovascular risk factors in the host also influence the course of CAV including older age, hypertension, smoking, and high BMI with dyslipidemia being the most important [137]. Control of lipid levels has a positive influence on the incidence of CAV [138]. Other drug therapies that may have an influence on CAV include statins, ACE-I, Ca-channel blockers, everolimus, and sirolimus [123]. Regular exercise has a positive effect on the development of CAV and is recommended to most transplant patients [139].

### 9.5.3 Histological Findings

CAV can affect large and small epicardial arteries, intramyocardial arteries [140], and veins with a diffuse degree of distribution [141]. Morphologically, it involves three types of lesions [142]:

#### Fibromuscular Intimal Hyperplasia

The principle histological findings are of a concentric fibromuscular intimal hyperplasia that distinguishes it from the normal eccentric pattern of conventional atherosclerosis. This is caused by accumulation of lymphocytes and macrophages beneath the endothelium ("endothelitis"). Intimal proliferation occurs, and the resultant lesions are composed of collagen, extracellular matrix proteins, and vascular smooth muscle cells.

#### Atheroma

These occur in the epicardial arteries of both adult and pediatric recipients. They demonstrate calcification and mural thrombus formation and share many similar processes to conventional atherosclerosis [143]. However, calcification is less frequent and not a marker of severity when present.

### Chronic Inflammation

Inflammation is seen to greater or lesser extent in the majority of graft vessels and can extend transmurally (unlike atherosclerosis which is limited to the intima). However, it is probably more active and disruptive in cases of CAV with elastic laminae and smooth muscle cell destruction.

## 9.5.4 Detection of CAV: Impact on the Macro- and Microvasculature

### Invasive Studies of the Macrovasculature

The primary pathology in CAV is a progressive encroachment into the lumen of the coronary vessel that is now known to occur throughout the entire coronary tree. As such, it has effects on both micro- and macrovasculature and can therefore be appreciated using a variety of complimentary and distinct investigative tools. Despite these potentially sophisticated techniques, as yet only angiography is largely used as the primary screening tool with recent ISHLT guidelines recommend annual or biannual angiography in both adult and pediatric patients [144]. In this setting, even the presence of mild-lesions is a marker of prognosis when recognized [145].

As a complimentary tool, IVUS provides more detailed information on the structure of the coronary arteries and may be able to recognize more subtle evidence of developing CAV. The initial rate of progression of intimal thickness as measured from two time points (baseline and 1 year) is a subtle way to recognize the development of CAV and correlates with outcome data at 5 years [146]. Several classification techniques exist to document the degree of CAV, the most widely accepted of which is the Stanford classification [147].

### Noninvasive Assessment Tools

While detection of CAV is not as reliable using ECG, exercise tolerance, arrhythmia monitoring, or echocardiography compared to angiography [148], they may have a role in certain scenarios [144].

The sensitivity of simple resting echocardiography is poor at less than 50 %. However, if regional dysfunction is present, it has a good specificity (>80 %) for CAV [149], and the application of tissue Doppler is also useful [150]. More widely used is stress echocardiography with a sensitivity of 72 % and specificity of 88 % for diagnosing Stanford class III or IV IVUS-CAV or any luminal irregularities [151]. Other echocardiographic techniques have been used including myocardial contrast echocardiography [152] and directly imaged coronary flow [153] with reasonable success.

Nuclear imaging is an alternative noninvasive technique for CAV screening. Dipyridamole myocardial scintigraphy has a good specificity (64–88 %) but a low sensitivity (21–58 %) for CAV. When exercise is used instead of pharmacological stimulation, sensitivity and specificity are increased, but it remains limited by the problem of achieving an adequate heart rate response [148]. SPECT perfusion defects have been recognized as a predictor for resultant CAV-related events during follow-up [154].

PET studies have revealed that resting myocardial blood flow is higher than in controls perhaps driven by the increased heart rate due to allograft vagal denervation [155]. Hyperemic flow is also lower than in controls and is inversely related to intimal thickness [156].

Other noninvasive options for assessing the presence of CAV include MRI or CT scanning. The presence of late gadolinium enhancement is correlated with the degree of CAV visible at angiography [157] as was strain rate seen with CMR tagging [158]. Recent work has suggested that CT may also be an alternative option to detect CAV [159].

## 9.5.5 Microvascular Assessment and Endothelial Function

While initial focus was placed on the documentation and diagnosis of CAV affecting the epicardial vessels, evidence is accumulating to demonstrate the effect of CAV on the microvasculature. PET and MRI have both confirmed the presence of CAV throughout the entire coronary tree, not just macrovasculature [156, 160]. Similarly, RV biopsies have shown a microvasculopathy as part of this disease entity and when present has adverse prognostic implications [140]. Therefore techniques to specifically investigate the microcirculation are both insightful and perhaps ultimately predictive.

Additionally, the process of CAV also affects endothelial function as has been recognized with PET scanning which may provide another target for diagnostic purposes [156]. Abnormal endothelial function is seen with invasive studies where vasoconstriction in response to acetylcholine is a predictor of the presence of coronary intimal thickening [161]. Both the rate of change of endothelial function when assessed serially [162] as well as the baseline endothelial function [163] appear to be good predictors of events.

Dipyridamole-induced CFR measured invasively during catheterization appears to have a role in predicting outcome in transplant patients mediated by CAV. Two years after catheterization, a CFR < 2.5 was a predictor for a decline in exercise ejection fraction [164]. However, as CFR is actually influenced by both epicardial and microvascular responses, it is interesting to note studies involving more specific investigative targets for the microcirculation.

As such, the index of microvascular resistance has been used to delineate the macro- and microvascular changes after transplantation. In a group of 25 patients, an improvement in IMR was noted over time in conjunction with deterioration in FFR (which was itself associated with plaque burden on IVUS) but an unchanging CFR [165]. This demonstrates the importance of separating the micro- and macrovascular domain and the fact that CFR is unable to distinguish between their divergent changes.

In those patients with an abnormal IMR (defined as >20) 1 year after transplantation, microvascular dysfunction was associated with a history of acute rejection and smaller donor hearts. Most interestingly, the majority of patients (86%) with impaired microvascular function in this study had no evidence of impaired epicardial function as demonstrated by FFR implying this process may originate before that of epicardial changes [166]. Therefore, there seems to be a spectrum of responses in the microcirculatory resistance following transplantation, and their recognition may prove helpful in assessing these patients.

The concept of resistance has been advanced through the use of another measure of microvascular function – IHDVPS (instantaneous hyperemic diastolic velocity pressure slope). This is a measure of conductance (the inverse of resistance) and is a reflection of the relationship between pressure and flow in mid-to-late diastole during hyperemia. While it was initially applied to macrovascular disease [167] in the absence of coronary artery lesions, it provides dedicated information on the microvasculature.

In an insightful series of experiments, Escaned et al. performed IHDVPS in transplant patients with simultaneous biopsies. The amount of arteriolar obliteration, as well as capillary density, at biopsy was significantly correlated with IHDVPS with a higher sensitivity over other measures of coronary resistance and reserve. Therefore, IHDVPS and other emerging dedicated measures of microvascular function are likely to be useful in the early diagnosis and perhaps monitoring of CAV [168].

### 9.5.6 Conclusion

CAV is one of the most concerning issues in the management of post-cardiac transplant patients. While many certainties are acknowledged, there remains a lot of debate particularly regarding the pathogenetic process. Importantly, it is now apparent that this is a disease not just of the epicardial vessels but also of the microvasculature, and in fact, it may even begin in this domain.

The resultant morbidity and mortality of this condition, combined with the worrying number of patients who present with sudden cardiac death, make risk stratification, early identification, and regular screening essential in these patients. At present, recommendations focus on the macrovascular appreciation of this disease. However, as intravascular microcirculatory assessment tools (such as IMR and IHDVPS) become more refined and sophisticated, it may become appropriate to employ these, along with IVUS and/or endothelial assessment techniques to provide a complex but detailed risk stratification and prognostication in these patients.

Encouragingly, some therapeutic options now exist with more on the horizon. It is key to target appropriate therapies to the higher-risk patients hopefully either preventing or slowing the progression of CAV. Identification of those patients most at risk perhaps using the above more complex screening strategy would allow a more bespoke approach to the treatment of CAV. As we begin to appreciate the diffuse pathological cardiac burden of this disease, more investigative strategies will emerge and guide therapy.

Regarding cardiomyopathies, the process by which the myocardium and coronary circulation interact cannot be ignored. Countless evidence has demonstrated the effect of the myocardium on driving coronary blood flow both in health and disease, and the disruption of this delicate interplay causes significant morbidity and mortality. Therefore, it should be of no surprise that the gross macro-pathology seen in the majority of cardiomyopathic processes significantly impacts on the normal micro- and macrovascular physiology.

The ultimately treatment goal for many patients affected by these diseases is heart transplantation. However, once undertaken, the unique process of cardiac allograft vasculopathy is an ever-present concern, this time with structural alterations affecting the walls of the coronary arteries themselves and with a significant resultant disease burden.

The options to investigate the domains of the microcirculation appear now to at least match those for the coronary domain, and their increasing application is producing fascinating information regarding the disease process and may even offer options for treatment. In many conditions, perhaps most significantly that of allograft vasculopathy, microcirculatory involvement may be appreciable before that of the macrocirculation allowing an earlier diagnosis and more timely instigation of therapy.

## References

1. Cannon 3rd RO, Schenke WH, Maron BJ, Tracy CM, Leon MB, Brush Jr JE, Rosing DR, Epstein SE. Differences in coronary flow and myocardial metabolism at rest and during pacing between patients with obstructive and patients with nonobstructive hypertrophic cardiomyopathy. J Am Coll Cardiol. 1987;10:53–62.
2. Maron BJ, Epstein SE, Roberts WC. Hypertrophic cardiomyopathy and transmural myocardial infarction without significant atherosclerosis of the extramural coronary arteries. Am J Cardiol. 1979;43:1086–102.
3. Pitcher D, Wainwright R, Maisey M, Curry P, Sowton E. Assessment of chest pain in hypertrophic cardiomyopathy using exercise thallium-201 myocardial scintigraphy. Br Heart J. 1980;44:650–6.
4. Cannon 3rd RO, Dilsizian V, O'Gara PT, Udelson JE, Schenke WH, Quyyumi A, Fananapazir L, Bonow RO. Myocardial metabolic, hemodynamic, and electrocardiographic significance of reversible thallium-201 abnormalities in hypertrophic cardiomyopathy. Circulation. 1991;83:1660–7.
5. Elliott PM, Rosano GM, Gill JS, Poole-Wilson PA, Kaski JC, McKenna WJ. Changes in coronary sinus pH during dipyridamole stress in patients with hypertrophic cardiomyopathy. Heart. 1996;75:179–83.
6. von Dohlen TW, Prisant LM, Frank MJ. Significance of positive or negative thallium-201 scintigraphy in hypertrophic cardiomyopathy. Am J Cardiol. 1989;64:498–503.
7. Udelson JE, Bonow RO, O'Gara PT, Maron BJ, Van Lingen A, Bacharach SL, Epstein SE. Verapamil prevents silent myocardial perfusion abnormalities during exercise in asymptomatic patients with hypertrophic cardiomyopathy. Circulation. 1989;79:1052–60.

8. Sorajja P, Chareonthaitawee P, Ommen SR, Miller TD, Hodge DO, Gibbons RJ. Prognostic utility of single-photon emission computed tomography in adult patients with hypertrophic cardiomyopathy. Am Heart J. 2006;151:426–35.
9. Elliott PM, Kaski JC, Prasad K, Seo H, Slade AK, Goldman JH, McKenna WJ. Chest pain during daily life in patients with hypertrophic cardiomyopathy: an ambulatory electrocardiographic study. Eur Heart J. 1996;17:1056–64.
10. Rigo F, Gherardi S, Galderisi M, Cortigiani L. Coronary flow reserve evaluation in stress-echocardiography laboratory. J Cardiovasc Med (Hagerstown). 2006;7:472–9.
11. Asami Y, Yoshida K, Hozumi T, Akasaka T, Takagi T, Kaji S, Kawamoto T, Ogata Y, Yagi T, Morioka S, Yoshikawa J. Assessment of coronary flow reserve in patients with hypertrophic cardiomyopathy using transthoracic color doppler echocardiography. J Cardiol. 1998;32:247–52.
12. Cortigiani L, Rigo F, Gherardi S, Galderisi M, Sicari R, Picano E. Prognostic implications of coronary flow reserve on left anterior descending coronary artery in hypertrophic cardiomyopathy. Am J Cardiol. 2008;102:1718–23.
13. Tesic M, Djordjevic-Dikic A, Beleslin B, Trifunovic D, Giga V, Marinkovic J, Petrovic O, Petrovic M, Stepanovic J, Dobric M, Vukcevic V, Stankovic G, Seferovic P, Ostojic M, Vujisic-Tesic B. Regional difference of microcirculation in patients with asymmetric hypertrophic cardiomyopathy: transthoracic doppler coronary flow velocity reserve analysis. J Am Soc Echocardiogr. 2013;26:775–82.
14. Iwakura K, Ito H, Takiuchi S, Taniyama Y, Nakatsuchi Y, Negoro S, Higashino Y, Okamura A, Masuyama T, Hori M, Fujii K, Minamino T. Alternation in the coronary blood flow velocity pattern in patients with no reflow and reperfused acute myocardial infarction. Circulation. 1996;94:1269–75.
15. Kawamoto T, Yoshida K, Akasaka T, Hozumi T, Takagi T, Kaji S, Ueda Y. Can coronary blood flow velocity pattern after primary percutaneous transluminal coronary angiography predict recovery of regional left ventricular function in patients with acute myocardial infarction? Circulation. 1999;100:339–45.
16. Watanabe N, Akasaka T, Yamaura Y, Akiyama M, Kaji S, Saito Y, Yoshida K. Intramyocardial coronary flow characteristics in patients with hypertrophic cardiomyopathy: non-invasive assessment by transthoracic doppler echocardiography. Heart. 2003;89:657–8.
17. Petersen SE, Jerosch-Herold M, Hudsmith LE, Robson MD, Francis JM, Doll HA, Selvanayagam JB, Neubauer S, Watkins H. Evidence for microvascular dysfunction in hypertrophic cardiomyopathy: new insights from multiparametric magnetic resonance imaging. Circulation. 2007;115:2418–25.
18. Knaapen P, van Dockum WG, Gotte MJ, Broeze KA, Kuijer JP, Zwanenburg JJ, Marcus JT, Kok WE, van Rossum AC, Lammertsma AA, Visser FC. Regional heterogeneity of resting perfusion in hypertrophic cardiomyopathy is related to delayed contrast enhancement but not to systolic function: a PET and MRI study. J Nucl Cardiol. 2006;13:660–7.
19. Choudhury L, Mahrholdt H, Wagner A, Choi KM, Elliott MD, Klocke FJ, Bonow RO, Judd RM, Kim RJ. Myocardial scarring in asymptomatic or mildly symptomatic patients with hypertrophic cardiomyopathy. J Am Coll Cardiol. 2002;40:2156–64.
20. Moon JC, Reed E, Sheppard MN, Elkington AG, Ho SY, Burke M, Petrou M, Pennell DJ. The histologic basis of late gadolinium enhancement cardiovascular magnetic resonance in hypertrophic cardiomyopathy. J Am Coll Cardiol. 2004;43:2260–4.
21. Papavassiliu T, Schnabel P, Schröder M, Borggrefe M. CMR scarring in a patient with hypertrophic cardiomyopathy correlates well with histological findings of fibrosis. Eur Heart J. 2005;26(22):2395.
22. Camici P, Chiriatti G, Lorenzoni R, Bellina RC, Gistri R, Italiani G, Parodi O, Salvadori PA, Nista N, Papi L, L'Abbate A. Coronary vasodilation is impaired in both hypertrophied and nonhypertrophied myocardium of patients with hypertrophic cardiomyopathy: a study with nitrogen-13 ammonia and positron emission tomography. J Am Coll Cardiol. 1991;17:879–86.
23. Lorenzoni R, Gistri R, Cecchi F, Olivotto I, Chiriatti G, Elliott P, McKenna WJ, Camici PG. Coronary vasodilator reserve is impaired in patients with hypertrophic cardiomyopathy and left ventricular dysfunction. Am Heart J. 1998;136:972–81.
24. Cecchi F, Olivotto I, Gistri R, Lorenzoni R, Chiriatti G, Camici PG. Coronary microvascular dysfunction and prognosis in hypertrophic cardiomyopathy. N Engl J Med. 2003;349:1027–35.
25. Olivotto I, Cecchi F, Gistri R, Lorenzoni R, Chiriatti G, Girolami F, Torricelli F, Camici PG. Relevance of coronary microvascular flow impairment to long-term remodeling and systolic dysfunction in hypertrophic cardiomyopathy. J Am Coll Cardiol. 2006;47:1043–8.
26. Gistri R, Cecchi F, Choudhury L, Montereggi A, Sorace O, Salvadori PA, Camici PG. Effect of verapamil on absolute myocardial blood flow in hypertrophic cardiomyopathy. Am J Cardiol. 1994;74:363–8.
27. Choudhury L, Elliott P, Rimoldi O, Ryan M, Lammertsma AA, Boyd H, McKenna WJ, Camici PG. Transmural myocardial blood flow distribution in hypertrophic cardiomyopathy and effect of treatment. Basic Res Cardiol. 1999;94:49–59.
28. Soliman OI, Knaapen P, Geleijnse ML, Dijkmans PA, Anwar AM, Nemes A, Michels M, Vletter WB, Lammertsma AA, ten Cate FJ. Assessment of intravascular and extravascular mechanisms of myocardial perfusion abnormalities in obstructive hypertrophic cardiomyopathy by myocardial contrast echocardiography. Heart. 2007;93:1204–12.
29. Krams R, Kofflard MJM, Duncker DJ, Von Birgelen C, Carlier S, Kliffen M, Cate FJ, Serruys PW. Decreased coronary flow reserve in hypertrophic cardiomyopathy is related to remodeling of the coronary microcirculation. Circulation. 1998;97:230–3.
30. Maron MS, Olivotto I, Maron BJ, Prasad SK, Cecchi F, Udelson JE, Camici PG. The case for myocardial ischemia in hypertrophic cardiomyopathy. J Am Coll Cardiol. 2009;54:866–75.
31. Schwartzkopff B, Mundhenke M, Strauer BE. Alterations of the architecture of subendocardial arterioles in patients with hypertrophic cardiomyopathy and impaired coronary vasodilator reserve: a possible cause for myocardial ischemia 1. J Am Coll Cardiol. 1998;31:1089–96.
32. Maron BJ, Wolfson JK, Epstein SE, Roberts WC. Intramural ("small vessel") coronary artery disease in hypertrophic cardiomyopathy. J Am Coll Cardiol. 1986;8:545–57.
33. Takemura G, Takatsu Y, Fujiwara H. Luminal narrowing of coronary capillaries in human hypertrophic hearts: an ultrastructural morphometrical study using endomyocardial biopsy specimens. Heart. 1998;79:78–85.
34. Kwon DH, Smedira NG, Rodriguez ER, Tan C, Setser R, Thamilarasan M, Lytle BW, Lever HM, Desai MY. Cardiac magnetic resonance detection of myocardial scarring in hypertrophic cardiomyopathy: correlation with histopathology and prevalence of ventricular tachycardia. J Am Coll Cardiol. 2009;54:242–9.
35. Kingsbury MP, Turner MA, Flores NA, Bovill E, Sheridan DJ. Endogenous and exogenous coronary vasodilatation are attenuated in cardiac hypertrophy: a morphological defect? J Mol Cell Cardiol. 2000;32:527–38.
36. Crabos M, Coste P, Paccalin M, Tariosse L, Daret D, Besse P, Bonoron-Adèle S. Reduced basal NO-mediated dilation and decreased endothelial NO-synthase expression in coronary vessels of spontaneously hypertensive rats. J Mol Cell Cardiol. 1997;29:55–65.
37. Mihaljevic T, Paul S, Cohn LH, Wechsler A. Pathophysiology of aortic valve disease *cardiac surgery in the adult*. New York: McGraw-Hil; 2003. p. 791–810.
38. Brilla CG, Janicki JS, Weber KT. Impaired diastolic function and coronary reserve in genetic hypertension. Role of interstitial fibrosis and medial thickening of intramyocardial coronary arteries. Circ Res. 1991;69:107–15.
39. Kalkman EAJ, Bilgin YM, Haren P, Suylen RJ, Saxena PR, Schoemaker RG. Determinants of coronary reserve in rats subjected to coronary artery ligation or aortic banding. Cardiovasc Res. 1996;32:1088–95.
40. Tomanek RJ, Wangler RD, Bauer CA. Prevention of coronary vasodilator reserve decrement in spontaneously hypertensive rats. Hypertension. 1985;7:533–40.

41. Opherk D, Mall G, Zebe H, Schwarz F, Weihe E, Manthey J, Kubler W. Reduction of coronary reserve: a mechanism for angina pectoris in patients with arterial hypertension and normal coronary arteries. Circulation. 1984;69:1–7.
42. Breisch EA, White FC, Nimmo LE, Bloor CM. Cardiac vasculature and flow during pressure-overload hypertrophy. Am J Phys – Heart Circ Phys. 1986;251:H1031–7.
43. Schwartzkopff B, Frenzel H, Diekerhoff J, Betz P, Flasshove M, Schulte HD, Mundhenke M, Motz W, Strauer BE. Morphometric investigation of human myocardium in arterial hypertension and valvular aortic stenosis. Eur Heart J. 1992;13:17–23.
44. Mueller TM, Marcus ML, Kerber RE, Young JA, Barnes RW, Abboud FM. Effect of renal hypertension and left ventricular hypertrophy on the coronary circulation in dogs. Circ Res. 1978;42:543–9.
45. Bishop SP, Powell PC, Hasebe N, Shen YT, Patrick TA, Hittinger L, Vatner SF. Coronary vascular morphology in pressure-overload left ventricular hypertrophy. J Mol Cell Cardiol. 1996;28:141–54.
46. Ecker T, Gobel C, Hullin R, Rettig R, Seitz G, Hofmann F. Decreased cardiac concentration of cGMP kinase in hypertensive animals. An index for cardiac vascularization? Circ Res. 1989;65:1361–9.
47. Rakusan K, Flanagan MF, Geva T, Southern J, Van Praagh R. Morphometry of human coronary capillaries during normal growth and the effect of age in left ventricular pressure-overload hypertrophy. Circulation. 1992;86:38–46.
48. Gould KL, Carabello BA. Why angina in aortic stenosis with normal coronary arteriograms? Circulation. 2003;107:3121–3.
49. O'Gorman DJ, Thomas P, Turner MA, Sheridan DJ. Investigation of impaired coronary vasodilator reserve in the guinea pig heart with pressure induced hypertrophy. Eur Heart J. 1992;13:697–703.
50. Rajappan K, Rimoldi OE, Dutka DP, Ariff B, Pennell DJ, Sheridan DJ, Camici PG. Mechanisms of coronary microcirculatory dysfunction in patients with aortic stenosis and angiographically normal coronary arteries. Circulation. 2002;105:470–6.
51. Villari B, Hess OM, Meier C, Pucillo A, Gaglione A, Turina M, Krayenbuehl HP. Regression of coronary artery dimensions after successful aortic valve replacement. Circulation. 1992;85:972–8.
52. Levy D, Garrison RJ, Savage DD, Kannel WB, Castelli WP. Prognostic implications of echocardiographically determined left ventricular mass in the Framingham Heart Study. N Engl J Med. 1990;322:1561–6.
53. Haider AW, Larson MG, Benjamin EJ, Levy D. Increased left ventricular mass and hypertrophy are associated with increased risk for sudden death. J Am Coll Cardiol. 1998;32:1454–9.
54. Levy D, Garrison RJ, Savage DD, Kannel WB, Castelli WP. Left ventricular mass and incidence of coronary heart disease in an elderly cohort. The Framingham Heart Study. Ann Intern Med. 1989;110:101–7.
55. Koren MJ, Devereux RB, Casale PN, Savage DD, Laragh JH. Relation of left ventricular mass and geometry to morbidity and mortality in uncomplicated essential hypertension. Ann Intern Med. 1991;114:345–52.
56. Wicker P, Tarazi RC, Kobayashi K. Coronary blood flow during the development and regression of left ventricular hypertrophy in renovascular hypertensive rats. Am J Cardiol. 1983;51:1744–9.
57. Sato F, Isoyama S, Takishima T. Normalization of impaired coronary circulation in hypertrophied rat hearts. Hypertension. 1990;16:26–34.
58. Kingsbury M, Mahnke A, Turner M, Sheridan D. Recovery of coronary function and morphology during regression of left ventricular hypertrophy. Cardiovasc Res. 2002;55:83–96.
59. Nunez E, Hosoya K, Susic D, Frohlich ED. Enalapril and losartan reduced cardiac mass and improved coronary hemodynamics in SHR. Hypertension. 1997;29:519–24.
60. Brilla CG, Janicki JS, Weber KT. Cardioreparative effects of lisinopril in rats with genetic hypertension and left ventricular hypertrophy. Circulation. 1991;83:1771–9.
61. Xu R, Zhang Y, Zhang M, Ge ZM, Li XC, Zhang W. Relationship between regression of hypertensive left ventricular hypertrophy and improvement of coronary flow reserve. Zhonghua Yi Xue Za Zhi. 2003;83:658–61.
62. Mizuno R, Fujimoto S, Saito Y, Okamoto Y. Optimal antihypertensive level for improvement of coronary microvascular dysfunction: the lower, the better? Hypertension. 2012;60:326–32.
63. Motz W, Strauer BE. Improvement of coronary flow reserve after long-term therapy with enalapril. Hypertension. 1996;27:1031–8.
64. Tomas JP, Moya JL, Barrios V, Campuzano R, Guzman G, Megias A, Ruiz-Leria S, Catalan P, Marfil T, Tarancon B, Muriel A, Garcia-Lledo A. Effect of candesartan on coronary flow reserve in patients with systemic hypertension. J Hypertens. 2006;24:2109–14.
65. Parodi O, Neglia D, Palombo C, Sambuceti G, Giorgetti A, Marabotti C, Gallopin M, Simonetti I, L'Abbate A. Comparative effects of enalapril and verapamil on myocardial blood flow in systemic hypertension. Circulation. 1997;96:864–73.
66. Zhu YH, Zhu YZ, Spitznagel H, Gohlke P, Unger T. Substrate metabolism, hormone interaction, and angiotensin-converting enzyme inhibitors in left ventricular hypertrophy. Diabetes. 1996;45:S59–65.
67. Just H, Frey M, Zehender M. Calcium antagonist drugs in hypertensive patients with angina pectoris. Eur Heart J. 1996;17:20–4.
68. Carpeggiani C, Neglia D, Paradossi U, Pratali L, Glauber M, L'Abbate A. Coronary flow reserve in severe aortic valve stenosis: a positron emission tomography study. J Cardiovasc Med. 2008;9:893–8.
69. Anversa P, Ricci R, Olivetti G. Coronary capillaries during normal and pathological growth. Can J Cardiol. 1986;2:104–13.
70. Antony I, Nitenberg A, Foult JM, Aptecar E. Coronary vasodilator reserve in untreated and treated hypertensive patients with and without left ventricular hypertrophy. J Am Coll Cardiol. 1993;22:514–20.
71. Brush JE, Cannon RO, Schenke WH, Bonow RO, Leon MB, Maron BJ, Epstein SE. Angina Due to coronary microvascular disease in hypertensive patients without left ventricular hypertrophy. N Engl J Med. 1988;319:1302–7.
72. Rodriguez-Porcel M, Zhu XY, Chade AR, Amores-Arriaga B, Caplice NM, Ritman EL, Lerman A, Lerman LO. Functional and structural remodeling of the myocardial microvasculature in early experimental hypertension. Am J Phys – Heart Circ Phys. 2006;290:H978–84.
73. McGoldrick RB, Kingsbury M, Turner MA, Sheridan DJ, Hughes AD. Left ventricular hypertrophy induced by aortic banding impairs relaxation of isolated coronary arteries. Clin Sci. 2007;113:473–8.
74. McAinsh AM, Turner MA, O'Hare D, Nithythyananthan R, Johnston DG, O'Gorman DJ, Sheridan DJ. Cardiac hypertrophy impairs recovery from ischaemia because there is a reduced reactive hyperaemic response. Cardiovasc Res. 1995;30:113–21.
75. Koyanagi S, Eastham CL, Harrison DG, Marcus ML. Increased size of myocardial infarction in dogs with chronic hypertension and left ventricular hypertrophy. Circ Res. 1982;50:55–62.
76. Yetman AT, McCrindle BW, MacDonald C, Freedom RM, Gow R. Myocardial bridging in children with hypertrophic cardiomyopathy--a risk factor for sudden death. N Engl J Med. 1998;339:1201–9.
77. Gori F, Basso C, Thiene G. Myocardial infarction in a patient with hypertrophic cardiomyopathy. N Engl J Med. 2000;342:593–4.
78. Davies JE, Sen S, Broyd C, Hadjiloizou N, Baksi J, Francis DP, Foale RA, Parker KH, Hughes AD, Chukwuemeka A, Casula R, Malik IS, Mikhail GW, Mayet J. Arterial pulse wave dynamics after percutaneous aortic valve replacement/clinical perspective. Circulation. 2011;124:1565–72.
79. Kyriakidis MK, Dernellis JM, Androulakis AE, Kelepeshis GA, Barbetseas J, Anastasakis AN, Trikas AG, Tentolouris CA, Gialafos JE, Toutouzas PK. Changes in phasic coronary blood flow velocity profile and relative coronary flow reserve in patients with hypertrophic obstructive cardiomyopathy. Circulation. 1997;96:834–41.
80. Cannon RO, McIntosh CL, Schenke WH, Maron BJ, Bonow RO, Epstein SE. Effect of surgical reduction of left ventricular outflow obstruction on hemodynamics, coronary flow, and myocardial metabolism in hypertrophic cardiomyopathy. Circulation. 1989;79:766–75.
81. Factor SM, Butany J, Sole MJ, Wigle ED, Williams WC, Rojkind M. Pathologic fibrosis and matrix connective tissue in the subaortic myocardium of patients with hypertrophic cardiomyopathy. J Am Coll Cardiol. 1991;17:1343–51.

82. Lombardi R, Betocchi S, Losi MA, Tocchetti CG, Aversa M, Miranda M, D'Alessandro G, Cacace A, Ciampi Q, Chiariello M. Myocardial collagen turnover in hypertrophic cardiomyopathy. Circulation. 2003;108:1455–60.
83. Tanaka M, Fujiwara H, Onodera T, Wu DJ, Hamashima Y, Kawai C. Quantitative analysis of myocardial fibrosis in normals, hypertensive hearts, and hypertrophic cardiomyopathy. Br Heart J. 1986;55:575–81.
84. Varnava A, Elliott P, Sharma S, McKenna W, Davies M. Hypertrophic cardiomyopathy: the interrelation of disarray, fibrosis, and small vessel disease. Heart. 2000;84:476–82.
85. Basso C, Thiene G, Corrado D, Buja G, Melacini P, Nava A. Hypertrophic cardiomyopathy and sudden death in the young: pathologic evidence of myocardial ischemia. Hum Pathol. 2000;31:988–98.
86. Dec GW, Fuster V. Idiopathic dilated cardiomyopathy. N Engl J Med. 1994;331:1564–75.
87. Koutalas E, Kanoupakis E, Vardas P. Sudden cardiac death in non-ischemic dilated cardiomyopathy: a critical appraisal of existing and potential risk stratification tools. Int J Cardiol. 2013;167:335–41.
88. Inoue T, Sakai Y, Morooka S, Hayashi T, Takayanagi K, Yamanaka T, Kakoi H, Takabatake Y. Coronary flow reserve in patients with dilated cardiomyopathy. Am Heart J. 1993;125:93–8.
89. Spoladore R, Fisicaro A, Faccini A, Camici PG. Coronary microvascular dysfunction in primary cardiomyopathies. Heart. 2014;100:806–13.
90. Treasure CB, Vita JA, Cox DA, Fish RD, Gordon JB, Mudge GH, Colucci WS, Sutton MG, Selwyn AP, Alexander RW, et al. Endothelium-dependent dilation of the coronary microvasculature is impaired in dilated cardiomyopathy. Circulation. 1990;81:772–9.
91. Neglia D, L'Abbate A. Coronary microvascular dysfunction and idiopathic dilated cardiomyopathy. Pharmacol Rep PR. 2005;57(Suppl):151–5.
92. Taylor AL, Ziesche S, Yancy C, Carson P, D'Agostino Jr R, Ferdinand K, Taylor M, Adams K, Sabolinski M, Worcel M, Cohn JN, African-American Heart Failure Trial I. Combination of isosorbide dinitrate and hydralazine in blacks with heart failure. New England J Med. 2004;351:2049–57.
93. Cohn JN, Johnson G, Ziesche S, Cobb F, Francis G, Tristani F, Smith R, Dunkman WB, Loeb H, Wong M, et al. A comparison of enalapril with hydralazine-isosorbide dinitrate in the treatment of chronic congestive heart failure. N Engl J Med. 1991;325:303–10.
94. Marcus FI, McKenna WJ, Sherrill D, Basso C, Bauce B, Bluemke DA, Calkins H, Corrado D, Cox MG, Daubert JP, Fontaine G, Gear K, Hauer R, Nava A, Picard MH, Protonotarios N, Saffitz JE, Sanborn DM, Steinberg JS, Tandri H, Thiene G, Towbin JA, Tsatsopoulou A, Wichter T, Zareba W. Diagnosis of arrhythmogenic right ventricular cardiomyopathy/dysplasia: proposed modification of the task force criteria. Circulation. 2010;121:1533–41.
95. Paul M, Rahbar K, Gerss J, Kies P, Schober O, Schafers K, Breithardt G, Schulze-Bahr E, Wichter T, Schafers M. Microvascular dysfunction in nonfailing arrhythmogenic right ventricular cardiomyopathy. Eur J Nucl Med Mol Imaging. 2012;39:416–20.
96. Wichter T, Schafers M, Rhodes CG, Borggrefe M, Lerch H, Lammertsma AA, Hermansen F, Schober O, Breithardt G, Camici PG. Abnormalities of cardiac sympathetic innervation in arrhythmogenic right ventricular cardiomyopathy : quantitative assessment of presynaptic norepinephrine reuptake and postsynaptic beta-adrenergic receptor density with positron emission tomography. Circulation. 2000;101:1552–8.
97. Almeida AG, Pinto FJ. Non-compaction cardiomyopathy. Heart. 2013;99:1535–42.
98. Jenni R, Wyss CA, Oechslin EN, Kaufmann PA. Isolated ventricular noncompaction is associated with coronary microcirculatory dysfunction. J Am Coll Cardiol. 2002;39:450–4.
99. Gianni M, Dentali F, Grandi AM, Sumner G, Hiralal R, Lonn E. Apical ballooning syndrome or takotsubo cardiomyopathy: a systematic review. Eur Heart J. 2006;27:1523–9.
100. Previtali M, Repetto A, Panigada S, Camporotondo R, Tavazzi L. Left ventricular apical ballooning syndrome: prevalence, clinical characteristics and pathogenetic mechanisms in a European population. Int J Cardiol. 2009;134:91–6.
101. Galiuto L, De Caterina AR, Porfidia A, Paraggio L, Barchetta S, Locorotondo G, Rebuzzi AG, Crea F. Reversible coronary microvascular dysfunction: a common pathogenetic mechanism in Apical Ballooning or Tako-Tsubo Syndrome. Eur Heart J. 2010;31:1319–27.
102. Patel SM, Lerman A, Lennon RJ, Prasad A. Impaired coronary microvascular reactivity in women with apical ballooning syndrome (Takotsubo/stress cardiomyopathy). Eur Heart J Acute Cardiovasc Care. 2013;2:147–52.
103. Martin EA, Prasad A, Rihal CS, Lerman LO, Lerman A. Endothelial function and vascular response to mental stress are impaired in patients with apical ballooning syndrome. J Am Coll Cardiol. 2010;56:1840–6.
104. Chambliss KL, Shaul PW. Estrogen modulation of endothelial nitric oxide synthase. Endocr Rev. 2002;23:665–86.
105. Wittstein IS, Thiemann DR, Lima JA, Baughman KL, Schulman SP, Gerstenblith G, Wu KC, Rade JJ, Bivalacqua TJ, Champion HC. Neurohumoral features of myocardial stunning due to sudden emotional stress. N Engl J Med. 2005;352:539–48.
106. Schultheiss HP, Kuhl U, Cooper LT. The management of myocarditis. Eur Heart J. 2011;32:2616–25.
107. Tschope C, Bock CT, Kasner M, Noutsias M, Westermann D, Schwimmbeck PL, Pauschinger M, Poller WC, Kuhl U, Kandolf R, Schultheiss HP. High prevalence of cardiac parvovirus B19 infection in patients with isolated left ventricular diastolic dysfunction. Circulation. 2005;111:879–86.
108. Schmidt-Lucke C, Spillmann F, Bock T, Kuhl U, Van Linthout S, Schultheiss HP, Tschope C. Interferon beta modulates endothelial damage in patients with cardiac persistence of human parvovirus b19 infection. J Infect Dis. 2010;201:936–45.
109. Elliott PM, Kindler H, Shah JS, Sachdev B, Rimoldi OE, Thaman R, Tome MT, McKenna WJ, Lee P, Camici PG. Coronary microvascular dysfunction in male patients with Anderson-Fabry disease and the effect of treatment with alpha galactosidase A. Heart. 2006;92:357–60.
110. Chimenti C, Morgante E, Tanzilli G, Mangieri E, Critelli G, Gaudio C, Russo MA, Frustaci A. Angina in fabry disease reflects coronary small vessel disease. Circ Heart Fail. 2008;1:161–9.
111. Tomberli B, Cecchi F, Sciagra R, Berti V, Lisi F, Torricelli F, Morrone A, Castelli G, Yacoub MH, Olivotto I. Coronary microvascular dysfunction is an early feature of cardiac involvement in patients with Anderson-Fabry disease. Eur J Heart Fail. 2013;15:1363–73.
112. Weidemann F, Niemann M, Breunig F, Herrmann S, Beer M, Stork S, Voelker W, Ertl G, Wanner C, Strotmann J. Long-term effects of enzyme replacement therapy on fabry cardiomyopathy: evidence for a better outcome with early treatment. Circulation. 2009;119:524–9.
113. Garcia-Pavia P, Tome-Esteban MT, Rapezzi C. Amyloidosis. Also a heart disease. Rev Esp Cardiol. 2011;64:797–808.
114. Modesto KM, Dispenzieri A, Gertz M, Cauduro SA, Khandheria BK, Seward JB, Kyle R, Wood CM, Bailey KR, Tajik AJ, Miller FA, Pellikka PA, Abraham TP. Vascular abnormalities in primary amyloidosis. Eur Heart J. 2007;28:1019–24.
115. Dorbala S, Vangala D, Bruyere Jr J, Quarta C, Kruger J, Padera R, Foster C, Hanley M, Di Carli MF, Falk R. Coronary microvascular dysfunction is related to abnormalities in myocardial structure and function in cardiac amyloidosis. JACC Heart Fail. 2014;2:358–67.
116. Di Carli MF, Bianco-Batlles D, Landa ME, Kazmers A, Groehn H, Muzik O, Grunberger G. Effects of autonomic neuropathy on coronary blood flow in patients with diabetes mellitus. Circulation. 1999;100:813–9.
117. Rahmani M, Cruz RP, Granville DJ, McManus BM. Allograft vasculopathy versus atherosclerosis. Circ Res. 2006;99:801–15.
118. Christie JD, Edwards LB, Kucheryavaya AY, Aurora P, Dobbels F, Kirk R, Rahmel AO, Stehlik J, Hertz MI. The Registry of the International Society for Heart and Lung Transplantation: twenty-seventh official

adult lung and heart-lung transplant report – 2010. J Heart Lung Transplant Off Publ Int Soc Heart Transplant. 2010;29:1104–18.
119. Stehlik J, Edwards LB, Kucheryavaya AY, Aurora P, Christie JD, Kirk R, Dobbels F, Rahmel AO, Hertz MI. The Registry of the International Society for Heart and Lung Transplantation: twenty-seventh official adult heart transplant report – 2010. J Heart Lung Transplant Off Publ Int Soc Heart Transplant. 2010;29:1089–103.
120. Ramzy D, Rao V, Brahm J, Miriuka S, Delgado D, Ross HJ. Cardiac allograft vasculopathy: a review. Can J Surg J canadien de chirurgie. 2005;48:319–27.
121. Waaga AM, Gasser M, Laskowski I, Tilney NL. Mechanisms of chronic rejection. Curr Opin Immunol. 2000;12:517–21.
122. Modjeski KL, Morrell CN. Small cells, big effects: the role of platelets in transplant vasculopathy. J Thromb Thrombolysis. 2014;37:17–23.
123. Benatti RD, Taylor DO. Evolving concepts and treatment strategies for cardiac allograft vasculopathy. Curr Treat Options Cardiovasc Med. 2014;16:278.
124. Schmauss D, Weis M. Cardiac allograft vasculopathy: recent developments. Circulation. 2008;117:2131–41.
125. Five-year findings of the hypertension detection and follow-up program. Prevention and reversal of left ventricular hypertrophy with antihypertensive drug therapy. Hypertension Detection and Follow-up Program Cooperative Group. Hypertension. 1985;7:105–12.
126. Fedoseyeva EV, Zhang F, Orr PL, Levin D, Buncke HJ, Benichou G. De novo autoimmunity to cardiac myosin after heart transplantation and its contribution to the rejection process. J Immunol. 1999;162:6836–42.
127. Nath DS, Ilias Basha H, Tiriveedhi V, Alur C, Phelan D, Ewald GA, Moazami N, Mohanakumar T. Characterization of immune responses to cardiac self-antigens myosin and vimentin in human cardiac allograft recipients with antibody-mediated rejection and cardiac allograft vasculopathy. J Heart Lung Transplant Off Publ Int Soc Heart Transplantat. 2010;29:1277–85.
128. Haque MA, Mizobuchi T, Yasufuku K, Fujisawa T, Brutkiewicz RR, Zheng Y, Woods K, Smith GN, Cummings OW, Heidler KM, Blum JS, Wilkes DS. Evidence for immune responses to a self-antigen in lung transplantation: role of type V collagen-specific T cells in the pathogenesis of lung allograft rejection. J Immunol. 2002;169:1542–9.
129. Grattan MT, Moreno-Cabral CE, Starnes VA, Oyer PE, Stinson EB, Shumway NE. Cytomegalovirus infection is associated with cardiac allograft rejection and atherosclerosis. JAMA. 1989;261:3561–6.
130. Subramanian AK, Quinn TC, Kickler TS, Kasper EK, Tucker PC. Correlation of chlamydia pneumoniae infection and severity of accelerated graft arteriosclerosis after cardiac transplantation. Transplantation. 2002;73:761–4.
131. Takada M, Nadeau KC, Hancock WW, Mackenzie HS, Shaw GD, Waaga AM, Chandraker A, Sayegh MH, Tilney NL. Effects of explosive brain death on cytokine activation of peripheral organs in the rat. Transplantation. 1998;65:1533–42.
132. Mehra MR, Uber PA, Ventura HO, Scott RL, Park MH. The impact of mode of donor brain death on cardiac allograft vasculopathy: an intravascular ultrasound study. J Am Coll Cardiol. 2004;43:806–10.
133. Mehra MR. Contemporary concepts in prevention and treatment of cardiac allograft vasculopathy. Am J Transplant Off J Am Soc Transplant Am Soc Transplant Surgeons. 2006;6:1248–56.
134. Weiss MJ, Madsen JC, Rosengard BR, Allan JS. Mechanisms of chronic rejection in cardiothoracic transplantation. Front Biosci J Virtual Library. 2008;13:2980–8.
135. Hauptman PJ, Nakagawa T, Tanaka H, Libby P. Acute rejection: culprit or coincidence in the pathogenesis of cardiac graft vascular disease? J Heart Lung Transplant Off Publ Int Soc Heart Transplant. 1995;14:S173–80.
136. Dhaliwal A, Thohan V. Cardiac allograft vasculopathy: the Achilles' heel of long-term survival after cardiac transplantation. Curr Atheroscler Rep. 2006;8:119–30.
137. Sanchez Lazaro IJ, Almenar Bonet L, Moro Lopez J, Sanchez Lacuesta E, Martinez-Dolz L, Aguero Ramon-Llin J, Andres Lalaguna L, Cano Perez O, Ortiz Martinez V, Buendia Fuentes F, Salvador Sanz A. Influence of traditional cardiovascular risk factors in the recipient on the development of cardiac allograft vasculopathy after heart transplantation. Transplant Proc. 2008;40:3056–7.
138. Kobashigawa JA, Katznelson S, Laks H, Johnson JA, Yeatman L, Wang XM, Chia D, Terasaki PI, Sabad A, Cogert GA, et al. Effect of pravastatin on outcomes after cardiac transplantation. N Engl J Med. 1995;333:621–7.
139. Nytroen K, Rustad LA, Erikstad I, Aukrust P, Ueland T, Lekva T, Gude E, Wilhelmsen N, Hervold A, Aakhus S, Gullestad L, Arora S. Effect of high-intensity interval training on progression of cardiac allograft vasculopathy. J Heart Lung Transplant Off Publ Int Soc Heart Transplantat. 2013;32:1073–80.
140. Hiemann NE, Wellnhofer E, Knosalla C, Lehmkuhl HB, Stein J, Hetzer R, Meyer R. Prognostic impact of microvasculopathy on survival after heart transplantation: evidence from 9713 endomyocardial biopsies. Circulation. 2007;116:1274–82.
141. Seki A, Fishbein MC. Predicting the development of cardiac allograft vasculopathy. Cardiovasc Pathol. 2014;23:253–60.
142. Lu W-h, Palatnik K, Fishbein GA, Lai C, Levi DS, Perens G, Alejos J, Kobashigawa J, Fishbein MC. Diverse morphologic manifestations of cardiac allograft vasculopathy: a pathologic study of 64 allograft hearts. J Heart Lung Transplant. 2011;30:1044–50.
143. Castellani C, Angelini A, de Boer OJ, van der Loos CM, Fedrigo M, Frigo AC, Meijer-Jorna LB, Li X, Ploegmakers HJ, Tona F, Feltrin G, Gerosa G, Valente M, Thiene G, van der Wal AC. Intraplaque hemorrhage in cardiac allograft vasculopathy. Am J Transplant Off J Am Soc Transplant Am Soc Transplant Surgeons. 2014;14:184–92.
144. Costanzo MR, Dipchand A, Starling R, Anderson A, Chan M, Desai S, Fedson S, Fisher P, Gonzales-Stawinski G, Martinelli L, McGiffin D, Smith J, Taylor D, Meiser B, Webber S, Baran D, Carboni M, Dengler T, Feldman D, Frigerio M, Kfoury A, Kim D, Kobashigawa J, Shullo M, Stehlik J, Teuteberg J, Uber P, Zuckermann A, Hunt S, Burch M, Bhat G, Canter C, Chinnock R, Crespo-Leiro M, Delgado R, Dobbels F, Grady K, Kao W, Lamour J, Parry G, Patel J, Pini D, Towbin J, Wolfel G, Delgado D, Eisen H, Goldberg L, Hosenpud J, Johnson M, Keogh A, Lewis C, O'Connell J, Rogers J, Ross H, Russell S, Vanhaecke J, International Society of H and Lung Transplantation G. The International Society of Heart and Lung Transplantation Guidelines for the care of heart transplant recipients. J Heart Lung Transplant Off Publ Int Soc Heart Transplant. 2010;29:914–56.
145. Zakliczynski M, Babinska A, Flak B, Nozynski J, Kamienska N, Szygula-Jurkiewicz B, Pacholewicz J, Przybylski R, Zembala M. Persistent mild lesions in coronary angiography predict poor long-term survival of heart transplant recipients. J Heart Lung Transplant Off Publ Int Soc Heart Transplant. 2014;33:618–23.
146. Kobashigawa JA, Tobis JM, Starling RC, Tuzcu EM, Smith AL, Valantine HA, Yeung AC, Mehra MR, Anzai H, Oeser BT, Abeywickrama KH, Murphy J, Cretin N. Multicenter intravascular ultrasound validation study among heart transplant recipients: outcomes after five years. J Am Coll Cardiol. 2005;45:1532–7.
147. St Goar FG, Pinto FJ, Alderman EL, Valantine HA, Schroeder JS, Gao SZ, Stinson EB, Popp RL. Intracoronary ultrasound in cardiac transplant recipients. In vivo evidence of "angiographically silent" intimal thickening. Circulation. 1992;85:979–87.
148. Fang JC, Rocco T, Jarcho J, Ganz P, Mudge GH. Noninvasive assessment of transplant-associated arteriosclerosis. Am Heart J. 1998;135:980–7.
149. Bax JJ, Kramer CM, Marwick TH, Wijns W. Cardiovascular imaging: a handbook for clinical practice. New York: John Wiley & Sons; 2009.
150. Dandel M, Hummel M, Müller J, Wellnhofer E, Meyer R, Solowjowa N, Ewert R, Hetzer R. Reliability of tissue doppler wall motion monitoring after heart transplantation for replacement of invasive routine screenings by optimally timed cardiac biopsies and catheterizations. Circulation. 2001;104:I-184–91.
151. Spes CH, Klauss V, Mudra H, Schnaack SD, Tammen AR, Rieber J, Siebert U, Henneke K-H, Überfuhr P, Reichart B, Theisen K, Angermann CE. Diagnostic and prognostic value of serial dobutamine stress echocardiography for noninvasive assessment of

cardiac allograft vasculopathy: a comparison with coronary angiography and intravascular ultrasound. Circulation. 1999;100:509–15.
152. Hacker M, Hoyer HX, Uebleis C, Ueberfuhr P, Foerster S, La Fougere C, Stempfle H-U. Quantitative assessment of cardiac allograft vasculopathy by real-time myocardial contrast echocardiography: a comparison with conventional echocardiographic analyses and [Tc99m]-sestamibi SPECT. Eur J Echocardiogr. 2008;9(4):494–500.
153. Tona F, Osto E, Tarantini G, Gambino A, Cavallin F, Feltrin G, Montisci R, Caforio AL, Gerosa G, Iliceto S. Coronary flow reserve by transthoracic echocardiography predicts epicardial intimal thickening in cardiac allograft vasculopathy. Am J Transplant Off J Am Soc Transplant Am Soc Transplant Surgeons. 2010;10:1668–76.
154. Wu YW, Yen RF, Lee CM, Ho YL, Chou NK, Wang SS, Huang PJ. Diagnostic and prognostic value of dobutamine thallium-201 single-photon emission computed tomography after heart transplantation. J Heart Lung Transplant Off Publ Int Soc Heart Transplantat. 2005;24:544–50.
155. Preumont N, Berkenboom G, Vachiery JL, Jansens JL, Antoine M, Wikler D, Damhaut P, Degré S, Lenaers A, Goldman S. Early alterations of myocardial blood flow reserve in heart transplant recipients with angiographically normal coronary arteries. J Heart Lung Transplant. 2000;19:538–45.
156. Kofoed KF, Czernin J, Johnson J, Kobashigawa J, Phelps ME, Laks H, Schelbert HR. Effects of cardiac allograft vasculopathy on myocardial blood flow, vasodilatory capacity, and coronary vasomotion. Circulation. 1997;95:600–6.
157. Steen H, Merten C, Refle S, Klingenberg R, Dengler T, Giannitsis E, Katus HA. Prevalence of different gadolinium enhancement patterns in patients after heart transplantation. J Am Coll Cardiol. 2008;52:1160–7.
158. Korosoglou G, Osman NF, Dengler TJ, Riedle N, Steen H, Lehrke S, Giannitsis E, Katus HA. Strain-encoded cardiac magnetic resonance for the evaluation of chronic allograft vasculopathy in transplant recipients. Am J Transplant Off J Am Soc Transplant Am Soc Transplant Surgeons. 2009;9:2587–96.
159. Mittal TK, Panicker MG, Mitchell AG, Banner NR. Cardiac allograft vasculopathy after heart transplantation: electrocardiographically gated cardiac CT angiography for assessment. Radiology. 2013;268:374–81.
160. Miller CA, Sarma J, Naish JH, Yonan N, Williams SG, Shaw SM, Clark D, Pearce K, Stout M, Potluri R, Borg A, Coutts G, Chowdhary S, McCann GP, Parker GJM, Ray SG, Schmitt M. Multiparametric cardiovascular magnetic resonance assessment of cardiac allograft vasculopathy. J Am Coll Cardiol. 2014;63:799–808.
161. Davis SF, Yeung AC, Meredith IT, Charbonneau F, Ganz P, Selwyn AP, Anderson TJ. Early endothelial dysfunction predicts the development of transplant coronary artery disease at 1 year posttransplant. Circulation. 1996;93:457–62.
162. Hollenberg SM, Klein LW, Parrillo JE, Scherer M, Burns D, Tamburro P, Bromet D, Satran A, Costanzo MR. Changes in coronary endothelial function predict progression of allograft vasculopathy after heart transplantation. J Heart Lung Transplant Off Publ Int Soc Heart Transplant. 2004;23:265–71.
163. Kubrich M, Petrakopoulou P, Kofler S, Nickel T, Kaczmarek I, Meiser BM, Reichart B, von Scheidt W, Weis M. Impact of coronary endothelial dysfunction on adverse long-term outcome after heart transplantation. Transplantation. 2008;85:1580–7.
164. Weis M, Hartmann A, Olbrich HG, Hor G, Zeiher AM. Prognostic significance of coronary flow reserve on left ventricular ejection fraction in cardiac transplant recipients. Transplantation. 1998;65:103–8.
165. Fearon WF, Hirohata A, Nakamura M, Luikart H, Lee DP, Vagelos RH, Hunt SA, Valantine HA, Fitzgerald PJ, Yock PG, Yeung AC. Discordant changes in epicardial and microvascular coronary physiology after cardiac transplantation: Physiologic Investigation for Transplant Arteriopathy II (PITA II) study. J Heart Lung Transplant Off Publ Int Soc Heart Transplant. 2006;25:765–71.
166. Haddad F, Khazanie P, Deuse T, Weisshaar D, Zhou J, Nam CW, Vu TA, Gomari FA, Skhiri M, Simos A, Schnittger I, Vrotvec B, Hunt SA, Fearon WF. Clinical and functional correlates of early microvascular dysfunction after heart transplantation. Circ Heart Fail. 2012;5:759–68.
167. Di Mario C, Krams R, Gil R, Serruys PW. Slope of the instantaneous hyperemic diastolic coronary flow velocity–pressure relation. A new index for assessment of the physiological significance of coronary stenosis in humans. Circulation. 1994;90:1215–24.
168. Escaned J, Flores A, Garcia-Pavia P, Segovia J, Jimenez J, Aragoncillo P, Salas C, Alfonso F, Hernandez R, Angiolillo DJ, Jimenez-Quevedo P, Banuelos C, Alonso-Pulpon L, Macaya C. Assessment of microcirculatory remodeling with intracoronary flow velocity and pressure measurements: validation with endomyocardial sampling in cardiac allografts. Circulation. 2009;120:1561–8.

# Practical Aspects of Intracoronary Pressure and Flow Measurements

*Arnold H. Seto and Morton J. Kern*




J. Escaned, J. Davies (eds.), *Physiological Assessment of Coronary Stenoses and the Microcirculation*,
DOI 10.1007/978-1-4471-5245-3_10

## 10.1 Introduction

Direct measurements of intracoronary pressure and flow are vital tools for determining the clinical significance of intermediate epicardial lesions and identifying microvascular dysfunction. Functional assessment of coronary artery disease complements the anatomical data obtained from coronary angiography and provides more reliable prognostic information. Noninvasive assessments of perfusion, including radionuclide myocardial perfusion scans but also more precise techniques such as positron emission tomography, suffer from well-recognized limitations in resolution, sensitivity, and specificity. Obtaining accurate intracoronary measurements may be straightforward in most cases, but can be fraught with technical pitfalls. Interpretation of the data should take into account both the physiologic and technical limitations of the various techniques and indices. In this chapter, we review the challenges that may affect intracoronary hemodynamic measurements.



## 10.2 Background on Pressure and Flow Indices

To appreciate the derivations of the commonly used physiology measurements, a brief review of coronary flow and pressure will be helpful. Myocardial ischemia results from an imbalance between the myocardial oxygen supply and demand. Coronary blood flow provides the required oxygen supply for any given myocardial oxygen demand, and normally increases automatically from a resting level to a maximum level in response to increases in myocardial oxygen demand from exercise, neurohumoral or pharmacologic hyperemic stimuli. There are three major resistance points to blood flow; the epicardial vessel (R1), the small arteries and arterioles (R2), and the intramyocardial capillary system (R3) (Fig. 10.1). In patients without atherosclerosis, the large epicardial vessel resistance (R1) is trivial. Adjustment of coronary resistance occurs principally at the arterioles (R2), which mediates the autoregulatory functions that maintain flow at a constant level in response to changing pressure conditions, and the hyperemic response to increasing demand. Atherosclerotic stenoses produce epicardial (R1) vessel resistance and can reduce coronary blood flow as described below. Several conditions, including left ventricular hypertrophy, myocardial ischemia, or diabetes can affect the microcirculation (R3 resistance), blunting maximal increases in coronary blood flow even in the absence of epicardial vessel narrowing.

### 10.2.1 Coronary Flow Reserve

Coronary flow reserve (CFR) is the ratio of maximal hyperemic to basal mean flow velocity in the target vessel obtained distal to the stenosis. CFR measures the capacity of the two-component system of the coronary artery and the supplied vascular bed to achieve maximal blood flow in response to a given hyperemic stimulation. Resting coronary flow is not impeded by mild or moderate stenoses and is maintained by normal vasodilatory regulation of the microcirculation. As shown by the classic experiments of Gould et al. [1], resting coronary blood flow remains constant up to the point where an epicardial coronary constriction exceeds 85–90 % of the normal segment diameter. However, unlike resting flow, maximal hyperemic coronary blood flow begins to decline when diameter stenosis exceeds 45–60 % (Fig. 10.2).

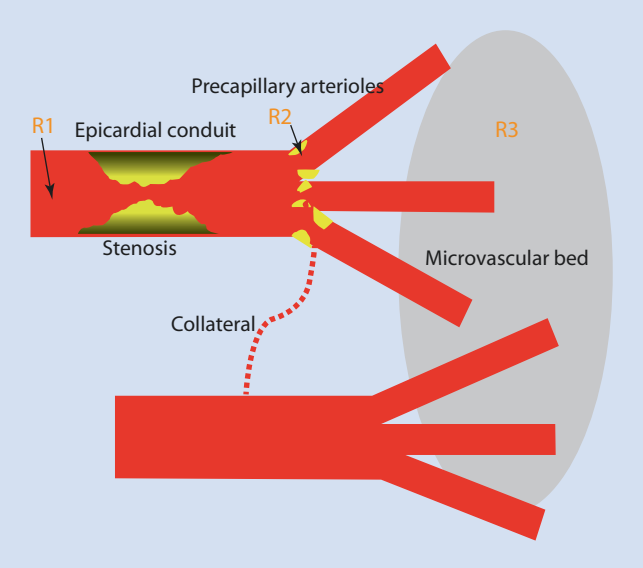


**Fig. 10.1** Diagram of coronary resistances. The epicardial arteries (*R1*) normally have negligible resistance until an atherosclerotic narrowing occurs (top artery). The precapillary arterioles (*R2*) regulate most of the coronary flow to the microvascular bed (*R3*). Diseased epicardial vessels are often connected to normal blood flow regions by collateral channels

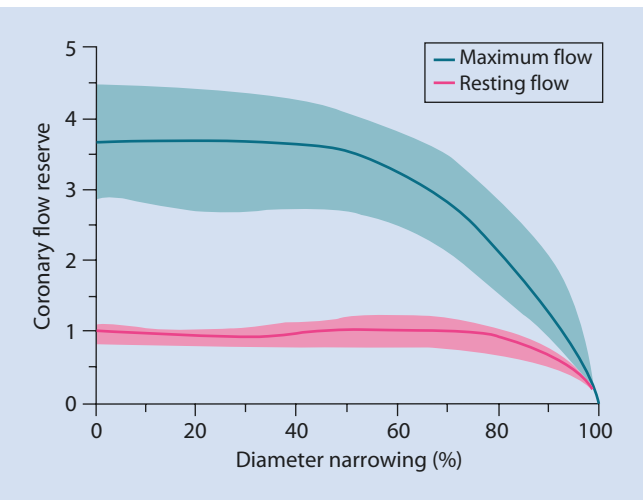


**Fig. 10.2** Coronary flow reserve expressed as ratio of maximum to resting flow plotted as a function of percent diameter narrowing. With progressive narrowing, resting flow does not change, whereas maximum potential increase in flow and coronary flow reserve begins to be impaired at approximately 50 % diameter narrowing. The *shaded area* represents the limits of variability of data about the mean (From Gould et al. [1])

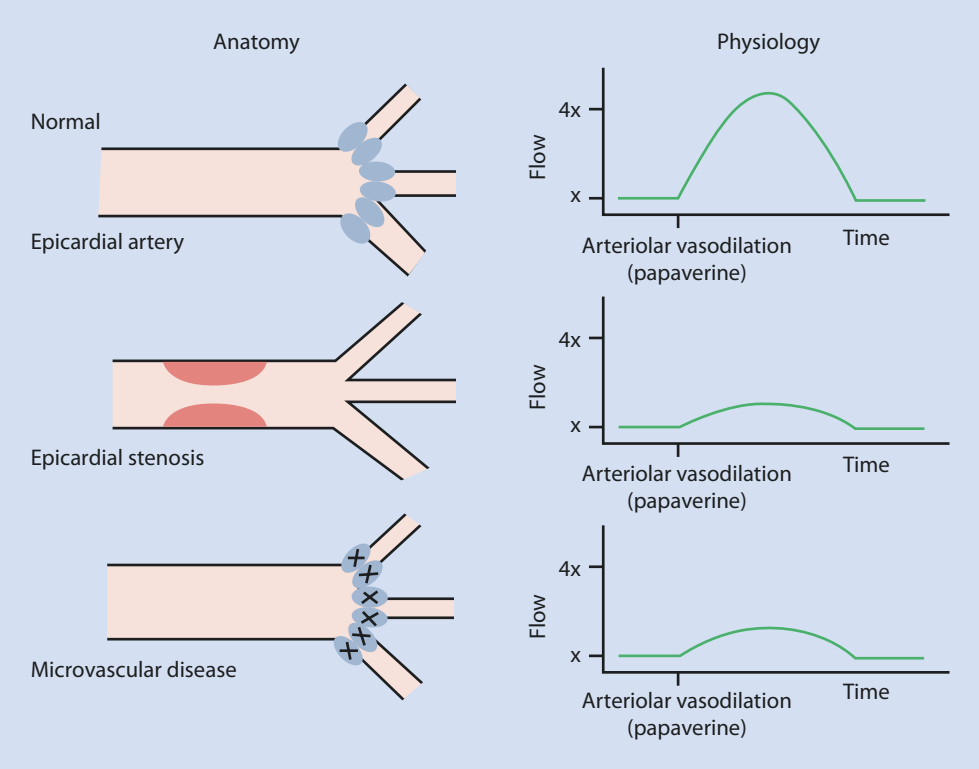


**Fig. 10.3** Limitations of CFR. A normal epicardial and microvascular bed results in a normal CFR (*top panel*). If either a stenosis or microvascular disease is present, then CFR is reduced (*middle and lower panels*) (From: Wilson [27])

Although early studies in animals and humans suggested a normal CFR of 3.5–5, clinical studies of patients undergoing cardiac catheterization have generally found a CFR of <2.0 to be the best threshold value for insufficient reserve [2]. As CFR reflects the summed response of both the epicardial artery and the microvasculature, an abnormal CFR cannot be used as the sole indicator of epicardial lesion significance (Fig. 10.3). Relative CFR (rCFR), the ratio of maximal flow in the coronary with stenosis to flow in a normal coronary without stenosis, may be an alternative but has limited applicability due to the need for a normal reference vessel and the assumption of a homogenous microcirculatory response [3].

## 10.2.2 Fractional Flow Reserve

In normal coronary arteries, there is minimal pressure loss along the length of the coronary artery. Therefore, in a normal epicardial coronary artery, the myocardial perfusion pressure equals aortic pressure ($P_a$) minus central venous pressure ($P_v$). In the presence of an epicardial stenosis, myocardial perfusion pressure is the poststenotic distal pressure ($P_d$) minus $P_v$.

Fractional flow reserve (FFR) is an index of the functional significance of coronary stenosis defined as the maximal flow in a vessel in the presence of a stenosis divided by the maximal flow in the theoretical absence of the stenosis (Fig. 10.4). Assuming flow is linearly related to pressure during hyperemia

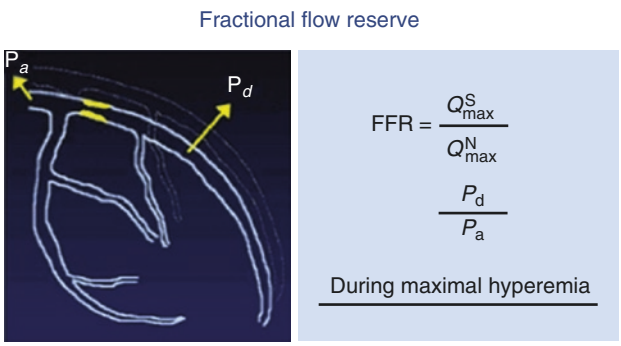


**Fig. 10.4** Fractional flow reserve (FFR) is derived from the ratio of myocardial flow ($Q_s$) across stenosis/myocardial flow ($Q_n$) without stenosis. Fractional flow reserve is the ratio of maximal myocardial perfusion in the stenotic territory divided by maximal hyperemic flow in the same region in the hypothetical case where the lesions were absent. Stated another way, FFR represents the fraction of hyperemic flow that still persists despite the presence of the stenosis. It has been demonstrated that this ratio of two flows could be calculated solely from the ratio of mean coronary pressure divided by mean aortic pressure provided both pressure are recorded under conditions of maximal hyperemia.

(when myocardial resistance is minimized), the translesional pressure ratio during hyperemia serves as a surrogate for the percent of normal flow possible in the absence of the stenosis. FFR can thus be estimated as $P_d - P_v/P_a - P_v$, or $\approx P_d/P_a$ as the effect of central venous pressure is usually negligible.

Unlike other physiologic indexes, FFR has a uniform normal value of 1.0 for every patient and every coronary

artery. FFR is not significantly influenced by changes in heart rate, blood pressure, or contractility [4]. A threshold value of 0.75 to define ischemia has been validated against a rigorous three-test standard of inducible ischemia [5]. Subsequent comparative studies of various single stress tests against FFR produced a range of values within a "gray zone" of uncertainty (0.75–0.80) such that high confidence for the presence or absence of ischemia is associated with FFR<0.75 and FFR>0.80, respectively. These cut-points were confirmed in prospective clinical trials such as DEFER, FAME, and FAME2 [6–8].

## 10.3 Basic Principles and Prerequisites for Measurements of Pressure and Flow

In previous chapters the clinical benefits of FFR have been well described. In order to obtain such benefits the importance of meticulous technique to ensure FFR measurements are accurately obtained and proper interpretation of tracing is key.

## 10.4 Measurement of Coronary Flow Velocity

### 10.4.1 Measurement of Coronary Flow Velocity by Intracoronary Doppler

Previous chapters have highlighted the importance of Doppler flow measurements to calculate CFR and indices of coronary resistance (Fig. 10.5).

## Doppler Flow Measurements: Technical Challenges

### Effect of Wire Position

Accurate flow velocity depends on a satisfactory velocity envelope. The Doppler wire transducer position must be adjusted to sample the correct volume of blood to optimize the velocity signal. The midstream signal should have the highest average peak velocity (APV). Poor Doppler signal acquisition may occur in 10–20 % of patients (even within normal arteries). Several different tip orientations interrogating the maximal velocity spectra are necessary (Fig. 10.6).

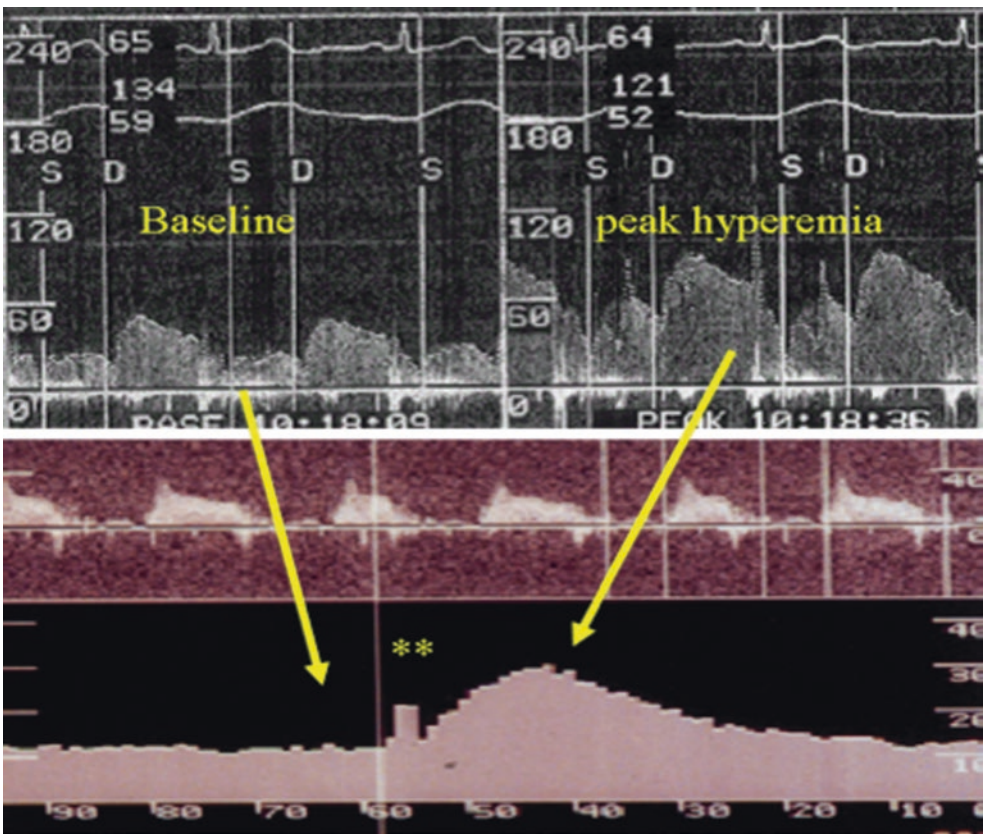


**Fig. 10.5** Coronary Doppler flow velocity signals used for the measurement of coronary flow velocity reserve in the cardiac catheterization laboratory. The *top panel* is divided into the baseline (*left*) and the peak hyperemic velocity (*right*) signals. Phasic flow velocity tracing is demarcated by systolic (*S*) and diastolic (*D*) markers, corresponding to the electrocardiogram and aortic pressure at top of panels. Diastolic flow predominates over systolic flow. Flow velocity scale is from 0 to 240 cm per second. Continuous trend plot of average peak velocity showing the baseline and time course of peak hyperemia (*bottom panel*). The intracoronary bolus adenosine injection can be seen by the square wave signal preceding the rapid increase in average peak velocity. The phasic peak hyperemic velocity signal was captured and displayed in the *upper right panel*. The trend plot scale is from 0 to 60 cm per second with a time base of 0 to 90 s (*bottom panel*). In this example, baseline flow is 13 cm per second and peak hyperemic flow is 30 cm per second for a coronary flow reserve of 2.3.

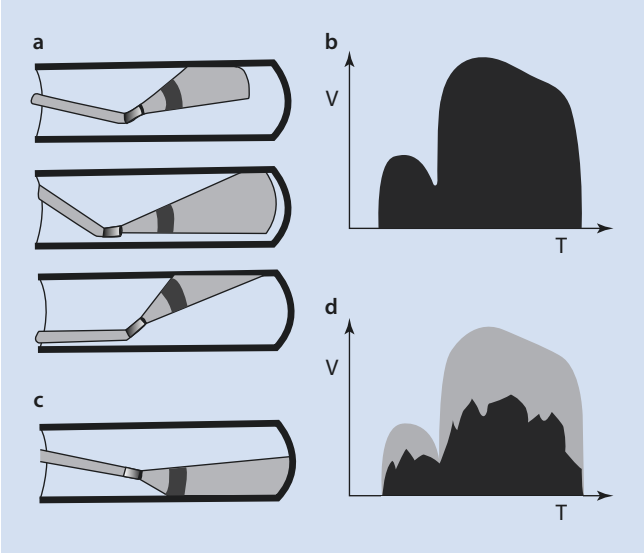


**Fig. 10.6** Effects of Doppler wire position. **a** Effective sampling of midstream blood flow leads to **b** good Doppler flow signals. **c** Doppler wire not sampling midstream, resulting in **d** poor Doppler flow signals (From Safian [28]).

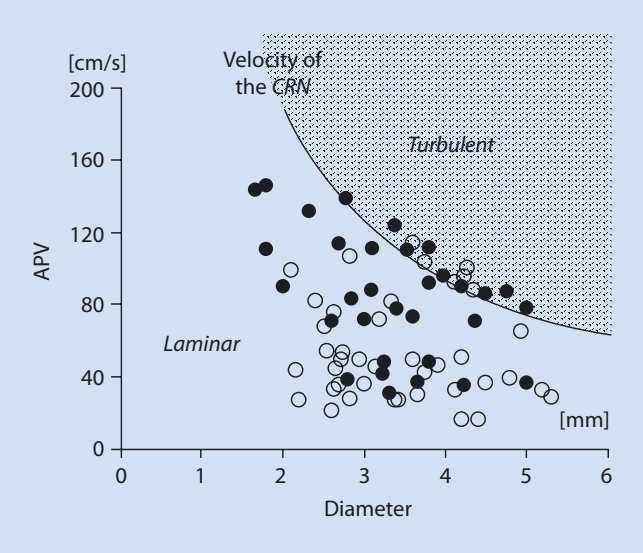


**Fig. 10.7** Maximum value of the average peak velocity APV in 43 patients before (○) or after an angiographically successful angioplasty of 32 patients (●). The highest values of APV were taken for each individual. The flow velocity at the critical Reynolds number (CRN) 500 describes the change from laminar to turbulent flow profile (From Ferrari [9])

Some operators recommend retroflexing the tip of the guide wire to a retrograde position to coronary blood flow.

The Doppler transducer measures the average peak velocity of coronary blood flow, as observed along the direct line or vector of the transducer. As in echocardiography, any difference in angulation (Ø) between the Doppler vector and the transducer reduces the measured velocity, particularly for angles greater than 30°. For tortuous vessels, the ability to measure an accurate blood flow velocity may be particularly impaired.

### Effect of Turbulent Flow

Quantification of coronary blood flow by Doppler presumes a laminar flow profile within the coronary artery. However, even in nonatherosclerotic coronary arteries turbulent flow patterns have been observed during open heart surgery studies. In an in vitro experiment, Ferrari et al. [9] determined that above a critical Reynolds number of 500, Doppler wire measurement underestimated actual volumetric flow by up to 22.5 %. In an accompanying in vivo experiment, the maximum APV exceeded this critical Reynolds value in 20 % of patients, indicating that the true flow velocity may be underestimated (Figs. 10.7 and 10.8). As hyperemic APV values are most likely to be in the turbulent zone than resting values, this potential underestimation should be kept in mind when calculating CFR.

### Effect of Epicardial Stenosis on Doppler Flow

A significant epicardial coronary stenosis will reduce the poststenotic APV and the diastolic/systolic flow velocity ratio while increasing the proximal/distal AVP. With hemodynamically significant stenoses, the Doppler signals distal to a stenosis may be difficult to detect above the background. APV should be measured sufficiently distal to the stenosis to avoid turbulence. If the transducer is not sufficiently distal to the stenosis, it may also inadvertently measure the acceleration of flow through a tight lesion. This higher flow velocity would not accurately describe the flow velocity in the vessel as a whole after laminar flow is restored.

## 10.4.2 Measurement of Coronary Flow by Thermodilution

The coronary thermodilution technique uses the piezoelectric pressure wire sensor as a thermistor. The shaft of the angioplasty pressure-monitoring guide wire (PressureWireCertus, St Jude Medical) has a temperature-dependent electrical resistance and acts as a proximal thermistor. Measurement of temperature change (arrival time to the thermistor) during injection of saline reflects coronary blood flow; thus the temperature curve at rest and during hyperemia can be used to determine coronary flow reserve. The pressure wire is connected to a dedicated interface with modified software for online analysis of the thermodilution curves (Fig. 10.9). Three milliliter of room temperature saline is injected via the guide catheter at rest and during peak hyperemia. These injections should be rapid, consistent, and performed in triplicate. Unlike in cardiac output measurements by thermodilution, the precise temperature and volume of the injection are relatively unimportant – only the timing of injection and the change in distal temperature is required.

Thermodilution CFR (CFRthermo) is defined as the ratio of hyperemic divided by resting coronary flow ($F$).

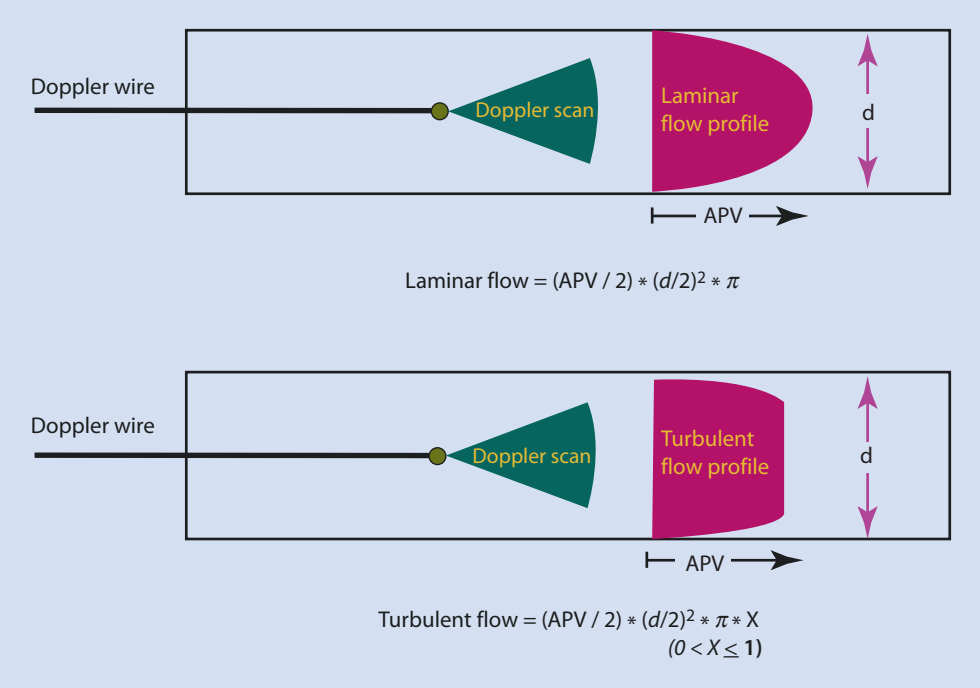


**Fig. 10.8** Flow profile under laminar and turbulent conditions. Under laminar flow the average peak velocity divided by 2 (APV/2) multiplied with the lamina area (vessel diameter = *d*) can be used for exact quantitative measurement of the blood flow. Under turbulent flow an underestimation of the blood flow occurs when measured with a Doppler wire (From Ferrari [9])

10

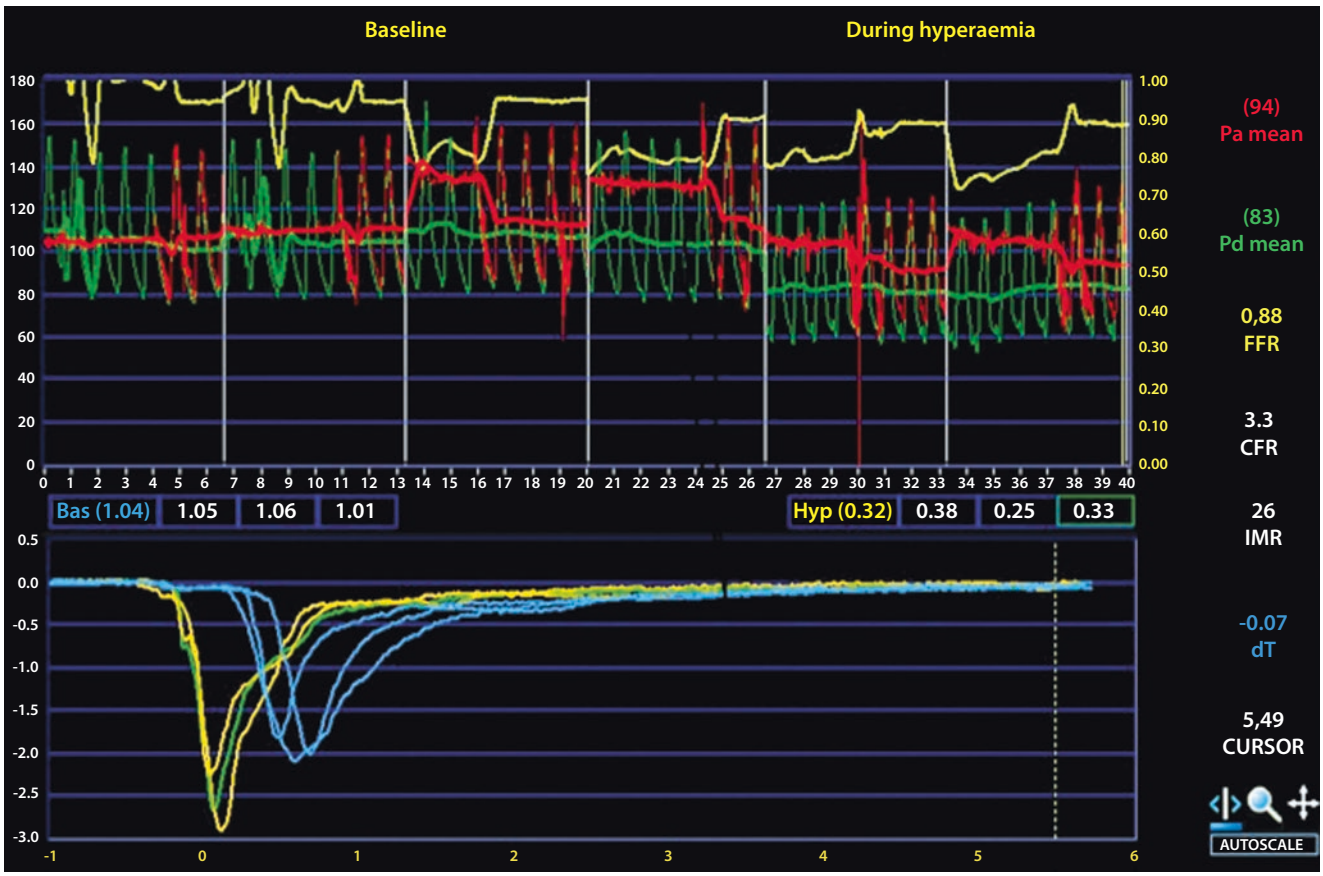


**Fig. 10.9** Thermodilution-derived transit time curves at baseline and during maximal hyperemia (From Varho [29])

$$CFR = \frac{F \text{ at hyperemia}}{F \text{ at rest}}$$

Flow is the ratio of the volume ($V$) divided by mean transit time ($T_{mn}$). Thus, CFR can be expressed as follows.

$$CFR = \frac{\left(\frac{V}{T_{mn}}\right) \text{at hyperemia}}{\left(\frac{V}{T_{mn}}\right) \text{at rest}}$$

Assuming the epicardial blood volume ($V$) remains unchanged, CFR can be calculated as follows.

$$CFR = \frac{T_{mn} \text{ at rest}}{T_{mn} \text{ at hyperemia}}$$

In animal experiments, a significant linear relation was found between flow velocity and $1/T_{mn}$. When comparing directly measured $CFR_{Doppler}$ and $CFR_{thermo}$, a good correlation was found ($r$ = 0.80) [10]. Simultaneous measurements of CFR and FFR can thus be obtained for research studies on coronary resistance. When combined with poststenotic pressure measurements, thermodilution measurements can provide a complete description of the pressure-flow relationship and the response of the microcirculation.

### Limitations of Thermodilution Flow Measurements

Measurement of coronary flow by thermodilution has the potential to be simpler than Doppler flow measurements. The technical success rate varies from 87 to 97 %, compared with a success rate of 69–91 % for successful Doppler CFR measurement, indicating that it may be easier to measure as wire position may be less critical. However, compared with $CFR_{Doppler}$ values, $CFR_{thermo}$ values are consistently higher, by up to 20 % [10].

CFR by thermodilution may be overestimated when large side branches are present. This especially occurs if such a side branch originates closely proximal to the stenosis and the sensor is located distal to the stenosis, and more of the coronary blood flow is directed toward the side branch. This limitation is not very important for proximal stenoses but may lead to overestimation of CFR by thermodilution in the case of stenoses in the mid or distal part of a coronary artery.

CFR by thermodilution requires steady-state hyperemia so that the repeated measurements of hyperemic flow are comparable. This precludes the use of intracoronary adenosine, and requires intravenous adenosine or papaverine. As discussed below, however, the hyperemic effects of intravenous adenosine are frequently not stable or consistent. This risks inaccurate thermodilution measurements of flow, as the coronary flow rate may change over the typical course of time to perform three thermodilution injections. In addition, the epicardial volume ($V$) can change in response to hyperemic vasodilation or spasm – this may violate the assumption of constant $V$ and lead to erroneous CFR calculations.

### 10.4.3 Variation of Coronary Flow

Coronary blood flow is autoregulated for myocardial demand. Moreover, coronary flow reserve is also variable depending on the flow status at the time of measurement. Hence, there is no absolute normal value for coronary blood flow. Flow may vary significantly between patients and within an individual depending on the conditions of measurement. Within the same individual, multiple factors can alter either basal or hyperemic flow. Tachycardia increases basal flow and reduces hyperemic flow; coronary flow reserve is reduced by 10 % for each 15 beats increase in heart rate [11–13]. Coronary flow reserve may be reduced in patients with essential hypertension and normal coronary arteries and in patients with aortic stenosis and normal coronary arteries. In some patients with moderate coronary artery disease, the stenosis configuration and surrounding vessel segments are subject to vasomotor stimuli. Thus, vasoconstrictor, neurologic or humoral influences, endothelial dysfunction, and extra vascular compression of intramural vessels may produce dynamic or episodic ischemia-related symptoms with activities of daily life such as exercise, emotional stress, or adrenergic stimulation.

## 10.5 Measurement of FFR and Pitfalls

Previous chapters have highlighted the background and methods of obtaining FFR measurements.

### 10.5.1 Technical Issues

#### Mechanical Issues: Transducers, Zeros, Connections

Measurement of aortic pressure through a fluid-filled guide catheter is subject to technical issues such as loose connections, leak in guide connections, and improper zeroing. Improper leveling of the systemic pressure transducer can over- or underestimate aortic pressure. Loose connections and malfunctioning pressure transducers can generate abnormal or moving systemic pressure measurements, mimicking wire drift. Most commonly, the Y-connector or Touhy-Borst may be inadequately tightened, or the needle introducer left in during measurement or normalization of pressures, leading to a decrease in measured aortic pressure (Fig. 10.10). Finally, a saline flush prior to any pressure measurement clears blood and radiographic contrast from the guide catheter, reducing the risk of a damped aortic pressure waveform (Fig. 10.11).


**Fig. 10.10** Loose connections. Equalized $P_a$ and $P_d$ pressures (*left panel*) become unequal when the Touhy-Borst introducer is not tightened (*right panel*), causing partial loss of aortic pressure. Leaving a needle introducer in place causes a similar loss of pressure

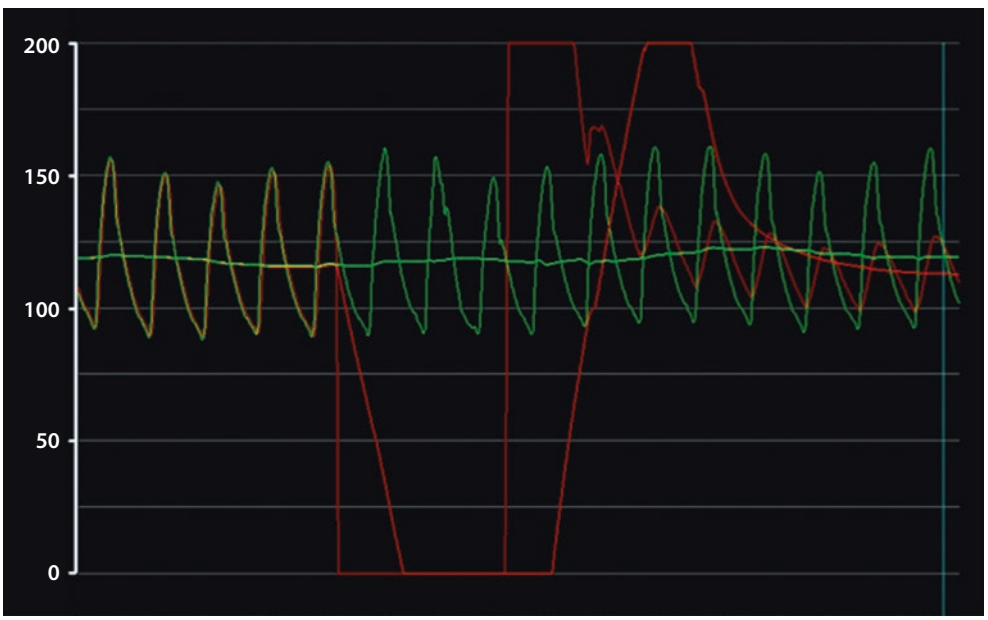


**Fig. 10.11** Contrast damping. Equalized $P_a$ and $P_d$ pressures (*left*) become unequal after an injection of radiographic contrast causes damping of the $P_a$ waveform (*right*) due to the viscosity of the contrast medium. This can also occur with blood and is accentuated by the use of small-caliber guides or diagnostic catheters

## Beat to Beat Variation

Physiologic pressure measurements may vary from one beat to another. These can result from spontaneous respiration, coughing (Fig. 10.12), arrhythmias (Fig. 10.13), or exaggerated respiratory activity (e.g., sleep apnea). The default setting for the commercial FFR software from Volcano and St Jude Medical is to take the lowest value of $P_d/P_a$ over a single beat resulting in an underestimated FFR. We and others recommend changing the settings of the software to measure the three or five-beat average FFR to minimize the impact of beat-to-beat variation (Fig. 10.14).


**Fig. 10.12** Cough. Transient rise in both $P_d$ and $P_a$ in response to coughing reflex (evident on ECG tracing) increasing intrathoracic pressure

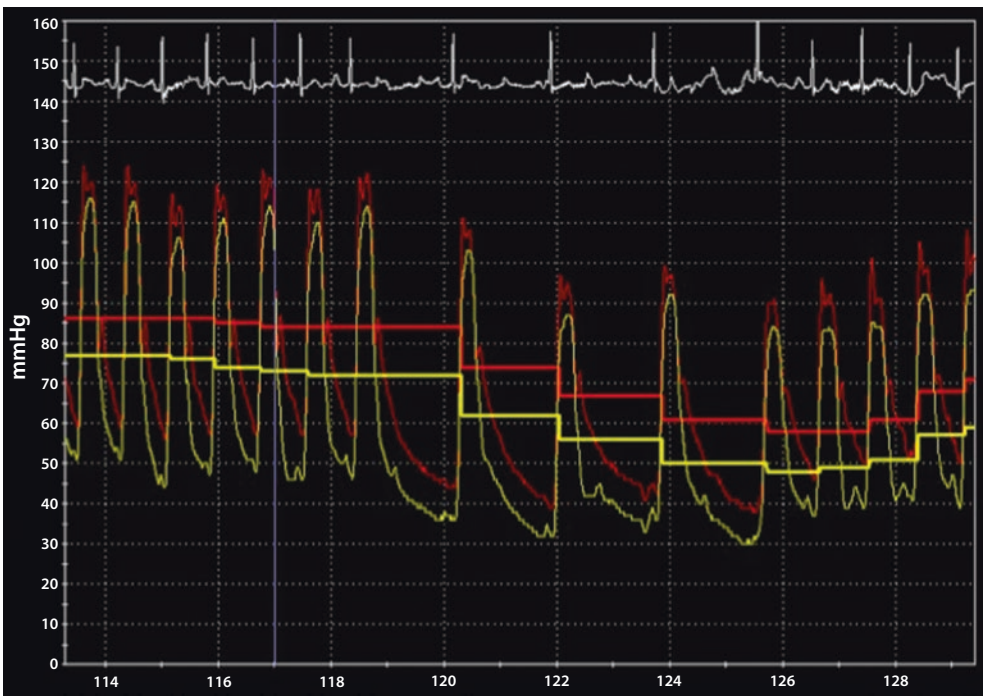


**Fig. 10.13** Arrhythmia. Transient heart block, PVCs, and irregular heart rhythms may all alter the $P_d/P_a$ relationship

## Catheters with Side Holes

Use of guide catheters with side holes in cases of aortic pressure damping introduces a potential source of error in that a pressure gradient through the guide side holes may be formed. A side-hole catheter may produce a pressure reading that is a combination of the aortic and coronary pressures, leading to a higher recorded value than the true proximal coronary pressure (Fig.10.15). The additional gradient may not be detected until hyperemia has occurred and hence FFR may be underestimated. If a guiding catheter with side holes is to be used, then it is mandatory to disengage the catheter from the coronary ostium before pressure measurements are made. The use of IC adenosine is not advised, given that part of the drug may be delivered into the aorta.

## Guide Wire Whipping

An uncommon artifact of the guide wire sensor is the phenomenon of "whipping". During cardiac contraction, the guide wire sensor may hit a moving coronary wall and produce an exaggerated and sharp increase in the pressure sig-

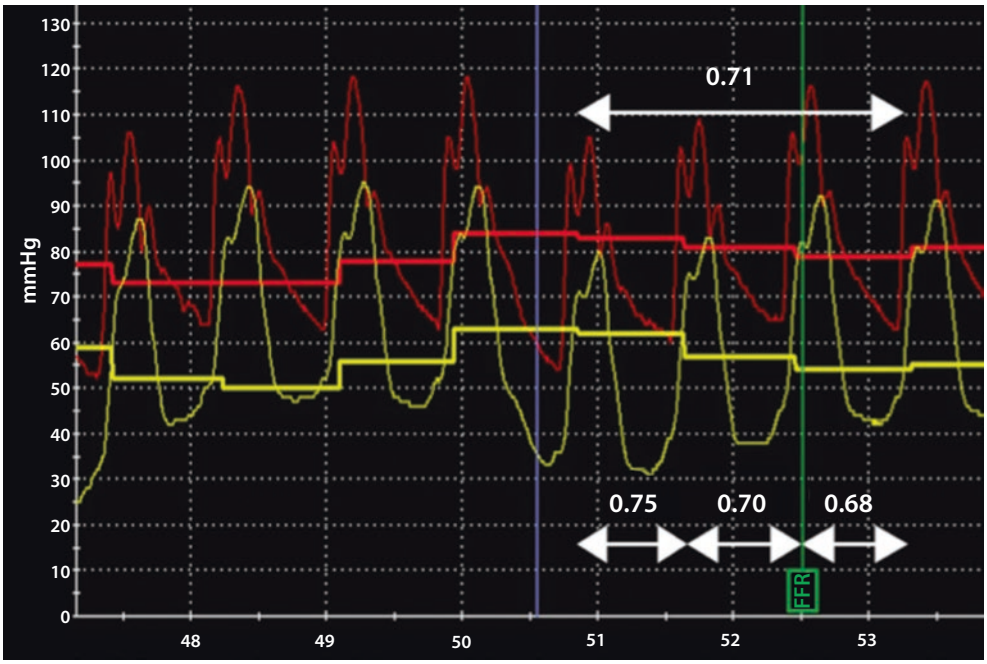


**Fig. 10.14** Measurement of FFR by one-beat vs. three-beat averages. The single-beat FFR varies from 0.68 to 0.75, whereas the three-beat average FFR attenuates these fluctuations and is preferred (From Seto et al. [25], reprinted with permission)



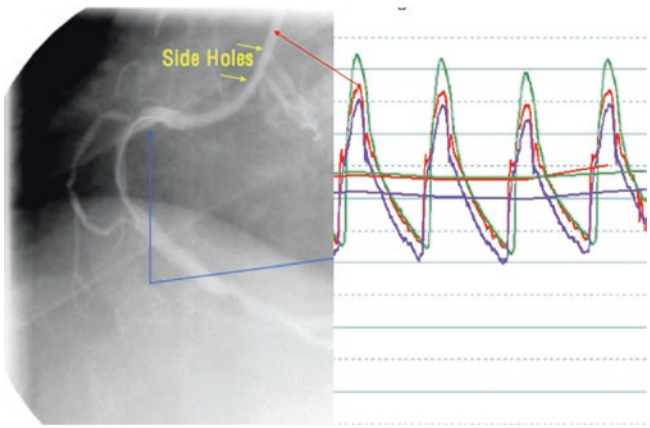


**Fig. 10.15** Confounding effects of guiding catheters with side holes. $P_a$ is represented by the *red pressure wave*, while the $P_d$ is represented by the *blue pressure wave*. The femoral artery pressure (*green*) is also recorded by the side arm of the arterial sheath. The sensor has been advanced to the tip of the guiding catheter and hyperemia has been induced. A gradient has developed between the femoral pressure and the $P_a$

nal (Fig. 10.16). Although this artifact increases the recorded coronary pressure, the nonphysiologic waveform is easily recognized. Correction of the whipping artifact is performed by withdrawing or advancing the wire a few millimeters and avoiding placement of the wire into small side branches.

## Wire Signal Drift

All piezoelectric pressure sensors are subject to electronic signal offset or drift during a procedure. Signal stability is confirmed by checking the matching of aortic and guide wire pressures at the guide catheter before and after the measurements. On occasion, after inserting the guide wire across a lesion a resting gradient with the aortic pressure may be noted. Several clues suggest that it is not a true pressure gradient and is instead the result of signal drift: (1) distal pressure is higher than aortic pressure; (2) the distal pressure signal is unstable and continues to drift higher or lower (Fig. 10.17); or (3) distal pressure is lower than aortic pressure but retains the identical waveform characteristics, including the dicrotic notch. A true significant stenosis acts like a high-frequency filter and obscures transmission of high-frequency signals responsible for the dicrotic notch in the aortic pressure. Therefore, when a translesional pressure gradient is present, but pressure recordings are identical in shape, signal drift should be suspected.

Signal drift occurs most commonly with the following:
Disconnection/reconnection of the wire, especially after PCI.
Prolonged use of the wire and exposure to blood.
Older generations (prior to 2013) of pressure wires. Note: Fiberoptic wires and catheters have less signal drift than piezoelectric sensors.

### 10.5.2 Physiologic Issues

## Effect of Hydrostatic Pressure

One assumption when comparing $P_d$ with $P_a$ is that both the distal and proximal pressures are at the same level in the heart relative to the pressure transducer. This is certainly the case at the time of equalization at the guide catheter tip; however, when the wire is advanced into the coronary circulation, there may be a small change in its position relative to the heart, which can result in a small change in pressure measured due to hydrostatic forces (e.g., gravity). This phenomenon occurs primarily in the distal RCA, posterior descending artery, and distal circumflex artery, and may result in a small 0.01–0.04 increase in FFR measurement. This effect is particularly evident in normal vessels where the resting $P_d/P_a$

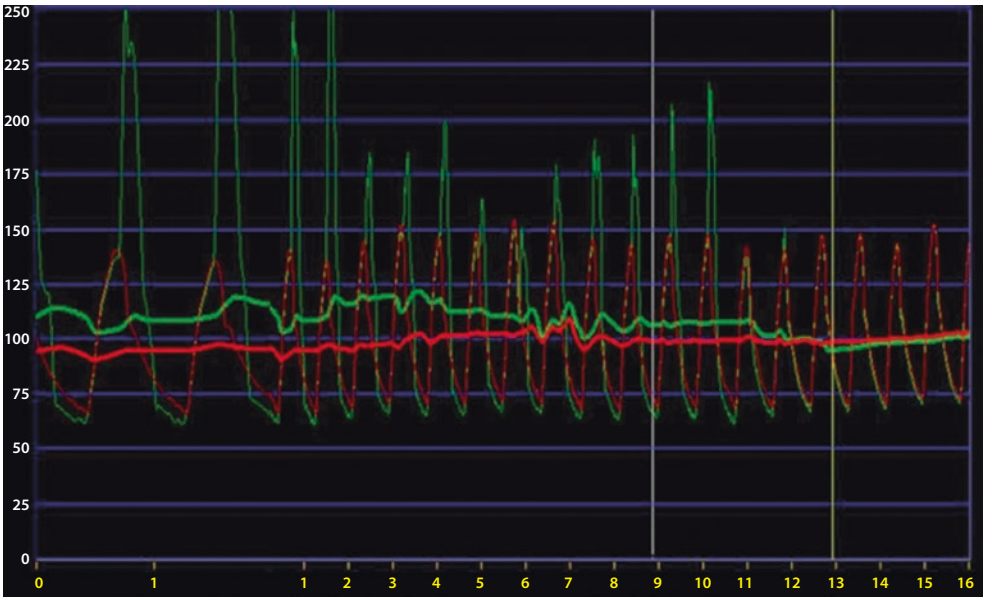


**Fig. 10.16** Wire sensor "whip". When the guide wire sensor is in direct contact with the coronary wall or myocardium, brief spikes in the pressure signal are measured by the wire

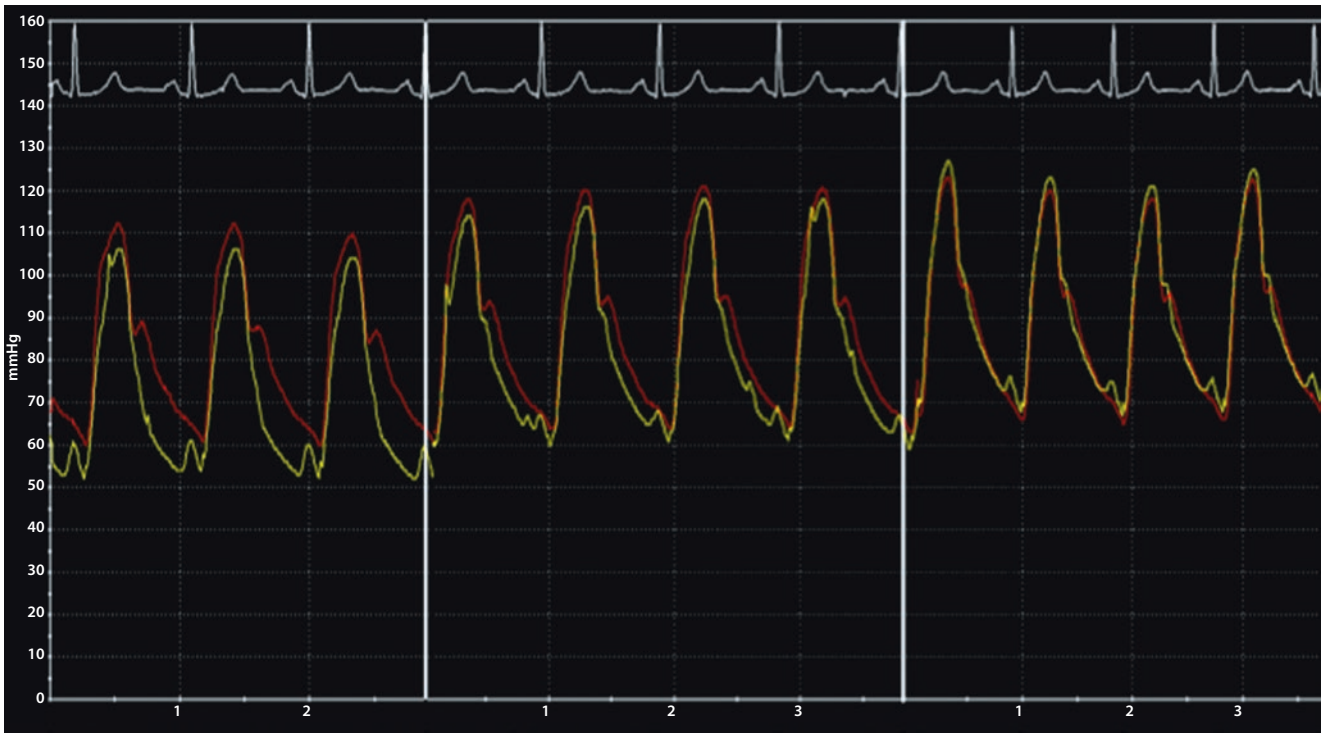


**Fig. 10.17** Wire drift. Electronic signal drift can occur with solid-state wires, whereby $P_d$ can increase/decrease without movement of the wire. The maximal and true gradient (*left panel*) decreases (*center panel*) and even reverses with wire drift (*right panel*), without any movement of the wire or change in the waveform

may be as high as 1.04. Pullback into the guide confirms the absence of wire signal drift and the physiologic basis of the change in distal pressure.

## Effects of Central Venous Pressure

FFR was formally derived and validated as $P_d - P_v / P_a - P_v$ during maximal hyperemia. In practice the effects of central venous pressure are typically presumed to be negligible, and FFR is assumed to be $\approx P_d / P_a$. However, in a study of 66 patients using invasive measurement of right atrial pressure ($P_v$) and an FFR cutoff of 0.75, Perera et al. demonstrated that 14 % of all lesions would be misclassified as insignificant when $P_v$ was ignored. Presuming a fixed $P_v$ value of 5, 8, or 10 mmHg improved sensitivity but decreased specificity [14]. In a mathematical analysis, Kumar showed that (1) any elevation in $P_v$ can only make the estimated FFR lower, so that there is no value to measuring $P_v$ when FFR is $\leq$0.80; (2) the effect of $P_v$ is less in hypertensive patients; and (3) the use of an FFR threshold value of $\leq$0.80 reduced the chance of a false-negative FFR compared with a threshold of $\leq$0.75 (Fig. 10.18) [15].

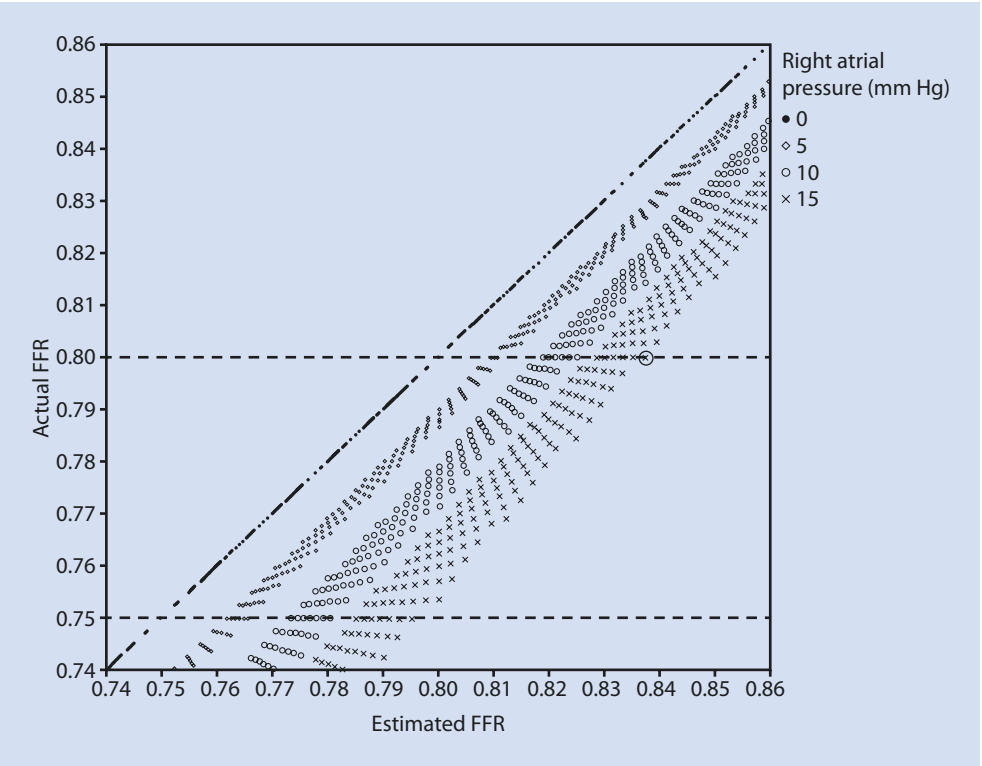


**Fig. 10.18** Effect of right atrial pressure (Pra) on FFR. Actual vs. estimated FFR for scenarios where $80 \leq P_a \leq 110$ mmHg showing progressive decrease in actual FFR with increasing Pra. At a Pra of 15 mmHg, an estimated FFR of 0.838 (*circled*) corrects to 0.80 (From Kumar [15])



The practice of ignoring the effect of $P_v$ has been validated by the clinical outcomes of the DEFER, FAME, and FAME2 trials, which did not require measurement of $P_v$ to estimate FFR in a selected population of stable angina patients. The use of the FFR ≤0.80 rather than <0.75 effectively captures most patients who might have had a false-negative FFR due to elevated $P_v$. However, in patients with hypotension or congestive heart failure, incorporation of $P_v$ measurements adheres more closely with the theory of FFR and may be clinically appropriate.

## Limitations of a Single Cutoff Value

Following multiple clinical trials including DEFER, FAME, and FAME 2, the FFR-guided approach has been shown to be superior to the angiographic approach to revascularization. Ultimately these studies supported FFR ≤0.80 as the threshold value for intervention. However, Petraco et al. [16] demonstrated the limitations of any single cutoff value when the method and tools have inherent imprecision. They found that in the gray area zone of 0.77–0.83, the chance of an FFR value crossing the threshold of 0.80 upon remeasurement of the same lesion 10 min later was 20 %. The closer the initial FFR value was to 0.80, the higher the likelihood of crossing the threshold value. Like any diagnostic test, FFR has an inherent coefficient of variation, largely due to the variable physiological response to adenosine.

A more nuanced approach is suggested by a patient-level meta-analysis of all FFR trials by Johnson et al. [17]. They found that the clinical outcome of patients was found to directly correlate with their FFR measurement, such that lower FFR values were associated with a higher risk of cardiovascular complications. Thus, rather than a simple binary outcome, FFR instead provides a continuum of risk based on the severity of the ischemia that can be demonstrated (Fig. 10.19). Patients with the most severe lesions would benefit most from revascularization, while more borderline lesions could be potentially deferred if the clinical situation suggests (i.e., a higher risk of PCI complications, or minimal symptoms). However, to test outcomes it is of value to employ a single cutoff understanding the limitations of applying such a value in clinical practice.

## 10.6 Technical Challenges Common to Pressure and Flow Measurements

### 10.6.1 Damping by Guiding Catheter

Because of the guide catheter size relative to the coronary ostium, a guide catheter can create a partial obstruction and a gradient between the aorta and the coronary artery often resulting in a distorted aortic pressure waveform (i.e., a damped pressure signal) and decreased flow. Damping is most common with larger guiding catheters (8 Fr), but can also occur with 6 Fr guide catheters in small coronary ostia or when the catheter is not coaxial with the artery. Extra backup guides are most commonly associated with damping, but any catheter that is deeply seated can create aortic pressure damping.

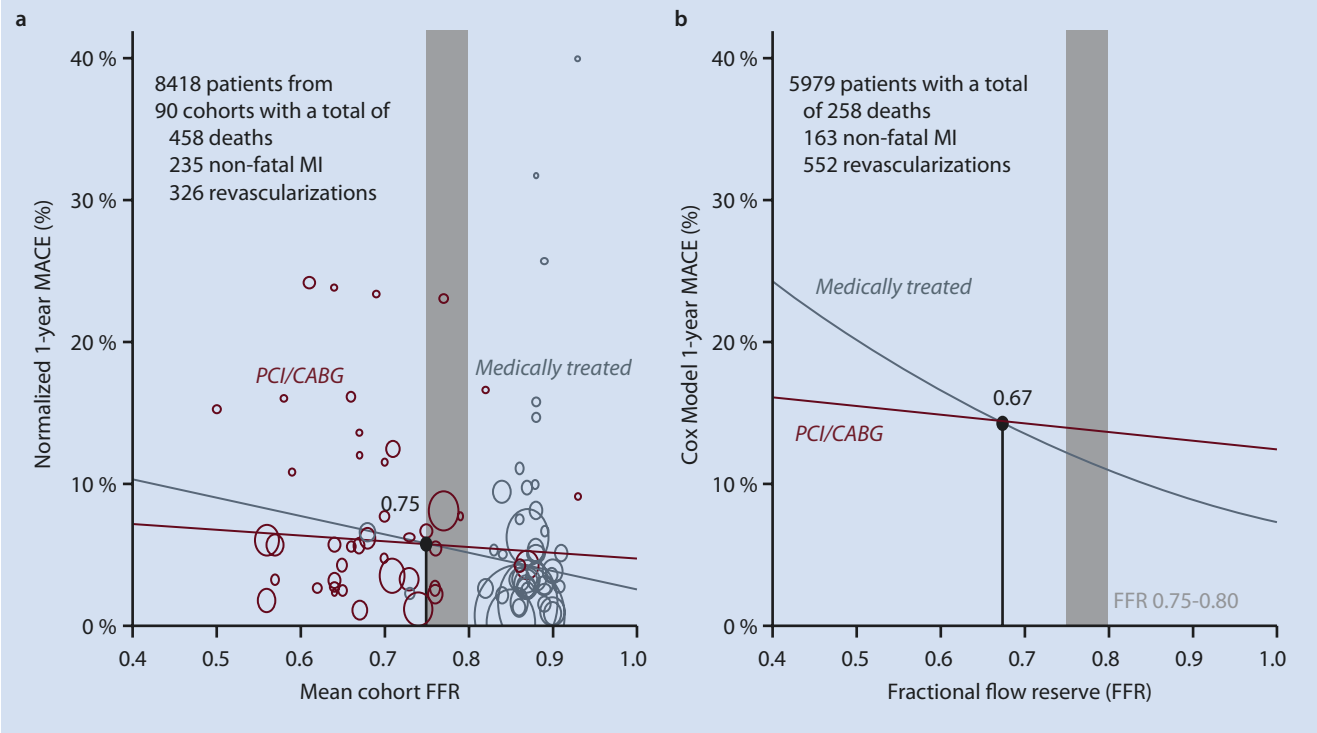


**Fig. 10.19** Outcomes as a function of FFR value. **a** Normalized 1-year major adverse cardiac event (MACE) rate for study-level analysis. **b** Cox model 1-year MACE rate for patient-level analysis. *Colored lines* depict the model fit for revascularization (*red*) or medical therapy (*slate*) treatment. These curves cross at the optimal FFR threshold, here shown for the unadjusted model. *FFR* fractional flow reserve, *MI* myocardial infarction (From Johnson et al. [17])

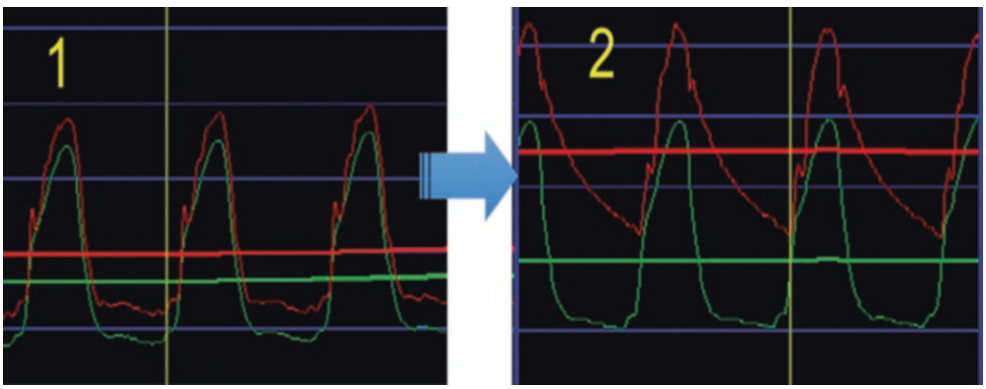


**Fig. 10.20** Guide catheter damping. When oversized or deep seated, a guide catheter can create a damped $P_a$ waveform (*Left panel*) that lacks a dicrotic notch. Disengagement of the guide reveals the true higher aortic pressure waveform (*Right panel*)

Aortic pressure damping will lower the measured $P_a$, underestimating the hyperemic gradient and lesion severity while overestimating the true FFR value (Fig. 10.20). The guiding catheter may also blunt maximum blood flow through the artery impairing accurate FFR. Pressure signal damping is best recognized by careful visual examination of the aortic pressure waveform, and prevented by disengaging the guide catheter from the ostium at the time of measurement. In a small study of 21 patients, even in the absence of clear ostial disease or dampening at baseline, the presence of the guide catheter caused the FFR value to be 0.04 higher than that measured with the guide disengaged, suggesting that routine guide catheter disengagement may be necessary for the precise measurement of FFR [18].

Damping of the guide catheter is also a concern with CFR measurements. This is especially the case with thermodilution measurements, where the guide catheter must be sufficiently engaged in the coronary artery to guarantee adequate delivery of the injectate into the vessel; but guide catheter obstruction can result in a decrease in coronary flow, resulting in underestimation of CFR. With Doppler flow measurements, damped flow in the coronary artery may be evident as a blunted coronary flow velocity profile that fails to increase with hyperemia, but is relieved with guide catheter disengagement.

**Fig. 10.21** Wire straightening artifact. The stiffness of the wire can straighten the tortuosity of a vessel, creating kinks in the artery (*arrow*) that may be hemodynamically significant

### 10.6.2 Wire Spasm and Pseudostenosis

Like any coronary guide wire, passing of a coronary pressure guide wire can induce vasoconstriction and spasm. Coronary spasm narrows the artery and can generate a pressure gradient consistent with a physiologic stenosis. To demonstrate that such a vasospastic stenosis is reversible, IC nitroglycerin (100–400 mcg) should be given prior to any intracoronary wire insertion. Even in the relatively hypotensive patient (systolic pressure 90–100 mmHg), 50–100 mcg of IC nitroglycerin is generally safe and well-tolerated.

Guide wires of all types can also create straightening artifacts in tortuous vessels, producing the so-called "accordion effect" (Fig. 10.21). This phenomenon occurs especially in the right coronary artery and with the use of stiffer wires or catheters. Guide wire straightening can create temporary obstructions or kinking with a pressure gradient that can decrease the FFR and flow measurements. The kinking or pseudostenoses are detected by observing the lesion after pulling back of the guide wire, or having only the most flexible wire tip portion in the tortuous section. In the presence of significant tortuosity and pseudostenosis, accurate measurements may be impossible.

### 10.6.3 Limitations of Adenosine as a Hyperemic Agent

FFR and CFR require the induction of a maximal hyperemic state to minimize the effect of microvascular resistance. The most commonly available agent, adenosine, is widely available and easy to use but may have an effect that can vary with the method of delivery, dose, the presence of interfering substances, and physiologic responses.

#### Methylxanthines and Adenosine Maximal Hyperemia

Methylxanthines such as caffeine, theobromine (from chocolate), and theophylline are competitive antagonists of the adenosine receptor. It is generally recommended that all such substances be held prior to studies using adenosine to obtain an optimal hyperemic response. Matsumoto et al. recently found that caffeine in the range of 1.8–4.6 mg/L inhibited the effect of IV adenosine (FFR 0.813 compared with 0.779 with papaverine), although larger doses of IV adenosine (210 mcg/kg/min) reduced the impact (Fig. 10.22) [19]. Avoidance of caffeine for several hours prior to a procedure may thus be advisable, but more severe restrictions are likely unnecessary.

#### Intracoronary Versus Intravenous Adenosine Induced Hyperemia

IV adenosine is regarded as the gold standard due to standardized dosing of 140 mcg/kg/min, but because of additional time and cost when giving IV adenosine, many operators prefer IC adenosine. The typical doses of IC adenosine produce submaximal hyperemia relative to IV adenosine in 10–15 % of patients, thus overestimating FFR and underestimating stenosis severity [20]. To compare the routes of adenosine administration, DeLuca et al. demonstrated a progressive, dose-dependent increase in the number of patients with FFR<0.75 with increasing IC adenosine doses up to 720 mcg (Fig. 10.23). These data show that IC adenosine is an effective alternative to the current standard IV adenosine, albeit at higher doses than typically administered clinically [21].

#### Peripheral Versus Central Intravenous Adenosine Infusion

Some controversy exists around the adequacy of adenosine delivery when given via a peripheral as compared with a central vein due to the short half-life and intravascular deactiva-

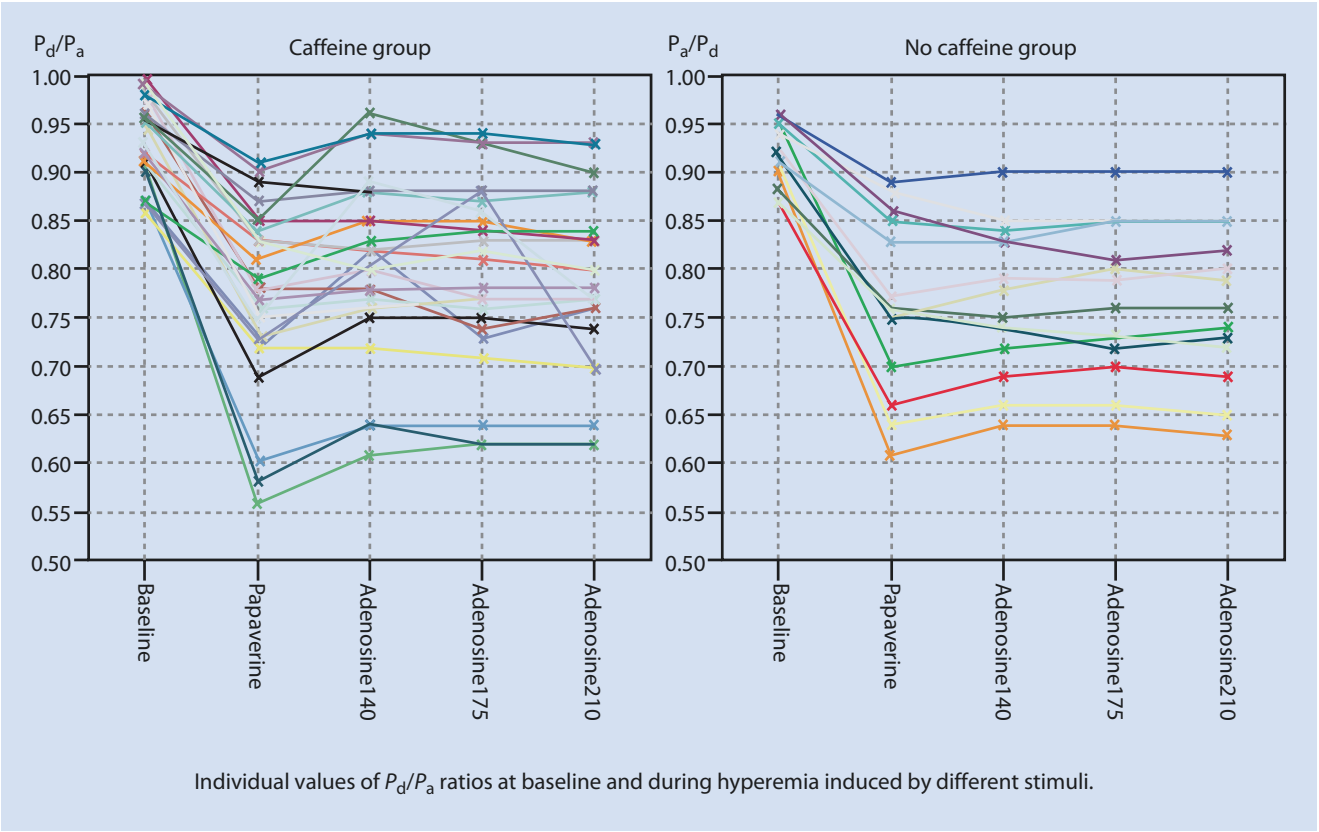


**Fig. 10.22** Caffeine effect. FFR measured with IV adenosine at 140, 175, 210 mcg/kg/min compared with papaverine in patients with and without caffeine. In patients with caffeine, FFR was overestimated with adenosine compared with papaverine (Matsumoto et al. [19], reprinted with permission from HMP Communications)

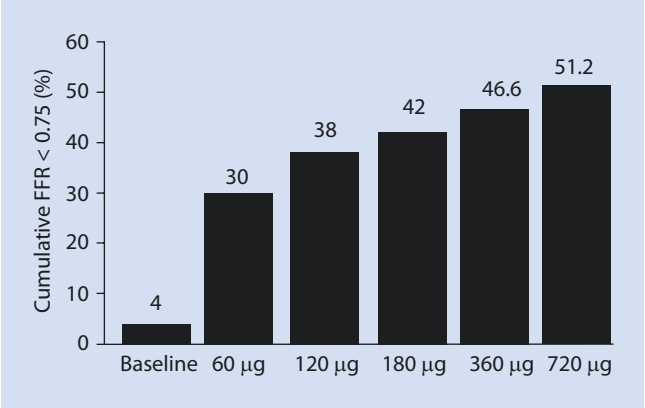


**Fig. 10.23** *Bar graph* shows the cumulative percentage of patients with fractional flow reserve (FFR) ≤0.75 with increasing dose of adenosine (From De Luca et al. [2], reprinted with permission)

tion of adenosine. However, multiple studies using antecubital, forearm, and hand venous access sites have documented that peripheral infusion of adenosine produces comparable FFR values to central infusion [22–24]. During peripheral IV adenosine administration, one must ensure that the blood pressure cuff is deflated or placed on the contralateral arm. Similarly, potential venous obstructions such as pacemakers, dialysis catheters, or deep venous thrombosis may interfere with venous flow, requiring central infusion to ensure adequate delivery.

## Variable Responses to IV Adenosine Infusion

Theoretically, once maximal hyperemia is achieved with an intravenous adenosine infusion, it should be sustained as a stable hyperemic state. Such a state would allow for accurate pullback measurements or multivessel assessment with FFR, with the presumption that stable hyperemia is sustained. Coronary flow measurements would also be stable, especially the repeated measurements required of the thermodilution technique.

However, we and others have shown that over the course of a single continuous intravenous adenosine infusion, the hyperemic effect varies significantly. Several patterns of pressure causing an FFR increase are identifiable. The most frequent pattern was that of $P_d$ rising more than the $P_a$ (Fig. 10.24) or fluctuating in a phasic pattern (Fig. 10.25). Using a combined pressure and flow wire, these patterns can be shown to be associated with an attenuation of the hyperemic response to continuous adenosine (Fig. 10.26), typically after 2 min of infusion. This phenomenon may be due to

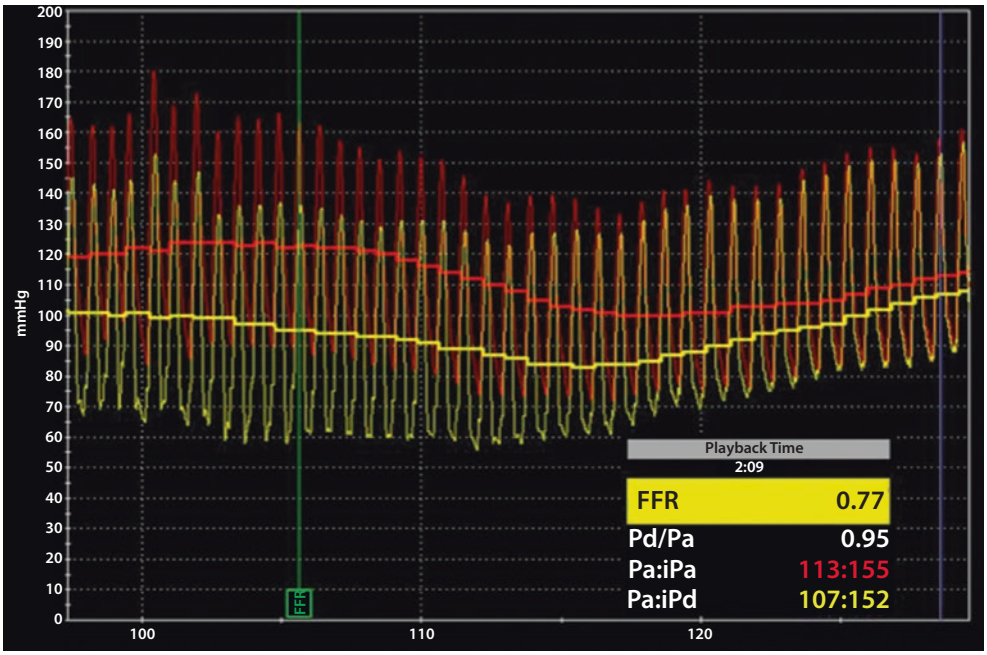


**Fig. 10.24** $P_d$ rising more than $P_a$ following maximal hyperemia during continuous adenosine infusion. This may reflect attenuation of adenosine hyperemia after prolonged (>90 s) infusion (Seto et al. [25], reprinted with permission)



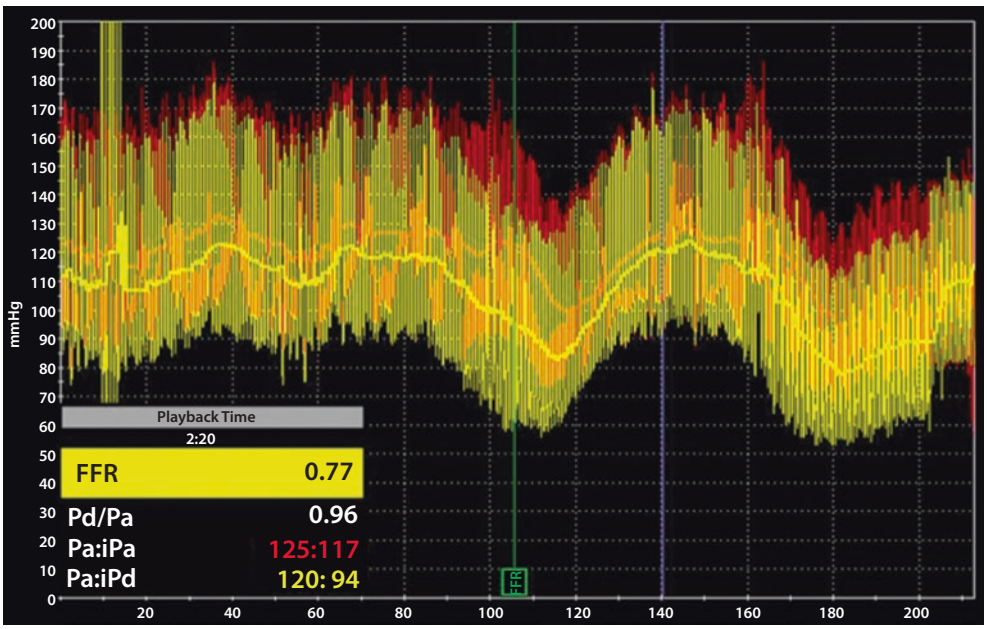


**Fig. 10.25** Phasic rises and falls in the $P_d/P_a$ ratio during continuous adenosine infusion (From Seto et al. [25], reprinted with permission)

inadequate delivery of IV adenosine, saturation of the vascular smooth muscle $A_{2A}$ receptor, or exhaustion of cAMP precursors.

A second pattern involves a sudden spike in $P_a$ pressure early at the onset of hyperemia (Fig. 10.27), causing the lowest $P_d/P_a$ value to occur prior to any significant drop in $P_d$. The last pattern of FFR change involves a fall in $P_a$ relative to $P_d$. Adenosine can cause variable degrees of systemic vasodilation in different individuals, occasionally causing more systemic than coronary vasodilation (Fig. 10.28).

Recently, Johnson et al. [26] found that among 190 complete paired FFR tracings obtained during adenosine

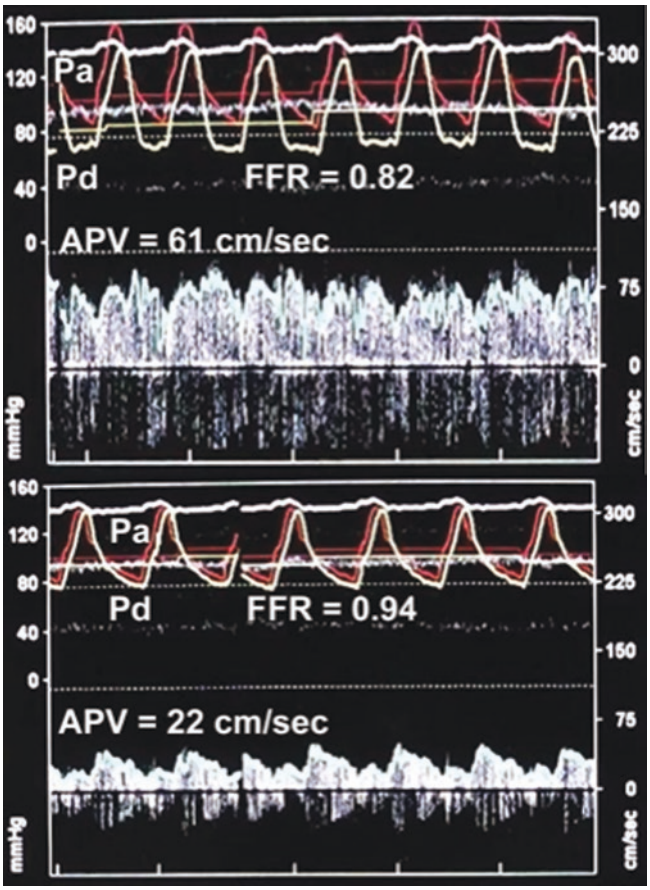


**Fig. 10.26** Instability of hyperemic flow with prolonged adenosine infusion. A combined pressure and flow wire (Combowire) measure an average peak velocity (*APV*) of 61 cm/s and a FFR value of 0.82 at maximal hyperemia (*top panel*). After continued adenosine infusion (*bottom panel*), the APV decreases to 22 cm/s and the FFR value increases to 0.94, indicating attenuation of adenosine hyperemia despite continued infusion. Phasic responses can also be demonstrated (From Seto et al. [25], reprinted with permission)

infusion, a stable hyperemic state was created in only 57 % of cases, with 39 % having a fluctuating hyperemic response as in Fig. 10.25. Even in the same patient and lesion, on repeated testing the pressure waveform patterns duplicated themselves only a minority of times. What was consistent on repeat testing was the lowest measured $P_d/P_a$ value ($r^2$ = 98.2 %), which did not differ from core lab analyses. Their conclusion, while contrary to classic teaching of FFR, is that the lowest value of $P_d/P_a$ should be used as the FFR rather than awaiting any stable value (Fig. 10.29). Similarly, the highest coronary flow velocity measured should be taken as the maximal hyperemic flow.

## 10.7 Conclusions

Invasive coronary hemodynamic evaluation is critical for a comprehensive understanding of coronary artery disease. CFR, either by Doppler or thermodilution, gives unique insight into the summed effect of the coronary arteries and microvasculature. FFR provides a simple and reliable technique to determine the functional significance of epicardial coronary stenoses. Understanding the potential technical challenges of pressure and flow measurements (Table 10.1) and the limitations of adenosine hyperemia will prepare the operator for any unexpected findings and avoid any miscalculations.

### Conflicts of Interest

Dr. Seto is a speaker for Volcano Corp, St Jude Medical, and consultant to Acist Inc. Dr. Kern is a speaker and consultant for Volcano Corp, St Jude Medical, and consultant to Acist Inc. and Opsens Inc.

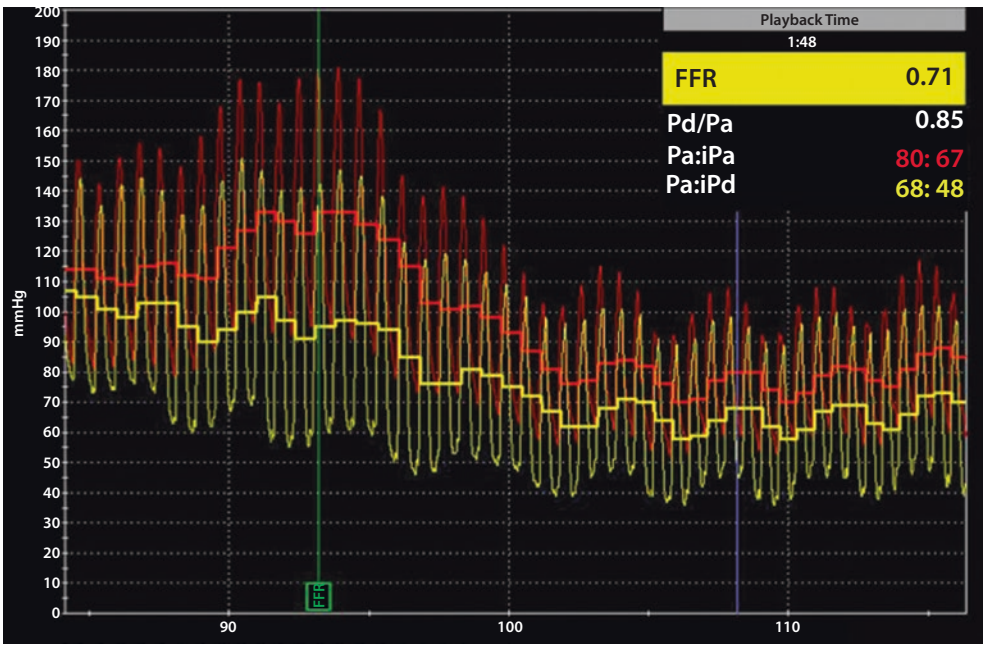


**Fig. 10.27** Sudden spike of $P_a$ early in the onset of hyperemia. This may reflect a neurologic reflex in response to the sensation of hyperemia (From Seto et al. [25], reprinted with permission)

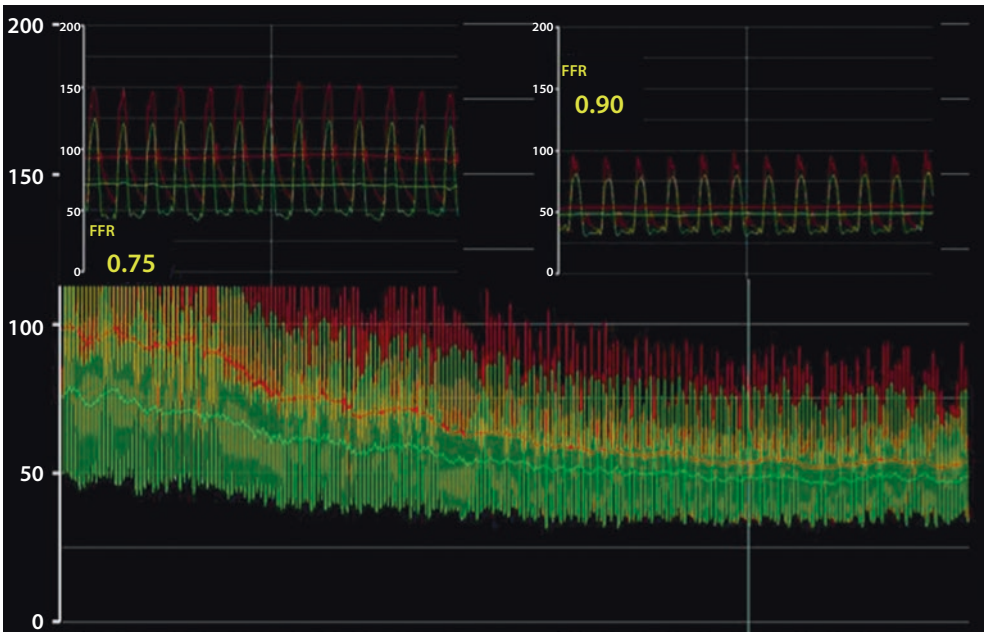


**Fig. 10.28** Systemic hypotension, with $P_a$ falling relative to the $P_d$ during continuous adenosine infusion. Adenosine can cause variable degrees of systemic vasodilation in different individuals, in some cases causing more systemic than coronary vasodilation (From Seto et al. [25], reprinted with permission)



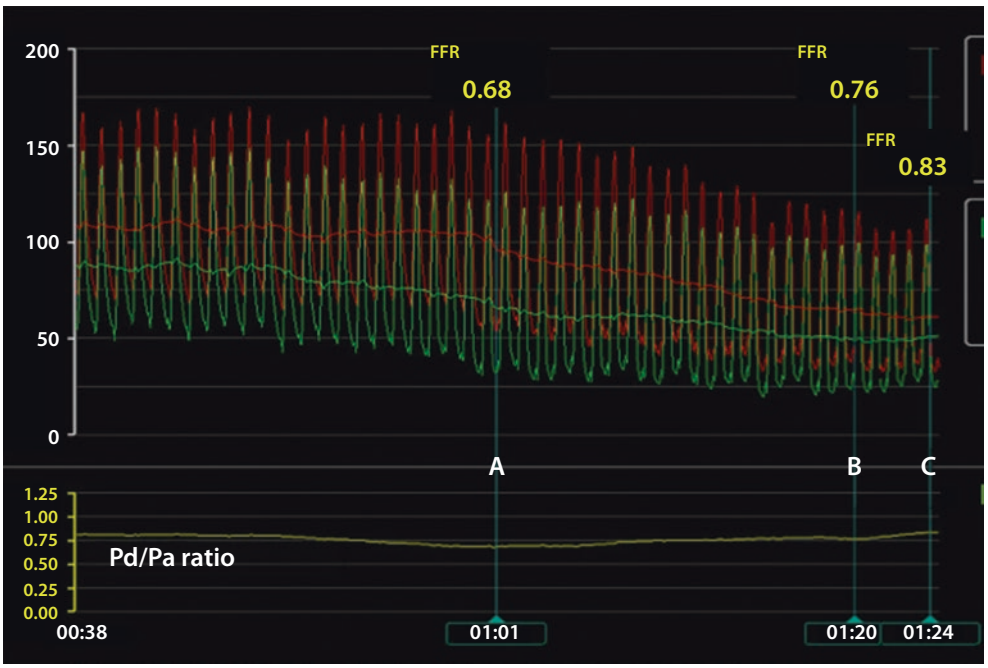


**Fig. 10.29** Typical coronary hemodynamic response to intravenous adenosine. The lowest single-beat $P_d/P_a$ (0.68) occurs early in hyperemia, at point *A*. Values obtained at the earliest nadir of $P_d$ (point B, 0.76) and during stable hyperemia (point *C*, 0.83–0.85) are significantly higher. The lowest average $P_d/P_a$ value (around point *A*) is the most reproducible FFR value

**Table 10.1** Limitations of intracoronary flow and presssure measurements

| Limitations of measurements | Comments |
|---|---|
| Doppler wire flow | |
| Difficulty sampling midstream flow | 10–20 % of procedures have poor quality measurements |
| Turbulent flow | Doppler may underestimate flow in 20 % of patients |
| Higher velocity near stenosis | Should measure well distal to the stenosis |
| Thermodilution flow | |
| Fixed bias | Generally 20 % higher than Doppler flow |
| Side branches | Large side branches cause flow to be overestimated |
| Need for stable hyperemia | Injections must be repeated during same hyperemic state |
| Technically challenging | |
| Pressure wire | |
| Zeroing and normalization | Ensure adequate flushing, equalization |
| Beat to beat variation | Use a five-beat average where possible |
| Guide catheter side holes | Transmits an inaccurate proximal pressure |
| Avoid the use of such guides | |
| Guide wire whipping | Move wire from small branch |
| Guide wire drift | Ensure equal pressures when wire pulled back to guide |
| Elevated central venous pressure | Measure CVP directly |
| Challenges common to pressure and flow measurements | |
| Guide catheter damping | May artifactually decrease coronary flow and pressure |
| Pseudostenosis | May make accurate measurements impossible with wires |
| Adenosine as hyperemic agent | May not cause maximal hyperemia depending on dose/route |
| | May not create stable hyperemic state |

## References

1. Gould KL, Lipscomb K, Hamilton GW. Physiologic basis for assessing critical coronary stenosis: instantaneous flow response and regional distribution during coronary hyperemia as measures of coronary flow reserve. Am J Cardiol. 1974;33:87–94.
2. Joye JD, Schulman DS, Lasorda D, Farah T, Donohue BC, Reichek N. Intracoronary Doppler guide wire versus stress single-photon emission computed tomographic thallium-201 imaging in assessment of intermediate coronary stenoses. J Am Coll Cardiol. 1994;24:940–7.
3. Gould KL, Kirkeeide RL, Buchi M. Coronary flow reserve as a physiologic measure of stenosis severity. J Am Coll Cardiol. 1990;15:459–74.
4. De Bruyne B, Bartunek J, Sys SU, et al. Simultaneous coronary pressure and flow velocity measurements in humans: feasibility, reproducibility, and hemodynamic dependence of coronary flow velocity reserve, hyperemic flow versus pressure slope index, and fractional flow reserve. Circulation. 1996;94:1842–9.
5. Pijls NH, De Bruyne B, Peels K, Van Der Voort PH, Bonnier HJ, Bartunek J, Koolen JJ, Koolen JJ. Measurement of fractional flow reserve to assess the functional severity of coronary-artery stenoses. N Engl J Med. 1996;334(26):1703–8.
6. Pijls NH, van Schaardenburgh P, Manoharan G, Boersma E, Bech JW, van't Veer M, Bär F, Hoorntje J, Koolen J, Wijns W, de Bruyne B. Percutaneous coronary intervention of functionally nonsignificant stenosis: 5-year follow-up of the DEFER Study. J Am Coll Cardiol. 2007;49(21):2105–11.
7. Tonino PA, De Bruyne B, Pijls NH, Siebert U, Ikeno F, van' t Veer M, Klauss V, Manoharan G, Engstrøm T, KG O, PN VL, PA MC, WF F, FAME Study Investigators. Fractional flow reserve versus angiography for guiding percutaneous coronary intervention. N Engl J Med. 2009;360(3):213.
8. De Bruyne B, Pijls NH, Kalesan B, Barbato E, Tonino PA, Piroth Z, Jagic N, Möbius-Winkler S, Rioufol G, Witt N, Kala P, MacCarthy P, Engström T, Oldroyd KG, Mavromatis K, Manoharan G, Verlee P, Frobert O, Curzen N, Johnson JB, Jüni P, WF F, FAME 2 Trial Investigators. Fractional flow reserve-guided PCI versus medical therapy in stable coronary disease. N Engl J Med. 2012;367(11):991–1001.
9. Ferrari M, Werner GS, Bahrmann P, Richartz BM, Figulla HR. Turbulent flow as a cause for underestimating coronary flow reserve measured by Doppler guide wire. Cardiovasc Ultrasound. 2006;4:14.
10. Pijls NH, De Bruyne B, Smith L, Aarnoudse W, Barbato E, Bartunek J, Bech GJ, Van De Vosse F. Coronary thermodilution to assess flow reserve: validation in humans. Circulation. 2002;105(21):2482–6.
11. McGinn AL, White CW, Wilson RF. Interstudy variability of coronary flow reserve: influence of heart rate, arterial pressure, and ventricular preload. Circulation. 1990;81:1319–30.
12. Hoffman JIE. Problems of coronary flow reserve. Ann Biomed Eng. 2000;28:884–96.
13. Chareonthaitawee P, Kaufmann PA, Rimoldi O, Camici PG. Heterogeneity of resting and hyperemic myocardial blood flow in healthy humans. Cardiovasc Res. 2001;50:151–61.
14. Perera D, Biggart S, Postema P, et al. Right atrial pressure: can it be ignored when calculating fractional flow reserve and collateral flow index? J Am Coll Cardiol. 2004;44(10):2089–91.
15. Kumar G. Letter to the editor: the influence of right atrial pressure on fractional flow reserve. J Invasive Cardiol. 2012;24(10):A43–4.
16. Petraco R, Sen S, Nijjer S, et al. Fractional flow reserve-guided revascularization: practical implications of a diagnostic gray zone and measurement variability on clinical decisions. JACC Cardiovasc Interv. 2013;6(3):222–5.

17. Johnson NP, Tóth GG, Lai D, Zhu H, Açar G, Agostoni P, Appelman Y, Arslan F, Barbato E, Chen SL, Di Serafino L, Domínguez-Franco AJ, Dupouy P, Esen AM, Esen OB, Hamilos M, Iwasaki K, Jensen LO, Jiménez-Navarro MF, Katritsis DG, Kocaman SA, Koo BK, López-Palop R, Lorin JD, Miller LH, Muller O, Nam CW, Oud N, Puymirat E, Rieber J, Rioufol G, Rodés-Cabau J, Sedlis SP, Takeishi Y, Tonino PA, Van Belle E, Verna E, Werner GS, Fearon WF, Pijls NH, De Bruyne B, Gould KL. Prognostic value of fractional flow reserve: linking physiologic severity to clinical outcomes. J Am Coll Cardiol. 2014;64(16):1641–1654.
18. Aminian A, Dolatabadi D, Lefebvre P, Khalil G, Zimmerman R, Michalakis G, Lalmand J. Importance of guiding catheter disengagement during measurement of fractional flow reserve in patients with an isolated proximal left anterior descending artery stenosis. Catheter Cardiovasc Interv. 2015;85(4):595–601.
19. Matsumoto H, Nakatsuma K, Shimada T, et al. Effect of caffeine on intravenous adenosine-induced hyperemia in fractional flow reserve measurement. J Invasive Cardiol. 2014;26(11):580–5.
20. Pijls NH, Kern MJ, Yock PG, et al. Practice and potential pitfalls of coronary pressure measurement. Catheter Cardiovasc Interv. 2000;49(1):1–16.
21. De Luca G, Venegoni L, Iorio S, et al. Effects of increasing doses of intracoronary adenosine on the assessment of fractional flow reserve. JACC Cardiovasc Interv. 2011;4(10):1079–84.
22. Seo MK, Koo BK, Kim JH, et al. Comparison of hyperemic efficacy between central and peripheral venous adenosine infusion for fractional flow reserve measurement. Circ Cardiovasc Interv. 2012;5(3):401–5.
23. Lindstaedt M, Bojara W, Holland-Letz T, et al. Adenosine-induced maximal coronary hyperemia for myocardial fractional flow reserve measurements: comparison of administration by femoral venous versus antecubital venous access. Clin Res Cardiol. 2009;98(11):717–23.
24. Scott P, Sirker A, Dworakowski R, Paul G, Candilio L, Jahagirdar N, Melikian N, Byrne J. Fractional flow reserve in the transradial era: will hand vein adenosine infusion suffice?: a comparative study of the extent, rapidity, and stability of hyperemia from hand and femoral venous routes of adenosine administration. JACC Cardiovasc Interv. 2015;8(4):527–35.
25. Seto AH, Tehrani DM, Bharmal MI, Kern MJ. Variations of coronary hemodynamic responses to intravenous adenosine infusion: implications for fractional flow reserve measurements. Catheter Cardiovasc Interv. 2014;84(3):416–25.
26. Johnson NP, Johnson DT, Kirkeeide RL, Berry C, De Bruyne B, Fearon WF, Oldroyd KG, Pijls NH, Gould KL. Repeatability of fractional flow reserve (FFR) despite variations in systemic and coronary hemodynamics. JACC Cardiovasc Interv. 2015;8:1018–27.
27. Wilson RF. Assessment of the human coronary circulation using a Doppler catheter. Am J Cardiol. 1991;67:44D–56D.
28. Safian, RD. The Device Guide. 2nd ed. Royal Oak: Physicians' Press; 1999. p. 278.
29. Varho V, Karjalainen PP, Ylitalo A, Airaksinen JK, Mikkelsson J, Sia J, Pietilä M, Kiviniemi TO. Transthoracic echocardiography for non-invasive assessment of coronary vasodilator function after DES implantation. Eur Heart J Cardiovasc Imaging. 2014 Sep;15(9):1029–34.

# Coronary Flow Reserve

## Contents

# Measurement of Coronary Flow Reserve in the Catheterization Laboratory

*Tim P. van de Hoef and Jan J. Piek*





J. Escaned, J. Davies (eds.), *Physiological Assessment of Coronary Stenoses and the Microcirculation*,
DOI 10.1007/978-1-4471-5245-3_11

## 11.1 Introduction

The coronary flow reserve (CFR) [1] is a well-validated physiological index that allows the identification of blood flow impairment in the coronary territory under investigation [1, 2]. This index summarizes flow impairment originating from focal epicardial, diffuse epicardial, and microcirculatory disease and therefore allows one to identify the overall available vasodilator capacity in the vasculature under investigation. The principle of CFR has been extensively applied to both invasive and noninvasive diagnostic techniques, including intracoronary Doppler- and thermodilution-derived flow [3–7], transthoracic echocardiography, positron emission tomography, and magnetic resonance imaging. All of these investigations have documented CFR to be a robust risk stratification tool [8–11]. Nonetheless, several limitations, including its sensitivity toward hemodynamic conditions, practical ambiguities associated with its assessment, and ambiguities related to its interpretation, have been important limitations toward its application in clinical practice. However, besides the well-documented prognostic information that can be derived from CFR, novel insights into its combined interpretation with fractional flow reserve (FFR), the contemporary physiological standard for functional stenosis assessment, have led to a renewed interest in this physiological index [9, 12, 13]. As such, ongoing developments on a technical level, as well as the development of novel concepts based on CFR theory, underscore the relevance of CFR in daily clinical practice.

This chapter will discuss the invasive assessment of CFR in the catheterization laboratory, starting from the physical aspects of currently available armamentarium to measure coronary flow invasively, toward clinical data, its application in daily clinical practice, and future outlooks regarding novel CFR-based concepts.

## 11.2 Invasive Assessment of Coronary Flow in the Cardiac Catheterization Laboratory

The ad hoc calculation of coronary flow reserve in the catheterization laboratory requires the invasive assessment of coronary flow. For this purpose, three modalities are currently available that will be reviewed in detail below.

### 11.2.1 Doppler Flow Velocity

#### Physical Principles

First described by Christian Andreas Doppler in 1842, the Doppler effect has found distinct practical expression cardiovascular medicine within ultrasound-based assessment of blood flow velocity. The principle described by Doppler is the apparent change in the frequency or wavelength of a wave when there is relative motion between the source of the wave and an observer. The observed frequency is higher (compared to the actual emitted frequency) when the source of the wave is moving toward the observer, and it is lower when the source of the wave is moving away from the observer. This apparent change in the pitch (or frequency) of sound is called Doppler effect or Doppler shift (Fig. 11.1) and can be used to determine the velocity of an object.

The currently available intracoronary Doppler flow velocity system (ComboMap, Volcano Corp., San Diego, CA) utilizes a piezoelectric crystal at the tip of a 0.014″ guide wire (ComboWire or FloWire, Volcano Corp., San Diego, CA), which serves as both the transmitter and receiver of a pulsed ultrasound signal and has a relatively large sample volume about 5 mm distal to the tip (Fig. 11.2a, b). The signal is emitted by the crystal in short bursts and is "echoed" by blood cells within the sample volume, which are moving away from

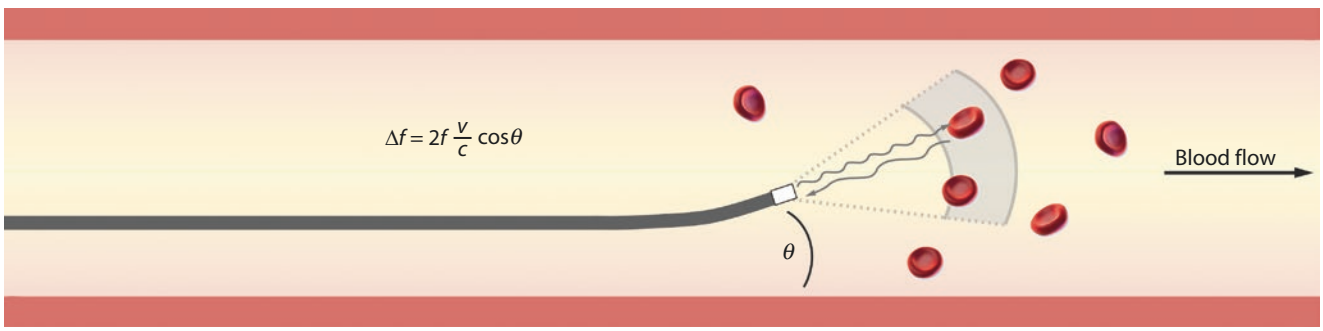


$f$ = transmitter frequency
$\Delta f$= frequency Doppler shift
$v$ = velocity of blood cells within sample volume
$c$ = speed of sound in blood
$\theta$ = angle between ultrasound beam and direction of blood flow

**Fig. 11.1** Intravascular velocity measurement by Doppler ultrasound. The ultrasound signal emitted by the Doppler crystal (*in white*) is reflected by red blood cells moving away from the transducer. The reflected sound waves, which have a lower frequency than the emitted waves, are received by the Doppler crystal. The console converts the received signal to velocity information expressed in cm/s

the transducer (Fig. 11.1). These echoes therefore return at the receiver at a lower frequency, and it is this Doppler shift that is detected by the instrumentation. When the Doppler beam is parallel to the bloodstream and given a constant transmitter frequency and a constant speed of sound in blood, this Doppler shift is directly proportional to the velocity of the blood cells within the sample volume (Fig. 11.1). When the Doppler beam is not parallel to the bloodstream, flow velocity may be underestimated. Nonetheless, such inaccuracy is limited to 6% when at a 20-degree angle, and it is therefore an accepted assumption that the ultrasound beam is relatively parallel to the main direction of the bloodstream.

The spectrum of frequencies received by the transmitter from the sample volume at any given moment represents a range of velocities at which the blood cells within the sample volume travel. The instrumentation then provides an overview of the frequency components of the Doppler signal converted to velocity, their relative intensity, and their variation in time. Flow velocity is extracted from these data by detecting the instantaneous peak velocity, which represents the maximum velocity within the sample volume (Fig. 11.2c). The average of instantaneous peak velocity over one or multiple heartbeats is termed average peak velocity and is the common parameter described in investigations using intracoronary Doppler flow velocity.

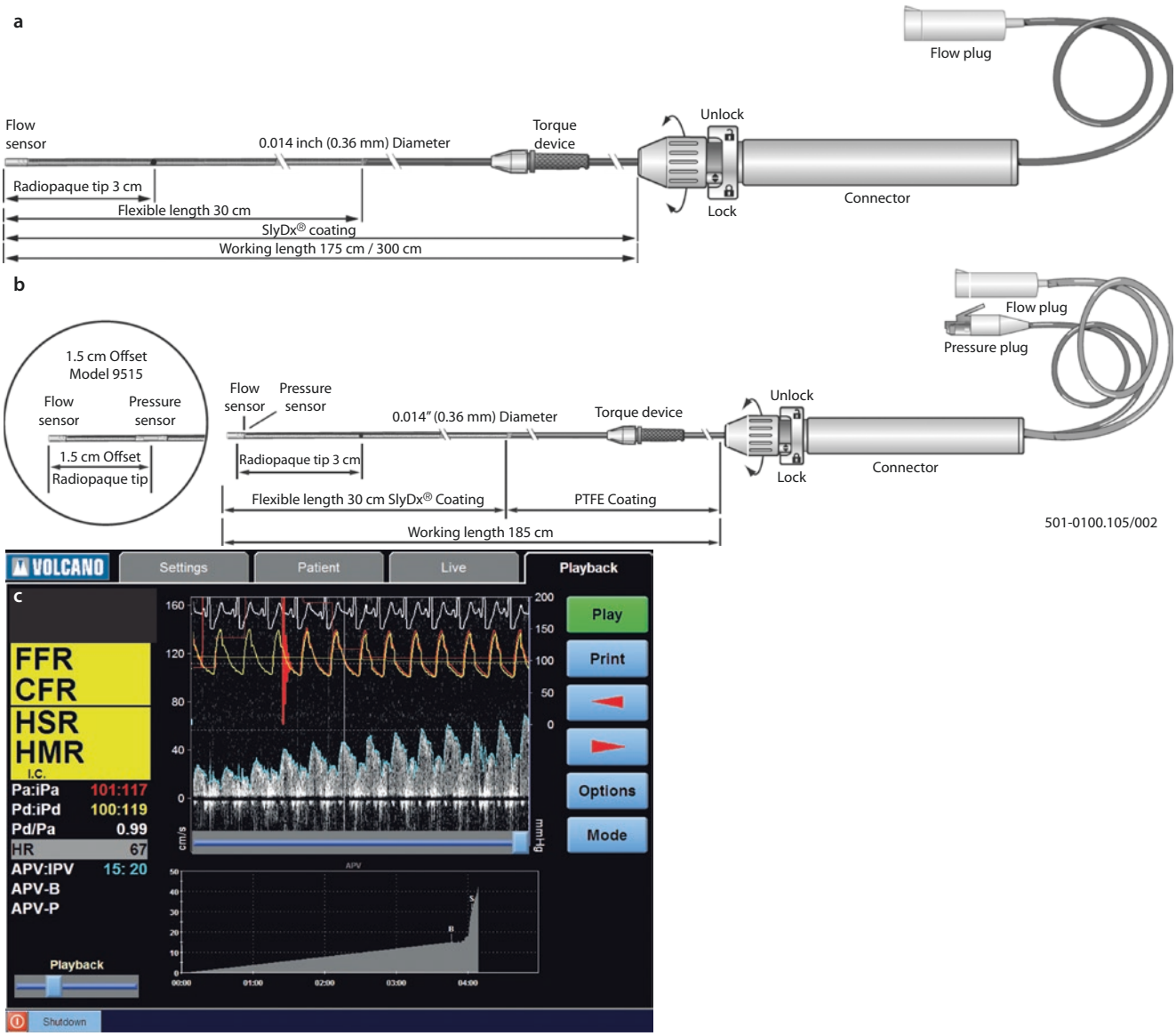


**Fig. 11.2** Doppler flow velocity instrumentation. **a** FloWire (Volcano-Philips). A 0.014″ guide wire with a Doppler crystal at the tip. **b** ComboWire (Volcano-Philips). A 0.014″ guide wire equipped with both a Doppler crystal at the tip and a pressure sensor either just distal or at 1.5 cm distal to the Doppler crystal. **c** ComboMap console display. Instrumentation displays temporal changes in coronary flow velocity (Doppler signal in *white*). The instantaneous peak velocity (the maximum velocity in the sample volume) is represented by the blue line on top of the Doppler signal. The console additionally displays ECG (*top white line*), aortic pressure (*red line*), and (in case of the ComboWire) distal coronary pressure (*yellow line*)

## Practical Aspects and Limitations

An advantage of Doppler flow velocity as a coronary flow parameter is that it is intrinsically normalized for the magnitude of perfused myocardial mass. This is due to the fact that nature normalizes coronary artery wall stress, which means that vessel diameter is directly related to the myocardial mass in its arterial distribution: the larger the perfused myocardial mass, the larger the supplying coronary artery [14, 15]. Where absolute flow (in mL/min) decreases with each branching of the coronary tree, the accommodating decrease in arterial diameter means that flow velocity is intrinsically corrected. This facilitates the interpretation of Doppler flow velocity values, since, despite its expression in cm/s, it is an accurate reflection of absolute flow per unit of perfused myocardial tissue.

As is illustrated by the description of the Doppler ultrasound technique above, the most important practical aspects of intracoronary Doppler flow velocity measurements are related to wire positioning to ensure optimal quality of the acquired signal and to ensure that these Doppler signals are representative of true blood flow velocity. Hence, operators are to be familiar with Doppler technology and should aim to manipulate wire position until a stable signal is obtained that is representative of the maximal cross-sectional velocity (Fig. 11.3). This aim is interfered by the natural tortuous vessel anatomy and cardiac motion, which can both degrade velocity signals. When inadequate signal quality is encountered despite wire position manipulation or when prolonged periods of stable velocity profiles are required, such as in extended research protocols, flipping of the wire tip can improve signal quality and ensures stable signals for prolonged recording times (Fig. 11.4). Nonetheless, the Doppler flow measurements remain technically difficult with the currently available measurement system, which leads to acquisition of Doppler signals of insufficient quality in up to 10–15 % of cases.



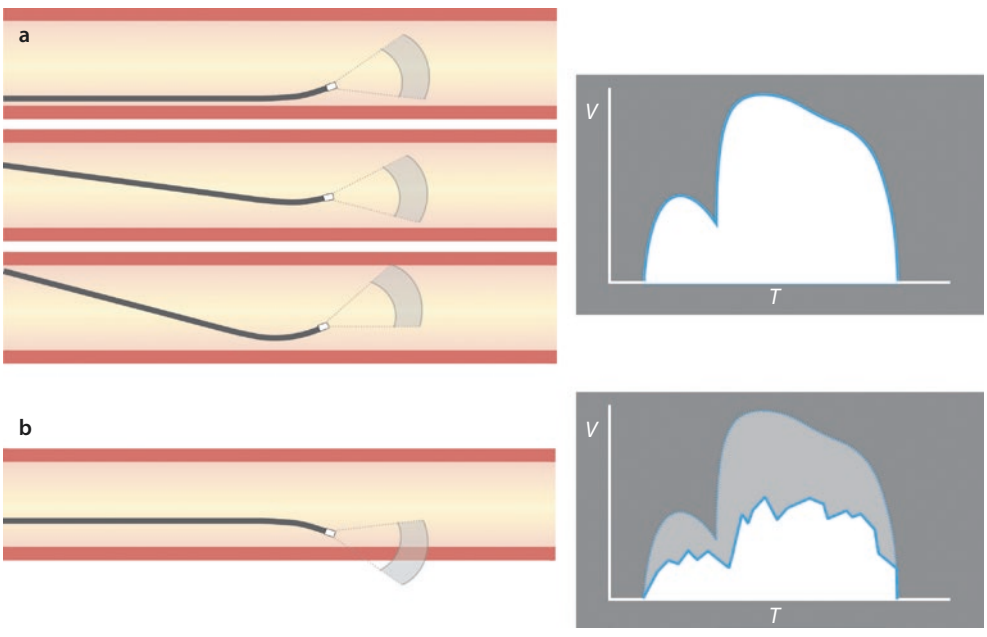


**Fig. 11.3** Wire positioning and Doppler flow velocity signal quality. Signal quality is determined by the location of the sample volume. Optimal signals are obtained when the sample volume is positioned midstream **a**. When the sample volume is directed toward the vessel wall, the Doppler signal is degraded **b**

### 11.2.2 Coronary Thermodilution-Derived Mean Transit Time

## Physical Principles

The indicator-dilution principle, first introduced by Stewart in 1897 for the measurement of cardiac output, has been validated for the invasive assessment of coronary flow as well. In short, the indicator-dilution theory dictates that injection of

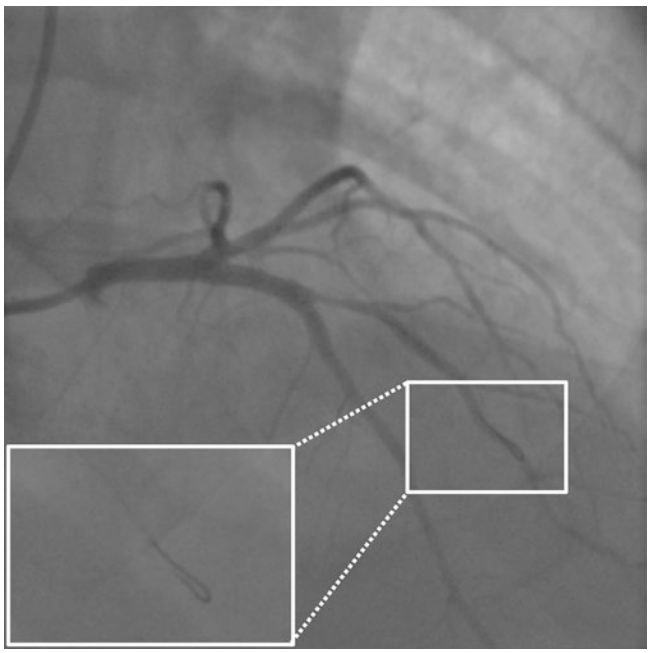

**Fig. 11.4** Flipping of the wire tip. When suboptimal signal quality is encountered despite wire manipulation, flipping of the wire tip may be performed. The Doppler signal is the obtained in a retrograde fashion, and such retrograde wire position frequently allows to obtain stable Doppler signals of higher quality (Adapted from van Lavieren et al. with permission [16])

a known amount of indicator into the bloodstream and measurement of the indicator concentration over time distal to the injection site allow quantification of coronary blood flow. This theory can be applied to the coronary circulation by exploiting the temperature sensitivity of sensor-equipped coronary guide wires [6, 7]. In this application, the shaft of the coronary guide wire serves as the proximal thermistor, allowing the identification of the start of the indicator injection. The temperature-sensitive sensor at the distal end of the guide wire then serves as the distal thermistor. While keeping the distance between the proximal and distal thermistor constant throughout the measurements, the volume of blood between the two remains equal. As such, the change in temperature over time can be registered and allows calculation of the mean transit time of the indicator from the proximal to the distal thermistor (Fig. 11.5a, b). Since greater magnitudes of coronary flow cause greater and more rapid dilution of the injected indicator, mean transit time of the

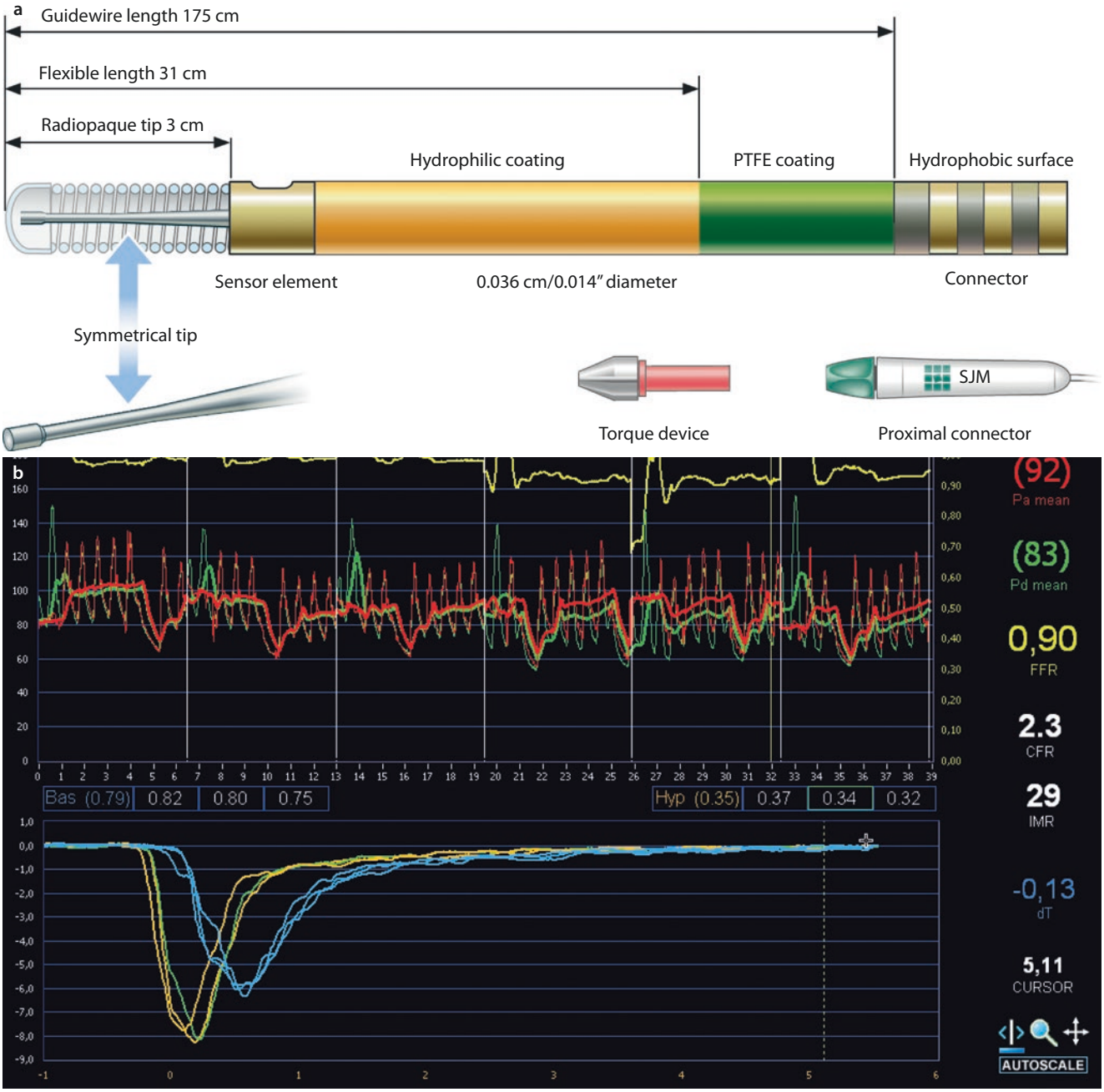


**Fig. 11.5** Coronary thermodilution instrumentation. **a** PressureWire (St Jude Medical). A 0.014″ guide wire equipped with a temperature-sensitive pressure sensor, which allows the assessment of both intracoronary pressure and coronary thermodilution curves. **b** RadiAnalyzer (St Jude Medical) console display. Instrumentation displays the thermodilution curves in performed in triplicate in resting (*blue curves*) and hyperemic (*yellow curves*) conditions. The mean transit time is calculated from these curves and is shown to decrease from resting to hyperemic conditions (Bas (0.79) to Hyp (0.35)). The console additionally displays the ECG (*top yellow line*), as well as aortic pressure (*red line*) and distal coronary pressure (*green line*) (Courtesy of Dr. J. Escaned, Hospital Clinico San Carlos, Madrid, Spain)

indicator will decrease with increasing blood flow. Since the amount of indicator injected is known and equal across measurements, mean transit time provides a measure of coronary blood flow defined as the inverse of mean transit time.

### Practical Aspects and Limitations

The contemporary application of coronary thermodilution in the catheterization laboratory requires the bolus injection of 3 cc of room-temperature saline as the indicator, which should be rapid and brisk. Since the timing of the injection during the cardiac cycle may influence the thermodilution curve, the latter is performed in triplicate, and the average mean transit time of these three injections is used for calculations. This is likely only clinically relevant when there is marked bradycardia, and it has been documented that ECG-controlled injection is generally not superior to manual injection of saline as the indicator [7].

Since saline boluses themselves cause significant transient reactive hyperemia [17], even in doses of 3 cc [18], it is important that sufficient time is allowed between repeated saline injections, especially during resting conditions. Otherwise, the repeated assessment of mean transit time is performed during a period of reactive hyperemia, which leads to overestimation of resting flow and therefore underestimation of CFR.



It is recommended that the distal thermistor, thus the guide wire sensor, be placed at least 6 cm distal from the injection site of the indicator, thus the catheter tip, to allow adequate mixing of blood and saline [7]. Neglecting this requisite leads to a larger variability in measurements and weaker correlation of the obtained mean transit time with absolute flow and therefore diminishes the accuracy of the measurements. This may not generally be a practical issue but should be considered while performing these measurements in clinical practice as coronary anatomy may not allow adherence to these guidelines and may therefore not allow accurate thermodilution flow measurements. Moreover, since the use of mean transit time as a surrogate for flow requires that the volume between the thermistors remains equal, catheter and wire position should remain the same throughout the measurements both during resting and hyperemic conditions for accurate flow measurements of flow and accurate calculation of CFR.

The measurement of coronary thermodilution-derived mean transit time during coronary hyperemia necessitates the induction of a hyperemic plateau long enough to perform the bolus injection and preferably long enough to perform these in triplicate. As such, thermodilution measurements cannot be performed with intracoronary adenosine administration, but requires the use of either intravenous adenosine administration, the administration of regadenoson, or the use of papaverine for the induction of a hyperemic plateau phase. In practice, the use of intravenously administered adenosine is customary for thermodilution measurements. The important consequences of this limitation will be discussed separately below.

Similar to Doppler flow velocity measurements, the assessment of adequate thermodilution curves is challenging, and sets of thermodilution curves of insufficient quality are also reported to occur in 10–15 % of cases, which mainly originate from cases where the distal thermistor cannot be placed distally enough to ensure a 6-cm distance between the two thermistors, leading to unacceptable variability in the repeated measurement of mean transit time to ensure accurate assessment of flow [6, 7].

## 11.2.3 Coronary Thermodilution-Derived Absolute Flow Measurement

The indicator-dilution theory also allows the assessment of absolute flow by coronary thermodilution, but this is much more complex and practically challenging. Nonetheless, using the same indicator-dilution theory, and the same 0.014-in. temperature-sensitive sensor-equipped coronary guide wire, the use of continuous infusion of room-temperature saline through a 2.8-F infusion catheter allows the measurement of absolute volumetric flow in mL/min directly in the catheterization laboratory [19, 20].

### Practical Aspects and Limitations

Besides the intrinsic limitations of absolute flow values for their interpretation and application in clinical practice [20], the requisite of continuous saline infusion for the assessment of absolute flow means that this technology does not allow to measure coronary flow reserve, since resting flow cannot be accurately assessed. Moreover, the setup and measurement process is much more complicated than for regular thermodilution or Doppler flow velocity measurements and therefore takes 10–15 min to complete [20]. Nonetheless, technical advancements may make absolute flow measurements less cumbersome in the catheterization laboratory and may lead to novel insights into their applicability and value in clinical practice.

## 11.3 Coronary Flow Reserve: Definition and Characteristics

### 11.3.1 Definition of Coronary Flow Reserve

The concept of coronary flow reserve relates to the ability of the coronary circulation to increase blood flow in response to alterations in oxygen demand. As such, coronary flow reserve is defined as the ratio of maximal flow during vasodilated conditions, termed hyperemic coronary flow, to flow during conditions of coronary autoregulation, termed resting or baseline coronary flow.

## 11.4 Coronary Flow Reserve: What's Normal and What's Not?

In healthy subjects, coronary flow is expected to increase more than 4.5-fold upon pharmacological induction of coronary hyperemia [21]. In contrast, in patients without

epicardial stenosis but known risk factor for cardiovascular disease, CFR was documented to amount to approximately 2.8 [3]. When assessed in vessels without epicardial coronary stenoses, CFR values below this threshold have consistently been associated with impaired clinical outcomes, including hard clinical end points such as myocardial infarction and death [10, 11, 22, 23]. CFR has additionally been investigated thoroughly in the setting of epicardial stenosis, where it is now generally accepted that a CFR of less than 2.0 should be considered a clinically relevant impairment of the vasodilator capacity of the coronary vasculature under investigation [24, 25]. In more detail, these data have documented a range of optimal cut points of invasively measured CFR for noninvasively assessed myocardial ischemia that lies from 1.7 to 2.1. In other words, a CFR below 1.7 should definitely be considered to reflect an impaired vasodilator capacity in the vasculature under investigation. A CFR in the range of 1.7–2.1 lies within the CFR range that is associated with myocardial ischemia and should also be considered clinically relevant, as it may clinically be associated with signs and symptoms of myocardial ischemia. A CFR between 2.1 and 2.8 lies above the CFR threshold that has been associated with myocardial ischemia and should be considered sufficient to prevent myocardial ischemia even though it is decreased compared with nonobstructed coronary arteries. Finally, as noted above, a CFR of 2.8 or higher can generally be considered normal for a patient population with risk factors for coronary artery disease.

These considerations borne in mind, the application of physiology techniques in both research and clinical practice is frequently dichotomous in nature. As such, the 2.0 CFR cutoff has become customary in the evaluation of adverse events in patients at risk for cardiovascular disease [26, 27]. This cutoff value is the most widely validated and allows robust risk stratification in patients at risk for cardiovascular events. Nonetheless, available data support that the spectrum of CFR values represents a risk continuum, where risk for adverse events becomes higher with decreasing CFR values: a risk stratification value that is likely not optimally reflected by a dichotomous interpretation.

### 11.4.1 Limitations of Coronary Flow Reserve

Despite the unequivocal prognostic information provided by CFR, several practical and intrinsic physiological limitations of this index need to be considered.

First and foremost, the assessment of coronary flow reserve requires the direct measurements of a surrogate of coronary flow in the catheterization laboratory, which is more challenging than, for example, pressure measurements. This is illustrated by the fact that flow data of insufficient quality for accurate calculations occurs in 10–15 % of cases for both Doppler- and thermodilution-derived flow, whereas insufficient data quality for pressure recordings occurs seldom. Obviously, operator experience with the specific armamentarium is crucial in this aspect, and, furthermore, technical advances are ongoing that may improve feasibility of flow measurements in the catheterization laboratory.

Second, CFR intrinsically provides insight into the overall impairment in coronary flow in the vasculature under investigation, regardless of its origin in the epicardial coronary artery, due to either focal stenosis or diffuse atherosclerosis, or in the microcirculation. Although such comprehensive assessment of flow impairment has distinct advantages and bears important prognostic information, CFR is intrinsically unable to differentiate between these domains to determine the dominant origin of blood flow impairment. Hence, solitary assessment of CFR does not allow identification of optimal treatment strategies in ischemic heart disease.

Third, CFR as an index of hyperemic to resting flow is sensitive toward alterations induced in either of these conditions [28]. Moreover, since flow during vasodilated conditions is determined by coronary perfusion pressure, changes in perfusion pressure also affect CFR. Figure 11.6 shows the effect of alterations in coronary hemodynamics on CFR on the basis of the pressure-flow relationships during resting and vasodilated conditions (e.g., during adenosine-induced coronary hyperemia). First, CFR is affected by changes in coronary perfusion pressure, which may occur secondary to the administration of vasodilators to induce hyperemia but may also occur in settings of elevated venous pressure (Fig. 11.6b). At lower perfusion pressure, autoregulated (rest) flow remains equivalent, while flow in vasodilated conditions may be significantly reduced due to the reduction in perfusion pressure, leading to a decrease in CFR. Second, CFR may be affected by alterations in resting flow. Elevated resting flows result in a decrease in CFR as shown in Fig. 11.6c and may occur in a variety of settings, which are shown in Table 11.1. Third, an increase in zero-flow pressure causes a rightward shift of the pressure-flow relationship and yields a decrease in CFR as shown in Fig. 11.6d. Such rightward shift may occur in various clinical settings, as shown in Table 11.3. Fourth, CFR may also decrease due to an increase in resistance to coronary flow in the vasodilated vessels. This increase in resistance leads to a decrease in coronary flow at maximal vasodilation as shown in Fig. 11.6e. Factors associated with a decrease in hyperemic coronary flow are noted in Table 11.3. Finally, the abovementioned factors may occur in combination, increasing the effect of both pathophysiological and physiological alterations in coronary hemodynamics on CFR. As can be derived from Tables 11.1–11.3, factors associated with a decrease in CFR represent both physiological and pathophysiological alterations in coronary hemodynamics. While it is the latter that likely drives the association of CFR with impaired clinical outcomes, one should be aware of the confounding effect of physiological adaptations on CFR to ensure its accurate interpretation.

These limitations accounted for, CFR has still been rigorously documented to provide robust prognostic information and risk stratification in a distinct number of populations and patient subsets, illustrating the clinical potential of this physiological index.

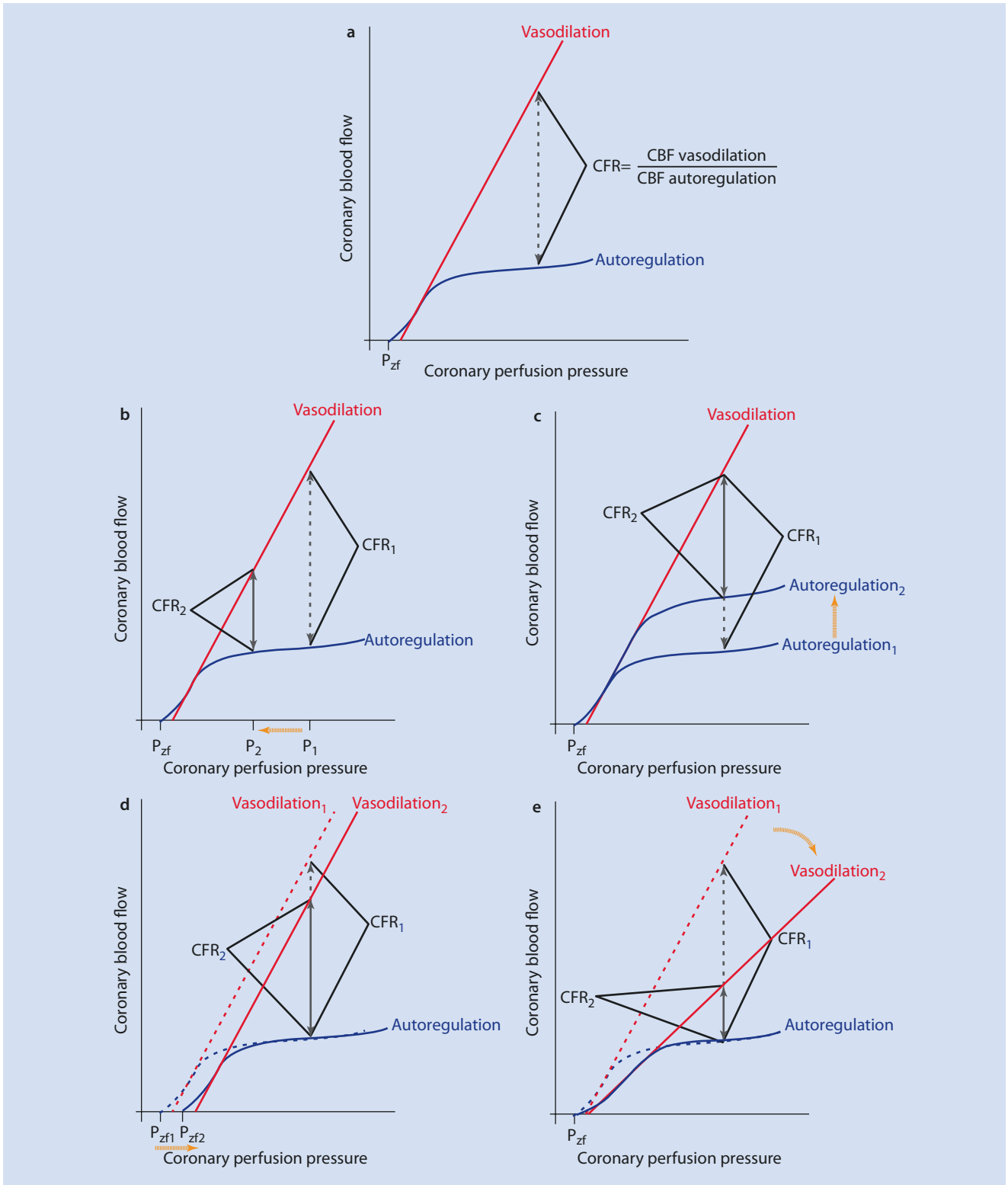


**Fig. 11.6** Coronary pressure-flow relations and coronary flow reserve. **a** Normal coronary circulation and definition of CFR. $P_{zf}$ indicates zero-flow pressure. **b** Effect of decreased perfusion pressure on CFR. Since maximal flow depends on perfusion pressure, CFR is sensitive toward changes in the latter. With a reduction in perfusion pressure, e.g., due to the intravenous administration of adenosine or regadenoson, CFR decreases from $CFR_1$ to $CFR_2$. **c** Effect of an increase in resting coronary flow on CFR. Since coronary autoregulation ensures resting flow accommodates myocardial demand, any increase in demand leads to increases in resting flow. Since CFR relates hyperemic to resting flow, increases in resting flow induce a decrease in CFR from $CFR_1$ to $CFR_2$. **d** Effect of elevated zero-flow pressure on CFR. An increase in zero-flow pressure results in a parallel rightward shift of the hyperemic pressure-flow relation from $vasodilation_1$ to $vasodilation_2$. As illustrated, this leads to a reduction in CFR from $CFR_1$ to $CFR_2$. **e** Effect of altered coronary resistance to flow on CFR. Alterations in coronary resistance to flow at vasodilation are characterized by a change in the slope of the hyperemic pressure-flow relation and are associated with a decrease in CFR as illustrated

**Table 11.1** Factors associated with an increase in autoregulated flow

| (Relative) increase in myocardial demand | Left shift of oxygen dissociation curve |
|---|---|
| Exercise[a] | Abnormal hemoglobins |
| Fever | Fetal hemoglobin |
| Increased inotropy[b] | Carboxyhemoglobin |
| Tachycardia[a,b] | Alkalosis |
| Thyrotoxicosis | |
| Ventricular hypertrophy[a,b] | |
| Hypoxemia | |
| Anemia | |

[a]May additionally increase zero-flow pressure
[b]May additionally reduced maximal flow

**Table 11.2** Factors associated with a rightward shift of zero-flow pressure

| |
|---|
| Increased left ventricular diastolic pressure[a] |
| Increased right ventricular diastolic pressure >10 mm Hg |
| Pericardial tamponade[a] |
| Increase in coronary sinus and venous pressure >10 mm Hg with normal right ventricular diastolic pressure |
| Beta-adrenergic blockade or alpha-adrenergic stimulation[a] |
| Left and right ventricular hypertrophy[a] |
| Tachycardia[a] |
| Several anesthetic agents |

[a]May additionally reduce maximal flow

**Table 11.3** Factors associated with a decrease in maximal flow

| *Small vessel disease* | *Abnormal cardiac function* |
|---|---|
| Hypertension | Ventricular hypertrophy[a,b] |
| Hypertrophic cardiomyopathy[a,b] | Tachycardia[a,b] |
| Diabetes mellitus | Decrease in aortic pressure |
| Cigarette smoking | Increased left ventricular diastolic pressure[a] |
| Aortic stenosis | Pericardial tamponade[a] |
| Systemic lupus erythematosus | Substantial increase in myocardial contractility[b] |
| *Large vessel disease* | *Increased blood viscosity* |
| Atherosclerosis | Polycythemia |
| Thrombosis | Macroglobulinemia |

[a]May additionally increase zero-flow pressure
[b]May also increase autoregulated flow

### 11.4.2 Induction of Coronary Hyperemia: Intracoronary Versus Systemic Vasodilation

For the assessment of CFR, flow values should be obtained during both resting and vasodilated conditions. Several agents are available for the induction of coronary hyperemia, such as adenosine, adenosine triphosphate (ATP), regadenoson, and papaverine, among which adenosine is the most commonly used agent in the catheterization laboratory. Whereas for Doppler flow velocity, measurements for either of these agents suffice; coronary thermodilution requires the administration of an agent that allows to create a hyperemic plateau during which the repeated bolus injections of saline can take place, such as intravenous administration of adenosine or ATP, regadenoson, or papaverine. It is important to realize that although intracoronary and intravenous adenosine administration, as well as the use of ATP, regadenoson, or papaverine, is generally considered interchangeable for the assessment of physiology techniques in clinical practice, this is not completely accurate for the assessment of maximal coronary flow at hyperemia. The administration of either of these agents is intended to induce coronary vasodilation and thereby to abolish coronary vasomotor tone. At coronary vasodilatation, coronary flow directly depends on the magnitude of the driving pressure. While intracoronary administration of adenosine does not alter systemic hemodynamics and therefore maintains equivalent driving pressure from resting to hyperemic conditions, intravenous infusion of adenosine/ATP or the use of regadenoson leads to significant decreases in aortic pressure at hyperemia of 10–15 % [29, 30]. Since maximal coronary flow at coronary hyperemia, and therefore CFR, depends on driving pressure, such a reduction in aortic pressure is associated with a proportional drop in maximal coronary flow (Fig. 11.6). Therefore, maximal flows and CFR assessed with the use of systemic vasodilation are prone to significant underestimation when these are determined using systemically administered vasodilators. It should therefore be considered to correct the obtained flow and CFR values for the accompanying drop in blood pressure by multiplying the CFR value with the ratio of resting to hyperemic mean aortic pressure, as was suggested previously [31].

## 11.5 Reintroduction of CFR in Clinical Practice: Combined Assessment of CFR and FFR

Although CFR is not routinely assessed in the clinical management of stable coronary artery disease, a setting where FFR is routinely applied to study the functional effect of a coronary stenosis [32], convincing data documents that the

impairment of coronary flow goes beyond the domain can be interrogated by fractional flow reserve [9, 12, 13]. As such, a strong body of evidence now supports the complementary nature of these two modalities, showing an important added diagnostic and prognostic value of CFR over FFR alone. Although FFR estimates whether a focal stenosis plays a dominant role in the impairment in myocardial perfusion [33–35], concomitant diffuse epicardial atherosclerosis or microvascular disease is not identified by this technique. The latter two conditions have been documented to be associated with a quantifiable risk for cardiovascular morbidity and mortality [8, 9] and thereby constitute an important area of interest both in clinical research and clinical practice settings. A wealth of data supports CFR as a tool to quantify the effect of both diffuse epicardial atherosclerosis and microvascular disease on myocardial perfusion, and CFR has been demonstrated to represent a robust risk stratification tool. Whether assessed invasively, as discussed in this chapter, or noninvasively, a normal CFR has repeatedly been associated with a low risk of cardiovascular events, with risk for such events increasing proportionally with decreasing CFR values. This ability of CFR to stratify risk for adverse cardiovascular events is independent of the presence of epicardial coronary artery disease and even of the presence or absence of stress-induced myocardial ischemia. Hence, CFR provides substantial incremental information over contemporary pressure-derived standards.

The combined assessment of FFR and CFR leads to challenges regarding the interpretation of the results, since disagreement occurs in over 30 % of cases (Fig. 11.7). When CFR and FFR agree, and they are both either in the normal range or in the abnormal range, interpretation of the results poses no difficulty. A stenosis yielding an abnormal FFR and normal CFR is by definition non-flow limiting, since flow can increase normally despite the atherosclerotic narrowing. Smalling et al. already documented that when coronary flow remains stable, coronary perfusion pressure may lower to FFR values below 0.5 without occurrence of myocardial ischemia [36]. Additionally, recent observational data suggests that the natural course of these non-flow-limiting stenoses is indeed associated with favorable clinical outcome [9]. Since non-flow-limiting stenoses are therefore likely not associated with myocardial ischemia and have a favorable clinical outcome, it is now debated whether these stenoses are optimally managed with percutaneous coronary intervention [37]. When FFR is normal and CFR is abnormal, two situations may (co)exist. First, this may represent the presence of dominant diffuse epicardial coronary artery disease, diminishing flow without inducing a significant pressure gradient due to the lack of flow acceleration and flow separation that dominates pressure gradients in focal disease [25, 38]. Second, this may be a representation of dominant microvascular disease, limiting the vasodilator reserve of the vasculature under investigation. Pure microvascular disease is more likely when the FFR value approaches 1.0, and these pathophysiological patterns may

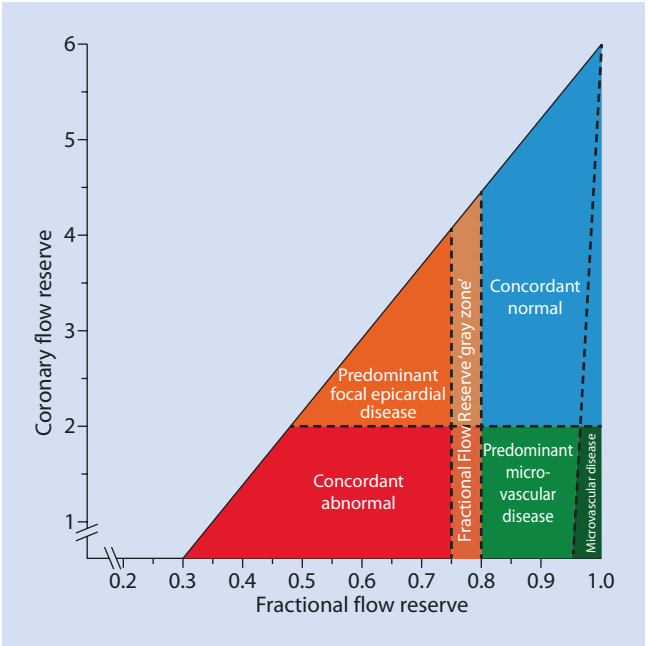


**Fig. 11.7** Conceptual plot of the fractional flow reserve (FFR)-coronary flow velocity reserve (CFR) relationship. Four main quadrants can be identified by applying the clinically applicable cutoff values for FFR and CFVR, indicated by the dotted lines. Patients in the upper right blue area are characterized by concordantly normal FFR and CFVR, and patients in the red lower left area are characterized by concordantly abnormal FFR and CFVR. Patients in the upper left orange area and lower right light green area are characterized by discordant results between FFR and CFVR, where the combination of an abnormal FFR and a normal CFVR indicates predominant focal epicardial but non-flow-limiting, coronary artery disease, and the combination of a normal FFR and an abnormal CFVR indicates predominant microvascular involvement in coronary artery disease. The small dark green region in the lower right is characterized by an FFR near 1 and an abnormal CFVR, indicating sole involvement of the coronary microvasculature. The FFR gray zone indicates the equivocal 0.75–0.80 FFR range (Reproduced from van de Hoef et al. [9])

coexist leading to the individual CFR-FFR pattern in a given patient. Importantly, this FFR-CFR pattern has been associated with a distinct risk for cardiovascular events [9, 39], and it was recently hypothesized that these patients may benefit from mechanical revascularization in specific situations [16].

## 11.6 Future Perspectives

CFR likely represents the most widely studied physiological index available, since its application is not restricted to invasive cardiology. Nonetheless, the limitations described above and lack of acknowledgement of its clinical potential have led to CFR being applied mainly as a research tool. Novel insights into the complexity of ischemic heart disease have now led to a renewed research and clinical interest, which is closely followed by technical partners that are improving flow assessment armamentarium. Hence, the clinical application of CFR

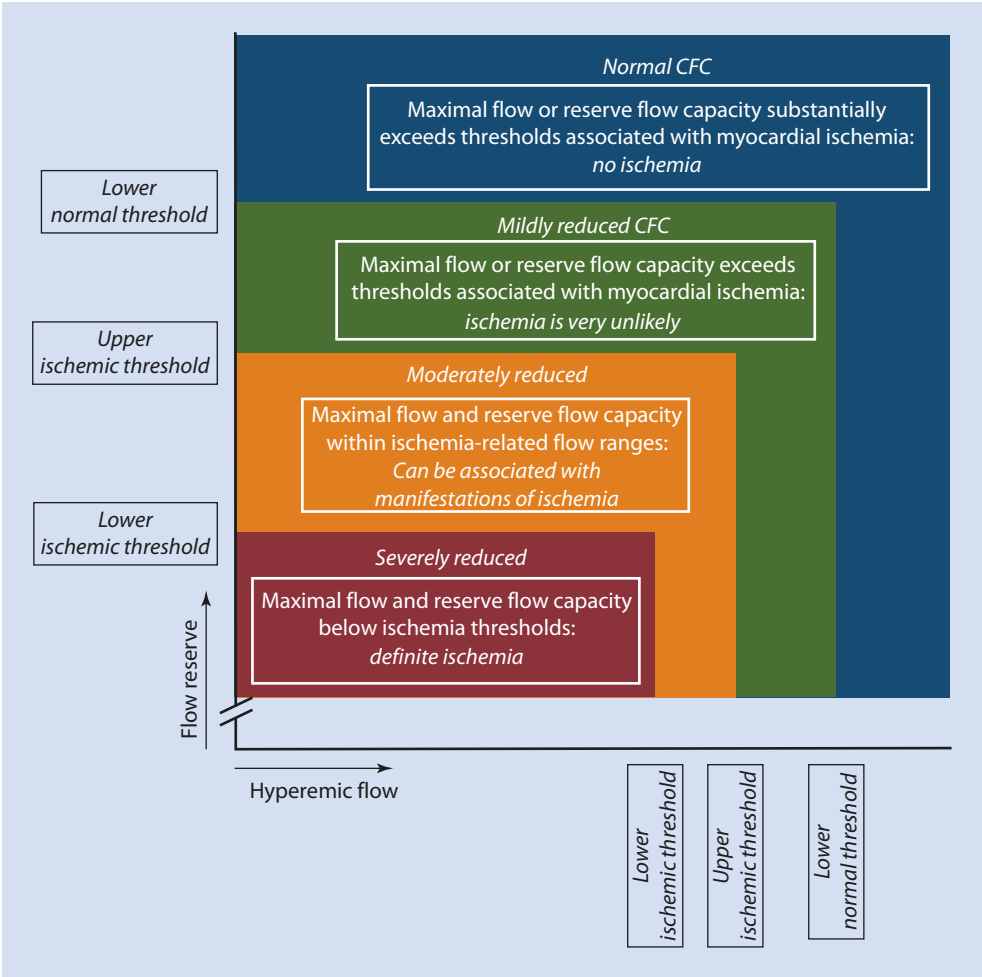


**Fig. 11.8** Coronary flow capacity concept. Since coronary flow reserve (CFR) equals hyperemic to baseline flow, a two-dimensional map of CFR versus hyperemic flow comprehensively describes the invasive flow characteristics of the coronary vasculature under investigation. Within this concept, four clinically meaningful categories are defined (coded with different colors in the graph) based on well-validated invasive CFR cutoff values and the corresponding hyperemic flow values (Reproduced from van de Hoef et al. [40])

is likely to become more important in the near future and will likely become more feasible as soon as industrial partners distribute updated measurement systems.

Moreover, concepts are now being developed that overcome part of the limitations associated with the use of CFR. One of these is the concept of coronary flow capacity, which incorporates CFR and maximal hyperemic flow in a comprehensive flow map of the coronary vasculature under investigation (Fig. 11.8) [40–42]. First applied to positron emission tomography, this coronary flow capacity concept was recently introduced based on invasive Doppler flow data and was documented to improve risk stratification characteristics of CFR. This is likely due to the fact that coronary flow capacity overcomes the limitations of CFR related to variations in the resting state.

Besides the improvement in the application of CFR and development of concepts that overcome its associated limitations, measurement systems nowadays allow to measure both pressure and flow simultaneously. Such techniques allow calculation and differentiation of the resistance to coronary blood flow induced by a stenosis or epicardial segment and the microcirculation [43, 44]. Ultimately, techniques that apply CFR or coronary flow capacity may therefore allow to evaluate whether clinically significant flow abnormalities occur in the vasculature under investigation, after which these novel technologies may be applied to identify the dominant source of flow impairment and to guide treatment strategies [37].

## 11.7 Conclusion

CFR is a well-validated physiological index that provides extensive diagnostic and prognostic information. Its assessment in the cardiac catheterization laboratory is associated with practical ambiguities that dominantly require operator experience with the specific armamentarium. For this purpose either intracoronary Doppler flow velocity or thermodilution can be used, both having their own practical and physiological advantages and limitations. Recent acknowledgement of the clinical pertinence of CFR will support reintroduction of CFR in the daily interventional cardiology, and the accompanying conceptual and technical advances may overcome many of the intrinsic and practical ambiguities associated with its assessment in the catheterization laboratory.

## References


1. Gould KL, Lipscomb K. Effects of coronary stenoses on coronary flow reserve and resistance. Am J Cardiol. 1974;34:48–55.
2. Gould KL, Kirkeeide RL, Buchi M. Coronary flow reserve as a physiologic measure of stenosis severity. J Am Coll Cardiol. 1990;15:459–74.
3. Kern MJ, Bach RG, Mechem CJ, et al. Variations in normal coronary vasodilatory reserve stratified by artery, gender, heart transplantation and coronary artery disease. J Am Coll Cardiol. 1996;28:1154–60.
4. Piek JJ, Boersma E, Di Mario C, et al. Angiographical and Doppler flow-derived parameters for assessment of coronary lesion severity and its relation to the results of exercise electrocardiography. Eur Heart J. 2000;21:466–74.
5. Doucette JW, Corl PD, Payne HM, et al. Validation of a Doppler guide wire for intravascular measurement of coronary artery flow velocity. Circulation. 1992;85:1899–911.
6. Pijls NHJ, De Bruyne B, Smith L, et al. Coronary thermodilution to assess flow reserve Validation in humans. Circulation. 2002;105:2482–6.
7. De Bruyne B, Pijls NHJ, Smith L, Wievegg M, Heyndrickx GR. Coronary thermodilution to assess flow reserve: experimental validation. Circulation. 2001;104:2003–6.
8. Murthy VL, Naya M, Foster CR, et al. Improved cardiac risk assessment with noninvasive measures of coronary flow reserve. Circulation. 2011;124:2215–24.
9. van de Hoef TP, van Lavieren MA, Damman P, et al. Physiological basis and long-term clinical outcome of discordance between fractional flow reserve and coronary flow velocity reserve in coronary stenoses of intermediate severity. Circ Cardiovasc Interv. 2014;7:301–11.
10. van de Hoef TP, Bax M, Meuwissen M, et al. Impact of coronary microvascular function on long-term cardiac mortality in patients with acute ST-segment-elevation myocardial infarction. Circ Cardiovasc Interv. 2013;6:207–15.
11. van de Hoef TP, Bax M, Damman P, et al. Impaired coronary autoregulation is associated with long-term fatal events in patients with stable coronary artery disease. Circ Cardiovasc Interv. 2013;6:329–35.
12. Johnson NP, Kirkeeide RL, Gould KL. Is discordance of coronary flow reserve and fractional flow reserve due to methodology or clinically relevant coronary pathophysiology? J Am Coll Cardiol Img. 2012;5:193–202.
13. Echavarria-Pinto M, Escaned J, Macias E, et al. Disturbed coronary hemodynamics in vessels with intermediate stenoses evaluated with fractional flow reserve: a combined analysis of epicardial and microcirculatory involvement in ischemic heart disease. Circulation. 2013;128:2557–66.
14. Seiler C, Kirkeeide RL, Gould KL. Measurement from arteriograms of regional myocardial bed size distal to any point in the coronary vascular tree for assessing anatomic area at risk. J Am Coll Cardiol. 1993;21:783–97.
15. Seiler C, Kirkeeide RL, Gould KL. Basic structure-function relations of the epicardial coronary vascular tree. Basis of quantitative coronary arteriography for diffuse coronary artery disease. Circulation. 1992;85:1987–2003.
16. van Lavieren MA, van de Hoef TP, Sjauw KD, et al. How should I treat a patient with refractory angina and a single stenosis with normal FFR but abnormal CFR? EuroIntervention. 2015;11:125–8.
17. Adjedj J, Toth GG, Johnson NP, et al. Intracoronary adenosine: dose–response relationship with hyperemia. J Am Coll Cardiol Intv. 2015;8:1422–30.
18. Emanuelsson H, Holmberg S, Selin K, Wallin J. Factors that modify the flow response to intracoronary injections. Circulation. 1985;72:287–91.
19. van't Veer M, Geven MC, Rutten MC, et al. Continuous infusion thermodilution for assessment of coronary flow: theoretical background and in vitro validation. Med Eng Phys. 2009;31:688–94.
20. Aarnoudse W, Van't Veer M, Pijls NH, et al. Direct volumetric blood flow measurement in coronary arteries by thermodilution. J Am Coll Cardiol. 2007;50:2294–304.
21. Wilson RF, Wyche K, Christensen BV, Zimmer S, Laxson DD. Effects of adenosine on human coronary arterial circulation. Circulation. 1990;82:1595–606.
22. Pepine CJ, Anderson RD, Sharaf BL, et al. Coronary microvascular reactivity to adenosine predicts adverse outcome in women evaluated for suspected ischemia results from the National Heart, Lung and Blood Institute WISE (Women's Ischemia Syndrome Evaluation) study. J Am Coll Cardiol. 2010;55:2825–32.
23. Britten MB, Zeiher AM, Schachinger V. Microvascular dysfunction in angiographically normal or mildly diseased coronary arteries predicts adverse cardiovascular long-term outcome. Coron Artery Dis. 2004;15:259–64.
24. Meuwissen M, Siebes M, Chamuleau SAJ, et al. Role of fractional and coronary flow reserve in clinical decision making in intermediate coronary lesions. Interv Cardiol. 2009;1:237–55.
25. van de Hoef TP, Meuwissen M, Escaned J, et al. Fractional flow reserve as a surrogate for inducible myocardial ischaemia. Nat Rev Cardiol. 2013;10:439–52.
26. Murthy VL, Naya M, Taqueti VR, et al. Effects of sex on coronary microvascular dysfunction and cardiac outcomes. Circulation. 2014;129:2518–27.
27. Murthy VL, Naya M, Foster CR, et al. Association between coronary vascular dysfunction and cardiac mortality in patients with and without diabetes mellitus. Circulation. 2012;126:1858–68.
28. Hoffman JI. Problems of coronary flow reserve. Ann Biomed Eng. 2000;28:884–96.
29. De Bruyne B, Pijls NH, Barbato E, et al. Intracoronary and intravenous adenosine 5'-triphosphate, adenosine, papaverine, and contrast medium to assess fractional flow reserve in humans. Circulation. 2003;107:1877–83.
30. Arumugham P, Figueredo VM, Patel PB, Morris DL. Comparison of intravenous adenosine and intravenous regadenoson for the measurement of pressure-derived coronary fractional flow reserve. EuroIntervention. 2013;8:1166–71.
31. Pijls NH, Aengevaeren WR, Uijen GJ, et al. Concept of maximal flow ratio for immediate evaluation of percutaneous transluminal coronary angioplasty result by videodensitometry. Circulation. 1991;83:854–65.
32. Windecker S, Kolh P, Alfonso F, et al. 2014 ESC/EACTS guidelines on myocardial revascularization. EuroIntervention. 2015;10:1024–94.
33. Tonino PA, De Bruyne B, Pijls NH, et al. Fractional flow reserve versus angiography for guiding percutaneous coronary intervention. N Engl J Med. 2009;360:213–24.
34. De Bruyne B, Pijls NH, Kalesan B, et al. Fractional flow reserve-guided PCI versus medical therapy in stable coronary disease. N Engl J Med. 2012;367:991–1001.
35. De Bruyne B, Fearon WF, Pijls NH, et al. Fractional flow reserve-guided PCI for stable coronary artery disease. N Engl J Med. 2014;371:1208–17.
36. Smalling RW, Kelley K, Kirkeeide RL, Fisher DJ. Regional myocardial function is not affected by severe coronary depressurization provided coronary blood flow is maintained. J Am Coll Cardiol. 1985;5:948–55.
37. van de Hoef TP, Siebes M, Spaan JA, Piek JJ. Fundamentals in clinical coronary physiology: why coronary flow is more important than coronary pressure. Eur Heart J. 2015;36:3312–9a.
38. van de Hoef TP, Nolte F, Rolandi MC, et al. Coronary pressure-flow relations as basis for the understanding of coronary physiology. J Mol Cell Cardiol. 2012;52:786–93.

39. Lee JM, Jung JH, Hwang D, et al. Coronary flow reserve and microcirculatory resistance in patients with intermediate coronary stenosis. J Am Coll Cardiol. 2016;67:1158–69.
40. van de Hoef TP, Echavarria-Pinto M, van Lavieren MA, et al. Diagnostic and prognostic implications of coronary flow capacity: a comprehensive cross-modality physiological concept in ischemic heart disease. JACC Cardiovasc Interv. 2015;8:1670–80.
41. Gould KL, Johnson NP, Bateman TM, et al. Anatomic versus physiologic assessment of coronary artery disease. Role of coronary flow reserve, fractional flow reserve, and positron emission tomography imaging in revascularization decision-making. J Am Coll Cardiol. 2013;62:1639–53.
42. Johnson NP, Gould KL. Integrating noninvasive absolute flow, coronary flow reserve, and ischemic thresholds into a comprehensive map of physiological severity. J Am Coll Cardiol Img. 2012;5:430–40.
43. Meuwissen M, Siebes M, Chamuleau SAJ, et al. Hyperemic stenosis resistance index for evaluation of functional coronary lesion severity. Circulation. 2002;106:441–6.
44. Meuwissen M, Chamuleau SA, Siebes M, et al. Role of variability in microvascular resistance on fractional flow reserve and coronary blood flow velocity reserve in intermediate coronary lesions. Circulation. 2001;103:184–7.

# Indices of Coronary Resistance

## Contents

# Stenosis Resistance Estimated from Pressure-Flow Relationships

*Guus A. de Waard, Nicolaas Westerhof, Koen M. Marques and Niels van Royen*




J. Escaned, J. Davies (eds.), *Physiological Assessment of Coronary Stenoses and the Microcirculation*,
DOI 10.1007/978-1-4471-5245-3_12

## 12.1 Introduction

The hemodynamic consequences of a coronary artery stenosis can be estimated either by assessment of coronary pressure, flow velocity, or their combination. In daily clinical practice, the fractional flow reserve (FFR) is used which is measured using a coronary guidewire equipped with a distal pressure sensor. FFR expresses the ratio of the maximal flow in a conduit vessel in the presence of a stenosis compared to the maximal flow in the hypothetical absence of the stenosis. It has been proven that FFR is equal to the ratio of distal coronary artery pressure and aortic pressure under hyperemia [1]. Given a solid underlying theoretical framework, extensive clinical validation, ease of measurement, and the fact there is a sharp cutoff value, FFR is currently the guideline recommended tool to guide revascularization for intermediate stenoses in patients with stable coronary artery disease [2–5]. However, in patients with impairment of coronary microvascular function or an exceptionally large autoregulatory reserve, the sharp cutoff value used for FFR may be inappropriate [6, 7]. These patients cannot be identified, however, without a more comprehensive physiological assessment of the coronary circulation, which can be obtained, by combined coronary blood flow or flow velocity and pressure measurements. Unfortunately, in clinical practice patients with an abnormal microvascular function where the rigid FFR cutoff value of 0.80 may not appropriately guide revascularization are not identified because coronary flow measurement is not part of standard clinical work-up. The coronary flow reserve (CFR) is defined as the ratio of hyperemic and resting coronary blood flow; it is dependent on both the severity of the epicardial stenosis as well as the microcirculatory function. When FFR and CFR both are below their respective cutoff points of 0.80 and 2.0, revascularization is clearly indicated. Similarly, when both FFR and CFR are negative, revascularization should be deferred. However, in approximately 25–40 % of patients, discordant FFR and CFR values are found (Fig. 12.1) [8, 9]. The discordant FFR and CFR result in these cases often originates from either abnormal microcirculatory function or a very large autoregulatory reserve. In these discordant cases, it is unclear whether revascularization should be performed or patients should have optimal medical treatment. Furthermore, it must be kept in mind that CFR is influenced by hemodynamic conditions and inotropic state, which further complicates the interpretation of discordant CFR and FFR results [10].

In an attempt to assess coronary stenoses severity independent on microcirculatory function, indices have been developed based on the combined information of both Doppler flow velocity together with proximal and distal coronary pressure. The resistance of the entire coronary perfusion territory is the sum of the epicardial and microcirculatory resistance. The resistance of the total coronary perfusion territory is the ratio of the mean aortic pressure and the mean Doppler flow velocity (Fig. 12.2). The coronary microcirculatory resistance is the ratio of coronary artery pressure distal to the stenosis and mean flow velocity. Finally, the epicardial stenosis resistance can be calculated as the ratio between the pressure gradient across the stenosis and the mean flow velocity.

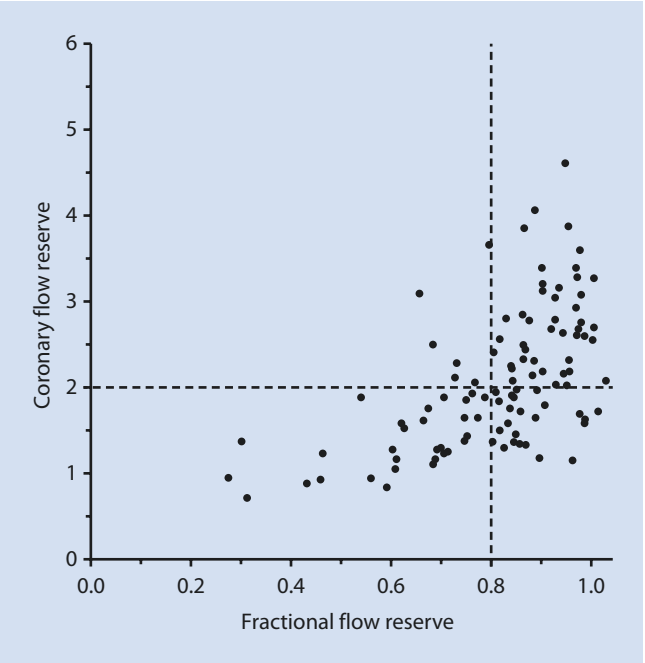


**Fig. 12.1** FFR and CFR are concordant in 60–75 % of cases, but a FFR and CFR discordance has been reported in 25–40 % of stenoses. From invasive combined pressure and Doppler flow velocity measurements in 106 stenoses, we established the FFR and CFR discordance to be in 29 % in this population. Data indicates that both a reduced CFR and FFR are associated with a poorer prognosis, as such it is difficult to determine the appropriate revascularization approach in discordant cases

In this chapter, we review the rationale and currently compiled scientific knowledge of stenosis resistance as a method to guide coronary intervention. Furthermore, we address the diastolic pressure gradient at a flow velocity of 50 cm/s ($dp_{v50}$), as different way to assess epicardial stenosis severity.

## 12.2 Pressure Loss Across a Stenosis

In 1974, Gould et al. postulated based on experimental data, a curvilinear relationship to determine the pressure gradient across a stenosis ($\Delta P$). This curvilinear relationship was described by the formula, $\Delta P = Av + Bv^2$, where $v$ is the (steady) flow velocity distal to the stenosis and terms $A$ and $B$ are a function of stenosis geometry and the rheological properties of blood [11, 12]. This formula takes into account the equations of Bernoulli and Hagen-Poiseuille, which are physical laws to describe fluid dynamics. Across the throat of the stenosis, there is frictional resistance to flow that contributes to the pressure loss and is described by the law of Hagen-Poiseuille. These frictional pressure losses are linearly related to flow and are described by term $A$ of the formula. Pressure

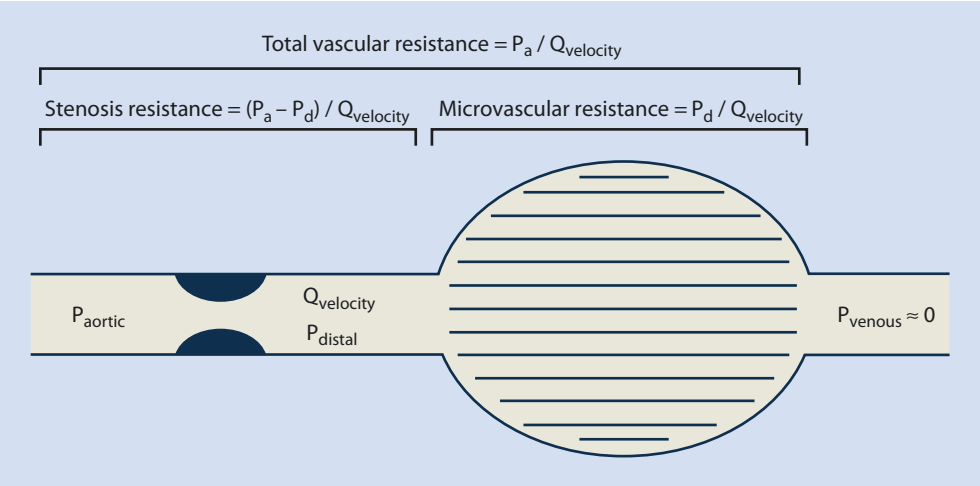


**Fig. 12.2** Schematic representation of a coronary artery with a stenosis and the microvascular bed. The total vascular resistance can be subdivided into the stenosis resistance over the epicardial coronary artery and the microvascular resistance specifically. The venous back pressure, left ventricular end-diastolic pressure, and collateral pressure are normally not assessed in clinical practice and typically neglected in the resistance equations. $P_a$ aortic pressure, $P_d$ distal coronary pressure, $P_{venous}$ venous pressure, $Q_{velocity}$ flow velocity

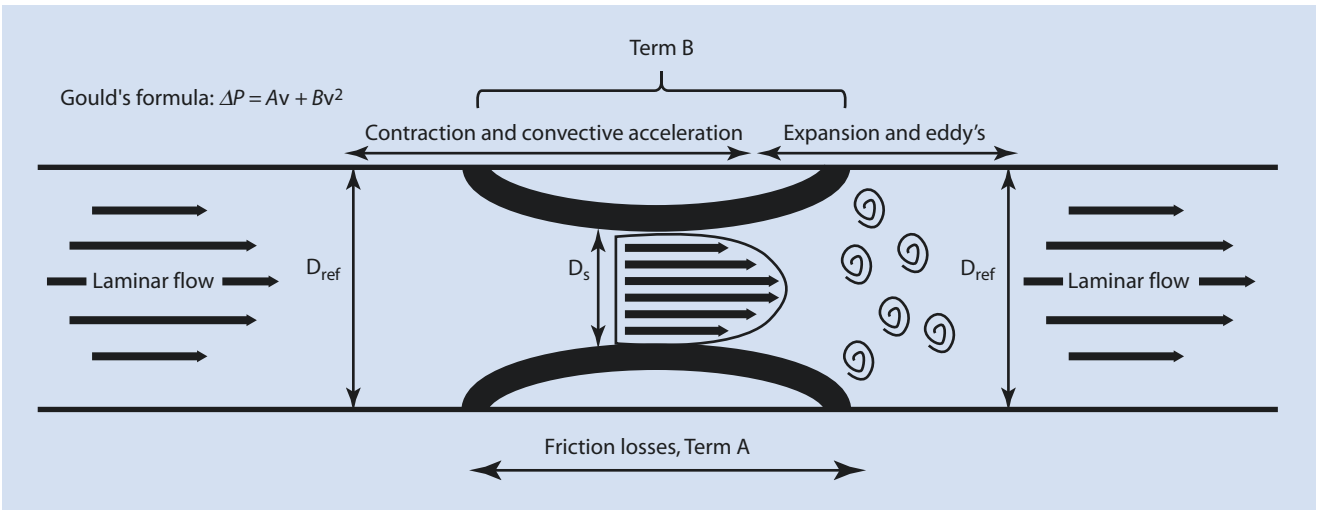


**Fig. 12.3** The total transstenotic pressure gradient ($\Delta P$) is calculated by $\Delta P = Av + Bv^2$. At the entrance and along the throat of the stenosis, pressure is lost by frictional resistance and determined by the law of Hagen-Poiseuille, which is translated into term *A*. Contraction, with subsequent convective acceleration of flow along the throat of the stenosis, causes pressure loss (law of Bernoulli). These losses are not recovered at the exit of the stenosis, due to flow separation and eddy formation, as described by term *B*. $A_s$ area of the stenosis, $A_{ref}$ area of the normal, reference segment

contraction with subsequent convective acceleration (according to the law of Bernoulli) causes pressure loss at the entrance of the stenosis. Due to eddy formation and flow separation, these pressure losses are not recovered at the exit of the stenosis. These pressure losses are included into Gould's formula as term *B* and increase with the square of flow velocity. Terms *A* and *B* are a function of stenosis geometry and the rheological properties of blood. As can be inferred from Gould's formula, however, the pressure gradient across the stenosis depends not only on coefficients *A* and *B* but also on the flow velocity. Because the flow velocity depends on aortic driving pressure, epicardial stenosis resistance, and microcirculatory resistance, these factors exert influence on the pressure gradient across the stenosis. Figure 12.3 clarifies the components that determine the pressure loss across a stenosis, while Fig. 12.4 represents the unique flow velocity and pressure gradient relationship for a stenosis as described by Gould's formula.

## 12.3 Advantages of Combining Coronary Pressure and Flow Velocity into Stenosis Resistance

The maximal, hyperemic flow rate depends on both the stenosis severity and on the microvascular resistance. Given a healthy microvasculature, with a large capacity to vasodilate as often is the case in trained athletes, flow can increase four- to fivefold in response to a hyperemic, vasodilating stimulus such as exogenous adenosine or exercise. According to Gould's formula, the pressure gradient across the stenosis increases along with the increase in flow when hyperemia is

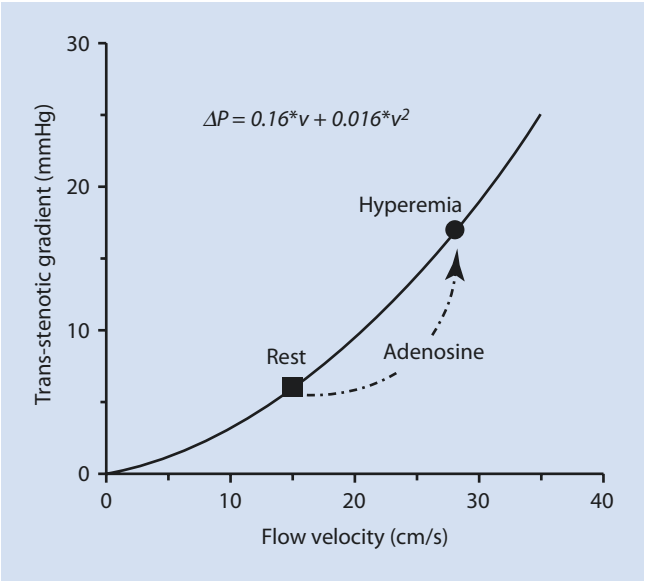


**Fig. 12.4** Each stenosis has a unique hemodynamic footprint that is derived primarily from stenosis geometry (although the rheological properties of blood also play a role). The curvilinear relationship between $\Delta P$ and flow velocity is depicted here under resting and hyperemic conditions. Through curve fitting, terms $A$ and $B$ of Gould's formula were calculated for the stenosis

established. For this reason, the pressure gradient across the stenosis is thus directly dependent on the functional status of the microvascular bed. Since this phenomenon also applies when microcirculatory function is impaired, this has important limitations for pressure-only assessment of functional stenosis significance by FFR. In case of a trivial stenosis but a healthy, preserved, microvascular function, flow increases dramatically when hyperemia is induced resulting in an exacerbated pressure gradient. Since flow rate is high, the large pressure gradient could lead to a positive FFR result, which is unlikely to be an expression of true myocardial ischemia [13]. Conversely, in the presence of impaired microvascular function with a small capacity to dilate, the increase in volumetric flow rate is limited in response to the hyperemic stimulus, and only a small pressure gradient will be produced. In this case, FFR remains relatively high, while myocardial perfusion can in fact be compromised [7]. Nevertheless, the theoretical framework of FFR is in fact not flawed, but the discrepancy between the FFR result and the presence of inducible myocardial ischemia arises from the use of a rigid cutoff value to indicate revascularization. As such, the FFR cutoff value of 0.75 may truly be the threshold for ischemia in some patients, but could very well be lower or higher for other patients depending on the functional status of their microcirculation. The theoretical framework of FFR describes that it is linearly related to the relative flow reserve, which is defined as the ratio between hyperemic myocardial flow in an obstructed and unobstructed territory [14]. The relative flow reserve assumes that microvascular function is similar across the entire myocardium, and it thus describes the flow impairment owing to a stenosis in relation to the theoretical absence of the stenosis independent of the microvascular status. For a patient with a very healthy microcirculatory function, an FFR of 0.75 may not indicate ischemia, while for a patient with an impaired microcirculatory function, the same FFR value can be indicative of deep myocardial ischemia. Nevertheless, the theoretical framework of FFR is not necessarily violated, since, in both patients, a 25 % reduction of myocardial blood flow exists in the presence of the stenosis in comparison to had that stenosis not been present.

Combined assessment of mean values for Doppler flow velocity, aortic driving pressure, and distal coronary artery pressure allows the calculation of stenosis resistance. The hyperemic stenosis resistance index (HSR) is defined as the ratio of hyperemic stenosis pressure gradient (mean aorta pressure-mean distal pressure) and hyperemic average peak-flow velocity (Fig. 12.2). In the absence of a stenosis, the pressure gradient across the stenosis is small or negligible, and consequently, the reference value of HSR is close to zero (HSR = 0 mmHg/cm per second). With increasing stenosis severity, the hyperemic pressure gradient increases, while hyperemic flow velocity simultaneously declines and HSR will rise accordingly. As mentioned above, not only the stenosis but also the microcirculation exerts effects on coronary flow, and by taking into account flow velocity, HSR thus corrects for the functional status of the microcirculation and is much more stenosis specific than FFR.

With these theoretical considerations in mind, HSR would provide a better representation of the functional consequences of an epicardial coronary artery stenosis than either CFR or FFR alone. Furthermore, because HSR may provide better guidance of revascularization in patients with a discordant CFR and FFR result [12]. An example of how the HSR can help to distinguish two stenoses with similar FFR, but a normal and abnormal perfusion, respectively, is shown in Fig. 12.5.

The above descriptions of the hypothetical positive aspects of HSR have primarily focused on the presumed advantages over pressure-only measures such as FFR. Flow-only-based parameters such as CFR and the hyperemic myocardial blood flow could also be used and provide an indication of ischemia at the myocardial level. However, these indices are unable to discern between the individual contributions of the epicardial coronary and the microvascular compartments (Fig. 12.2). As such, it can be difficult to assess the impact of stenosis revascularization on the reduction of myocardial ischemia based on CFR alone. In contrast, HSR reflects solely the epicardial coronary segment and distinguishes clearly between the epicardial coronary artery and the downstream microvasculature. Based on these considerations, HSR appears to be a very robust physiological invasive index at present for guidance of revascularization. However, as will be described in the section below, obtaining stenosis resistance has some notable disadvantages and comes with its own set of difficulties as well.

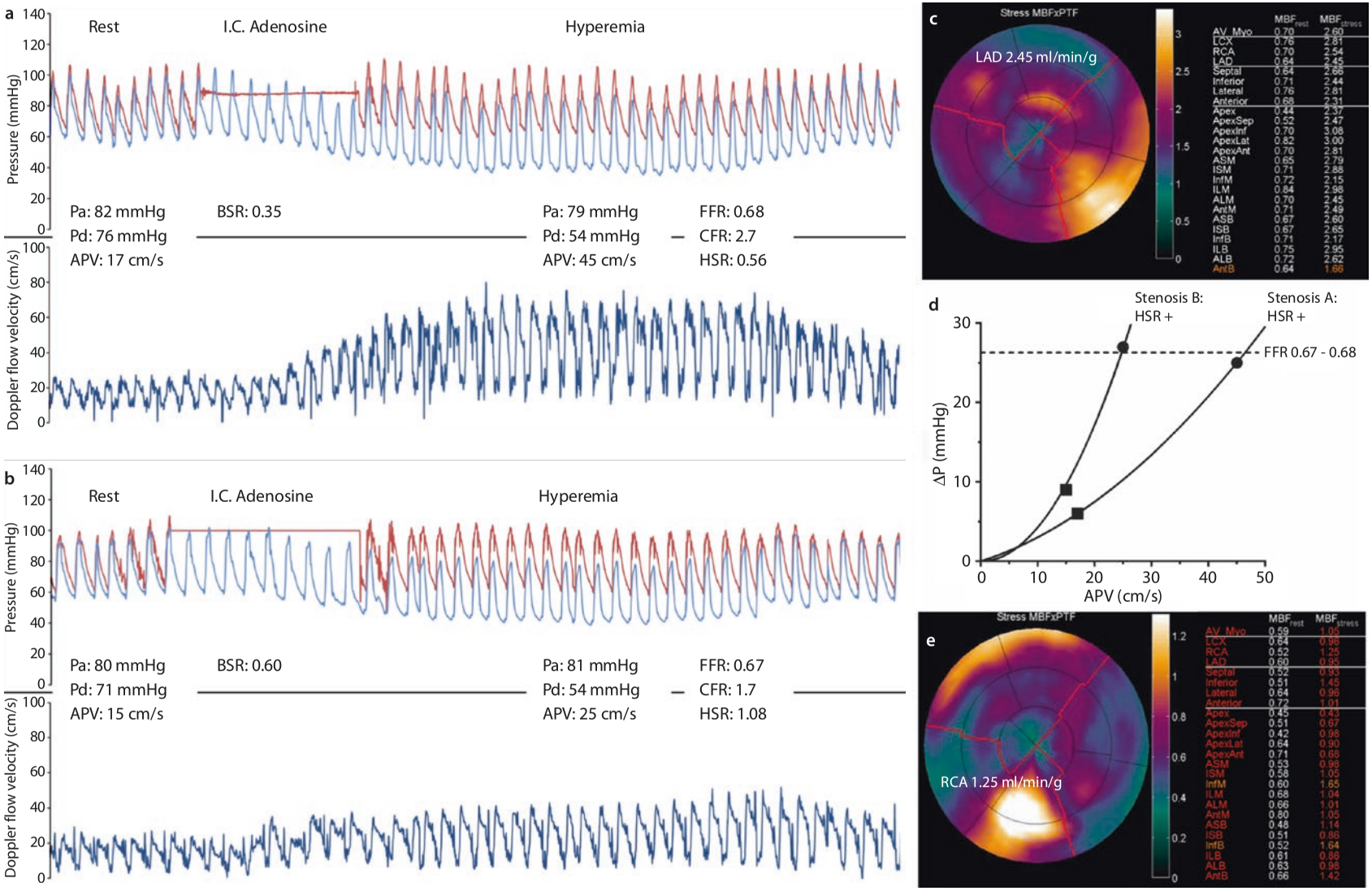


**Fig. 12.5** Simultaneous Doppler flow velocity and pressure traces are depicted for two different stenoses under resting and hyperemic conditions in panel (**a** and **b**). Both stenoses have a similar FFR value. However *stenosis A* has a normal LAD perfusion of 2.45 ml/g/min in the subtending myocardium (panel **c**) as indicated by $H_2{}^{15}O$ PET perfusion imaging (reference value 2.3 ml/min/g or more), while the RCA perfusion is impaired for stenosis B (panel **e**, 1.25 ml/min/g). A high-flow velocity mediates the low FFR value in stenosis A across the stenosis, which results in a large pressure gradient. Because HSR corrects the pressure gradient for flow velocity, HSR remains negative for *stenosis A*. While *stenosis B* is clearly severe as all physiological parameters in addition to PET are positive and in agreement, *stenosis A* is nonischemic despite having the same FFR value. Why the FFR value can be similar for both stenoses can be understood by judging the flow velocity and pressure gradient relationships depicted in panel **d**. *APV* average peak Doppler flow velocity, *IC* intracoronary, *PET* positron emission tomography

## 12.4 Hyperemic Stenosis Resistance (HSR)

The first report providing insight into the assessment of stenosis resistance in humans was published by Meuwissen et al. in 2002 [15]. In their study, distal pressure and Doppler flow velocity measurements were obtained using two separate wires for 181 lesions in 151 patients with either one- or two-vessel coronary artery disease. From these measurements, HSR, FFR, and CFR were calculated, and the predictive power of these indices to assess the presence of a reversible perfusion defect as defined by myocardial perfusion scintigraphy (MPS) was evaluated. A significantly higher area-under-the-receiver-operator curve to predict a reversible perfusion deficit was found for HSR in comparison to either FFR or CFR. The cutoff point, yielding the optimal combined test sensitivity and specificity for the presence of MPS-defined myocardial ischemia, was determined at a HSR value of 0.80 mmHg/cm per second or more. Using this value, the diagnostic improvement obtained with HSR was pronounced in vessels where discordant results between FFR and CFR were observed. These findings underline the hypothetical advantages of HSR outlined in the paragraph above and suggest that it is perhaps a better discriminator for the identification of coronary artery stenosis that would benefit most from revascularization than either FFR or CFR.

The interpretation of the obtained HSR value and the optimal cutoff point somewhat differs from the interpretation of FFR. Firstly, higher values of HSR represent incremental resistance and severity, whereas for FFR, higher values correspond to smaller stenosis severity. Secondly, the optimal cutoff point for HSR represents the ischemic threshold, which corresponds to an FFR value of 0.75. The fractional flow reserve versus Angiography for Multivessel Evaluation (FAME) trials (2;3) used a higher cutoff value of 0.80, which consequently became the cutoff point used to guide revascularization in contemporary clinical practice. It can be envisaged that if HSR would be introduced into clinical practice, a more aggressive approach to revascularization would be chosen, similar to what has been done for FFR, by lowering the HSR threshold of 0.80 mmHg/cm per second.

Circumstantial evidence that HSR appears to be a more stenosis-specific measure than FFR can be inferred from a study investigating the impact of opening a chronic total obstruction on the intracoronary physiology of large collateral donor vessels [16]. It was shown that after opening of the occlusion, FFR in the predominant donor vessel significantly increased, while no intervention was performed in that vessel leaving stenosis geometry unaltered. The increased FFR was likely mediated by a decreased hyperemic flow velocity paired with an increased hyperemic microvascular resistance, since the amount of myocardium subtended by the donor vessel decreases after revascularization. If we recall the Gould's formula, it becomes apparent that with the reduction of hyperemic flow velocity, the pressure gradient falls and FFR increases. Importantly, HSR remained numerically and statistically equivalent in the large donor vessel after opening of the occlusion, since the decreased hyperemic flow velocity corrects for the decreased pressure gradient. These findings provide supporting evidence that HSR is more stenosis-specific than FFR, but do not inform about whether or not HSR is also a better indicator of myocardial ischemia.

## 12.5 Baseline Stenosis Resistance (BSR)

The administration of a pharmacological agent with microvascular vasodilating properties to establish the hyperemic state, such as adenosine, maximizes flow velocity and mimics exhaustion of the autoregulatory reserve of the microcirculation as would be induced by physical exercise [17]. Although strictly speaking, pharmacological induction of hyperemia allows for greater vasodilation than can be established by exercise, while exogenous administration also does not increase myocardial contractility and systemic blood pressure as exercise does. The establishment of true microvascular hyperemia is crucial for reliable assessment of FFR and CFR. As can be inferred from the theoretical framework for the evaluation of stenosis resistance outlined above, HSR is less dependent on the establishment of true maximal hyperemia since the magnitude of flow velocity somewhat corrects for the pressure gradient across the stenosis. Nevertheless, in their original work, Meuwissen et al. dismissed the option to assess stenosis resistance under resting conditions, due to the concern of hemodynamic variability under resting conditions, which might negatively affect the test reliability. Recently, however, physiological lesion assessment without hyperemia has gained renewed attention [18]. The primary reason for this appears to be the low penetrance of FFR despite guidelines explicitly advocating the use of FFR in clinical practice [19]. It was assumed that a significant contributing factor of the poor guideline adherence could be the requirement of pharmacological induction of the hyperemic state, which frequently causes temporary yet undesirable side effects and is contraindicated in patients with severe COPD or asthma. In the wake of the recent introduction of the instantaneous wave-free ratio (iFR) as a hyperemia-independent physiological alternative to FFR, the baseline stenosis resistance (BSR) was proposed by van de Hoef et al. in 2012 as the hyperemia-free alternative to HSR [20]. The computation of BSR is identical to that of HSR and calculated as the transstenotic pressure gradient divided by flow velocity, with the only difference being the omission of the administration of a hyperemic agent. In the study by van de Hoef et al., BSR, HSR, CFR, and FFR were compared against MPS-defined myocardial ischemia. It was found that BSR, CFR, and FFR had an equal diagnostic performance, but HSR significantly trumped the other physiological indices. The optimal cutoff point for BSR was determined at 0.66 mmHg/cm per second. Later, the same authors confirmed the diagnostic equivalence between BSR and FFR, when tested against stenosis-specific (and thus microcirculatory independent) myocardial ischemia, defined as the presence of both MPS- and HSR-positive stenoses [21]. While these results challenge the true necessity for adenosine-induced hyperemia to

unmask the hemodynamic significance of coronary artery disease, BSR still underperformed compared to HSR. Furthermore, the results teach us that the optimal ischemic cutoff points for BSR and HSR are not identical, and in fact, BSR values are consistently lower than HSR values. This difference in BSR and HSR values is unlikely to be explained by hemodynamic variability, but again Gould's formula may provide the explanation. Since term *B* is squared by flow velocity, the relationship between pressure gradient and flow velocity is not linear, but quadratic. As such, the computed stenosis resistance will increase with higher flow velocity, as is the case when hyperemia is induced. Despite these two parameters of stenosis resistance are not numerically identical, this should not necessarily impact diagnostic accuracy, since the threshold for a positive test result for BSR is lower than it is for HSR. However, the assumption that diagnostic accuracy is equivalent only holds true when the data acquired is very robust and not prone to measurement variability or inaccuracy. In reality, Doppler flow velocity is in fact prone to measurement variability, and an optimal flow envelope cannot always be obtained. With induction of hyperemia, flow velocity increases, and the impact of the measurement deviation proportionally reduces, presumably making HSR more robust than BSR.

## 12.6 Diastolic Pressure Gradient at Flow Velocity of 50 cm/s ($dp_{v50}$)

While stenosis resistance is less reliant on microcirculatory function than FFR and CFR, the degree of hyperemia achieved still affects the measured stenosis resistance, and achieving submaximal hyperemia may underestimate the HSR. Marques et al. proposed the pressure gradient at flow velocity of 50 cm/s ($dp_{v50}$) in 2006 as a way to assess hemodynamic stenosis significance that is not influenced by either microcirculatory function, the requirement of achieving maximal hyperemia, or hemodynamic variability that may occur under resting conditions [22]. The $dp_{v50}$ is derived from the relationship between flow velocity and the pressure gradient across the stenosis during diastole. To calculate $dp_{v50}$, instantaneous diastolic values of coronary flow velocity on the x-axis and the pressure gradient at the y-axis are plotted in graph and involve cardiac cycles between peak hyperemia and resting conditions (Fig. 12.6a). A regression line according to the Gould's formula is drawn to fit the data points on the graph, and the $dp_{v50}$ is determined as the pressure gradient at a coronary flow velocity of 50 cm/s (Fig. 12.6b) [23]. The optimal cutoff point for $dp_{v50}$ to predict myocardial ischemia as defined by either MPS or dobutamine stress echocardiography was found at 22.4 mmHg by receiver-operator-characteristic analysis. Using this cutoff value, $dp_{v50}$ had a diagnostic accuracy of 95 % compared with myocardial ischemia, which was higher than FFR at 91 % and CFR at 75 %. The stellar diagnostic performance of $dp_{v50}$ does not come as a surprise, given $dp_{v50}$ is solely determined by stenosis geometry. By normalizing the flow velocity at 50 cm/s, variable factors that may influence flow velocity such as the degree of hyperemia, the functional status of the microcirculation, and hemodynamic variability will have no influence on $dp_{v50}$. For these reasons, $dpv_{50}$ could even be superior to HSR and may well be the optimal method to quantify stenosis severity specifically. Unfortunately, no algorithm that automatically constructs the curves and calculates $dp_{v50}$ is commercially available at present. Constructing the curves manually is cumbersome and not feasible to immediately perform at the catheterization laboratory. In conclusion, while $dp_{v50}$ may be theoretically superior to any other existing

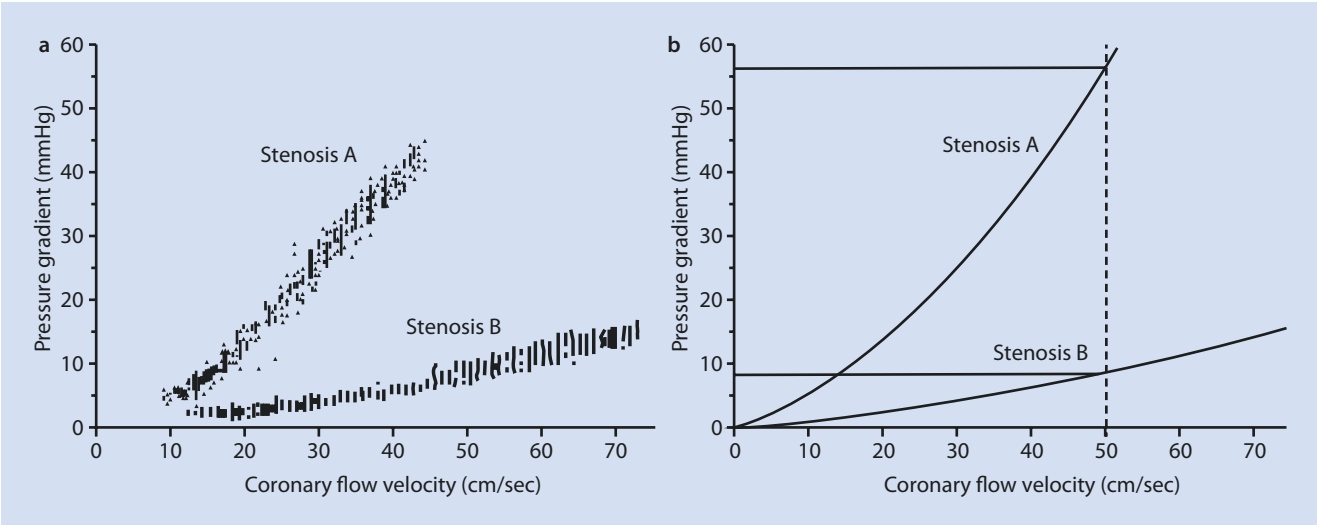


**Fig. 12.6** Panel **a**: To calculate $dp_{v50}$, the coronary flow velocity and pressure gradient during middiastole are first plotted for cardiac cycles during resting conditions and after administration of adenosine. Panel **b**: A regression line is then plotted that represents the relationship between flow velocity and pressure gradient. For stenosis A, the $dp_{v50}$ is 56 mmHg and for stenosis B $dp_{v50}$ is 9 mmHg. The cutoff value for $dp_{v50}$ is 22.4 mmHg, indicating that stenosis A is hemodynamically significant, while stenosis B is not severe; $dp_{v50}$ = diastolic pressure gradient at flow velocity of 50 cm/s (Reprinted with permission from Marques [22])

physiological index, the difficulties in calculating $dp_{v50}$ and obtaining high-fidelity Doppler flow velocity signals preclude clinical use.

## 12.7 Hypothetical Limitations of Stenosis Resistance

While comprehensive assessment of the coronary circulation by measuring stenosis resistance has many advantages, the validation of the indices that describe stenosis resistance has been less extensive than for FFR and has not been done in specific subsets of patients. Firstly, in patients with a previous myocardial infarction, interpreting the different indices that estimate stenosis resistance (HSR, BSR, and $dp_{v50}$) may be treacherous. In the presence of a prior myocardial infarction, less viable myocardium remains, and myocardial flow demand is decreased. While, the theoretical framework of FFR is not violated and still applies, this may not be the case for stenosis resistance indices [24]. These indices estimate the true resistance across the stenosis and do not account for the myocardial demand. As such, while the resistive capacity of a stenosis may be severe, the remaining subtended viable myocardium has little flow demand, and myocardial blood flow may still be adequate even in the presence of a severe stenosis. Secondly, coronary flow velocity is not the same as absolute coronary blood flow, and this may hamper accurate assessment of stenosis resistance in specific subsets of patients. In the presence of diffuse epicardial coronary artery disease, the measured hyperemic flow velocity is preserved, while absolute hyperemic coronary flow velocity is inadequate because of the narrow luminal diameter. Flow velocity may thus underestimate stenosis resistance. Conversely, when the segment distal to the stenosis where the measurement is done is aneurysmatic, flow velocity is low, while absolute coronary blood flow may be higher. In this case, stenosis resistance calculated from flow velocity is relatively higher than it would be when calculated from absolute coronary blood flow. Ideally, quantitative coronary blood flow is available to accurately assess true stenosis resistance.

## 12.8 Future of Stenosis Resistance as a Clinical Tool

At the time Meuwissen et al. published their first report on HSR, it was cumbersome to obtain measurements of Doppler flow velocity and distal coronary artery pressure. Two consecutive measurements using both a pressure and a Doppler flow velocity wire, with subsequent induction of the hyperemic state, were required. Furthermore, for the calculation of HSR, it is imperative that the variables of flow velocity, aortic, and distal pressure are obtained under consistent hemodynamic conditions and stenosis morphology. However, heart rate, proximal aortic driving pressure, microvascular resistance, and epicardial vessel tone are in a constant state of flux in order to maintain homeostasis. Albeit minor hemodynamic adaptations, imperfections in the computation of HSR are inevitable when two separate wires are used in succession. Taken together, these difficulties have precluded widespread clinical application and further larger-scale trials at the time.

Ongoing technological advances have allowed for smaller sensors, however, which now permit the incorporation of both a Doppler flow velocity and a pressure sensor at the tip of a single 0.014-in. guidewire (Fig. 12.7). With the use of this specific wire, all parameters required for the computation of HSR can be obtained simultaneously, and a built-in algorithm in the console allows for instantaneous estimation of HSR during the catheterization procedure. With this contemporary wire, much of the aforementioned barriers hindering clinical adaptation and further scientific examination appear to be solved. Nevertheless, as operators who frequently use wires equipped with flow velocity sensors can

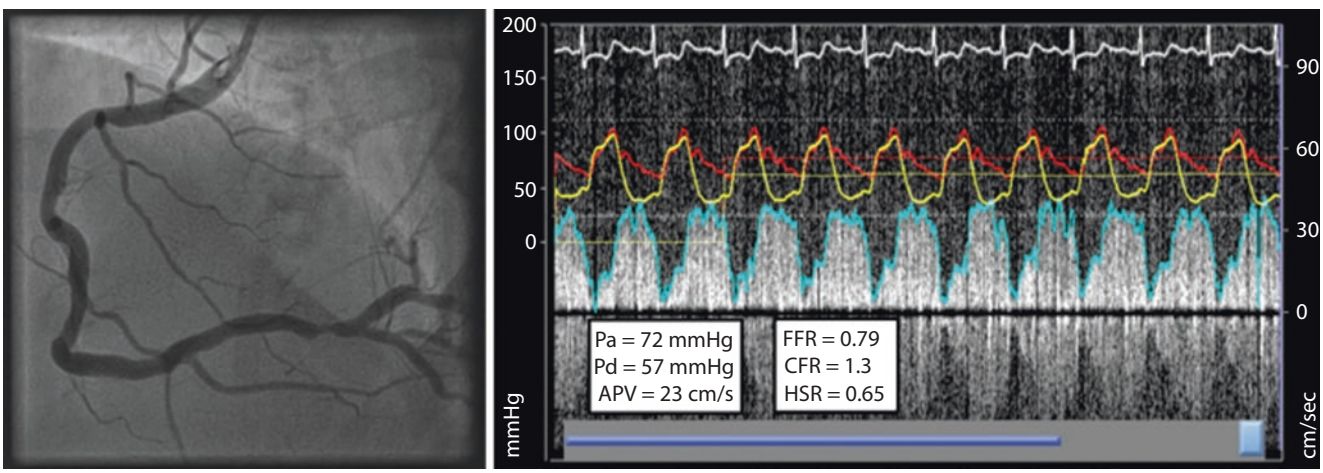


**Fig. 12.7** Simultaneous combined intracoronary pressure and Doppler flow velocity measurements obtained in the distal part of the right coronary artery. This measurement was obtained during stable hyperemia induced by intravenous administration of 140 μg/kg/min of adenosine. *APV* average peak Doppler flow velocity

undoubtedly attest, obtaining stable and representative Doppler flow velocity signals with this wire can be difficult and sometimes requires extensive maneuvering. Although not reported in literature, stenosis resistance could also theoretically be calculated using coronary thermodilution in combination with distal coronary pressure, which could perhaps solve the aforementioned quality issues that can arise with Doppler flow velocity (although thermodilution may come with its own theoretical and practical drawbacks) [25]. Further clinical trials investigating the potential advantage of a combined flow velocity and pressure-based approach to determine stenosis resistance and guide coronary revascularization are eagerly awaited before adoption into clinical guidelines can be considered.

**Disclosures** None of the authors have a potential conflict of interest to disclose.

## References

1. Pijls NH, van Son JA, Kirkeeide RL, De Bruyne B, Gould KL. Experimental basis of determining maximum coronary, myocardial, and collateral blood flow by pressure measurements for assessing functional stenosis severity before and after percutaneous transluminal coronary angioplasty. Circulation. 1993;87(4):1354–67.
2. Tonino PA, De Bruyne B, Pijls NH, Siebert U, Ikeno F, van't Veer M, et al. Fractional flow reserve versus angiography for guiding percutaneous coronary intervention. N Engl J Med. 2009;360(3):213–24.
3. De Bruyne, Pijls NH, Kalesan B, Barbato E, Tonino PA, Piroth Z, et al. Fractional flow reserve-guided PCI versus medical therapy in stable coronary disease. N Engl J Med. 2012;367(11):991–1001.
4. Montalescot G, Sechtem U, Achenbach S, Andreotti F, Arden C, Budaj A, et al. 2013 ESC guidelines on the management of stable coronary artery disease: the task force on the management of stable coronary artery disease of the European society of cardiology. Eur Heart J. 2013;34(38):2949–3003.
5. Fihn SD, Gardin JM, Abrams J, Berra K, Blankenship JC, Dallas AP, et al. 2012 ACCF/AHA/ACP/AATS/PCNA/SCAI/STS Guideline for the diagnosis and management of patients with stable ischemic heart disease: a report of the American College of Cardiology Foundation/American Heart Association Task Force on Practice Guidelines, and the American College of Physicians, American Association for Thoracic Surgery, Preventive Cardiovascular Nurses Association, Society for Cardiovascular Angiography and Interventions, and Society of Thoracic Surgeons. J Am Coll Cardiol. 2012;60(24):e44–164.
6. Echavarria-Pinto M, Escaned J, Macias E, Medina M, Gonzalo N, Petraco R, et al. Disturbed coronary hemodynamics in vessels with intermediate stenoses evaluated with fractional flow reserve: a combined analysis of epicardial and microcirculatory involvement in ischemic heart disease. Circulation. 2013;128(24):2557–66.
7. van de Hoef TP, Nolte F, Echavarria-Pinto M, van Lavieren MA, Damman P, Chamuleau SA, et al. Impact of hyperaemic microvascular resistance on fractional flow reserve measurements in patients with stable coronary artery disease: insights from combined stenosis and microvascular resistance assessment. Heart. 2014;100(12):951–9.
8. Meuwissen M, Chamuleau SA, Siebes M, Schotborgh CE, Koch KT, de Winter RJ, et al. Role of variability in microvascular resistance on fractional flow reserve and coronary blood flow velocity reserve in intermediate coronary lesions. Circulation. 2001;103(2):184–7.
9. Johnson NP, Kirkeeide RL, Gould KL. Is discordance of coronary flow reserve and fractional flow reserve due to methodology or clinically relevant coronary pathophysiology? JACC Cardiovasc Imaging. 2012;5(2):193–202.
10. McGinn AL, White CW, Wilson RF. Interstudy variability of coronary flow reserve. Influence of heart rate, arterial pressure, and ventricular preload. Circulation. 1990;81(4):1319–30.
11. Gould KL, Lipscomb K, Hamilton GW. Physiologic basis for assessing critical coronary stenosis. Instantaneous flow response and regional distribution during coronary hyperemia as measures of coronary flow reserve. Am J Cardiol. 1974;33(1):87–94.
12. Kern MJ, Lerman A, Bech JW, De Bruyne B, Eeckhout E, Fearon WF, et al. Physiological assessment of coronary artery disease in the cardiac catheterization laboratory: a scientific statement from the American Heart Association Committee on diagnostic and interventional cardiac catheterization. Circulation. 2006;114(12):1321–41.
13. Petraco R, van de Hoef TP, Nijjer S, Sen S, van Lavieren MA, Foale RA, et al. Baseline instantaneous wave-free ratio as a pressure-only estimation of underlying coronary flow reserve: results of the JUSTIFY-CFR study (Joined Coronary Pressure and Flow Analysis to Determine Diagnostic Characteristics of Basal and Hyperemic Indices of Functional Lesion Severity-Coronary Flow Reserve). Circ Cardiovasc Interv. 2014;7(4):492–502.
14. De Bruyne, Baudhuin T, Melin JA, Pijls NH, Sys SU, Bol A, et al. Coronary flow reserve calculated from pressure measurements in humans. Validation with positron emission tomography. Circulation. 1994;89(3):1013–22.
15. Meuwissen M, Siebes M, Chamuleau SA, van Eck-Smit BL, Koch KT, de Winter RJ, et al. Hyperemic stenosis resistance index for evaluation of functional coronary lesion severity. Circulation. 2002;106(4):441–6.
16. Ladwiniec A, Cunnington MS, Rossington J, Mather AN, Alahmar A, Oliver RM, et al. Collateral donor artery physiology and the influence of a chronic total occlusion on fractional flow reserve. Circ Cardiovasc Interv. 2015;8(4). pii: e002219. doi: 10.1161/CIRCINTERVENTIONS.114.002219.
17. Nijjer SS, de Waard GA, Sen S, van de Hoef TP, Petraco R, Echavarria-Pinto M, et al. Coronary pressure and flow relationships in humans: phasic analysis of normal and pathological vessels and the implications for stenosis assessment: a report from the Iberian-Dutch-English (IDEAL) collaborators. Eur Heart J. 2015;37:2069–80.
18. Sen S, Escaned J, Malik IS, Mikhail GW, Foale RA, Mila R, et al. Development and validation of a new adenosine-independent index of stenosis severity from coronary wave-intensity analysis: results of the ADVISE (ADenosine Vasodilator Independent Stenosis Evaluation) study. J Am Coll Cardiol. 2012;59(15):1392–402.
19. Dattilo PB, Prasad A, Honeycutt E, Wang TY, Messenger JC. Contemporary patterns of fractional flow reserve and intravascular ultrasound use among patients undergoing percutaneous coronary intervention in the United States: insights from the National Cardiovascular Data Registry. J Am Coll Cardiol. 2012;60(22):2337–9.
20. van de Hoef TP, Nolte F, Damman P, Delewi R, Bax M, Chamuleau SA, et al. Diagnostic accuracy of combined intracoronary pressure and flow velocity information during baseline conditions: adenosine-free assessment of functional coronary lesion severity. Circ Cardiovasc Interv. 2012;5(4):508–14.
21. van de Hoef TP, Meuwissen M, Escaned J, Sen S, Petraco R, van Lavieren MA, et al. Head-to-head comparison of basal stenosis resistance index, instantaneous wave-free ratio, and fractional flow reserve: diagnostic accuracy for stenosis-specific myocardial ischaemia. EuroIntervention. 2014;11:914–25.
22. Marques KM, van Eenige MJ, Spruijt HJ, Westerhof N, Twisk J, Visser CA, et al. The diastolic flow velocity–pressure gradient relation and dpv50 to assess the hemodynamic significance of coronary stenoses. Am J Physiol Heart Circ Physiol. 2006;291(6):H2630–5.
23. Marques KM, Spruijt HJ, Boer C, Westerhof N, Visser CA, Visser FC. The diastolic flow-pressure gradient relation in coronary stenoses in humans. J Am Coll Cardiol. 2002;39(10):1630–6.
24. Marques KM, Knaapen P, Boellaard R, Westerhof N, Lammertsma AA, Visser CA, et al. Hyperaemic microvascular resistance is not increased in viable myocardium after chronic myocardial infarction. Eur Heart J. 2007;28(19):2320–5.
25. Amier RP, Teunissen PF, Marques KM, Knaapen P, van Royen. Invasive measurement of coronary microvascular resistance in patients with acute myocardial infarction treated by primary PCI. Heart. 2014;100(1):13–20.

# Measurements of Microcirculatory Resistance

*Nicola Ryan, Mauro Echavarría-Pinto, Alicia Quirós, Hernán Mejía-Rentería, María Del Trigo, Pilar Jiménez-Quevedo, and Javier Escaned*




J. Escaned, J. Davies (eds.), *Physiological Assessment of Coronary Stenoses and the Microcirculation*,
DOI 10.1007/978-1-4471-5245-3_13

## 13.1 Introduction

The coronary microvasculature is an extremely dynamic system that responds to multiple physiological conditions in order to maintain adequate myocardial perfusion [1, 2], modulation of microcirculatory resistance plays a key role in this regulatory process. The underling pathophysiology and adaptive mechanisms of the microcirculation are fully described in other chapters in this book. In patients with ischemic heart disease (IHD), obstructive lesions in epicardial vessels are not a prerequisite for myocardial ischemia [3], which may arise from microcirculatory dysfunction (MCD). It has been shown that MCD is an independent predictor of poorer clinical outcomes in various clinical scenarios [4, 5] and, therefore, outlining its presence in such clinical situations might be important. However, the diagnosis of MCD is hampered by the lack of standardized methodologies.

The microcirculation is often referred to as a "blackbox" largely because, while the major epicardial coronary arteries are easily visualized and treated using coronary angiography alone, the microcirculation cannot be visualized in vivo, and only surrogate measures of its function can be appreciated using more sophisticated techniques. In previous chapters of this book, we have explored different measurements and theoretical frameworks to assess the coronary circulation. Coronary flow reserve (CFR) provides a global evaluation of the coronary circulation both the macro-and microvasculature using the concept of flow. Pressure drop across a stenosis can be used as a surrogate of myocardial flow impairment, allowing fractional flow reserve (FFR) and the instantaneous wave-free ratio (iFR) to evaluate the physiological impact of obstructive coronary disease. A third potential framework is vascular resistance, which requires measurements of pressure and flow for its calculation and is particularly suitable for the assessment of the coronary microcirculation.

In this chapter we will focus on resistive physiological measurements in the coronary microvasculature, paying attention to two indices that have been used in the clinical field: the index of microcirculatory resistance (IMR) and the hyperemic microcirculatory resistance (HMR). We will also discuss how the coronary microvasculature can be evaluated by assessing diastolic conductance (the inverse of resistance) and how to estimate the coronary pressure at which flow ceases, named zero-flow pressure ($P_{zf}$) (Fig. 13.1)

## 13.2 Invasive Physiology Measurements

Resistance can be calculated in the catheterization laboratory by combining coronary pressure with measurements of flow, using one of the two commercially available physiology wires to assess the latter: Doppler or thermodilution. Doppler-tipped guidewires estimate coronary flow velocity [6] while thermal sensitive guidewires, based on the thermodilution method, estimate mean transit time, an index of absolute coronary flow [7]. Following acquisition of the pressure and flow measurements at baseline and during hyperemia, several

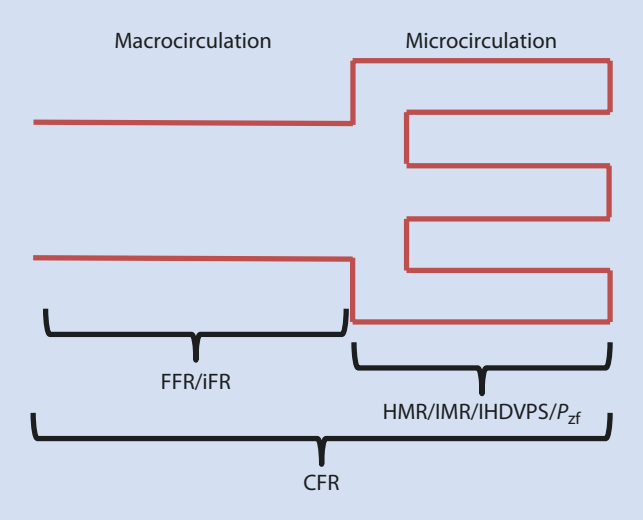


**Fig. 13.1** Coronary circulation

physiological indices can be obtained by relating Ohm's law to fluid flow [8] (Figs. 13.2 and 13.3). Volumetric flow requires the calculation of absolute luminal cross-sectional area and Doppler flow velocity. However, the close correlation between volumetric flow and average peak flow velocity by Doppler has allowed the use of flow velocity as a surrogate measure of coronary flow [9]. Since the sampling rates of the Doppler and pressure sensors rarely exceed heart rate frequency, Doppler flow allows calculation of mean indices based on the entire cardiac cycle or phasic measurements within the cardiac cycle. Using the thermodilution method to estimate coronary flow provides an index of absolute flow, the mean transit time. Disadvantages of thermodilution include an inability to provide a whole cycle estimate of flow, and its calculation is also affected by the presence of side branches.

## 13.3 Index of Microcirculatory Resistance (IMR)

The index of microcirculatory resistance (IMR) was first proposed by Fearon et al. [10] and is calculated from thermodilution-derived estimates of coronary flow and intracoronary pressure measured during maximal coronary hyperemia [11]. For its validation, the authors used a porcine model where they compared the true microcirculatory resistance (TMR), defined as distal coronary pressure divided by absolute coronary flow at hyperemia, with the IMR in both normal and disrupted microcirculations, as well as in the presence and absence of epicardial stenoses. The authors observed that IMR was significantly correlated with TMR ($r=0.54$, $P<0.0001$) and that the presence of epicardial stenosis did not significantly affected the values of TMR or IMR.

As IMR uses distal coronary flow in its calculation, it can be used to selectively interrogate the coronary microvasculature [10, 12, 13]. For its clinical measurement, the physiology guidewire is advanced into the coronary artery of interest, where the pressure sensor of the wire acts as a distal thermistor, and the shaft of the

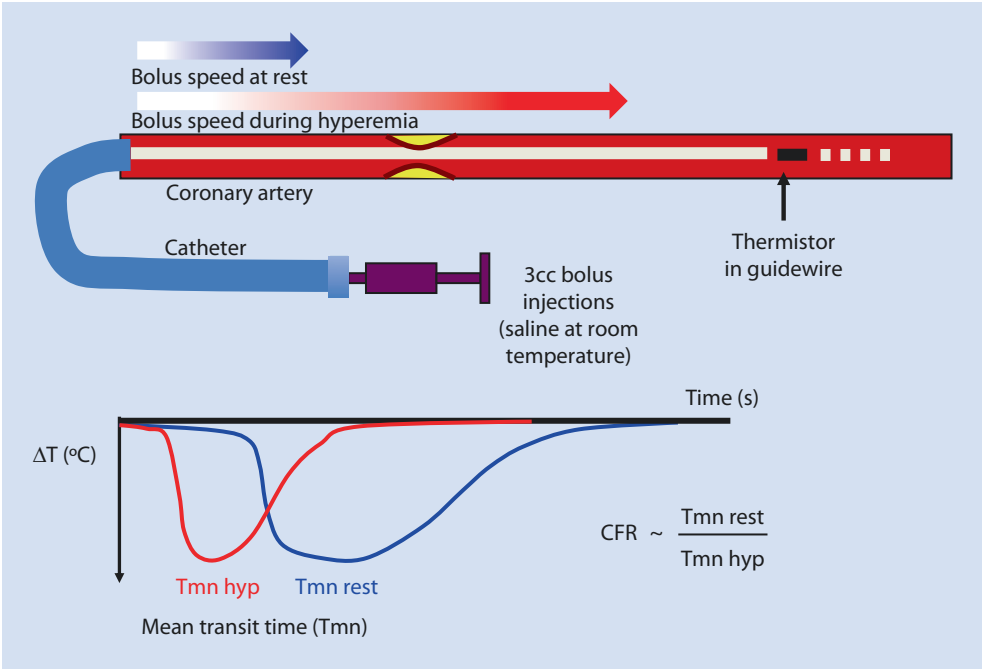


**Fig. 13.2** Combined pressure and flow wire using thermodilution


**Fig. 13.3** Combined pressure and flow wire using Doppler

wire acts as a proximal thermistor. Following injection of intracoronary boluses of saline at room temperature, the mean transit time ($T_{mn}$) of the saline bolus is derived from the recorded coronary thermodilution curve. Using the distal pressure ($P_d$) and the $T_{mn}$, IMR is then calculated, using the equation

$$\text{IMR} = P_d * T_{mn}.$$

In the presence of an epicardial stenosis, collateral flow can be a confounding factor in the determination of microvascular resistance. Therefore, it has been proposed that it was necessary to invasively measure coronary wedge pressure ($P_w$), as a measurement of collateral flow, in order to account for its possible impact on the estimated resistance [14, 15]. While the confounding effect of collateral flow in the calculation of microvascular resistance is still controversial [16], recent work by Yong et al. [17] has proposed an equation aimed to simplify the calculation of the IMR in the presence of a significant coronary stenosis without the need to invasively measure $P_w$. Other investigators have found that the IMR is only influenced by $P_w$ in the presence of a severe stenosis (FFR <0.6) [16].

As such, IMR can be described as the apparent IMR ($IMR_{app}$) calculated directly without the measurement of $P_w$

$$IMR_{app} = P_d * T_{mn}.$$

Application of Yong's formula aims to account for the presence of epicardial stenosis and provides a corrected IMR ($IMR_{corr}$)

$$IMR_{corr} = P_a * T_{mn} * \left(\left[1.35 * P_d / P_a\right] - 0.32\right)$$

$T_{mn}$ – mean transit time
$P_d$ – distal arterial pressure
$P_a$ – proximal arterial pressure

### 13.3.1 Prognostic Value of IMR

The potential clinical value of IMR to assess microcirculatory injury in patients undergoing primary percutaneous intervention (PPCI) for STEMI was first demonstrated in a small group of patients ($n = 29$) [18]. Using a cutoff value, 32 IMR correlated with peak CK and CK-MB ($r = 0.61$, $p = 0.0005$, $r = 0.67$, $p < 0.0001$) and larger infarction size. Measured immediately, post PPCI IMR predicted left ventricular function (LVF), as assessed using a wall motion score, at 3 months as well as recovery of LVF at 3 months. This initial study demonstrating the ability of IMR to predict LV recovery and discriminate viability has further been supported by studies using CMR [19, 20], single positron emission tomography [21], and PET [22]. A large study ($n = 253$) evaluating the prognostic value of IMR in the context of acute myocardial infarction demonstrated that an IMR > 40 post PPCI (the median IMR value of the study population) was associated with a fourfold increase in mortality risk, with IMR the only independent predictor of death alone (hazard ratio, 4.3 $p = 0.02$) [23]. Furthermore, in the same study, patients with IMR >40 had higher rates of hospitalization for cardiac failure in the first year. Therefore IMR appears to be a useful tool in identifying patients who may require closer follow-up post STEMI.

To date no cutoff value for abnormal IMR has been established in patients with stable ischemic heart disease (IHD). Recent work by Lee et al. [24] based on an international IMR registry investigated the distribution and determinants of IMR values in 1,452 vessels in 1,096 patients with stable IHD. All patients enrolled in the registry underwent measurement of both FFR and IMR in coronary vessels with stenosis. Given that the distribution of IMR varied, a cutoff of the 75th percentile in each of the major coronary arteries was taken to define high IMR, being 22, 24, and 28 in the left anterior descending artery, circumflex, and right coronary artery, respectively. $IMR_{corr}$ was calculated using Yong's formula, and all patients with at least one elevated IMR were classified as having high microvascular resistance. No correlation was found between $IMR_{corr}$ and FFR or $IMR_{corr}$ and angiographic diameter stenosis ($r = 0.01$, $p = 0.62$, $r = -0.03$, $p = 0.25$). Overall 17 % of patients had a stenosis with nonischemic FFR values (FFR >0.8) but abnormally high microvascular resistance suggesting that MCD was the predominant contributor to myocardial ischemia. Similarly on a per-vessel level analysis, one quarter (26 %) of vessels had an FFR >0.8 with an abnormal IMR. Predictors of high IMR which included previous myocardial infarction, right coronary artery, female, and obesity were different to those of ischemic FFR. Overall these findings suggest that IMR provides valuable additional information to that provided by FFR; hence, there is a need to integrate IMR with FFR when evaluating patients with myocardial ischemia. Recently Lee et al. evaluated the long-term outcome of 313 patients (663 vessels) with >1 coronary stenosis with an FFR >0.80. Concomitant measurements of CFR and IMR were performed to investigate whether they could predict the patient-oriented composite outcome (POCO) of any death, myocardial infarction, and revascularization [13]. The authors found that patients with high IMR and low CFR had the highest POCO ($p = 0.002$). This work highlights the benefit of integrating IMR and CFR in the evaluation of patients with a normal FFR to improve risk stratification and target medical therapy. Interestingly, an abnormal IMR with normal CFR did not identify patients with worse prognosis.

In summary, evaluation of IMR post STEMI appears to be beneficial in predicting poorer prognosis and may be useful to identify patients who should receive stricter clinical follow-up. In the stable IHD population without myocardial infarction, integration of IMR should be considered to fully evaluate the cause of the ischemia and appropriately target therapies. A major obstacle in the integration of the concept of IMR into clinical practice has been the lack of well-validated normal ranges. To date no large study has shown the distribution of IMR values in a healthy population without clinical symptoms or evidence of ischemia on noninvasive testing. Of note although the IMR international registry used the $IMR_{corr}$, there was negligible difference between the $IMR_{corr}$ and $IMR_{app}$, and using $IMR_{app}$ did not change any of the results obtained using $IMR_{corr}$; therefore in the absence of a severe stenosis, $IMR_{app}$ may be a more practical way to assess the microcirculation in routine clinical practice [24].

## 13.4 Hyperemic Microvascular Resistance (HMR)

Hyperemic microvascular resistance (HMR) is a vascular resistance index calculated from Doppler and pressure measurements. In clinical practice HMR is easily obtained with pressure guidewires fitted with both pressure and Doppler sensors and is calculated as the ratio of hyperemic mean distal coronary pressure to mean distal coronary flow velocity. Similar to IMR it has been argued that

HMR might overestimate the true microvascular resistance in the presence of a flow limiting stenosis, as it fails to account for the contribution of collateral flow to total myocardial blood flow [14, 15]. Nolte et al. [25] studied 228 patients with intermediate coronary stenosis by QCA (40–70 %) and evaluated the association between high HMR in the target vessel and reversible perfusion defects on myocardial perfusion scintigraphy (MPS). HMR does not have a validated clinical cutoff or normal range; therefore in this study the median HMR was used to define high and low HMR. Epicardial disease severity as assessed by the FFR was not significantly different between the high and low HMR groups (0.81 [0.7–0.89] vs 0.79 [0.79–0.88] $p = 0.46$). However, lesions with high HMR demonstrated significantly more reversible myocardial ischemia on MPS (37 % vs 19 % $p$ <0.001) than those with low HMR. When the analysis was restricted to lesions with an FFR >0.6, where the contribution of collateral flow is unlikely, the results did not change, thus implying the HMR allows identification of microcirculatory dysfunction in the presence of a coronary stenosis without the need to account for collateral flow.

### 13.4.1 Prognostic Value of HMR

Similarly to IMR, the HMR value post primary PCI in acute myocardial infarction has been found to be correlated to peak creatine kinase-MB (CK-MB) and infarct size as assessed by cardiac magnetic resonance (CMR) [26, 27]. HMR has also been found to be an independent predictor of left ventricle (LV) remodeling at 8 months post PPCI, defined as an increase in LV end-diastolic volume >20 % on CMR [28]. Teunissen et al. [27] evaluated 60 patients immediately post PPCI with intracoronary pressure–flow measurements and performed CMR and $H_2{}^{15}O$ positron emission tomography (PET). An HMR cutoff point of 2.5 mmHg/cm/sec was shown to predict the development of CMR-defined microvascular impairment and PET-derived flow impairment in the days immediately after PPCI. Elevated HMR was also associated with increased final infarct size and impaired LV ejection fraction as assessed by CMR at 3 months follow-up. Finally Yoon et al. showed that HMR was correlated to myocardial viability at 7 days and recovery of LV contractility as assessed by fluorodeoxyglucose PET [29].

HMR has been less extensively evaluated in patients with stable IHD, and, similarly to IMR, to date well-defined cutoffs for HMR in the healthy population, stable IHD, and acute coronary syndromes have not been established.

In summary high HMR post PPCI is predictive of poorer outcomes and may be useful in identifying patients at higher risk. Similarly in patients with stable IHD, high HMR correlated with ischemia demonstrated on noninvasive testing and may be useful in identifying patients in whom aggressive medical treatment should be initiated.

## 13.5 Instantaneous Hyperemic Diastolic Velocity–Pressure Slope

The instantaneous hyperemic diastolic velocity–pressure slope (IHDVPS) was first proposed by Mancini et al. [30] in 1989 as an alternative method to CFR to assess stenosis severity. As such, IHDVPS was based on aortic pressure and coronary flow measured during maximal coronary hyperemia. The concept was translated to the study of coronary microcirculation by Escaned et al. by using either aortic pressure in the absence of obstructive epicardial disease or intracoronary pressure distal to the stenosis in case of obstructive disease [31].

IHDVPS constitutes an estimate of mid- and late-diastolic microcirculatory conductance. The effects on coronary flow of extravascular systolic compression of the microcirculation, as well as the early diastolic modification of coronary capacitance, are thus negated. In animal and human models, IHDVPS, used to estimate stenosis severity, was found to be independent of heart rate, aortic pressure ($P_a$), preload, myocardial contractility, and basal blood flow [32, 33].

The calculation of IHDVPS can be envisaged as part of intracoronary pressure–flow velocity loops analysis (Fig. 13.4). IHDVPS is defined as the slope of the relation between distal pressure ($P_d$) and flow velocity (FV) in the mid- to late diastolic segment of the loop obtained during maximal hyperemia. The mid- to late diastolic interval (DI) used to calculate IHDVPS is defined from the maximal diastolic velocity to the onset of the rapid decline of coronary FV due to myocardial contraction (Fig. 13.4). Recent clinical studies using IHDVPS have incorporated automated methods for the calculation of IHVDPS and $P_{zf}$ that are likely to circumvent the relatively high degree of variability associated with manual calculation [33]. Currently there are no commercially available systems to calculate IHDVPS.

### 13.5.1 Prognostic Value of IHDVPS

Escaned et al. [31] evaluated the value of IHDVPS and other intracoronary indices to detect changes in the microcirculation in patients post heart transplantation, chosen as a model for microcirculatory dysfunction (related to cardiac allograft vasculopathy). In brief they compared intracoronary physiology with cardiac biopsies in patients undergoing routine screening. They found that both arteriolar obliteration and capillary rarefaction have an independent influence on microcirculatory hemodynamics and that IHDVPS was the index that best reflected the influence of the abnormalities ($r = 0.84$, $P = 0.0002$). Lower IHDVPS values were found in patients who developed cardiac events during follow-up.

In a large study evaluating the relationship between Doppler-derived invasive physiological measures in patients post STEMI and microvascular impairment, Teunissen et al. confirmed the expected inverse relationship between HMR and IHVDPS ($r = -0.52$, $p = 0.004$); however they failed to

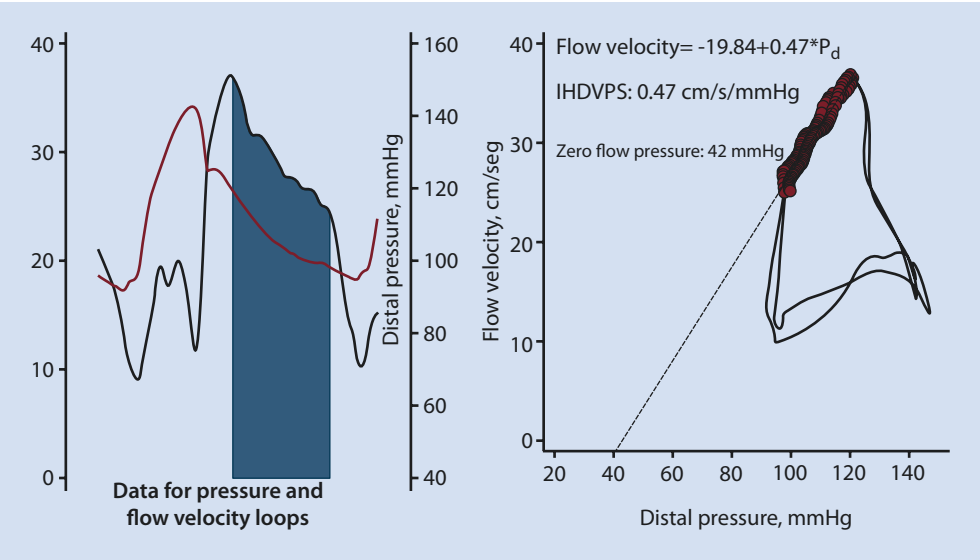


**Fig. 13.4** Illustration of IHDVPS and $P_{zf}$ indices estimation from physiology data. The diastolic interval is defined from the maximal diastolic velocity to the onset of the rapid decline of coronary flow velocity due to myocardial contraction or simply as late diastole. Formally, if the diastolic pressure–flow velocity relationship is determined by a regression line ($y = a + bx$), then IHDVPS is defined to be equal to the slope, b, and $P_{zf} = -a/b$, i.e., the intercept of the line with the pressure axis

show a relationship between IHVDPS and microvascular injury as demonstrated using CMR [27].

In summary, IHVDPS is a reliable measurement of capacitance, the inverse of resistance, and can be used to evaluate the microcirculation in both stable IHD and patients with ACS. To date the calculation of IHDVPS has been tedious requiring the manual selection of cardiac cycles and fitting of regression lines meaning easy integration into decision making at the time of invasive investigation is difficult. The development of an automatic algorithm to calculate IHVDPS would allow the calculation of IHDVPS with increased speed and accuracy, which may increase its incorporation into everyday clinical practice.

## 13.6 Zero-Flow Pressure ($P_{zf}$)

The concept of zero-flow pressure ($P_{zf}$), which can be described as the backpressure in the coronary circulation, has its origin in the vascular waterfall theory [34]. In practical terms, $P_{zf}$ can be thought of as the calculated pressure at which coronary flow would cease. Of note, the value of $P_{zf}$ is typically higher than that of central venous or right atrial pressure, and it could be the result of closure of collapsible elements of the coronary circulation (mainly capillaries) under the effect of extravascular compression (including intramyocardial and intraventricular pressures). As it is not possible to measure $P_{zf}$ in vivo, it is extrapolated from pressure–flow velocity loops obtained in the manner described in the IHDVPS section (Fig. 13.4).

### 13.6.1 Prognostic Value of $P_{zf}$

In 2003 Shimada et al. first reported the correlation between $P_{zf}$ and myocardial viability. In 27 patients with acute anterior, they found that $P_{zf}$ correlated with myocardial viability as assessed by FDG–PET ($r = -0.696$, $p = <0.001$) [35]. A later study showed that $P_{zf}$ is increased post myocardial infarction [36]. In a study evaluating HMR, $P_{zf}$ and CFR (Doppler) in patients post anterior myocardial infarction all correlated with infarct size in early (13 days) CMR, with $P_{zf}$ higher in patients with >75 % transmural infarct [26].

More recently work from our group evaluated the predictive effect of intracoronary physiology indices for the occurrence of microvascular injury and microvascular perfusion defects post successful PPCI. It was found that measurement of $P_{zf}$ provided useful prognostic information [27], since $P_{zf}$ was significantly higher in patients with microvascular injury (45.68 ± 13.72 vs 34.01 ± 13.67 mmHg, $p = 0.009$). These findings were subsequently supported by the OxAMI study [37], aimed to assess which invasive measure of the microcirculation at the time of PPCI best predicted the extent of left ventricular infarction as determined by CMR 6 months post STEMI. They found the $P_{zf}$ was superior to HMR and IMR for predicting a greater than 24 % infarction (area under the receiver operating curve: 0.94 vs 0.74 ($p = 0.04$) vs 0.54 ($p = 0.003$), respectively). $P_{zf}$ was also found to have significant direct relationships with troponin area under the curve (rho = 0.55, $p = 0.002$), final infarct mass (rho = 0.75, $p < 0.001$), percent transmurality of infarction (rho = 0.74, $p = <0.001$), percent of LV infarction (rho 0.77, $p = <0.001$), and inverse relationships with myocardial salvage index (rho = −0.53, $p = -0.01$) and 6-month ejection fraction (rho = −0.73, $p = -0.0001$).

In summary the clinical application of $P_{zf}$ has been limited due to the technical difficulties in obtaining stable Doppler signals as well as the fact that it is technically tedious and time consuming to reconstruct pressure volume loops. However given that $P_{zf}$ has been shown to be an accurate predictor of outcome post myocardial infarction, the development of automated algorithms to allow its calculation should increase its integration into clinical practice allowing the targeting of therapies in patients at increased risk of poorer outcomes.

## 13.7 Summary

The evidence supporting the prognostic value of microvascular impairment is mounting. Both elevated HMR and IMR are predictive of poorer outcomes in the setting of STEMI evaluated using biomarkers, echocardiography, CMR, and PET testing, with elevated IMR shown to be associated with increased mortality. Similarly in stable coronary artery disease, elevated IMR and HMR have been shown to be associated with myocardial ischemia on noninvasive imaging in the absence of functionally significant epicardial stenosis. All invasive measures of the microvasculature have suffered from a lack of well-validated normal ranges. To date no large study has shown the distribution of values in a healthy population without clinical symptoms or evidence of ischemia on noninvasive testing. Both IHVDPS and $P_{zf}$ have been shown to accurately assess the microcirculation and act as predictors of poorer prognosis; however to date the clinical applications of these measures have been limited due to several factors including the technical difficulties in obtaining stable Doppler signals, the fact that it is technically tedious and time consuming to reconstruct pressure volume loops, and a lack of standardization across studies.

## References

1. Crea F, Camici PG, Bairey Merz CN. Coronary microvascular dysfunction: an update. Eur Heart J. 2014;35(17):1101–11.
2. Pries AR, Badimon L, Bugiardini R, Camici PG, Dorobantu M, Duncker DJ, et al. Coronary vascular regulation, remodelling, and collateralization: mechanisms and clinical implications on behalf of the working group on coronary pathophysiology and microcirculation. Eur Heart J. 2015;36:3134–46;ehv100.
3. Camici PG, Crea F. Coronary microvascular dysfunction. N Engl J Med. 2007;356(8):830–40.
4. Lanza GA, Crea F. Primary coronary microvascular dysfunction: clinical presentation, pathophysiology, and management. Circulation. 2010;121(21):2317–25.
5. van de Hoef TP, Bax M, Meuwissen M, Damman P, Delewi R, de Winter RJ, et al. Impact of coronary microvascular function on long-term cardiac mortality in patients with acute ST-segment-elevation myocardial infarction. Circ Cardiovasc Interv. 2013;6(3):207–15.
6. Serruys PW, Di Mario C, Meneveau N, de Jaegere P, Strikwerda S, de Feyter PJ, et al. Intracoronary pressure and flow velocity with sensor-tip guidewires: a new methodologic approach for assessment of coronary hemodynamics before and after coronary interventions. Am J Cardiol. 1993;71(14):41D–53.
7. De Bruyne B, Pijls NH, Smith L, Wievegg M, Heyndrickx GR. Coronary thermodilution to assess flow reserve: experimental validation. Circulation. 2001;104(17):2003–6.
8. Kern MJ, Lerman A, Bech J-W, De Bruyne B, Eeckhout E, Fearon WF, et al. Physiological assessment of coronary artery disease in the cardiac catheterization laboratory: a scientific statement from the American heart association committee on diagnostic and interventional cardiac catheterization. Circulation. 2006;114(12):1321–41.
9. Kern MJ, Deligonul U, Vandormael M, Labovitz A, Gudipati CV, Gabliani G, et al. Impaired coronary vasodilator reserve in the immediate postcoronary angioplasty period: Analysis of coronary artery flow velocity indexes and regional cardiac venous efflux. J Am Coll Cardiol. 1989;13(4):860–72.
10. Fearon WF, Balsam LB, Farouque HMO, Robbins RC, Fitzgerald PJ, Yock PG, et al. Novel index for invasively assessing the coronary microcirculation. Circulation. 2003;107(25):3129–32.
11. Yong ASC, Ho M, Shah MG, Ng MKC, Fearon WF. Coronary microcirculatory resistance is independent of epicardial stenosis. Circ Cardiovasc Interv. 2012;5(1):103–8, S1–2.
12. Ng MKC. Invasive assessment of the coronary microcirculation: superior reproducibility and less hemodynamic dependence of index of microcirculatory resistance compared with coronary flow reserve. Circulation. 2006;113(17):2054–61.
13. Lee JM, Jung J-H, Hwang D, Park J, Fan Y, Na S-H, et al. Coronary flow reserve and microcirculatory resistance in patients with intermediate coronary stenosis. J Am Coll Cardiol. 2016;67(10):1158–69.
14. Aarnoudse W. Epicardial stenosis severity does not affect minimal microcirculatory resistance. Circulation. 2004;110(15):2137–42.
15. Fearon WF, Aarnoudse W, Pijls NHJ, De Bruyne B, Balsam LB, Cooke DT, et al. Microvascular resistance is not influenced by epicardial coronary artery stenosis severity: experimental validation. Circulation. 2004;109(19):2269–72.
16. Verhoeff B-J, van de Hoef TP, Spaan JAE, Piek JJ, Siebes M. Minimal effect of collateral flow on coronary microvascular resistance in the presence of intermediate and noncritical coronary stenoses. Am J Physiol Heart Circ Physiol. 2012;303(4):H422–8.
17. Yong AS, Layland J, Fearon WF, Ho M, Shah MG, Daniels D, et al. Calculation of the index of microcirculatory resistance without coronary wedge pressure measurement in the presence of epicardial stenosis. JACC Cardiovasc Interv. 2013;6(1):53–8.
18. Fearon WF, Shah M, Ng M, Brinton T, Wilson A, Tremmel JA, et al. Predictive value of the index of microcirculatory resistance in patients with ST-segment elevation myocardial infarction. J Am Coll Cardiol. 2008;51(5):560–5.
19. McGeoch R, Watkins S, Berry C, Steedman T, Davie A, Byrne J, et al. The index of microcirculatory resistance measured acutely predicts the extent and severity of myocardial infarction in patients with ST-segment elevation myocardial infarction. JACC Cardiovasc Interv. 2010;3(7):715–22.
20. Payne AR, Berry C, Doolin O, McEntegart M, Petrie MC, Lindsay MM, et al. Microvascular resistance predicts myocardial salvage and infarct characteristics in ST-Elevation myocardial infarction. J Am Heart Assoc. 2012;1(4):e002246. Available from: http://jaha.ahajournals.org/content/1/4/e002246.abstract.
21. Sezer M, Aslanger EK, Cimen AO, Yormaz E, Turkmen C, Umman B, et al. Concurrent microvascular and infarct remodeling after successful reperfusion of ST-elevation acute myocardial infarction. Circ Cardiovasc Interv. 2010;3(3):208–15.
22. Lim H-S, Yoon M-H, Tahk S-J, Yang H-M, Choi B-J, Choi S-Y, et al. Usefulness of the index of microcirculatory resistance for invasively assessing myocardial viability immediately after primary angioplasty for anterior myocardial infarction. Eur Heart J. 2009;30(23):2854–60.
23. Fearon WF, Low AF, Yong AS, McGeoch R, Berry C, Shah MG, et al. Prognostic value of the index of microcirculatory resistance measured after primary percutaneous coronary intervention. Circulation. 2013;127(24):2436–41.
24. Lee JM, Layland J, Jung J-H, Lee H-J, Echavarria-Pinto M, Watkins S, et al. Integrated physiologic assessment of ischemic heart disease in real-world practice using index of microcirculatory resistance and fractional flow reserve insights from the international index of microcirculatory resistance registry. Circ Cardiovasc Interv. 2015;8(11):e002857.
25. Nolte F, van de Hoef TP, Meuwissen M, Voskuil M, Chamuleau SAJ, Henriques JPS, et al. Increased hyperaemic coronary microvascular resistance adds to the presence of myocardial ischaemia. EuroIntervention J Eur Collab Work Group Interv Cardiol Eur Soc Cardiol. 2014;9(12):1423–31.
26. Kitabata H, Imanishi T, Kubo T, Takarada S, Kashiwagi M, Matsumoto H, et al. Coronary microvascular resistance index immediately after primary percutaneous coronary intervention as a predictor of the

transmural extent of infarction in patients with ST-segment elevation anterior acute myocardial infarction. JACC Cardiovasc Imaging. 2009;2(3):263–72.
27. Teunissen PFA, de Waard GA, Hollander MR, Robbers LFHJ, Danad I, Biesbroek PS, et al. Doppler-derived intracoronary physiology indices predict the occurrence of microvascular injury and microvascular perfusion deficits after angiographically successful primary percutaneous coronary intervention. Circ Cardiovasc Interv. 2015;8(3):e001786.
28. Kitabata H, Kubo T, Ishibashi K, Komukai K, Tanimoto T, Ino Y, et al. Prognostic value of microvascular resistance index immediately after primary percutaneous coronary intervention on left ventricular remodeling in patients with reperfused anterior acute ST-segment elevation myocardial infarction. JACC Cardiovasc Interv. 2013;6(10):1046–54.
29. Yoon M-H, Tahk S-J, Yang H-M, Woo S-I, Lim H-S, Kang S-J, et al. Comparison of accuracy in the prediction of left ventricular wall motion changes between invasively assessed microvascular integrity indexes and fluorine-18 fluorodeoxyglucose positron emission tomography in patients with ST-elevation myocardial infarction. Am J Cardiol. 2008;102(2):129–34.
30. Mancini GB, McGillem MJ, DeBoe SF, Gallagher KP. The diastolic hyperemic flow versus pressure relation. A new index of coronary stenosis severity and flow reserve. Circulation. 1989;80(4):941–50.
31. Escaned J, Flores A, Garcia-Pavia P, Segovia J, Jimenez J, Aragoncillo P, et al. Assessment of microcirculatory remodeling with intracoronary flow velocity and pressure measurements: validation with endomyocardial sampling in cardiac allografts. Circulation. 2009;120(16):1561–8.
32. Di Mario C, Krams R, Gil R, Serruys PW. Slope of the instantaneous hyperemic diastolic coronary flow velocity–pressure relation. A new index for assessment of the physiological significance of coronary stenosis in humans. Circulation. 1994;90(3):1215–24.
33. de Bruyne B, Bartunek J, Sys SU, Pijls NH, Heyndrickx GR, Wijns W. Simultaneous coronary pressure and flow velocity measurements in humans. Feasibility, reproducibility, and hemodynamic dependence of coronary flow velocity reserve, hyperemic flow versus pressure slope index, and fractional flow reserve. Circulation. 1996;94(8):1842–9.
34. Bellamy RF. Diastolic coronary artery pressure-flow relations in the dog. Circ Res. 1978;43(1):92–101.
35. Shimada K, Sakanoue Y, Kobayashi Y, Ehara S, Hirose M, Nakamura Y, et al. Assessment of myocardial viability using coronary zero flow pressure after successful angioplasty in patients with acute anterior myocardial infarction. Heart. 2003;89(1):71–6.
36. Van Herck PL, Carlier SG, Claeys MJ, Haine SE, Gorissen P, Miljoen H, et al. Coronary microvascular dysfunction after myocardial infarction: increased coronary zero flow pressure both in the infarcted and in the remote myocardium is mainly related to left ventricular filling pressure. Heart. 2007;93(10):1231–7.
37. Patel N, Petraco R, Dall'Armellina E, Kassimis G, De Maria GL, Dawkins S, et al. Zero-flow pressure measured immediately after primary percutaneous coronary intervention for ST-segment elevation myocardial infarction provides the best invasive index for predicting the extent of myocardial infarction at 6 months: an OxAMI study (Oxford Acute Myocardial Infarction). JACC Cardiovasc Interv. 2015;8(11):1410–21.

# Fractional Flow Reserve (FFR)

## Contents

# Understanding Fractional Flow Reserve

*Antonio Maria Leone, Giancarla Scalone, and Giampaolo Niccoli*




J. Escaned, J. Davies (eds.), *Physiological Assessment of Coronary Stenoses and the Microcirculation*,
DOI 10.1007/978-1-4471-5245-3_14

## 14.1 Introduction

Limitations of coronary angiography in the assessment of the severity of a coronary stenosis are well known [1]. In particular, the use of a luminogram to determine treatment strategies explains the observed dissociation between stenosis assessment by coronary angiography and clinical manifestation [2]. This particularly holds true for angiographically intermediate stenoses [3]. Thus, in the late 1980s, the search for an index of functional stenosis severity began. Of note, this index would have to be easy to use, reproducible, and able to identify ischemia-producing lesions. Intracoronary (IC) Doppler and pressure guidewires were tested, and eventually fractional flow reserve (FFR) was developed and validated as an invasive index of functional stenosis severity [4–6]. Nowadays, FFR has a high class of recommendation and level of evidence in guidelines for myocardial revascularization [7]. In this chapter we will describe the basic aspects of FFR including development of the concept and formula, validation against ischemia tests, and some practical aspects to be borne in mind in the catheterization laboratory (Figs. 14.1, 14.2, and 14.3).

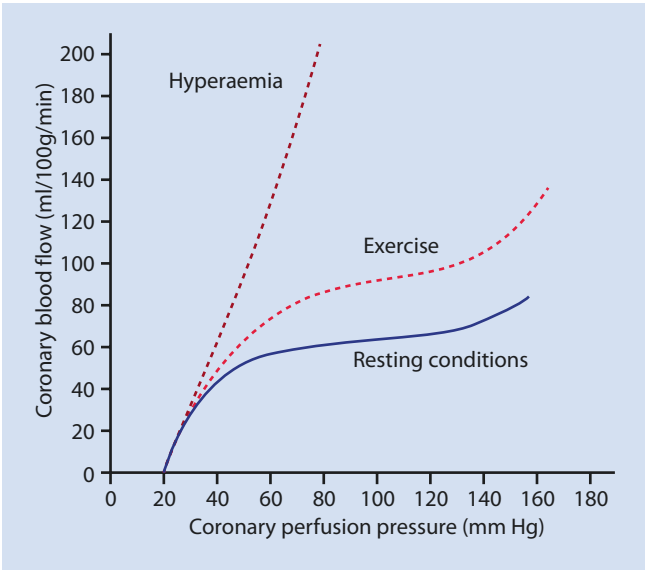


**Fig. 14.1** Coronary pressure–flow relationship. At a constant myocardial oxygen consumption level, coronary flow is autoregulated: coronary blood flow is constant within a physiological range of perfusion pressures (resting conditions). An increase in myocardial oxygen demand causes an increase in the autoregulatory plateau, called metabolic adaptation (exercise). During hyperemia, the relationship between coronary pressure and flow tends toward a linear relationship although it does not pass through the origin and has a slightly concave course (hyperemia) (Adapted from Ref. [12])

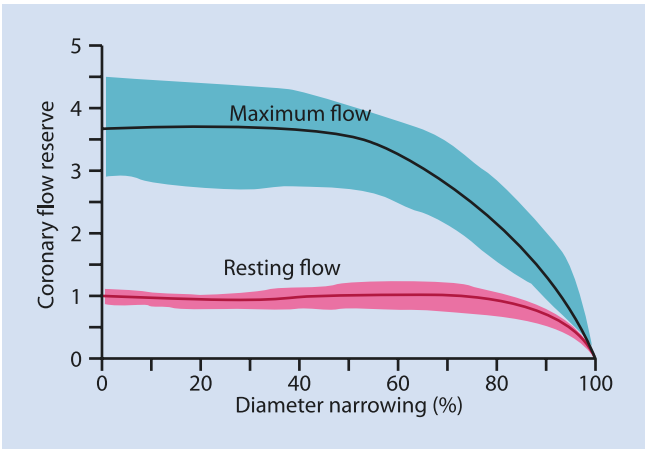


**Fig. 14.3** The figure illustrates coronary flow reserve (CFR) vs. arteriographic percent diameter stenosis in canine experimental model. Because of the autoregulation phenomenon, the flow remains constant as stenosis severity increases. In particular, hyperemic coronary flow begins to decline when a short 50 % diameter stenosis is present (75 % cross-sectional area). However, the resting flow does not change until a tight narrowing of at least 80–85 % in diameter is reached (Adapted from Ref. [13])

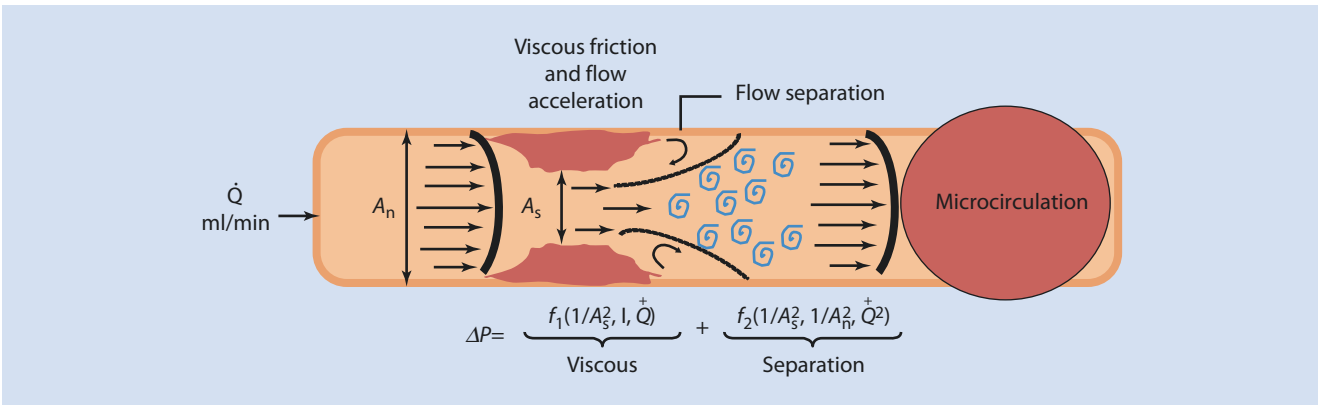


**Fig. 14.2** Total pressure loss derives from two sources: frictional losses along the entrance and throat and inertial losses stemming from the sudden expansion, causing flow separation and eddies (exit losses). Frictional losses are linearly related to flow, *Q* (law of Poiseuille), and exit losses increase with the square of the flow caused by convective acceleration in the narrowed segment (law of Bernoulli). Total pressure gradient ($\Delta P$) is the sum of the two: $\Delta P$ ($f1 \times Q$) + ($f2 \times Q^2$). The loss coefficients *f*1 and *f*2 are a function of stenosis geometry and rheologic properties of blood (viscosity and density). *As* indicates area of the stenosis, *An* area of the normal segment

## 14.2 Principles

### 14.2.1 Principles of FFR

FFR is defined as the ratio of hyperemic flow in the index myocardial territory to hyperemic flow in the same territory, in the hypothetical case that the epicardial vessel was completely normal. FFR relies on the principle that during maximal hyperemia, the pressure–flow relationship in the coronary tree becomes linear [8–10]. This makes it possible to use a pressure gradient for the assessment of stenosis severity in terms of flow impairment. Accordingly, when the pressure–flow relationship is linear, the ratio between two coronary pressures is identical to the ratio between coronary flows corresponding to these pressures. This concept is applied to pressure proximal and distal to a stenosis (Fig. 14.4). In other words, FFR represents the fraction of maximum flow that is maintained despite the presence of the stenosis or the maximum flow expressed as fraction of its normal value.

$$\text{FFR} = \text{Maximum myocardial flow in the presence of a stenosis} / \text{Normal maximum flow.}$$

More generally, normal maximum myocardial blood flow (QN) is given by $QN = (P_a - P_v)/R$, where $R$ is myocardial resistance at maximum vasodilation and $P_a$ and $P_v$ represent mean aortic pressure and mean central venous pressure, respectively. Actual maximum blood flow in the presence of the stenosis is given by $Q = (P_d - P_v)/R$ where $P_d$ represents hyperemic distal coronary pressure. As the myocardial vascular bed is maximally vasodilated, its resistance is minimal and constant. Therefore, FFR defined Q/QN and is given by $FFR = P_d - P_v / P_a - P_v$ where $P_a$, $P_d$, and $P_v$ represent mean aortic, distal coronary, and central venous pressure, obtained at maximum coronary hyperemia. This equation can be further simplified to [14–18]:

$$\text{FFR} = P_d / P_a \text{ during maximal hyperaemia.}$$

Suppose that we have a system consisting of a coronary artery and its dependent myocardium studied at maximum vasodilation, corresponding to maximum coronary and myocardial hyperemia when myocardial resistance is minimal (and therefore constant) and blood flow is proportional to driving pressure. In the absence of a coronary stenosis, the perfusion pressure over the myocardium would be 100 mmHg (Fig. 14.5, panel A) [19]. In the presence of a coronary stenosis, resulting in a hyperemic gradient of 30 mmHg, the perfusion pressure decreases to 70 mmHg. Therefore, maximum attainable blood flow to the myocardium in the presence of stenosis is only 70 % of normal maximum flow. We now say that the FFR of the myocardium supplied by this artery is 70 % or 0.7 (Fig. 14.5, panel B).

Thus, we state that FFR is defined as the ratio of the hyperemic flow in the index myocardial territory to the hyperemic flow in that same territory in the hypothetical case the epicardial vessel was completely normal [20, 21]. In other words, FFR expresses maximal hyperemic blood flow in the myocardial territory as a fraction of its normal value, or more simply, FFR expresses the extent to which maximal myocardial blood flow is limited by the presence of an epicardial stenosis. For example, if FFR is 0.60, it means that maximal myocardial blood flow reaches only 60 % of its normal value.

Of note, FFR is independent of heart rate, blood pressure, and contractility [6, 21, 22] with an unequivocal normal value of 1.0. In the initial definition, FFR was termed myocardial FFR ($FFR_{myo}$) as this index takes into account the contribution of the collateral flow and consequently expresses the FFR for a

- FFR is the ration of myocardial flow in the stenotic epicardial artery ($Qs^{max}$) to normal myocardial flow ($Qn^{max}$) during maximal hyperemia

$$FFR = \frac{Qs^{max}}{Qn^{max}}$$

- Flow (Q) is calculated by the ration of the pressure (*P*) difference across the coronary stenosis and divided by coronary resistance (*R*)

$$FFR = \frac{(P_d - P_v)/RS^{max}}{(P_a - P_v)/RN^{max}}$$

- Resistance within the coronary artery is minimal due to maximal hyperemia and therefore can be omitted from the equation

$$FFR = \frac{(P_d - P_v)}{(P_a - P_v)}$$

- For practical purposes, $P_v$ is omitted as it is negligible in the coronary arteries

$$FFR = \frac{(P_d)}{(P_a)}$$

**Fig. 14.4** Mathematical derivation and equation of fractional flow reserve. FFR fractional flow reserve, $P_a$ aortic pressure, $P_d$ distal coronary pressure, *Pv* venous pressure, $Qn^{max}$ hyperemic myocardial blood flow in the normal artery, $Qs^{max}$ hyperemic myocardial blood flow in the stenotic artery, $Rn^{max}$ hyperemic myocardial resistance in the normal territory, $Rs^{max}$ hyperemic myocardial resistance in the stenotic artery

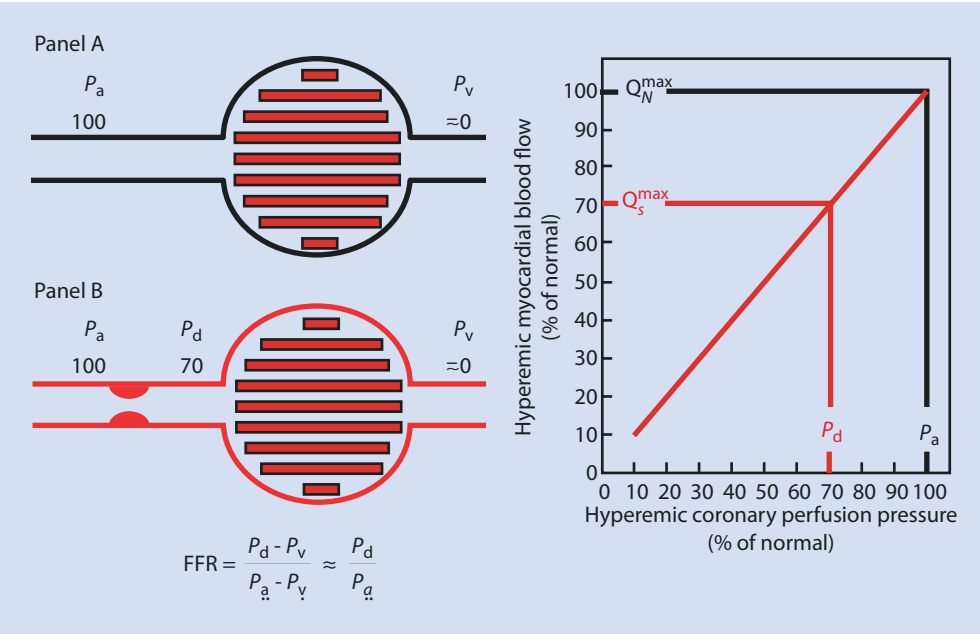


**Fig. 14.5** When no epicardial stenosis is present (*panel A*), the driving pressure $P_a$ determines a normal (100 %) maximal myocardial blood flow. In case of stenosis responsible for a hyperemic pressure gradient of 30 mmHg (*panel B*), the driving pressure will no longer be 100 mmHg but instead will be 70 mmHg ($P_d$). Because the relationship between driving pressure and myocardial blood flow is linear during maximal hyperemia, myocardial blood flow will only reach 70 % of its normal value. This numerical example shows how a ratio of two pressures ($P_d/P_a$) corresponds to a ratio of two flows (QS max/QN max). $P_v$ central venous pressure (Adapted from Ref. [19])

given myocardial territory. The term coronary FFR ($FFR_{cor}$) refers to the ratio of maximal blood flow in the target coronary artery to the hypothetical maximal blood flow in the same artery in the absence of a stenosis. Its calculation requires the exclusion of contributions to myocardial blood flow other than the main coronary vessel, such as coronary collaterals or bypass graft. Therefore, $FFR_{cor}$ is defined as $(P_d - P_w)/(P_a - P_w)$, where *Pa* represents the mean aortic pressure, $P_d$ represents the mean distal coronary pressure, and $P_w$ can be considered the coronary wedge pressure, which is assumed to be an estimate of collateral flow supply and is measured at coronary occlusion [20–23]. The difference between $FFR_{myo}$ and $FFR_{cor}$ represents the contribution of collateral flow to total myocardial perfusion and is called fractional collateral flow [20–23]. Because $FFR_{myo}$ reflects both anterograde and collateral contribution to maximum myocardial perfusion, it is the most important flow index from a clinical point of view and for this reason gained the definition of "FFR."

### 14.2.2 Potential Limitations of FFR

Due to its ease of use, FFR is increasingly utilized worldwide. However, interventionalists should be aware of some potential limitations that are intrinsic with the assumptions on which FFR has been developed. First, the actual pressure–flow relationship at hyperemia is not linear but actually curvilinear, namely, it is incremental linear in the physiological range of perfusion pressures but has a nonzero pressure intercept because coronary blood flow ceases at a perfusion pressure of approximately 20 mmHg [24]. Venous back pressure, collateral flow, epicardial capacitance (which describes the effect of blood storage in epicardial vessels during systole and its subsequent discharge into subendocardial vessels during diastole), and intramyocardial compliance contribute to the intercept pressure [11, 20]. Venous pressure was subtracted from both aortic and distal coronary pressure in the experimental validation of FFR [25]. However, this correction is not often performed in daily clinical practice as venous pressure is usually very low, and its influence is consequently considered negligible in comparison with the other determinants of the nonzero pressure intercept. In patients with myocardial dysfunction and heart failure, the contribution of venous pressure should be taken into account.

As stated above the same degree of stenosis may produce different FFR results in the presence of microvascular dysfunction as it may reduce the pressure gradient leading to overestimation of FFR and underestimation of stenosis severity (Fig. 14.6). This possibility should be considered when microvascular dysfunction is suspected due to clustering of many risk factors including diabetes or in patients with an acute coronary syndrome where the microcirculation may be affected [26]. Interestingly, coronary flow reserve (CFR) and FFR may be discordant in such scenario with "normal" FFR (>0.80) but reduced coronary flow reserve (<2.0) due to microvascular dysfunction (putative false-negative FFR) [27–30]. This patient group seems to carry a high risk of cardiovascular events in long-term follow-up [31, 32]. Less commonly, coronary flow reserve may be normal but FFR abnormal due to a large (supernormal) increase in flow in the presence of moderate stenosis leading to greater gradient and lower FFR values (putative false-positive FFR) [27, 31, 32].

Finally, coronary steal may occur when a collateral supplying vessel is stenoses [33]. In this scenario distal pressure will be lower due to steal phenomenon; indeed when distal resistance in the territory of the second vessel decreases (e.g., after administration of a vasodilatory stimulus), blood flow increases, and as a result distal coronary pressure decreases, resulting in a lower perfusion pressure over the collaterals and decreased collateral flow to the territory of the first artery, leading to greater transtenotic gradients and lower FFR values. Theoretically, infusing vasodilators via an

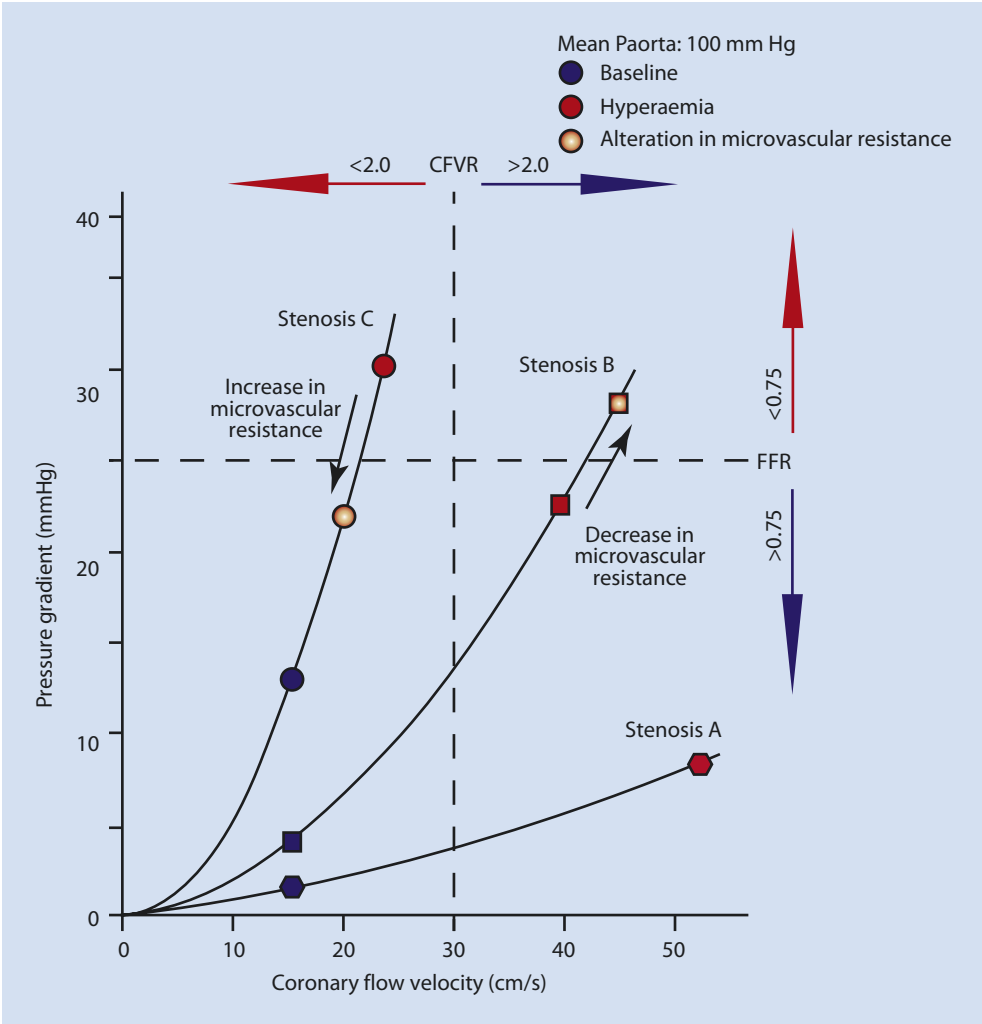


**Fig. 14.6** Pressure gradient–flow velocity relationship. Pressure loss over a normal epicardial segment can be considered negligible and therefore does not change significantly with increasing flow velocity (reference vessel). With increasing stenosis severity (increasing stenosis severity from stenoses A to C), the pressure gradient–flow velocity ($\Delta P$–$v$) curve becomes steeper, reflecting a higher perfusion pressure loss over the stenosis with increasing flow velocity. Changes of microvascular resistance may explain the dissociation between FFR and CFR observed in some cases by modulation flow velocity (Adapted from Ref. [12])

intracoronary (IC) route in the interrogated vessel should lead to higher FFR as distal pressure will not be reduced by coronary steal and collateral pressure contribution will be maintained. However, large studies in this area are lacking.

## 14.3 Validations of FFR and Ischemic Thresholds

FFR has been validated for its accuracy in identifying coronary stenoses associated with reversible myocardial ischemia detected by noninvasive stress testing [21, 34–58]. Table 14.1 shows the principal studies comparing FFR with non-invasive exercise or pharmacological stress testing to assess myocardial ischemia [21, 37–60]. Initially, an FFR cutoff value of 0.66 was proposed by De Bruyne and colleagues, as this value most accurately reflected the results of electrocardiographic exercise tolerance testing, with an associated sensitivity and specificity of approximately 86% [35]. Subsequently, Pijls et al. suggested a second cutoff value of 0.74 on the basis of a comparison of FFR with inducible ischemia during stress testing. Importantly, in this study patients were only enrolled if the positive stress test was associated with the presence of single-vessel disease and the stress test was negative after successful treatment of the stenosis with balloon angioplasty [21]. Thereafter, a cutoff value of 0.75 was proposed, as a result of multitest comparison with electrocardiographic exercise tolerance testing, stress echocardiography, and myocardial perfusion imaging [36]. This cutoff value was adopted in the first decision-making trial using FFR, the DEFER study [59]. Other studies were unable to reproduce the high diagnostic accuracy of the 0.75 FFR cutoff observed by Pijls et al. in the exercise tolerance testing and the multitest study (97% and 93%, respectively) [21, 36]. However, it should be acknowledged that a large number of these studies did not enroll patients with documented relief of ischemia after a successful revascularization (a Bayesian approach) but simply correlated noninvasive tests to FFR values. This may have influenced the accuracy of FFR by enrolling patients with false-positive ischemia during noninvasive stress testing. An FFR < 0.75 has a 100% specificity, 88% sensitivity, 100% positive predictive value, and 93% overall accuracy for ischemia. However, in order to improve the sensitivity (>90%) at the price of more false-positive results and less specificity, recent large-scale FFR trials have moved the cutoff to perform percutaneous coronary intervention (PCI) to 0.80 [60]. By using this cutoff, clinical outcome was improved by FFR both in the FAME and in the

**Table 14.1** Studies comparing FFR with noninvasive stress testing to assess myocardial ischemia

| Year | Author | Lesions (n) | Hyperemic stimulus | Ischemic test | Best FFR cut-off value | Accuracy (%) | Clinical setting |
|---|---|---|---|---|---|---|---|
| 1995 | Pijls [21] | 60 | IV adenosine infusion (140 μg/kg/min) | EST, SPECT, DSE | 0.74 | 97 | Single vessel CAD |
| 1995 | Tron [44] | 70 | IC adenosine bolus (up to 40–60 μg) | SPECT | 0.69 | 67 | Multivessel CAD |
| 1995 | De Bruyne [37] | 60 | IC papaverine (up to 8–12 μg) and adenosine bolus (up to 12–18 μg) | EST, SPECT | 0.66 | 87 | Single vessel CAD |
| 1996 | Pijls [38] | 45 | IV adenosine infusion (140 μg/kg/min) | DSE | 0.75 | 93 | Single vessel CAD |
| 1996 | Bartunek [52] | 75 | IC papaverine (up to 8–12 μg) and adenosine bolus (up to 12–18 μg) | DSE | 0.75 | 81 | Single vessel CAD |
| 1997 | Bartunek [45] | 37 | IC adenosine bolus (up to 40–60 μg) | DSE | 0.67 | 90 | Single vessel CAD |
| 2000 | Caymaz [46] | 40 | IC adenosine bolus (up to 40–60 μg) | SPECT | 0.75 | 95 | Single vessel CAD |
| 2000 | Fearon [47] | 10 | IC adenosine bolus (up to 40–60 μg) | SPECT | 0.75 | 95 | Single vessel CAD |
| 2000 | Abe [53] | 46 | IV ATP infusion (150 μg/kg/min) | SPECT | 0.75 | 91 | Single vessel CAD |
| 2001 | Jimenez-Navarro [40] | 21 | IV adenosine infusion (140 μg/kg/min) | SPECT, DSE | 0.75 | 90 | Single vessel CAD |
| 2001 | Chamuleau [48] | 161 | IC adenosine bolus (up to 40–60 μg) | SPECT | 0.74 | 77 | Multivessel CAD |
| 2001 | De Bruyne [54] | 57 | IV adenosine infusion (150 μg/kg/min; IC adenosine bolus (40 μg); IC ATP bolus (40 μg) | SPECT | 0.78 | 85 | Previous MI |
| 2002 | Seo [49] | 25 | IC adenosine bolus (up to 40–60 μg) | SPECT | 0.75 | 60 | Previous MI |
| 2002 | Yanagisawa [55] | 194 | IC papaverine (up to 8–12 μg) | SPECT | 0.75 | 76 | Previous MI |
| 2004 | Zlaee [56] | 55 | IV adenosine infusion (140 μg/kg/min; IC adenosine bolus (up to 30–50 μg) | EST, SPECT, DSE | 0.75 | 88 | Ostial lesions |
| 2004 | Rieber [41] | 48 | IV adenosine infusion (140 μg/kg/min) | SPECT | 0.75 | 76-81 | Multivessel CAD |
| 2004 | Morishima [57] | 20 | IC ATP bolus (40 μg) | SPECT | 0.75 | 85 | Single vessel CAD |
| 2005 | Erhard [42] | 47 | IV adenosine infusion (140 μg/kg/min) | SPECT, DSE | 0.75 | 77 | Multivessel CAD |
| 2005 | Hacker [43] | 50 | IV adenosine infusion (140 μg/kg/min) | SPECT | 0.75 | 86 | Single vessel CAD |
| 2005 | Kruger [50] | 42 | IC adenosine bolus (up to 40–60 μg) | SPECT | 0.75 | 88 | ISR |
| 2005 | Kobori [58] | 156 | IC papaverine (up to 8–12 μg) | SPECT | 0.75 | 70 | ISR |

(continued)

**Table 14.1** Studies comparing FFR with noninvasive stress testing to assess myocardial ischemia

| Year | Author | Lesions (n) | Hyperemic stimulus | Ischemic test | Best FFR cut-off value | Accuracy (%) | Clinical setting |
|---|---|---|---|---|---|---|---|
| 2006 | Samady [51] | 48 | IC adenosine bolus (up to 40–60 μg) | SPECT, DSE | 0.78 | 92 | Previous MI |
| 2007 | Ragosta [59] | 36 | IC adenosine bolus (up to 30–100 μg) | SPECT | 0.75 | 69 | Multivessel CAD |
| 2012 | Van der Hoef [60] | 299 | IC adenosine bolus (up to 40–60 μg) | SPECT | 0.76 | 74 | Multivessel CAD |

*ATP* adenosine triphosphate disodium, *CAD* coronary artery disease, *DES* dobutamine stress echocardiogram, *EST* exercise stress test, *IC* intracoronary, *ISR* instent restenosis, *IV* intravenous, *MI* myocardial infarction, *SPECT* single-photon emission scintigraphy

**Table 14.2** Drugs used to achieve hyperemia during FFR evaluation in the catheterization laboratory

| Method of administration | Dose range | Plateau | Half-life | Side effects |
|---|---|---|---|---|
| Papaverine IC | 8–20 mg | 2 min | 2 h | QT prolongation, T-wave changes; ventricular dysrhythmias |
| Adenosine IC and IV | 60–600 μg IC, 140 μg/kg/min IV | 30–60 sec | 1–2 min 10 sec | IC: AV block; IV: hypotension; burning or angina-like chest pain during infusion |
| NTP IC | 0.3–0.9 μg/kg | 1 min | 2 min | Headache, hypotension, cyanide toxicity |
| ATP IC and IV | 20–40 mg IC, 140 μg/kg/min IV | 30–60 sec | 1–2 min 60–120 sec | IC: AV block; IV: hypotension; burning or angina-like chest pain during infusion |

*ATP* adenosine triphosphate disodium, *AV* atrioventricular, *CM* contrast medium, *h* hours, *IC* intracoronary, *IV* intravenous, *min* minutes, *NTP* sodium nitroprusside, *sec* seconds

FAME 2 studies [60, 61]. However, the concept of a fixed cut-off has been recently challenged by a meta-analysis suggesting that FFR demonstrates a continuous and independent relationship with subsequent outcomes, with lesions having lower FFR values receive larger absolute benefits from revascularization [62].

Finally, it should be emphasized that FFR has a high reproducibility as shown in a study with serial FFR measurement in 325 patients in whom FFR was measured twice within a 10-min interval (*R* of correlation = 0.983) [37].

## 14.4 Practicalities

FFR can be measured using one of the commercially available pressure wires produced by two companies: St. Jude Medical and the Volcano Corporation. Both systems employ 0.014-in wires with pressure sensors positioned 3 cm from the tip of the wire at the junction of the radiopaque and radiolucent portion of the wire. Recently, a micro-catheter system (ACIST|RXi™ Rapid Exchange FFR System, Acist Medical Systems, Minnesota, USA) mounted on a standard coronary guidewire has been proposed for FFR assessment, but needs to be validated in large clinical studies. Most operators prefer to use 6-French guiding catheters, but FFR can be measured through 5- and 4-French systems. Intracoronary nitroglycerin at 100–200 μg is administered to induce epicardial vasodilation; this attenuates resistance induced by epicardial vascular tone. The pressure wire is connected to the system's console, and it is calibrated and advanced out of the guiding catheter until the sensor is positioned at the catheter's ostium. In this position, the pressure wire is equalized to the guiding catheter pressure. The wire is then advanced to the distal two-thirds of the vessel being investigated. Once the sensor is distal to the stenosis, a maximum hyperemic stimulus is administered for complete evaluation of the physiologic significance of the lesions and FFR assessment. It is important to remember that the greater the flow across a particular stenosis, the greater the gradient and the lower the FFR. Thus, achieving maximal hyperemia is of paramount importance for FFR accuracy. Several drugs, administered IC or IV, have been shown to induce hyperemia suitable for invasive evaluation of coronary stenosis; among these, adenosine, in particular administered intravenously, is currently considered the reference standard (Table 14.2).

### 14.4.1 Inducing Hyperemia

## Adenosine

FFR was originally validated using IV adenosine administered via a central vein at a dose of 140 μg/kg/min [63–65]. Adenosine is a natural nucleoside synthesized by the heart, by dephosphorylation of adenosine triphosphate (ATP) or cyclic adenosine monophosphate, under physiological conditions due to an increase in metabolic demand or in pathological conditions due to ischemia, and it is responsible for angina pain due to stimulation of cardiac-sensitive nerve fibers [65]. By binding to A2 receptors on smooth muscle cells of arterioles, it causes vasodilatation of the microvascular bed [65]. Due to its short half-life (< 20 s), an IV infusion allows longer hyperemia. When given intravenously, it induces hyperemia relatively rapidly (within 60–90 s after the start of the infusion), and hyperemia persists for the duration of the infusion, with an effect that disappears within 1 min after cessation of administration. This allows careful study of long lesions or multiple stenoses using the pullback technique or ostial stenosis, by disengaging the guiding catheter. Patients often experience chest discomfort, shortness of breath, and a rather characteristic facial flush during the infusion, and these may limit the tolerability of the test. These effects, absolutely normal and related to the mechanisms of action of adenosine, should never be confused with those characteristics of myocardial ischemia [65]. Due to its bronchoconstrictive action, IV adenosine should be avoided in patients with a history of severe chronic obstructive pulmonary disease or asthma. Atrioventricular blocks are not very common with continuous infusion of adenosine intravenously. The hemodynamic response to IV adenosine is generally characterized by a pressure drop of 10–20% and an increase in heart rate, unless overridden by the direct effect of heart rate lowering of adenosine itself. In general a central vein ensures a greater stability in hyperemia. However, use of a peripheral vein has an efficacy comparable to that obtained with IV adenosine via the central route using the dose of 140 μg/kg/min [63, 64]. The dosage may be increased to 170–180 μg/kg/min [64] (Tables 14.3 and 14.4) to ensure maximum hyperemia is achieved. It is important to ensure the patient avoids deep breathing (common temptation to alleviate the sensation of breathlessness typical of the adenosine) to avoid altering the venous return to the heart. Tables 14.3 and 14.4 show the methods of preparation and administration of various compositions of adenosine.

There is a large body of evidence on the safety and the efficacy of adenosine administered IC [66–68]. It is well known that the effect of IC adenosine reaches a peak within 10 s of administration, but the duration of action is less than 20 s. Intracoronary adenosine allows a more rapid and economic induction of hyperemia, free from a series of systemic effects of IV adenosine described above but has a not negligible rate of transient atrioventricular blocks (especially in the administration in the right coronary artery). Despite the wealth of data available and the extensive use made of it in the real world instead of IV adenosine, surprisingly the optimal dosage of IC adenosine is not yet well established. However, it is evident that doses initially proposed (15–20 μg for the right coronary artery and 18–24 μg for the left coronary artery) [66–69] are associated with an overestimation of FFR value in

**Table 14.3** Nomogram for intravenous administration of adenosine (galenic preparation) and adenoscan vials during FFR evaluation in the catheterization laboratory

| Adenosine (galenic preparation – 200 mg of adenosine in a 100ml bag of NaCl) | |
|---|---|
| Weight of patient (Kg) | Infusion rate (ml/h) |
| 50 | 210 |
| 60 | 252 |
| 70 | 294 |
| 80 | 336 |
| 90 | 378 |
| 100 | 420 |
| **ADENOSCAN® vials (30 mg of adenosine in 10 ml)** | |
| Weight of patient (Kg) | Length of infusion: 2min |
| 50 | 2.3 |
| 60 | 2.8 |
| 70 | 3.3 |
| 80 | 3.7 |
| 90 | 4.2 |
| 100 | 4.7 |

**Table 14.4** Nomogram for intravenous administration of vials of Adenocor or Krenosin during FFR evaluation in the catheterization laboratory

| Adenocor or Krenosin vials (6 mg of adenosine in 2 ml) | | | | |
|---|---|---|---|---|
| N of vials for 140 μg/Kg/min | | | | |
| N of vials for 180 μg/Kg/min | | | | |
| Posiology | | | | |
| Weight of patient (Kg) | Length of infusion: 2min | Length of infusion: 3min | Length of infusion: 2min | Length of infusion: 3min |
| 50 | 2.3 | 3.5 | 3.0 | 4.5 |
| 60 | 2.8 | 4.2 | 3.6 | 5.4 |
| 70 | 3.3 | 4.9 | 4.2 | 6.3 |
| 80 | 3.7 | 5.6 | 4.8 | 7.2 |
| 90 | 4.2 | 6.3 | 5.4 | 8.1 |
| 100 | 4.7 | 7.0 | 6.0 | 9.0 |
| Vials diluted in 0.9% saline up to 60 ml of solution, infused in 2 or 3 minutes by hand | | | | |

up to 10 % of cases [66, 67]. Recent studies demonstrate that the use of high doses of adenosine up to 600 μg is safe and has a comparable efficacy to IV adenosine notwithstanding that progressive increases in doses increase the likelihood of transient atrioventricular block [69, 70]. A prudent approach may be to administer incremental doses of IC adenosine (e.g., from 60–600 μg) moving to the IV route if atrioventricular block develops or in cases close to the threshold of significance (i.e., between 0.81 and 0.83) [70]. From a practical point of view, it is necessary to emphasize the need to avoid the use of catheters with side holes, to limit the interruption of the $P_a$ signal, given the short duration of action of adenosine IC and to flush the catheter as rapidly as possible. Finally, it is important that the mean signal should not be averaged for more than three beats to avoid erroneous FFR readings.

It should be noted that methylxanthines such as caffeine, by blocking the receptors for A2A, prevent the hyperemic response to adenosine [71]. Therefore, although there is sparse evidence on the effect of caffeine on FFR, it is prudent to advise patients to avoid consuming coffee or tea for at least 24 h before the procedure [71].

## Papaverine

The IC injection of papaverine induces an effective and stable maximal coronary hyperemia; the peak effect is reached after 10–30 s, and the duration of the plateau is around 45–60 s [72]. The recommended dose is 12–16 mg in the right coronary and 16–20 mg in the left coronary artery. Papaverine was one of the first hyperemia-inducing drugs tested. Despite a vast body of evidence supporting the mode of action and effectiveness, the use of papaverine is limited by its proarrhythmic action. Indeed, it can prolong the QT interval, potentially leading to polymorphic ventricular tachycardia and ventricular fibrillation (1–2 % of cases) [73, 74]. For this reason it is mandatory to correct hypokalemia before the procedure and to advise patients to not take other medicines that lengthen the QT interval, to minimize the risk of these potentially fatal arrhythmias. In addition, coadministration with some contrast media may cause crystallization [74]. However, its prolonged duration of action allows pullback maneuvers, but this also means that at least 5 min is required between measurements to allow the $P_d/P_a$ to return to baseline. In conclusion papaverine is considered a second-level hyperemic agent reserved for carefully considered cases with absolute contraindication to adenosine.

## Sodium Nitroprusside

As its action does not depend on any specific adrenergic receptor, unlike antagonists of the sympathetic system, sodium nitroprusside does not change the regional distribution of blood flow [75, 76]. In the coronary arteries, this drug acts as an inducer of vasodilation, through the stimulation of the release of nitric oxide [77]. Its use was initially restricted to the treatment of the phenomenon of no reflow, rather than the evaluation of coronary stenosis. For measurement of FFR, the dose of 0.6 μg/Kg has been proven to document mean FFR values and FFR ≤0.80 comparable to IC adenosine with a duration of maximal hyperemia 25 % higher than that obtained with IC adenosine. Unfortunately, these favorable effects are counterbalanced by a significant reduction in blood pressure, although rapidly reversible, that can not only make this drug uncomfortable for the patient but also affect the accuracy of FFR assessment [78]. Finally, nitroprusside lacks validation in large clinical trials [6]. Overall sodium nitroprusside should be seen as second-choice hyperemic agent to be reserved for cases with absolute contraindication to adenosine.

## Other Vasodilators

Adenosine 5′-triphosphate (ATP) has a short plasma half-life and is rapidly degraded to ADP, AMP, and adenosine. Although the effects of ATP depend on its degradation to adenosine, it cannot be ruled out a direct action on adenosine receptors or on purine receptors P2. Indeed, doses between 15 and 50 μg of IC ATP induce the same degree of vasodilation as 10 mg of papaverine without any change in hemodynamics or in the electrocardiographic waveform [79, 80]. The use of IC ATP was first described by Japanese investigators and mostly used in Japan. It produces less chest discomfort as compared to adenosine, with similar blood pressure reduction (10–15 %) and heart rate increase (10–15 %).

Drugs that are widely used for noninvasive stress testing such as dobutamine (10–40 μg/Kg per minute) or dipyridamole (0.56–0.84 mg/kg) have been occasionally used for FFR assessment but due to practical reasons (longer time for induction of hyperemia for dobutamine, side effects) are not commonly used in the catheterization laboratory [81, 82].

Finally, there is ongoing interest in the development of an easy to administer, effective, and safe hyperemic inducer based on synthetic derivatives selective for the adenosine A2A receptor, such as regadenoson [83–85]. This would have the advantage of avoiding the side effects; dependent receptor stimulation of A1, A2B, and A3A receptors; and characteristics of adenosine such as bronchospasm, dyspnea, and chrono- and dromotropic negative effects. Despite the vast experience available in the field of nuclear medicine, there is little data available regarding their use in FFR. However, it appears they have comparable effectiveness to IV adenosine, with fewer side effects, a more rapid action, and a fixed dose independent of the weight [85].

Nonionic radiographic contrast medium, routinely used during coronary angiography, has been demonstrated to induce hyperemia, although inferior to adenosine [86]. Thus, it is conceivable that the *Pd*/*Pa* ratio registered by pressure wire during reactive hyperemia induced by IC injection of conventional nonionic contrast medium may be sufficient for the assessment of physiological severity of stenosis in a large number of cases, avoiding the drawbacks of adenosine injection. In this context, the RINASCI study [87] demonstrated that contrast medium-induced $P_d/P_a$ ratio (CMR), a novel index calculated as $P_d/P_a$ after the induction of submaximal hyperemia using IC injection of standard radiographic contrast medium, is accurate in predicting the functional significance of intermediate coronary artery stenosis assessed by FFR. Moreover, in

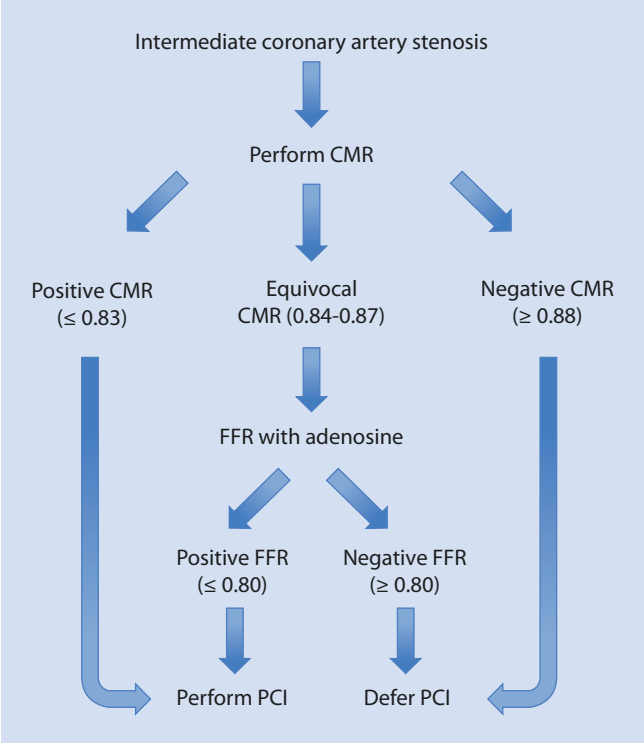


**Fig. 14.7** Algorithm proposed by the RINASCI study for the measurement of fractional flow reserve (FFR) with sequential utilization of contrast medium and intracoronary (IC) and intravenous (IV) adenosine to obtain maximal coronary vasodilation.

A contrast medium-induced $P_d/P_a$ ratio (CMR) value ≤ 0.83 is considered significant, and consequently performing percutaneous coronary intervention (PCI) is recommended; a CMR value ≥ 0.88 is judged not significant and therefore deferring PCI is suggested; a CMR value between 0.84 and 0.87 is considered doubtful, therefore requiring to induce maximal hyperemia using IC or IV adenosine for FFR assessment; finally, if FFR measured during intravenous adenosine is ≤ 0.80, PCI is recommended (Adapted from Ref. [87])

this study, the authors proposed an algorithm for the measurement of FFR using sequential utilization of CMR and IC and IV adenosine to obtain maximal coronary vasodilation. In particular, a CMR value ≤ 0.83 is considered significant and consequently performing PCI is recommended; a CMR value ≥ 0.88 is judged not significant and therefore deferring PCI is suggested; a CMR value between 0.84 and 0.87 is considered doubtful, therefore requiring induction of maximal hyperemia using IC or IV adenosine for FFR assessment; finally, if FFR measured during IV adenosine is ≤0.80, PCI is recommended (Fig. 14.7) showing that contrast induced Pd/Pa (also called cFFR) provides diagnostic performance superior to that of resting indexes for predicting FFR [88, 89].

## 14.4.2 Avoiding Practical Pitfalls

### Needles, Y-Connector, and Equalization

Reduction of fluid-filled pressure (aortic) due to backflow either through the introducer needle or the Y-connector should be avoided as they may produce falsely high FFR. Thus, the needle introducer should be withdrawn and the Y-connector tightly closed during FFR measurement to avoid loss of aortic pressure [4, 19]. Importantly, once the pressure wire has reached the coronary ostium, pressure measured by the catheter end hole and that measured by the wire needs to be equalized [4, 19, 90]. The radiopaque marker of the wire should be positioned 1–2 mm outside of the catheter tip. Differences in aortic and wire pressures may be due to inappropriate height of the fluid-filled pressure transducer that should be positioned 5 cm below the patient's sternum (the estimated location of the aortic root). Electronic equalization should be done after proper flushing and is essential in order to start the vessel interrogation with the same pressure at the origin of the coronary [4, 19, 90].

### Guiding Catheter

When performing coronary pressure measurements, it is advisable to use at most a 6-F catheter. If using a larger guide, an additional gradient between the aorta and the proximal coronary artery will be created either at rest or during maximum hyperemia by the presence of the guiding catheter. This situation is recognized by damping or ventricularization of the pressure signal recorded by the guiding catheter [91]. It is important to stress that this "damping" is often only unmasked by hyperemia, leading to an underestimation of the hyperemic gradient across the coronary artery stenosis and a corresponding overestimation of FFR. Disengaging the guiding catheter, leaving the pressure wire in the distal vessel, and using an IV instead of an IC hyperemic stimulus can prevent this. This should also be considered with smaller guiding catheters in the presence of ostial disease or an anatomically small ostium.

Catheters with side holes should be avoided when using IC hyperemic stimuli, as the delivered dose of the drug will be unpredictable. Furthermore, the pressure measured by the fluid-filled transducers will be influenced by the pressure at the tip of the catheter (coronary pressure) and by the pressure at the side holes (aortic pressure). Thus, if guiding catheters with side holes are the only option, one should remember to disengage the guiding catheter after injection of the hyperemic stimuli; however preferably IV hyperemic agents should be used.

### Intra-Procedural Pitfalls: Drift, Whipping, Accordion Effect

Particularly after long procedures, a gradient between aortic and distal pressures may occur; this however is not a true pressure gradient. This phenomenon is known as electronic drift. In order to differentiate a true gradient from a drift, one should check the morphology of the distal pressure curve. If the shape of the curves is almost identical, this is a clear evidence of drift as distal pressure usually ventricularizes in case of a true gradient. In particular, if the aortic notch is present in the distal pressure signal with an important gradient, drift should be suspected. Due to preferential contribution of the diastolic flow in the left coronary system as compared to the right coronary system (where a systolic contribution is well

recognized), drift may be more difficult to be identified in the right coronary artery. In this case, it may be useful to pull back the guidewire, check for the presence of drift, and eventually re-equalize the pressure tracings, or, if rechecking the stenosis is not possible, the value of the drift can be inserted into the FFR formula and FFR manually calculated (e.g., FFR = $P_d \pm$ drift value/$P_a$). Post-PCI current large clinical studies suggest that a drift of ±2 mmHg is tolerated. Otherwise, it is better to re-equalize and check distal pressure under hyperemia for more accurate FFR values. Flushing the guiding catheter with saline to remove contrast will occasionally eliminate this apparent drift. Finally, pullback studies during IV adenosine may help clarify the presence of drift (by comparing the pressure just distal to the stenosis of interest to the pressure proximal to that stenosis) and the significance of an apparently "new" gradient after stenting (drift vs. unmasking the hemodynamic effects of proximal plaques due to increased blood flow).

Whipping is easily recognized by the presence of a spike in the pressure tracing due to the hit of the wire against the coronary wall. Changing wire position usually solves this artifact. Furthermore, the accordion effect due to folds of the vessel walls in tortuous vessels that is induced by the wire may cause false pressure gradients. Again, pulling back the wire solves this phenomenon.

### Guidewire Disconnection for PCI

The FFR wire can be disconnected, used as a PCI wire, and reconnected in order to assess post-PCI FFR values. It is important to clean the distal 2.5 cm (where the electrodes are positioned) with wet gauzes and dry thoroughly before reconnection to the interface connector; otherwise measurements may be inaccurate.

### Modulation of Stenosis Severity by Vasoconstriction

In some cases patients may have a moderate stenosis (non-ischemia producing) that is aggravated by exertion (becoming ischemia producing) causing abnormal stress test results. However, when measuring FFR with a hyperemic stimulus, vasoconstriction does not occur, and FFR will be non-ischemic. This should be considered when there are discrepancies between stress testing and FFR in the case of a single-vessel moderate stenosis [91].

## 14.5 Conclusion

Due to limitations in the assessment of coronary stenosis severity, coronary angiography is increasingly supported by invasive functional evaluation of coronary stenosis especially when such narrowings are deemed angiographically intermediate. FFR was introduced and validated in the late 1980s and early 1990s and is currently recommended in the guidelines on myocardial revascularization. However, an appropriate understanding of the basic principles and assumptions leading to FFR calculation is necessary in order to avoid mistakes in patient management. In particular, the role of hyperemia is of paramount importance for FFR assessment. Finally, some practical points regarding the use of guidewires and the steps in FFR acquisition should be borne in mind in order to appropriately diagnose and treat patients affected by coronary artery disease.

## References

1. Mintz GS, Popma JJ, Pichard AD, Kent KM, Satler LF, Chuang YC, DeFalco RA, Leon MB. Limitations of angiography in the assessment of plaque distribution in coronary artery disease: a systematic study of target lesion eccentricity in 1446 lesions. Circulation. 1996;93:924–31.
2. Topol EJ, Nissen SE. Our preoccupation with coronary luminology. The dissociation between clinical and angiographic findings in ischemic heart disease. Circulation. 1995;92:2333–42.
3. Tobis J, Azarbal B, Slavin L. Assessment of intermediate severity coronary lesions in the catheterization laboratory. J Am Coll Cardiol. 2007;49:839–48.
4. Kern MJ, Lerman A, Bech JW, De Bruyne B, Eeckhout E, Fearon WF, Higano ST, Lim MJ, Meuwissen M, Piek JJ, Pijls NH, Siebes M, Spaan JA, American Heart Association Committee on Diagnostic and Interventional Cardiac Catheterization, Council on Clinical Cardiology. Physiological assessment of coronary artery disease in the cardiac catheterization laboratory: a scientific statement from the American Heart Association Committee on Diagnostic and Interventional Cardiac Catheterization, Council on Clinical Cardiology. Circulation. 2006;114:1321–41.
5. Van de Hoef TP, Meuwissen M, Escaned J, Davies JE, Siebes M, Spaan JA, Piek JJ. Fractional flow reserve as a surrogate for inducible myocardial ischaemia. Nat Rev Cardiol. 2013;10:439–52.
6. Fearon WF. Invasive coronary physiology for assessing intermediate lesions. Circ Cardiovasc Interv. 2015;8:001942.
7. Task Force on Myocardial Revascularization of the European Society of Cardiology (ESC) and the European Association for Cardio-Thoracic Surgery (EACTS), European Association for Percutaneous Cardiovascular Interventions (EAPCI), Wijns W, Kolh P, Danchin N, Di Mario C, Falk V, Folliguet T, Garg S, Huber K, James S, Knuuti J, Lopez-Sendon J, Marco J, Menicanti L, Ostojic M, Piepoli MF, Pirlet C, Pomar JL, Reifart N, Ribichini FL, Schalij MJ, Sergeant P, Serruys PW, Silber S, Sousa Uva M, Taggart D. Guidelines on myocardial revascularization. Eur Heart J. 2010;31:2501–55.
8. Deussen A, Ohanyan V, Jannasch A, Yin L, Chilian W. Mechanisms of metabolic coronary flow regulation. J Mol Cell Cardiol. 2012;52:794–801.
9. Mosher P, Ross Jr J, Mcfate PA, Shaw RF. Control of coronary blood flow by an autoregulatory mechanism. Circ Res. 1964;14:250–9.
10. Di Mario C, Krams R, Gil R, Serruys PW. Slope of the instantaneous hyperemic diastolic coronary flow velocity-pressure relation. A new index for assessment of the physiological significance of coronary stenosis in humans. Circulation. 1994;90:1215–24.
11. Spaan JA. Coronary diastolic pressure-flow relation and zero flow pressure explained on the basis of intramyocardial compliance. Circ Res. 1985;56:293–309.
12. van de Hoef TP, Meuwissen M, Piek JJ. Fractional flow reserve and beyond. Heart. 2013;99:1699–705.
13. Gould KL, Lipscomb K, Hamilton GW. Physiologic basis for assessing critical coronary stenosis. Instantaneous flow response and regional distribution during coronary hyperemia as measures of coronary flow reserve. Am J Cardiol. 1974;33:87–94.
14. Baumgart D, Haude M, Liu F, Ge J, Goerge G, Erbel R. Current concepts of coronary flow reserve for clinical decision making during cardiac catheterization. Am Heart J. 1998;136:136–49.
15. Gould KL, Kirkeeide RL, Buchi M. Coronary flow reserve as a physiologic measure of stenosis severity. J Am Coll Cardiol. 1990;15:459–74.

16. Chareonthaitawee P, Kaufmann PA, Rimoldi O, Camici PG. Heterogeneity of resting and hyperemic myocardial blood flow in healthy humans. Cardiovasc Res. 2001;50:151–61.
17. McGinn AL, White CW, Wilson RF. Interstudy variability of coronary flow reserve: influence of heart rate, arterial pressure, and ventricular preload. Circulation. 1990;81:1319–30.
18. Hoffman JI. Problems of coronary flow reserve. Ann Biomed Eng. 2000;28:884–96.
19. Pijls NH, Sels JW. Functional measurement of coronary stenosis. J Am Coll Cardiol. 2012;59:1045–57.
20. Pijls NH, van Son JA, Kirkeeide RL, De Bruyne B, Gould KL. Experimental basis of determining maximum coronary, myocardial, and collateral blood flow by pressure measurements for assessing functional stenosis severity before and after percutaneous transluminal coronary angioplasty. Circulation. 1993;87:1354–67.
21. Pijls NH, Van Gelder B, Van der Voort P, Peels K, Bracke FA, Bonnier HJ, el Gamal MI. Fractional flow reserve. A useful index to evaluate the influence of an epicardial coronary stenosis on myocardial blood flow. Circulation. 1995;92:3183–93.
22. de Bruyne B, Bartunek J, Sys SU, Pijls NH, Heyndrickx GR, Wijns W. Simultaneous coronary pressure and flow velocity measurements in humans. Feasibility, reproducibility, and hemodynamic dependence of coronary flow velocity reserve, hyperemic flow versus pressure slope index, and fractional flow reserve. Circulation. 1996;94:1842–9.
23. Pijls NH, De Bruyne B. Coronary pressure. 2nd ed. Dordrecht: Kluwer Academic Publisher; 2000.
24. Grattan MT, Hanley FL, Stevens MB, Hoffman JI. Transmural coronary flow reserve patterns in dogs. Am J Physiol. 1986;250:H276–83.
25. Spaan JA, Piek JJ, Hoffman JI, Siebes M. Physiological basis of clinically used coronary hemodynamic indices. Circulation. 2006;113:446–55.
26. Meuwissen M, Chamuleau SA, Siebes M, Schotborgh CE, Koch KT, de Winter RJ, Bax M, de Jong A, Spaan JA, Piek JJ. Role of variability in microvascular resistance on fractional flow reserve and coronary blood flow velocity reserve in intermediate coronary lesions. Circulation. 2001;103:184–7.
27. Johnson NP, Kirkeeide RL, Gould KL. Is discordance of coronary flow reserve and fractional flow reserve due to methodology or clinically relevant coronary pathophysiology? J Am Coll Cardiol Img. 2012;5:193–202.
28. Van de Hoef TP, Nolte F, Echavarria Pinto M, van Lavieren MA, Damman P, Chamuleau SAJ, Voskuil M, Verberne HJ, Henriques JPS, van Eck-Smit BLF, Koch KT, de Winter RJ, Spaan JAE, Siebes M, Tijssen JGP, Meuwissen M, Piek JJ. Impact of hyperaemic microvascular resistance on fractional flow reserve measurements in patients with stable coronary artery disease: insights from combined stenosis and microvascular resistance assessment. Heart. 2014;100:951–9.
29. Echavarria-Pinto M, van de Hoef TP, Serruys PW, Piek JJ, Escaned J. Facing the complexity of ischaemic heart disease with intracoronary pressure and flow measurements: beyond fractional flow reserve interrogation of the coronary circulation. Curr Opin Cardiol. 2014;29:564–70.
30. Echavarria-Pinto M, Escaned J, Macias E, Medina M, Gonzalo N, Petraco R, Sen S, Jimenez-Quevedo P, Hernandez R, Mila R, Ibanez B, Nunez-Gil IJ, Fernandez C, Alfonso F, Banuelos C, Garcia E, Davies J, Fernandez-Ortiz A, Macaya C. Disturbed coronary hemodynamics in vessels with intermediate stenoses evaluated with fractional flow reserve: a combined analysis of epicardial and microcirculatory involvement in ischemic heart disease. Circulation. 2013;128:2557–66.
31. van de Hoef TP, van Lavieren MA, Damman P, Delewi R, Piek MA, Chamuleau SA, Voskuil M, Henriques JP, Koch KT, de Winter RJ, Spaan JA, Siebes M, Tijssen JG, Meuwissen M, Piek JJ. Physiological basis and long-term clinical outcome of discordance between fractional flow reserve and coronary flow velocity reserve in coronary stenoses of intermediate severity. Circ Cardiovasc Interv. 2014;7:301–11.
32. van de Hoef TP, Bax M, Damman P, Delewi R, Hassell ME, Piek MA, Chamuleau SA, Voskuil M, van Eck-Smit BL, Verberne HJ, Henriques JP, Koch KT, de Winter RJ, Tijssen JG, Piek JJ, Meuwissen M. Impaired coronary autoregulation is associated with long-term fatal events in patients with stable coronary artery disease. Circ Cardiovasc Interv. 2013;6:329–35.
33. Gross GJ, Warltier DC. Coronary steal in four models of single or multiple vessel obstruction in dogs. Am J Cardiol. 1981;48:84–92.
34. Christou MA, Siontis GC, Katritsis DG, Ioannidis JP. Meta-analysis of and fractional flow reserve versus quantitative coronary angiography noninvasive imaging for evaluation of myocardial ischemia. Am J Cardiol. 2007;99:450–6.
35. De Bruyne B, Bartunek J, Sys SU, Heyndrickx GR. Relation between myocardial fractional flow reserve calculated from coronary pressure measurements and exercise-induced myocardial ischemia. Circulation. 1995;92:39–46.
36. Pijls NH, De Bruyne B, Peels K, Van Der Voort PH, Bonnier HJ, Bartunek J, Koolen JJ, Koolen JJ. Measurement of fractional flow reserve to assess the functional severity of coronary-artery stenoses. N Engl J Med. 1996;334:1703–8.
37. Bech GJ, De Bruyne B, Pijls NH, de Muinck ED, Hoorntje JC, Escaned J, Stella PR, Boersma E, Bartunek J, Koolen JJ, Wijns W. Fractional flow reserve to determine the appropriateness of angioplasty in moderate coronary stenosis: a randomized trial. Circulation. 2001;103:2928–34.
38. Jiménez-Navarro M, Alonso-Briales JH, Hernández García MJ, Rodríguez Bailón I, Gómez-Doblas JJ, de Teresa Galván E. Measurement of fractional flow reserve to assess moderately severe coronary lesions: correlation with dobutamine stress echocardiography. J Interv Cardiol. 2001;14:499–504.
39. Rieber J, Jung P, Erhard I, Koenig A, Hacker M, Schiele TM, Segmiller T, Stempfle HU, Theisen K, Siebert U, Klauss V. Comparison of pressure measurement, dobutamine contrast stress echocardiography and SPECT for the evaluation of intermediate coronary stenoses. The COMPRESS trial. Int J Cardiovasc Intervent. 2004;6:142–7.
40. Erhard I, Rieber J, Jung P, Hacker M, Schiele T, Stempfle HU, König A, Baylacher M, Theisen K, Siebert U, Klauss V. The validation of fractional flow reserve in patients with coronary multivessel disease: a comparison with SPECT and contrast-enhanced dobutamine stress echocardiography. Z Kardiol. 2005;94:321–7.
41. Hacker M, Rieber J, Schmid R, Lafougere C, Tausig A, Theisen K, Klaus V, Tiling R. Comparison of Tc-99m sestamibi SPECT with fractional flow reserve in patients with intermediate coronary artery stenoses. J Nucl Cardiol. 2005;12:645–54.
42. Tron C, Donohue TJ, Bach RG, Aguirre FV, Caracciolo EA, Wolford TL, Miller DD, Kern MJ. Comparison of pressure-derived fractional flow reserve with poststenotic coronary flow velocity reserve for prediction of stress myocardial perfusion imaging results. Am Heart J. 1995;130:723–33.
43. Bartunek J, Van Schuerbeeck E, de Bruyne B. Comparison of exercise electrocardiography and dobutamine echocardiography with invasively assessed myocardial fractional flow reserve in evaluation of severity of coronary arterial narrowing. Am J Cardiol. 1997;79:478–81.
44. Caymaz O, Fak AS, Tezcan H, Inanir SS, Toprak A, Tokay S, Turoglu T, Oktay A. Correlation of myocardial fractional flow reserve with thallium-201 SPECT imaging in intermediate-severity coronary artery lesions. J Invasive Cardiol. 2000;12:345–50.
45. Fearon WF, Takagi A, Jeremias A, Yeung AC, Joye JD, Cohen DJ, Chou TM, Kern MJ, Yock PG. Use of fractional myocardial flow reserve to assess the functional significance of intermediate coronary stenoses. Am J Cardiol. 2000;86:1013–4.
46. Chamuleau SA, Meuwissen M, van Eck-Smit BL, Koch KT, de Jong A, de Winter RJ, Schotborgh CE, Bax M, Verberne HJ, Tijssen JG, Piek JJ. Fractional flow reserve, absolute and relative coronary blood flow velocity reserve in relation to the results of technetium-99m sestamibi single-photon emission computed tomography in patients with two-vessel coronary artery disease. J Am Coll Cardiol. 2001;37:1316–22.
47. Seo JK, Kwan J, Suh JH, Kim DH, Lee KH, Hyun IY, Choe WS, Park KS, Lee WH. Early dipyridamole stress myocardial SPECT to detect residual stenosis of infarct related artery: comparison with coronary angiography and fractional flow reserve. Korean J Intern Med. 2002;17:7–13.
48. Krüger S, Koch KC, Kaumanns I, Merx MW, Schäfer WM, Buell U, Hanrath P, Hoffmann R. Use of fractional flow reserve versus stress perfusion scintigraphy in stent restenosis. Eur J Intern Med. 2005;16:429–31.
49. Samady H, Lepper W, Powers ER, Wei K, Ragosta M, Bishop GG, Sarembock IJ, Gimple L, Watson DD, Beller GA, Barringhaus KG.

Fractional flow reserve of infarct-related arteries identifies reversible defects on noninvasive myocardial perfusion imaging early after myocardial infarction. J Am Coll Cardiol. 2006;47:2187–93.
50. Bartunek J, Marwick TH, Rodrigues AC, Vincent M, Van Schuerbeeck E, Sys SU, de Bruyne B. Dobutamine-induced wall motion abnormalities: correlations with myocardial fractional flow reserve and quantitative coronary angiography. J Am Coll Cardiol. 1996;27:1429–36.
51. Abe M, Tomiyama H, Yoshida H, Doba N. Diastolic fractional flow reserve to assess the functional severity of moderate coronary artery stenoses: comparison with fractional flow reserve and coronary flow velocity reserve. Circulation. 2000;102:2365–70.
52. De Bruyne B, Pijls NH, Bartunek J, Kulecki K, Bech JW, De Winter H, Van Crombrugge P, Heyndrickx GR, Wijns W. Fractional flow reserve in patients with prior myocardial infarction. Circulation. 2001;104:157–62.
53. Yanagisawa H, Chikamori T, Tanaka N, Hatano T, Morishima T, Hida S, Iino H, Amaya K, Takazawa K, Yamashina A. Correlation between thallium-201 myocardial perfusion defects and the functional severity of coronary artery stenosis as assessed by pressure-derived myocardial fractional flow reserve. Circ J. 2002;66:1105–9.
54. Ziaee A, Parham WA, Herrmann SC, Stewart RE, Lim MJ, Kern MJ. Lack of relation between imaging and physiology in ostial coronary artery narrowings. Am J Cardiol. 2004;93:1404–7.
55. Morishima T, Chikamori T, Hatano T, Tanaka N, Takazawa K, Yamashina A. Correlation between myocardial uptake of technetium-99m-sestamibi and pressure-derived myocardial fractional flow reserve. J Cardiol. 2004;43:155–63.
56. Kobori Y, Tanaka N, Takazawa K, Yamashina A. Usefulness of fractional flow reserve in determining the indication of target lesion revascularization. Catheter Cardiovasc Interv. 2005;65:355–60.
57. Ragosta M, Bishop AH, Lipson LC, Watson DD, Gimple LW, Sarembock IJ, Powers ER. Comparison between angiography and fractional flow reserve versus single-photon emission computed tomographic myocardial perfusion imaging for determining lesion significance in patients with multivessel coronary disease. Am J Cardiol. 2007;99:896–902.
58. Van de Hoef TP, Nolte F, Damman P, Delewi R, Bax M, Chamuleau SA, Voskuil M, Siebes M, Tijssen JG, Spaan JA, Piek JJ, Meuwissen M. Diagnostic accuracy of combined intracoronary pressure and flow velocity information during baseline conditions: adenosine-free assessment of functional coronary lesion severity. Circ Cardiovasc Interv. 2012;5:508–14.
59. Pijls NH, van Schaardenburgh P, Manoharan G, Boersma E, Bech JW, van't Veer M, bar F, Hoorntje J, Koolen J, Wijns W, de Bruyne B. Percutaneous coronary intervention of functionally non significant stenosis: 5-year follow-up of the DEFER Study. J Am Coll Cardiol. 2007;49:2015–111.
60. Tonino PA, De Bruyne B, Pijls NH, Siebert U, Ikeno F, van't Veer M, Klauss V, Manoharan G, Engstrøm T, Oldroyd KG, Ver Lee PN, MacCarthy PA, Fearon WF, FAME Study Investigators. Fractional flow reserve versus angiography for guiding percutaneous coronary intervention. N Engl J Med. 2009;360:213–24.
61. De Bruyne B, Pijls NH, Kalesan B, Barbato E, Tonino PA, Piroth Z, Jagic N, Möbius-Winkler S, Rioufol G, Witt N, Kala P, MacCarthy P, Engström T, Oldroyd KG, Mavromatis K, Manoharan G, Verlee P, Frobert O, Curzen N, Johnson JB, Jüni P, Fearon WF, FAME 2 Trial Investigators. Fractional flow reserve-guided PCI versus medical therapy in stable coronary disease. N Engl J Med. 2012;367:991–1001.
62. Johnson NP, Tóth GG, Lai D, Zhu H, Açar G, Agostoni P, Appelman Y, Arslan F, Barbato E, Chen SL, Di Serafino L, Domínguez-Franco AJ, Dupouy P, Esen AM, Esen OB, Hamilos M, Iwasaki K, Jensen LO, Jiménez-Navarro MF, Katritsis DG, Kocaman SA, Koo BK, López-Palop R, Lorin JD, Miller LH, Muller O, Nam CW, Oud N, Puymirat E, Rieber J, Rioufol G, Rodés-Cabau J, Sedlis SP, Takeishi Y, Tonino PA, Van Belle E, Verna E, Werner GS, Fearon WF, Pijls NH, De Bruyne B, Gould KL. Prognostic value of fractional flow reserve: linking physiologic severity to clinical outcomes. J Am Coll Cardiol. 2014;64:1641–54.
63. Seo MK, Koo BK, Kim JH, Shin DH, Yang HM, Park KW, Lee HY, Kang HJ, Kim HS, Oh BH, Park YB. Comparison of hyperemic efficacy between central and peripheral venous adenosine infusion for fractional flow reserve measurement. Circ Cardiovasc Interv. 2012;5:401–5.
64. Lindstaedt M, Bojara W, Holland-Letz T, Yazar A, Fadgyas T, Müller L, Mügge A, Germing A. Adenosine-induced maximal coronary hyperemia for myocardial fractional flow reserve measurements: comparison of administration by femoral venous versus antecubital venous access. Clin Res Cardiol. 2009;98:717–23.
65. Wilson RF, Wyche K, Christensen BV, Zimmer S, Laxson DD. Effects of adenosine on human coronary arterial circulation. Circulation. 1990;82:1595–606.
66. Jeremias A, Whitbourn RJ, Filardo SD, Fitzgerald PJ, Cohen DJ, Tuzcu EM, Anderson WD, Abizaid AA, Mintz GS, Yeung AC, Kern MJ, Yock PG. Adequacy of intracoronary versus intravenous adenosine-induced maximal coronary hyperaemia for fractional flow reserve measurements. Am Heart J. 2000;140:651–7.
67. Murtagh B, Higano S, Lennon R, Mathew V, Holmes Jr DR, Lerman A. Role of incremental doses of intracoronary adenosine for fractional flow reserve assessment. Am Heart J. 2003;146:99–105.
68. Casella G, Leibig M, Schiele TM, Schrepf R, Seelig V, Stempfle HU, Erdin P, Rieber J, König A, Siebert U, Klauss V. Are high doses of intracoronary adenosine an alternative to standard intravenous adenosine for the assessment of fractional flow reserve? Am Heart J. 2004;148:590–5.
69. De Luca G, Venegoni L, Iorio S, Giuliani L, Marino P. Effects of increasing doses of intracoronary adenosine on the assessment of fractional flow reserve. JACC Cardiovasc Interv. 2011;4:1079–84.
70. Leone AM, Porto I, De Caterina AR, Basile E, Aurelio A, Gardi A, Russo D, Laezza D, Niccoli G, Burzotta F, Trani C, Mazzari MA, Mongiardo R, Rebuzzi AG, Crea F. Maximal hyperemia in the assessment of fractional flow reserve: intracoronary adenosine versus intracoronary sodium nitroprusside versus intravenous adenosine: the NASCI (Nitroprussiato versus Adenosina nelle Stenosi Coronariche Intermedie) study. JACC Cardiovasc Interv. 2012;5:402–8.
71. Raed AA, Gilbert JZ, Trimm JR, Baldwin SA, Iskandrian AE. Effect of caffeine administered intravenously on intracoronary-administered adenosine-induced coronary hemodynamics in patients with coronary artery disease. Am J Cardiol. 2004;93:343–6.
72. Wilson RF, White CW. Intracoronary papaverine: an ideal coronary vasodilator for studies of the coronary circulation in conscious humans. Circulation. 1986;73:444–51.
73. Inoue T, Asahi S, Takayanagi K, Morooka S, Takabatake Y. QT prolongation and possibility of ventricular arrhythmias after intracoronary papaverine. Cardiology. 1994;84:9–13.
74. Vrolix M, Piessens J, De Geest H. Torsades de pointes after intracoronary papaverine. Eur Heart J. 1991;12:273–6.
75. Gmeiner R, Riedl J, Baumgartner H. Effect of sodium nitroprusside on myocardial performance and venous tone. Eur J Pharmacol. 1975;31:287–91.
76. Cohn JN, Burke LP. Nitroprusside. Ann Intern Med. 1979;91:752–7.
77. Bates JN, Baker MT, Guerra Jr R, et al. Nitric oxide generation from nitroprusside by vascular tissue: evidence that reduction of the nitroprusside ion and cyanide loss are required. Biochem Pharmacol. 1991;42:S157–65.
78. Parham WA, Bouhasin A, Ciaramita JP, Khoukaz S, Herrmann SC, Kern MJ. Coronary hyperemic dose responses of intracoronary sodium nitroprusside. Circulation. 2004;109:1236–43.
79. De Bruyne B, Pijls NH, Barbato E, Bartunek J, Bech JW, Wijns W, Heyndrickx GR. Intracoronary and intravenous adenosine 5′-triphosphate, adenosine, papaverine, and contrast medium to assess fractional flow reserve in humans. Circulation. 2003;15:1877–83.
80. Sonoda S, Takeuchi M, Nakashima Y, Kuroiwa A. Safety and optimal dose of intracoronary adenosine 5′-triphosphate for the measurement of coronary flow reserve. Am Heart J. 1998;135:621–7.
81. Homma S, Gilliland Y, Guiney TE, Strauss HW, Boucher CA. Safety of intravenous dipyridamole for stress testing with thallium imaging. Am J Cardiol. 1987;59:152–4.
82. Bartunek J, Wijns W, Heyndrickx GR, de Bruyne B. Effects of dobutamine on coronary stenosis physiology and morphology: comparison with intracoronary adenosine. Circulation. 1999;100:243–9.
83. Arumugham P, Figueredo VM, Patel PB, Morris DL. Comparison of intravenous adenosine and intravenous regadenoson for the

measurement of pressure-derived coronary fractional flow reserve. EuroIntervention. 2013;8:1166–71.
84. Nair PK, Marroquin OC, Mulukutla SR, Khandhar S, Gulati V, Schindler JT, Lee JS. Clinical utility of regadenoson for assessing fractional flow reserve. JACC Cardiovasc Interv. 2011;4:1085–92.
85. Prasad A, Zareh M, Doherty R, Gopal A, Vora H, Somma K, Mehra A, Clavijo LC, Matthews RV, Shavelle DM. Use of regadenoson for measurement of fractional flow reserve. Catheter Cardiovasc Interv. 2014;83:369–74.
86. Baile EM, Paré PD, D'yachkova Y, Carere RG. Effect of contrast media on coronary vascular resistance: contrast-induced coronary vasodilation. Chest. 1999;116:1039–45.
87. Leone AM, Scalone G, De Maria GL, Tagliaferro F, Gardi A, Clemente F, Basile E, Cialdella P, De Caterina AR, Porto I, Aurigemma C, Burzotta F, Niccoli G, Trani C, Rebuzzi AG, Crea F. Efficacy of contrast medium induced Pd/Pa ratio in predicting functional significance of intermediate coronary artery stenosis assessed by fractional flow reserve: insights from the RINASCI study. EuroIntervention. 2014;11:421–7.
88. Johnson NP, Jeremias A, Zimmermann FM, Adjedj J, Witt N, Hennigan B, Koo BK, Maehara A, Matsumura M, Barbato E, Esposito G, Trimarco B, Rioufol G, Park SJ, Yang HM, Baptista SB, Chrysant GS, Leone AM, Berry C, De Bruyne B, Gould KL, Kirkeeide RL, Oldroyd KG, Pijls NH, Fearon WF. Continuum of vasodilator stress from rest to contrast medium to adenosine hyperemia for fractional flow reserve assessment. JACC Cardiovasc Interv. 2016;9:757–67.
89. Leone AM, Martin-Reyes R, Baptista SB, Amabile N, Raposo L, Franco Pelaez JA, Trani C, Cialdella P, Basile E, Zimbardo G, Burzotta F, Porto I, Aurigemma C, Rebuzzi AG, Faustino M, Niccoli G, Abreu PF, Slama MS, Spagnoli V, Telleria Arrieta M, Amat Santos IJ, de la Torre Hernandez JM, Lopez Palop R, Crea F. The Multi-center Evaluation of the Accuracy of the Contrast MEdium INduced Pd/Pa RaTiO in Predicting FFR (MEMENTO-FFR) Study. EuroIntervention. 2016;12:708–15.
90. Pijls NH, De Bruyne B, Bech GJ, Liistro F, Heyndrickx GR, Bonnier HJ, Koolen JJ. Coronary pressure measurement to assess the hemodynamic significance of serial stenoses within one coronary artery: validation in humans. Circulation. 2000;102:2371–7.
91. Pijls NH, Kern MJ, Yock PG, De Bruyne B. Practice and potential pitfalls of coronary pressure measurement. Catheter Cardiovasc Interv. 2000;49:1–16.

# FFR as a Clinical Tool and Its Applications in Specific Scenarios

*David Neves, Ruben Ramos, Luís Raposo, Sérgio Baptista, and Pedro de Araújo Gonçalves*




J. Escaned, J. Davies (eds.), *Physiological Assessment of Coronary Stenoses and the Microcirculation*,
DOI 10.1007/978-1-4471-5245-3_15

## 15.1 Intermediate Stenosis

Angiographically intermediate stenoses, usually defined as a 40–70 % diameter narrowing, are frequent findings at coronary angiography. They pose a dilemma to the operator as their functional severity is unknown, lesions with very similar angiographic appearances can be both significant and not, and only those truly significant are likely to benefit from angioplasty (Figs. 15.1 and 15.2). Intracoronary imaging can provide relevant morphological information and clarify anatomical severity. However it does not provide information about the myocardial repercussions of such stenoses, which, in a clinically stable context, is probably the most important information. Intracoronary imaging and physiologic assessment may be complementary when evaluating coronary lesions [1]. FFR has emerged as the most frequently used physiological tool to assess functional severity of coronary stenoses, and intermediate stenoses have been the most important subset in which it has been evaluated.

Pivotal studies, such as DEFER [2], FAME [3], and FAME 2 [4], included patients with coronary lesions causing ≥50 % stenosis. In this context, it has been shown that:

- It is safe to defer PCI in lesions with an FFR ≥0.75 [2].
- FFR-guided PCI improves outcomes [3].
- PCI of lesions with FFR ≤0.80 leads to better outcomes than medical therapy alone [4].

Most importantly, these studies have demonstrated that treatment based on functional assessment performed with FFR translates into improved clinical outcomes, and the cost-effectiveness of PCI in lesions with a low FFR in FAME 2 appears favorable [5]. It has recently been demonstrated that not only does FFR have the ability to distinguish stenosis significance in a meaningful dichotomize manner but also its value is continuously related to clinical outcomes, and lesions with the lowest FFR values seem to benefit the most with revascularization [6].

In a recent meta-analysis involving data from 49,517 patients, FFR-guided PCI has shown to be associated with

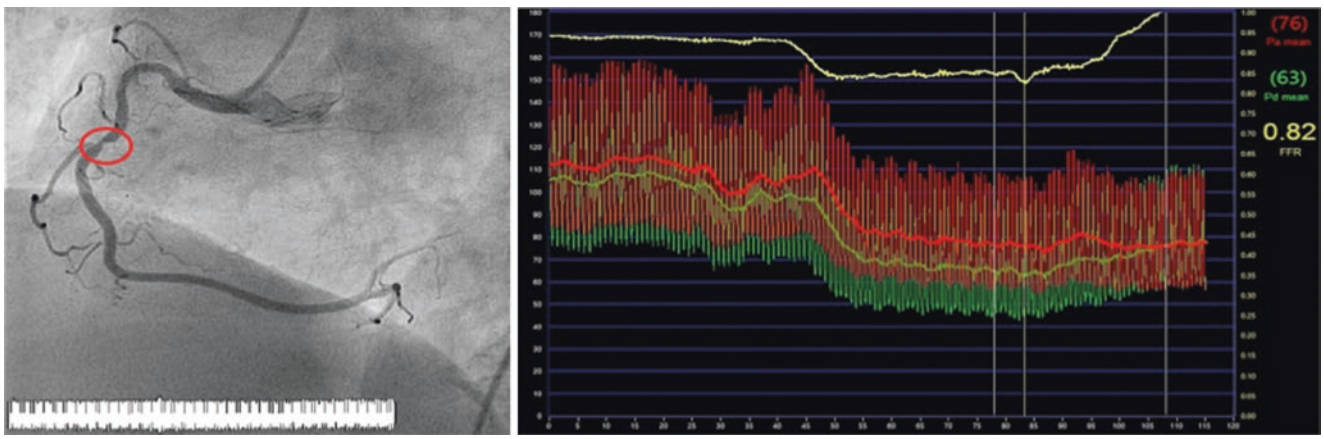


**Fig. 15.1** A 64-year-old man referred for angiography for stable angina. An intermediate stenosis in mid-RCA was noted. FFR was negative (0.82). Revascularization was deferred. *RCA* right coronary artery

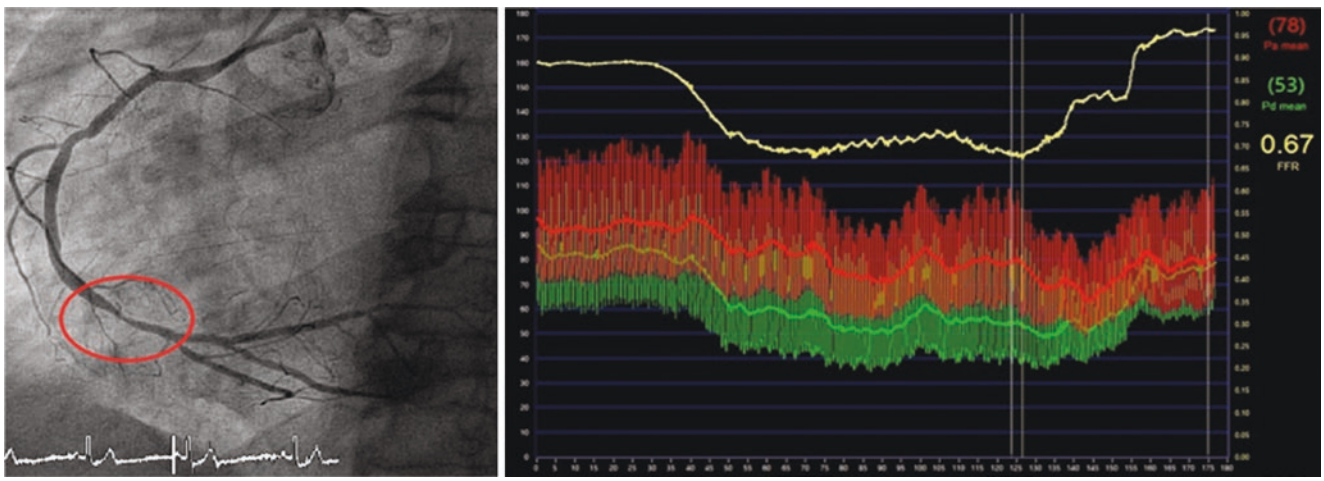


**Fig. 15.2** A 57-year-old woman referred for angiography for stable angina. An intermediate stenosis in distal-RCA was noted. FFR was positive (0.67). Revascularization performed with PCI. *RCA* right coronary artery

improved clinical outcomes, i.e., lower MACE/MACCE, death, MI, and repeat revascularization, when compared to angiography-guided PCI [7]. Diabetes mellitus is associated with microvascular disease, with consequent anatomical and functional changes that may lead to a decreased reliability of intracoronary pressure in assessing stenosis significance. Although not completely resolved, several studies have demonstrated that the presence of diabetes mellitus does not seem to significantly affect the value of FFR measurements [8–11].

## 15.2 Multivessel Disease

The definite management strategy for stable ischemic heart disease is not completely established, and the specific subgroup of patients with multivessel disease (MVD) can be particularly challenging. In general, cardiovascular risk stratification based on anatomical estimates of atherosclerotic burden (obstructive or not) provides important prognostic information in symptomatic or asymptomatic patients [12, 13]. However, major management decisions ultimately depend on whether or not revascularization can improve outcomes when compared with medical therapy (OMT) alone for any given anatomic scenario. For stable MVD, landmark clinical trials have suggested that revascularization of all anatomically significant stenosis or vessels is not necessarily associated with better results compared to OMT alone [14, 15]. These findings coupled with the observations that reduction of ischemic burden (by OMT, revascularization or both) is associated with improved outcomes have laid the foundations for the yet unproven hypothesis that ischemia-guided revascularization decreases death and MI rates [16, 17].

Unfortunately, noninvasive identification of lesions or vessels causing ischemia is intricate and largely unreliable for revascularization guidance since most of the methods currently available lack adequate spatial resolution [18]. Therefore, pressure wire-derived index technologies, by providing real-time, vessel-level specificity, ease of use, and interpretation, are now widely accepted as the preferred methods for selection of target lesions or vessels for revascularization [19]. More importantly, physiologically guided revascularization has proven to be safe and associated with improvement in the rate of unplanned urgent revascularization [17]. Advantages of physiologically guided revascularization in the context of MVD are numerous. It allows only ischemia causing lesions to be exposed to the risks and benefits of revascularization (Fig. 15.3). The FAME study has persuasively shown the merits of PCI deferral based on FFR guidance in MVD. In this randomized international trial, percutaneous revascularization guided by FFR was associated with a significant 5.1 % absolute risk reduction in a composite measure of death, MI or any repeat revascularization

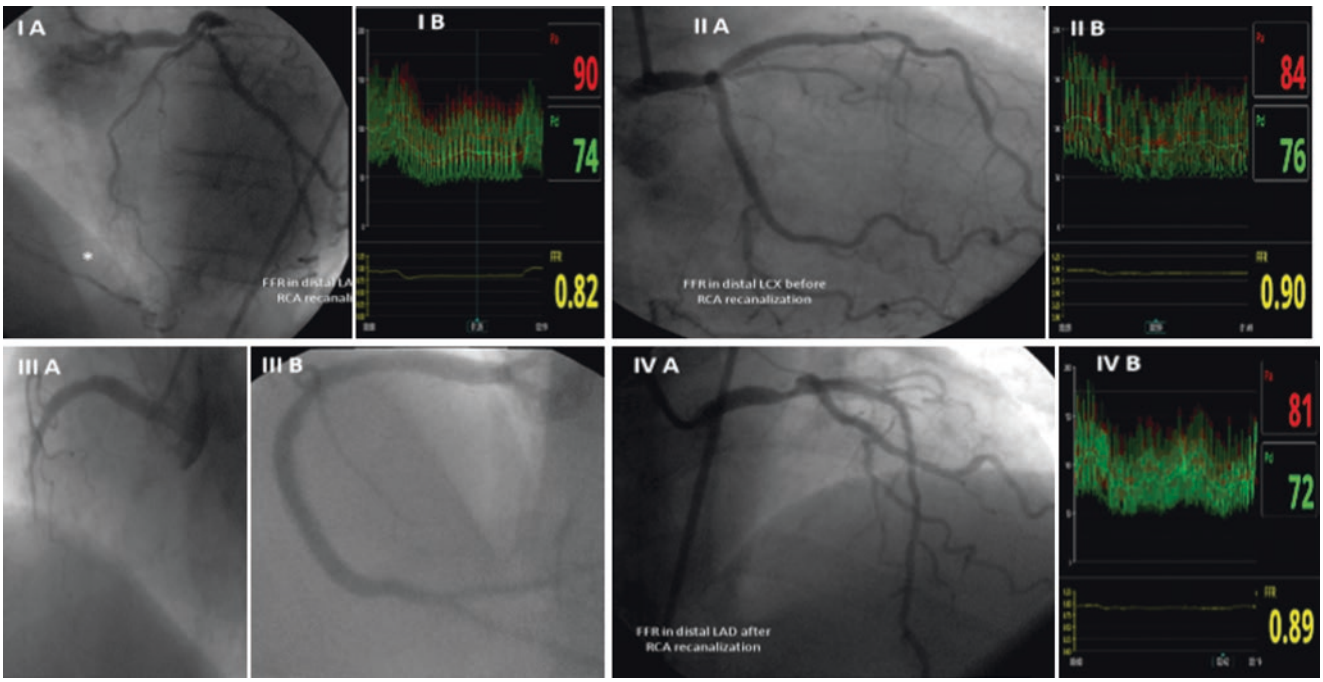


**Fig. 15.3** An 85-year-old female referred for CABG after diagnostic coronary angiography documenting an intermediate stenosis in distal LM coronary artery (50–70 %) and chronic total occlusion in mid-RCA. Distal RCA was supplied mainly from left coronary collaterals (*). The patient refused surgery and percutaneous coronary revascularization was suggested. Before RCA recanalization FFR in distal LAD was 0.82 (panel **I**) and 0.90 in distal LCX (panel **II**) suggesting a larger contribution of collateral circulation from LAD. After successful revascularization of RCA (panel **III**), FFR was again measured and increased from 0.82 to 0.89 in distal LAD (panel **IV**) and remained practically unchanged in LCX (0.92) (not shown). *CABG* coronary artery bypass graft surgery, *FFR* fractional flow reserve, *LAD* left anterior descendent artery, *LCX* left circumflex artery, *LM* left main, *RCA* right coronary artery

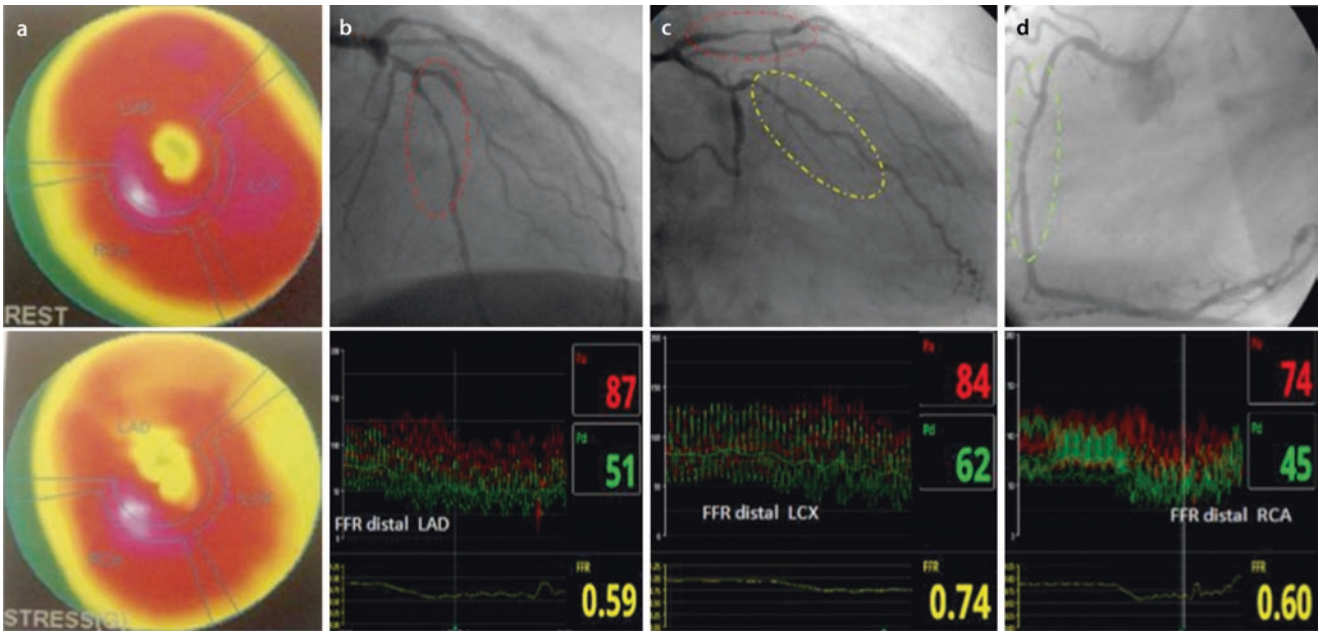


**Fig. 15.4** A 56-year-old, diabetic asymptomatic male with moderate anterior and mild lateral myocardial wall perfusion defects (panel **a**) and moderate LV systolic dysfunction (LVEF = 48 %). Coronary angiography revealed diffuse angiographically moderate lesions in all, small-caliber, epicardial vessels: proximal and mid-LAD (*red circles* in panels **b** and **c**), OM1 (*yellow circle* in panel **c**), and proximal to mid-RCA (*green circle* in panel **d**). All lesions were physiologically significant by FFR assessment and the patient was referred for CABG. The LCX and RCA lesions were underappreciated because of the relatively more severe compromise of the LAD lesion. *CABG* coronary artery bypass graft surgery, *FFR* fractional flow reserve, *LAD* left anterior descendent artery, *LCX* left circumflex artery, *LM* left main, *LVEF* left ventricular ejection fraction, *OM1* first obtuse marginal branch, *RCA* right coronary artery

at 12 months as compared to angiography-guided revascularization [20]. Two years after the intervention, the initial 30 % relative risk reduction was maintained, and importantly, for lesions deferred on the basis of FFR >0.80, the rate of myocardial infarction or revascularization was only 0.2 % and 3.2 %, respectively [21].

Complete anatomical revascularization of MVD in patients with moderate to severe ischemia is encouraged by international recommendations. However, clinical data from trials and registries have repeatedly shown that real-time combined anatomy and physiology assessment has the potential for CAD severity reclassification and consequent reorientation of the management strategy (Fig. 15.4). In a large French registry, investigators were asked to define prospectively their revascularization strategy based on angiography in patients for whom FFR could be performed. After performing FFR the final management strategy changed in 42 % of cases. Importantly 1-year outcomes, for patients reclassified by FFR, were equivalent to those without reclassification, underlying the safety of the FFR-based decision-making process. This safety was maintained irrespective of baseline risk category [22]. Another retrospective study using data from the FFR-guided PCI arm calculated the functional SYNTAX score (SYNTAX score including only physiologically significant lesions). Again, over 40 % of patients with an anatomic SYNTAX score >22 (usual recommendation for CABG) were reclassified to a score <22 (recommendation for PCI). Also, the functional score was more important than the anatomic score as a predictor of subsequent ischemic events [23]. Botman et al. previously studied this concept in a small cohort of patients with anatomic MVD. They compared the 2-year outcomes of PCI versus CABG guided by FFR. Surgical revascularization was selected for functionally significant three-vessel disease or two-vessel disease including proximal LAD and with PCI (using bare-metal stents) in the remaining scenarios. In contrast to most studies comparing PCI with CABG, there were no significant differences between groups at all endpoints, including repeat revascularization [24]. The ongoing FAME 3 trial (NCT02100722) is currently recruiting patients with three-vessel disease for comparison of PCI vs. CABG revascularization. However, in this trial, FFR-guided PCI (using a second-generation drug-eluting stents) will be compared to anatomy-guided CABG.

Often-quoted disadvantages of routine invasive physiological assessment are that it is mostly used by inexperienced operators to rule out significant stenosis and that it is time-consuming and expensive. Each of these points has been systematically discredited. It has been eloquently proven that regardless of operator experience, concordance between FFR and angiogram rarely exceeds 60 %. Moreover, even in intermediate lesions (50–70 % stenosis), more than a third will have an FFR value <0.8 [25] (Fig. 15.5). For experienced operators the interventional procedure is not significantly prolonged [20], and for patients with MVD, the FFR strategy has been proven to be cost-effective [26]. Notwithstanding the described advantages and guideline recommendations, penetration of invasive physiological

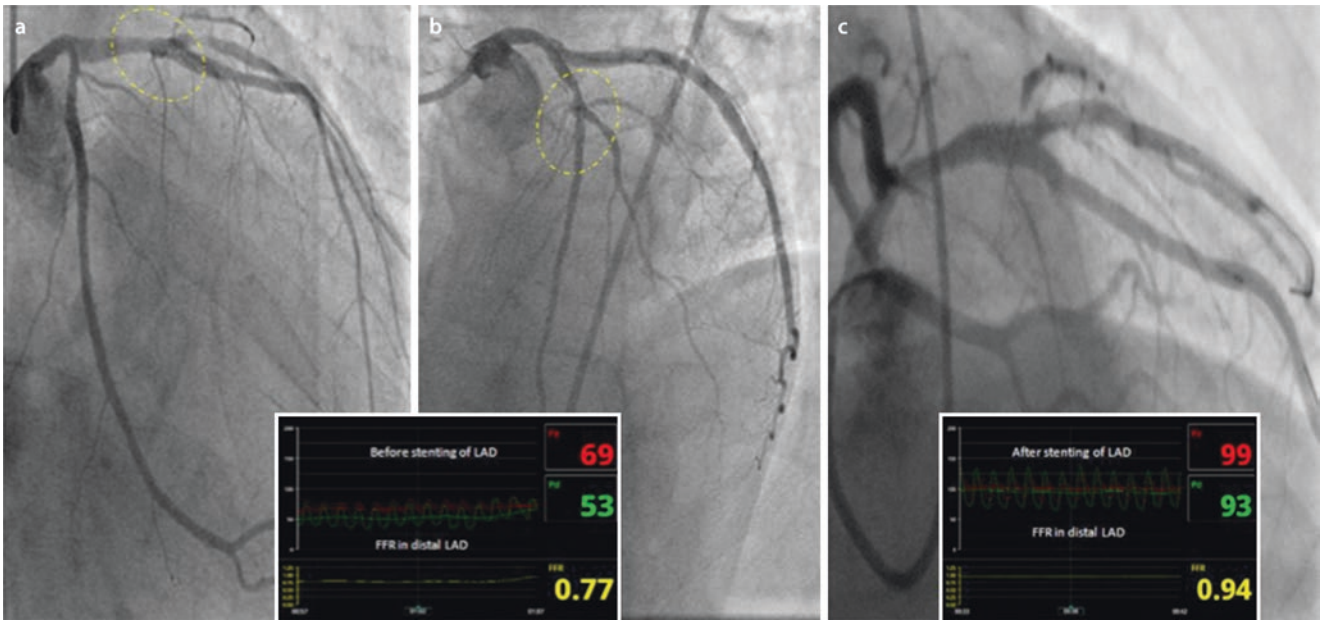


**Fig. 15.5** Symptomatic 46-year-old female with angiographically mild to moderate stenosis in mid-LAD in two orthogonal views (circle in panels **a** and **b**). Invasive physiological assessment with FFR proved that the lesion was hemodynamically significant (FFR = 0.77). After LAD stenting FFR value increased to 0.94 (panel **c**). *FFR* fractional flow reserve, *LAD* left anterior descendent artery

evaluation in clinical practice is perceived to be exceedingly low [27]. Further technology refinements, such as adenosine-free iFR, described in other chapters in this book, are expected to be important contributors to more widespread adoption of these techniques.

## 15.3 Unprotected Left Main Disease

### 15.3.1 Clinical Background

Significant left main lesions (≥50 % diameter stenosis) are present in 3–5 % of patients with coronary artery disease undergoing coronary angiography, frequently in association with multivessel disease [28, 29], and are linked to a dire clinical outcomes when medically treated [30]. In early studies of myocardial revascularization, coronary bypass grafting was shown to confer a mortality benefit over medical therapy in this setting [30, 31], and thus LMS disease has been universally accepted as an indication for CABG for many years. Recently, percutaneous stent implantation (especially in the era of DES) has proved to be a viable alternative to CABG in suitable patient subsets and angiographic scenarios and is being increasingly used [32–35]. Although the exact mechanism by which revascularization reduces mortality in patients with left main disease is largely unknown, it has been suggested that a link may exist between the severity of flow limitation and the risk of plaque instability and subsequent ischemic events, as for other coronary plaques [36]. However, a significant discrepancy between the angiographic findings and true anatomic features of left main lesions, especially the severity of the stenosis, has been recognized [37]. Therefore, the ability of angiography to predict the extent to which coronary flow is truly compromised and thus to anticipate the potential benefits of revascularization is limited. Of note, in the long-term follow-up of the CASS registry, CABG failed to prolong survival in the subgroup of patients with lesions 50–59 % by visual estimate [31], raising the question of whether or not these lesions were actually ischemic in the first place. Even for experienced operators, the accuracy of estimating the severity of angiographic stenosis and predicting functional significance of intermediate left main lesions (taking FFR as the gold standard) has been shown by Lindstaedt et al. [38] to be no more than 50 %; in the same report, unanimous classification (as significant or nonsignificant) by four different observers was achieved in only one third of all cases. In addition, obstructive disease elsewhere in the coronary tree may limit the accuracy of noninvasive testing to discriminate between inducible ischemia caused by a LMCA stenosis or by other coronary abnormalities (Fig. 15.6). Finally, mid- to long-term bypass patency has been shown to be affected by baseline FFR [39], and thus, confirmation of true hemodynamic significance of left main disease is of paramount importance if a sustained benefit from revascularization is to be expected.

### 15.3.2 Outcomes of Unprotected Left Main Revascularization Based on FFR Evaluation

To date, no adequately powered prospective randomized trials have been conducted to specifically address the issue of FFR-guided management of unprotected left main disease (ULMD). Also, and importantly, patients with angiographically significant LMD have been systematically excluded from the most important randomized trials, namely, the DEFER [2], FAME [3],

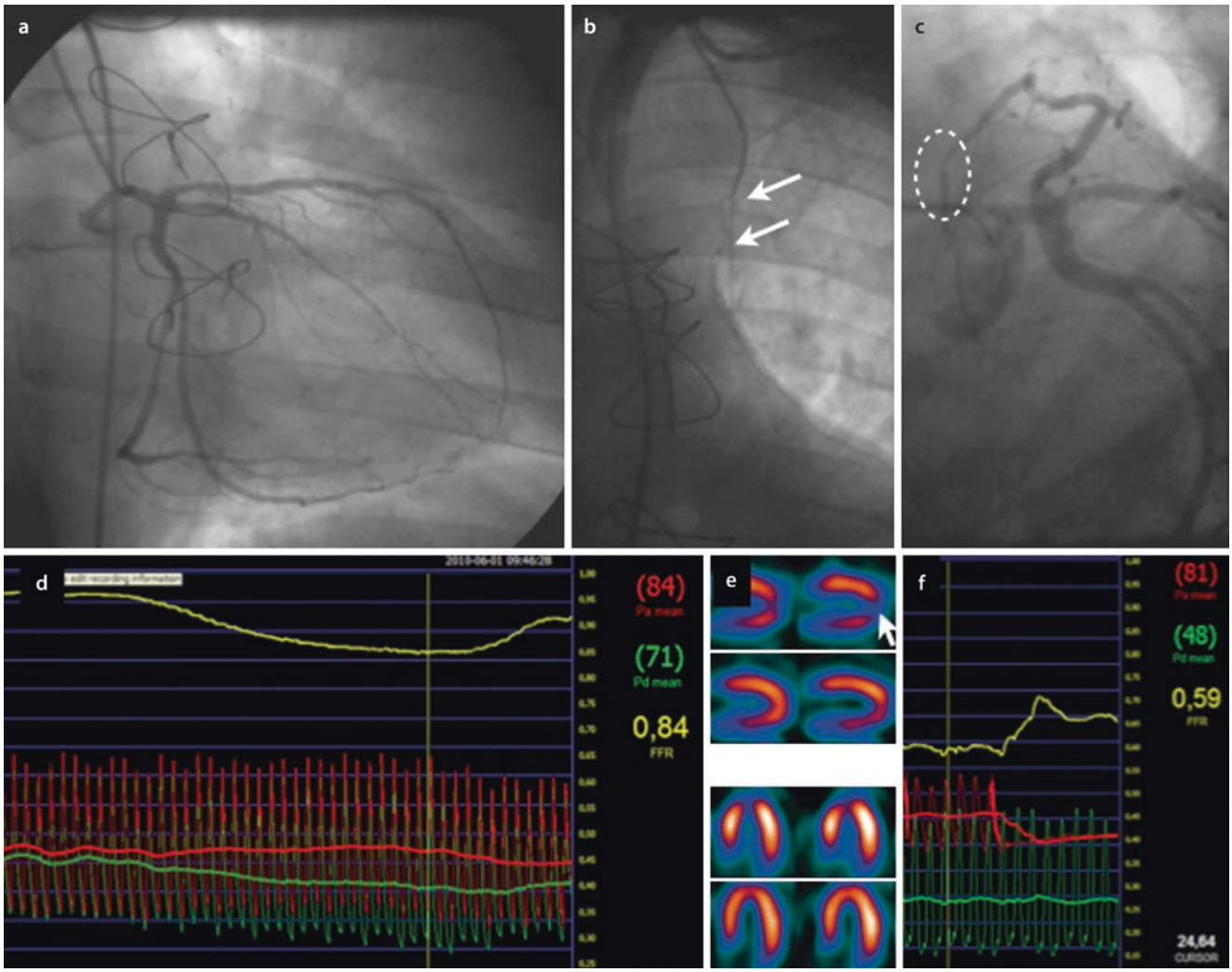


**Fig. 15.6** Illustrative case of a patient that had initially underwent CABG because of left main disease in the setting of a positive SPECT. Follow-up repeat angiography 3 years after original surgery, driven by a new positive SPECT (apical reversible defect in panel **e**), showed an occluded left internal mammary artery graft (*arrows* in panel **b**), an FFR of 0.84 in the left circumflex, and an eccentric lesion on the distal LAD (*circle* on panel **c**) with an FFR 0f 0.59. This lesion most likely was overlooked during the original angiography (prior to surgery) and justifies the apical ischemia. Patient was treated medically (Source: Raposo, L, MD; Personal Presentation, EuroPCR 2014, Paris)

15

and FAME 2 [17] studies. The outcome of patients whose treatment of intermediate/equivocal ULMD was deferred based on an FFR above the accepted "ischemic thresholds" – clinically validated in the DEFER (≥0.75) and in the FAME 2 (>0.80) trials – has been examined in small observational cohort studies including only stable patients [40–43]. Mid- to long-term survival of medically treated patients, with left main FFR above 0.75 to 0.80, was excellent and at least as good as those for whom surgery was deemed necessary based on an FFR below 0.75 to 0.80 (Table 15.1). Typically, an early hazard was observed in surgically treated patients, due to CABG-related mortality. Most of the ischemic events were revascularizations driven by progression of atherosclerosis, persistent symptoms, and positive stress tests, as the rate of myocardial infarction in deferred patients was remarkably low (≤1 %). However, when considered individually, these studies have limited power to detect statistically meaningful differences between study groups. In a recently published meta-analysis of six cohort studies including 525 patients (41 % undergoing revascularization based on usual FFR thresholds), Mallidi et al. [44] reported no statistically significant differences between groups concerning the rates of the primary composite endpoint of death from all causes, nonfatal myocardial infarctions and subsequent revascularizations ($p=0.15$), all-cause mortality ($p=0.06$), or nonfatal myocardial infarctions ($p=0.76$). However, there was a significant increase in the rate of subsequent revascularizations in the deferred patients ($p=0.002$).

### 15.3.3 Technical Aspects of FFR Evaluation of Left Main Lesions

Given its unique anatomy, the left main poses special challenges to operators performing invasive pressure measurements. Small vessel caliber (<3 mm) as well as the presence of ostial disease and angulation will frequently make stable cannulation

**Table 15.1** Summary of most relevant observational cohort studies addressing FFR-guided management of equivocal or intermediate unprotected left main lesions

| | Bech et al., *Heart* (2001) [49] | | Lindstaedt et al., *Am Heart J* (2006) [50] | | Hamilos et al., *Circulation* (2009) [52] | | Courtis et al., *Am Heart J* (2009) [51] | |
|---|---|---|---|---|---|---|---|---|
| Total pt. number | 54 | | 51 | | 213 | | 142 | |
| Follow-up (months) [mean ± SD] | 29 ± 15 | | 29 ± 16 | | 35 ± 25 | | 14 ± 11 | |
| Management groups and FFR threshold | FFR ≥0.75 Medical (*n* = 24) | FFR <0.75 CABG (*n* = 30) | FFR >0.80 Medical[a] (*n* = 24) | FFR <0.75 CABG[a] (*n* = 27) | FFR ≥0.80 Medical (*n* = 138) | FFR <0.80 CABG (*n* = 75) | FFR >0.80 Medical[a] (*n* = 82) | FFR <0.75 CABG[a] (*n* = 60) |
| Total survival | 100 % | 97 % | 100 % | 81 % | 89.8 % | 85.4 % | 96.3 % | 95 % |
| MACE-free survival | 76 % | 83 % | 69 % | 66 % | 74.2 % | 82.8 % | 87 % | 93 % |

[a]Patients in the "gray zone" of 0.75 to 0.80 were treated according to additional evidence and clinical considerations for each individual case

cumbersome. There is also the risk of damping pressure curves and subsequent limitation of maximal hyperemic flow, which will likely overestimate FFR. In our experience, the use of a second wire allows disengagement of the guide catheter, while still allowing adequate manipulation of the pressure wire, without significantly interfering with pressure gradients.

Another important limitation of FFR evaluation in LM disease is that the presence of downstream lesions in the left anterior descending and the circumflex may cause an overestimation of the hyperemic pressure gradient across the left main stem stenosis [45]. Currently there is no completely validated method that accurately predicts FFR in sequential lesions without the need for transient occlusion of the distal vessel for obtaining hyperemic wedge pressures [46]. Emerging resting indexes, which minimize the impact of flow on pressure gradients, may prove to be of value in this setting, as will be discussed further in this chapter.

## 15.4 Bifurcations

Bifurcation lesions are frequent targets for PCI, accounting for 15–20 % of treated lesions [47], and always represent a challenge to the operator for several reasons. Firstly, the relevance of this subgroup is well illustrated, by the fact that bifurcation lesions are independent predictors of periprocedural myocardial infarction [48] and stent thrombosis [49] and they are associated with lower success and higher restenosis, cost, and complication rates [50]. Secondly, at an anatomical level, the bifurcation lesion is difficult to evaluate by any imaging technique. The plaque is frequently not only eccentric and with a complex structure, but it is also dynamic during main branch PCI (e.g., plaque shift, dissection, thrombus, spasm, stent struts, etc.). Thirdly, at a physiological level, significance may be difficult to access due to many factors, namely, the subtended myocardium to a side branch, which is, in principle, smaller than the main branch's, but is highly variable and not necessarily related to the vessel diameter.

Bifurcation lesions' severity is more difficult to estimate based on angiography than non-bifurcation lesions. Even with dedicated 3D quantitative analysis integrating fractal laws, angiography has limited diagnostic accuracy for physiologic significance [51]. Intracoronary imaging such as IVUS and OCT may play a role, but their accuracy in this subset is reported to be relatively low [52–54]. Difficult measurements and variable myocardial mass related to any given intracoronary measurements are probably among the main reasons for intracoronary imaging inaccuracy. Full understanding of patient-level coronary physiology is very complex and unlikely to be fully predicted only by anatomical criteria [55].

FFR has been demonstrated to be useful in this setting, providing important physiologic information to guide treatment. Since the provisional one-stent approach has generally been accepted as the preferred technique for the majority of situations [47, 56], FFR may be useful in determining the need to treat a side branch once the main branch has been stented. FFR of a side branch before PCI is unlikely to be useful, given the complexity of the anatomic substrate and its dynamic behavior during PCI [50]. The bifurcation atheroma is usually contiguous with the main branch, with the possibility of creating a tandem-lesion effect, which will be difficult to evaluate even with careful pullback.

More often than not, jailed side-branch lesions are nonsignificant when assessed by FFR [57, 58], and their severity is frequently overestimated by angiography. In one series with 94 lesions, less than 1/3 of the jailed side-branch lesions with >75 % stenosis had an FFR <0.75 [59]. FFR in this context has shown to be relatively easy, safe, and a reliable measure that does not change significantly over time, from immediately after PCI to 6–8-month follow-up [60, 61]. To date, no randomized study has proven that FFR-guided PCI of a jailed side branch is clinically superior to angiography-guided PCI [61], but it has been demonstrated that FFR guidance reduces side-branch stenting, with very similar clinical outcomes, as recently demonstrated in the DKCRUSH-VI study [62]. DKCRUSH-VI was a randomized multicenter study, comparing FFR-guided and angiography-guided provisional stenting of true bifurcation lesions in

**Table 15.2** Summary of studies directly addressing the usefulness of FFR in ACS

| Paper | Year | Sample size[a] | ACS type[b] | Time from symptom onset to FFR | FFR threshold to treat | Major findings |
|---|---|---|---|---|---|---|
| De Bruyne et al. [105] | 2001 | 57 | Q wave 34 (60%), non-Q wave 23 (40%) | ≥6 days (20 ± 27) | <0.75 | 85% concordance with SPECT |
| Tamita et al. [5] | 2002 | 33 | STEMI | 310 ± 134 min | ND | FFR higher in AMI culprit than in SA for the same stenosis severity |
| Leesar et al. [106] | 2003 | 35 | NSTEMI 24 (69%); UA 11 (31%) | ≤48 h | <0.75 | FFR associated with lower costs, without differences in clinical outcomes |
| McClish et al. [108] | 2004 | 43 | STEMI/Q wave 36 (84%); NSTEMI/ non-Q wave 8 (16%) | 1–5 days | ND | FFR correlates to diameter stenosis by angiography in AMI as in SA |
| Samady H et al. [109] | 2006 | 48 | STEMI 36 (75%); NSTEMI 12 (25%) | STEMI >3 days; NSTEMI >2 days (total 3.7 ± 1.3) | ≤0.75 | 91% concordance with SPECT (for "true reversibility") |
| Potvin et al. [110] | 2006 | 124 | STEMI 11 (9%); NSTEMI 31 (25%); UA 82 (66%) | STEMI 48 h (IQR 24–144); NSTEACS 24 h (IQR 2–144) | <0.75 | No different cardiac events from SA patients at 2 years |
| López-Palop et al. [111] | 2010 | 106 | STEMI 14 (13%); NSTEACS 92 (87%) | ND | ≤0.75 | Low event rate at 1 year in patients with PCI deferred due to negative FFR (mortality 1.9%, nonfatal MI 0%, TLR 0.9%, cardiac cause hospital admission 4.7%) |
| Ntalianis et al. [101] | 2010 | 101 | STEMI 75 (74%); NSTEMI 26 (26%) | STEMI 230 ± 201 min; NSTEMI 52 ± 45 h | <0.80 | FFR reproducible ($r = 0.91$, $p < 0.0001$) between acute phase and follow-up (35 ± 4 days) in nonculprit artery lesions |
| Sels et al. [104] | 2011 | 150 | UA and NSTEMI | ND | ≤0.80 | Similar benefit of FFR-guided PCI as in SA |
| Layland et al. [107] | 2014 | 350 | NSTEMI | 3 (IQR 2, 5) days | ≤0.80 | FFR changed treatment in 21.6% patients |

Lower revascularization in FFR-guided strategy ($p = 0.054$)
*IQR* interquartile range (expressed as first quartile, third quartile), *ND* not defined, *SA* stable angina
[a]Sample size refers to the number of ACS patients included in that particular study in which the clinical decision was performed based on FFR
[b]Number of patients with each ACS type: UA (unstable angina), NSTEMI (non-ST-elevation myocardial infarction), NSTEACS (non-ST-elevation acute coronary syndrome, includes UA and NSTEMI), STEMI (ST-elevation myocardial infarction)

320 patients. In the FFR group, side-branch stenting was attempted less frequently than in the angiography group (25.9 vs. 38.1 %, respectively; $p = 0.01$), with identical 1-year endpoint rates (death, MI, TLR, TVR, stent thrombosis, and composite MACE). As myocardial territory from a side branch is usually smaller than that from the main branch, it will probably be very difficult to ever demonstrate a clinical benefit in this subset [63] such as that demonstrated in FAME [4] and FAME 2 [17].

Care must be taken when interpreting FFR values in specific patients. For example, a negative FFR in a side branch does not necessarily mean it doesn't need treatment, as anatomical considerations must also to be taken into account, for example, an important side branch in a young patient. A significantly diseased branch may also have a higher FFR value due to the ability to redirect hyperemic blood flow to an unobstructed branch. Likewise, an FFR measurement on a small side branch may be positive, but its clinical meaning will be unclear.

In summary, bifurcation lesions are difficult to assess by any method. FFR can help determine the need for side-branch treatment after main branch PCI. In this context FFR has demonstrated to lower the rates of side-branch treatment, with similar clinical outcomes. Risks of further lesion manipulation should always be outweighed by the potential benefits, so FFR guidance is proposed only in clinically significant side branches, which may be determined by careful integrated angiographic assessment.

## 15.5 Sequential Stenosis and Diffuse Disease

Diffuse and serial/tandem intermediate coronary lesions are common in patients with coronary artery disease, and functional evaluation can be particularly challenging in these cases. In the presence of consecutive lesions in the same vessel, the fluid-dynamic interaction between the stenosis alters their relative severity and impedes determination of FFR from the simple hyperemic ratio of pressure across each single stenosis. Because hyperemic flow declines significantly whenever any 50 % reduction in lumen diameter is observed, even mild secondary lesions can affect hyperemic pressure indexes. Identifying the most appropriate stenosis to be treated out of several in sequence is an important interventional decision. Several approaches have been developed to try to overcome this limitation, including equations for predicting independent FFR values, hyperemic pullback, and resting pullback with evaluation of pressure gradient in the wave-free period (iFR).

### 15.5.1 Equations for Predicting FFR of Individual Lesion

In an animal model, De Bruyne and colleagues derived an equation for predicting the FFR value for two sequential lesions in the same vessel [64]. This equation includes, besides the distal (Pd) and proximal pressures (Pa), also the pressure measured between the lesions (Pm) and the coronary wedge pressure (Pw). The equation was tested in humans, and the predicted FFR value for one lesion showed a good correlation with the "true" FFR, measured after angioplasty of the other lesion ($r = 0.92$, $\Delta\% = 4 \pm 0\%$) [46]. Importantly, the authors confirmed that without accounting for stenosis interaction, the value of FFR for each stenosis would have been significantly overestimated, both for the proximal and the distal lesions.

This approach was again tested more recently in an in vitro model of several sequential lesions. Two different complex equations were mathematically derived to predict true FFR of each stenosis in multiple sequential stenoses and to predict the true FFR after releasing a given stenosis in multiple sequential stenoses. Both equations showed excellent correlation with "true" FFR values ($R^2 = 0.92$ and 0.97, respectively) [65]. However, these theoretical models are time-consuming and difficult to implement in daily clinical practice.

### 15.5.2 Hyperemic Pressure Wire Pullback

In order to quantify lesion severity in a diffusely affected coronary vessel, a live pressure pullback curve can be used. In this technique, the pressure guidewire is manually withdrawn from a distal position during steady-state maximum hyperemia, resulting in a curve that represents the pressure gradient over the entire length of the vessel. Performing the pullback together with angiographic visualization identifies the vessel segments where the pressure "jump" is more important, thus allowing spot stenting in the presence of long and diffuse lesions. This strategy was tested in a small study, including 131 patients with multiple intermediate stenoses within the same coronary artery, assessed by FFR with pullback pressure tracings, in which the stenosis that caused the largest pressure step-up was stented first. The technique was safe and effective and was associated with a very low event rate; of note, there were no events related to deferred lesions. However, prolonged adenosine hyperemia (required for the pullback) may have unexpected consequences with changing pressure ratios [66], which may go unnoticed during a pullback and affect its interpretation. This effect may be particularly relevant when profound hypotension occurs [67, 68]. While more studies are needed to clarify the clinical role of hyperemic pullback, these pitfalls must be understood when performing this technique, in order to avoid erroneous lesion functional classification.

## 15.6 Post PCI

Although FFR is mainly a tool for decision-making regarding the need for revascularization, it has also been studied in the setting of post-intervention. It has been demonstrated that there is an inverse association between post-PCI FFR and the restenosis rate [69, 70]. After successful PCI, no significant gradient should be present across the stent [71], and values >0.90 [69] and >0.95 [72] have been associated with lower event rates in the follow-up. In a large multicenter registry, evaluating FFR after stenting, a residual gradient (FFR <0.90) was present in nearly 1/3 of the patients and was associated with a significantly higher event rate in the follow-up. This might be due to the presence of diffuse disease and higher atherosclerotic burden rather than the stent itself and is in line with more recent evidence from coronary CT angiography that diffuses disease, and higher atherosclerotic burden has important prognostic implications [73, 74]. The type of implanted stent may have an impact on the consequent FFR measurement. In a small study comparing FFR values in a sirolimus-eluting stent (SES) and a BMS, FFR immediately after stenting was the same (0.88 vs. 0.9, respectively; $p = 0.55$) but different at 6-month follow-up, favoring the SES (0.91 vs. 0.83, $p = 0.027$) [71]. In the presence of in-stent restenosis (ISR), FFR does not have conclusive data on hard endpoints. However, in this context, angiographic quantification seems to be even less reliable in estimating functional significance given a relatively poor correlation with FFR [75, 76]. Angio-guided PCI in ISR thus has the potential to lead to an inappropriate decision in a significant proportion of patients [77]. An FFR value of 0.75 in the ISR context has shown an agreement of 88 % with stress perfusion myocardial scintigraphy to detect functional significance in a 42-patient sample with a single ISR lesion of intermediate angiographic significance (40–70 % diameter stenosis) [78]. From available data, translation of FFR-guided PCI in ISR into better clinical outcomes has not been formally proven, but may be expected.

## 15.7 CABG

FFR has been evaluated in the context of coronary artery bypass graft surgery (CABG). In planning the procedure, FFR can help on the correct identification of the number of vessels/lesions with functional stenosis, and therefore it is expected to be associated with a lower number of grafts and higher patency in the follow-up. It has been prospectively demonstrated that failure of grafts implanted on coronaries with no flow-limiting stenosis (FFR >0.8, blinded to the surgeon) can be up to three times higher than in those with FFR <0.8 in the first year after surgical revascularization [39]. In another study, angiography-guided and FFR-guided CABG were compared in a single-center retrospective analysis [79]. At 3 years the rate of MACE was similar between the groups. However, the FFR guidance was associated with lower numbers of grafts used, higher rate of off-pump surgery, higher rate of venous graft patency, and less angina. In order to prospectively confirm these findings, the ongoing GRAFFITI trial [NCT01810224] is currently randomizing patients with MVD already committed to surgical revascularization (based on LM/LAD anatomy) to one of the two alternative strategies of revascularization for the remaining vessels. In the FFR arm, only coronaries with FFR <0.8 will be grafted. In the angiography arm, all lesions >70 % will be grafted. The primary endpoint is graft patency at 12 months. FFR may also be used to evaluate hemodynamic significance of bypass graft stenosis. In a small study including patients with lesions in saphenous vein grafts, there was a reasonable specificity and negative predictive value as compared to myocardial perfusion imaging, although further research is needed in this field [80].

## 15.8 Valve Disease

About 20–50 % patients with severe valvular heart disease have concomitant coronary artery disease (CAD) [81]. European and American guidelines recommend myocardial revascularization at the time of valvular surgery when a stenosis >50 % is present in a major epicardial artery. In contrast to other groups of patients with stable coronary artery disease, demonstration of functional significance of such lesions is not currently endorsed in this context. Evidence supporting revascularization in this context is fragile and mostly based in observational studies suggesting a negative impact of non-revascularized CAD in postoperative outcomes [19, 82].

Generally, provocative ischemia test is considered unsafe in the setting of severe symptomatic VHD, particularly for aortic stenosis (AS) [82]. However, the use of intravenous adenosine to induce maximal hyperemia has been shown to be safe and accurate in patients with AS in the context of noninvasive assessment [83] (Fig. 15.7). Similarly, anecdotal reports of



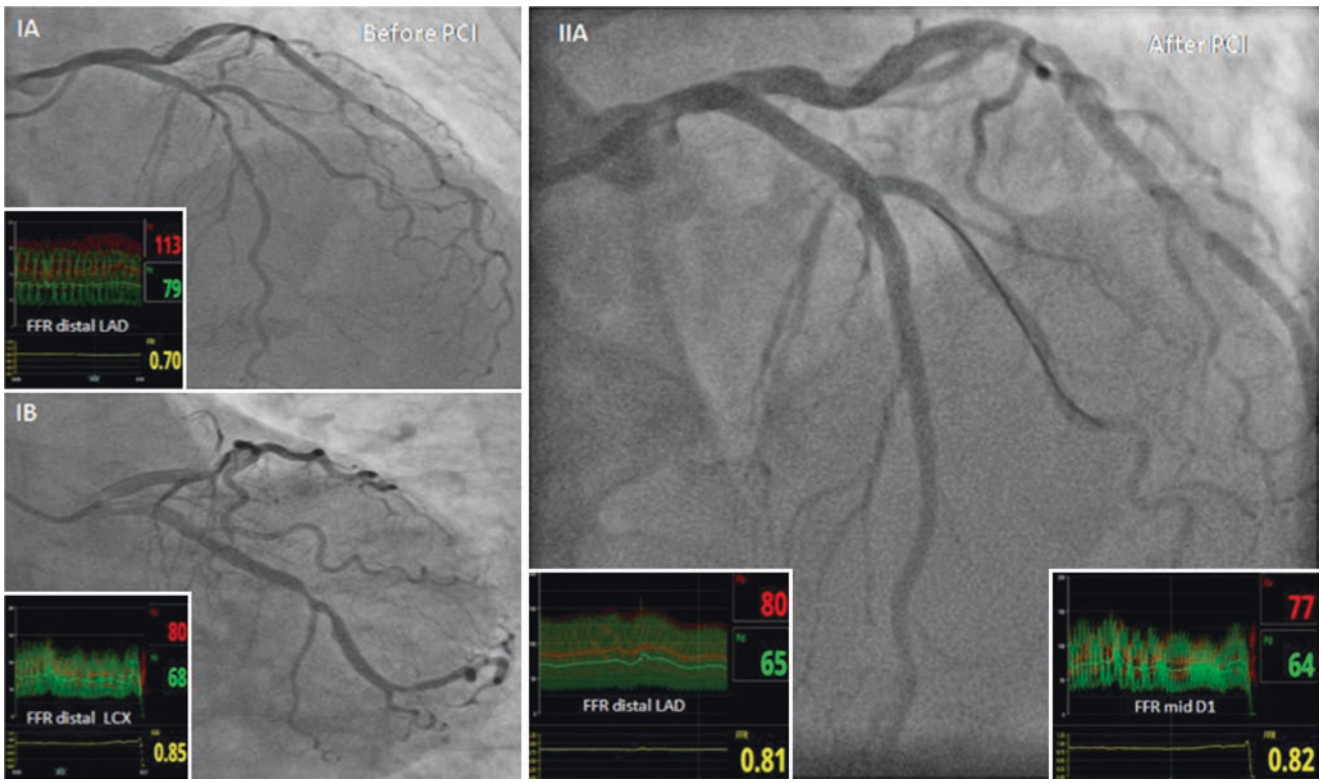


**Fig. 15.7** A 79-year-old female patient with severe aortic stenosis and angiographically significant stenosis in mid-LAD (panel **Ia**) and LCX (panel **Ib**) considered for TAVI procedure. Only the LAD lesion was shown to be hemodynamically significant under IV adenosine administration. After successful LAD stenting, the hyperemic flow increased from 0.7 to 0.81. The same FFR value was obtained in disease-free D1 suggesting residual diffuse myocardial ischemia possibly related to supply/demand imbalance in the context of severe valvular disease. *D1* first diagonal, *FFR* fractional flow reserve, *LAD* left anterior descendent artery, *LCX* left circumflex artery, *TAVI* transaortic valve implantation

invasive physiologic assessment of CAD using FFR in patients with severe AS have been described to be safe and have been effectively applied to guide percutaneous revascularizations before transaortic valve implantation [84, 85]. It is plausible that not all patients and not all vessels with anatomically significant stenosis require revascularization during valvular surgery. To date all major studies showing benefits of FFR-guided revascularization in comparison to angiography-guided revascularization have excluded patients with significant VHD. Thus, the validity of these pressure-derived physiological surrogates of myocardial ischemia requires further investigation before its routine use can be recommended to guide percutaneous or surgical revascularization in patients with significant VHD.

## 15.9 Conclusion

FFR is a useful tool in a wide range of clinical scenarios for the evaluation of the severity of coronary stenosis. It is important to bear in mind that the utility of FFR is situation dependent with each clinical scenario having its own benefits and limitations that have to be considered when applying the results of FFR evaluation.

## References

1. Tobis J, Azarbal B, Slavin L. Assessment of intermediate severity coronary lesions in the catheterization laboratory. J Am Coll Cardiol. 2007;49(8):839–48.
2. Pijls NHJ, van Schaardenburgh P, Manoharan G, Boersma E, Bech JW, van't Veer M, et al. Percutaneous coronary intervention of functionally nonsignificant stenosis. 5-year follow-up of the DEFER study. J Am Coll Cardiol. 2007;49(21):2105–11.
3. Pijls NHJ, Fearon WF, Tonino PAL, Siebert U, Ikeno F, Bornschein B, et al. Fractional flow reserve versus angiography for guiding percutaneous coronary intervention in patients with multivessel coronary artery disease: 2-Year follow-up of the FAME (fractional flow reserve versus angiography for multivessel evaluation) study. J Am Coll Cardiol. Elsevier Inc. 2010;56(3):177–84.
4. De Bruyne B, Fearon WF, Pijls NHJ, Barbato E, Tonino P, Piroth Z, et al. Fractional flow reserve–guided PCI for stable coronary artery disease. N Engl J Med. 2014;371:1208–17.
5. Fearon WF, Shilane D, Pijls NHJ, Boothroyd DB, Tonino PAL, Barbato E. Cost-effectiveness of percutaneous coronary intervention in patients with stable coronary artery disease and abnormal fractional flow reserve. Circulation. 2013;128(12):1335–40.
6. Johnson NP, Tóth GG, Lai D, Zhu H, Açar G, Agostoni P, et al. Prognostic value of fractional flow reserve linking physiologic severity to clinical outcomes. J Am Coll Cardiol. 2014;64(16):1641–54.
7. Zhang D, Lv S, Song X, Yuan F, Xu F, Zhang M, et al. Fractional flow reserve versus angiography for guiding percutaneous coronary intervention: a meta-analysis. Heart. 2015;101(6):455–62.
8. Yanagisawa H, Chikamori T, Tanaka N, Usui Y, Takazawa K, Yamashina A. Application of pressure-derived myocardial fractional flow reserve in assessing the functional severity of coronary artery stenosis in patients with diabetes mellitus. Circ J. 2004;68(11):993–8.
9. Domínguez-Franco AJ, Jiménez-Navarro MF, Muñoz-García AJ, Alonso-Briales JH, Hernández-García JM, de Teresa Galván E. Long-term prognosis in diabetic patients in whom revascularization is deferred following fractional flow reserve assessment. Rev Esp Cardiol. 2008;61(4):352–9.
10. Reith S, Battermann S, Hellmich M, Marx N, Burgmaier M. Impact of type 2 diabetes mellitus and glucose control on fractional flow reserve measurements in intermediate grade coronary lesions. Clin Res Cardiol. 2014;103(3):191–201.
11. Sahinarslan A, Kocaman SA, Olgun H, Kunak T, Kiziltunç E, Ozdemir M, et al. The reliability of fractional flow reserve measurement in patients with diabetes mellitus. Coron Artery Dis. 2009;20(5):317–21.
12. Min JK, Shaw LJ, Devereux RB, Okin PM, Weinsaft JW, Russo DJ, et al. Prognostic value of multidetector coronary computed tomographic angiography for prediction of all-cause mortality. J Am Coll Cardiol. 2007;50(12):1161–70.
13. Cho I, Chang H-J, Sung JM, Pencina MJ, Lin FY, Dunning AM, et al. Coronary computed tomographic angiography and risk of all-cause mortality and nonfatal myocardial infarction in subjects without chest pain syndrome from the CONFIRM registry (Coronary CT Angiography Evaluation for Clinical Outcomes: An International Mult. Circulation. 2012;126(3):304–13.
14. Boden W, O'Rourke R. Optimal medical therapy with or without PCI for stable coronary disease william. N Engl J Med. 2007;356(15):1503–16.
15. Frye RL, August P, Brooks MM, Hardison RM, Kelsey SF, MacGregor JM, et al. A randomized trial of therapies for type 2 diabetes and coronary artery disease. N Engl J Med. 2009;360(24):2503–15.
16. Shaw LJ, Berman DS, Maron DJ, Mancini GBJ, Hayes SW, Hartigan PM, et al. Optimal medical therapy with or without percutaneous coronary intervention to reduce ischemic burden: results from the Clinical Outcomes Utilizing Revascularization and Aggressive Drug Evaluation (COURAGE) trial nuclear substudy. Circulation. 2008;117(10):1283–91.
17. De Bruyne B, Pijls NHJ, Kalesan B, Barbato E, Tonino PAL, Piroth Z, et al. Fractional flow reserve–guided PCI versus medical therapy in stable coronary disease. N Engl J Med. 2012;367(11):991–1001.
18. Schwartz JG, Fearon WF. Functional assessment of multivessel coronary artery disease: ischemia-guided percutaneous coronary intervention. Coron Artery Dis. 2014;25(6):521–8.
19. Windecker S, Kolh P, Alfonso F, Collet J-P, Cremer J, Falk V, et al. 2014 ESC/EACTS Guidelines on myocardial revascularization: the Task Force on Myocardial Revascularization of the European Society of Cardiology (ESC) and the European Association for Cardio-Thoracic Surgery (EACTS) * Developed with the special contribution. Eur Heart J. 2014;35(37):2541–619.
20. Tonino PAL, De Bruyne B, Pijls NHJ, Siebert U, Ikeno F, Van Veer MT, et al. Fractional flow reserve versus angiography for guiding percutaneous coronary intervention. N Engl J Med. 2009;360(3):213–24.
21. Pijls NHJ, Fearon WF, Tonino PAL, Siebert U, Ikeno F, Bornschein B, et al. Fractional flow reserve versus angiography for guiding percutaneous coronary intervention in patients with multivessel coronary artery disease: 2-Year follow-up of the FAME (fractional flow reserve versus angiography for multivessel evaluation) study. J Am Coll Cardiol. 2010;56(3):177–84.
22. Van Belle E, Rioufol G, Pouillot C, Cuisset T, Bougrini K, Teiger E, et al. Outcome impact of coronary revascularization strategy reclassification with fractional flow reserve at time of diagnostic angiography: Insights from a large french multicenter fractional flow reserve registry. Circulation. 2014;129(2):173–85.
23. Nam CW, Mangiacapra F, Entjes R, Chung IS, Sels JW, Tonino PAL, et al. Functional SYNTAX score for risk assessment in multivessel coronary artery disease. J Am Coll Cardiol. Elsevier Inc. 2011;58(12):1211–8.
24. Botman KJ, Pijls NHJ, Bech JW, Aarnoudse W, Peels K, Van Straten B, et al. Percutaneous coronary intervention or bypass surgery in multivessel disease? A tailored approach based on coronary pressure measurement. Catheter Cardiovasc Interv. 2004;63(2):184–91.
25. Toth GG, Toth B, Johnson NP, De Vroey F, Di Serafino L, Pyxaras S, et al. Revascularization decisions in patients with stable angina and intermediate lesions: results of the international survey on interventional strategy. Circ Cardiovasc Interv. 2014;7(6):751–9.

26. Fearon WF, Bornschein B, Tonino PAL, Gothe RM, De Bruyne B, Pijls NHJ, et al. Economic evaluation of fractional flow reserve-guided percutaneous coronary intervention in patients with multivessel disease. Circulation. 2010;122(24):2545–50.
27. Park S-J, Ahn J-M. Should we be using fractional flow reserve more routinely to select stable coronary patients for percutaneous coronary intervention? Curr Opin Cardiol. 2012;27(6):675–81.
28. Giannoglou GD, Antoniadis AP, Chatzizisis YS, Damvopoulou E, Parcharidis GE, Louridas GE. Prevalence of narrowing ≥50% of the left main coronary artery among 17,300 patients having coronary angiography. Am J Cardiol. 2006;98(9):1202–5.
29. Soleimani A, Abbasi A, Kazzazi EH, Hosseini K, Salirifar M, Darabian S, et al. Prevalence of left main coronary artery disease among patients with ischemic heart disease: insights from the Tehran Angiography Registry. Minerva Cardioangiol. 2009;57(2):175–83.
30. Yusuf S, Zucker D, Peduzzi P, Fisher LD, Takaro T, Kennedy JW, et al. Effect of coronary artery bypass graft surgery on survival: overview of 10-year results from randomised trials by the Coronary Artery Bypass Graft Surgery Trialists Collaboration. Lancet. 1994;344(8922):563–70.
31. Caracciolo EA, Davis KB, Sopko G, Kaiser GC, Corley SD, Schaff H, et al. Comparison of surgical and medical group survival in patients with left main equivalent coronary artery disease. Long-term CASS experience. Circulation. 1995;91(9):2335–44.
32. Dores H, Raposo L, Almeida MS, Brito J, Santos PG, Sousa PJ, et al. Percutaneous coronary intervention of unprotected left main disease: five-year outcome of a single-center registry. Rev Port Cardiol. 2013;32(12):997–1004.
33. Kappetein AP, Feldman TE, Mack MJ, Morice M-C, Holmes DR, Ståhle E, et al. Comparison of coronary bypass surgery with drug-eluting stenting for the treatment of left main and/or three-vessel disease: 3-year follow-up of the SYNTAX trial. Eur Heart J. 2011;32(17):2125–34.
34. Ahn J-M, Roh J-H, Kim Y-H, Park D-W, Yun S-C, Lee PH, et al. Randomized trial of stents versus bypass surgery for left main coronary artery disease: five-year outcomes of the PRECOMBAT study. J Am Coll Cardiol. 2015;65(20):2198–206.
35. Park D-W, Seung KB, Kim Y-H, Lee J-Y, Kim W-J, Kang S-J, et al. Long-term safety and efficacy of stenting versus coronary artery bypass grafting for unprotected left main coronary artery disease 5-year results from the MAIN-COMPARE (Revascularization for Unprotected Left Main Coronary Artery Stenosis: Comparison of Per. J Am Coll Cardiol. 2010;56(2):117–24.
36. Park H-B, Heo RÓ, Hartaigh B, Cho I, Gransar H, Nakazato R, et al. Atherosclerotic plaque characteristics by CT angiography identify coronary lesions that cause ischemia: a direct comparison to fractional flow reserve. JACC Cardiovasc Imaging. 2015;8(1):1–10.
37. Isner JM, Kishel J, Kent KM, Ronan JA, Ross AM, Roberts WC. Accuracy of angiographic determination of left main coronary arterial narrowing. Angiographic–histologic correlative analysis in 28 patients. Circulation. 1981;63(5):1056–64.
38. Lindstaedt M, Spiecker M, Perings C, Lawo T, Yazar A, Holland-Letz T, et al. How good are experienced interventional cardiologists at predicting the functional significance of intermediate or equivocal left main coronary artery stenoses? Int J Cardiol. 2007;120(2):254–61.
39. Botman CJ, Schonberger J, Koolen S, Penn O, Botman H, Dib N, et al. Does stenosis severity of native vessels influence bypass graft patency? A prospective fractional flow reserve-guided study. Ann Thorac Surg. 2007;83(6):2093–7.
40. Bech GJ, Droste H, Pijls NH, De Bruyne B, Bonnier JJ, Michels HR, et al. Value of fractional flow reserve in making decisions about bypass surgery for equivocal left main coronary artery disease. Heart. 2001;86(5):547–52.
41. Lindstaedt M, Yazar A, Germing A, Fritz MK, Holland-Letz T, Mügge A, et al. Clinical outcome in patients with intermediate or equivocal left main coronary artery disease after deferral of surgical revascularization on the basis of fractional flow reserve measurements. Am Heart J. 2006;152(1):156.e1–9.
42. Courtis J, Rodés-Cabau J, Larose E, Potvin JM, Déry JP, De Larochellière R, et al. Usefulness of coronary fractional flow reserve measurements in guiding clinical decisions in intermediate or equivocal left main coronary stenoses. Am J Cardiol. 2009;103(7):943–9.
43. Hamilos M, Muller O, Cuisset T, Ntalianis A, Chlouverakis G, Sarno G, et al. Long-term clinical outcome after fractional flow reserve-guided treatment in patients with angiographically equivocal left main coronary artery stenosis. Circulation. 2009;120(15):1505–12.
44. Mallidi J, Atreya AR, Cook J, Garb J, Jeremias A, Klein LW, et al. Long-term outcomes following fractional flow reserve-guided treatment of angiographically ambiguous left main coronary artery disease: a meta-analysis of prospective cohort studies. Catheter Cardiovasc Interv. 2015;86(1):12–8.
45. Daniels DV, Van'T Veer M, Pijls NHJ, Van Der Horst A, Yong AS, De Bruyne B, et al. The impact of downstream coronary stenoses on fractional flow reserve assessment of intermediate left main disease. JACC Cardiovasc Interv. 2012;5(10):1021–5.
46. Pijls NH, De Bruyne B, Bech GJ, Liistro F, Heyndrickx GR, Bonnier HJ, et al. Coronary pressure measurement to assess the hemodynamic significance of serial stenoses within one coronary artery: validation in humans. Circulation. 2000;102(19):2371–7.
47. Latib A, Colombo A. Bifurcation disease. What do we know, what should we do? JACC Cardiovasc Interv. 2008;1(3):218–26.
48. Park D-W, Kim Y-H, Yun S-C, Ahn J-M, Lee J-Y, Kim W-J, et al. Frequency, causes, predictors, and clinical significance of peri-procedural myocardial infarction following percutaneous coronary intervention. Eur Heart J. 2013;34(22):1662–9.
49. Van Werkum JW, Heestermans AA, Zomer AC, Kelder JC, Suttorp MJ, Rensing BJ, et al. Predictors of coronary stent thrombosis. The Dutch Stent Thrombosis Registry. J Am Coll Cardiol. American College of Cardiology Foundation. 2009;53(16):1399–409.
50. Park SH, Koo B-K. Clinical applications of fractional flow reserve in bifurcation lesions. J Geriatr Cardiol. 2012;9(3):278–84.
51. Tu S, Pyxaras SA, Lam MK, Li Y. Fractional flow reserve and coronary bifurcation anatomy. JACC Cardiovasc Interv. 2015;8(4):564–74.
52. Stankovic G, Lefevre T, Chieffo A, Hildick-Smith D, Lassen JF, Pan M, et al. Consensus from the 7th European Bifurcation Club meeting. EuroIntervention. 2013;9(1):36–45.
53. Koh JS, Koo BK, Kim JH, Yang HM, Park KW, Kang HJ, et al. Relationship between fractional flow reserve and angiographic and intravascular ultrasound parameters in ostial lesions: major epicardial vessel versus side branch ostial lesions. JACC Cardiovasc Interv. 2012;5(4):409–15.
54. Ha J, Kim J-S, Mintz GS, Kim B-K, Shin D-H, Ko Y-G, et al. 3D OCT versus FFR for jailed side-branch ostial stenoses. JACC Cardiovasc Imaging. American College of Cardiology Foundation; 2014;7(2):204–5.
55. Johnson NP, Kirkeeide RL, Gould KL. Coronary anatomy to predict physiology fundamental limits. Circ Cardiovasc Imaging. 2013;6(5):817–32.
56. Behan MW, Holm NR, Curzen NP, Erglis A, Stables RH, De Belder AJ, et al. Simple or complex stenting for bifurcation coronary lesions: a patient-level pooled-analysis of the Nordic bifurcation study and the British bifurcation coronary study. Circ Cardiovasc Interv. 2011;4(1):57–64.
57. Bellenger NG, Swallow R, Wald DS, Court I, Calver AL, Dawkins KD, et al. Haemodynamic significance of ostial side branch nipping following percutaneous intervention at bifurcations: a pressure wire pilot study. Heart. 2007;93(2):249–50.
58. Ahn JM, Lee JY, Kang SJ, Kim YH, Song HG, Oh JH, et al. Functional assessment of jailed side branches in coronary bifurcation lesions using fractional flow reserve. JACC Cardiovasc Interv. 2012;5(2):155–61.
59. Koo BK, Kang HJ, Youn TJ, Chae IH, Choi DJ, Kim HS, et al. Physiologic assessment of jailed side branch lesions using fractional flow reserve. J Am Coll Cardiol. 2005;46(4):633–7.
60. Kumsars I, Narbute I, Thuesen L, Niemelä M, Steigen TK, Kervinen K, et al. Side branch fractional flow reserve measurements after main vessel stenting: a Nordic-Baltic Bifurcation study III substudy. EuroIntervention. 2012;7(10):1155–61.

61. Koo BK, Park KW, Kang HJ, Cho YS, Chung WY, Youn TJ, et al. Physiological evaluation of the provisional side-branch intervention strategy for bifurcation lesions using fractional flow reserve. Eur Heart J. 2008;29(6):726–32.
62. Chen S, Zhang J, Xu T, Liu Z, Ge Z, You W, et al. Randomized comparison of FFR-guided and angiography-guided provisional stenting of true coronary bifurcation lesions. 2015:1–12.
63. Strategy I, Clinical I. Fractional flow reserve for coronary. 2015:1–3.
64. De Bruyne B, Pijls NH, Heyndrickx GR, Hodeige D, Kirkeeide R, Gould KL. Pressure-derived fractional flow reserve to assess serial epicardial stenoses: theoretical basis and animal validation. Circulation. 2000;101(15):1840–7.
65. Saito N, Matsuo H, Kawase Y, Watanabe S, Bao B, Yamamoto E, et al. In vitro assessment of mathematically-derived fractional flow reserve in coronary lesions with more than two sequential stenoses. J Invasive Cardiol. 2013;25(12):642–9.
66. Seto AH, Tehrani DM, Bharmal MI, Kern MJ. Variations of coronary hemodynamic responses to intravenous adenosine infusion: implications for fractional flow reserve measurements. Catheter Cardiovasc Interv. 2014;84(3):416–25.
67. Echavarría-Pinto M, Gonzalo N, Ibañez B, Petraco R, Jimenez-Quevedo P, Sen S, et al. Low coronary microcirculatory resistance associated with profound hypotension during intravenous adenosine infusion implications for the functional assessment of coronary stenoses. Circ Cardiovasc Interv. 2014;7(1):35–42.
68. Tarkin JM, Nijjer S, Sen S, Petraco R, Echavarria-Pinto M, Asress KN, et al. Hemodynamic response to intravenous adenosine and its effect on fractional flow reserve assessment: results of the adenosine for the functional evaluation of coronary stenosis severity (AFFECTS) study. Circ Cardiovasc Interv. 2013;6(6):654–61.
69. Pijls NHJ, Klauss V, Siebert U, Powers E, Takazawa K, Fearon WF, et al. Coronary pressure measurement after stenting predicts adverse events at follow-up: a multicenter registry. Circulation. 2002;105(25):2950–4.
70. Jensen LO, Thayssen P, Thuesen L, Hansen HS, Lassen JF, Kelbaek H, et al. Influence of a pressure gradient distal to implanted bare-metal stent on in-stent restenosis after percutaneous coronary intervention. Circulation. 2007;116(24):2802–8.
71. Van't Veer M, Pijls NHJ, Aarnoudse W, Koolen JJ, Van De Vosse FN. Evaluation of the haemodynamic characteristics of drug-eluting stents at implantation and at follow-up. Eur Heart J. 2006;27(15):1811–7.
72. Klauss V, Erdin P, Rieber J, Leibig M, Stempfle H-U, König A, et al. Fractional flow reserve for the prediction of cardiac events after coronary stent implantation: results of a multivariate analysis. Heart. 2005;91(2):203–6.
73. Bittencourt MS, Hulten E, Ghoshhajra B, O'Leary D, Christman MP, Montana P, et al. Prognostic value of nonobstructive and obstructive coronary artery disease detected by coronary computed tomography angiography to identify cardiovascular events. Circ Cardiovasc Imaging. 2014;7(2):282–91.
74. Mushtaq S, De Araujo GP, Garcia-Garcia HM, Pontone G, Bartorelli AL, Bertella E, et al. Long-term prognostic effect of coronary atherosclerotic burden: validation of the computed tomography-Leaman score. Circ Cardiovasc Imaging. 2015;8(2):e002332.
75. Lopez-Palop R, Pinar E, Lozano Í, Saura D, Picó F, Valdés M. Utility of the fractional flow reserve in the evaluation of angiographically moderate in-stent restenosis. Eur Heart J. 2004;25(22):2040–7.
76. Yamashita J, Tanaka N, Fujita H, Akasaka T, Takayama T, Oikawa Y, et al. Usefulness of functional assessment in the treatment of patients with moderate angiographic paclitaxel-eluting stent restenosis. Circ J. 2013;77(5):1180–5.
77. Wilson SJS, Hunter G, Okane P, Swallow R, Talwar S, Levy T. Fractional flow reserve assessment for in-stent restenosis: providing the courage to defer target lesion revascularisation in angiographic significant lesions. EuroIntervention. 2012;8(Suppl N):Abstract 228.
78. Krüger S, Koch KC, Kaumanns I, Merx MW, Schäfer WM, Buell U, et al. Use of fractional flow reserve versus stress perfusion scintigraphy in stent restenosis. Eur J Intern Med. 2005;16(6):429–31.
79. Toth G, De Bruyne B, Casselman F, De Vroey F, Pyxaras S, Di Serafino L, et al. Fractional flow reserve-guided versus angiography-guided coronary artery bypass graft surgery. Circulation. 2013;128(13):1405–11.
80. Aqel R, Zoghbi GJ, Hage F, Dell'Italia L, Iskandrian AE. Hemodynamic evaluation of coronary artery bypass graft lesions using fractional flow reserve. Catheter Cardiovasc Interv. 2008;72(4):479–85.
81. Rapp AH, Hillis LD, Lange RA, Cigarroa JE. Prevalence of coronary artery disease in patients with aortic stenosis with and without angina pectoris. Am J Cardiol. Elsevier. 2001;87(10):1216–7.
82. Nishimura RA, Otto CM, Bonow RO, Carabello BA, Erwin JP, Guyton RA, et al. 2014 AHA/ACC guideline for the management of patients with valvular heart disease: executive summary: a report of the American College of Cardiology/American Heart Association Task Force on Practice Guidelines. Circ. 2014;129(23):2440–92.
83. Burgstahler C, Kunze M, Gawaz MP, Rasche V, Wöhrle J, Hombach V, et al. Adenosine stress first pass perfusion for the detection of coronary artery disease in patients with aortic stenosis: a feasibility study. Int J Cardiovasc Imaging. 2008;24(2):195–200.
84. Stähli BE, Maier W, Corti R, Lüscher TF, Altwegg LA. Fractional flow reserve evaluation in patients considered for transfemoral transcatheter aortic valve implantation: a case series. Cardiology. 2012;123(4):234–9.
85. Camuglia A, Poon K, Raffel O, Incani A, Savage M, Walters D. Fractional flow reserve assessment of epicardial coronary artery stenosis in the setting of severe degenerative valvular aortic stenosis. Lung and Circulation: Heart; 2012. p. S236–7.

# Instantaneous Wave Free Ratio (iFR)

Contents

# Validation of iFR: Clinical Registries

*Ricardo Petraco, Javier Escaned, and Justin Davies*




J. Escaned, J. Davies (eds.), *Physiological Assessment of Coronary Stenoses and the Microcirculation*,
DOI 10.1007/978-1-4471-5245-3_16

Initial landmark studies on coronary physiology presented the theory of coronary wave intensity analysis [1] and introduced the concept of instantaneous wave-free ratio (iFR) as an index of coronary stenosis severity [2]. Whilst these earlier studies set the physiological foundations for iFR and demonstrated its close relationship with fractional flow reserve (FFR), they were limited in their ability to directly reflect the performance of iFR in clinical practice, as their samples were not selected solely from patients undergoing FFR measurement in clinical practice [3]. For instance, ADVISE evaluated iFR's performance across a broad range of coronary stenosis severities, which included tight and mild coronary lesions, in the same line as pioneering studies of FFR [4] and other perfusion modalities [5]. However, in everyday practice, and in agreement with clinical practice guideline recommendations [6], functional intracoronary assessment of stenosis severity is predominantly used to interrogate intermediate stenoses of unclear severity. It was likely that these different strategies of lesion selection could influence the agreement between iFR and FFR on classifying coronary stenoses. Therefore, the next step in the validation of iFR as a clinically applicable index was to study its performance against FFR in clinical registries. In this chapter, we aim to demonstrate the importance of clinical registries on the initial validation of iFR and explain how they more closely reflect the true clinical performance of an index when directly applied to patients. Finally, we present the initially proposed approach to use iFR and FFR in a hybrid diagnostic pathway, a concept derived from combined clinical registries.

## 16.1 Diagnostic Performance and Disease Severity: The Importance of Clinical Samples

The diagnostic accuracy of a test is largely dependent on the distribution of disease severity in the underlying sample being studied [3]. Figure 16.1 demonstrates why accuracy is high at the extremes but falls close to intermediate values of disease severity. In the case of iFR and coronary disease, studies that include more severe stenoses in their samples are bound to present higher values of diagnostic accuracy against FFR – or indeed any other reference gold standard. This was the case for ADVISE, a study formed by a wide range of stenosis severities and which reported an agreement between iFR and FFR of 88 % with an AUROC curve of 93 % [2]. Therefore, following ADVISE, it was essential for the relationship between iFR and FFR to be tested in clinical registries, studies which are formed by patients solely selected by clinicians and which reflect the daily applicability of physiology in clinical practice.

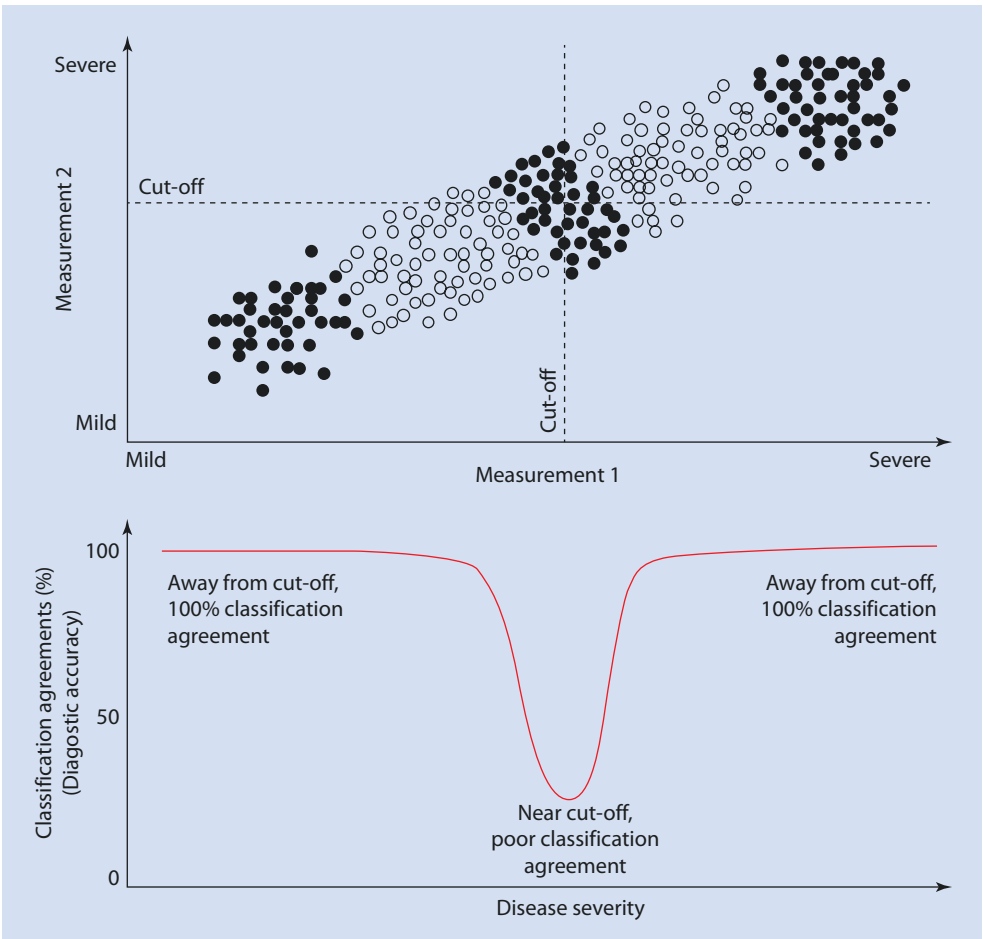


**Fig. 16.1** Schematic representation of the relationship between disease severity in a study sample (*x* axis) and the accuracy of a diagnostic method being evaluated (*y* axis). This is a universal principle also applicable to the validation of iFR. Study samples made of intermediate forms of disease severity such as clinical registries will result in lower values of overall accuracy than pilot studies which include a wider range of disease severity

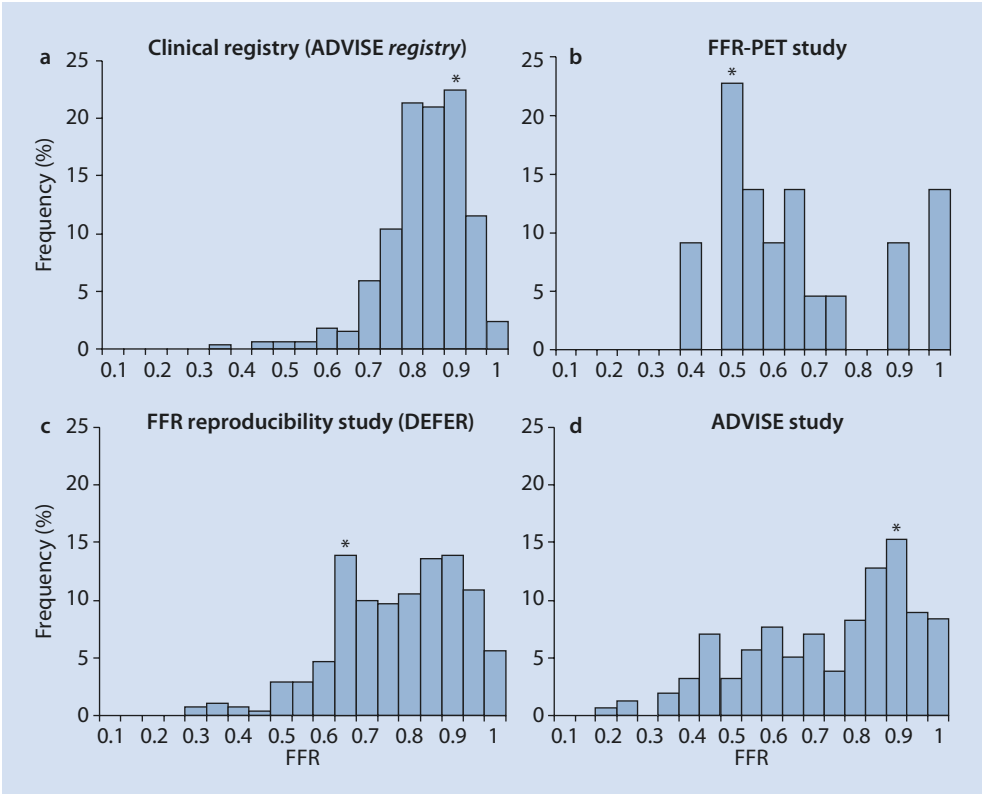


**Fig. 16.2** Distribution of FFR values in different studies of coronary physiology. Clinical registries such as the ADVISE Registry **a** are formed by a cluster of physiologically intermediate stenoses around the ischaemic cut-off of 0.80, because lesions are selected based on clinical grounds. Landmark validation studies often display a different pattern of FFR distribution, in a case-control fashion away from the cut-off **b** or with a wide range of ischaemic lesions **c**, **d**

## 16.2 The Concept of Physiologically Intermediate Stenoses

Different from early validation studies, which include stenoses with a wide range of FFR values, clinical registries are formed by samples of intermediate physiological severity, with lesions clustering around the FFR cut-off of 0.80 (Fig. 16.2). For instance, 72 % of lesions in the ADVISE *in practice* study [7] had FFR values between 0.70 and 0.90 with only 1 % being lower than 0.50. This phenomenon was originally observed in the ADVISE Registry and subsequently described in the ADVISE II [8] and other independent clinical registries [9, 10]. The finding that registries are formed predominantly by stenoses close to the ischaemic cut-off, with less extreme disease, not only has implications to the diagnostic accuracy of new indices being evaluated but also demonstrates that clinicians, when selecting *anatomically* intermediate lesions to interrogate with physiology, are relatively accurate at identifying those which are *physiologically* intermediate.

## 16.3 Lesion Distribution and the Agreement Between iFR and FFR

The first clinical registry published on iFR, the ADVISE Registry, reported a classification agreement between iFR and FFR of 80 % with an AUROC curve of 86 % [3]. These slightly lower values of accuracy than originally reported in ADVISE do not reflect any worsening in the numerical relationship between the indices. Indeed, the standard error of the estimate (SEE) between iFR and FFR in ADVISE Registry was slightly *lower* than in ADVISE (0.06 versus 0.09), reflecting a closer overall numerical agreement between the indices. The lower values of agreement (80 % versus 88 %) solely reflected the differences in sample distribution between the studies. For instance, whilst 41 % of the patients in ADVISE had FFR values < 0.7, in ADVISE Registry most FFR values (81 %) fell between 0.60 and 0.90, a pattern found in data from the three participating institutions (Fig. 16.2) and in other published clinical registries [8].

Following the publication of ADVISE Registry, many other independent studies have been published describing the relationship between iFR and FFR in clinical samples [7, 9–11]. Table 16.1 summarises the findings of all clinical registries published to date and demonstrates the consistency of reported diagnostic agreement across all studies, independently from sample size or study location. Amongst these studies, three are particularly relevant as they brought new insights into the utilisation of iFR in clinical practice. Firstly, the ADVISE *in practice* was the first to report the performance of live iFR, with values obtained from clinical consoles and reported by operators from catheter laboratories around Europe, Africa and Asia. Its results, therefore, demonstrated the feasibility of iFR utilisation by the clinical community and confirmed the applicability of earlier offline core lab reports to clinical practice. Secondly, an Italian registry presented by Fede et al. demonstrated very

**Table 16.1** List of iFR clinical registries published to date

| Study | Author, year | Size (N) | Reported iFR-FFR agreement (%) | Optimal iFR cut-off |
|---|---|---|---|---|
| ADVISE Registry | Petraco, 2012 | 339 | 80 | 0.89 |
| South Korean Registry | Park, 2013 | 238 | 82 | 0.90 |
| ADVISE *in practice* | Petraco, 2014 | 392 | 80 | 0.90 |
| Italian Registry I | Indolfi, 2015 | 123 | 80 | 0.89 |
| Italian Registry II | Fede, 2015 | 89 | 85 | 0.89 |
| German Registry | Harle, 2015 | 151 | 83 | 0.90 |
| ADVISE II | Escaned, 2015 | 690 | 83 | 0.89 |

high reproducibility for three sequential measurements of iFR from clinical consoles [10]. Finally, Indolfi et al. independently demonstrated the potential for iFR utilisation in non-culprit lesions of patients presenting with acute coronary syndrome [11].

## 16.4 Reproducibility of FFR Stenosis Classification Is Also Affected by Study Sample

Initial iFR validation studies, including clinical registries, used FFR as a reference ischaemic modality. Therefore, it was equally important to explore the limitations of the gold standard and understand how frequently FFR disagrees with itself in repeated measurements. The ADVISE Registry demonstrated that, similar to the relationship between iFR and FFR, FFR reproducibility of lesion classification also falls close to the 0.80 cut-off (Fig. 16.3) [3]. As a result, FFR intrinsic agreement – when FFR is measured 10 min apart in the same lesion – is also dependent on the underlying sample distribution, with clinical populations of physiologically intermediate stenoses showing lower values than studies with wider lesion distribution [12]. For instance, it can be estimated that, in clinical registries, in 15 % of cases in which FFR is measured twice, 10 min apart, there will be disagreement between the first and the second measurement, with respect to being below or above the 0.80 cut-off. This intrinsic FFR accuracy of 85 % is relevant because it represents a ceiling against which other modalities cannot improve upon in lesion classification when tested against FFR.

## 16.5 Clinical Registries and Optimal iFR Cut-Off

Another important step in iFR validation derived from clinical registries was the establishment of its optimal cutpoint to match a clinical FFR cut-off of 0.80. The ADVISE study, as a pilot physiological study, reported an optimal iFR cut-off of 0.83 to match an FFR value of 0.80 [2]. However, as we discussed before, ADVISE was underpowered in the physiologically intermediate range of FFR values, precisely the region which influences AUROC-derived cut-offs. All subsequent studies on iFR performed in clinical samples reported an optimal iFR cut-off of 0.89–0.90 (Table 16.1), a finding later prospectively validated in the ADVISE II study [8].

## 16.6 The Hybrid iFR-FFR Approach to Decision-Making

Clinical registries which directly compared the classification of intermediate coronary stenoses by iFR and FFR revealed a consistent pattern of agreement between the two methods: outside of the intermediate range of iFR and FFR values agreement is very high (>90 %), whilst disagreements are concentrated in the zone near their cut-offs [3]. This pattern of high classification agreement between iFR and FFR outside of the intermediate zone provided the opportunity for the introduction into clinical practice of a staged, hybrid iFR-FFR decision-making strategy, in which only patients within a certain range of intermediate iFR values would require FFR measurement. In a combined analysis of the ADVISE Registry and a South Korean registry, the hybrid iFR-FFR strategy was compared with an FFR-only strategy, in which all patients would undergo FFR measurements [13]. About 519 stenoses were included in the original study, with results summarised in Fig. 16.4: if an iFR value is >0.93, it can be used to defer treatment, and an iFR value of <0.86 can be used to confirm the need for revascularisation. Values in between 0.86 and 0.93 would require FFR measurement for revascularisation decision. With such approach, 57 % of stenoses would be spared from vasodilator administration with a 95 % classification agreement with an FFR-to-all strategy. This strategy permitted the benefits of both techniques to be immediately applied to patients: the safety and prognostic implications of a high agreement with FFR classification of lesions (95 %) and a significant reduction (57 %) in the need for vasodilator administration. In practice, it meant that soon after the introduction of iFR into clinical practice, a three-vessel physiological assessment could be performed with adenosine only being given to one interrogation. The ADVISE II study later prospectively validated the hybrid iFR-FFR approach in a larger, multicentre study including centres in the USA (see below). The hybrid approach has since been applied clinically in man centres around Europe, Asia and Africa, a strategy likely to become established until outcome data for iFR is available.

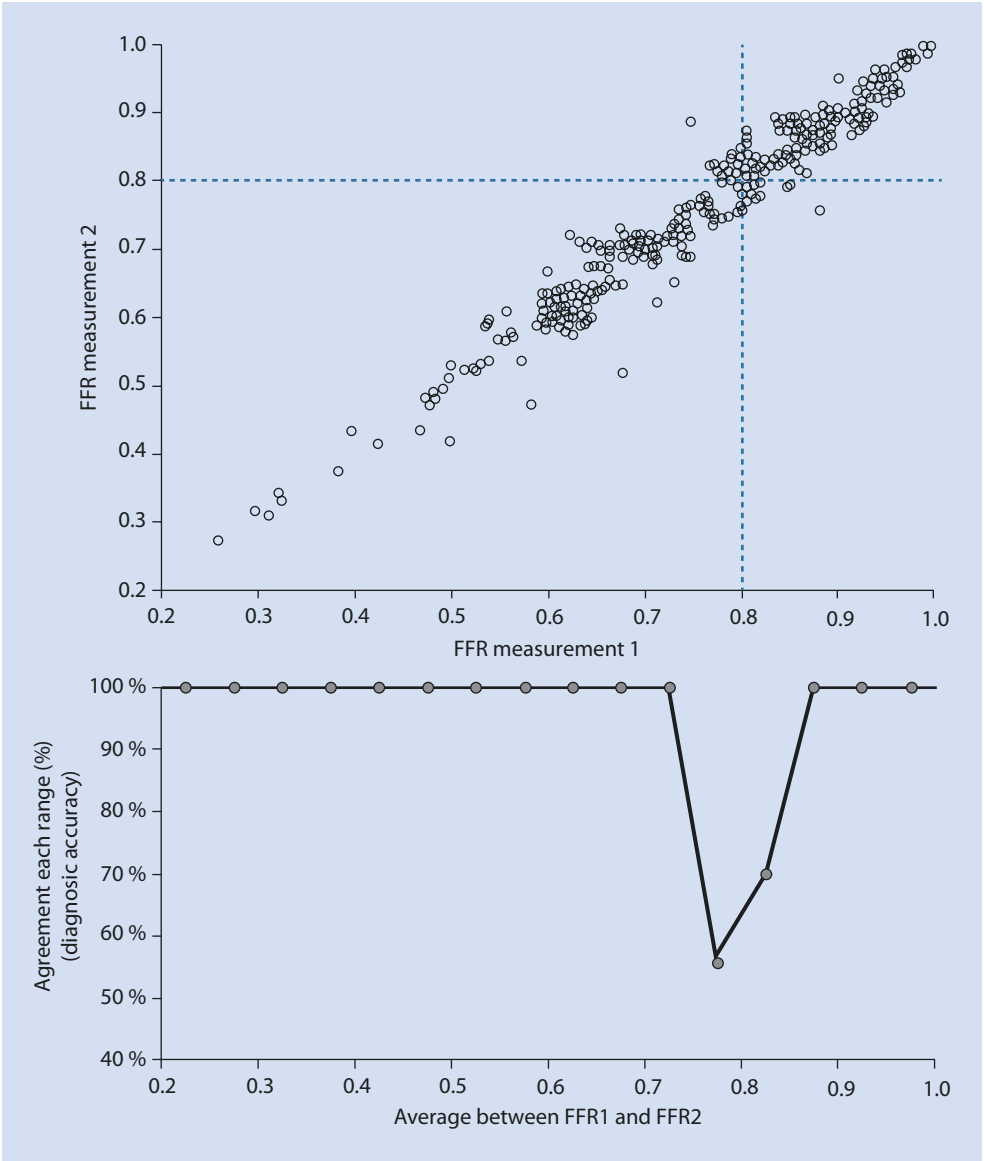


**Fig. 16.3** The reproducibility scatter plot from the DEFER study (top panel, two FFR measurements, 10 min apart) is presented together with the classification agreement between repeated FFR measurements (bottom panel). Agreement between repeated FFR measurements falls in the intermediate range of FFR values (close to 0.80 cut-off). In populations such as found in clinical registries, formed predominantly by intermediate stenoses, FFR reproducibility in lesion classification is approximately 85 %

## 16.7 The Limitation of iFR Clinical Registries: FFR as a Gold Standard for Ischaemia

Clinical registries were an essential step in the validation of iFR as a novel index of disease severity as they evaluated the relationship between iFR and FFR in clinical practice. However, all iFR registries shared a common fundamental limitation, which is the utilisation of FFR as a reference gold standard. Although over the last 20 years FFR has been established as the most widely used methodology for invasive lesion interrogation in clinical practice, its utilisation as a true biological reference for ischaemia could be challenged [14, 15]. For instance, contemporary metro-analysis of FFR performance in clinical practice reported an overall agreement between FFR and other perfusion modalities to 76 % [16], similar to the overall 80–90 % performance of iFR. Indeed, subsequent steps in iFR validation have since determined that despite its overall 10–20 % disagreement with FFR in lesion classification, it has equal ability to detect ischaemia [17] and flow limitation [18, 19] when other perfusion modalities are used as differentiators.

## 16.8 ADVISE II: Prospective Validation of the Hybrid iFR-FFR Approach in Clinical Practice

The first studies that reported the initial performance of iFR in clinical samples were all retrospective analysis of previously collected data, originally used for clinical decision-making. This methodology represents one of the strengths of clinical registries with respect to the meaningfulness of their results to clinical practice. However, the lack of prospective protocols for data collection and, most importantly, the absence of a core lab for data analysis were inevitable limitations of such studies. Also, most initially reported iFR registry studies were single-centre experiences from outside the USA (mostly Europe, Asia and

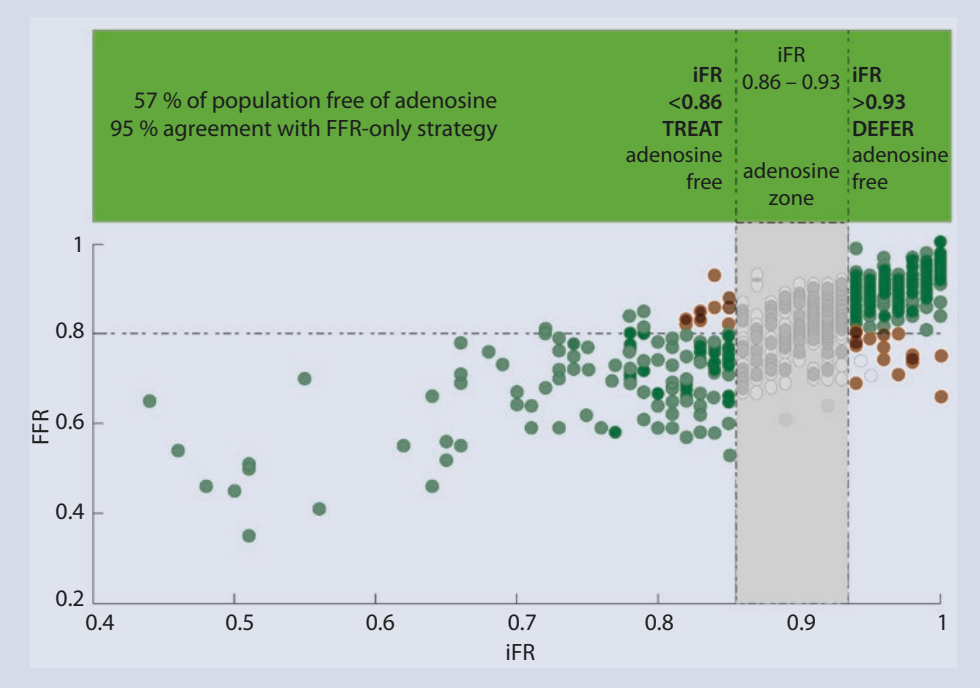


**Fig. 16.4** Proposed hybrid strategy for clinical decision-making, in which iFR and FFR are used in a staged approach. iFR is initially measured in all stenoses. If iFR is >0.93, lesion is deferred without the need for FFR measurement. If iFR is <0.86, lesion is treated without the need for FFR measurement. If iFR falls in between 0.86 and 0.93, FFR is measured and used to guide revascularisation. This approach provides an overall 95 % agreement with an FFR-only strategy whilst sparing 57 % of stenosis interrogation from the need for vasodilator and FFR measurement. The hybrid iFR-FFR approach has been used in catheter laboratories around the world until outcome data is available to judge the merits of using iFR as a sole guide to decision-making

Africa). Finally, the initially proposed hybrid iFR-FFR strategy was also a retrospective analysis of two independent cohorts.

The ADVISE II study was an investigator-led, multicentre study with an independent core lab, designed to overcome all of the above limitations [8]. It aimed to corroborate the results of previously reported registries and, most importantly, provide a prospective validation of the hybrid iFR-FFR strategy. ADVISE II differed from previous landmark FFR studies as it recruited only patients undergoing physiological interrogation of stenosis based on clinical grounds, hence providing a clinical distribution of disease severity. ADVISE II results confirmed all previous retrospective reports, by demonstrating, across 45 centres and in 690 lesions, an overall 83 % agreement between iFR and FFR using a prespecified iFR cut-off of 0.89. Also, it prospectively confirmed the findings of the initial retrospective hybrid analysis, showing that 69 % of stenoses could be interrogated without vasodilator, whilst maintaining a high 94 % agreement with FFR. Importantly, ADVISE II presented its FFR data distribution and confirmed its role as the first prospective physiological study performed with a clinical distribution of ischemia, making its results immediately applicable to clinical practice. ADVISE II results led to iFR being approved by FDA in a hybrid strategy with FFR.

## 16.9 Chapter Summary: Lessons from iFR Clinical Registries

- Study samples can significantly affect the diagnostic accuracy of new indices (Fig. 16.1);
- Clinical iFR registries are formed predominantly by physiologically intermediate lesions, clustered around the FFR cut-off of 0.80 (Fig. 16.2);
- Reproducibility of FFR in lesion classification is also affected by disease distribution of the underlying sample, being approximately 85 % in clinical registries (Fig. 16.3);
- Agreement between iFR and FFR in clinical samples ranges from 80 to 85 % (Table 16.1);
- The optimal iFR cut-off to match an FFR of 0.80 is 0.89 (Table 16.1);
- The hybrid iFR-FFR strategy can spare 57–69 % of stenoses from the need for vasodilator whilst maintaining a 94–95 % agreement with FFR (Fig. 16.4);
- The ADVISE II study prospectively validated across 45 centres the results of previous clinical registries and confirmed the applicability of iFR in clinical practice;

## References

1. Davies JE, Whinnett ZI, Francis DP, Manisty CH, Aguado-Sierra J, Willson K, Foale RA, Malik IS, Hughes AD, Parker KH, Mayet J. Evidence of a dominant backward-propagating "suction" wave responsible for diastolic coronary filling in humans, attenuated in left ventricular hypertrophy. Circulation. 2006;113:1768–78.
2. Sen S, Escaned J, Malik IS, Mikhail GW, Foale RA, Mila R, Tarkin J, Petraco R, Broyd C, Jabbour R, Sethi A, Baker CS, Bellamy M, Al-Bustami M, Hackett D, Khan M, Lefroy D, Parker KH, Hughes AD, Francis DP, Di Mario C, Mayet J, Davies JE. Development and validation of a new adenosine-independent index of stenosis severity from coronary wave-intensity analysis: results of the advise (adenosine vasodilator independent stenosis evaluation) study. J Am Coll Cardiol. 2012;59:1392–402.
3. Petraco R, Escaned J, Sen S, Nijjer S, Asrress KN, Echavarria-Pinto M, Lockie T, Khawaja MZ, Cuevas C, Foin N, Broyd C, Foale RA, Hadjiloizou N, Malik IS, Mikhail GW, Sethi A, Kaprielian R, Baker CS, Lefroy D, Bellamy M, Al-Bustami M, Khan MA, Hughes AD, Francis DP, Mayet J, Di Mario C, Redwood S, Davies JE. Classification performance of instantaneous wave-free ratio (ifr) and fractional flow reserve in a clinical

population of intermediate coronary stenoses: results of the advise registry. Eurointervention. 2013;9:91–101.
4. De Bruyne B, Baudhuin T, Melin JA, Pijls NH, Sys SU, Bol A, Paulus WJ, Heyndrickx GR, Wijns W. Coronary flow reserve calculated from pressure measurements in humans. Validation with positron emission tomography. Circulation. 1994;89:1013–22.
5. Pijls NHJ, de Bruyne B, Peels K, van der Voort PH, Bonnier HJRM, Bartunek J, Koolen JJ. Measurement of fractional flow reserve to assess the functional severity of coronary-artery stenoses. N Engl J Med. 1996;334:1703–8.
6. Windecker S, Kolh P, Alfonso F, Collet JP, Cremer J, Falk V, Filippatos G, Hamm C, Head SJ, Juni P, Kappetein AP, Kastrati A, Knuuti J, Landmesser U, Laufer G, Neumann FJ, Richter DJ, Schauerte P, Sousa Uva M, Stefanini GG, Taggart DP, Torracca L, Valgimigli M, Wijns W, Witkowski A. 2014 esc/eacts guidelines on myocardial revascularization: the task force on myocardial revascularization of the european society of cardiology (esc) and the european association for cardio-thoracic surgery (eacts)developed with the special contribution of the european association of percutaneous cardiovascular interventions (eapci). Eur Heart J. 2014;35:2541–619.
7. Petraco R, Al-Lamee R, Gotberg M, Sharp A, Hellig F, Nijjer SS, Echavarria-Pinto M, van de Hoef TP, Sen S, Tanaka N, Van Belle E, Bojara W, Sakoda K, Mates M, Indolfi C, De Rosa S, Vrints CJ, Haine S, Yokoi H, Ribichini FL, Meuwissen M, Matsuo H, Janssens L, Katsumi U, Di Mario C, Escaned J, Piek J, Davies JE. Real-time use of instantaneous wave–free ratio: results of the advise in-practice: an international, multicenter evaluation of instantaneous wave–free ratio in clinical practice. Am Heart J. 2014;168:739–48.
8. Escaned J, Echavarría-Pinto M, Garcia-Garcia HM, van de Hoef TP, de Vries T, Kaul P, Raveendran G, Altman JD, Kurz HI, Brechtken J, Tulli M, Von Birgelen C, Schneider JE, Khashaba AA, Jeremias A, Baucum J, Moreno R, Meuwissen M, Mishkel G, van Geuns R-J, Levite H, Lopez-Palop R, Mayhew M, Serruys PW, Samady H, Piek JJ, Lerman A. Prospective assessment of the diagnostic accuracy of instantaneous wave-free ratio to assess coronary stenosis relevance: results of advise ii international, multicenter study (adenosine vasodilator independent stenosis evaluation ii). JACC Cardiovasc Interv. 2015;8:824–33.
9. Härle T, Bojara W, Meyer S, Elsässer A. Comparison of instantaneous wave-free ratio (ifr) and fractional flow reserve (ffr) — first real world experience. Int J Cardiol. 2015;199:1–7.
10. Fede A, Zivelonghi C, Benfari G, Pesarini G, Pighi M, Ferrara A, Piccoli A, Ariotti S, Ferrero V, Mura DD, Battistoni M, Vassanelli C, Ribichini F. Ifr-ffr comparison in daily practice: a single-center, prospective, online assessment. J Cardiovasc Med. 2015;16:625–31.
11. Indolfi C, Mongiardo A, Spaccarotella C, Torella D, Caiazzo G, Polimeni A, Sorrentino S, Micieli M, Sabatino J, Curcio A, De Rosa S. The instantaneous wave-free ratio (ifr) for valuation of non-emculprit lesions in patients with acute coronary syndrome and multivessel disease. Int J Cardiol. 2015;178:46–54.
12. Petraco R, Sen S, Nijjer S, Echavarria-Pinto M, Escaned J, Francis DP, Davies JE. Fractional flow reserve-guided revascularization: practical implications of a diagnostic gray zone and measurement variability on clinical decisions. JACC Cardiovasc Interv. 2013;6:222–5.
13. Petraco R, Park JJ, Sen S, Nijjer SS, Malik IS, Echavarria-Pinto M, Asrress KN, Nam CW, Macias E, Foale RA, Sethi A, Mikhail GW, Kaprielian R, Baker CS, Lefroy D, Bellamy M, Al-Bustami M, Khan MA, Gonzalo N, Hughes AD, Francis DP, Mayet J, Di Mario C, Redwood S, Escaned J, Koo BK, Davies JE. Hybrid ifr-ffr decision-making strategy: Implications for enhancing universal adoption of physiology-guided coronary revascularisation. Eurointervention. 2013;8:1157–65.
14. Plein S, Motwani M. Fractional flow reserve as the reference standard for myocardial perfusion studies: fool's gold? Eur Heart J Cardiovasc Imaging. 2013;14(12):1211-3. doi: 10.1093/ehjci/jet110. Epub 2013 Jun 21.
15. Petraco R, Escaned J, Nijjer S, Sen S, Echavarria-Pinto M, Francis DP, Davies JE. Reply fractional flow reserve: a good or a gold standard? JACC Cardiovasc Interv. 2014;7:228–9.
16. Christou MAC, Siontis GCM, Katritsis DG, Ioannidis JPA. Meta-analysis of fractional flow reserve versus quantitative coronary angiography and noninvasive imaging for evaluation of myocardial ischemia. Am J Cardiol. 2007;99:450–6.
17. van de Hoef TP, Meuwissen M, Escaned J, Sen S, Petraco R, van Lavieren MA, Echavarria-Pinto M, Nolte F, Nijjer S, Chamuleau SA, Voskuil M, van Eck-Smit BL, Verberne HJ, Henriques JP, Koch KT, de Winter RJ, Spaan JA, Siebes M, Tijssen JG, Davies JE, Piek JJ. Head-to-head comparison of basal stenosis resistance index, instantaneous wave-free ratio, and fractional flow reserve: diagnostic accuracy for stenosis-specific myocardial ischaemia. EuroIntervention. 2015;11(8):914-25. doi: 10.4244/EIJY14M08_17.
18. Petraco R, van de Hoef TP, Nijjer S, Sen S, van Lavieren MA, Foale RA, Meuwissen M, Broyd C, Echavarria-Pinto M, Foin N, Malik IS, Mikhail GW, Hughes AD, Francis DP, Mayet J, Di Mario C, Escaned J, Piek JJ, Davies JE. Baseline instantaneous wave-free ratio as a pressure-only estimation of underlying coronary flow reserve: results of the justify-cfr study (joined coronary pressure and flow analysis to determine diagnostic characteristics of basal and hyperemic indices of functional lesion severity–coronary flow reserve). Circ Cardiovasc Interv. 2014;7:492–502.
19. Sen S, Asrress KN, Nijjer S, Petraco R, Malik IS, Foale RA, Mikhail GW, Foin N, Broyd C, Hadjiloizou N, Sethi A, Al-Bustami M, Hackett D, Khan MA, Khawaja MZ, Baker CS, Bellamy M, Parker KH, Hughes AD, Francis DP, Mayet J, Di Mario C, Escaned J, Redwood S, Davies JE. Diagnostic classification of the instantaneous wave-free ratio is equivalent to fractional flow reserve and is not improved with adenosine administration: results of clarify (classification accuracy of pressure-only ratios against indices using flow study). J Am Coll Cardiol. 2013;61:1409–20.

# Application of iFR in Clinical Scenarios

*Sukhjinder Nijjer and Justin Davies*




J. Escaned, J. Davies (eds.), *Physiological Assessment of Coronary Stenoses and the Microcirculation*,
DOI 10.1007/978-1-4471-5245-3_17

## 17.1 Introduction

The instantaneous wave-free ratio (iFR) is a clinical tool that uses a pressure wire to guide whether a stenosis in a coronary artery is sufficiently severe to benefit from stenting.

iFR is a resting pressure-only index of stenosis severity which measures coronary pressures during a specific part of diastole, known as the wave-free period [1]. During this period, the flow in a coronary vessel is at its highest and resistance the lowest, relative to other parts of the cycle during rest (Fig. 17.1) [2]. In studies of physiologically important stenoses, the flow over the wave-free period is statistically not different from flow measured during adenosine-mediated hyperemia [2]. Similarly, the translesional pressure gradient is the largest at rest over the wave-free period, and pressure-flow curves generated from large datasets while resting flow is relatively preserved across stenosis severities, can readily distinguish between stenosis severities [3].

The nature of iFR is that it quantifies the impact of a stenosis upon the coronary microcirculation [3]. Important coronary stenoses cause natural resting microcirculatory dilatation, causing a reduction in microvascular resistance. This preserves resting coronary flow to maintain homeostasis, but it occurs at the expense of distal coronary pressure. The reduction in transtenotic gradient over the wave-free period is directly related to the physiological importance of the stenosis. These findings are true in both focal and diffuse stenoses, as well tandem disease [3]. The relative preservation of resting flow within a vessel means that pressure gradients measured at specific points in the vessel are valid for the stenoses proximal to measurement point. This enables interesting clinical applications when the iFR is measured using a pressure pullback and measured after coronary intervention [4–6].

This chapter discusses iFR and its determination, practical considerations when making a pressure wire assessment, and its applications in common clinical scenarios.

## 17.2 Clinical Measurement of iFR

### 17.2.1 Calculation of iFR

iFR is a pressure-only index that is measured during the wave-free period in diastole. The wave-free period was determined using wave-intensity analysis [1], and is a period where the conflicting forces the control blood flow are quiescent, and microcirculatory resistance is at its lowest value compared to the whole cardiac cycle at rest. Since resistance is stable, pressure and flow are linearly related over the wave-free period, enabling a resting pressure index to assess stenosis severity without the need of an exogenous vasodilator (Fig. 17.1).

iFR is calculated in the same manner as other pressure-only-based pressure wire techniques. Once the pressure sensor beyond the stenosis is in question, iFR can be calculated over a single heartbeat calculation or more typically as average of several beats. Activating the iFR calculation on the console will trigger the algorithm to make a measurement over several heartbeats – when the calculation is consistently stable, the value is reported: this is typically over five heartbeats (Fig. 17.2).

### 17.2.2 Dealing with Variable Heart Rhythms

Algorithms within the commercial consoles are capable of excluding inappropriate beats with a wide variability. When significant variability is detected on a beat-to-beat basis, the console will typically measure over more heartbeats to provide a more reliable average iFR value. The algorithm relies upon both pressure and ECG gating to ensure the correct time period in diastole is isolated. This means that iFR is not affected by beat-to-beat variability or atrial arrhythmias. Measurements are accurate within heart rates typical for performing physiological assessment (40–130 bpm). Physiological assessment at heart rates beyond these values is unlikely to be helpful – patients with such bradycardia or tachycardias will have other clinical priorities that require treatment first.

ECG monitoring has been recommended to correctly elucidate the diastolic wave-free period; the console systems should be linked to the hemodynamic system using the catheter laboratory. New advances mean that newer pressure-only algorithms can accurately measure iFR without ECG connection and this will further simplify the setup required. This may be of value when patients are found to have unreliable ECG recordings or if the catheter lab in question is unable to output ECG data to the pressure wire console.

### 17.2.3 Performing an iFR Pullback

iFR can be plotted throughout the vessel during gentle pressure wire pullback to identify focal and diffuse disease throughout the vessel (Fig. 17.3). The degree of information observed will depend partly upon the speed of pullback; about 20–30 s typically suffices. Since this information is acquired at rest, the degree of flow interaction that can occur between multiple stenoses during hyperemia is minimized. This provides an additional advantage of an iFR pullback approach, since it becomes possible to predict the hemodynamic effect of removing a stenosis. The residual resting gradients typically remain the same after coronary intervention since resting flow velocity changes little. This novel additional information may facilitate a more physiologically guided coronary intervention than hitherto possible.

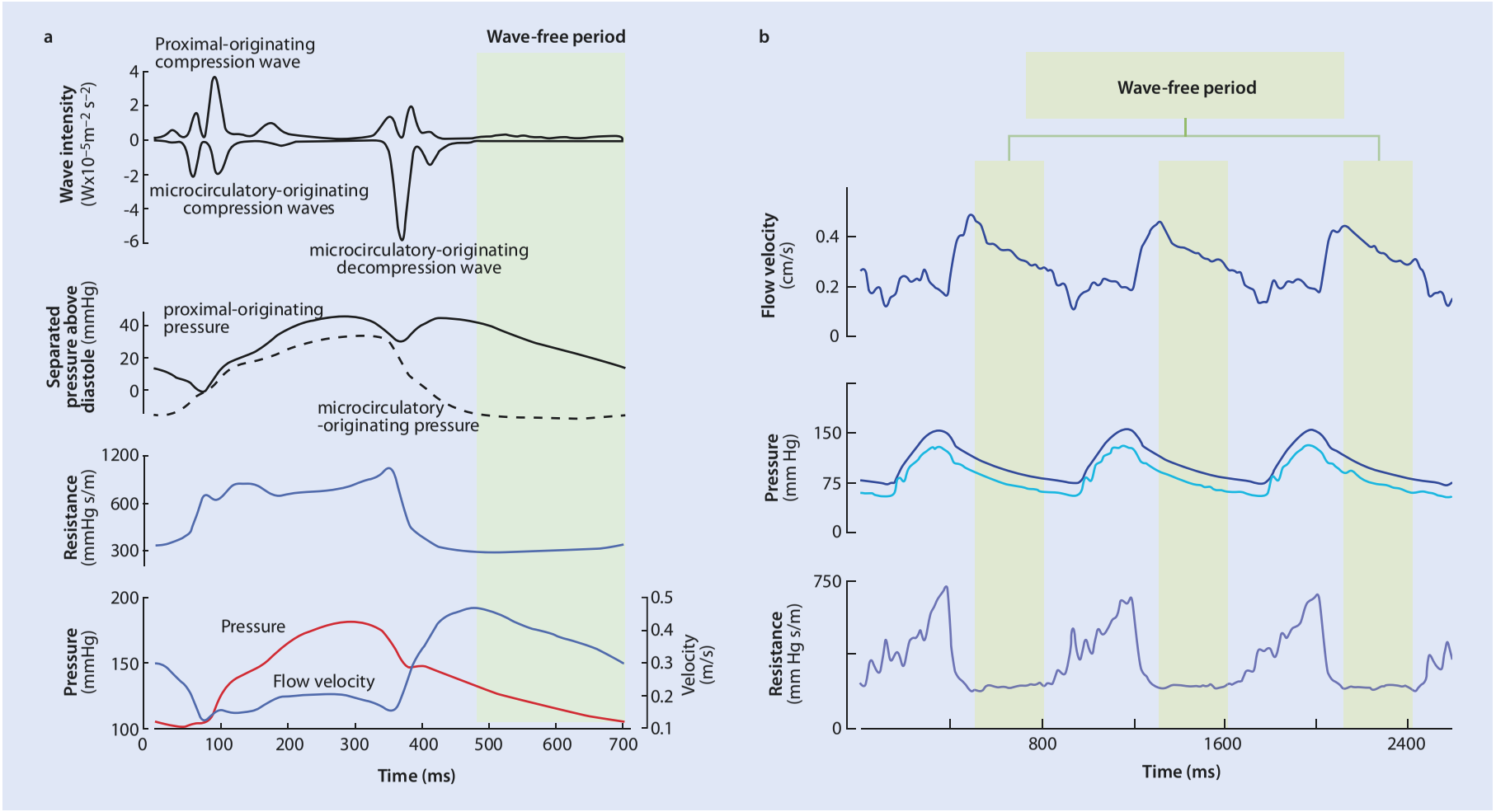


**Fig. 17.1** iFR and the wave-free period. **a** Wave-intensity analysis figure. Panel **a** is adapted from (Sen, "Development and Validation of a New Adenosine-Independent Index of Stenosis Severity From Coronary Wave–Intensity Analysis", 2012). Wave-intensity analysis (*upper most panel*) demonstrates the proximal and microcirculatory (distal) originating waves generated during the cardiac cycle. A wave-free period can be seen in diastole when no new waves are generated (*shaded green*). This corresponds to a time period in which there is minimal microcirculatory (distal) originating pressure (*second panel*), minimal and constant resistance (*third panel*), and a nearly constant rate of change in flow velocity (*fourth panel*). **b** Multiple heartbeats are shown, including systole and diastole. The green-shaded areas show the wave-free period is reproducible from beat to beat. Resistance is constant, while flow velocity is higher than over the whole cycle


**Fig. 17.2** Example of iFR. Example of iFR calculation. The ratio of pressures over the wave-free period (shown in *green*) are averaged over five beats. A value of <0.90 suggests the presence of ischemia. Note an ECG is attached and used to gate the detection of the wave-free period. The quality of the ECG should be checked

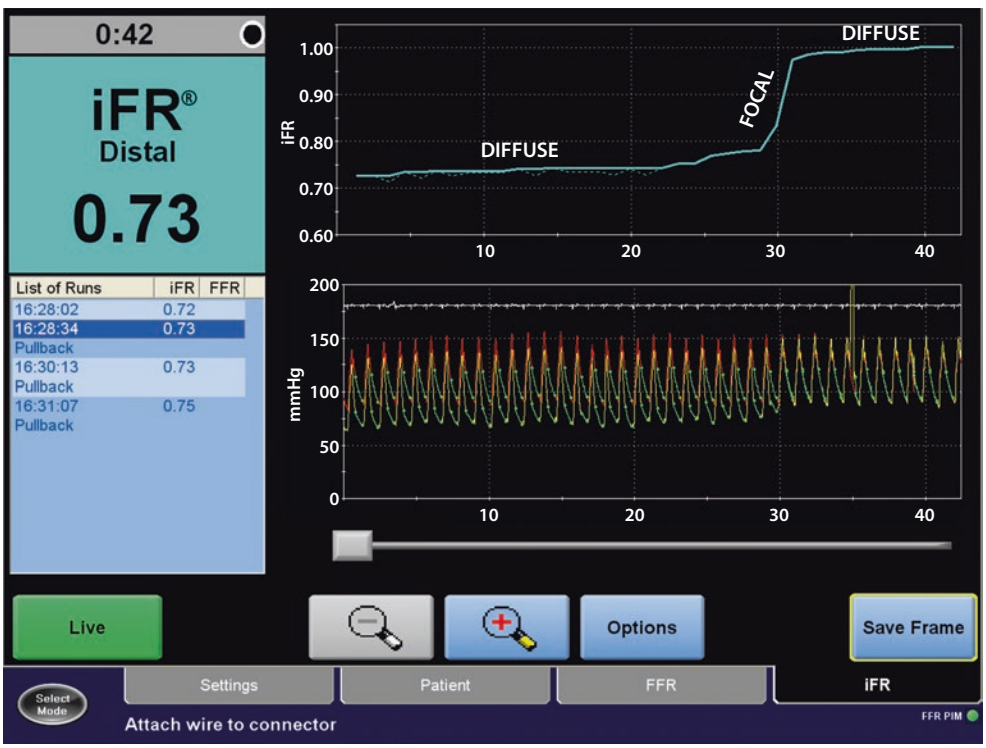


**Fig. 17.3** Example of iFR pullback. The operator should observe the line while watching the wire position on fluoroscopy. A novel innovation is the inclusion of a dotted raw iFR line, and the sold line which never falls back below the last calculated iFR value. A great deal of information can be observed on the solid blue line compared to the raw pressure trace it is acquired from (*lower panel*)

### 17.2.4 Using iFR During Adenosine Infusions

It is also possible to measure iFR during the administration of a vasodilator such as adenosine (referred to as iFRa). This will consistently produce lower iFR values, and in the IDEAL study, 87 % of iFRa values were lower than the FFR in the same vessel. However, there is no additional diagnostic advantage with similar diagnostic accuracies between iFR and FFR when compared against a third-party gold stand such as hyperemic stenosis resistance [2].

## 17.3 Practical Considerations of Pressure Wire Measurement

### 17.3.1 Aortic Pressure Measurement

It is typical to measure aortic pressure (Pa) continuously throughout intracoronary procedures utilizing the fluid-filled hollow guide catheters. Pressure is transmitted through the column of fluid from the tip of the guiding catheter through a connecting tube to a pressure transducer integrated into the catheter laboratory hemodynamic system. The height of transducer system was adjusted according to the patient size and position on the catheter table, typically 5 cm below the sternum and then fixed for each case. This position estimates the location of the aortic root (Fig. 17.4). The transducer system and the console were simultaneously zeroed by opening the ports to air at the beginning of every case and during the case when adjustments to patient position or a new pressure wire were required. All the tubing and manifold system was flushed and kept clear of any bubbles that may interfere with pressure tracings.

### 17.3.2 Challenges in Optimizing Pressure Recordings

1. Transducer height: Transducer height should be placed at the level of the aortic root, since when it is above the heart, the aortic pressure trace will be *below* that of the coronary pressure trace (Fig. 17.4). This error is commonly and easily recognized. If, however, the transducer is below the heart, then the aortic pressure trace is above the distal coronary pressure to give the appearance of an apparent transtenotic pressure gradient. This is more challenging to recognize and if missed can lead to erroneously positive results. However, it is readily resolved by performing normalization at the beginning of the case and checking for equalization of pressures whenever the sensor is returned to the vessel ostium.
2. Pressure signal drift: Iterations of pressure wire technology have reduced pressure wire drift, but it remains a recognized issue that must be actively sought. This can be identified at the end of the distal pressure recording when the sensor is returned to the ostium. Provided there is no drift, the Pd/Pa ratio should remain at 1.0. If the value differs from 1.0, then drift has occurred – a result of electrical charge developing on the pressure sensor. Drift may also be identified when the wire is distal to a stenosis since the pressure waveform may take on the appearance of the aortic trace. Measurements should be repeated if drift exceeds 2 mmHg. Drift is a dynamic problem as a result of electrical phenomenon and is more likely if the wire is used rapidly after activation. To prospectively counter this, early activation of the wire with a heparinized saline flush is recommended. Allowing a longer period of inactivity between activation and clinical usage should minimize early wire drift.

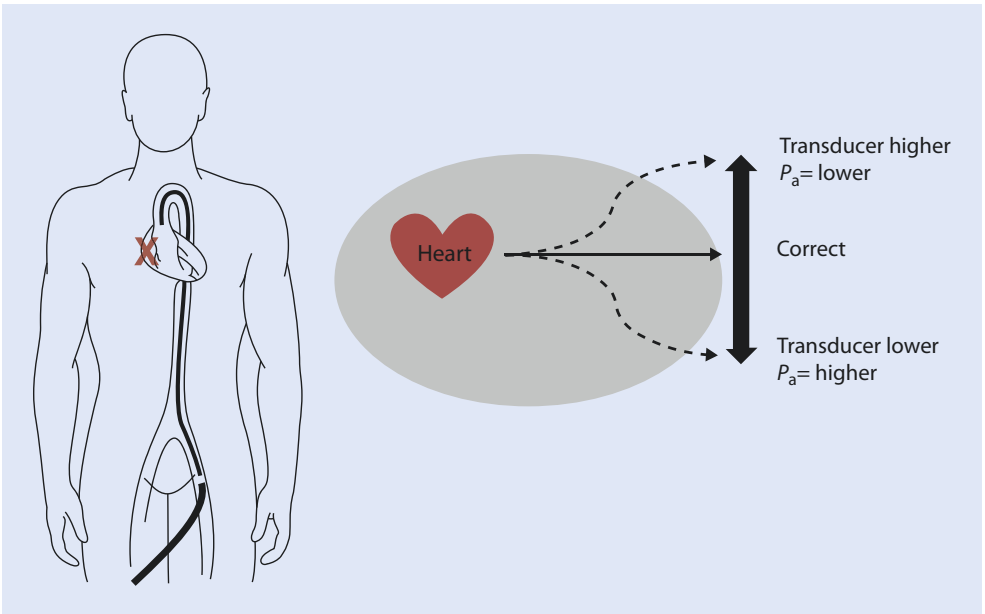


**Fig. 17.4** Transducer height. Position the transducer height at the level of the heart. When the transducer is above the heart, the Pa pressure trace is artificially lower. If it is below the heart, the Pa trace is higher and can give the impression of a transtenotic gradient

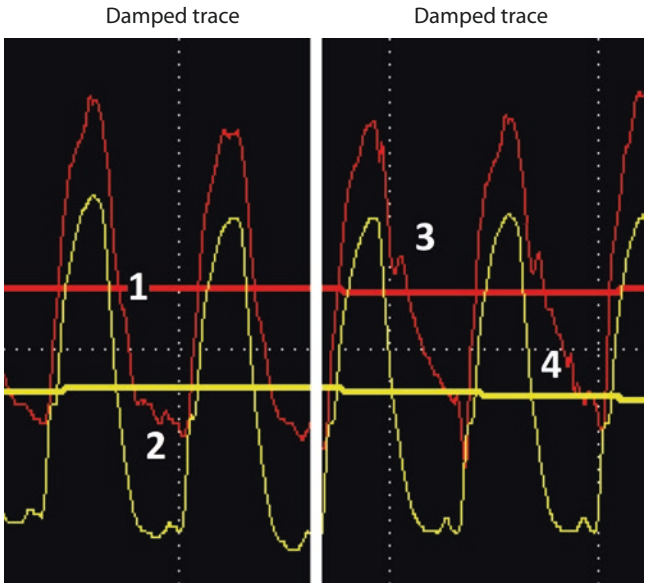


**Fig. 17.5** Damping of pressure traces. Two traces are compared. On the *left*, a damped trace due to deep engagement of the guiding catheter. The dicrotic notch is lost and the aortic pressure takes on a ventricular morphology rather than an aortic morphology. On the *right*, the guiding catheter has been withdrawn slightly causing the dicrotic notch to return and a normal decline in aortic pressure over diastole

3. Guide catheter damping: All guiding catheters will produce a degree of ostial stenosis for the vessel. This is particularly problematic for 8Fr and 7Fr catheters and may be observed as damping of the aortic pressure signal with loss of the dicrotic notch (Fig. 17.5). 5Fr and 6Fr catheters are less likely to cause significant damping, but if it occurs, the wire should be normalized in the aortic root, and then the catheter should be disengaged once the wire is passed distal to the stenosis. Caution is also required during intravenous adenosine infusion since the increase in intracoronary flow and altered aortic hemodynamics mean that the guiding catheter can be drawn into the vessel: this will cause damping with a reduction of flow and underestimation of distal stenosis significance. Catheters with side holes should be avoided since although they appear to generate a normal aortic pressure waveform, the catheter pressure is not truly representative of aortic pressure.
4. Whipping artifact: Whipping may be observed if the pressure sensor is against the vessel wall or is repeatedly striking it. This can be overcome by withdrawing the wire slightly.
5. Erroneous console determination of indices: It is common for pressure wire consoles to compute FFR values when the pressure ratio is at its lowest. However, FFR should be calculated when there is stable hyperemia, and this may not be the lowest ratio. This issue is accentuated when using intracoronary adenosine injections where recording or calculation during the injection phase can give an artifactual aortic pressure trace and therefore an erroneous FFR value. Manual adjustment of the recorded ratio will resolve this. During iFR recording, ectopy or erroneous ECG tracings may affect iFR calculation. Errors can be identified by assessing when the wave-free period has been calculated and making a repeat measure.

### 17.3.3 Practical Tips and Best Practice Considerations for iFR Measurement

When performing resting physiological assessment, a rigorous standardized approach is necessary.

Physiological assessment requires the use of adequately sized guiding catheters to engage the vessel of interest. Six French catheters are suitable although some prefer to utilize five French guiding catheters, in particular when using a radial approach. Caution is required to ensure there is no damping of the pressure signal after engagement, since this will compromise all measurements. Catheters with side holes should be avoided; although the side hole can improve the appearance of the pressure trace, there remains a relative ostial obstruction such that the pressure trace on the screen does not represent the true proximal pressure. In the event of pressure damping or the presence of important ostial disease, it is appropriate to perform measurements with the guiding catheter disengaged. This, however, obviates the possibility of using intracoronary vasodilators or injectants for thermodilution.

In general, experts and local practice suggests that guiding catheters are used in preference over diagnostic catheters. One practical reason is for the management of wire-related complications. Although infrequent, wire-related complications such as wire-related coronary dissection or vessel occlusion can occur at the rate of 0.5–1.0 % [7]. These events would be more rapidly treated if a guiding catheter was utilized rather than a diagnostic catheter.

An essential step is to administer intracoronary nitrates. Nitrates are required for all physiological assessments in order to stabilize epicardial resistance. This will counter the impact wire-induced coronary vasospasm that occurs whenever any wire is introduced into the vessel. Doses vary, but typically 300 mcg to 1 mg according to the systemic pressure should be administered as soon as the guiding catheter is engaged and before the pressure wire is passed into the vessel. If time has elapsed between the last administration and a recording, it is recommended to readminister nitrate doses. Nitrates do not cause significant or long-lived hyperemia. Shortly after injection, it will be noted that translational gradients will increase because there is a temporary increase in flow; however, the flow returns to baseline state within 30 s. To mitigate against confusion this may cause, it is best practice to administer the nitrate before the pressure wire is passed.

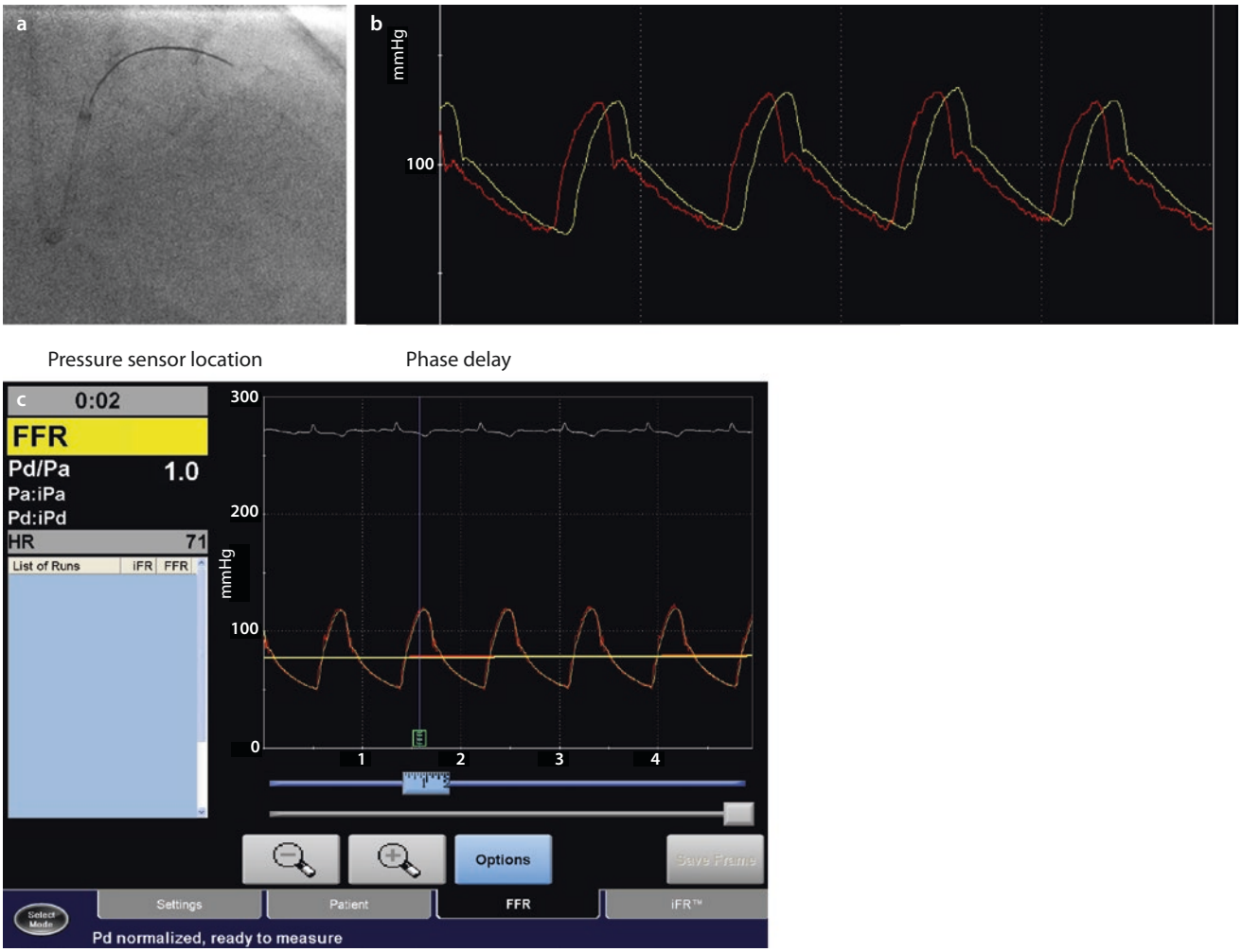


**Fig. 17.6** Normalization of pressure wire. **a** The pressure wire sensor should be normalized at the ostium of the vessel. The sensor is placed at the junction between the radio-opaque marker and the rest of wire (3 cm proximal to the end of the wire). **b** There was initial phase delay between proximal aortic pressure (Pa, *red*) and distal wire pressure (Pd, *yellow*); while the Pd/Pa ratio over the whole cycle is 1.0, during the wave-free period in diastole, the ratio is an erroneous 1.08 at the ostium. Therefore any measurements taken would be erroneous. **c** After activating the formal normalization process on the console, the distal pressure trace (Pd) is aligned with the aortic trace (Pa) in terms of both pressure values and also in phase throughout the cardiac cycle

17

"Normalization" of the pressure wire at the vessel ostium is an essential that should never be omitted (Fig. 17.6). This ensures that intracoronary pressure measurements are made in comparison to the aortic pressure. Furthermore, it gives the operator a further chance to review the aortic pressure traces and ensure they are not damped in appearance. Knowledge of the waveform is essential, and in general, an anacrotic and dicrotic notch should be present. In the majority of cases, the guiding catheter will not damp the pressure trace, and the normalization can be performed with the pressure sensor placed at the ostium of the vessel. Good practice includes fluoroscopic documentation of the wire position during normalization. Normalization should be performed with the introducer needle removed, since this can create an offset of 1–2 mmHg which may be important for borderline stenoses. Active normalization will not only ensure the pressure ratios are 1.0 but also ensure there is no time delay between proximal and distal pressure tracings. This is pertinent for phasic pressure analysis such as iFR, since time offsets will generate incorrect calculation. iFR-based systems utilize a prospective normalization technology to ensure accurate normalization. Should the traces not be aligned, or remain out of phase, normalization should be repeated until the errors are removed.

When ostial stenoses are present and/or there is damping of the pressure trace, it is appropriate to normalize the pressure wire in the aorta. The guiding catheter should remain disengaged and the pressure wire advanced until the sensor is within the aorta. Once normalized, the wire can be withdrawn, and the guiding catheter can be engaged in the normal manner. Once the pressure wire is located in the correct distal location, the guiding catheter should be disengaged again to remove the decamping effect.

Pressure wires should be placed with the sensor at least 2 vessel diameters from the lesion in question; this may be

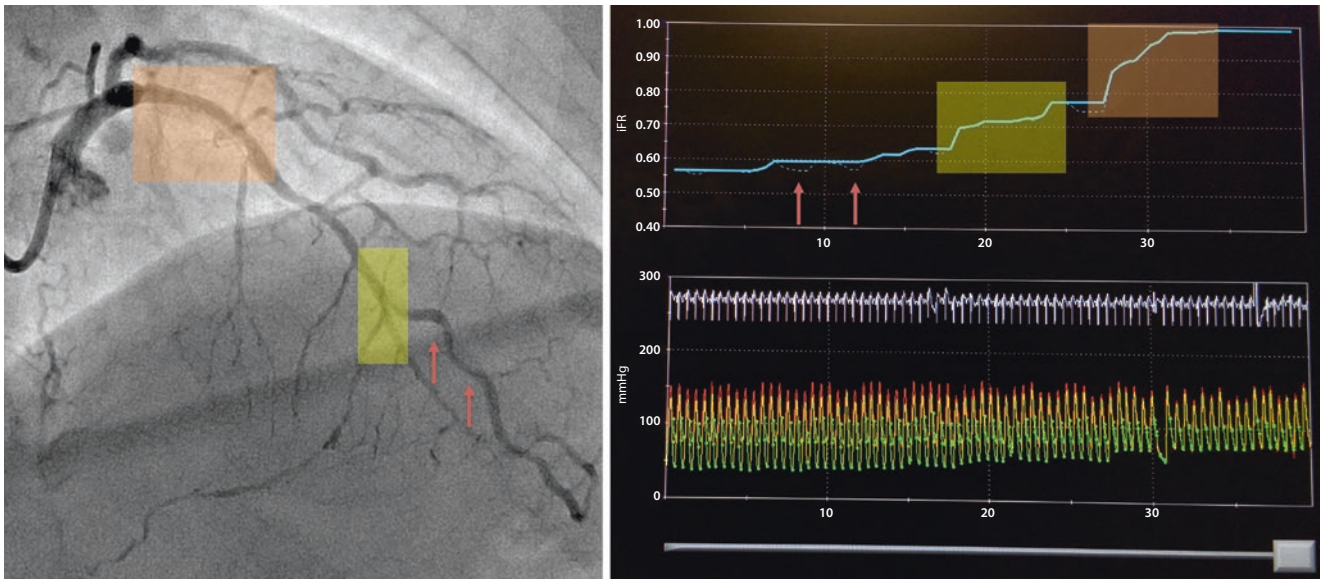


**Fig. 17.7** iFR pullback in a vessel with multiple stenoses and subtle pressure recovery. In this LAD vessel, there is moderate in-stent restenosis of a previously placed proximal stent; there is further atheromatous disease in the mid-vessel and two more tandem lesions in a tortuous segment distally. Two areas of pressure recovery (*dotted blue line* dips below the *solid blue line*), marked with *red arrows*, are noted: they correspond to the atheroma marked in *red* on the angiogram. The steps marked in *yellow* and *orange boxes* correspond to the equivalently marked boxes on the angiogram: if pullback speed is not consistent, then additional care is required to mentally co-register the steps with angiographic appearances

practical limitation in very distal lesions but remains necessary as flow turbulence close to the stenosis can alter the pressures measured.

Finally, once the wire has been positioned in the location for measurement, there should be no further touching of the pressure wire. For optimal resting assessment, additional contrast injections should be avoided immediately before the measurement of iFR. For most, documenting wire position without contrast is sufficient. If there remains doubt and contrast injection becomes necessary, then it is recommended that 20 s is allowed to elapse to allow the impact of submaximal hyperemia to subside.

In the post-PCI state, either after ballooning or stenting, resting flow states have typically resumed by the time the balloon is withdrawn or the catheters have been flushed. In practical terms, there is no delay in the time required to make a resting measurement.

Overall, an optimal physiological approach can be encapsulated by the "3Ns": nitrates, normalize, and no touch.

### 17.3.4 Performing an Optimal Pressure Wire Pullback

Modern iFR consoles have the capacity to perform an iFR pullback. Pullback assessment can be particularly useful when multiple coronary stenoses are present or if there is additional diffuse disease that may modulate the likelihood of hemodynamic improvement after coronary intervention.

iFR and iFR pullback can be used to determine the resting pressure loss caused by each individual stenosis. The iFR value calculated at any given location in the vessel is the iFR value caused by all the stenoses proximal to the pressure sensor; unlike FFR, the iFR value is only trivially affected by the presence of more distal disease. If a stenosis can be removed perfectly, with minimal pressure loss across the treated segment, then it should be possible to predict the post-PCI iFR value. This could be done simply by placing the pressure sensor proximal to the stenosis in question: the value calculated there will be that which would be achieved if all the distal stenoses were removed.

This is further simplified if iFR is plotted continuously throughout the vessel during an iFR pullback. As the pressure sensor crosses a stenosis, a step in pressure trace will be observed. Since the operator may not be intending to remove all stenoses distally, or that there may be diffuse disease distally, then the iFR post-PCI will not simply be the iFR value proximal to the stenosis. The iFR pullback trace can help significantly. The stented segment would remove the pressure loss in the area of interest; the residual disease continues to cause the pressure loss.

The speed of wire movement will determine if the step change is very shallow or very steep. When a consistent pullback speed is utilized, steep steps tend to represent focal disease while more shallow changes represent diffuse disease. Even in focal disease, the pressure steps can be small or large; a single stenosis may in fact cause several different areas of pressure change. If the wire is moved too quickly through the stenosis, such granularity may be lost, but the important aspect of observing the step will remain true.

The iFR pullback trace is made up of two separate lines: (1) the dotted line which represents the raw iFR value at the given location and (2) the solid line which represents a processed value that prevents the iFR pullback line from falling below what has already been plotted (Fig. 17.7). In many

cases, both lines overlap and may not be visible. In some cases, it is possible to see that the dotted line falls significantly at the outlet of a stenosis before returning to the solid line. This is a fascinating demonstration of the pressure loss caused by turbulence of blood, which must accelerate to pass through a stenosis and the subsequent pressure recovery that is observed within a few millimeters of the stenosis outlet. No previous pressure wire technologies have had sufficient fidelity to demonstrate these known physiological concepts in routine clinical practice.

### 17.3.5 Practical Tips and Tricks of Performing the iFR Pullback

When performing an iFR pullback assessment, a short period of time should be allowed from the moment the pullback is activated to when the pullback is started. This will enable a steady line for pullback to be displayed on the console.

Effort should be made to ensure the Y connector is closed; the wire can normally be withdrawn without opening the O-ring. The wire should be withdrawn at a steady pace while observing the position of the pressure sensor on angiography. When pressure steps are noted on the pullback trace, fluoroscopy should be stored to help identify the location of pressure changes. This will aid the interpretation of small or steep changes in pressure and help the operator co-localize the pressure changes with angiographic appearances.

The pressure sensor should be moved to the ostium of the vessel as part of the pullback. This means that any drift can be identified. The pullback systems automatically reformat the pressure trace for small degrees of pressure wire drift, which assists in interpreting the data collected.

### 17.3.6 Co-registration of iFR Pullback with Angiographic Data

With the advent of advanced computational systems, it is now feasible for the pressure wire tip to be tracked during continuous fluoroscopy. This would facilitate co-registration between pressure changes and angiographic disease and enable operators to move the wire freely. At present, detailed co-registration requires a careful approach of using a motorized pullback device to move the wire at a fixed speed. Using continuous tracking of the wire position removes this need and provides confidence for physicians in identifying stenoses causing the pressure loss. As systems advance, such co-registered approaches enable advanced planning of coronary intervention: stenoses of interest can be removed from the pressure trace using "virtual-PCI": the iFR pullback can be recalculated after stenoses are selectively removed from the co-registered angiographic image. This can produce a predicted post-PCI iFR value, and operators can consider which stenting approach will achieve an optimal hemodynamic result while balancing risk of potentially complex coronary intervention.

## 17.4 Common Clinical Applications

Common clinical applications for iFR include assessment of stenosis significance in stable coronary artery disease and during acute coronary syndromes.

iFR can also be used to assess the success of coronary angioplasty and be used in the planning of coronary intervention using iFR pullback approaches such as iFR-Scout.

iFR has attraction in simplifying stenosis assessment by removing the absolute need for a vasodilator. This likely reduces cost, time, and patient discomfort from vasodilators. There are additional potential uses one example being cases where patients cannot be given a vasodilator, such as those with allergy, severe airways disease, or with conditions which cannot tolerate hypotension – including aortic stenosis. Multivessel assessment and physiologically planned coronary intervention with assessment after intervention provide further potential scenarios.

### 17.4.1 Coronary Stenoses at Rest

The widest application of iFR is the assessment of coronary stenoses within native coronary arteries in patients with stable coronary disease.

To date, much of the validation work of iFR has been to compare the diagnostic classification of a stenosis (whether ischemic or nonischemic) according to iFR to other ischemic parameters. Much of this work has been in patients with stable coronary disease and by extension it remains the most applicable clinical setting for iFR to be applied.

In stable patients, iFR can be readily measured in any major epicardial artery to determine the hemodynamic significance of a stenosis. The pressure wire can be passed past the stenosis in question and the iFR calculated after following the appropriate steps of wire preparation and application of intracoronary nitrates.

## 17.5 iFR in Clinical Trials

iFR has been compared to FFR most notably the ADVISE family of studies. The degree of classification match is strongly dependent upon the distribution of lesions included with clinical cohorts demonstrating 80–88 % match. The limit of match is driven by the capacity for FFR to match itself when repeated. This varies according to the technique and analysis route chosen but can be as much as 15 % change in classification match when FFR is close to its threshold. When compared to third-party markers of ischemia, including HSR, CFR, SPECT, and PET imaging, iFR and FFR are equal in their capacity to detect ischemia. These assessments are perhaps the fairest assessment of iFR, since while FFR is an accepted clinical standard, its capacity to detect ischemia was itself inferred by comparisons to noninvasive tests such as exercise testing and stress echocardiography in a relatively small dataset.

Clinical outcome studies are underway in very large randomized controlled trials: DEFINE-FLAIR and the iFR-SWEDEHEART studies will compare clinical outcomes when patients are undergoing revascularization based upon either iFR or FFR. At the time of writing, both studies have finished enrolment and are expected to report soon.

### 17.5.1 The iFR-FFR Hybrid Approach

While awaiting outcome data, a prudent application of iFR in the clinical setting is to apply the Hybrid iFR-FFR strategy [8]. The aim is to achieve a high diagnostic agreement with FFR, which has outcome data, while reducing the need to administer adenosine. iFR is measured in all patients; if the value found is within a narrow range, then adenosine is administered to calculate FFR. Multiple different Hybrid iFR-FFR approaches are possible according to classification match sought: a match of 95 % requires adenosine if iFR values are between 0.86 and 0.93, sparing almost 60–70 % of patients' adenosine [8].

External validity of the iFR-FFR hybrid approach has been provided by ADVISE-II and the ADVISE-In-Practice studies. ADVISE-II was a prospective global double-blind multicenter study of 690 truly intermediate stenoses (mean FFR 0.83 ± 0.11) [9]. Nearly 70 % of stenoses could avoid adenosine using the Hybrid approach while maintaining 94 % overall classification match with an FFR-only approach.

ADVISE-in-practice was the first study to employ the commercially available iFR console [10]. In this international, multicenter study of 392 stenoses in 313 patients, iFR had a high classification match with FFR (80 % using the FFR 0.80 cut point; 88 % with ischemic threshold of 0.75 and 92 % if the FFR gray zone was accounted for) [10]. Using the Hybrid approach, 61 % of the patients could be spared from adenosine with a 94 % classification match with FFR [10].

The Hybrid approach has been adopted in routine clinical practice and is being used in SYNTAX-II (NCT 02015832) (European Cardiovascular Research Institute 2014) in which three-vessel disease on angiography will undergo revascularization according to physiological findings on iFR-FFR assessment. Since physiological assessment can convert angiographic three-vessel disease to lesser severities [7, 11], SYNTAX-II may show rapid assessment with iFR-FFR can assist in focusing revascularization to functionally important stenoses in cases otherwise treated surgically.

Clinicians experienced in using iFR are increasingly using it alone as a single physiological parameter, with a single threshold of significance (an iFR <0.90 is treated with revascularization, while iFR ≥0.90 are deferred). These thresholds were determined against an FFR threshold of 0.80 in the large and independent RESOLVE study which combined many different datasets [12]. The validity and safety of such approach is being assessed in two international studies, DEFINE-FLAIR (Imperial College London 2013) and the iFR-SWEDEHEART (Uppsala University 2014).

## 17.6 iFR in Acute Coronary Syndromes

### 17.6.1 Non-culprit Vessels in ACS

At present, iFR has very limited data in the setting of ACS, but it raises the interesting prospect of guiding intervention to non-culprit vessels. In the ACS setting, the microcirculatory bed may be less responsive to exogenous hyperemic agents which may lead to the underestimation of lesion severity. By removing the need for an exogenous hyperemic agent, then the variability of responsive to the agent is removed, and it may simplify assessment. The added value of non-culprit assessment at the time of ACS treatment is that patients with multivessel may be spared multiple procedures and therefore reduce costs and risks.

The FORECAST study is an independent study, using offline iFR calculation, which demonstrated it is feasible to make iFR measurements in non-culprit vessels in ACS [13]. In 123 stenoses in 82 patients with ACS and stable disease, an iFR threshold of 0.92 best matched an FFR of 0.80 with a diagnostic concordance with FFR of 81.3 % [13]. No difference in diagnostic efficiency between ACS patients and those with stable disease was found and all apparent discrepancies were within the FFR 0.75–0.80 gray zone [13]. Furthermore, when using a Hybrid iFR-FFR approach, they found 68 % of patients would be spared adenosine.

Further significant data will come from the DEFINE-FLAIR study which has included a large proportion of patients with ACS. FLAIR will provide the clinical outcomes of ACS patients having non-culprit vessel therapy guided by iFR or FFR and confirm whether using iFR in this setting is sufficiently safe for routine use.

### 17.6.2 Culprit Vessels in ACS

For culprit vessels, the application of physiological assessment to guide stenting remains a difficult concept; vessels which have had a thrombotic occlusion or stepwise change in lesion severity following plaque rupture are likely best treated with coronary stents since significant clinical benefit has been repeatedly shown in studies who selected patients without physiological assessment. The risk of physiological assessment in the culprit vessel is that a non-occlusive ruptured plaque may not cause sufficient flow limitation to reach a fixed threshold (e.g., an FFR of 0.80 or iFR 0.90, both of which were determined in stable disease) but may still progress rapidly and cause further events. It is well recognized that patients with ACS have the highest rate of further events and therefore deferring an angiographically significant stenosis that is consistent with clinical presentation of ACS may pose a risk to the patient. The FAMOUS Study used FFR to assess both culprit and non-culprit vessels [14]. Unfortunately the data was not presented in a manner that allowed determination of whether the major adverse events occurring in

deferred patients did so in the deferred culprit vessels. However, it is clear from the Kaplan-Meier plot that all patients deferred from stenting based upon the FFR had an event by the end of the follow-up, suggesting that deferring may not be the optimal result.

## 17.7 Coronary Artery Bypass Grafts

### 17.7.1 Using Physiology to Guide PCI or CABG

In general, the findings of angiographic multivessel disease may lead referral for coronary artery bypass grafting (CABG) but should automatically lead to physiological assessment.

Much of the historical data for the value of coronary artery bypass surgery has been based upon studies in patients with angiographically defined disease, without the use of intracoronary physiology. This has remained true even in recent history, such as BARI [15] and CARDIA [16] but also in the more modern era of studies such as SYNTAX [17] and FREEDOM [18] – both of which demonstrated a benefit of CABG over PCI in patient cohorts defined only angiographically. Conceptually, many of the vessels treated will not have been ischemic and therefore were conferred no advantage from either PCI or bypass surgery. While the presence of an unnecessary bypass graft may go clinically undetected (vein graft occlusion will be asymptomatic if the native is non-flow limiting), the presence of unnecessary stents in nonischemic vessels poses the risks of late stent thrombosis and in-stent restenosis that can count against PCI.

The FAME study demonstrated that FFR-guided PCI in the multivessel setting (where CABG was not being offered) was safer than stenting all stenoses >50 % [19]. In the FAME study, patients were already selected for PCI as opposed to surgical revascularization. However, as an extension of these findings, it has been suggested that physiology can be used to reclassify angiographic disease from, say, three-vessel disease to two or even one vessel based upon the presence or absence of ischemia [7, 19, 20]. This may spare a significant proportion of patients from surgical treatment and simplify a potential PCI approach, reducing the number of vessels requiring intervention.

The SYNTAX-II study has prospectively enrolled patients with multivessel disease who are in equipoise between a surgical or PCI approach. Patients undergo multivessel iFR/FFR assessment using the Hybrid approach, and only vessels that are physiologically significant are treated and stents are IVUS optimized. The outcomes of the cohort will be compared to a historical cohort from the SYNTAX I study. FAME 3 follows a similar concept, randomizing patients with three-vessel disease to FFR-guided PCI or to angiographic-guided CABG. Both studies will add considerably to our knowledge of converting patients otherwise destined for surgery into PCI candidates.

### 17.7.2 Guiding Surgery with Physiology

There is data to suggest that bypass grafts have a higher rate of occlusion if the native vessel is nonischemic or non-flow limiting. There is biological plausibility: normal flow in the native vessel would mean insufficient demand upon the vein graft and ultimately lead to the occlusion of a vein graft or cause atresia of a mammary artery. Much of this work has been performed with FFR [21]. Conceptually the findings should hold true for iFR also although studies remain to be done.

### 17.7.3 Graft Physiological Assessment

There remains limited data for the application of intracoronary physiology in the assessment of bypass grafts. Venous grafts demonstrate an aggressive type of atherosclerosis that is more likely to progress rapidly or have plaque rupture; the outcomes of deferring stenoses based upon physiological assessment in vein grafts remains a speculative and untested paradigm.

## 17.8 Pullback and Planning PCI Using iFR Pullback and Virtual PCI

Advances in how the wave-free period can be calculated upon a beat-to-beat nature means that iFR can be calculated live during a pressure wire pullback. This enables to the identification of stenoses and their physiological significance at rest without the need for a long infusion of hyperemic agent. Commercial systems are already in testing, and early data suggests important advantages to performing a resting pullback [5, 6].

A controlled pullback, using a mechanized device, enables the plotting of changes in iFR along the vessel length on an angiogram. Data can be plotted as a simple change in gradient or more visually integrated with angiogram, such as more intuitively understood graphical markers plotted directly onto the vessel. If plotted as intensity, that is, the change in iFR per millimeter, then the stenoses causing the greatest pressure drop in the vessel can be readily identified. This may help an interventionalist identify which stenosis is causing the greatest physiological effect, which is particularly pertinent as coronary disease becomes increasingly complex and frequently tandem.

In lieu of a pullback device, co-registration systems that can track the movement of pressure wire will allow manual hand-guided pressure wire pullbacks. The advanced tracking software will compute the speed of wire movement and location at a given time-point to plot the physiological data directly upon the angiogram. This is under active development and remains an area of great growth, reliant upon integrated physiology, x-ray, and advanced computing systems.

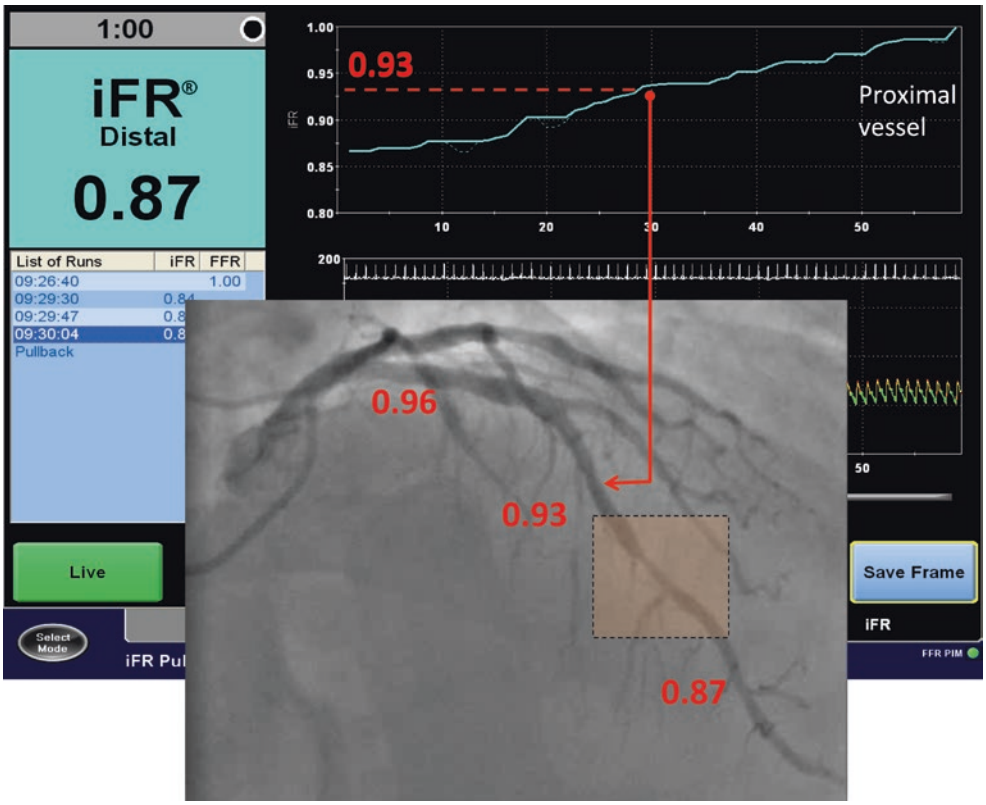


**Fig. 17.8** Example of iFR pullback being used to predict post-PCI iFR results. The LAD has diffused disease proximally and in the mid-segment with a focal lesion in the mid-to-distal segment. Pressure wire shows the vessel has an iFR 0.87 suggesting ischemia. Just proximal to the focal stenosis, an iFR of 0.93 is observed. Therefore, if the stenosis could be removed completely without residual gradient, then the iFR in the distal vessel would be 0.93

A key advantage of a resting pressure wire pullback, such as the iFR pullback, is the limited interaction between stenoses, such that the effect of distal disease upon proximal stenoses is minimized or mitigated. The presence of cross talk between stenoses under hyperemic conditions is well established – the presence of a distal stenosis will mean maximal hyperemia is not achieved, such that the significance of a proximal stenosis is underestimated. Since hyperemia is limited by stenoses of even trivial severity and more diffuse disease, then it is possible that many hyperemic assessments are confounded by this interaction between diseased segments. In the resting state, it has been observed that the resting coronary flow velocity is preserved despite the presence of even severe stenoses. The result is that the transtenotic pressure drop observed distal to the stenosis is resultant only due stenoses proximal to the pressure sensor. In the context of a resting pressure wire pullback, the gradient observed at a given point will be valid for that physical location in the vessel.

This leads to an exciting new domain. It is possible for computer algorithms to "remove" a stenosis on an iFR pullback trace [5, 6]. Using "virtual-PCI," removal of a stenosis will lead to a recalculation of the pullback trace to compute what the expected iFR would be if the selected intervention was performed in the real world. The expected iFR value is computed under the assumption that the intervention is ideal without any residual gradient in the treated segment. In the first iFR pullback study, it was found that process could predict a post-PCI iFR value with high accuracy and without a significant systematic bias [5, 6]. In that regard, it can provide a target physiological value for the real-world intervention (Fig. 17.8). It can also permit multiple different stenting strategies to evaluate their potential physiological benefit.

It can be seen that such an advance would elevate physiologically guided intervention to a truly physiologically directed process with more intelligent approach to stenting complex vessels. It may be that an iFR pullback reveals that an acceptable physiological result can be achieved by a more limited stenting approach rather than a more extensive stenting; this may help long-term with reduced in-stent restenosis or stent-related complications.

This is an area of intense interest, and it is expected this will continue to advance with the simultaneous advancements in both pressure wires, computing power and integrated approaches with angiographic imaging.

## 17.9 Post-PCI Assessment

Physiological indices can provide an assessment of the success of coronary intervention. Both FFR and iFR may be used to assess the hemodynamic improvement after a stent [4, 22, 23].

### 17.9.1 Measuring FFR Post-PCI

According to FFR theory, if a stenosis is successfully treated with PCI without a residual pressure gradient across the treated segment, then the flow should be restored to normal

and the post-PCI FFR value should be 1.0. Any residual stenosis will cause a residual pressure loss and give a lower FFR value suggesting further intervention is required.

In reality, it is uncommon to achieve an FFR value of 1.0 post-PCI because even angiographically unobstructed vessels can produce a pressure drop under hyperemia: cases have been reported previously and the IDEAL study demonstrated FFR values as low as 0.85 in unobstructed reference vessels [3]. How does this occur? In the presence of hyperemia, blood flow may lose energy and therefore pressure due to resistance along mild diffuse atheroma. A much larger energy loss is observed secondary to turbulence generated by an irregularities or stenoses within the vessel. A stent may also cause a significant turbulence, and this may be accentuated if the stent is inadequately deployed, for example, if stent struts remain unopposed.

Opposing these factors, there may be a relative resistance of the microcirculation to respond to adenosine or other exogenous hyperemic agents. Long balloon inflations cause relative ischemia which is potent vasodilator, and additional adenosine during this phase will be unable to achieve additional hyperemia which can be falsely interpreted as increased microvascular resistance due to micro-embolization. This can often be resolved by waiting for a short period to allow the normal resting state to return, but there may still be doubts of the responsiveness to adenosine giving a falsely elevated FFR value.

A further complex and poorly appreciated phenomena may also occur post-PCI under hyperemic conditions. Since any stenosis of more than 30–40 % severity will limit hyperemic flow, then even mild more proximal stenoses will prevent more distal stenoses from experiencing the same degree of hyperemic flow velocity. The more significant the proximal stenosis, the greater the reduction in proximal flow velocity. Since the pressure drop across a stenosis is a function of the flow velocity, then proximal stenoses can cause underestimation of the importance of distal stenoses. Removing a stenosis will increase hyperemic flow velocity in the vessel and thereby unmask the significance of the distal stenoses. In the post-PCI setting, this can account for unexpectedly low FFR values. In some cases, the FFR value can be even lower than the pre-PCI value which can be concerning to the operating physician.

If this phenomenon is observed, it would be recommended to ensure that the stent has been optimally deployed and then remeasure the FFR. If the low value remains, it suggests an important stenosis remains elsewhere in the vessel. Since the FFR value of a even a mild-to-moderate stenosis cannot be predicted, then a detailed pullback assessment is required to determine which segment of the vessel is responsible for the pressure loss.

Clinical outcome studies suggest that post-PCI FFR values exceeding 0.90 are associated with improved outcomes – with fewer events observed the higher the FFR value. Post-PCI values of >0.95 had the least events, in particular re-PCI or acute myocardial infarction [23]. Conceptually this is in keeping with FFR theory – vessels with less residual ischemia will cause less symptoms or events in patients.

### 17.9.2 Measuring iFR Post-PCI

iFR can also be measured post-PCI in the same manner as FFR although clinical outcome data is still awaited. The changes in iFR values across a broad range of stenoses was statistically similar to the change observed in FFR [4]. The change in iFR and FFR was significantly larger than that observed for Pd/Pa suggesting there was greater fidelity of information when using the wave-free period as compared to the whole cycle average. The advantage of this is that residual disease would be more readily detected using iFR and FFR than Pd/Pa.

The change in iFR after PCI can be observed rapidly during the procedure. Although it is well established that balloon inflation or stent deployment will cause relative ischemia and that can disrupt resting physiology, it is observed that in the time taken to remove the interventional balloons, flush the catheters, readminister intracoronary nitrates, and prepare the pressure wire to make a measurement, there is stabilization of the resting state.

Since iFR is based upon resting physiology, there is some added advantage over FFR. Since resting flow velocity has evolved to be remarkably consistent in the presence and absence of stenoses and that it has been demonstrated that it changes little after coronary intervention to most moderate-to-severe stenoses, then it is expected that there will be little change in flow velocity in the vessel after PCI to a given stenosis. If there are multiple stenoses present in a vessel, each will produce a degree of pressure loss that is relatively independent of each other. Removing a given stenosis will resolve the pressure loss in that segment but leave the remaining areas unaffected. This is best observed when using iFR pullback: an iFR pullback measurement made after coronary intervention will feature the same steps in the pressure trace in the untreated segments [5, 6].

## 17.10 Other Clinical Applications

### 17.10.1 Aortic Stenosis

Other conditions in which iFR may find use include the assessment of stenosis significance in severe aortic stenosis (AS). In patients with severe AS, it is preferable to avoid the large hemodynamic changes that may occur during vasodilator infusion. Drugs such as adenosine cause a significant fall in peripheral pressure which will lead to a dangerous rise in aortic gradient and risk hemodynamic collapse. As such, iFR may provide an attractive alternative to assess stenoses without vasodilators. iFR should be measured in the typical fashion and a single cut point could be used to guide therapy. However, it should be recognized that there is a paucity of data to support the use of any physiological parameter in the management of coronary disease in patients with aortic stenosis.

Until recently, there was little need for the approach: patients with angiographically significant stenoses with severe aortic stenosis would be offered surgical aortic valve replacement with concomitant bypass grafting. With the advent of transcatheter aortic valve implantation (TAVI), not only are whole cohorts of patients previously unsuitable for valve replacement being treated, but also there is a paradigm shift in how aortic valve disease is managed. The management of concomitant coronary disease remains controversial [24] and is limited that many of the TAVI studies have treated the presence of coronary disease in a binary manner. Furthermore, there is no agreement on how to define ischemia in aortic stenosis – which is known to cause microvascular ischemia even in the absence of epicardial coronary disease.

At present, FFR remains the principle physiological tool utilized when judging coronary stenoses in patients with aortic stenosis. However, there are a number of factors that suggest that FFR will underestimate stenosis severity in aortic stenosis.

Firstly, aortic stenosis itself likely behaves as a critical proximal tandem stenosis which will drive significant cross talk between it and stenoses within the vessels under hyperemic conditions. Therefore stenoses may be underestimated.

Secondly, patients with aortic stenosis have a reduced coronary flow reserve even in the absence of stenosis [25]. This is likely to be partly secondary to left ventricular hypertrophy in response to the aortic stenosis which causes a degree of fixed microvascular resistance. This means there is a relative failure to respond to hyperemic agents causing a fall in the flow reserve. Simultaneously, a number of vasoconstrictors, such as angiotensin and vasopressin, are elevated in aortic stenosis to preserve blood pressure: all of these counter the effects of infused vasodilators such as adenosine. The combined consequence is that stenosis severity may be underestimated.

Thirdly, in aortic stenosis systole is prolonged, and measures that rely upon whole cycle averaging of pressure data, such as FFR, will become confounded. Since the purpose of stenosis assessment is to keep microvascular resistance minimal and constant, any involvement of systole which has the most variance in microvascular resistance will impair the capacity of a marker to detect a significant stenosis.

These factors strongly suggest that a resting physiological approach such as iFR has advantages over a hyperemic approach in aortic stenosis. However, further work is required to confirm the validity and long-term safety of such approach.

### 17.10.2 Heart Failure

Coronary disease in the context of heart failure can be a challenge to assess physiologically. Elevated left ventricular end diastolic pressures, increased wall strain, and elevated right atrial pressures can mean that distal coronary pressures are falsely elevated even in the presence of a significant stenosis. For hyperemic indices, there is an additional complexity, as microvascular dilatation in response to exogenous vasodilators requires preserved myocardial function. Therefore, stenoses may be underestimated when assessed by any intracoronary physiological index in the context of severe heart failure. In this cohort of patients, where complete revascularization may offer the patient an improvement in pump function, a complete clinical picture should be sought rather than a single coronary parameter. The opposite is also true: when a physiological parameter is significant in the presence of severe LV impairment, it suggests the degree of flow limitation is truly significant and revascularization should be considered.

### 17.10.3 Peripheral Artery Stenoses

Peripheral artery disease remains a common cause of morbidity, but identification of important stenoses remains a challenge. The lack of a good understanding of hyperemia in the peripheral circulation means that resting physiology is the principle approach employed. Resting parameters such as iFR have been suggested to quantify stenosis severity in the peripheral vasculature. An important limitation is that iFR, as a diastolic measure, may have limited utility in the peripheries where flow is predominantly systolic. A whole cycle average pressure tracing may have greater utility.

## References

1. Sen S, Escaned J, Malik IS, et al. Development and validation of a new adenosine-independent index of stenosis severity from coronary wave–intensity analysis. J Am Coll Cardiol. 2012;59:1392–402. doi:10.1016/j.jacc.2011.11.003.
2. Sen S, Asrress KN, Nijjer S, et al. Diagnostic classification of the instantaneous wave-free ratio is equivalent to fractional flow reserve and is not improved with adenosine administration. Results of CLARIFY (Classification Accuracy of Pressure-Only Ratios Against Indices Using Flow Study). J Am Coll Cardiol. 2013;61:1409–20. doi:10.1016/j.jacc.2013.01.034.
3. Nijjer SS, Waard GA de, Sen S, et al. Coronary pressure and flow relationships in humans: phasic analysis of normal and pathological vessels and the implications for stenosis assessment: a report from the Iberian–Dutch–English (IDEAL) collaborators. Eur Heart J. 2015:ehv626. doi:10.1093/eurheartj/ehv626.
4. Nijjer SS, Sen S, Petraco R, et al. Improvement in coronary haemodynamics after percutaneous coronary intervention: assessment using instantaneous wave-free ratio. Heart. 2013;99:1740–8. doi:10.1136/heartjnl-2013-304387.
5. Nijjer SS, Sen S, Petraco R, et al. Pre-angioplasty instantaneous wave-free ratio pullback provides virtual intervention and predicts hemodynamic outcome for serial lesions and diffuse coronary artery disease. JACC Cardiovasc Interv. 2014;7:1386–96. doi:10.1016/j.jcin.2014.06.015.
6. Nijjer SS, Sen S, Petraco R, et al. The Instantaneous wave-Free Ratio (iFR) pullback: a novel innovation using baseline physiology to optimise coronary angioplasty in tandem lesions. Cardiovasc Revasc Med. 2015;16:167–71. doi:10.1016/j.carrev.2015.01.006.
7. Curzen N, Rana O, Nicholas Z, et al. Does routine pressure wire assessment influence management strategy at coronary angiography for diagnosis of chest pain? The RIPCORD Study. Circ Cardiovasc Interv. 2014:CIRCINTERVENTIONS.113.000978. doi:10.1161/CIRCINTERVENTIONS.113.000978.
8. Petraco R, Park JJ, Sen S, et al. Hybrid iFR-FFR decision-making strategy: implications for enhancing universal adoption of physiology-guided coronary revascularisation. EuroIntervention. 2013;8:1157–65. doi:10.4244/EIJV8I10A179.

9. Escaned J, Echavarría-Pinto M, Garcia-Garcia HM, et al. Prospective assessment of the diagnostic accuracy of instantaneous wave-free ratio to assess coronary stenosis relevance: results of ADVISE II international, multicenter study (ADenosine Vasodilator Independent Stenosis Evaluation II). JACC Cardiovasc Interv. 2015;8:824–33. doi:10.1016/j.jcin.2015.01.029.
10. Petraco R, Al-Lamee R, Gotberg M, et al. Real-time use of instantaneous wave-free ratio: results of the ADVISE in-practice: an international, multicenter evaluation of instantaneous wave-free ratio in clinical practice. Am Heart J. 2014;168:739–48. doi:10.1016/j.ahj.2014.06.022.
11. Nam C-W, Mangiacapra F, Entjes R, et al. Functional SYNTAX score for risk assessment in multivessel coronary artery disease. J Am Coll Cardiol. 2011;58:1211–8. doi:10.1016/j.jacc.2011.06.020.
12. Jeremias A, Maehara A, Généreux P, et al. Multicenter core laboratory comparison of the instantaneous wave-free ratio and resting Pd/Pa with fractional flow reserve: the RESOLVE study. J Am Coll Cardiol. 2014;63:1253–61. doi:10.1016/j.jacc.2013.09.060.
13. Indolfi C, Mongiardo A, Spaccarotella C, et al. The instantaneous wave-free ratio (iFR) for evaluation of non-culprit lesions in patients with acute coronary syndrome and multivessel disease. Int J Cardiol. 2014;178C:46–54. doi:10.1016/j.ijcard.2014.03.210.
14. Layland J, Oldroyd KG, Curzen N, et al. Fractional flow reserve vs. angiography in guiding management to optimize outcomes in non-ST-segment elevation myocardial infarction: the British Heart Foundation FAMOUS–NSTEMI randomized trial. Eur Heart J. 2014:ehu338. doi:10.1093/eurheartj/ehu338.
15. BARI 2D Investigators. A randomized trial of therapies for type 2 diabetes and coronary artery disease. N Engl J Med. 2009;360:2503–15. doi:10.1056/NEJMoa0805796.
16. Kapur A, Hall RJ, Malik IS, et al. Randomized comparison of percutaneous coronary intervention with coronary artery bypass grafting in diabetic patients: 1-year results of the CARDia (coronary artery revascularization in diabetes) trial. J Am Coll Cardiol. 2010;55:432–40. doi:10.1016/j.jacc.2009.10.014.
17. Serruys PW, Morice M-C, Kappetein AP, et al. Percutaneous coronary intervention versus coronary-artery bypass grafting for severe coronary artery disease. N Engl J Med. 2009;360:961–72.
18. Farkouh ME, Domanski M, Sleeper LA, et al. Strategies for multivessel revascularization in patients with diabetes. N Engl J Med. 2012;367:2375–84. doi:10.1056/NEJMoa1211585.
19. Tonino PAL, De Bruyne B, Pijls NHJ, et al. Fractional flow reserve versus angiography for guiding percutaneous coronary intervention. N Engl J Med. 2009;360:213–24. doi:10.1056/NEJMoa0807611.
20. Van Belle EV, Rioufol G, Pouillot C, et al. Outcome impact of coronary revascularization strategy reclassification with fractional flow reserve at time of diagnostic angiography insights from a large french multicenter fractional flow reserve registry. Circulation. 2014;129:173–85. doi:10.1161/CIRCULATIONAHA.113.006646.
21. Botman CJ, Schonberger J, Koolen S, et al. Does stenosis severity of native vessels influence bypass graft patency? A prospective fractional flow reserve–guided study. Ann Thorac Surg. 2007;83:2093–7. doi:10.1016/j.athoracsur.2007.01.027.
22. Bech GJ, Pijls NH, De Bruyne B, et al. Usefulness of fractional flow reserve to predict clinical outcome after balloon angioplasty. Circulation. 1999;99:883–8.
23. Pijls NHJ, Klauss V, Siebert U, et al. Coronary pressure measurement after stenting predicts adverse events at follow-up: a multicenter registry. Circulation. 2002;105:2950–4.
24. Danson E, Hansen P, Sen S, et al. Assessment, treatment, and prognostic implications of CAD in patients undergoing TAVI. Nat Rev Cardiol. Published Online First: 11 February 2016. doi:10.1038/nrcardio.2016.9.
25. Rajappan K, Rimoldi OE, Dutka DP, et al. Mechanisms of coronary microcirculatory dysfunction in patients with aortic stenosis and angiographically normal coronary arteries. Circulation. 2002;105:470–6.

# Multimodality Assessment of the Coronary Circulation

## Contents

# Comprehensive Assessment of the Coronary Circulation Using Pressure and Flow Measurements

*Hernan Mejia-Rentería, Nicola Ryan, Fernando Macayo, Ivan Nuñéz-Gil, Luis Nombela-Franco, and Javier Escaned*




J. Escaned, J. Davies (eds.), *Physiological Assessment of Coronary Stenoses and the Microcirculation*,
DOI 10.1007/978-1-4471-5245-3_18

## 18.1 Introduction

The coronary circulation is an intricate and dynamic network composed of the large epicardial vessels and the microvasculature. This network is controlled by multiple physiological mechanisms that maintain adequate myocardial perfusion despite ever-changing hemodynamic conditions [1–3]. The underlying pathophysiology and adaptive mechanisms of the coronary circulation, beyond the scope of this chapter, are fully described in other chapters in this book. Epicardial vessels, and therefore epicardial stenoses, can be visualized and assessed using one of most the fundamental tools of interventional cardiology, the coronary angiogram; the microcirculation however cannot be directly visualized in vivo and requires more sophisticated techniques to assess its function. Importantly, a comprehensive view of the origin of myocardial ischemia, and its relationship with the different domains of the coronary circulation, has to be borne in mind when applying and interpreting the results of both invasive and noninvasive functional tests (Fig. 18.1).

Several different measurements and theoretical frameworks exist to assess the coronary circulation including flow, coronary flow reserve (CFR), pressure as a surrogate of flow, instantaneous wave-free ratio (iFR) and fractional flow reserve (FFR), and vascular resistance, which is calculated using measurements of pressure and flow giving the index of microcirculatory resistance (IMR) and the hyperemic microcirculatory resistance (HMR). The development of the coronary angiogram along with pioneering work from Gould et al. [4], who identified disturbed coronary flow in the presence of epicardial stenosis >85 % and >50 % at rest and during hyperemia, respectively, leads to the initial belief that there was a cause and effect relationship between coronary stenosis and myocardial ischemia. Significant progress has ensued in the intervening years, and we now appreciate that myocardial ischemia is not a single entity but a disease spectrum that may be due to a focal epicardial stenosis, diffuse coronary artery disease, microvascular dysfunction (MCD), or a combination of these.

Therefore, in order to comprehensively assess and target treatment, in individual patients, a thorough understanding of the underlying etiology of the myocardial ischemia is required. In this chapter we will discuss how, when used in combination, invasive measurements of pressure and flow complement each other and allow us to clearly delineate the underlying etiology of myocardial ischemia as well as providing prognostic information.

### 18.1.1 Fractional Flow Reserve and Coronary Flow Reserve: Friends, Not Foes

Fractional flow reserve (FFR) was first proposed by Pijls et al. [5, 6] and is calculated as the ratio of invasively measured coronary pressures, distal (Pd) and proximal (Pa) to an epicardial stenosis, under hyperemic conditions, usually obtained with adenosine. It is assumed that the Pd/Pa ratio acts as a surrogate for the fractional peak flow across the lesion given that hyperemia induces minimal and constant myocardial resistance [7]. Several large clinical trials, most notably DEFER [8], FAME [9], and FAME II [10], have shown FFR to be both safe and efficacious in predicting the functional significance of a coronary stenosis, with a cutoff value of 0.75–0.8. The relative ease and simplicity with which FFR can be obtained during daily clinical practice and its inclusion in the current guidelines [11, 12] means it is a commonly used tool for investigating the functional significance of a coronary stenosis.

It is important to note that FFR guidance does not confer absolute protection against the development of cardiovascular events. A significant percentage of patients included in pivotal FFR studies presenting an initial normal FFR develop major adverse cardiovascular events (MACE) at long-term follow-up. In the DEFER study [7], which evaluated the appropriateness of stenting functionally nonsignificant stenoses, the deferred group (PCI deferred as FFR >0.75) had excellent 5-year outcomes. Nonetheless, there was a MACE rate of 21 % (all-cause mortality, cardiac death, and any type of revascularization), and one third of patients had ongoing chest pain during 5-year follow-up. The FAME trial demonstrated that limiting PCI to significant hemodynamically coronary stenoses based on FFR resulted in a significant decrease in target vessel revascularization, myocardial infarction, and death, compared to the angiography-based decision arm. However, 20 % of patients with an epicardial coronary artery stenosis with deferred PCI (FFR > 0.80) had recurrent angina during 2-year follow-up [9].



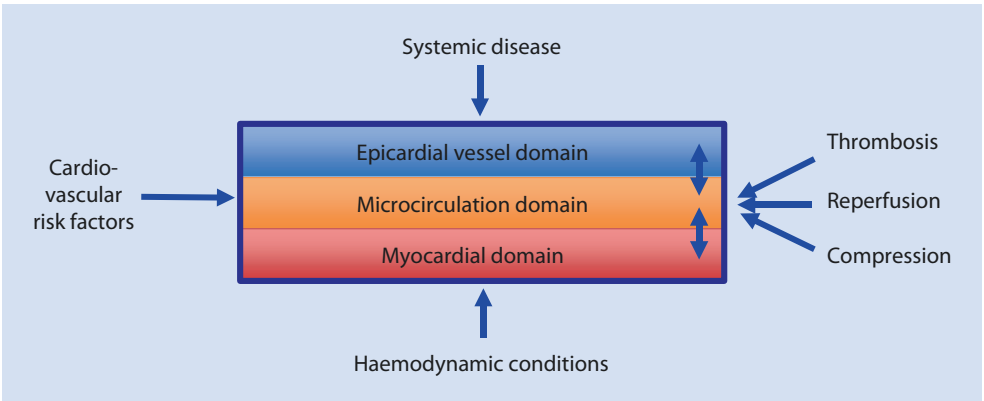


**Fig. 18.1** Schematic representation of the origin of myocardial ischemia in ischemic heart disease. Ischemias may have an origin in the epicardial of microcirculatory domains of the coronary circulation or in the myocyte itself, and it is influenced by additional factors including systemic disease, cardiovascular risk factors, hemodynamic conditions, or thrombosis, reperfusion, and compression in acute coronary syndromes

Another point to bear in mind is that FFR only provides surrogate data about coronary flow in the presence of an epicardial stenosis. An FFR will only vary from one in the presence of coronary stenosis and flow disturbance causing a drop in the distal coronary pressure. In the absence of an epicardial stenosis, an FFR value of one will be documented, independent of the perfusion pressure. Therefore, FFR cannot be used to evaluate the coronary circulation in the absence of CAD [19] and does not evaluate other domains contributing to myocardial ischemia. This is an important concept, since FFR is often described as the "gold standard" in invasive evaluation of ischemia, while in reality it provides information on the contribution of the interrogated stenosis to myocardial ischemia (if present). FFR itself was validated against a number of noninvasive assessment tools, each with varying sensitivity and specificity [13]. Importantly, to be included in that study, patients in whom PCI was performed had to demonstrate a lack of detectible ischemia in subsequent ischemia testing (i.e., demonstrate that the ischemia was clearly linked to the presence of the interrogated stenosis).

Structural and functional microcirculatory abnormalities may significantly limit the maximal myocardial flow due to an increase in the resistances of arterioles and capillaries, which in turn provokes a smaller distal pressure drop. Consequently, the pressure gradient (distal pressure/aortic pressure) across an epicardial stenosis in presence of MCD may be closer to one. For example, an FFR >0.80 could be obtained in an epicardial lesion with significant MCD limiting the coronary flow, while it may be possible that the same epicardial lesion in absence of high microcirculatory resistances could result in an FFR ≤0.80.

While FFR-guided percutaneous coronary intervention (PCI) circumvents many of the limitations of angiography in assessing stenosis severity and has improved the patient outcomes, its utility is limited to the assessment of the epicardial coronary artery stenosis. Other important contributors to myocardial ischemia are not assessed using FFR. Therefore in order to comprehensively evaluate and risk stratify patients with IHD, the combination of pressure and flow measurements aims to obtain valuable information about the coronary circulation beyond focal epicardial disease.

Coronary flow reserve (CFR) has long been established as providing a global invasive and noninvasive assessment of the microcirculation, evaluating the ability of the coronary vasculature to increase its flow in response to increasing myocardial oxygen demand [4, 6, 15]. In the absence of an obstructive epicardial coronary artery stenosis, the coronary vasculature can increase its flow up to four times above baseline with an intact autoregulatory system [16]. Therefore failure of the coronary vasculature to increase its flow in the absence of a focal coronary stenosis implies that there is either diffuse coronary artery disease, which may not always be appreciated at coronary angiography, or the presence of MCD. Despite it being the initial tool in the invasive assessment of ischemia, CFR has fallen out of favor in recent years due to the perceived difficulties in its measurement. While obtaining stable Doppler signals can be difficult with a little experience, CFR can be reliably obtained and adds significantly to the toolkit in the assessment of ischemia.

Studies comparing FFR and CFR in the evaluation of the functional significance of epicardial stenoses have frequently reported discordance, 30–60 % of lesions, between these measurements [17–20]. Integrating both PET and invasive physiology, Johnson et al. proposed classifying coronary vessels into four quadrants based on the cutoff values of CFR (>2) and FFR (<0.8) [21] (■ Fig. 18.2). Understanding these

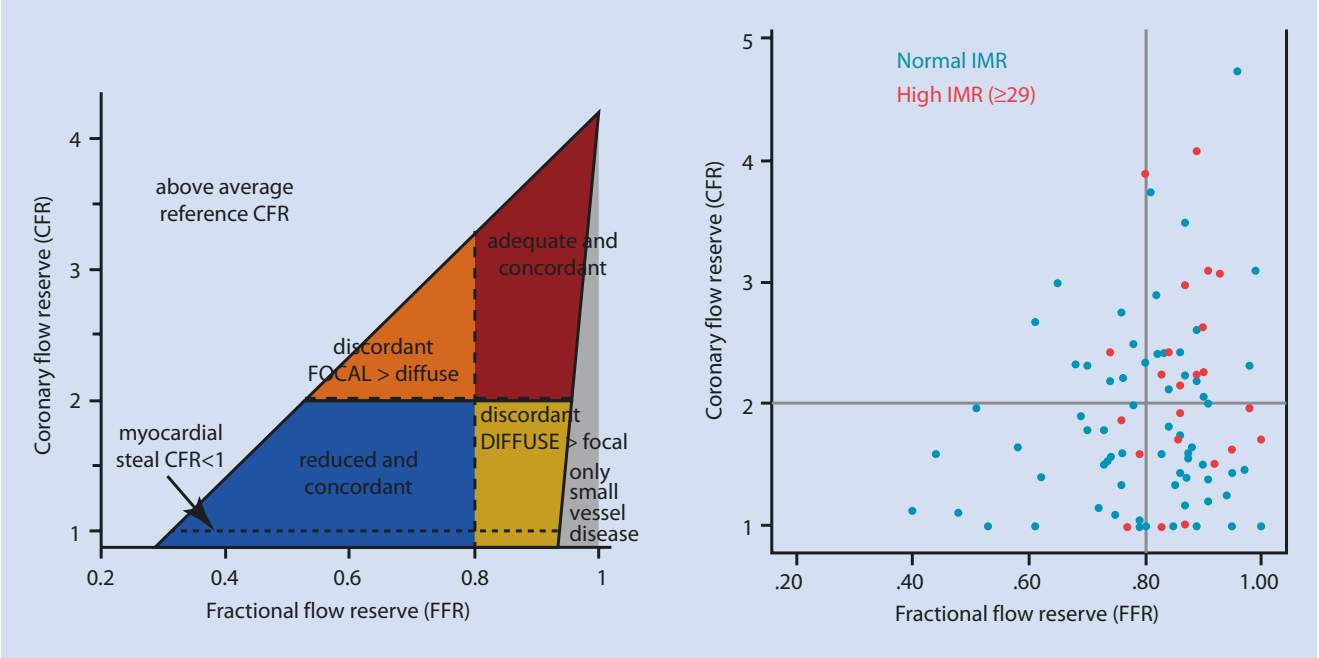


■ **Fig. 18.2** Conceptual plot of FFR and CFR values used in multimodal physiology (Johnson et al. [21])

four quadrants is key to understanding the complementary information that CFR and FFR provide. The concordance between CFR and FFR when evaluating the coronary circulation can be relatively easily interpreted; if both are normal (CFR >2, FFR >0.80), it can be assumed that myocardial ischemia is unlikely as there is no significant limitation to flow through the epicardial artery or impediment to the microvasculature in appropriately increasing flow. When both the CFR and FFR are abnormal, myocardial ischemia occurs due to an inability of the autoregulatory mechanisms of the microvasculature to augment flow in response to increased resistance caused by the epicardial stenosis. In this case revascularization of the coronary stenosis should restore flow through the coronary artery; however, if there is coexisting MCD revascularization will not restore the autoregulatory mechanisms, discordance between CFR and FFR leads clinicians to question which result is providing the correct answer. When one considers the underlying physiological principles of these techniques, it can be easily understood why apparently discordant results can be obtained. With this understanding rather than questioning which technique is providing us with the "correct" answer, one should view them as complementary physiological indices [22] and incorporate the information provided from both techniques in order to provide the best possible treatment to our patients. In the following paragraphs, we will discuss the discordant groups and how the addition of resistance can further classify ischemia in these groups.

## 18.2 Normal FFR with Abnormal CFR

This pattern of coronary hemodynamics can perhaps be most easily explained by the presence of microvascular disease causing a decreased CFR with normal or nonobstructive epicardial vessels reflecting the normal FFR values. Structural microcirculatory remodeling or microcirculatory plugging may exist, therefore limiting the maximal myocardial flow due to increased resistance in the arterioles and capillaries which leads to a reduced distal pressure drop, and thus a higher FFR would be obtained in the absence of MCD [23]. This is supported by the work of Meuwissen et al. who assessed CFR, FFR, and minimal microvascular resistance, a velocity-based index of microvascular resistance during maximal hyperemia, in 150 intermediate coronary lesions [24]. When the two discordant groups were analyzed, there were no significant differences found in the clinical or angiographic characteristics; however in the group with a normal FFR but abnormal CFR, there was a significantly higher minimal microvascular resistance when compared to the group with an abnormal FFR but normal CFR (2.42 ± 60.77 vs. 1.91 ± 60.70 $p$ <0.05), thus implying the presence of microvascular disease in the group with the normal FFR and abnormal CFR. The presence of diffuse epicardial coronary disease, which limits hyperemic flow to the point that the pressure gradient across the stenosis is low or nonexistent, is an alternative cause for this scenario. In the presence of diffuse atherosclerotic disease, there is a lack of convective accelerative flow and flow separation loss. This causes minimal pressure drop (normal FFR) in the flow-limiting coronary segment, despite its effect on vessel conductance, which is reflected as a low CFR. Due to low flow, the pressure gradient through the stenosis is limited and therefore FFR remains relatively normal despite the presence of angiographically significant stenosis. Gould et al. described the hemodynamic effects of diffuse coronary artery disease on coronary flow in patients with angiographically mild CAD without myocardial perfusion defects using dipyridamole positron emission tomography (PET) [25]. Despite demonstrating no segmental myocardial perfusion defects, which in this instance can be interpreted as a surrogate of normal FFR, they found a graded, longitudinal base to apex myocardial perfusion gradient significantly different to that observed in healthy subjects. This work was further supported by De Bruyne et al. who measured FFR in patients with non-stenotic CAD and controls without atherosclerosis; in coronary arteries with diffuse atherosclerosis and no focal stenosis, they found a pressure gradient along the length of the artery, a phenomenon that was not seen in normal coronary arteries [26]. These findings can be interpreted as diffuse atherosclerosis causing increased flow resistance, therefore promoting myocardial ischemia. Echavarría-Pinto et al. [27] eloquently integrated microcirculatory resistance, using IMR, along with FFR and CFR into the investigation of intermediate coronary artery stenosis in order to further elicit this discordance. They found a high frequency of abnormal CFR and/or IMR in arteries with normal FFR (63 % of cases). Furthermore, in vessels with FFR > 0.80 and CFR < 2 ($n$ = 28, 39 %), IMR had a wide dispersion. Given that high IMR reflects increased microvascular resistance and thus is a marker of MCD, this can thus lead and allow us to differentiate ischemia predominantly due to MCD (normal FFR, low CFR, high IMR) from ischemia predominantly due to diffuse coronary artery disease (normal FFR, low CFR, low IMR) (Fig. 18.3).

## 18.3 Abnormal FFR with Normal CFR

A key aspect to bear in mind is that in FFR it is assumed that the Pd/Pa ratio acts as a surrogate for the fractional peak flow across the lesion given that hyperemia induces minimal and constant myocardial resistance; however myocardial function depends on coronary blood flow, and not coronary perfusion pressure alone [28]. The simplest explanation for this phenomenon is that even a mild stenosis can generate a significant trans-lesional pressure gradient if coronary flow increases sufficiently. This scenario occurs most commonly in proximal stenoses or those which have a large subtended myocardial mass. The presence of virtually no pressure gradient at rest, but a significant gradient during hyperemia, should alert the operator to the possibility of this phenomenon [29].

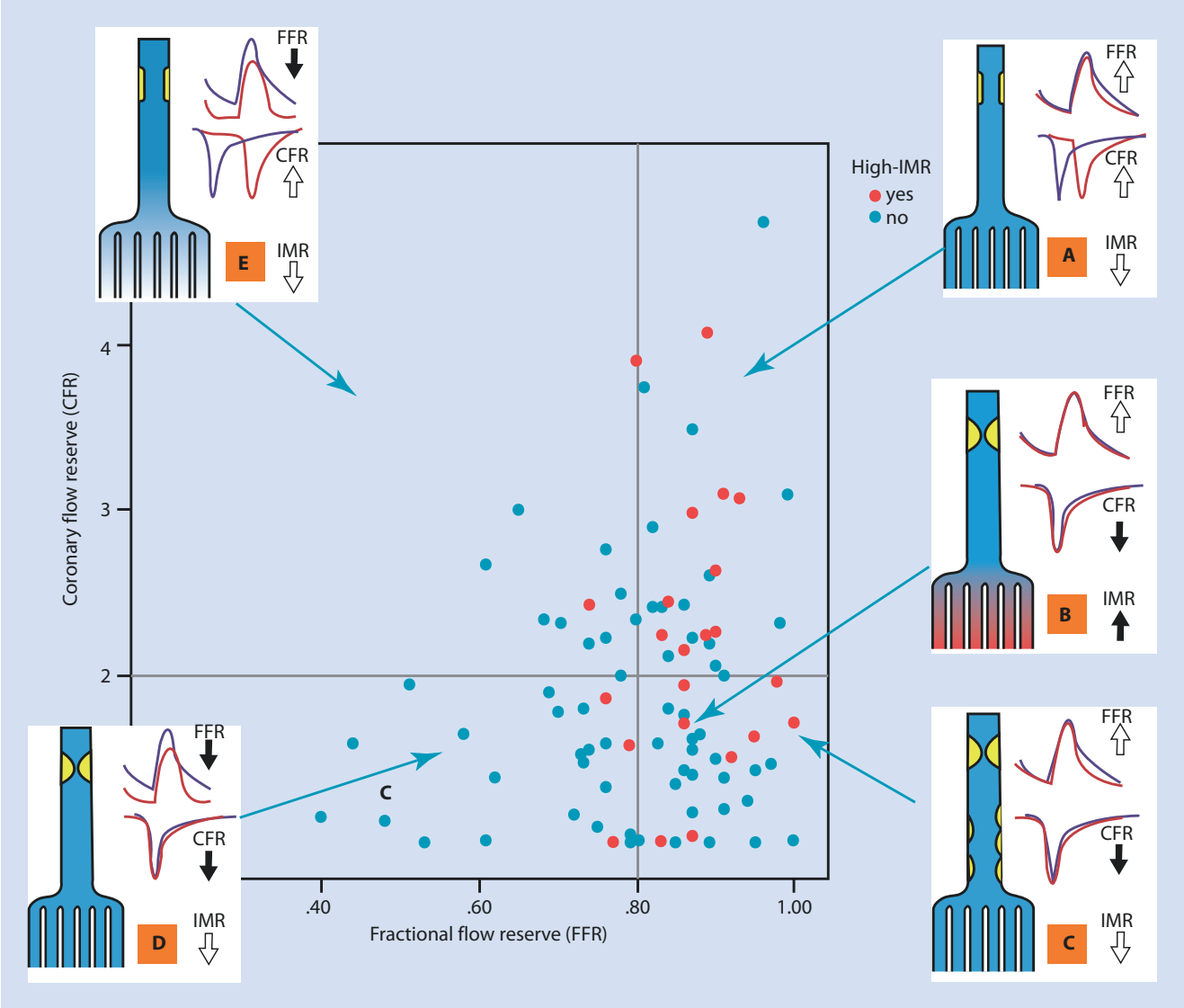


**Fig. 18.3** Conceptual and documented plots of the FFR/CFR relationship with schematic representation of the coronary hemodynamic patterns. Conceptual plot of the FFR/CFR relationship showing the four different quadrants. Scatterplot of FFR and CFR with IMR values (in red high IMR [>29.1U]). A schematic representation of the coronary hemodynamic patterns in the presence of focal epicardial stenosis is superposed. A, Vessel with a non-severe focal stenosis (FFR>0.80) without associated DCA or MCD (normal CFR [>2.0] and normal IMR [>29U]). B, Vessel with a non-severe focal stenosis but depressed CFR in presence of high values of IMR, due to predominant MCD as the cause of ischemia. C, Vessel with a non-severe focal stenosis but depressed CFR; despite a normal FFR, an abnormal CFR with low IMR suggests that DCA is the predominantly affected compartment, which would account for the discrepancy between FFR and CFR. D, Vessel with depressed CFR as a result of predominant physiologically significant epicardial stenosis. E, Vessel with physiologically significant epicardial stenosis (abnormal FFR) but preserved CFR as a result of functional microcirculation (normal [low] IMR) and the absence of significant DCA. The abnormal hemodynamics illustrated in B and C can be only identified by combining information of FFR, CFR, and microcirculatory resistance (Adapted from Mauro Echavarria-Pinto et al. [27], with permission of the publisher) *CFR* coronary flow reserve, *CMVD* coronary microvascular dysfunction, *DCA* diffuse coronary atherosclerosis, *IMR* index of microcirculatory resistance, *FFR* fractional flow reserve

Echavarría-Pinto et al.'s [27] work once again provides us with an understanding of this group by incorporating the IMR measurements. In this case, the epicardial lesion limits the conduction of blood through the vessel (FFR ≤0.80), although the overall myocardial blood supply in the territory is not significantly impaired as shown by the normal CFR. The lowest IMR values were found in this group supporting a functional microcirculation (Fig. 18.3).

### 18.3.1 Prognostic Value of CMR, FFR, and Resistance

Although CFR was first used for the assessment of epicardial stenosis severity [4], its utility in providing a global assessment of the coronary circulation and in stratifying cardiovascular risk has been extensively investigated using both invasive and noninvasive techniques [18, 27, 30, 31]. A good

example of this is the work of Murthy [31], evaluating myocardial perfusion and CFR in patients with and without coronary artery disease (CAD) with positron electron tomography (PET). These authors found that an impaired CFR was associated with an adjusted 3.2- and 4.9-fold increase in the rate of cardiac death in diabetic and nondiabetic patients, respectively ($p$ 0.0004). Interestingly diabetes has always been considered a cardiovascular risk factor; however in this study, diabetic patients without CAD with an impaired CFR experienced a similar rate of cardiac death to nondiabetic patients with CAD (2.8 vs. 2.0 %/year $p$ 0.33). In contrast diabetic patients without CAD with a preserved CFR had a very low rate of cardiac mortality similar to patients without diabetes or CAD and a preserved CFR (0.3 vs. 0.5 %/year $p$ 0.65). It must also be borne in mind that while FFR is now widely used in clinical practice, there was a MACE rate of approximately 20 % at long-term follow-up in the patients with deferred PCI in both DEFER [8] and FAME [10]. These along with other studies [24, 32–34] highlight the importance of looking beyond the epicardial stenosis when attempting to risk stratify patients.

The combined prognostic value of CFR, FFR, and resistance was evaluated by Meuwissen et al. in 2008, who investigated deferral of PCI in 186 intermediate stenoses interrogated with FFR, CFR, and HMR. In this study the authors found a significantly higher rate of MACE in the group with concordantly abnormal CFR and FFR when compared to the discordant groups or the concordantly normal group (33.3 % vs. 19.7 % vs. 5.4 %, $p$ 0.008). This initial work showing the additional prognostic benefit of adding CFR to FFR regenerated interest in researching the complementary information these two measures can provide. Recent work from van de Hoef et al. provides us with long-term follow-up, mean 11.7 years, of 157 patients with intermediate stenosis studied with FFR and CFVR [18, 20]. Interestingly they divided the patients into four quadrants using both a FFR cutoff value of 0.75, the original proposed value, and the currently widely accepted value of 0.80. When an FFR value of 0.75 was used, discordant results, FFR >0.75, CFVR <2, and FFR <0.75, CFVR > 2, were found in 14 % and 16 % of patients, respectively. Using the cutoff value of 0.8 for FFR, discordant results were found in 6.4 % and 30.6 % of patients, FFR >0.8, CFVR <2, and FFR <0.8, CFVR > 2, respectively. Discordance between FFR and CFVR was associated with an overall higher incidence of MACE than in the group with normal FFR and CFVR. The combination of a normal FFR with an abnormal CFVR leads to significantly more MACE early in the study and this increased MACE rate remained significant throughout follow-up. In contrast when a normal CFVR was associated with an abnormal FFR, the MACE rate was equivalent to that in patients with a normal FFR and CFVR up to 3 years and 10 years with cutoff points of 0.75 and 0.8, respectively. Interestingly the combination of a normal FFR and abnormal CFVR had a significantly higher MACE rate than the group with an abnormal FFR and normal CFVR up to 3 years and 10 years using the cutoff points of 0.75 and 0.8, respectively (Fig. 18.2). The key message this study adds is that while discordance with a normal FFR and abnormal CFVR is associated with adverse clinical outcomes compared to concordance, discordance with an abnormal FFR and normal CFVR has an equivalent clinical outcome to concordance. The authors also integrated the measurements of HMR into the interpretation of these concordant groups. In the group with a normal FFR but abnormal CFVR, the HMR was high implying an impairment of the vasodilatory response of the microcirculation during hyperemia, i.e., MCD. Conversely in the group with an abnormal FFR but normal CFVR, the HMR was low implying that despite the presence of a focal epicardial stenosis, the vasodilatory mechanisms of the microcirculation remain intact, and thus myocardial perfusion is preserved. The increased MACE rate when an FFR cutoff value of 0.75 was used is in keeping with prior studies support the concept that FFR values are a spectrum rather than a fixed cutoff point; the lower the FFR value of the cutoff point, the higher the event rates [10, 14, 35, 36]. This study highlights the importance of combining measurements of pressure and flow not only to fully elicit the ischemic potential in the coronary circulation but importantly to provide prognostic information and thus assist in optimizing the treatment of the individual. This concept that it is clinically safe and efficacious to defer stenting in arteries with an abnormal FFR but normal CFR is currently being prospectively investigated in the ongoing multicenter clinical trial DEFINE-FLOW (NCT02328820), in which patients with clinical intermediate stenosis are being investigated with pressure wire measurements with deferral of stenting when the FFR is <0.80 with an CFR >2. Recruitment is expected to finish in December 2018.

Lee et al. aimed to investigate prognostic implications of CFR and IMR in patients undergoing investigation with FFR [17]. In total 663 vessels in 313 patients undergoing clinically indicated coronary angiography were evaluated. Given that there are no well-accepted values for IMR, they used an $IMR_{corr}$ >75 % percentile as a high IMR, in this case >23 U. About 230 patients, 516 vessels, with a normal FFR were divided into groups based on low and high CFR and then subdivided into four groups: (A) high CFR with low IMR, (B) high CFR with high IMR, (C) low CFR with low IMR, and (D) low CFR with high IMR. The primary outcome was patient-oriented composite outcome (POCO), a combination of all-cause mortality, any MI, and any revascularization, with the individual components of POCE as the secondary outcomes. Patients were followed for a median of 658 days (IQR 503.8–1139.3). This group, once again, show that patients with a normal FFR and low CFR had a higher incidence of POCE (HR 4.189, 95 % CI 1.117–15.715, $p$ 0.034). When looking at the subgroups, the cumulative incidence of POCE was 9.5 %, 0 %, 7 %, and 27.9 % for groups A, B, C, and D, respectively ($p$ 0.002). Thus patients with impaired flow due to microvascular disease (low CFR, high IMR) had the worst outcomes. As all patients had similar clinical and angiographic characteristics, the measurement of flow and resistance provided additional

prognostic information in this group who by FFR alone would have been characterized as not having functionally significant disease (Fig. 18.4). Clinical examples of the combined use of pressure, flow, and resistance are shown in Figs. 18.5 and 18.6.

### 18.3.2 Future Perspectives

The instantaneous wave-free index (iFR) differs from FFR as it is not intended to estimate the maximal myocardial blood flow with pressure and therefore does not require hyperemia for its calculation; instead, the iFR is the ratio of the mean

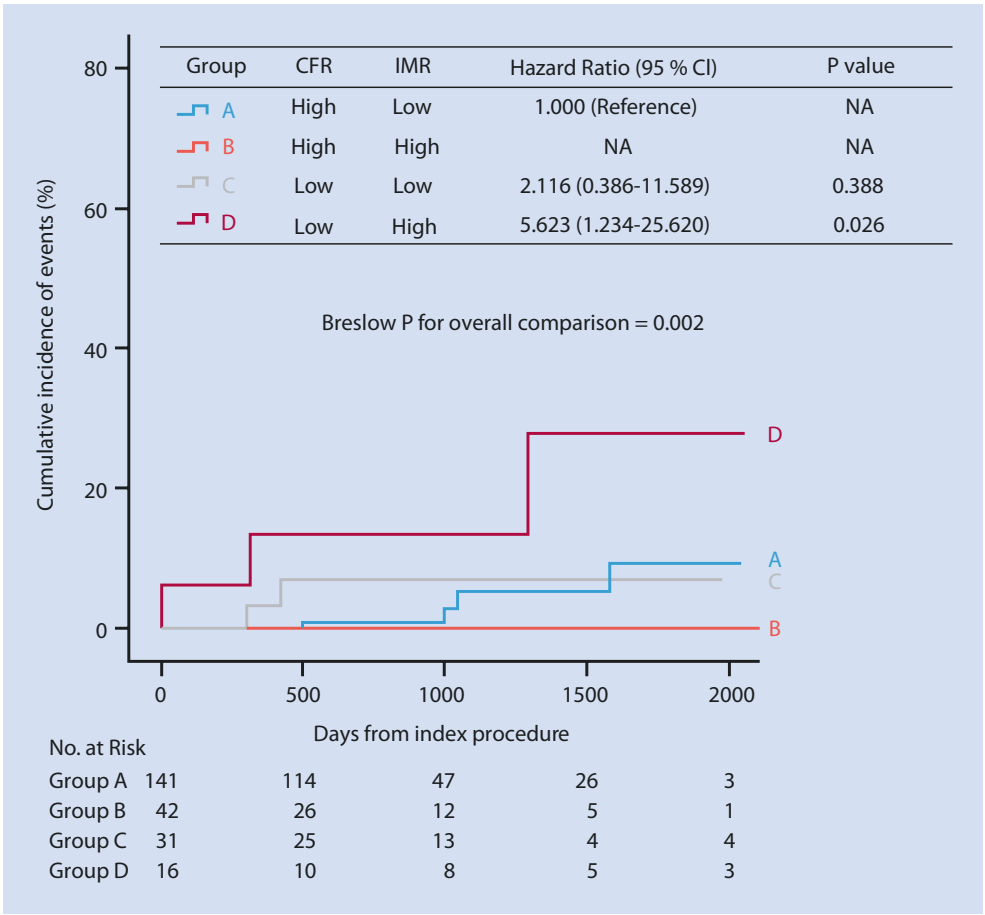


**Fig. 18.4** Clinical outcomes in patients with FFR>0.80 according to patterns of microvascular status, defined with CFR and IMR. The cumulative incidence of patient-oriented composite outcomes was compared among four groups divided according to CFR and IMR values (*NA* not available; with permission from Lee et al. [17])

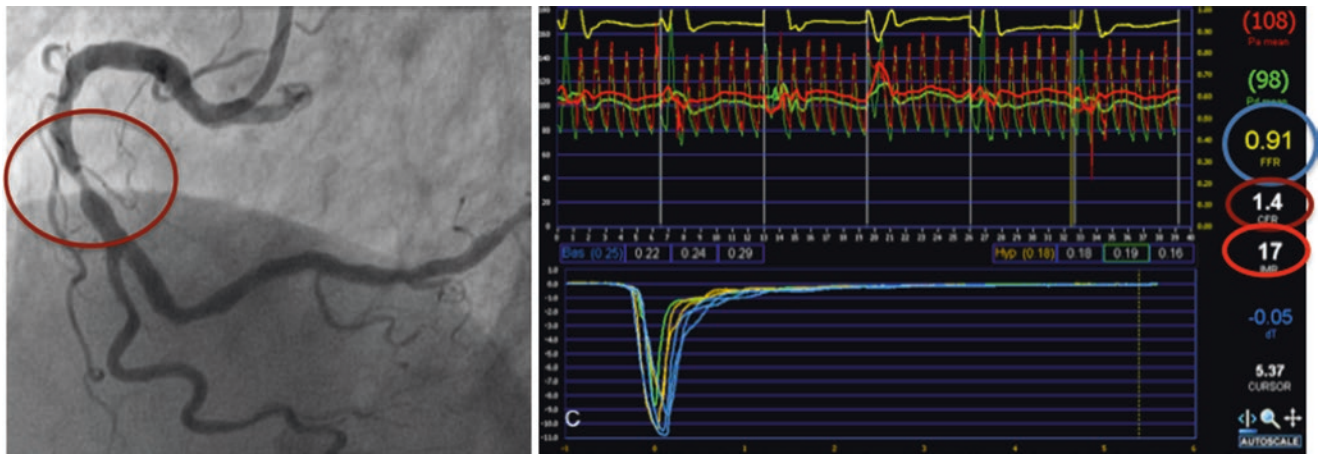


**Fig. 18.5** Combined measurement of pressure and thermodilution-derived flow in a 70-year-old patient with stable angina. *Left panel* shows an intermediate lesion in the mid-segment of the right coronary artery. The right shows the curves of the distal (in *green*) and the proximal (in *red*) hyperemic trans-stenotic pressures, obtaining an FFR of 0.91. At the bottom the mean transit times of Doppler-derived flow velocities, obtaining a CFR of 1.4 and IMR of 17 U, are shown. The results of this multimodal physiological approach are in concordance with physiologically nonsignificant epicardial lesion but depressed CFR, suggesting the presence of diffuse coronary artery disease (normal IMR)

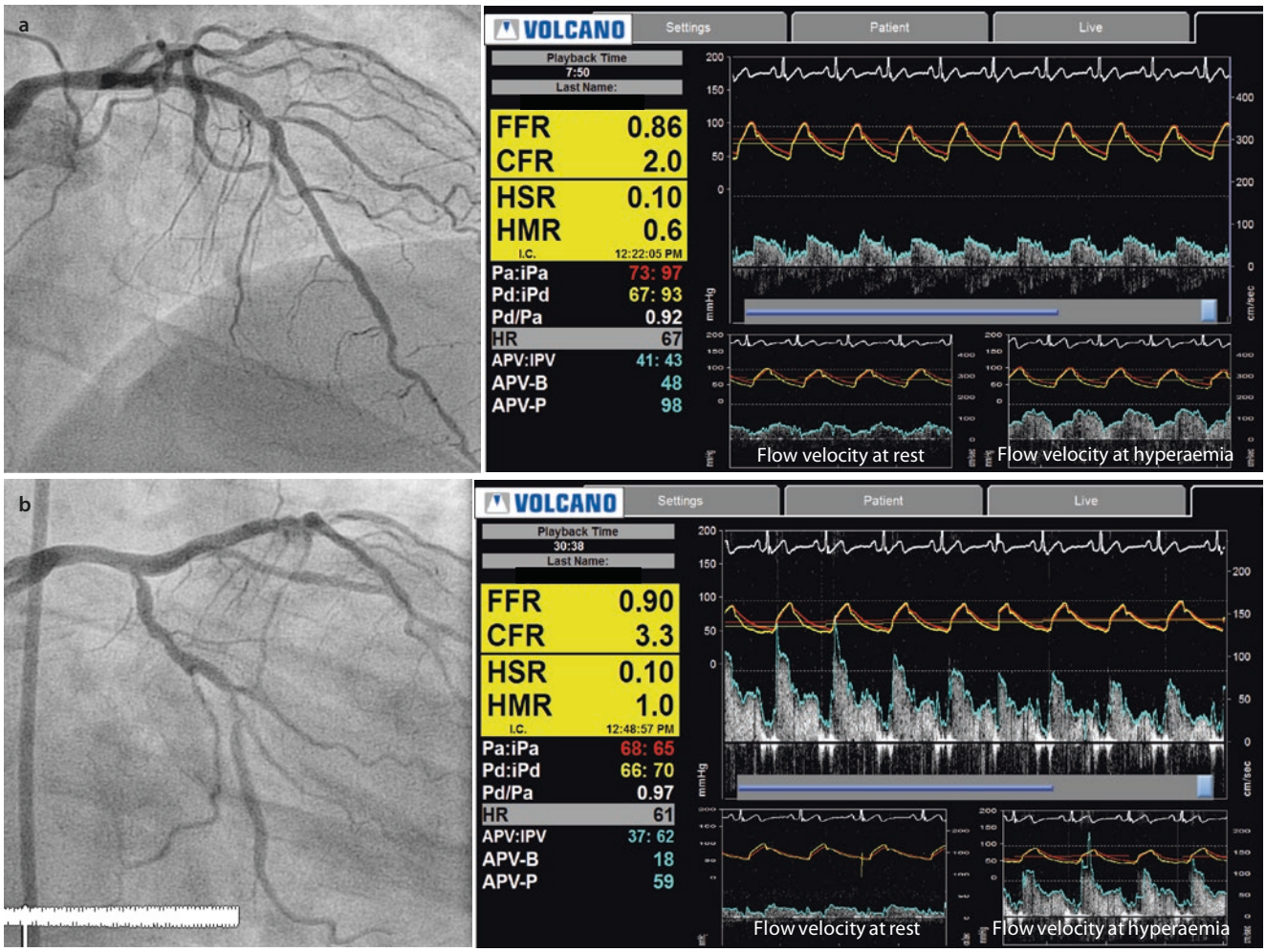


**Fig. 18.6** Comprehensive assessment of intracoronary pressure and Doppler-derived flow in a 65-year-old gentleman with stable angina and intermediate multivessel coronary disease. **a** Left panel is an angiographic projection focused to the left main stem and the left anterior descending (LAD) showing angiographic intermediate multisegment disease. *Right panel* shows the Doppler flow velocity traces (*blue curve*) and trans-stenotic distal (*yellow curve*) and proximal (*red curve*) pressures obtained with a combowire located in the distal LAD. The *bottom boxes* of the *right panel* show the flow velocity during adenosine-induced hyperemia and flow velocity at rest. An FFR (0.86) and CFR (2.0) were concordantly normal, thus implying physiologically nonsignificant epicardial lesions in this vessel. Furthermore normal CFR and HMR (0.6) reflect a preserved coronary microcirculation in the subtended myocardial territory of LAD. **b** Same patient as figure **a**. **b** *Left panel* shows an angiographic projection focused to the left circumflex coronary artery (LCx) showing an ostial calcified lesion with intermediate stenosis, and the mid-segment with other lesion angiographically unlikely significant. Right panel shows the Doppler flow velocity trace (blue curve) and trans-stenotic distal (*yellow curve*) and proximal (*red curve*) pressures obtained with a combowire located in the distal LCx. The bottom boxes of the right panel show the flow velocity during adenosine-induced hyperemia and flow velocity at rest. FFR (0.90) and CFR (3.3) were normally concordant implying physiologically non-significant lesions. Furthermore, normal CFR and HMR (1.0) reflect a preserved coronary. Following the physiological results in both major vessels, no PCI was performed, and medical treatment was optimized. *CFR* coronary flow reserve, *FFR* fractional flow reserve, *HSR* hyperemic stenosis resistance, *HMR* hyperemic microcirculatory resistance, *Pa* aortic pressure, *Pd* distal pressure, *APV-B* average of peak velocity at rest, *APV-P* average of peak velocity at hyperemia, *PCI* percutaneous coronary intervention



wave-free period distal to the stenosis to the mean wave-free period in the aorta. Although iFR is known to have a close pressure relationship to FFR [37], it is relatively insensitive to non-flow-limiting coronary stenosis; this can easily be explained by the fact that it is calculated during basal conditions and therefore the large pressure gradient during hyperemia that results from a large increase in coronary flow and thus a low FFR is not observed with iFR. Therefore iFR may provide a closer correlation with CFR and thus better prognostic information. This hypothesis was investigated by the JUSTIFY-CFR study [38] where invasive pressure, iFR and FFR, and flow velocity CFVR were measured in 216 stenoses in 186 patients scheduled for routine coronary angiography. The relationship between the pressure and flow indices was then compared; iFR showed a stronger correlation with CFVR than FFR (iFR–CFVR, $\rho$ =0.68 vs. FFR–CFVR, $\rho$ =0.50; $P$ <0.001) and agreed more closely with CFVR than FFR in stenosis classification (iFR area under the receiver operating characteristic curve, 0.82 vs. FFR area under the receiver operating characteristic curve, 0.72; $P$ <0.001, for a

CFVR of 2). This study also identified an iFR value of 0.85 as the cutoff with maximal accuracy to detect a flow-limiting stenosis, similar to the 0.86 value reported in the CLARIFY study [39]. While prognostic implications were not evaluated in this study, the closer association between iFR and CFR implies that iFR may provide better insights into the prognostic significance of ischemic heart disease than FFR alone; however further studies are required in this regard.

## 18.4 Conclusions

The evidence supporting the complementary prognostic value of CFR and FFR is mounting, with additional benefit when measurements of resistance are added to provide a comprehensive global assessment of the coronary circulation. While FFR has long been held up as a "gold standard" in evaluating the functional significance of a coronary stenosis, the presence of a negative FFR does not imply that the individual patient does not have myocardial ischemia and therefore a poorer clinical prognosis. Instead of viewing FFR, CFR, and measures of resistance as competing tools, the concept of multimodal physiology combining the information provided by all three indices in order to achieve our ultimate goal, providing the best clinical outcomes to every patient, should be adopted. Ongoing prospective clinical trials will provide us with further information on the prognostic value of this multimodal physiology approach.

## References

1. Chareonthaitawee P, Kaufmann PA, Rimoldi O, Camici PG. Heterogeneity of resting and hyperemic myocardial blood flow in healthy humans. Cardiovasc Res. 2001;50(1):151–61.
2. Camici PG, Crea F. Coronary microvascular dysfunction. N Engl J Med. 2007;356(8):830–40.
3. Camici PG, d'Amati G, Rimoldi O. Coronary microvascular dysfunction: mechanisms and functional assessment. Nat Rev Cardiol. 2014;12(1):48–62.
4. Gould KL, Lipscomb K. Effects of coronary stenoses on coronary flow reserve and resistance. Am J Cardiol. 1974;34(1):48–55.
5. Pijls NH, van Son JA, Kirkeeide RL, De Bruyne B, Gould KL. Experimental basis of determining maximum coronary, myocardial, and collateral blood flow by pressure measurements for assessing functional stenosis severity before and after percutaneous transluminal coronary angioplasty. Circulation. 1993;87(4):1354–67.
6. De Bruyne B, Baudhuin T, Melin JA, Pijls NH, Sys SU, Bol A, et al. Coronary flow reserve calculated from pressure measurements in humans. Validation with positron emission tomography. Circulation. 1994;89(3):1013–22.
7. Kakouros N, Rybicki FJ, Mitsouras D, Miller JM. Coronary pressure-derived fractional flow reserve in the assessment of coronary artery stenoses. Eur Radiol. 2013;23(4):958–67.
8. Zimmermann FM, Ferrara A, Johnson NP, van Nunen LX, Escaned J, Albertsson P, et al. Deferral vs. performance of percutaneous coronary intervention of functionally non-significant coronary stenosis: 15-year follow-up of the DEFER trial. Eur Heart J. 2015;36(45):3182–8.
9. Tonino PAL, Fearon WF, De Bruyne B, Oldroyd KG, Leesar MA, Ver Lee PN, et al. Angiographic versus functional severity of coronary artery stenoses in the FAME study. J Am Coll Cardiol. 2010;55(25):2816–21.
10. De Bruyne B, Pijls NHJ, Kalesan B, Barbato E, Tonino PAL, Piroth Z, et al. Fractional flow reserve–guided PCI versus medical therapy in stable coronary disease. N Engl J Med. 2012;367(11):991–1001.
11. Windecker S, Kolh P, Alfonso F, Collet J-P, Cremer J, Falk V, et al. 2014 ESC/EACTS Guidelines on myocardial revascularization: the Task Force on Myocardial Revascularization of the European Society of Cardiology (ESC) and the European Association for Cardio-Thoracic Surgery (EACTS) * Developed with the special contribution. Eur Heart J. 2014;35(37):2541–619.
12. Patel MR, Dehmer GJ, Hirshfeld JW, Smith PK, Spertus JA. ACCF/SCAI/STS/AATS/AHA/ASNC/HFSA/SCCT 2012 Appropriate use criteria for coronary revascularization focused update: a report of the American College of Cardiology Foundation Appropriate Use Criteria Task Force, Society for Cardiovascular Angiography and Interventions, Society of Thoracic Surgeons, American Association for Thoracic Surgery, American Heart Association, American Society of Nuclear Cardiology, and the Society of Cardiovascular Computed Tomography. J Am Coll Cardiol. Elsevier Inc. 2012;59(9):857–81.
13. Pijls NH, de Bruyne B, Peels K, van der Voort PH, Bonnier HJ, Bartunek J, et al. Measurement of fractional flow reserve to assess the functional severity of coronary-artery stenoses. N Engl J Med. 1996;334(26):1703–8.
14. Petraco R, Sen S, Nijjer S, Echavarria-Pinto M, Escaned J, Francis DP, et al. Fractional flow reserve-guided revascularization: Practical implications of a diagnostic gray zone and measurement variability on clinical decisions. JACC Cardiovasc Interv. Elsevier Inc. 2013;6(3):222–5.
15. Serruys PW, Di Mario C, Meneveau N, de Jaegere P, Strikwerda S, de Feyter PJ, et al. Intracoronary pressure and flow velocity with sensor-tip guidewires: a new methodologic approach for assessment of coronary hemodynamics before and after coronary interventions. Am J Cardiol. 1993;71(14):41D–53.
16. Pries AR, Badimon L, Bugiardini R, Camici PG, Dorobantu M, Duncker DJ, et al. Coronary vascular regulation, remodelling, and collateralization: mechanisms and clinical implications on behalf of the working group on coronary pathophysiology and microcirculation. Eur Heart J. 2015;36(45):3134–46.
17. Lee JM, Jung J-H, Hwang D, Park J, Fan Y, Na S-H, et al. Coronary flow reserve and microcirculatory resistance in patients with intermediate coronary stenosis. J Am Coll Cardiol. 2016;67(10):1158–69.
18. van de Hoef TP, van Lavieren MA, Damman P, Delewi R, Piek MA, Chamuleau SAJ, et al. Physiological basis and long-term clinical outcome of discordance between fractional flow reserve and coronary flow velocity reserve in coronary stenoses of intermediate severity. Circ Cardiovasc Interv. 2014;7(3):301–11.
19. Meuwissen M, Siebes M, Chamuleau SAJ, van Eck-Smit BLF, Koch KT, de Winter RJ, et al. Hyperemic stenosis resistance index for evaluation of functional coronary lesion severity. Circulation. 2002;106(4):441–6.
20. Meuwissen M, Chamuleau SAJ, Siebes M, de Winter RJ, Koch KT, Dijksman LM, et al. The prognostic value of combined intracoronary pressure and blood flow velocity measurements after deferral of percutaneous coronary intervention. Catheter Cardiovasc Interv Off J Soc Card Angiogr Interv. 2008;71(3):291–7.
21. Johnson NP, Kirkeeide RL, Gould KL. Is discordance of coronary flow reserve and fractional flow reserve due to methodology or clinically relevant coronary pathophysiology? JACC Cardiovasc Imaging. 2012;5(2):193–202.
22. Escaned J, Echavarría-Pinto M. Moving beyond coronary stenosis: has the time arrived to address important physiological questions not answered by fractional flow reserve alone? Circ Cardiovasc Interv. 2014;7(3):282–4.
23. Tamita K, Akasaka T, Takagi T, Yamamuro A, Yamabe K, Katayama M, et al. Effects of microvascular dysfunction on myocardial fractional flow reserve after percutaneous coronary intervention in patients with acute myocardial infarction. Catheter Cardiovasc Interv Off J Soc Card Angiogr Interv. 2002;57(4):452–9.

24. Meuwissen M, Chamuleau SA, Siebes M, Schotborgh CE, Koch KT, de Winter RJ, et al. Role of variability in microvascular resistance on fractional flow reserve and coronary blood flow velocity reserve in intermediate coronary lesions. Circulation. 2001;103(2):184–7.
25. Gould KL, Nakagawa Y, Nakagawa K, Sdringola S, Hess MJ, Haynie M, et al. Frequency and clinical implications of fluid dynamically significant diffuse coronary artery disease manifest as graded, longitudinal, base-to-apex myocardial perfusion abnormalities by noninvasive positron emission tomography. Circulation. 2000;101(16):1931–9.
26. De Bruyne B, Hersbach F, Pijls NH, Bartunek J, Bech JW, Heyndrickx GR, et al. Abnormal epicardial coronary resistance in patients with diffuse atherosclerosis but "Normal" coronary angiography. Circulation. 2001;104(20):2401–6.
27. Echavarria-Pinto M, Escaned J, Macías E, Medina M, Gonzalo N, Petraco R, et al. Disturbed coronary hemodynamics in vessels with intermediate stenoses evaluated with fractional flow reserve: a combined analysis of epicardial and microcirculatory involvement in ischemic heart disease. Circulation. 2013;128(24):2557–66.
28. Gould KL, Johnson NP, Bateman TM, Beanlands RS, Bengel FM, Bober R, et al. Anatomic versus physiologic assessment of coronary artery disease. J Am Coll Cardiol. 2013;62(18):1639–53.
29. Echavarría-Pinto M, van de Hoef TP, van Lavieren MA, Nijjer S, Ibañez B, Pocock S, et al. Combining baseline distal-to-aortic pressure ratio and fractional flow reserve in the assessment of coronary stenosis severity. JACC Cardiovasc Interv. 2015;8(13):1681–91.
30. Herzog BA, Husmann L, Valenta I, Gaemperli O, Siegrist PT, Tay FM, et al. Long-term prognostic value of 13 N-ammonia myocardial perfusion positron emission tomography added value of coronary flow reserve. J Am Coll Cardiol. 2009;54(2):150–6.
31. Murthy VL, Naya M, Foster CR, Hainer J, Gaber M, Di Carli G, et al. Improved cardiac risk assessment with noninvasive measures of coronary flow reserve. Circulation. 2011;124(20):2215–24.
32. Cannon III RO, Epstein SE. "Microvascular angina" as a cause of chest pain with angiographically normal coronary arteries. Am J Cardiol. 1988;61(15):1338–43.
33. Fearon WF, Low AF, Yong AS, McGeoch R, Berry C, Shah MG, et al. Prognostic value of the index of microcirculatory resistance measured after primary percutaneous coronary intervention. Circulation. 2013;127(24):2436–41.
34. van de Hoef TP, Echavarría-Pinto M, van Lavieren MA, Meuwissen M, Serruys PWJC, Tijssen JGP, et al. Diagnostic and prognostic implications of coronary flow capacity. JACC Cardiovasc Interv. 2015;8(13):1670–80.
35. Depta JP, Patel JS, Novak E, Gage BF, Masrani SK, Raymer D, et al. Risk model for estimating the 1-year risk of deferred lesion intervention following deferred revascularization after fractional flow reserve assessment. Eur Heart J. 2015;36(8):509–15.
36. Van Belle E, Rioufol G, Pouillot C, Cuisset T, Bougrini K, Teiger E, et al. Outcome impact of coronary revascularization strategy reclassification with fractional flow reserve at time of diagnostic Angiography clinical perspective: insights from a large French multicenter fractional flow reserve registry. Circulation. 2014;129(2):173–85.
37. Escaned J, Echavarría-Pinto M, Garcia-Garcia HM, van de Hoef TP, de Vries T, Kaul P, et al. Prospective assessment of the diagnostic accuracy of instantaneous wave-free ratio to assess coronary stenosis relevance. JACC Cardiovasc Interv. 2015;8(6):824–33.
38. Petraco R, van de Hoef TP, Nijjer S, Sen S, van Lavieren MA, Foale RA, et al. Baseline instantaneous wave-free ratio as a pressure-only estimation of underlying coronary flow reserve: results of the JUSTIFY-CFR study (Joined Coronary Pressure and Flow Analysis to Determine Diagnostic Characteristics of Basal and Hyperemic Indices of Functional Lesion Severity-Coronary Flow Reserve). Circ Cardiovasc Interv. 2014;7(4):492–502.
39. Sen S, Asrress KN, Nijjer S, Petraco R, Malik IS, Foale RA, et al. Diagnostic classification of the instantaneous wave-free ratio is equivalent to fractional flow reserve and is not improved with adenosine administration. Results of CLARIFY (classification accuracy of pressure-only ratios against indices using flow study). J Am Coll Cardiol. 2013;61(13):1409–20.

# Wave Intensity Analysis

## Contents

# Wave Intensity Patterns in Coronary Flow in Health and Disease

*Christopher J. Broyd, Kim Parker, and Justin Davies*




J. Escaned, J. Davies (eds.), *Physiological Assessment of Coronary Stenoses and the Microcirculation*,
DOI 10.1007/978-1-4471-5245-3_19

## 19.1 Introduction

Wave intensity analysis is a technique that has emerged from the field of gas dynamics and has found marked applicability in assessing coronary physiology. It is particularly useful in this system as it cannot only quantify the phasic forces acting within a single cardiac cycle but can also separate them according to their point of origin. While it remains a useful tool to investigate the systemic circulation, its application to the coronary circulation has demonstrated its unique strength: in this system both the proximal (aortic) and distal (myocardial) arterial ends are potentially active and wave intensity analysis allows their individual contributions to be measured even when they occur simultaneously (Fig. 19.1).

Wave intensity is derived from simultaneously acquired pressure and flow waveforms, which can be measured using a dual-tipped Doppler- and pressure-sensor wire. Using this system, six dominant waves are evident per cardiac cycle in both health and disease. The most clinically relevant wave is the backward decompression wave (BDW), which is generated in the blood vessels in the myocardium at the start of diastole. This wave has the most significant impact on coronary flow velocity, causing the acceleration that is evident at this time in the cardiac cycle. It is created by the re-expansion of the intramyocardial blood vessels that have been compressed during systole producing a distal "suction" effect. The BDW, therefore, provides information on the health and efficiency of the myocardium in its ability to effectively generate its own blood flow.

Wave intensity in the coronary arteries has been investigated in a number of disease states including left ventricular hypertrophy, aortic stenosis, heart failure, and ischemic heart

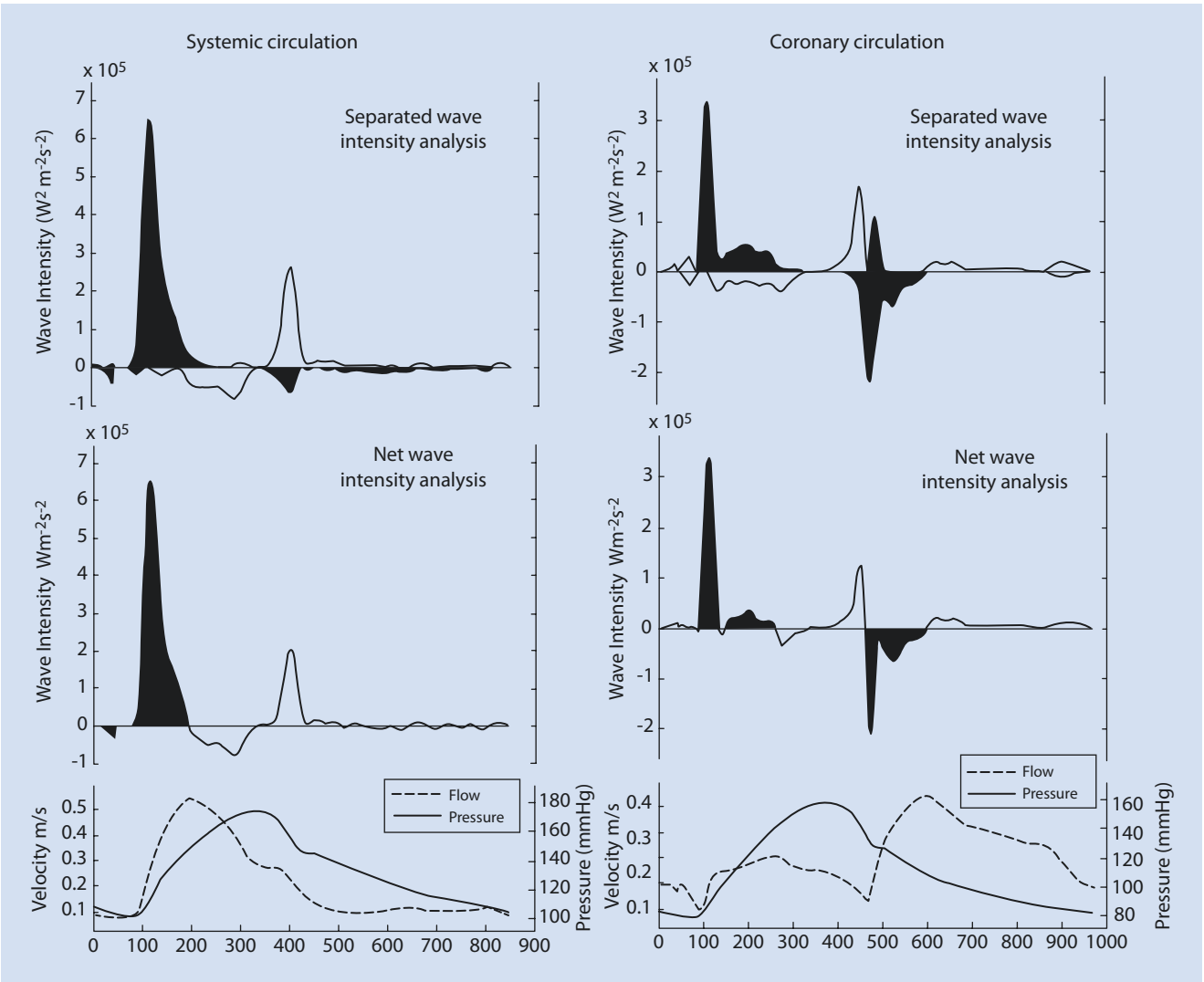


**Fig. 19.1** The importance of separated wave intensity analysis in the coronary circulation: pressure, velocity, net and separated wave intensity in the aorta (*left*) and coronary (*right*) arteries. In the systemic circulation there are very few coincident waves largely because the distal end of the vasculature is passive. Therefore net wave-intensity is very similar to separated wave-intensity. However, in the coronary system there are several coincident waves due to the 'active' nature of the myocardium. These waves can only be identified and correctly quantified using separated wave-intensity analysis. Shaded waves have an accelerating effect and unshaded have a decelerating effect. Waves above the zero-line originate proximally and below the zero line distally

disease to provide insightful, diagnostic, and prognostic information on the function of the myocardium and microcirculation. It has also been directly involved in the construction of adenosine-free measures of epicardial coronary stenoses due to the identification of regular, wave-free parts of the cardiac cycle. Its clinical applicability is currently hampered by its need to be assessed using invasive tools; however, once this issue is resolved it has the potential to be applied to larger cohort-based studies and transferred more broadly into the clinical environment.

## 19.2 Mathematical Concepts

### 19.2.1 Wave Intensity Analysis: Conceptual Theory

Although the geometry of arterial structures is complex, when dealing with wave intensity they can be regarded as one-dimensional tubes. As a result wave intensity analysis cannot provide information on local shear stress distribution or variation in velocity across the cross-section of a vessel but it can provide detailed information on axial pressure and velocity changes.

Wave intensity analysis is a technique that involves waveform decomposition. In mathematics, "decomposition" refers to ways to express a function (such as a waveform) as a combination of simpler components. There are numerous ways to achieve this but within the cardiovascular system Fourier analysis is one of the more widely applied decomposition tools, first described to simplify the study of heat transfer. It uses sinusoidal wave trains of different frequencies as its basis functions. It can be shown that a periodic function can be represented as the summation of sinusoidal waves with frequencies equal to the fundamental frequency and its harmonics. Fourier analysis, therefore, decomposes the measured pressure and flow waveforms into sinusoidal waves with the appropriate amplitudes and phases. Although this technique has proven useful in countless applications the transformation of the problem from the temporal to the frequency domain has some drawbacks. Notably, it is impossible to ascribe aspects of a frequency-based waveform decomposition to a particular moment in the (time-based) cardiac cycle.

In wave intensity analysis, the basis functions are incremental wavefronts. The measured pressure and flow waveforms are decomposed into the summation of successive wavefronts of different amplitudes, either positive or negative. For application to coronary studies, wave intensity analysis has two advantages: it is carried out in the time domain making it easy to relate its results to particular times in the cardiac cycle and it makes no assumption about periodicity so it can be used to analyze transient conditions where Fourier analysis is invalid.

The simplest definition of a wave is a "disturbance that propagates in space and time" and invariably, this propagation involves the exchange of energy. In the cardiovascular system, this exchange is between the kinetic energy of the blood and the potential energy stored in the walls of the elastic vessels. In arteries it is observed that these waves travel at a speed that is always larger than the velocity of the blood. For example, a wave generated by the contraction of the left ventricle travels to the wrist (where it can be appreciated as the radial pulse), approximately 1 m from the root of the aorta, in about 0.1 s; giving an average wave speed of 10 m/s. The mean velocity of blood in the arteries of the arm, at rest, is approximately 20 cm/s, 50 times slower than the wave speed. Similar ratios are found in the coronary arteries. This means that the elastic vessel waves can travel forward, from proximal to distal vessels, or backward, from distal to proximal vessels.

Accordingly these waves influence the medium in which they pass in three potential ways, all of which can be assessed:

Direction of travel – originating either proximally (forward waves) or distally (backward waves)
Effect on pressure – either compressive (increasing pressure) or decompressive (decreasing pressure)
Effect on velocity – either causing acceleration or deceleration

It is important to realize that coincident waves with opposing effects will have a summative result so that if a forward acceleration wave meets a backward deceleration wave of the same magnitude there will be no net change in the velocity.

### 19.2.2 Wave Intensity Analysis: Mathematical Derivation

Wave intensity analysis is based on the solution of the fundamental equations for the conservation of mass and momentum in the blood vessel. The solution is based on the method of characteristics which involves rather subtle mathematics, which are presented elsewhere in detail [1]. Given the complexity of the mathematics, the results are surprisingly simple and intuitive.

The fundamental definition of wave intensity ($I$) is

$$I = dP\,dU$$

where $dP$ is the change in pressure and $dU$ the change in velocity across a wave. The "width" of the wavefront is implicitly defined as one sampling time.

Wave intensity has the units $Wm^{-2}$ and its sign conveys the direction of the dominant wave such that a positive value reflects the dominance of the wave originating proximally and negative the dominance of the wave originating distally. A disadvantage of this definition is that its magnitude is determined by the sampling frequency (Fig. 19.2). Therefore, either a universal sampling frequency needs to be adopted for standardization or, more conveniently, the definition of wave intensity can incorporate the sampling rate as:

$$I' = \left(\frac{dP}{dt}\right)\left(\frac{dU}{dt}\right)$$

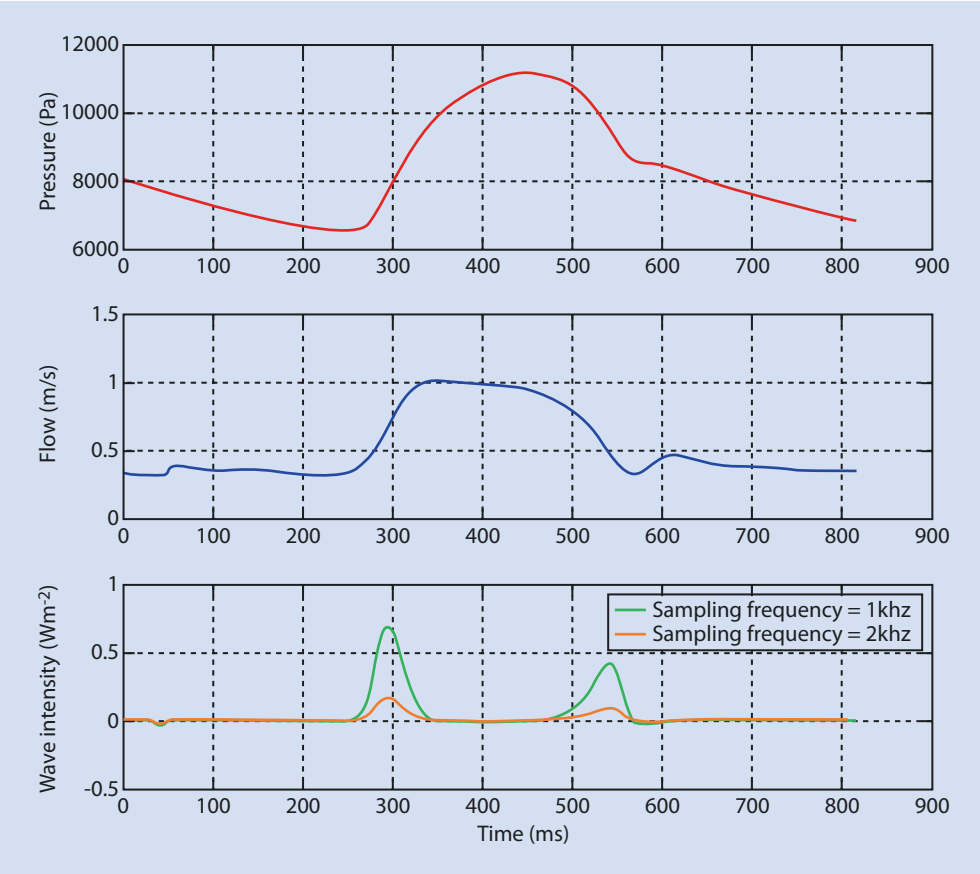


**Fig. 19.2** Pressure, flow and wave intensity recorded from a human renal artery with differing sampling frequencies. The data was processed from the same waveforms but at both 1000Hz and 2000Hz. Whilst both the pressure and flow waveforms are unchanged, net wave intensity (*dPdU*) is increased with lower sampling frequencies. Therefore it is suggested that wave intensity is calculated from *dP*/*dt* and *dU*/*dt* which makes wave intensity independent of the sampling time

In this case, the units are now $Wm^{-2}\ s^{-1}$.

The first step in calculating separated wave intensity is the observation that the pressure and velocity changes in each elemental wavefront must be related to each other for mass and momentum to be conserved. The method of characteristics solution gives this relationship, which are known as the "water hammer" equations, as

$$dP_+ = \rho c\, dU_+$$

for forward waves (subscript "+") and

$$dP_- = -\rho c\, dU_-$$

for backward waves (subscript "−"). Here $\rho$ is the density of blood and $c$ is the wave speed.

Since our decomposition of the measured waveforms into successive incremental wavefronts assumed that the wavefronts are additive and only forward and backward waves are present, at any point at any time in the artery

$$dP = dP_+ + dP_-$$
$$dU = dU_+ + dU_-$$

These equations and the water hammer equations give us four equations for the four unknowns, $dP_+$, $dP_-$, $dU_+$, and $dU_-$, in terms of the known changes in pressure and velocity, $dP$ and $dU$.

Solving first for $dP_+$

$$dP_+ = dP - dP_- = dP + \rho c\, dU_-$$
$$= dP + \rho c\left(dU - dU_+\right) = dP + \rho c dU - dP_+$$

Thus

$$dP_+ = \frac{1}{2}\left(dP + \rho c\, dU\right)$$

Solving for $dP_-$ in the same way

$$dP_- = \frac{1}{2}\left(dP - \rho c\, dU\right)$$

The forward and backward velocity changes follow directly from the water hammer equations

$$dU_+ = \frac{1}{2\rho c}\left(dP + \rho c\, dU\right)$$
$$dU_- = \frac{-1}{2\rho c}\left(dP - \rho c\, dU\right)$$

The separated wave intensities are defined in the same way as the net wave intensity so that

$$I_+ \equiv dP_+ dU_+ = \frac{1}{4\rho c}\left(dP + \rho c\, dU\right)^2$$
$$I_- \equiv dP_- dU_- = \frac{-1}{4\rho c}\left(dP - \rho c\, dU\right)^2$$

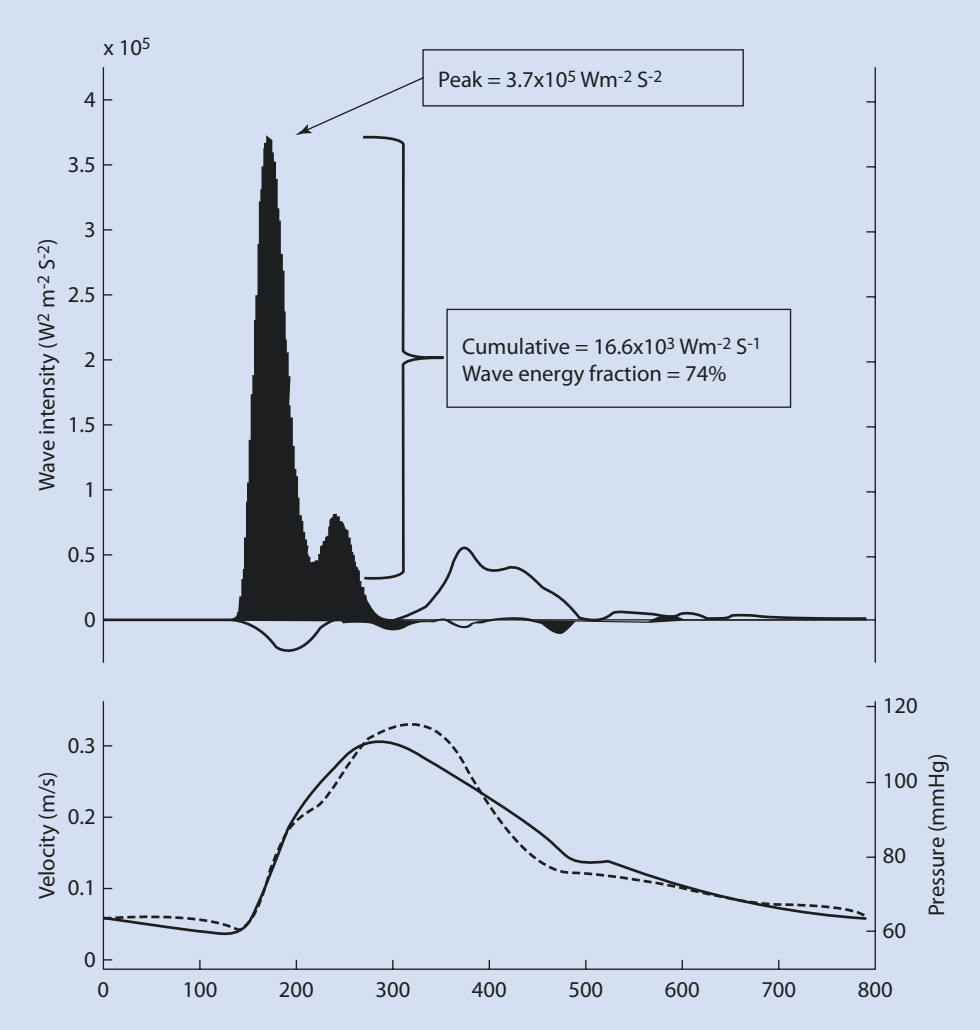


**Fig. 19.3** Measurements of wave intensity analysis: pressure, flow and separated wave intensity calculated from measurements in a human carotid artery. The three ways to express wave intensity are demonstrated. Peak is the largest value of a particular wave (units = $Wm^{-2}\ s^{-2}$). Cumulative wave intensity is calculated for each wave by measuring the area under the peak of wave intensity versus time curve (units = $Wm^{-2}\ s^{-1}$). Wave energy fraction is the cumulative intensity of an individual wave as a proportion of the total cumulative wave intensity over the cardiac cycle (units = %). Shaded waves are accelerative and non-shaded waves decelerative

Inspection of these results shows, because of the square term, $dI_+ > 0$ and $dI_- < 0$ which explains why wave intensity easily differentiates between forward and backward waves.

Another property of the separated wave intensity is that the forward and backward wave intensity sum to the net wave intensity, a useful result that is not immediately apparent.

$$\begin{aligned} I_+ + I_- &= \frac{1}{4\rho c}\left[\left(dP + \rho c\, dU\right)^2 - \left(dP - \rho c\, dU\right)^2\right] \\ &= \frac{1}{4\rho c}[\left(dP^2 + 2\rho c\, dP dU + \left(\rho c\, dU\right)^2\right) \\ &\qquad -\left(dP^2 - 2\rho c\, dP dU + \left(\rho c\, dU\right)^2\right)\} \\ &= dP dU = I \end{aligned}$$

From these derivations, we see that both the forward and backward wave intensities can easily be separated from the pressure and velocity measured in the cardiac catheterization laboratory.

Necessary for the calculation of wave intensity is knowledge of the wave speed. Given the inherent length of coronary arteries, a foot-to-foot approach to measuring the wave speed is not appropriate and an alternative means for deriving wave speed is required. An alternate method has been proposed and validated as well as it could be in the absence of an independent definitive measure of coronary artery wave speed. The derivation of the sum-of-squares method, which is beyond the scope of this book, yields the following formula (Fig. 19.3)

$$c = \frac{1}{\rho}\sqrt{\frac{\sum dP^2}{\sum dU^2}}$$

where the summations must be taken over the whole cardiac cycle.

Given the uncertainties in the estimation of $c$, it is important to note that the net wave intensity does not require any knowledge of $c$, depending directly on the measured $P$ and $U$, and so any diagnostic conclusions that can be drawn from the net wave intensity alone are more reliable. Quantitative calculation of the separated wave intensities, which can be particularly informative in the coronary arteries, does introduce an increased level of uncertainty into the analysis.

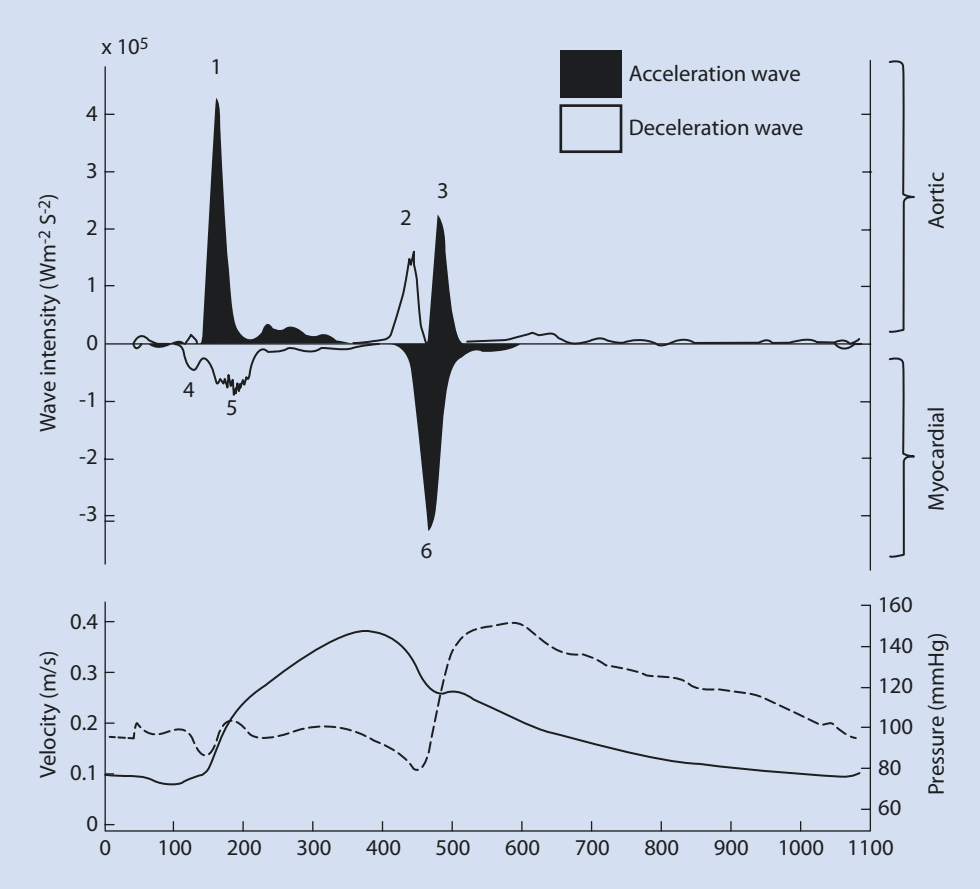


**Fig. 19.4** Coronary wave intensity profile. Six waves are usually evident in the coronary arteries. Three originate from the aortic end (*1–3*) and three originate from the myocardium (*4–6*). Each wave has either an accelerating (*1*, *3*, *6*) or decelerating (*2*, *4*, *5*) effect on coronary blood as indicated by the *black* and *white* shading

The wave intensity derived and calculated as above is defined throughout the cardiac cycle and the final step is to find clinically useful ways to characterize this function (see examples of clinically derived wave intensities Figures 1, 4, 5 and 6). The wave intensity is invariably characterized as a number of distinct peaks, each of which is interpreted as an individual wave. Six individual waves are identified in Fig. 19.4, which are common to all of our coronary artery results. Waves 1–3 are forward waves originating in the coronary sinuses and 4–6 are backward waves originating in the myocardium. These waves are either acceleration waves (1, 3, 6) or deceleration waves (2, 4, 5) as indicated by the shading. From the water hammer equations, or simply looking at the slope of the pressure at the time of the wave, we see that (1, 4, 5) are compressive waves and (2, 3, 6) are decompressive waves.

The wave intensity peaks can be expressed in three different but related ways: Firstly, the "peak wave intensity" is defined as the maximum value of the wave intensity, which has the units ($W/m^2$) and is a measure of the flux of energy carried by the wave. Second, the "cumulative wave intensity" is defined as the area under the wave intensity versus time curve. The cumulative wave intensity has units $J/m^2$ and is a measure of the energy of the wave and accounts for the duration of the wave as well as its peak value. Finally, the "wave energy fraction" is defined as the cumulative wave intensity for a particular wave divided by the integral of the wave intensity over the cardiac period. It is dimensionless and represents the fraction of the wave energy of a particular wave relative to the net wave energy generated throughout the cardiac cycle. The wave energy fraction can be useful to differentiate, for example, between changes due to a particular mechanism and changes due to an overall change of heart function.

## 19.3 Coronary Wave Intensity Analysis in Health

Through the above derivation, separated wave intensity can be calculated from simultaneously acquired pressure and velocity waveforms. These measurements are achieved through either individual pressure and velocity sensor wires or, more recently, combined pressure- and flow-sensor tipped wire (Fig. 19.5).

Initial work in patients with unobstructed coronary arteries demonstrated a repeating pattern of six waves per cardiac cycle evident in all major epicardial arteries [3]. Three waves originate proximally and three distally with variable compressing/decompressing and accelerating/decelerating effects (Fig. 19.4).

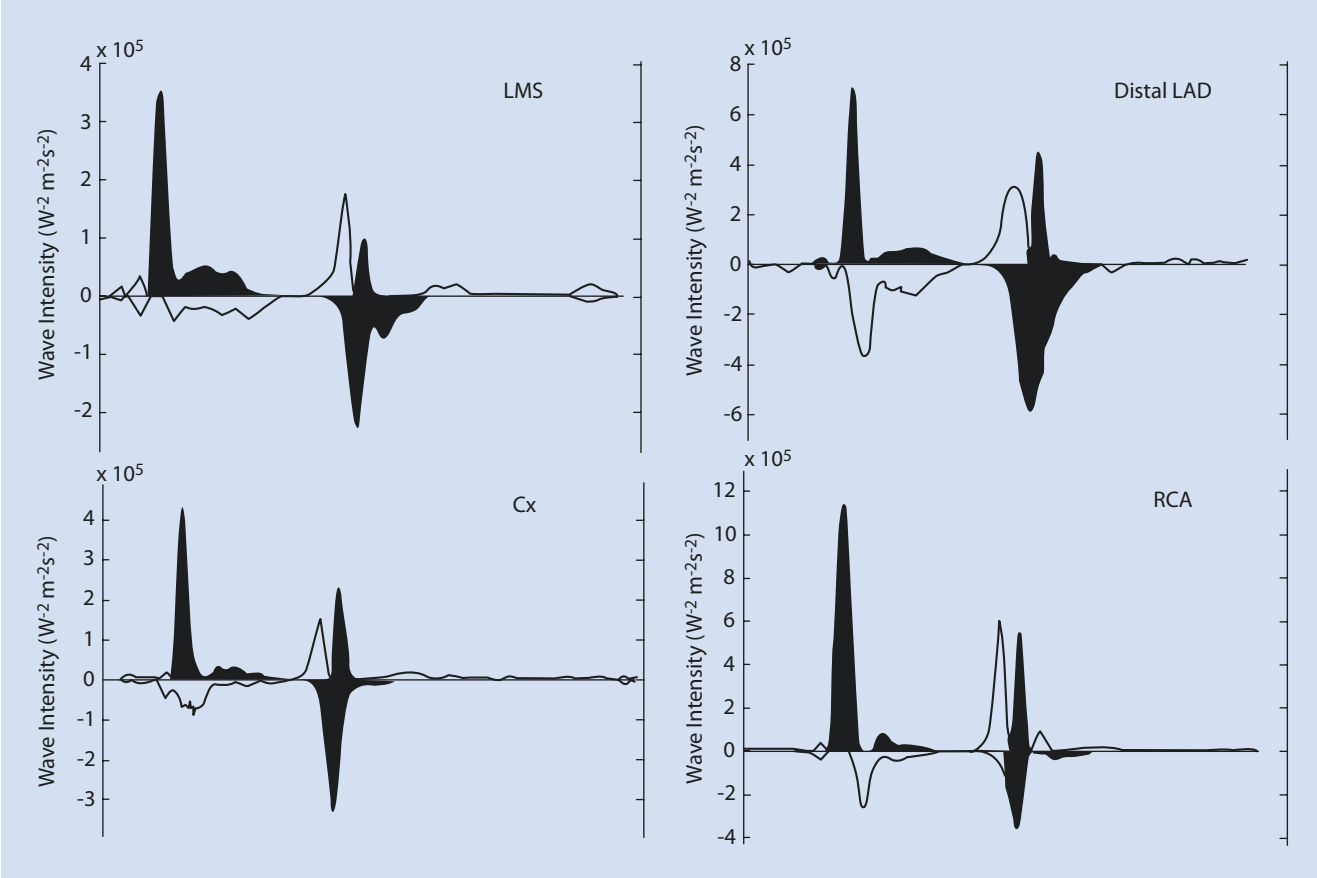


**Fig. 19.5** Wave intensity in the left main stem (*LMS*), distal left anterior descending (*LAD*), circumflex (*Cx*), and right coronary artery (*RCA*). Although the magnitude of the wave intensity profile varies, particularly in the right coronary artery, the pattern of six repeating waves is consistent (Note the different *y*-axis scales)

### 19.3.1 Proximally ("Aortic") Originating Waves

These waves originate from the aortic end of the coronary circulation and are conventionally described as "forward traveling".

### 19.3.2 Forward Compression Wave

Contraction of the left ventricle with an open aortic valve results in expulsion of blood into the proximal aorta and coronary sinuses. This generates a wave that originates in the left ventricle, is transmitted into the aorta, and thus down the coronary artery in an antegrade direction. This forward compressive wave results in an accelerative force.

### 19.3.3 Forward Decompression Wave

As systole concludes, the slowing of ventricular contraction creates a suction effect in the aorta at the proximal end of the coronary artery. This produces a forward decompressive wave causing a decelerating force.

### 19.3.4 Late Forward Compression Wave

With the transition to diastole, the aortic valve closes creating a short-lived proximal-to-distal compression wave during early diastole. This has an accelerative effect on blood flow.

### 19.3.5 Distally ("Myocardial") Originating Waves

These waves originate from the myocardial end of the coronary artery and are therefore "backward traveling".

### 19.3.6 Early Backward Compression Wave

In early systole, prior to the aortic valve opening, the period of isovolemic contraction results in compression of the intramyocardial blood vessels that generates a distal-to-proximal compression wave that has a decelerating effect.

### 19.3.7 Late Backward Compression Wave

A second distal-to-proximal compressive wave is generated in early systole by the continuing compression of the microcirculation. Additionally, as the forward compression wave meets bifurcation sites or compressed microvasculature, reflection of this wave occurs contributing to the late backward compression wave. The net effect is a distally originating compression wave again with a decelerating influence.

### 19.3.8 Backward Decompression Wave

The backward decompression wave (BDW) occurring at the end of systole is perhaps the most clinically relevant wave. It originates from the myocardium but is decompressive; therefore it causes an accelerative force to be applied to blood flow. This wave is created by the re-expansion of the compressed intramyocardial blood vessels. This wave has also been called a "suction" wave as it draws in blood from aorta akin to a dry sponge being squeezed and immersed in water before being released.

The two waves, which dominate in terms of magnitude, are the forward compression wave and the backward decompression wave – both cause an accelerative force to be applied to the coronary circulation. However, during systole this force has an attenuated effect on blood velocity due to the high myocardial pressure from ventricular contraction as well as the wave's own reflection from the distal vascular bed (Table 19.1).

## 19.4 Coronary Wave Intensity in Different Healthy Arteries

While the magnitude of the individual waves within each coronary artery is variable, the pattern of six waves is consistent (Fig. 19.4). Of note, the arteries subtending the left ventricle from the right coronary artery display different flow patterns with a higher systolic:diastolic flow ratio. A smaller BDW is seen in the right coronary artery accounting for the lower diastolic velocity rates. This is due to the right ventricle having lower peak cavity pressures and the resultant diastolic relaxation (and thus the myocardial "suction" force) is less.

## 19.5 Coronary Wave Intensity Analysis in Disease

Coronary wave intensity analysis has been applied to a number of disease states. The most informative wave in this setting has proven to be the BDW. As outlined above, this is caused by the re-expansion of the intramyocardial blood vessels, which are compressed by ventricular contraction during systole. This compression reduces the volume of blood within them, giving rise to the backward compressive wave, and simultaneously increases their resistance to flow significantly. This increased resistance is, in part, responsible for the failure of the forward compression wave to cause a significant increase in coronary flow velocity (similar to a car driver trying to accelerate by simultaneously pressing both the accelerator and brake pedals). However, once myocardial relaxation begins this "brake" is removed and the forces acting on blood velocity are much less opposed. Therefore, as this network of vessels reopens, driven in part by the expanding myocardial fibers and in part through their elastic recoil, a proximal-to-distal pressure ("decompression") gradient is created resulting in an accelerative force and an increase in coronary velocity.

Conceptually, several processes could affect this wave. First, relaxation of an increased ventricular force should cause a larger "suction" effect from the myocardium resulting in a larger BDW. Second, if the interrogated artery had an increased density of subtended vessels the BDW would also increase. Third, the efficiency with which the intramyocardial vessels themselves re-expand will also govern the relative magnitude of the BDW. Fourth, the efficiency with which the ventricle relaxes will also have an important effect on the BDW. Changes in the BDW have been observed in a variety of pathological states, which can be explained through one or more of these processes (Fig. 19.6).

## 19.6 Left Ventricular Hypertrophy

Previous large-scale retrospective and prospective studies have demonstrated the unfavorable independent effect of left ventricular hypertrophy (LVH) on prognosis [4–6]. For every increment of 50 g/m height in LV mass the relative risk of cardiovascular disease increases approximately 1.5-fold,



**Table 19.1** Nomenclature for the potential waves that may travel within the coronary circulation and their origin, effect of pressure, and velocity

| Wave | Origin | Pressure effect | Resultant effect on velocity |
|---|---|---|---|
| Forward compression | Aorta | Increase | Acceleration |
| Forward decompression | Aorta | Decrease | Deceleration |
| Backward compression | Intramyocardial blood vessels | Increase | Deceleration |
| Backward decompression | Intramyocardial blood vessels | Decrease | Acceleration |

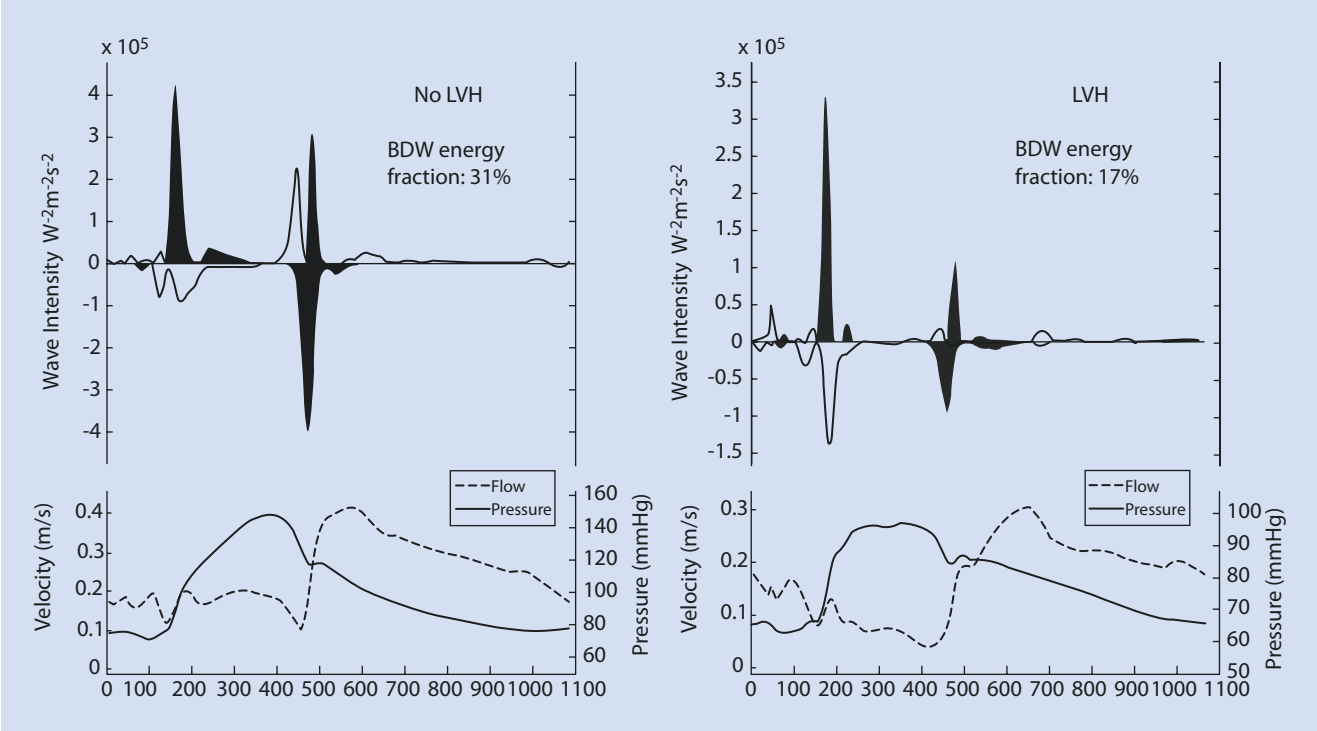


**Fig. 19.6** Example of wave intensity profile in individuals with no left ventricular hypertrophy (*left*) and with left ventricular hypertrophy (*right*). With increasing left ventricular hypertrophy there is a decrease in the BDW energy fraction. Additionally, the exchange of energy between the forward compression wave and BDW becomes less effective (*BDW* backward decompression wave; *LVH* left ventricular hypertrophy)

independent from any blood pressure effect [7], possibly leading to the development of heart failure [8, 9].

At a structural level, myocardial hypertrophy leads to a distortion of myocardial architecture with additional development of fibrotic changes over time [10]; this disorganization can be appreciated using conventional coronary physiology. Animal models have demonstrated that the induction of LVH has a negative effect on coronary flow reserve, largely driven by an attenuated and recovered hyperemic response [11–13], whereas regression of LVH has a positive effect. Similarly, pharmacological treatment of spontaneously hypertensive animal models can improve coronary flow reserve along with an appreciable regression of left ventricular hypertrophy [14, 15]. Equivalent results have also been seen in humans where pharmacological treatment can improve CFR [16] such that an 8 % reduction in LV mass is associated with a 43 % increase in coronary flow reserve [17].

Wave intensity has allowed an even more detailed insight into this pathophysiological state [3]. In patients with unobstructed arteries and no evidence of alular disease, obvious changes are recognizable in the wave intensity profile with increasing left ventricular wall thickness. Particularly a decrease in the BDW energy fraction is noted. There is also a reduction in the ratio of the forward compression wave to the backward decompression wave highlighting a reduced transfer of energy between the two.

Importantly, this disease also gives us a first glimpse of the relative sensitivity of wave intensity analysis where abnormalities in its profile are recognizable without induction of hyperemia. One can imagine that with exercise or pharmacological stimulus this disruption becomes magnified to the point where coronary flow velocity abnormalities are appreciable.

## 19.7 Aortic Stenosis

Aortic stenosis is also associated with left ventricular hypertrophy. However, in contrast to nonalular left ventricular hypertrophy there is also a marked coexisting outflow tract gradient. In fact, the development of hypertrophy in this condition is related to the degree of systolic outflow pressure [18] and is considered one of the most important mechanisms in adapting to the hemodynamic overload of aortic stenosis [19] according to Laplace's law [20]:

$$\text{Wall stress} = \text{Pressure} \times \text{Radius} / \text{Thickness}$$

Physiological dysfunction has been demonstrated in a variety of ways over the last 50 years in aortic stenosis, including through measurement of the levels of lactic acid production [21], thallium scans [22], ST segment shift on 24-h Holter monitors [23], CFR [24], myocardial contrast echocardiography [25], stress echocardiography [26], and PET scanning [27]. However, despite this wealth of information it remains difficult to tease out the relative contributions

of myocardial hypertrophy and the stenotic pressure to this pathophysiology, which is where wave intensity analysis is able to shed some light.

The first striking finding in severe aortic stenosis is the dramatically increased BDW (both cumulative and peak). This relates to the increased systolic ventricular contractive force required to expel blood through a significant outflow tract obstruction. When the stenotic valve closes and diastole commences, the myocardium relaxes with a similarly increased magnitude. There is, therefore, a larger decompressive force generated distally and the proximal-to-distal pressure gradient is more marked. This effect swiftly reverses following interventional treatment of aortic stenosis.

The ability to pace a heart with aortic stenosis and/or hypertrophy for research purposes has been explored in animal models (where abnormalities in blood flow have been demonstrated [28]) and historic studies in humans (reproducing symptoms of angina [29]). However, by using the clinically necessary pacing wire in patients undergoing transcutaneous aortic valve implantation (TAVI), a more modern slant on this approach is feasible. Prior to replacement of the valve, with pacing at successive increments in heart rate, a progressive decrease in the BDW is seen in untreated severe aortic stenosis (Fig. 19.7). This is reversed after TAVI returning to what is felt to be the physiological norm [30, 31]. It has been proposed that this reflects a "decoupling" of the normal ventricular-coronary mechanisms essential for maintaining normal coronary perfusion. It is also possible to suggest that this now recognizable decoupling is the process through which angina occurs in patients with aortic stenosis and why there is an instantaneous reduction in mortality following aortic valve replacement [3].

## 19.8 Heart Failure and Resynchronization Therapy

While the effect of resynchronization in patients with heart failure and a left bundle branch block (LBBB) are well documented in terms of symptom and prognostic improvements, the effect on coronary physiology is not so well studied. Both invasive catheter studies and PET scanning techniques have failed to show a marked change in coronary flow rates at rest. However, as illustrated above, wave intensity has the sensitivity to look beyond resting flow rates and demonstrate more subtle changes. Additionally, with advances in biventricular pacemaker optimization it is possible to measure wave intensity at different "degrees" of atrio-ventricular (AV) optimization at identical heart rates.

Using this approach, an obvious change in the wave intensity profile has been noted with different pacing protocols [32]. The BDW increases with AV optimization producing an increased coronary velocity time integral. Additionally, in a suboptimally paced heart no demonstrable differences in the BDW are noted when compared with an unpaced heart (Fig. 19.8). In heart failure, therefore, wave intensity analysis informs us that:

1. Ventricular-ventricular coordination is important in improving coronary hemodynamics by ensuring that all parts of the myocardium relax, as well as contract, simultaneously.
2. Atrio-ventricular coordination is as important, ensuring adequate ventricular filling and thus optimum LV contraction and relaxation.

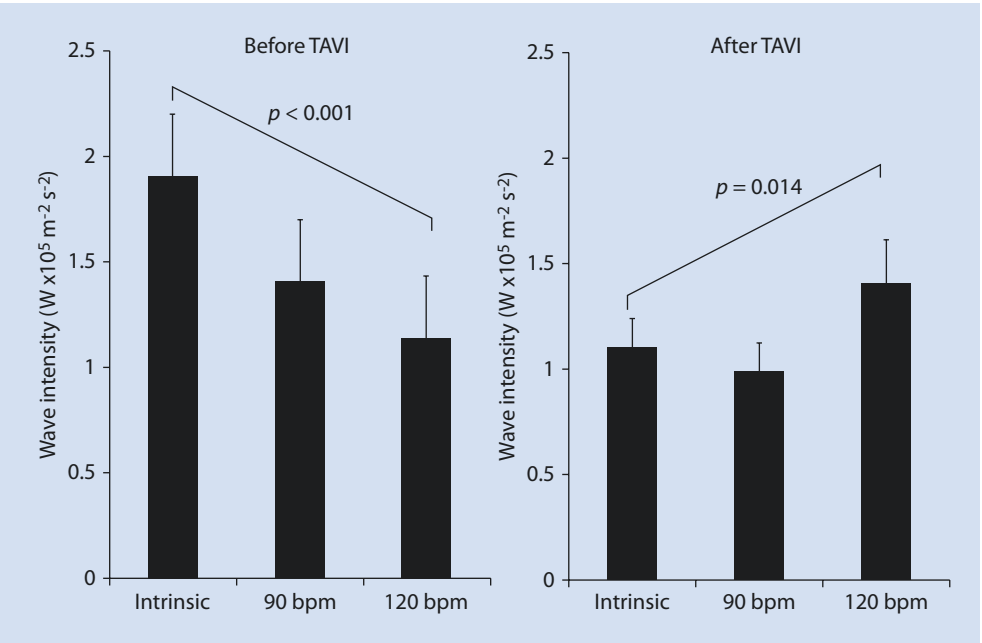


**Fig. 19.7** The peak backward decompression wave in response to successive pacing before and after transcatheter aortic valve replacement (*TAVI*). In the presence of severe aortic stenosis a decline is seen the backward decompression wave in response to pacing. This reverses and returns to the physiological norm following transcatheter valve implantation (Reproduced with permission from Davies et al. [39])

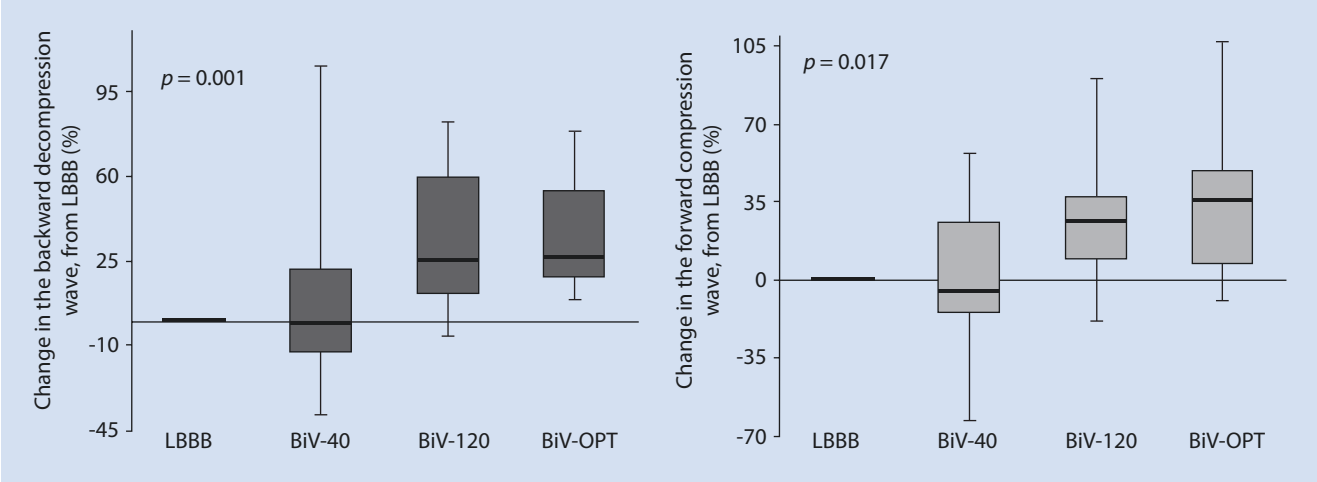


**Fig. 19.8** Changes in the backward decompression wave (*left*) and forward compression wave (*right*) from left bundles branch block (*LBBB*) with 40 ms AV delay (*BiV-40*), 120 ms AV delay (*BiV 120*), and optimized AV delay (*BiV-OPT*). Both the forward compression and backward decompression waves are significantly increased at BiV-Opt ($p = 0.022$ and $p = 0.005$, respectively) in comparison with LBBB. The intensities of the waves at BiV-40 were not different from LBBB ($p = 0.386$ and $p = 0.799$, respectively) (Reproduced with permission from Kyriacou et al. [32])

## 19.9 Warm-Up Angina

The phenomenon of warm-up angina has interested scientists for 50 years. It was first recognized as an increased exercise tolerance after inducing a bout of exercise-induced angina on treadmill testing [33] and furthered by documentation of reduced electrocardiographic evidence of ischemia in this setting [34]. At the time, invasive studies were undertaken but failed to reach a conclusion due to the relative crudity of the available techniques.

Wave intensity has now been applied to this phenomenon. In an elegant series of experiments, wave intensity analysis performed distal to a coronary lesion during two successive periods of exertion has shown a relative increase in the BDW with the second phase [31]. It appears that this "preconditioning" of the heart results in an improved cardiac–coronary interaction resulting in this improved performance. This feature interacts with other favorable "warm-up" cardiovascular changes including a reduction in central aortic pressure augmentation and reduced coronary microvascular resistance resulting in a summative or even synergistic effect.

## 19.10 Myocardial Infarction and Functional Recovery

While coronary revascularization following acute myocardial ischemia is the "corner stone" of modern cardiology treatment, significant numbers of patients go on to develop myocardial cell infarction despite optimal interventional and pharmacological therapy. The integrity of the microvasculature is a key determinant of myocardial viability and tissue perfusion as demonstrated with PET [35] or myocardial contrast echocardiography [36]. Additionally, a number of unusual patterns of coronary flow have been acknowledged as potential markers for microvascular dysfunction [37, 38]. This stimulated the use of wave intensity analysis to explore this field and examine for different predictive markers of outcome.

First, it is interesting to note that the peri-infarct BDW magnitude is inversely correlated with both biochemical and MRI markers of infarct severity in the infarct related, but not in the reference, vessel. There is also a reasonable correlation between the forward compression wave and ejection fraction but not the BDW perhaps implying a relative inefficiency in energy exchange between these two similar to that seen in left ventricular hypertrophy. The backward compression wave appropriately was also related to left ventricular function.

Recovery of left ventricular function can be assessed by measuring improvements in wall thickening over a period of months and in fact correlates well with BDW values measured at the time of percutaneous treatment. Therefore, wave intensity analysis measured at the time of infarction is both a marker of infarct size and also conveys information on myocardial integrity, an important predictor of functional recovery.

## 19.11 Conclusion

Coronary wave intensity analysis has emerged as a powerful tool to investigate the coronary system and particularly in the distal intramyocardial blood vessels. It is able to recognize subtle abnormalities in resting coronary physiology that are imperceptible through simple velocity or pressure measures and that can otherwise only be unmasked with an appropriate hemodynamic stimulus. While the magnitude of waves

varies in both health and disease, the six waves identified in Fig. 4 are almost always evident, providing temporal information on the cardiac cycle.

While initially a research tool, wave intensity has now provided important mechanistic insights into a group of heterogeneous conditions all of which could be ultimately implemented clinically. Additionally, recognition of the waves (and thus wave-free periods) of the cardiac cycle has led to the development of the instantaneous wave-free ratio (iFR) as discussed elsewhere in this book.

With improvements in technology, it is possible that coronary wave intensity could be moved out of the invasive catheter laboratory environment and into the noninvasive domain. This will allow larger studies to be undertaken perhaps with sequential follow-up in patients enhancing the applicability of techniques. Ultimately, it may be used for prognostication in a variety of conditions including hypertension, HCM, aortic stenosis, and heart failure.

## References


1. Parker KH. An introduction to wave intensity analysis. Med Biol Eng Comput. 2009;47:175–88.
2. Davies JE, Whinnett ZI, Francis DP, Willson K, Foale RA, Malik IS, Hughes AD, Parker KH, Mayet J. Use of simultaneous pressure and velocity measurements to estimate arterial wave speed at a single site in humans. Am J Physiol –Heart Circ Physiol. 2006;290:H878–85.
3. Davies JE, Whinnett ZI, Francis DP, Manisty CH, Aguado-Sierra J, Willson K, Foale RA, Malik IS, Hughes AD, Parker KH, Mayet J. Evidence of a dominant backward-propagating "suction" wave responsible for diastolic coronary filling in humans, attenuated in left ventricular hypertrophy. Circulation. 2006;113:1768–78.
4. Levy D, Garrison RJ, Savage DD, Kannel WB, Castelli WP. Prognostic implications of echocardiographically determined left ventricular mass in the framingham heart study. N Engl J Med. 1990;322:1561–6.
5. Haider AW, Larson MG, Benjamin EJ, Levy D. Increased left ventricular mass and hypertrophy are associated with increased risk for sudden death. J Am Coll Cardiol. 1998;32:1454–9.
6. Levy D, Garrison RJ, Savage DD, Kannel WB, Castelli WP. Left ventricular mass and incidence of coronary heart disease in an elderly cohort. The framingham heart study. Ann Intern Med. 1989;110:101–7.
7. Koren MJ, Devereux RB, Casale PN, Savage DD, Laragh JH. Relation of left ventricular mass and geometry to morbidity and mortality in uncomplicated essential hypertension. Ann Intern Med. 1991;114:345–52.
8. Drazner MH, Rame JE, Marino EK, Gottdiener JS, Kitzman DW, Gardin JM, Manolio TA, Dries DL, Siscovick DS. Increased left ventricular mass is a risk factor for the development of a depressed left ventricular ejection fraction within five years: the cardiovascular health study. J Am Coll Cardiol. 2004;43:2207–15.
9. Gardin JM, McClelland R, Kitzman D, Lima JA, Bommer W, Klopfenstein HS, Wong ND, Smith VE, Gottdiener J. M-mode echocardiographic predictors of six- to seven-year incidence of coronary heart disease, stroke, congestive heart failure, and mortality in an elderly cohort (the cardiovascular health study). Am J Cardiol. 2001;87:1051–7.
10. Schwartzkopff B, Frenzel H, Diekerhoff J, Betz P, Flasshove M, Schulte HD, Mundhenke M, Motz W, Strauer BE. Morphometric investigation of human myocardium in arterial hypertension and valvular aortic stenosis. Eur Heart J. 1992;13:17–23.
11. Sato F, Isoyama S, Takishima T. Normalization of impaired coronary circulation in hypertrophied rat hearts. Hypertension. 1990;16:26–34.
12. Kingsbury M, Mahnke A, Turner M, Sheridan D. Recovery of coronary function and morphology during regression of left ventricular hypertrophy. Cardiovasc Res. 2002;55:83–96.
13. Wicker P, Tarazi RC, Kobayashi K. Coronary blood flow during the development and regression of left ventricular hypertrophy in renovascular hypertensive rats. Am J Cardiol. 1983;51:1744–9.
14. Nunez E, Hosoya K, Susic D, Frohlich ED. Enalapril and losartan reduced cardiac mass and improved coronary hemodynamics in shr. Hypertension. 1997;29:519–24.
15. Brilla CG, Janicki JS, Weber KT. Cardioreparative effects of lisinopril in rats with genetic hypertension and left ventricular hypertrophy. Circulation. 1991;83:1771–9.
16. Xu R, Zhang Y, Zhang M, Ge ZM, Li XC, Zhang W. relationship between regression of hypertensive left ventricular hypertrophy and improvement of coronary flow reserve. Zhonghua yi xue za zhi. 2003;83:658–61.
17. Motz W, Strauer BE. Improvement of coronary flow reserve after long-term therapy with enalapril. Hypertension. 1996;27:1031–8.
18. Gaasch WH. Left ventricular radius to wall thickness ratio. Am J Cardiol. 1979;43:1189–94.
19. Grossman W, Jones D, McLaurin LP. Wall stress and patterns of hypertrophy in the human left ventricle. J Clin Invest. 1975;56:56–64.
20. Gould KL, Carabello BA. Why angina in aortic stenosis with normal coronary arteriograms? Circulation. 2003;107:3121–3.
21. Fallen EL, Elliott WC, Gorlin RICH. Mechanisms of angina in aortic stenosis. Circulation. 1967;36:480–8.
22. Kupari M, Virtanen KS, Turto H, Viitasalo M, Mänttäri M, Lindroos M, Koskela E, Leinonen H, Pohjola-Sintonen S, Heikkilä J. Exclusion of coronary artery disease by exercise thallium-201 tomography in patients with aortic valve stenosis. Am J Cardiol. 1992;70:635–40.
23. Scheler S, Motz W, Strauer BE. Transient myocardial ischaemia in hypertensives: Missing link with left ventricular hypertrophy. Eur Heart J. 1992;13:62–5.
24. Marcus ML, Doty DB, Hiratzka LF, Wright CB, Eastham CL. Decreased coronary reserve – a mechanism for angina pectoris in patients with aortic stenosis and normal coronary arteries. N Engl J Med. 1982;307:1362–6.
25. Galiuto L, Lotrionte M, Crea F, Anselmi A, Biondi-Zoccai GGL, De Giorgio F, Baldi A, Baldi F, Possati G, Gaudino M, Vetrovec GW, Abbate A. Impaired coronary and myocardial flow in severe aortic stenosis is associated with increased apoptosis: a transthoracic doppler and myocardial contrast echocardiography study. Heart. 2006;92:208–12.
26. Hildick-Smith DJR, Shapiro LM. Coronary flow reserve improves after aortic valve replacement for aortic stenosis: an adenosine transthoracic echocardiography study. J Am Coll Cardiol. 2000;36:1889–96.
27. Vinten-Johansen J, Weiss HR. Oxygen consumption in subepicardial and subendocardial regions of the canine left ventricle. The effect of experimental acute valvular aortic stenosis. Circ Res. 1980;46:139–45.
28. Bache RJ, Vrobel TR, Ring WS, Emery RW, Andersen RW. Regional myocardial blood flow during exercise in dogs with chronic left ventricular hypertrophy. Circ Res. 1981;48:76–87.
29. Fifer MA, Bourdillon PD, Lorell BH. Altered left ventricular diastolic properties during pacing-induced angina in patients with aortic stenosis. Circulation. 1986;74:675–83.
30. Sun YH, Anderson TJ, Parker KH, Tyberg JV. Wave-intensity analysis: a new approach to coronary hemodynamics. J Appl Physiol. 2000;89:1636–44.
31. Lockie TP, Rolandi MC, Guilcher A, Perera D, De Silva K, Williams R, Asrress KN, Patel K, Plein S, Chowienczyk P, Siebes M, Redwood SR, Marber MS. Synergistic adaptations to exercise in the systemic and coronary circulations that underlie the warm-up angina phenomenon. Circulation. 2012;126:2565–74.
32. Kyriacou A, Whinnett ZI, Sen S, Pabari PA, Wright I, Cornelussen R, Lefroy D, Davies DW, Peters NS, Kanagaratnam P, Mayet J, Hughes AD, Francis DP, Davies JE. Improvement in coronary blood flow

velocity with acute biventricular pacing is predominantly due to an increase in a diastolic backward-travelling decompression (suction) wave. Circulation. 2012;126:1334–44.
33. Macalpin RN, Kattus AA. Adaptation to exercise in angina pectoris: the electrocardiogram during treadmill walking and coronary angiographic findings. Circulation. 1966;33:183–201.
34. Jaffe MD, Quinn NK. Warm-up phenomenon in angina pectoris. Lancet. 1980;2:934–6.
35. Maes A, Van de Werf F, Nuyts J, Bormans G, Desmet W, Mortelmans L. Impaired myocardial tissue perfusion early after successful thrombolysis: impact on myocardial flow, metabolism, and function at late follow-up. Circulation. 1995;92:2072–8.
36. Iliceto S, Galiuto L, Marchese A, Colonna P, Oliva S, Rizzon P. Functional role of microvascular integrity in patients with infarct-related artery patency after acute myocardial infarction. Eur Heart J. 1997;18(4):618–24.
37. Furber AP, Prunier F, Nguyen HCP, Boulet S, Delépine S, Geslin P. Coronary blood flow assessment after successful angioplasty for acute myocardial infarction predicts the risk of long-term cardiac events. Circulation. 2004;110:3527–33.
38. Kawamoto T, Yoshida K, Akasaka T, Hozumi T, Takagi T, Kaji S, Ueda Y. Can coronary blood flow velocity pattern after primary percutaneous transluminal coronary angiography predict recovery of regional left ventricular function in patients with acute myocardial infarction? Circulation. 1999;100:339–45.
39. Davies JE, Sen S, Broyd C, Hadjiloizou N, Baksi J, Francis DP, Foale RA, Parker KH, Hughes AD, Chukwuemeka A, Casula R, Malik IS, Mikhail GW, Mayet J. Arterial pulse wave dynamics after percutaneous aortic valve replacement / clinical perspective. Circulation. 2011;124:1565–72.

# Assessment of Endothelial Dysfunction

Contents

# Coronary Vasomotor Responses to Intracoronary Acetylcholine

*Peter Ong and Udo Sechtem*



The authors declare that no conflict of interest exists in conjunction with the preparation of this chapter.


J. Escaned, J. Davies (eds.), *Physiological Assessment of Coronary Stenoses and the Microcirculation*,
DOI 10.1007/978-1-4471-5245-3_20

1) Pharmaceutical product: Miochol-E© (Bausch&Lomb) = 20mg acetylcholine chloride (powder) and 2ml solvent

2) Preparation

**Important: Prepare ACH-solutions only immediately before application (solution not usable for more than 2 hours after preparation!)**

a) Mix 20mg acetylcholine + 2ml solvent + 98ml NaCl 0,9% (=0,2 mg/ml)

→ this is stock solution 1

b) Mix 9ml of stock solution 1 + 91ml NaCl 0, 9% (=18µg/ml)

→ this is stock solution 2

**c) Label 3 perfusion syringes (each of 50ml) with„high", „medium" and „low":**

- Perfusion syringe 1 „high" = „ACH $10^{-5}$" (high dose):

→ 40ml of stock solution II (=18µg/ml)

- Perfusion syringe 2 „medium"= „ACH $10^{-6}$" (medium dose):

→ 8ml perfusion syringe 1 + 32ml NaCl 0,9% (=3,6µg/ml)

- Perfusion syringe „low", „ACH $10^{-7}$" (low dose):

→ 4ml perfusion syringe 2 + 36ml NaCl 0,9% (=0,36µg/ml)

**Fig. 20.1** Preparation protocol for acetylcholine provocation test

## 20.1 Introduction

Coronary artery disease is a dynamic process with structural as well as functional vascular alterations affecting the whole coronary tree including the coronary microcirculation. The structural alterations of the epicardial arteries can be examined by visualization of the vessels using invasive or noninvasive coronary angiography. However, the functional alterations are more difficult to detect especially when the coronary microcirculation is involved. Clinically, patients seek medical attention because of various forms of chest discomfort occurring at rest or effort or both, with different locations and characters (e.g., burning, squeezing, etc.). However, the clinical presentation alone does not allow the clinician to predict the underlying (coronary) pathology. Indeed, studies have shown that despite signs and symptoms of myocardial ischemia up to 60 % of patients do not have any relevant epicardial stenosis upon diagnostic coronary angiography [1]. Moreover, functional coronary vasomotor abnormalities such as epicardial or microvascular spasm have been shown to be present especially in patients with angina pectoris and unobstructed coronary arteries [2]. One established method to assess these functional disorders is intracoronary acetylcholine provocation testing. It can be useful in various clinical scenarios and some are described in more detail in this chapter.

## 20.2 Intracoronary Acetylcholine Provocation Testing

Acetylcholine is a neurotransmitter of the parasympathetic nervous system. However, muscarinic acetylcholine receptors are also expressed in the endothelium as well as the vascular smooth muscle layer of the coronary arteries. When binding to the endothelium, acetylcholine induces a nitric oxide dependent vasodilatation, whereas binding with receptors in the vascular smooth muscle layer induces vasoconstriction [3]. Depending on the integrity of the endothelium the net effect is a slight vasodilatation as described in individuals without angina and without coronary stenoses [4] or marked vasoconstriction and spasm as in patients with vasospastic angina.

After introduction of acetylcholine provocation testing in the 1980s [5], the test was widely used for the assessment of coronary artery spasm. However, after introduction of percutaneous coronary intervention in 1986 the interest in functional coronary vasomotor disorders declined considerably at least in Europe and the United States. Still today, acetylcholine testing has a class IIa recommendation by the European Society of Cardiology Guidelines for stable coronary artery disease for the detection of coronary spasm in patients with angina and unobstructed coronary arteries [6].

Preparation of acetylcholine solutions for intracoronary injection is easy and catheterization laboratory staff can be trained to prepare the solutions in short time. Usually, commercially available Miochol-E is used for preparation of the intracoronary ACH solutions as it can be purchased from the pharmacy. The protocol for preparation of ACH solutions is shown in Fig. 20.1. Of note, once prepared, the solutions should be used within 2 h and then discarded or newly prepared for the next patient. Details regarding the preparation of the acetylcholine solutions can be found elsewhere [7].

## 20.3 Intracoronary Injection of Acetylcholine

Acetylcholine injection is performed via the diagnostic coronary catheter. We always commence with the LCA-catheter as two vessels can be challenged at the same time. It is of

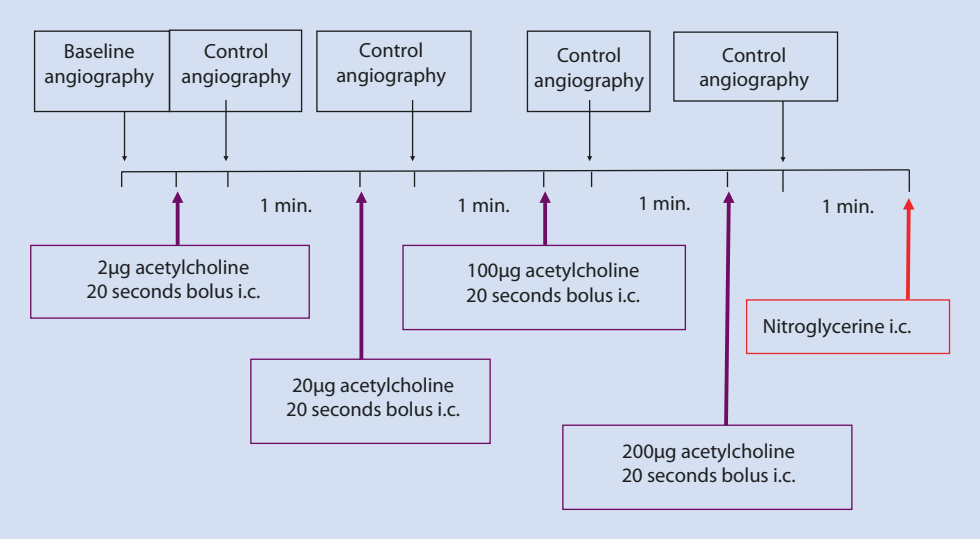


**Fig. 20.2** Acetylcholine provocation protocol for the left coronary artery

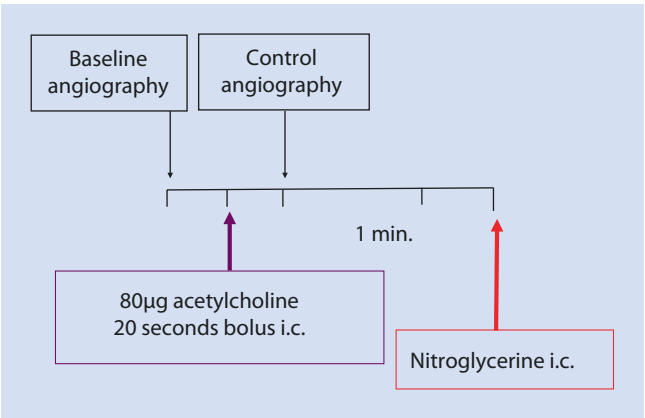


**Fig. 20.3** Acetylcholine provocation protocol for the right coronary artery

utmost importance to follow a stepwise approach with increasing dosages starting at 2 µg (and then increasing to 20, 100, and 200 µg as the maximum dose for the LCA) as some patients may develop severe coronary spasm at the lower dosages. If assessment of the LCA is uneventful, the RCA should be challenged with 80 µg. The injection period and time frames are shown in Figs. 20.2 and 20.3. Usually the manual injection should be performed over a period of 20 s. It is important to have a continuous 12-lead ECG registration throughout the test and the patient should be asked about any symptoms occurring after completion of every dose of ACH. In case of severe angina or ischemic ECG shifts nitroglycerine is injected into the respective vessel (standard dose is 200 µg) following angiographic documentation of coronary vasospasm. This almost always reverts the pathologic findings. Sometimes a second dose of nitroglycerine is necessary. In the rare case of refractory spasm, atropine (e.g., 1 mg intravenously) should be given as this is the direct antagonist of acetylcholine. The most frequent side effect of intracoronary acetylcholine injection is bradycardia. Thus, some centers prefer to have a temporary pacemaker inserted into the right ventricle before the ACH-test is started. It should, however, be mentioned that duration of bradycardia is only short when the speed of the manual injection is slowed down.

## 20.4 Definition of Acetylcholine Testing Results

Epicardial coronary spasm: Focal or diffuse epicardial vasoconstriction ≥90 % in comparison to the relaxed state after intracoronary nitroglycerine administration together with ischemic ECG shifts and reproduction of the patient's symptoms.

Microvascular spasm: Reproduction of the patient's symptoms together with ischemic ECG shifts (usually ST-segment depression) without epicardial vasoconstriction ≥90 % (Fig. 20.4). A more detailed description of the acetylcholine test can be found elsewhere [8].

## 20.5 Clinical Scenarios Where ACH-Testing Can Be Helpful

### 20.5.1 ACH-Testing as a Spasm Test

The clinical suspicion that coronary spasm may be the cause of the patient's symptoms is of great importance. The most frequent clinical presentation is angina pectoris at rest (often with a preserved exercise capacity) and smoking has been shown to be an important risk factor for epicardial spasm [2]. Coronary angiography is recommended in such patients to determine the degree of underlying epicardial coronary artery disease. Moreover, acetylcholine provocation testing should be performed to determine the site and mode of spasm. Focal spasm (i.e., ≥90 % vasoconstriction in one isolated coronary segment, usually complete occlusion) with transient ST-segment elevation and reproduction of angina is one form of vasospastic angina that is called Prinzmetal's variant angina. However, studies on Caucasian patients have shown that distal and diffuse spasm

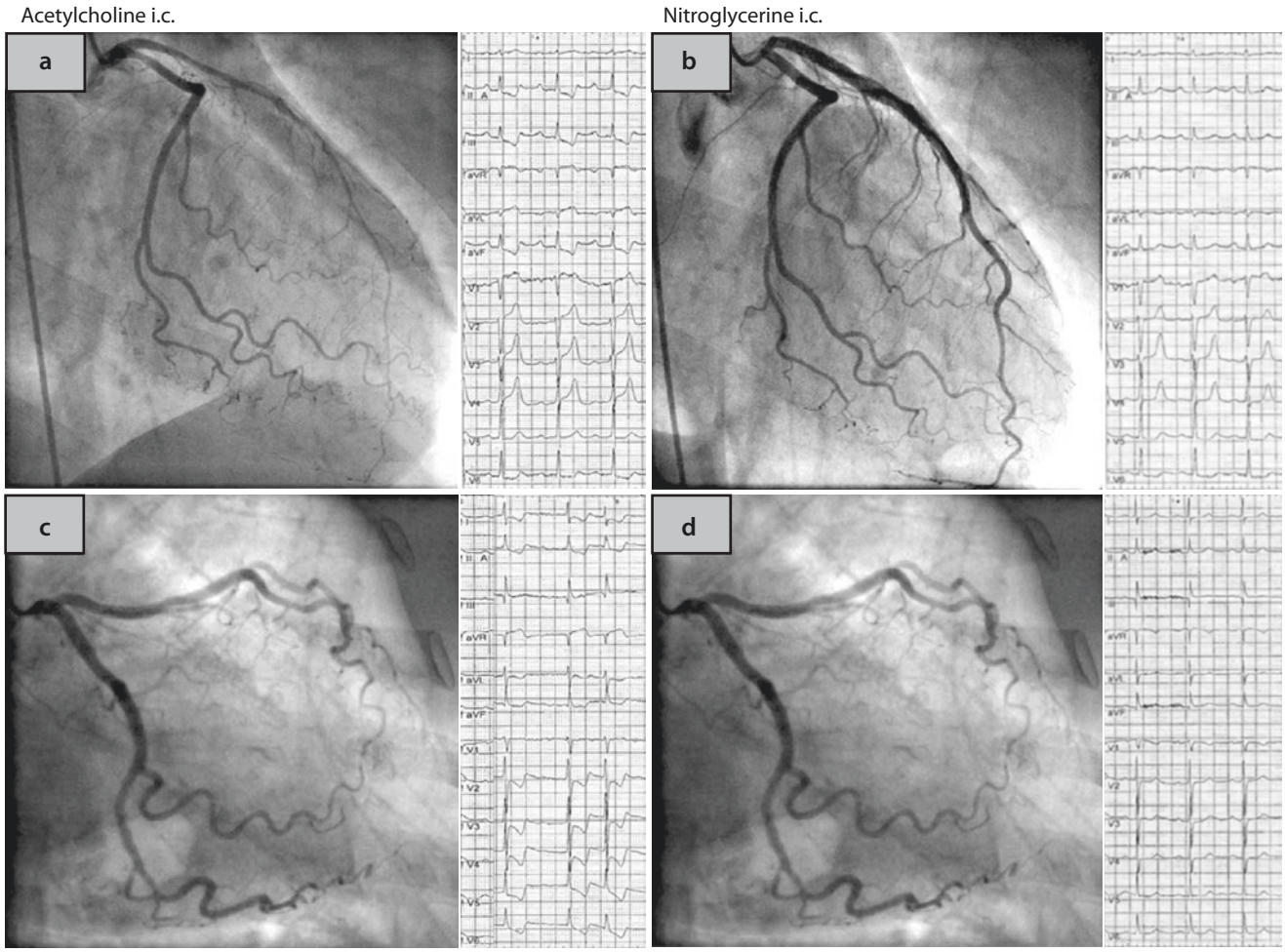


**Fig. 20.4** The upper panels show left coronary artery angiograms and electrocardiograms (ECGs) in a patient with epicardial spasm. Note the diffuse but distally accentuated narrowing of the left anterior descending coronary artery (wraps around the apex) during acetylcholine infusion together with ischemic ECG shifts in the precordial and inferior leads (**a**) and resolution of both findings after intracoronary nitroglycerin (**b**). The lower panels show an example of a patient with microvascular spasm. During acetylcholine infusion the patient had reproduction of chest pain and ischemic ECG changes but no epicardial vasoconstriction (**c**). After intracoronary nitroglycerin, chest pain and ECG changes resolved (**d**) (With permission from *J Am Coll Cardiol*. 2012;59:655–62.) Will send permission in a separate email.

usually with ST-segment depression on the ECG in response to acetylcholine is by far the most frequent finding [9]. The distinction between focal and diffuse epicardial coronary artery spasm is important as the type of spasm has been shown to carry prognostic relevance. In an Asian study, Sato et al. found that patients with focal spasm had a worse prognosis compared to patients with diffuse spasm [10].

20

### 20.5.2 ACH-Testing as a Test for the Coronary Microcirculation

Acetylcholine provocation testing can also detect abnormal coronary vasomotion of the coronary microcirculation. Frequently acetylcholine testing showed no epicardial spasm but patients reported reproduction of their usual symptoms and the simultaneously recorded 12-lead ECG showed ischemic shifts. Thus coronary microvascular spasm was assumed to be the pathophysiologic correlate [11]. Recent studies have shown that microvascular spasm can be found in ~ 30 % of patients with angina and unobstructed coronary arteries [2]. Clinically there may be patients with resting angina in whom the ACH-test reveals coronary microvascular spasm. However, there are also patients with pure effort-induced angina in whom the acetylcholine test reveals microvascular "spasm". Whether microvascular "spasm" is the cause for the effort-induced angina in everyday life still needs to be determined but it is also plausible that the abnormal ACH-test is a marker for a more general dysfunction of the coronary microcirculation with impaired vasodilatation as the main mechanism for effort angina [12, 13].

### 20.5.3 ACH-Testing in the Presence of Coronary Stenoses

In patients with epicardial coronary atherosclerosis ACH-testing may indicate the site of future development of epicardial stenoses [14]. However, this has not been consistently

shown. Another interesting aspect is the presence of coronary spasm at the site of an intermediate plaque contributing to transient occlusion of the vessel. In such cases, stenting may abolish spasm at the site of the activated atherosclerotic plaque [15]. Moreover, spasms at the site of activated plaques have been associated with worse outcomes [16]. Finally, patients with previous successful PCI but recurrent or ongoing angina frequently suffer from coronary spasm, which are often diffuse and occur usually distal to the stent [17, 18]. The reasons for this phenomenon are still not understood but they may involve interruption of vascular communication due to the stent [19]. Whether or not this pathologic response may be prevented by the use of bioresorbable vascular scaffold stents is still under debate [20, 21].

## 20.6 Clinical Implications

Acetylcholine provocation testing has been shown to be safe [9] with a complication rate similar to that of diagnostic coronary angiography [22]. Moreover, the test is cheap and can be performed immediately after diagnostic angiography with an additional time frame of approximately 15 min. The diagnostic information arising from the test is multiple. First, the patient can be reassured that a cardiac cause for the symptoms is found. Second, if a coronary vasomotor disorder is diagnosed, targeted treatment with calcium channel blockers, nitrates, and other drugs to improve coronary vasomotion (e.g., nicorandil) can be initiated [23]. Nevertheless, approximately 30 % of patients have refractory symptoms [24] underpinning the need for a better understanding of the pathophysiology and the need for the development of new therapeutic strategies.

## 20.7 Conclusion

Intracoronary acetylcholine provocation testing is a safe and reliable technique for the assessment of coronary vasomotor disorders. It is useful to detect epicardial and microvascular spasm, which can be found in up to 60 % of patients with angina and unobstructed coronary arteries. Establishing such a diagnosis enables the physician to reassure the patient that a cause for the clinical presentation is found. Moreover, targeted medical treatment approaches with calcium channel blockers and nitrates can be initiated.

## References

1. Patel MR, Peterson ED, Dai D, Brennan JM, Redberg RF, Anderson HV, Brindis RG, Douglas PS. Low diagnostic yield of elective coronary angiography. N Engl J Med. 2010;362:886–95.
2. Ong P, Athanasiadis A, Borgulya G, Mahrholdt H, Kaski JC, Sechtem U. High prevalence of a pathological response to acetylcholine testing in patients with stable angina pectoris and unobstructed coronary arteries. The ACOVA Study (Abnormal COronary VAsomotion in patients with stable angina and unobstructed coronary arteries). J Am Coll Cardiol. 2012;59:655–62.
3. Furchgott RF, Zawadzki JV. The obligatory role of endothelial cells in the relaxation of arterial smooth muscle by acetylcholine. Nature. 1980;288:373–6.
4. Shimizu H, Lee JD, Ogawa K, Hara A, Nakamura T. Coronary artery vasoreactivity to intracoronary acetylcholine infusion test in patients with chest pain syndrome. Intern Med. 1992;31:22–7.
5. Yasue H, Horio Y, Nakamura N, Fujii H, Imoto N, Sonoda R, Kugiyama K, Obata K, Morikami Y, Kimura T. Induction of coronary artery spasm by acetylcholine in patients with variant angina: possible role of the parasympathetic nervous system in the pathogenesis of coronary artery spasm. Circulation. 1986;74:955–63.
6. Task Force Members; Montalescot G, Sechtem U, Achenbach S, Andreotti F, Arden C, Budaj A, Bugiardini R, Crea F, Cuisset T, Di Mario C, Ferreira JR, Gersh BJ, Gitt AK, Hulot JS, Marx N, Opie LH, Pfisterer M, Prescott E, Ruschitzka F, Sabaté M, Senior R, Taggart DP, van der Wall EE, Vrints CJ; ESC Committee for Practice Guidelines; Zamorano JL, Achenbach S, Baumgartner H, Bax JJ, Bueno H, Dean V, Deaton C, Erol C, Fagard R, Ferrari R, Hasdai D, Hoes AW, Kirchhof P, Knuuti J, Kolh P, Lancellotti P, Linhart A, Nihoyannopoulos P, Piepoli MF, Ponikowski P, Sirnes PA, Tamargo JL, Tendera M, Torbicki A, Wijns W, Windecker S; Document Reviewers; Knuuti J, Valgimigli M, Bueno H, Claeys MJ, Donner-Banzhoff N, Erol C, Frank H, Funck-Brentano C, Gaemperli O, Gonzalez-Juanatey JR, Hamilos M, Hasdai D, Husted S, James SK, Kervinen K, Kolh P, Kristensen SD, Lancellotti P, Maggioni AP, Piepoli MF, Pries AR, Romeo F, Rydén L, Simoons ML, Sirnes PA, Steg PG, Timmis A, Wijns W, Windecker S, Yildirir A, Zamorano JL. 2013 ESC guidelines on the management of stable coronary artery disease: the Task Force on the management of stable coronary artery disease of the European Society of Cardiology. Eur Heart J. 2013;34:2949–3003.
7. Ong P, Athanasiadis A, Sechtem U. Intracoronary acetylcholine provocation testing for assessment of coronary vasomotor disorders. J Vis Exp 2016;114. doi: 10.3791/54295. In Press.
8. Ong P, Athanasiadis A, Sechtem U. Patterns of coronary vasomotor responses to intracoronary acetylcholine provocation. Heart. 2013;99:1288–95.
9. Ong P, Athanasiadis A, Borgulya G, Vokshi I, Bastiaenen R, Kubik S, Hill S, Schäufele T, Mahrholdt H, Kaski JC, Sechtem U. Clinical usefulness, angiographic characteristics, and safety evaluation of intracoronary acetylcholine provocation testing among 921 consecutive white patients with unobstructed coronary arteries. Circulation. 2014;129:1723–30. In Press.
10. Sato K, Kaikita K, Nakayama N, Horio E, Yoshimura H, Ono T, Ohba K, Tsujita K, Kojima S, Tayama S, Hokimoto S, Matsui K, Sugiyama S, Yamabe H, Ogawa H. Coronary vasomotor response to intracoronary acetylcholine injection, clinical features, and long-term prognosis in 873 consecutive patients with coronary spasm: analysis of a single-center study over 20 years. J Am Heart Assoc. 2013;2(4):e000227. doi:10.1161/JAHA.113.000227.
11. Mohri M, Koyanagi M, Egashira K, Tagawa H, Ichiki T, Shimokawa H, Takeshita A. Angina pectoris caused by coronary microvascular spasm. Lancet. 1998;351:1165–9.
12. Reis SE, Holubkov R, Conrad Smith AJ, Kelsey SF, Sharaf BL, Reichek N, Rogers WJ, Merz CN, Sopko G, Pepine CJ; WISE Investigators. Coronary microvascular dysfunction is highly prevalent in women with chest pain in the absence of coronary artery disease: results from the NHLBI WISE study. Am Heart J. 2001;141:735–41.
13. Ong P, Athanasiadis A, Hill S, Schäufele T, Mahrholdt H, Sechtem U. Coronary microvascular dysfunction assessed by intracoronary acetylcholine provocation testing is a frequent cause of ischemia and angina in patients with exercise-induced electrocardiographic changes and unobstructed coronary arteries. Clin Cardiol. 2014;37:462–7.
14. Schächinger V, Britten MB, Zeiher AM. Prognostic impact of coronary vasodilator dysfunction on adverse long-term outcome of coronary heart disease. Circulation. 2000;101:1899–906.
15. Bentz K, Ong P, Sechtem U. Unstable angina pectoris – combination of an epicardial stenosis and a Prinzmetal spasm. Dtsch Med Wochenschr. 2013;138:2546–9.

16. Ishii M, Kaikita K, Sato K, Tanaka T, Sugamura K, Sakamoto K, Izumiya Y, Yamamoto E, Tsujita K, Yamamuro M, Kojima S, Soejima H, Hokimoto S, Matsui K, Ogawa H. Acetylcholine-provoked coronary spasm at site of significant organic stenosis predicts poor prognosis in patients with coronary vasospastic angina. J Am Coll Cardiol. 2015;66:1105–15.
17. Ito S, Nakasuka K, Morimoto K, Inomata M, Yoshida T, Tamai N, Suzuki S, Murakami Y, Morino A, Shimizu Y, Sato K. Angiographic and clinical characteristics of patients with acetylcholine-induced coronary vasospasm on follow-up coronary angiography following drug-eluting stent implantation. J Invasive Cardiol. 2011;23:57–64.
18. Ong P, Athanasiadis A, Perne A, Mahrholdt H, Schäufele T, Hill S, Sechtem U. Coronary vasomotor abnormalities in patients with stable angina after successful stent implantation but without in-stent restenosis. Clin Res Cardiol. 2014;103:11–9.
19. Tran CH, Welsh DG. The differential hypothesis: a provocative rationalization of the conducted vasomotor response. Microcirculation. 2010;17:226–36.
20. Lindemann H, Sechtem U, Ong P. Recurrent angina due to epicardial coronary artery spasm after successful bioresorbable vascular scaffold implantation. Circ J. 2015;79:1853–4.
21. Serruys PW, Ormiston JA, Onuma Y, Regar E, Gonzalo N, Garcia-Garcia HM, et al. A bioabsorbable everolimus-eluting coronary stent system (ABSORB): 2-year outcomes and results from multiple imaging methods. Lancet. 2009;373:897–910.
22. Noto Jr TJ, Johnson LW, Krone R, Weaver WF, Clark DA, Kramer Jr JR, Vetrovec GW. Cardiac catheterization 1990: a report of the Registry of the Society for Cardiac Angiography and Interventions (SCA&I). Cathet Cardiovasc Diagn. 1991;24:75–83.
23. Ong P, Athanasiadis A, Sechtem U. Pharmacotherapy for coronary microvascular dysfunction. Eur Heart J Cardiovasc Pharmacother. 2015;1:65–71. doi:10.1093/ehjcvp/pvu020.
24. Ong P, Konopka N, Mahrholdt H, Schumm J, Athanasiadis A, Sechtem U. 4-year follow-up of patients with stable angina, unobstructed coronary arteries and proof of coronary artery spasm: the ACOVA study follow-up. Clin Res Cardiol. 2013;102(Suppl 1):P478. doi:10.1007/s00392-013-1100-1.

# Research Models

## Contents

# Comparative Physiology and Pathophysiology of the Coronary Circulation

## Relevant Differences in the Coronary Circulation in Humans and Experimental Animal Models

*Ilkka H. A. Heinonen, Oana Sorop, Daphne Merkus, and Dirk J. Duncker*




J. Escaned, J. Davies (eds.), *Physiological Assessment of Coronary Stenoses and the Microcirculation*,
DOI 10.1007/978-1-4471-5245-3_21

## 21.1 Introduction

Over the last 50 years, a tremendous amount of knowledge pertaining to the structure and control mechanisms that govern function of the coronary circulation has been obtained through invasive studies in experimental animal models [1–5]. The major factors determining coronary blood flow (CBF) and myocardial oxygen delivery that were established in the experimental laboratory several decades ago have been incorporated into the management of ischemic heart disease [6–8]. The basic understanding of the fluid mechanical behavior of coronary stenoses as studied in the experimental setting has also been translated to the cardiac catheterization laboratory where measurements of coronary pressure distal to a stenosis and CBF are routinely obtained [7, 9, 10]. These physiological concepts that were originally studied in the experimental animal laboratory now facilitate routine clinical decision-making in a fashion that favorably impacts outcomes [11, 12].

Notwithstanding these major achievements, there is growing concern that animal models have limited translational value for complex disease processes such as ischemic heart disease [13–15]. Understanding the interspecies differences in coronary anatomy and physiology, as well as the limitations of experimental animal models of ischemic heart disease is essential to properly appreciate the translational value of animal studies. In this chapter we highlight relevant differences in coronary anatomy and physiology between humans and experimental animals and address the benefits and limitations of experimental animal models of ischemic heart disease. Since most experimental studies pertaining to the coronary circulation have been performed in large animals, most notably dogs and swine, focus will be particularly on these species.

## 21.2 Comparative Anatomy of the Coronary Circulation

**Epicardial Coronary Arteries** Ventricular blood flow is supplied by the left and right epicardial coronary arteries, which originate from the ostia in the left and right sinuses of Valsalva, respectively. The main branches of the left coronary artery are the left anterior descending artery (LAD) and the left circumflex coronary artery (LCx). The LAD supplies the left ventricular (LV) anterior wall and anterior two-thirds of the interventricular septum, equivalent to ~40 % of the LV myocardial mass, while the LCx supplies the lateral LV wall (~20 % of LV mass). The RCA supplies the right ventricle and in typically right dominant species (humans and swine) the LV posterior wall and septum, comprising ~40 % of the LV myocardial mass. In contrast, in left dominant species (dogs, goats, ruminants) the LCx supplies both the lateral and posterior LV wall as well as the posterior LV septum comprising ~60 % of the LV myocardial mass. Although variations in left versus right dominance are also observed within a particular species, a LCx stenosis or occlusion will in general yield a markedly greater area of ischemia in dogs than in swine [4].

**Coronary Collateral Arteries** Considerable interspecies differences exist with respect to the presence of innate coronary inter-arterial anastomoses, i.e. coronary collaterals [16, 17]. Thus, while species such as rat, rabbit, sheep, and swine have a negligible innate coronary collateral circulation, dogs, cats, and particularly guinea pigs have an extensive innate collateral circulation (Fig. 21.1; [17]). Consequently, a coronary artery occlusion in cats and dogs results in significantly slower development of myocardial necrosis, while collateral flow in guinea pigs is so high that necrosis is virtually absent even during

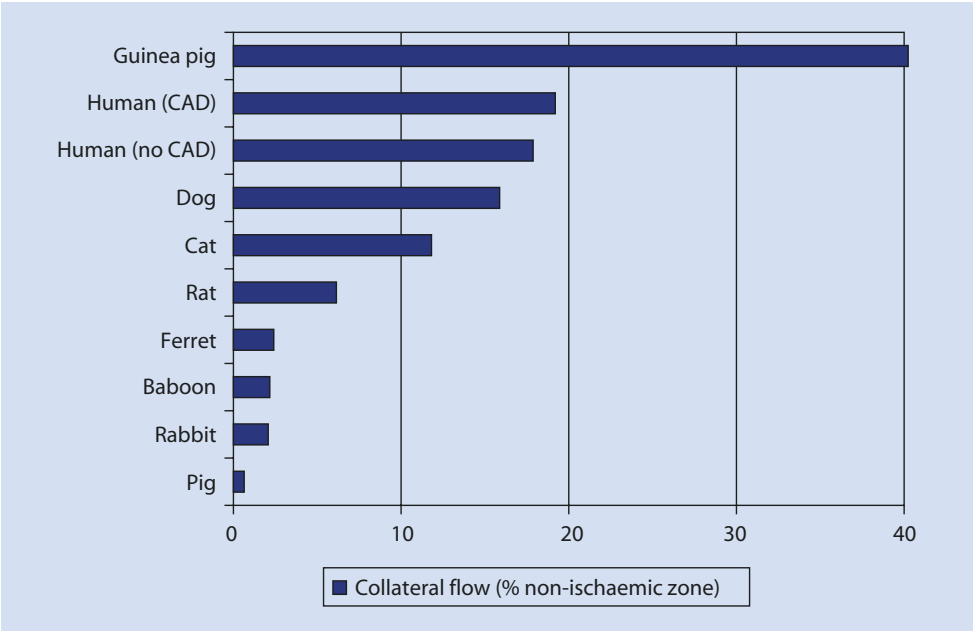


**Fig. 21.1** Interspecies differences in coronary collateral flow relative to normal flow in the nonoccluded vessel (Reproduced with permission from Seiler et al. [17])

sustained coronary occlusions [17, 18]. Even in pigs, in which collaterals are absent in the normal heart, coronary collaterals can be readily induced following placement of a (progressive) proximal coronary artery stenosis or repetitive brief (2 min) coronary artery occlusions [3, 16]. Recent evidence from clinical studies suggests that in humans there may be considerable collateral blood flow capacity even in healthy individuals, reaching collateral blood flow levels similar to those observed in dogs [17]. Moreover, coronary collateral supply can be further increased in patients by physical exercise training, where there is a dose–response relation between coronary collateral flow augmentation and improvement in exercise capacity [17]. Conversely, classical risk factors, including diabetes and hypertension, hamper collateral formation [19, 20]. Moreover, genetic factors also influence the growth response of collateral blood vessels [20] and together with the environmental factors may explain why significant interindividual variations in collateral blood flow capacity in patients with coronary artery disease are observed [21]. This indicates that both collateral-rich and collateral-deficient species are useful in ischemia–reperfusion studies, representing patients with high (e.g., dogs) or low (e.g., swine) collateral blood flow capacity.

### 21.2.1 Comparative Physiology of the Coronary Circulation

**Epicardial Coronary Arteries** Epicardial conduit arteries do not normally contribute significantly to coronary vascular resistance, yet arterial diameter is modulated by a wide variety of factors, including neurohumoral (norepinephrine, acetylcholine), paracrine (platelet-derived), and mechanical (shear stress) factors [7]. The net effect of many of these factors depends critically on the presence of a functional endothelium. Furchgott and Zawadski originally demonstrated that acetylcholine normally dilates arteries via an endothelium-dependent mechanism, which was later identified as nitric oxide (NO) [22]. When the endothelium is removed, the dilation to acetylcholine is converted to vasoconstriction, reflecting the effect of muscarinic vascular smooth muscle contraction. In experimental animal models as well as patients undergoing an intravascular coronary procedure, acetylcholine is the gold standard for testing epicardial coronary endothelial function [23]. However, in swine the vascular smooth muscle constrictor effects of acetylcholine outweigh its endothelium-dependent vasodilator effects, making acetylcholine unsuitable for investigating endothelial-dependent vasodilation in this species [3].

**Coronary Microvasculature and the Regulation of Coronary Blood Flow** The principal locus of coronary vascular resistance resides in microvessels smaller than 200 micron in diameter, termed arterioles [3, 24]. Regulation of tone in these microvessels is the result of a balance between a myriad of vasodilator and vasoconstrictor signals exerted by metabolic signals from the myocardium, the endothelium, and neurohormonal influences [3, 24]. These signals enable the heart to match the coronary blood supply to the need for oxygen and nutrients, while maintaining a consistently high and near maximum level of oxygen extraction (60–80%) [1, 3]. As a result of the high oxygen extraction under resting baseline conditions, an increase in myocardial oxygen demand such as during dynamic exercise increases CBF in proportion to the heart rate, with peak values during maximal exercise typically three to five times the resting level [25]. The strong correlation between coronary flow and heart rate occurs because heart rate is a common multiplier for the other determinants of myocardial oxygen demand (contractility and cardiac work), which are computed per beat. Regression analysis of published LV myocardial blood flow data against heart rate demonstrates remarkably similar relationships between canine, equine, human, porcine, and even rodent data during dynamic exercise (Fig. 21.2).

Although the increases in CBF during exercise are comparable among large mammalian species, the mechanisms controlling coronary vascular resistance – including differences in autonomic, endothelial, and metabolic control – can vary markedly as is highlighted in Table 21.1. There is evidence that CBF regulation follows a nonlinear redundancy design in the dog [26], whereas coronary flow regulation appears to follow a linear additive design in the pig [27], demonstrating that significant species differences exist [3]. It is presently

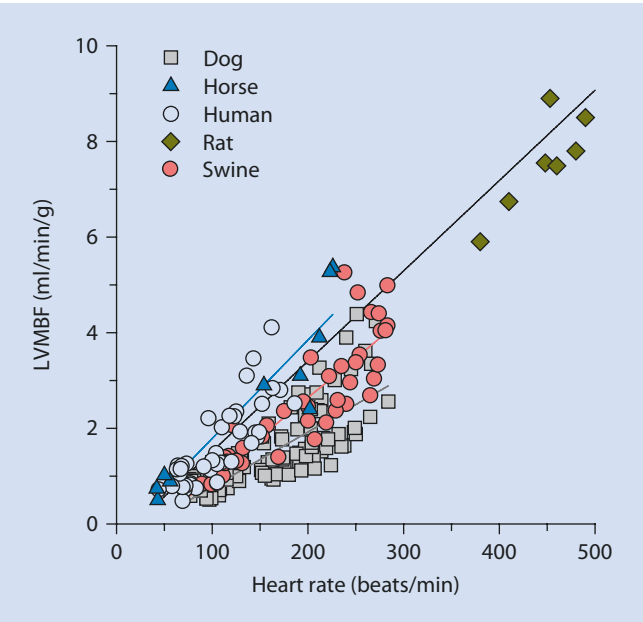


**Fig. 21.2** Relations between heart rate and left ventricular myocardial blood flow (LVMBF) at rest and during treadmill exercise in dogs, horses, humans, and swine. Data from humans were obtained principally from young healthy male subjects performing upright bicycle exercise. Data from rats have been added (*solid diamonds*) to illustrate that the high LVMBF values in this species are the result of the high heart rates, so that the rat data fall close to the regression line for the human data (Reproduced from Duncker et al. [28], with permission from Elsevier)

**Table 21.1** Mechanisms demonstrated to be involved in the regulation of coronary vascular resistance in dogs, swine, and humans in vivo

| | Dog | Swine | Human |
|---|---|---|---|
| Neurohumoral control | | | |
| Alpha-adrenergic | + | – | +a |
| Beta-adrenergic | + | + | + |
| Muscarinic | +b | +b | ? |
| Angiotensin II | | | |
| Endothelial mediators | – | + | + |
| Nitric oxide | + | –c | + |
| Prostanoids | – | + | – |
| Endothelin | + | + | + |
| Metabolic regulators | | | |
| Adenosine | – | + | + |
| KATP channels | + | + | +c |
| KV channels | + | + | ? |

unclear whether control of the human coronary circulation follows a redundancy or additive design [28].

Species differences clearly exist with respect to neurohumoral control of CBF. For example, swine lack significant alpha-adrenergic control of CBF [29, 30], whereas the exercise-induced increase in CBF is impeded by an increase in alpha-adrenergic tone in dogs [5, 31], and the role of alpha-adrenergic constriction in healthy humans during exercise remains uncertain [32]. Conversely, beta-adrenergic vasodilation occurs in all three species [3]. Species differences are also noted for parasympathetic control of the coronary circulation, with parasympathetic tone exerting a coronary vasodilator influence in resting dogs but a vasoconstrictor influence in resting swine [3]. Similarly, angiotensin II contributes to coronary vascular tone in resting swine, but not in resting dogs or humans [19, 28].

Endothelial control of CBF also demonstrates significant differences between species [28]. For example, inhibition of nitric oxide synthase results in coronary vasoconstriction in resting humans and swine and to a lesser extent in dogs, while inhibition of prostanoid production produces coronary vasoconstriction in swine, but not in dogs or humans. Conversely, endothelin exerts a vasoconstrictor influence in awake resting swine, dogs, and healthy humans (insert Table -).

Interestingly, an interaction exists between NO and prostanoids in the canine coronary circulation [33]. These findings indicate an increased contribution of prostanoids when NO synthase activity is blunted and could explain why clinical studies of patients with (minimal) coronary artery disease reported a role for vasodilator prostanoids [34–36], whereas the single study in healthy human volunteers failed to observe such a role [37]. In swine, the contribution of prostanoids to the regulation of coronary vascular tone was not enhanced by inhibition of NO synthesis [38] suggesting that in the porcine heart, prostanoids and NO do not act in a compensatory manner when one of these pathways is blocked. As the effects of endogenous prostanoids decrease with age both in pigs [39] and humans [40], the discrepancy between porcine versus human/canine studies may reflect a difference in age-dependent contribution of prostanoids to regulation of coronary resistance vessel tone. These examples highlight the importance of taking the presence of risk factors or coronary artery disease into account when interpreting data from older patients with (minimal) disease versus studies in young healthy animals.

### 21.2.2 Comparative Pathophysiology of the Coronary Circulation in Coronary Artery Disease

**Coronary Artery Disease in Humans Versus Experimental Animal Models** Ischemic heart disease in humans is the result of long-term exposure to risk factors that predispose to the development of atherosclerosis in the arterial vessels. Atherosclerosis can start as early as the second decade of life [41, 42] but often does not become symptomatic until the sixth or seventh decade of life. Symptoms of myocardial ischemia occur when an atherosclerotic plaque obstructs the vascular lumen by more than 75 % of its cross-sectional area to produce a hemodynamically significant coronary artery stenosis or when a (hemodynamically insignificant) plaque ruptures and a thrombus causes the arterial vessel to become suddenly occluded [7]. A coronary artery stenosis can eventually result in chronic myocardial stunning and hibernation, whereas a sudden thrombotic occlusion poses an acute threat to myocardial viability [7].

In the majority of experimental studies, myocardial ischemia has been studied in anesthetized animals, either open- or closed chest, in the acute setting [18]. Acute severe ischemia is almost invariably produced by complete occlusion of a coronary artery. In open-chest animals, this can be accomplished by ligation of the vessel or occluding the vessel by inflation of a balloon placed around the vessel. In closed-chest animals, intracoronary devices can be used to occlude a vessel. This approach has the advantage that surgical trauma produced by the thoracotomy is avoided. The most frequently employed method is inflation of a balloon placed at the tip of a catheter [18, 43]. Studies into novel strategies to protect the heart against irreversible ischemia–reperfusion damage have provided us with a wealth of information on the mechanisms of ischemia–reperfusion damage [44], including a role for the coronary microcirculation [45, 46]. To date, however, this has not yet yielded a proven and established novel therapy against ischemia–reperfusion injury [47–49]. There are several explanations for the disparity between experimental and clinical studies,

including methodological limitations in clinical studies but also lack of risk factors, comorbidities, and co-medication in animal studies. For an in-depth review of this issue, the reader is referred to several excellent review articles elsewhere [47–49].

In order to produce mild or moderate ischemia, the flow in the coronary artery must be reduced rather than completely abolished. In open-chest anesthetized animals, this can be achieved through a hydraulic occluder positioned around the coronary artery, tightening a J-shaped screw clamp or other mechanical devices [18]. Flow reductions can also be achieved by intracoronary placement of a cylinder attached to a catheter [50]. The lumen of a hole drilled in the length of the cylinder provides the partial perfusion when the catheter is so far advanced into the coronary artery that the cylinder occludes the vessel completely. An advantage of this method is that it can be used in closed-chest animals and that the lumen of the catheter provides an opportunity to obtain post-stenosis pressure measurements. A disadvantage of all above-described methods is that they produce concentric stenoses, while in man the majority (~70 %) of stenoses are eccentric. Vessels with a fixed concentric constriction do not respond to vasodilators, while vessels with eccentric stenoses are capable to increase their lumen, thereby enlarging coronary blood flow. Consequently, some investigators have attempted to mimic an eccentric stenosis by partially inflating an intraluminal balloon [51].

Over the past 20 years, investigators have begun to use more chronic models of ischemia, for example, to study post-infarct remodeling [52, 53] and chronic myocardial stunning and hibernation [54–56]. In infarct studies mechanical approaches to coronary artery ligations have been employed either to permanently occlude a coronary artery or produce a transient coronary artery occlusion (1–2-h balloon occlusion) to mimic reperfusion therapy of myocardial infarction [43, 57]. To study chronic myocardial stunning and hibernation, investigators have implanted small (C-shaped) occluder devices sutured around the coronary artery in young growing swine [54–56, 58]. Over time, the initially mild stenosis increases in severity as the animals grow leading to severe narrowing and even occlusion in subsets of animals [56].

Notwithstanding the usefulness of direct mechanical approaches to coronary artery obstructions in all of the aforementioned studies, a limitation of these experimental models is that they typically involve young healthy animals with no risk factors or comorbidities. For this purpose, several research groups have begun studying the influence of high-fat diet, familial hypercholesterolemia, metabolic syndrome, and diabetes mellitus on coronary atherosclerosis and coronary microvascular dysfunction [59–61]. Swine appear to be particularly useful as their blood lipid profile is similar to humans and atherosclerosis can be easily induced [60, 62]. Although studies in swine are very expensive as they often require large amounts of specific (high-fat) diets and housing over an extended period of time to produce coronary atherosclerosis, they allow the study of functional and structural alterations in the coronary microvasculature, which are now recognized as an integral part of ischemic heart disease [63–65]. The coronary atherosclerosis produced in most large animal models typically represents early stage plaques, with only very few studies reporting advanced complex plaques [66, 67]. Furthermore, no study has, to our knowledge, demonstrated yet that spontaneous coronary plaque rupture does actually occur, but recent advances in transgene technology in swine may soon yield a valid human model of vulnerable plaque formation and possibly coronary microvascular dysfunction [68].

**Coronary Microvascular Dysfunction in Humans Versus Experimental Animal Models** It is well appreciated that atherosclerosis of conduit epicardial arteries is often the culprit underlying the complications of coronary heart disease [7]. For instance, it has been demonstrated by coronary angiography in several studies that there is a close relationship between the severity and extent of coronary artery disease and patient survival. However, a growing body of literature indicates that the coronary microcirculation also contributes substantially to the pathophysiology of cardiovascular disease [40, 63, 65, 69]. In addition, cardiovascular events in patients presenting with acute coronary syndromes, and undergoing successful coronary intervention, were equally attributable to culprit and non-culprit lesion sites, indicating that coronary artery disease is a diffuse and systemic disease affecting all coronary macro- and microvessels, even when only a single flow-limiting stenosis is present [70]. Consequently, understanding the exact mechanisms that regulate coronary microvascular function in health and how it is altered in disease states is essential, particularly as regulatory mechanisms can vary substantially across species and vascular beds [25, 71].

Assessment of coronary microvascular function in humans has been somewhat hampered to date due to the fact that no technique allows the direct visualization of coronary microcirculation in vivo in humans [65]. Several measurements that rely on the quantification of blood flow through the coronary circulation, such as intracoronary thermodilution or intracoronary Doppler wire in large proximal coronary arteries, are commonly used to assess function of the coronary microvasculature. However, these techniques still provide only indirect information about the flow through the coronary microvasculature. Somewhat more direct information regarding human coronary artery microvascular (dys)function has been obtained by positron emission tomography, which is a functional imaging tool applying short-lived radioisotopes to measure myocardial blood flow noninvasively and in absolute terms [72]. These studies have revealed that myocardial flow reserve is impaired in several clinical conditions such as in patients at high risk for CAD [73], hypercholesterolemia [74], hypertriglyceridemia [75], hypertension [76], chronic kidney disease [77], LV hypertrophy [78], and diabetes [79, 80]. Importantly, in all these studies, reduced myocardial blood flow reserve was detected in anatomically normal coronary

arteries highlighting the importance of coronary microvascular dysfunction that accompanies many common comorbidities. Recent evidence also indicates that microvascular dysfunction is an independent predictor of adverse clinical events following coronary revascularization [81].

To complement the studies addressing coronary microvascular function in humans, numerous animal studies have provided important mechanistic information on the topic. It is of note that particularly large animal studies have recapitulated many clinical features of coronary microvascular dysfunction as described above. For instance, several large animal models with features of metabolic syndrome have recently addressed alterations in coronary (micro)vascular function and structure. In Ossabaw swine with metabolic syndrome, coronary arterial enlargement with diffuse coronary artery disease was present in the absence of severe focal stenosis [82]. Moreover, hypertrophic inward remodeling of coronary resistance microvessels and capillary rarefaction occurred in the myocardium, which contributed to decreased coronary flow and myocardial ischemia [60]. Furthermore, a reduction in nitric oxide bioavailability and impairment of the endothelin-1 vasoconstrictor responses were observed in coronary microvessels from a pre-atherosclerotic diabetes mellitus porcine model with type 2 characteristics [59]. This reduction in coronary microvascular NO bioavailability is similar to that observed in human coronary arteries [40] and results in a loss of the "normal" contribution of NO to shear stress-dependent vasodilation in CAD patients [40]. It is highly plausible that this reduced NO bioavailability is due to increased production of reactive oxygen species which are elevated in practically all cardiovascular disease states [40]. Interestingly, shear stress-mediated vasodilation was still present in CAD patients, but an increased contribution of a so-called endothelium-derived hyperpolarizing factor (EDHF) compensated for the loss of NO [40]. There are several possible EDHFs that act to compensate and maintain coronary artery dilation in CAD and other disease conditions, not only in response to shear stress but also bradykinin-induced vasodilation in human coronary arteries [40]. Taken together, human and animal studies show many similarities in terms of regulation of vascular tone in the coronary microvasculature and in terms of alteration regulation of vascular tone in disease states.

## 21.3 Concluding Remarks

Over the last 50 years, a vast amount of knowledge pertaining to the structure and control mechanisms that govern function of the coronary circulation has been obtained through invasive studies in experimental animal models [1–5, 7]. Thus, the major factors determining myocardial oxygen delivery and the fluid mechanical behavior of coronary artery stenoses have been elucidated, and this knowledge has been successfully incorporated into the management of patients with ischemic heart disease [7, 9, 10]. Notwithstanding the importance of large animal studies for our current understanding of coronary physiology, there is a need to further develop animal models of coronary artery disease in order to continue to successfully translate knowledge from the experimental laboratory to the clinical arena. Most notably, we should generate animal models that more closely mimic the clinical situation, including long-term exposure to comorbidities to recapitulate human coronary artery disease. Such animal models are critical in order to further improve the treatment of patients with ischemic heart disease.



## References


1. Feigl EO. Coronary physiology. Physiol Rev. 1983;63:1–205.
2. Duncker DJ, Bache RJ. Regulation of coronary vasomotor tone under normal conditions and during acute myocardial hypoperfusion. Pharmacol Ther. 2000;86:87–110.
3. Duncker DJ, Bache RJ. Regulation of coronary blood flow during exercise. Physiol Rev. 2008;88:1009–86.
4. Tomanek RJ. Coronary vasculature: development, structure-function, and adaptations. New York: Springer; 2013.
5. Tune JD. Coronary circulation. Williston: Morgan & Claypool Life Sciences; Williston, Vermont; 2014.
6. Hoffman JIE, Spaan JAE. Pressure-flow relations in coronary circulation. Physiol Rev. 1990;70:331–90.
7. Canty Jr JM, Duncker DJ. Coronary blood flow and myocardial ischemia. In: Bonow RO, Mann DL, Zipes DP, Libby P, editors. Braunwald's heart disease. 10th ed. Philadelphia: Elsevier; 2014.
8. Duncker DJ, Koller A, Merkus D, Canty Jr JM. Regulation of coronary blood flow in health and ischemic heart disease. Prog Cardiovasc Dis. 2015;57:409–22.
9. Pijls NH, Sels JW. Functional measurement of coronary stenosis. J Am Coll Cardiol. 2012;59:1045–57.
10. van de Hoef TP, Nolte F, Rolandi MC, Piek JJ, van den Wijngaard J, Spaan JAE, Siebes M. Coronary pressure-flow relations as basis for the understanding of coronary physiology. J Mol Cell Cardiol. 2012;52:786–93.
11. Tonino PA, De Bruyne B, Pijls NH, Siebert U, Ikeno F, van' t Veer M, Klauss V, Manoharan G, Engstrom T, Oldroyd KG, Ver Lee PN, MacCarthy PA, Fearon WF. Fractional flow reserve versus angiography for guiding percutaneous coronary intervention. N Engl J Med. 2009;360:213–24.
12. De Bruyne B, Pijls NH, Kalesan B, Barbato E, Tonino PA, Piroth Z, Jagic N, Mobius-Winkler S, Rioufol G, Witt N, Kala P, MacCarthy P, Engstrom T, Oldroyd KG, Mavromatis K, Manoharan G, Verlee P, Frobert O, Curzen N, Johnson JB, Juni P, Fearon WF. Fractional flow reserve-guided PCI versus medical therapy in stable coronary disease. N Engl J Med. 2012;367:991–1001.
13. Ludman AJ, Yellon DM, Hausenloy DJ. Cardiac preconditioning for ischaemia: lost in translation. Dis Model Mech. 2010;3:35–8.
14. Schwartz BG, Kloner RA. Coronary no reflow. J Mol Cell Cardiol. 2012;52:873–82.
15. Pecoraro V, Moja L, Dall'Olmo L, Cappellini G, Garattini S. Most appropriate animal models to study the efficacy of statins: a systematic review. Eur J Clin Invest. 2014;44:848–71.
16. Schaper W. Collateral circulation: past and present. Basic Res Cardiol. 2009;104:5–21.
17. Seiler C, Stoller M, Pitt B, Meier P. The human coronary collateral circulation: development and clinical importance. Eur Heart J. 2013;34:2674–82.
18. Verdouw PD, van den Doel MA, de Zeeuw S, Duncker DJ. Animal models in the study of myocardial ischaemia and ischaemic syndromes. Cardiovasc Res. 1998;39:121–35.
19. Chilian WM, Penn MS, Pung YF, Dong F, Mayorga M, Ohanyan V, Logan S, Yin L. Coronary collateral growth--back to the future. J Mol Cell Cardiol. 2012;52:905–11.

20. Teunissen PF, Horrevoets AJ, van Royen N. The coronary collateral circulation: genetic and environmental determinants in experimental models and humans. J Mol Cell Cardiol. 2012;52:897–904.
21. Seiler C. Assessment and impact of the human coronary collateral circulation on myocardial ischemia and outcome. Circ Cardiovasc Interv. 2013;6:719–28.
22. Furchgott RF, Zawadzki JV. The obligatory role of endothelial cells in the relaxation of arterial smooth muscle by acetylcholine. Nature. 1980;288:373–6.
23. Gutierrez E, Flammer AJ, Lerman LO, Elizaga J, Lerman A, Fernandez-Aviles F. Endothelial dysfunction over the course of coronary artery disease. Eur Heart J. 2013;34:3175–81.
24. Zhang C, Rogers P, Merkus D, Knudson P, Chilian WM. Regulation of coronary microvascular resistance in health and disease. In: Tuma RF, Duran WN, Ley K, editors. Microcirculation. 2nd ed. Boston: Elsevier; 2008. p. 521.
25. Laughlin MH, Davis MJ, Secher NH, vLJ J, Arce-Esquivel AA, Simmons GH, Bender SB, Padilla J, Bache RJ, Merkus D, Duncker DJ. Peripheral circulation. Compr Physiol. 2012;2:321–447.
26. Ishibashi Y, Bache RJ, Zhang J. ATP-sensitive K+ channels, adenosine, and nitric oxide-mediated mechanisms account for coronary vasodilation during exercise. Circ Res. 1998;82:346–59.
27. Merkus D, Haitsma DB, Fung TY, Assen YJ, Verdouw PD, Duncker DJ. Coronary blood flow regulation in exercising swine involves parallel rather than redundant vasodilator pathways. Am J Physiol – Heart Circ Physiol. 2003;285:H424–33.
28. Duncker DJ, Bache RJ, Merkus D. Regulation of coronary resistance vessel tone in response to exercise. J Mol Cell Cardiol. 2012;52:802–13.
29. Schulz R, Oudiz RJ, Guth BD, Heusch G. Minimal $a_1$- and $a_2$-adrenoceptor-mediated coronary vasoconstriction in the anaesthetized swine. Naunyn Schmiedebergs Arch Pharmacol. 1990;342:422–8.
30. Duncker DJ, Stubenitsky R, Verdouw PD. Autonomic control of vasomotion in the porcine coronary circulation during treadmill exercise. Evidence for feed-forward b-adrenergic control. Circ Res. 1998;82:1312–22.
31. Bache RJ, Dai X-Z, Herzog CA, Schwartz JS. Effects of nonselective and selective a1-adrenergic blockade on coronary blood flow during exercise. Circ Res. 1987;61(suppl. II):II-36–II-41.
32. Heusch G, Baumgart D, Camici P, Chilian W, Gregorini L, Hess O, Indolfi C, Rimoldi O. a-adrenergic coronary vasoconstriction and myocardial ischemia in humans. Circulation. 2000;101:689–94.
33. Puybasset L, Bea ML, Ghaleb B, Giudicelli JF, Berdeaux A. Coronary and systemic hemodynamic effects of sustained inhibition of nitric oxide synthesis in conscious dogs. Evidence for cross talk between nitric oxide and cyclooxygenase in coronary vessels. Circ Res. 1996;79:343–57.
34. Duffy SJ, Castle SF, Harper RW, Meredith IT. Contribution of vasodilator prostanoids and nitric oxide to resting flow, metabolic vasodilation, and flow-mediated dilation in human coronary circulation. Circulation. 1999;100:1951–7.
35. Friedman PL, Brown Jr EJ, Gunther S, Alexander RW, Barry WH, Mudge Jr GH, Grossman W. Coronary vasoconstrictor effect of indomethacin in patients with coronary-artery disease. N Engl J Med. 1981;305:1171–5.
36. Pacold I, Hwang MH, Lawless CE, Diamond P, Scanlon PJ, Loeb HS. Effects of indomethacin on coronary hemodynamics, myocardial metabolism and anginal threshold in coronary artery disease. Am J Cardiol. 1986;57:912–5.
37. Edlund A, Sollevi A, Wennmalm A. The role of adenosine and prostacyclin in coronary flow regulation in healthy man. Acta Physiol Scand. 1989;135:39–46.
38. Merkus D, Houweling B, Zarbanoui A, Duncker DJ. Interaction between prostanoids and nitric oxide in regulation of systemic, pulmonary, and coronary vascular tone in exercising swine. Am J Physiol Heart Circ Physiol. 2004;286:H1114–23.
39. Willis AP, Leffler CW. NO and prostanoids: age dependence of hypercapnia and histamine-induced dilations of pig pial arterioles. Am J Physiol. 1999;277:H299–307.
40. Beyer AM, Gutterman DD. Regulation of the human coronary microcirculation. J Mol Cell Cardiol. 2012;52:814–21.
41. Stary HC. Evolution and progression of atherosclerotic lesions in coronary arteries of children and young adults. Arteriosclerosis. 1989;9:I19–32.
42. Tuzcu EM, Kapadia SR, Tutar E, Ziada KM, Hobbs RE, McCarthy PM, Young JB, Nissen SE. High prevalence of coronary atherosclerosis in asymptomatic teenagers and young adults: evidence from intravascular ultrasound. Circulation. 2001;103:2705–10.
43. Moelker AD, Baks T, van den Bos EJ, van Geuns RJ, de Feyter PJ, Duncker DJ, van der Giessen WJ. Reduction in infarct size, but no functional improvement after bone marrow cell administration in a porcine model of reperfused myocardial infarction. Eur Heart J. 2006;27:3057–64.
44. Heusch G. Molecular basis of cardioprotection: signal transduction in ischemic pre-, post-, and remote conditioning. Circ Res. 2015;116:674–99.
45. Fordyce CB, Gersh BJ, Stone GW, Granger CB. Novel therapeutics in myocardial infarction: targeting microvascular dysfunction and reperfusion injury. Trends Pharmacol Sci. 2015;36:605–16.
46. Betgem RP, de Waard GA, Nijveldt R, Beek AM, Escaned J, van Royen N. Intramyocardial haemorrhage after acute myocardial infarction. Nat Rev Cardiol. 2015;12:156–67.
47. Bolli R, Becker L, Gross G, Mentzer Jr R, Balshaw D, Lathrop DA. Ischemia NWGotToTfPtHf. Myocardial protection at a crossroads: the need for translation into clinical therapy. Circ Res. 2004;95:125–34.
48. Dirksen MT, Laarman GJ, Simoons ML, Duncker DJ. Reperfusion injury in humans: a review of clinical trials on reperfusion injury inhibitory strategies. Cardiovasc Res. 2007;74:343–55.
49. Kloner RA. Current state of clinical translation of cardioprotective agents for acute myocardial infarction. Circ Res. 2013;113:451–63.
50. Gewirtz H, Most AS. Production of a critical coronary arterial stenosis in closed chest laboratory animals: Description of a new nonsurgical method based on standard cardiac catheterization techniques. Am J Cardiol. 1981;47:589–96.
51. Ichikawa Y, Yokoyama M, Akita H, Fukuzaki H. Constriction of a large coronary artery contributes to serotonin-induced myocardial ischemia in the dog with pliable coronary stenosis. J Am Coll Cardiol. 1989;14:449–59.
52. Merkus D, Duncker DJ. Coronary microvascular dysfunction in post-infarct remodelled myocardium. Eur Heart J. 2014;16:A74–9.
53. Heinonen I, Sorop OE, de Beer VJ, Duncker DJ, Merkus D. What can we learn about treating heart failure from the heart's response to acute exercise: Focus on the coronary microcirculation. J Appl Physiol. 2015;119:934–43.
54. McFalls EO, Baldwin D, Palmer B, Marx D, Jaimes D, Ward HB. Regional glucose uptake within hypoperfused swine myocardium as measured by positron emission tomography. Am J Physiol. 1997;272:H343–9.
55. Canty Jr JM, Fallavollita JA. Hibernating myocardium. J Nucl Cardiol. 2005;12:104–19.
56. Canty Jr JM, Suzuki G. Myocardial perfusion and contraction in acute ischemia and chronic ischemic heart disease. J Mol Cell Cardiol. 2012;52:822–31.
57. Moelker AD, Baks T, Wever KM, Spitskovsky D, Wielopolski PA, van Beusekom HM, van Geuns RJ, Wnendt S, Duncker DJ, van der Giessen WJ. Intracoronary delivery of umbilical cord blood derived unrestricted somatic stem cells is not suitable to improve LV function after myocardial infarction in swine. J Mol Cell Cardiol. 2007;42:735–45.
58. Sorop O, Merkus D, de Beer VJ, Houweling B, Pistea A, McFalls EO, Boomsma F, van Beusekom HM, van der Giessen WJ, VanBavel E, Duncker DJ. Functional and structural adaptations of coronary microvessels distal to a chronic coronary artery stenosis. Circ Res. 2008;102:795–803.
59. van den Heuvel M, Sorop O, Koopmans SJ, Dekker R, de Vries R, van Beusekom HM, Eringa EC, Duncker DJ, Danser AH, van der Giessen WJ. Coronary microvascular dysfunction in a porcine model of early atherosclerosis and diabetes. Am J Physiol Heart Circ Physiol. 2012;302:H85–94.

60. Trask AJ, Katz PS, Kelly AP, Galantowicz ML, Cismowski MJ, West TA, Neeb ZP, Berwick ZC, Goodwill AG, Alloosh M, Tune JD, Sturek M, Lucchesi PA. Dynamic micro- and macrovascular remodeling in coronary circulation of obese Ossabaw pigs with metabolic syndrome. J Appl Physiol. 2012;113:1128–40.
61. de Chantemele EJ B, Stepp DW. Influence of obesity and metabolic dysfunction on the endothelial control in the coronary circulation. J Mol Cell Cardiol. 2012;52:840–7.
62. Bender SB, de Beer VJ, Tharp DL, van Deel ED, Bowles DK, Duncker DJ, Laughlin MH, Merkus D. Reduced contribution of endothelin to the regulation of systemic and pulmonary vascular tone in severe familial hypercholesterolaemia. J Physiol. 2014;592:1757–69.
63. Marzilli M, Merz CN, Boden WE, Bonow RO, Capozza PG, Chilian WM, DeMaria AN, Guarini G, Huqi A, Morrone D, Patel MR, Weintraub WS. Obstructive coronary atherosclerosis and ischemic heart disease: an elusive link! J Am Coll Cardiol. 2012;60:951–6.
64. Crea F, Camici PG, Bairey Merz CN. Coronary microvascular dysfunction: an update. Eur Heart J. 2014;35:1101–11.
65. Camici PG, d'Amati G, Rimoldi O. Coronary microvascular dysfunction: mechanisms and functional assessment. Nat Rev Cardiol. 2015;12:48–62.
66. Granada JF, Kaluza GL, Wilensky RL, Biedermann BC, Schwartz RS, Falk E. Porcine models of coronary atherosclerosis and vulnerable plaque for imaging and interventional research. EuroIntervention. 2009;5:140–8.
67. Vilahur G, Padro T, Badimon L. Atherosclerosis and thrombosis: insights from large animal models. J Biomed Biotechnol. 2011; 2011:907575.
68. Al-Mashhadi RH, Sorensen CB, Kragh PM, Christoffersen C, Mortensen MB, Tolbod LP, Thim T, Du Y, Li J, Liu Y, Moldt B, Schmidt M, Vajta G, Larsen T, Purup S, Bolund L, Nielsen LB, Callesen H, Falk E, Mikkelsen JG, Bentzon JF. Familial hypercholesterolemia and atherosclerosis in cloned minipigs created by DNA transposition of a human PCSK9 gain-of-function mutant. Sci Transl Med. 2013;5:166ra161.
69. Pries AR, Badimon L, Bugiardini R, Camici PG, Dorobantu M, Duncker DJ, Escaned J, Koller A, Piek JJ, de Wit C. Coronary vascular regulation, remodelling, and collateralization: mechanisms and clinical implications on behalf of the working group on coronary pathophysiology and microcirculation. Eur Heart J. 2015;36:3134–46 (ePub ahead of print).
70. Stone GW, Maehara A, Lansky AJ, de Bruyne B, Cristea E, Mintz GS, Mehran R, McPherson J, Farhat N, Marso SP, Parise H, Templin B, White R, Zhang Z, Serruys PW, Investigators P. A prospective natural-history study of coronary atherosclerosis. N Engl J Med. 2011;364: 226–35.
71. Heinonen I, Kalliokoski KK, Hannukainen JC, Duncker DJ, Nuutila P, Knuuti J. Organ-specific physiological responses to acute physical exercise and long-term training in humans. Physiology (Bethesda). 2014;29:421–36.
72. Kajander SA, Joutsiniemi E, Saraste M, Pietila M, Ukkonen H, Saraste A, Sipila HT, Teras M, Maki M, Airaksinen J, Hartiala J, Knuuti J. Clinical value of absolute quantification of myocardial perfusion with (15)O-water in coronary artery disease. Circ Cardiovasc Imaging. 2011;4:678–84.
73. Dayanikli F, Grambow D, Muzik O, Mosca L, Rubenfire M, Schwaiger M. Early detection of abnormal coronary flow reserve in asymptomatic men at high risk for coronary artery disease using positron emission tomography. Circulation. 1994;90:808–17.
74. Pitkanen OP, Raitakari OT, Niinikoski H, Nuutila P, Iida H, Voipio-Pulkki LM, Harkonen R, Wegelius U, Ronnemaa T, Viikari J, Knuuti J. Coronary flow reserve is impaired in young men with familial hypercholesterolemia. J Am Coll Cardiol. 1996;28:1705–11.
75. Yokoyama I, Ohtake T, Momomura S, Yonekura K, Kobayakawa N, Aoyagi T, Sugiura S, Sasaki Y, Omata M. Altered myocardial vasodilatation in patients with hypertriglyceridemia in anatomically normal coronary arteries. Arterioscler Thromb Vasc Biol. 1998;18:294–9.
76. Parodi O, Neglia D, Sambuceti G, Marabotti C, Palombo C, Donato L. Regional myocardial blood flow and coronary reserve in hypertensive patients. The effect of therapy. Drugs. 1992;44 Suppl 1:48–55.
77. Murthy VL, Naya M, Foster CR, Hainer J, Gaber M, Dorbala S, Charytan DM, Blankstein R, Di Carli MF. Coronary vascular dysfunction and prognosis in patients with chronic kidney disease. JACC Cardiovasc Imaging. 2012;5:1025–34.
78. Choudhury L, Rosen SD, Patel D, Nihoyannopoulos P, Camici PG. Coronary vasodilator reserve in primary and secondary left ventricular hypertrophy. A study with positron emission tomography. Eur Heart J. 1997;18:108–16.
79. Pitkänen OP, Nuutila P, Raitakari OT, Rönnemaa T, Koskinen PJ, Iida H, Lehtimaki TJ, Laine HK, Takala T, Viikari JS, Knuuti J. Coronary flow reserve is reduced in young men with IDDM. Diabetes. 1998;47: 248–54.
80. Chen WJ, Danad I, Raijmakers PG, Halbmeijer R, Harms HJ, Lammertsma AA, van Rossum AC, Diamant M, Knaapen P. Effect of type 2 diabetes mellitus on epicardial adipose tissue volume and coronary vasomotor function. Am J Cardiol. 2014;113:90–7.
81. Taqueti VR, Hachamovitch R, Murthy VL, Naya M, Foster CR, Hainer J, Dorbala S, Blankstein R, Di Carli MF. Global coronary flow reserve is associated with adverse cardiovascular events independently of luminal angiographic severity and modifies the effect of early revascularization. Circulation. 2015;131:19–27.
82. Choy JS, Luo T, Huo Y, Wischgoll T, Schultz K, Teague SD, Sturek M, Kassab GS. Compensatory enlargement of ossabaw miniature swine coronary arteries in diffuse atherosclerosis. IJC Heart Vasc. 2015;6:4–11.

# Computational Analysis of Multislice CT Angiography

*Carlos Collet, Chrysafios Girasis, Charles Taylor, Patrick W. Serruys, and Yoshinobu Onuma*




J. Escaned, J. Davies (eds.), *Physiological Assessment of Coronary Stenoses and the Microcirculation*,
DOI 10.1007/978-1-4471-5245-3_22

## 22.1 Introduction

In the last two decades, coronary computed tomography angiography (CTA) has been introduced as a noninvasive alternative for the assessment of coronary anatomy [1]. Since its introduction, the technology has undergone rapid scientific advances with improvements in resolution, acquisition times, reduction in contrast volume, and radiation doses, going from an 8-slice CT system in 2000 to 16-slice (2002), 64-slice (2004), and more recently 128-slice and 256-slice CT systems. The new-generation 256-slice CT system enables imaging of the entire heart in a single heart beat, with the rapid speed of the scan facilitating a substantial reduction in both contrast volumes and radiation dosage [2].

The landmark multicenter CORE-64 study investigated the diagnostic ability of coronary CTA, utilizing 64-slice scanners, compared to invasive angiography in 291 consecutive patients. Coronary CTA (area under the receiver-operator curve [AUC] 0.84, 95 % CI 0.79–0.88) was demonstrated to be similar to conventional invasive angiography in its ability to identify patients who subsequently underwent revascularization. Further patient-based analyses demonstrated coronary CTA was highly accurate for the diagnosis of patients with at least one coronary stenosis of 50 % or more, as assessed by invasive quantitative coronary angiography (QCA), with an AUC 0.93 (95 % confidence interval [CI], 0.90–0.96). In a vessel-based analysis, the AUC was 0.91 (95 % confidence interval [CI], 0.88–0.93) demonstrating that 64-slice coronary CTA had a good diagnostic capacity [3].

More recently, the PROMISE and SCOT-HEART trials collectively investigating over 14,000 patients demonstrated the potential incremental value of coronary CTA over conventional practice in investigating patients with suspected angina due to coronary heart disease [4, 5]. In the PROMISE study, coronary CTA was shown to be non-inferior to functional testing over a median follow-up of 2 years and allowed for better understanding of the coronary anatomy and presence of obstructive disease before the patient entered the catheterization laboratory. This in turn was shown to reduce the likelihood of the patient undergoing invasive angiography demonstrating no obstructive CAD, as well as improving secondary prevention [4]. SCOT-HEART showed similar results, namely, that the addition of coronary CTA to standard medical therapy leads to an incremental benefit. In particular, a noninvasive understanding of the presence of obstructive disease reduced the likelihood of the patient undergoing invasive angiography demonstrating no obstructive CAD. Furthermore, coronary CTA allowed for the appropriate targeting of revascularization strategies and secondary prevention [5].

Beyond luminography and tissue characterization, multislice CT (MSCT) was unable to provide a functional assessment of the severity of the epicardial narrowings. Over the last 15 years, research in the field has made major progress and some landmark discoveries, including the introduction and validation of patient-specific 3-D blood flow analysis, the development of adaptive finite-element models for simulating cardiovascular blood flow, the definition of physiologically realistic inflow and outflow boundary conditions, as well as the coupled description of blood flow and vessel wall dynamics. These advances have allowed the development of algorithms to calculate FFR noninvasively using coronary CTA ($FFR_{CT}$).

## 22.2 Fractional Flow Reserve

Fractional flow reserve (FFR), the ratio of maximal blood flow on either side of a coronary artery stenosis (distal vessel pressure divided by proximal vessel pressure), was introduced almost two decades ago [6]. FFR has been intensively validated and has demonstrated its clinical utility in deferring percutaneous treatment in non-flow-limiting stenoses [7]. Furthermore, recent studies have reported that FFR-guided coronary revascularization leads to improved clinical outcomes and reduced costs compared with angiography-guided coronary revascularization alone [8]. The current guidelines emphasize the role of invasive FFR to determine the functional significance of a coronary stenosis [9].

In clinical practice, the interventional cardiologist has information derived from noninvasive angiography studies suggesting the presence of additional coronary lesions above those involved in the etiology of an ischemic condition. The functional effects of a lesion rather than the degree of narrowing predict the potential benefit of revascularization. These tests (radio-nuclear, echocardiography, magnetic resonance imaging) constitute a severe financial burden for society [10, 11]. The desire to have a single diagnostic modality providing all the information in one single noninvasive assessment is long awaited [12].

## 22.3 Principles of Noninvasive FFR Assessment with MSCT

$FFR_{CT}$ technology is based on three key underlying principles for the generation of physiologic models of coronary blood flow.

According to the first principle, baseline coronary blood flow is met by myocardial demand for oxygen at rest. Allometric scaling laws in the form $Q_c^{rest} \propto M_{myo}\, k$ can be used to estimate physiological parameters, for instance, coronary flow ($Q_c$), under baseline conditions given an organ mass $M_{myo}$; $k$ is the scaling factor [13, 14]. Adherence to this principle enables calculation of total resting coronary blood flow relative to patient-specific left and right ventricular mass quantified from the same MSCT scan. Naturally, this assumption does not apply to patients with angina at rest, and therefore $FFR_{CT}$ technology cannot be utilized in this group.

The second principle claims that the resistance of the microcirculatory vascular bed at rest is inversely, but not linearly, proportional to the size of the feeding vessel as demonstrated in prior morphometry, shear stress autoregulation, and compensatory remodeling research [15–20]. In other

words, healthy and diseased blood vessels adapt to the amount of flow they carry. Power law relationships in the form $r_p^k = r_{d1}^k + r_{d2}^k$ apply to the coronary arteries; autoregulation of wall shear stress provides the mechanism to explain observed power laws inherent in flow-diameter relationships [17, 18].

The third principle states that the coronary microcirculation has a predictable response to adenosine, which is produced as soon as the heart lacks $O_2$. Exogenous administration of adenosine elicits the maximum hyperemic responses by producing complete relaxation of the smooth muscle cells lining the resistance arterioles. Importantly, $FFR_{CT}$ technology does not require any modifications in CCTA acquisition protocols, additional imaging, or administration of additional drugs.

## 22.4 Cardiovascular Computational Fluid Dynamics

Any application of computational fluid dynamics to structures as small as the coronary circulation bed requires unique capabilities for finite-element mesh generation and modification [21]. Flow of an incompressible fluid, such as blood, submitted to a high driving pressure (e.g., 100 mmHg) may be highly accelerated when a small additional gradient of pressure is applied. This can generate significant changes in wall shear stress that require custom solving tools. Within current algorithms, finite-element meshes can iteratively adapt their resolution in an anisotropic fashion; the distribution of element size and density can be modified according to computation requirements [22, 23]. In areas of less complex flow, the mesh elements may be coarser and less dense. Structured layers of elements are required near the vessel wall (boundary layers), in order to enhance the accuracy of wall shear stress computations, especially in highly/exceedingly curved vessels [24]. On the other hand, flow-pressure variations in the coronary arteries cannot be directly measured, as they are inherently part of the solution. Coronary flow distribution is modulated by both the resistance of the downstream vascular bed and the intramyocardial pressure due to ventricular myocardium contraction [25]. Flow is not always proportional to pressure; thus, their relationship at the outlets of the coronaries is better expressed in the form of outflow boundary conditions coupling the 3-D epicardial domain to the microvasculature. Conversely, the influence of preload, heart rate, contractility, and cardiac output can be modeled in appropriately set inflow boundary conditions [26].

## 22.5 Calculation of $FFR_{CT}$

Based upon the aforementioned three principles for the generation of physiologic models of coronary blood flow, proprietary algorithms using cardiovascular computational flow dynamics were created. The anatomy of the coronary arterial bed of a particular patient is not known a priori and has to be extracted from a patient-specific medical imaging dataset;

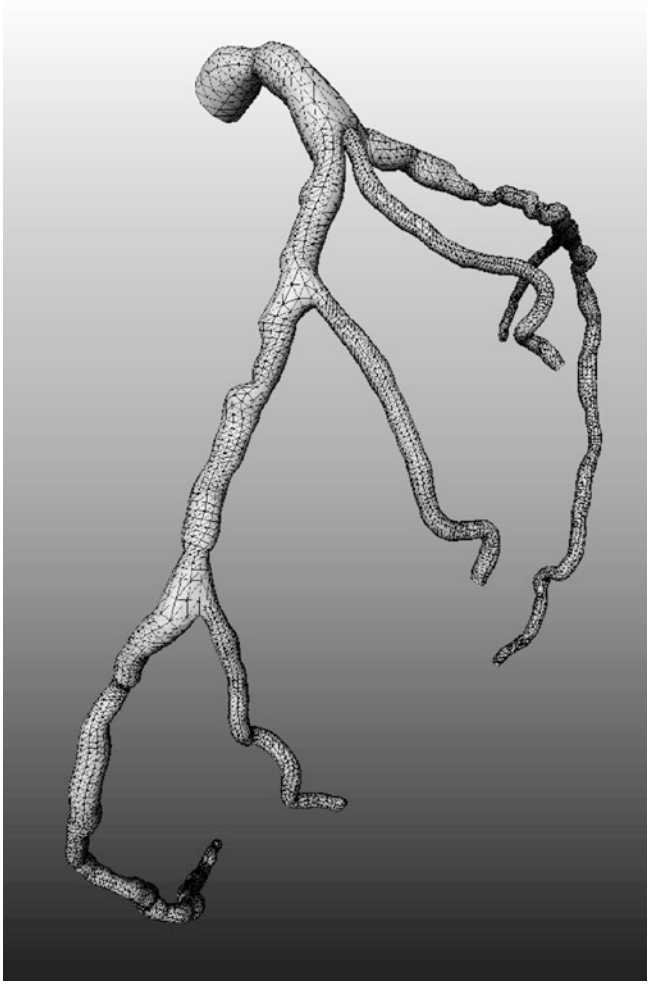

**Fig. 22.1** Finite element mesh. The distribution of element size and density can be iteratively adapted to computation requirements

MSCT can provide an accurate coronary geometric model, including branching and pathology specific to a patient. Based upon this geometric information, a volumetric finite-element mesh with anisotropic refinement and boundary layers is generated in order to compute numerical results (Fig. 22.1). Using a proprietary algorithm, the heart-vessel interaction can be defined and time-varying coronary resistance for each coronary branch determined relative to intramyocardial pressure and microvasculature impedance. This latter component can be represented by a so-called lumped (zero-dimensional) parameter model, which resembles an electric circuit, including resistive and capacitive elements (Fig. 22.2) [25]. Finally, the complex fluid properties of the blood are integrated/entered into the model, in order to refine/complete the computations.

Upon completion of the blood flow analysis, mean coronary pressure is extracted from the computer analysis performed under maximum hyperemic conditions. The $FFR_{CT}$ is defined as the computed mean coronary pressure distal to a lesion divided by the computed mean blood pressure in the aorta under conditions of simulated maximum hyperemia. This allows for a measure of lesion-specific ischemia.

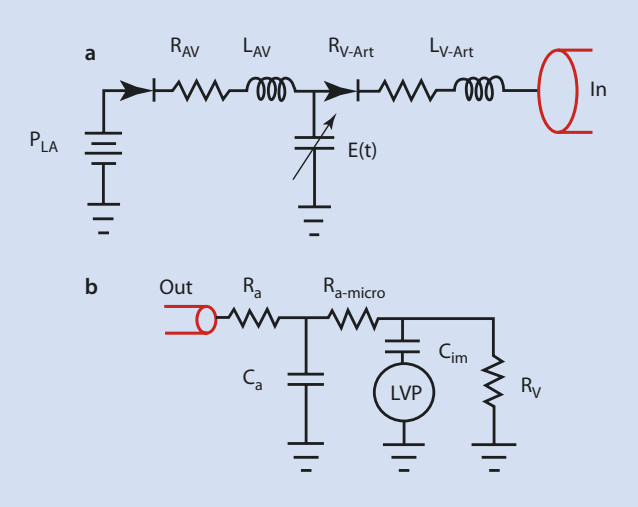


**Fig. 22.2** Lumped (zero-dimensional) parameter models used in cardiovascular blood flow simulations. (**a**) Lumped parameter heart model coupling the left heart side to the aortic inlet (In) of a closed loop system comprising the systemic and pulmonary circulation. The left heart model consists of left atrial pressure PLA, mitral valve, atrio-ventricular valvular resistance RAV, atrio-ventricular inductance LAV, aortic valve, ventriculo-arterial valvular resistance RV-Art, ventriculo-arterial inductance LV-Art, and left ventricular (LV) pressure. The LV pressure is modeled with time-varying LV elastance E(t). (**b**) Lumped parameter coronary vascular bed model coupled to a coronary branch outlet (Out). This model consists of coronary arterial and venous resistance (Ra and Rv respectively), coronary arterial microcirculation resistance Ra-micro, coronary arterial compliance Ca, myocardial compliance Cim, and LV pressure; LV pressure stands for intra-myocardial pressure for branches emerging from the left coronary artery

## 22.6 Clinical Validation of $FFR_{CT}$

The first iteration of this technology was evaluated in the DISCOVER-FLOW (diagnosis of ischemia-causing stenoses obtained via noninvasive fractional flow reserve) trial and DeFACTO (determination of fractional flow reserve by anatomic computed tomographic angiography) trial [27, 28]. The main finding of these studies was the incremental accuracy of $FFR_{CT}$ above coronary CTA stenosis, with an observed diagnostic specificity and accuracy of $FFR_{CT}$ vs. stenosis quantification (stenosis >50 %) of 54 % (95 % CI, 46 %–83 %) vs. 42 % (95 % CI, 34 %–51 %) and 73 (95 % CI, 67 %–78 %) vs. 64 % (95 % CI, 58 %–70 %), respectively. The NeXt sTeps study aimed to assess the diagnostic performance of FFRCT by using invasive FFR as the reference standard in patients referred for **non-emergent** invasive coronary angiography. In this study, improved $FFR_{CT}$ technology (updated proprietary software with quantitative image quality analysis, improved image segmentation, refined physiological models, and increased automation) was used. The primary endpoint was per-patient diagnostic performance as assessed by the area AUC of $FFR_{CT}$ (≤0.80) versus coronary CTA (stenosis >50 %) for the diagnosis of hemodynamically significant stenosis with an invasive FFR ≤ 0.80 in patients with coronary CTA stenosis of 30–90 %. 365 patients were screened and 251 patients were included. Per-patient and per-vessel AUC for $FFR_{CT}$ were 0.90 (95 % CI: 0.87–0.94) and 0.93 (95 % CI: 0.91–0.95), respectively. There was a high correlation at per-vessel level between $FFR_{CT}$ to FFR (Pearson's correlation

**Fig. 22.3** Diagnostic performance of FFRCT in the NXT trial compared to invasive FFR and non-invasive diagnostic cases. *CCTA* coronary CT angiography, *FFR* fractional flow reserve, *SPECT* Single-photon emission computed tomography, *IVUS* Intravascular Ultrasound, *TAG* Transattenuation Gradient

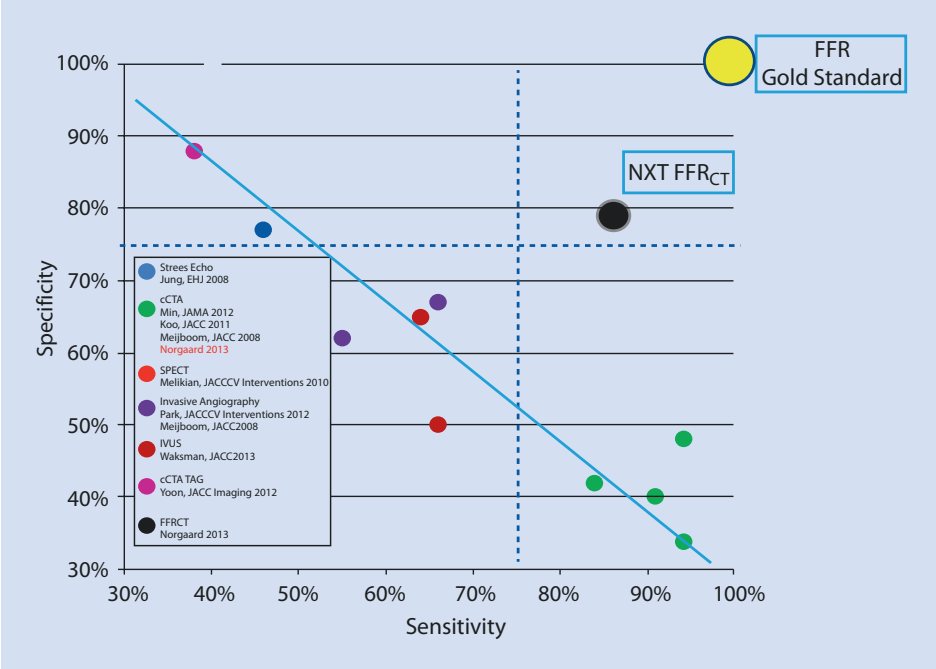

coefficient 0.82; $p < 0.001$), with a slight underestimation of $FFR_{CT}$ compared to FFR. In this study, $FFR_{CT}$ demonstrated a substantial improvement in diagnostic performance, high sensitivity, specificity, and negative and positive predictive value (per vessel 86 % and 95 %, respectively) becoming an attractive alternative compared to other noninvasive modalities. $FFR_{CT}$ was superior to every diagnostic test except conventional FFR for diagnosing functional disease of the coronary arteries (Fig. 22.3). Table 22.1 summarizes the main evidence supporting $FFR_{CT}$.

Following three major validation studies comparing the diagnostic accuracy of $FFR_{CT}$ with invasive FFR, the

**Table 22.1** Literature on noninvasive FFR derivation

| First author | Year | Journal | Title |
|---|---|---|---|
| *Patient-specific 3D blood flow analysis and treatment planning* | | | |
| Taylor CA | 1998 | *Computer Methods in Applied Mechanics and Engineering* | Finite-element modeling of blood flow in arteries |
| Taylor CA | 1999 | *Computer Aided Surgery* | Predictive medicine: Computational techniques in therapeutic decision-making |
| *Validation of patient-specific blood flow analysis* | | | |
| Ku JP | 2002 | *Annals of Biomedical Engineering* | In vivo validation of numerical prediction of blood flow in arterial bypass grafts |
| Ku JP | 2005 | *Annals of Biomedical Engineering* | Comparison of CFD and MRI flow and velocities in an in vitro *l*arge artery bypass graft model |
| Steele BN | 2003 | *IEEE Transactions on Biomedical Engineering* | In vivo validation of an one-dimensional finite-element method for predicting blood flow in cardiovascular bypass grafts. |
| Steele BN | 2007 | *Computer Methods in Biomechanics and Biomedical Engineering* | Fractal network model for simulating abdominal and lower extremity blood flow during resting and exercise conditions |
| *Anisotropic, adaptive and boundary layer mesh generation for cardiovascular flow* | | | |
| Müller J | 2005 | *Computer Methods in Biomechanics and Biomedical Engineering* | Anisotropic adaptive finite-element method for modeling blood flow |
| Sahni O | 2006 | *Computer Methods in Applied Mechanics and Engineering* | Efficient anisotropic adaptive discretization of the cardiovascular system |
| Sahni O | 2008 | *Engineering with Computers* | Adaptive boundary layer meshing for viscous flow simulations |
| Sahni O | 2009 | *Engineering with Computers* | Automated adaptive cardiovascular flow simulations |
| *Physiologically realistic outflow boundary conditions and Coupled blood flow-wall dynamics* | | | |
| Vignon-Clementel IE | 2006 | *Computer Methods in Applied Mechanics and Engineering* | Outflow boundary conditions for three-dimensional finite-element modeling of blood flow and pressure in arteries |
| Spilker RL | 2010 | *Annals of Biomedical Engineering* | Tuning multi-domain hemodynamic simulations to match physiological measurements |
| Figueroa CA | 2006 | *Computer Methods in Applied Mechanics and Engineering* | A coupled momentum method for modeling blood flow in three-dimensional deformable arteries |
| Vignon-Clementel IE | 2010 | *Computer Methods in Biomechanics and Biomedical Engineering* | Outflow boundary conditions for 3D simulations of non-periodic blood flow and pressure fields in deformable arteries |
| *Direct 3D image segmentation and geometric modeling* | | | |
| Bekkers EJ | 2008 | *IEEE Transactions on Medical Imaging* | Multiscale vascular surface model generation from medical imaging data using hierarchical features. |
| Xiong G | 2011 | *International Journal for Numerical Methods in Biomedical Engineering* | Simulation of blood flow in deformable vessels using subject-specific geometry and spatially varying wall properties |

(continued)

**Table 22.1** Literature on noninvasive FFR derivation

| First author | Year | Journal | Title |
|---|---|---|---|
| *Development of methods for modeling coronary flow and autoregulatory mechanisms* | | | |
| Kim HJ | 2009 | *Computer Methods in Applied Mechanics and Engineering* | Augmented Lagrangian method for constraining the shape of velocity profiles at outlet boundaries for three-dimensional finite-element simulations of blood flow |
| Kim HJ | 2009 | *Annals of Biomedical Engineering* | On coupling a lumped parameter heart model and a three-dimensional finite-element aorta model |
| Kim HJ | 2010 | *Finite Elements in Analysis and Design* | Developing computational methods for three-dimensional finite-element simulations of coronary blood flow |
| Kim HJ | 2010 | *Annals of Biomedical Engineering* | Patient-specific modeling of blood flow and pressure in human coronary arteries |
| Kim HJ | 2010 | *Annals of Biomedical Engineering* | Incorporating autoregulatory mechanisms of the cardiovascular system in three-dimensional finite-element models of arterial blood flow |
| *Clinical validation studies* | | | |
| Koo BK | 2011 | *Journal American College of Cardiology* | Diagnosis of ischemia-causing coronary stenoses by noninvasive fractional flow reserve computed from coronary computed tomographic angiograms. Results from the prospective multicenter DISCOVER-FLOW (diagnosis of ischemia-causing stenoses obtained via noninvasive fractional flow reserve) study |
| Min JK | 2012 | *JAMA* | DeFacto study: Diagnostic accuracy of fractional flow reserve from anatomic CT angiography |
| Norgaard BL | 2014 | *Journal American College of Cardiology* | Diagnostic performance of noninvasive fractional flow reserve derived from coronary CT angiography in suspected coronary artery disease: The NXT trial |
| Douglas P | 2015 | *European Heart Journal* | Clinical outcomes of FFRCT-guided diagnostic strategies versus usual care in patients with suspected coronary artery disease: the PLATFORM study |

*3D* three dimensional, *CFD* computational fluid dynamics, *FFR* fractional flow reserve, *MRI* magnetic resonance imaging

PLATFORM trial (clinical outcomes of fractional flow reserve by computed tomographic angiography-guided diagnostic strategies vs. usual care in patients with suspected coronary artery disease: the prospective longitudinal trial of $FFR_{CT}$ – outcome and resource impacts study) was the first to evaluate the performance of this technology in the real-world workup of stable patients with suspected coronary artery disease (CAD). Using a comparative effectiveness observational design, this trial included symptomatic patients with planned invasive or noninvasive evaluation for the presence of obstructive CAD. Two cohorts (planned invasive or noninvasive approach) were sequentially subdivided to receive the usual care or $CTA/FFR_{CT}$. In the primary endpoint, the rate of invasive coronary angiography with no obstructive CAD within 90 days was significantly higher in patients allocated usual care versus the $FFR_{CT}$ strategy (73.3 % vs. 12.4 %, risk difference 60.8 % CI 53.0–68.7 %, $p < 0.001$). $FFR_{CT}$ also led to more ischemia-guided revascularization (95 % $CTA/FFR_{CT}$ vs. 55 % usual care) complying with current guidelines. These findings support the use of $FFR_{CT}$ as a triage tool before patients are referred for invasive angiography.

## 22.7 Future Applications of $FFR_{CT}$

### 22.7.1 Virtual Stenting

Initial studies with coronary $CTA/FFR_{CT}$ have focused on patients with suspected CAD; however, given the comprehensive assessment of anatomical and functional characteristics at the per-lesion level, this technology could be further expanded to patients with known CAD. In patients with sequential coronary stenosis, virtually stenting one lesion and reassessment of $FFR_{CT}$ afterward may help identify the culprit lesion causing myocardial ischemia (Fig. 22.4). Preprocedural planning with this technique could optimize treatment strategies and functional outcomes before the

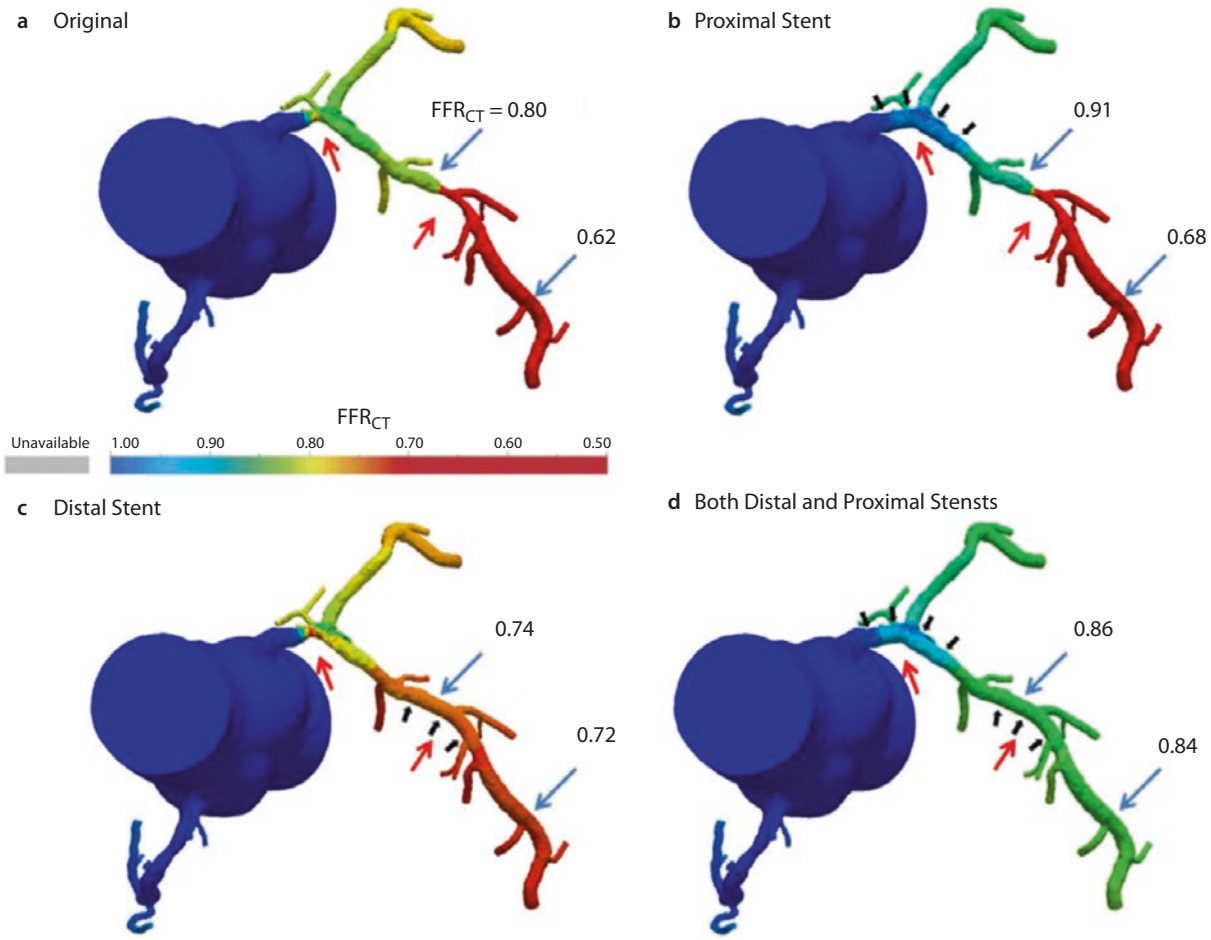


**Fig. 22.4** Virtual revascularization on 3-dimensional model with FFRCT. Red arrows show serial stenoses in left anterior descending artery. Blue arrows show simulated FFRCT values at indicated locations. Black arrows show positions of simulated stents. Before simulated stent implantation FFRCT positive (0.62) (**a**). After simulated stent implantation for distal or proximal stenosis lesion, neither stent implantation for distal nor proximal narrowing in the model gives a negative FFR (0.72 with stent for distal and 0.68 with stent for proximal) (**b** and **c**). After simulated stent implantation for both distal and proximal stenosis lesions, vessel FFRCT is negative (0.84) in this scenario (**d**). FFRCT: Computed fractional flow reserve

invasive procedure. However, further large prospective studies are necessary to validate this tool [29, 30].

### 22.7.2 Three-Vessel Disease with or Without LMS Disease: Heart-Team Clinical Decision-Making Based on MSCT

The latest coronary CTA technology with the addition of FFR$_{CT}$ is capable of identifying patients with functionally significant multivessel disease. This noninvasive evaluation has the potential to reclassify the patients to a lower risk group (i.e., one or two vessels) disease. Furthermore, in patients referred for surgical revascularization, anatomical characteristics at the graft anastomosis site (e.g., vessel wall calcifications, intramyocardial course, etc.) may aid the surgeon in the decision-making process. In this population, current guidelines recommend (IB) risk stratification based on the extent and severity of the CAD [9]. For this purpose, the anatomical SYNTAX (SYNergy between percutaneous coronary intervention with TAXus and cardiac surgery) score has proven to be a valuable and reproducible tool using both coronary angiography and MSCT [31, 32, 33]. Moreover, the addition of clinical variables to the anatomic score (angiography or coronary CTA based) to calculate the SYNTAX II score further enhances the decision-making process between CAGB and PCI for an individual patient [34]. The SYNTAX III REVOLUTION trial will include patients with multivessel disease with or without left main disease and will randomize two Heart Teams who, with guidance of the SYNTAX II score, will make a decision between surgical or percutaneous treatment based on either a conventional angiography or MSCT angiography with the incremental value of FFR$_{CT}$. This study will set the foundations for the integration of coronary CTA in the decision-making process in patients with complex coronary artery disease.

## 22.8 Conclusion

Over the past decade, noninvasive imaging using MSCT has made major progress with luminography and tissue characterization improving, due to a continuous increase in spatial

(16, 64, 128, 256, and 320 detectors/slices) and temporal resolution, despite some inherent limitations of X-ray regarding tissue characterization. The addition of functional assessment for flow-limiting lesions is a quantum leap in the noninvasive evaluation of patients prior to PCI with the option of virtual treatment planning. Therefore, a single MSCT study will ultimately provide us with comprehensive "one-stop" noninvasive evaluation of the coronaries able to guide interventional and surgical revascularization.

## 22.9 Example Clinical Cases

### Case 1

A 65-year-old male patient with stable angina; coronary risk factors included hypertension and hypercholesterolemia. MSCT angiography showed two stenotic lesions, one in the ostium of the left anterior descending (LAD) coronary artery and one in the midportion of the right coronary artery (RCA), respectively. The $FFR_{CT}$ distal to the RCA lesion was 0.88, while the invasive FFR was 0.89. The mid-LAD had a $FFR_{CT}$ of 0.70 vs. 0.74 with the invasive approach (Fig. 22.5). Virtual PCI of the LAD ostium resulted in a limited improvement, $FFR_{CT}$ increasing from 0.77 to 0.80. The striking observation was a drop in $FFR_{CT}$ along the left main stem (LMS) measuring 0.81 in its midportion. Virtual treatment of LMS normalized $FFR_{CT}$ in the mid-LAD ($FFR_{CT} = 0.90$). The combined treatment of the LMS and ostial LAD resulted in further improvement of the $FFR_{CT}$ to a value of 0.93.

### Case 2

A bioresorable everolimus-eluting scaffold was implanted in the proximal RCA 5 years previously. At 6- and 24-month follow-up, the conventional angiography did not show any significant stenosis in the scaffolded segment. At 5-year

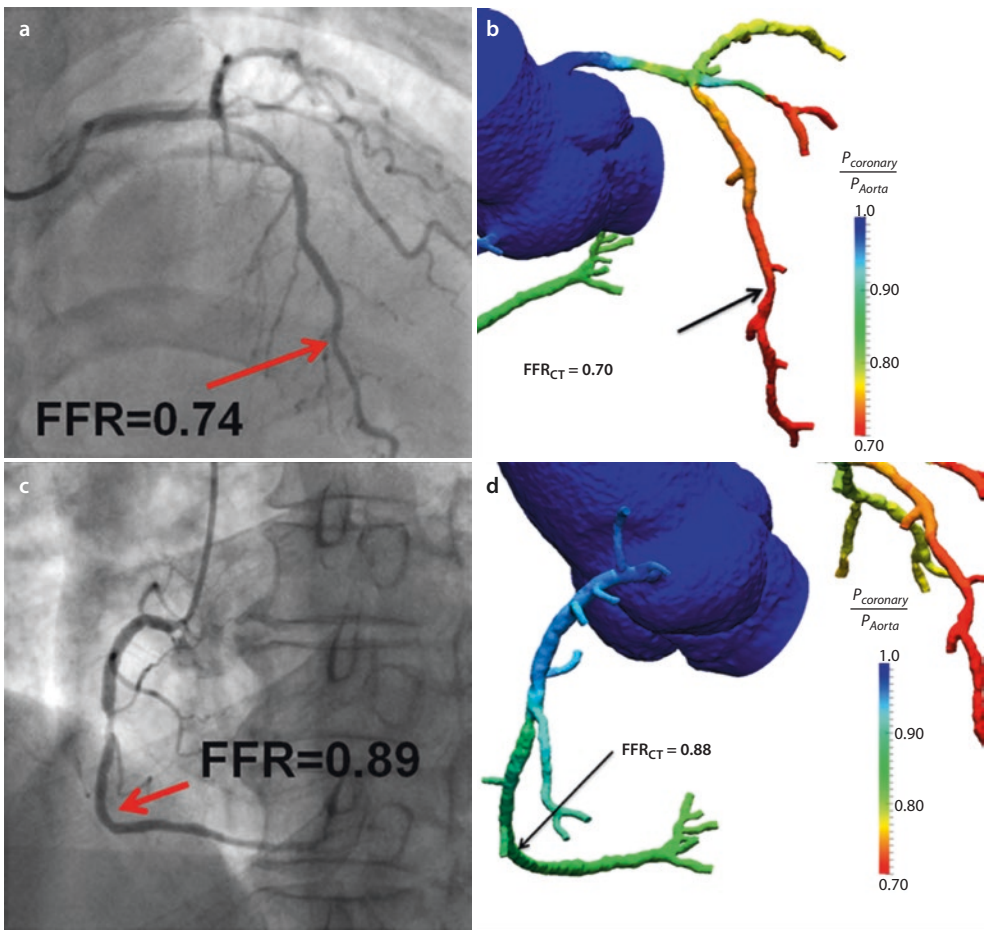


**Fig. 22.5** Clinical case 1. Invasive vs. non-invasive FFR values in a left anterior descending (**a**, **b**) and a right coronary artery (**c**, **d**). Using the invasive FFR as a reference standard and a cut-off of <0.80, FFRCT provides a true positive and a true negative result respectively. Right sided images show CCTA based reconstructions of the respective vessels; the color scale is based on the FFRCT values. *CCTA* coronary CT angiography, *FFR* fractional flow reserve

follow-up, MSCT scan showed a patent, non-stenotic scaffolded area demarcated by the two radiopaque platinum markers (black arrows [Fig. 22.6]). On the maximum intensity projection, two small calcified plaques are visible distal to the scaffold. Noninvasive functional assessment showed that all three vessels exhibit $FFR_{CT}$ values distally above the threshold of 0.80.

## Case 3

A 64-year-old male with a history of hypertension presented with typical stable angina CCS II. Left ventricular ejection fraction was 70 % with no regional wall motion abnormalities. MSCT with $FFR_{CT}$ was performed with anatomical and functional three-vessel disease and an anatomic Syntax score of 13. Syntax II score predicted a 4-year mortality of 4 % for CABG and 3 % for PCI. The patient subsequently underwent invasive angiography with FFR assessment. There was a severe ischemic lesion in the midportion of the RCA, detected noninvasively with $FFR_{CT}$ and confirmed by invasive FFR. In the mid-LAD, there was a severe lesion with positive $FFR_{CT}$ and invasive FFR. In the small circumflex artery, a severe ischemic lesion was identified by $FFR_{CT}$ and confirmed by invasive measurement of FFR. In this case, perfect agreement at the per-lesion level was found (Fig. 22.7).

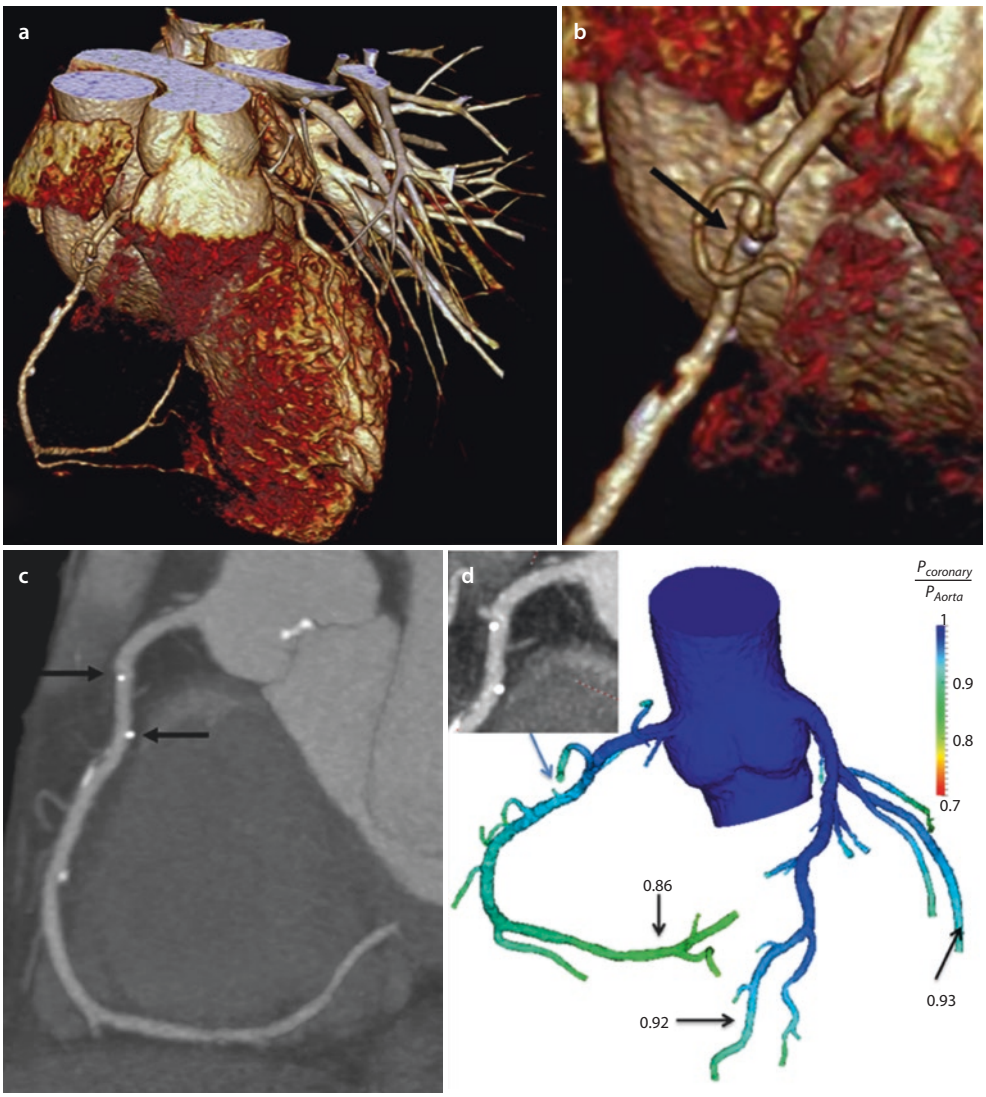


**Fig. 22.6** Clinical case 2. (**a**) Three-dimensional volume-rendered CT angiogram of a right coronary artery. Magnification of the proximal artery segment in the volume-rendered image (**b**) and a curved multi-planar image (**c**) show the platinum markers of the resorbed stent (*black arrows*). (**d**) Non-invasive FFR derivation did not show ischemia in any of the coronary arteries

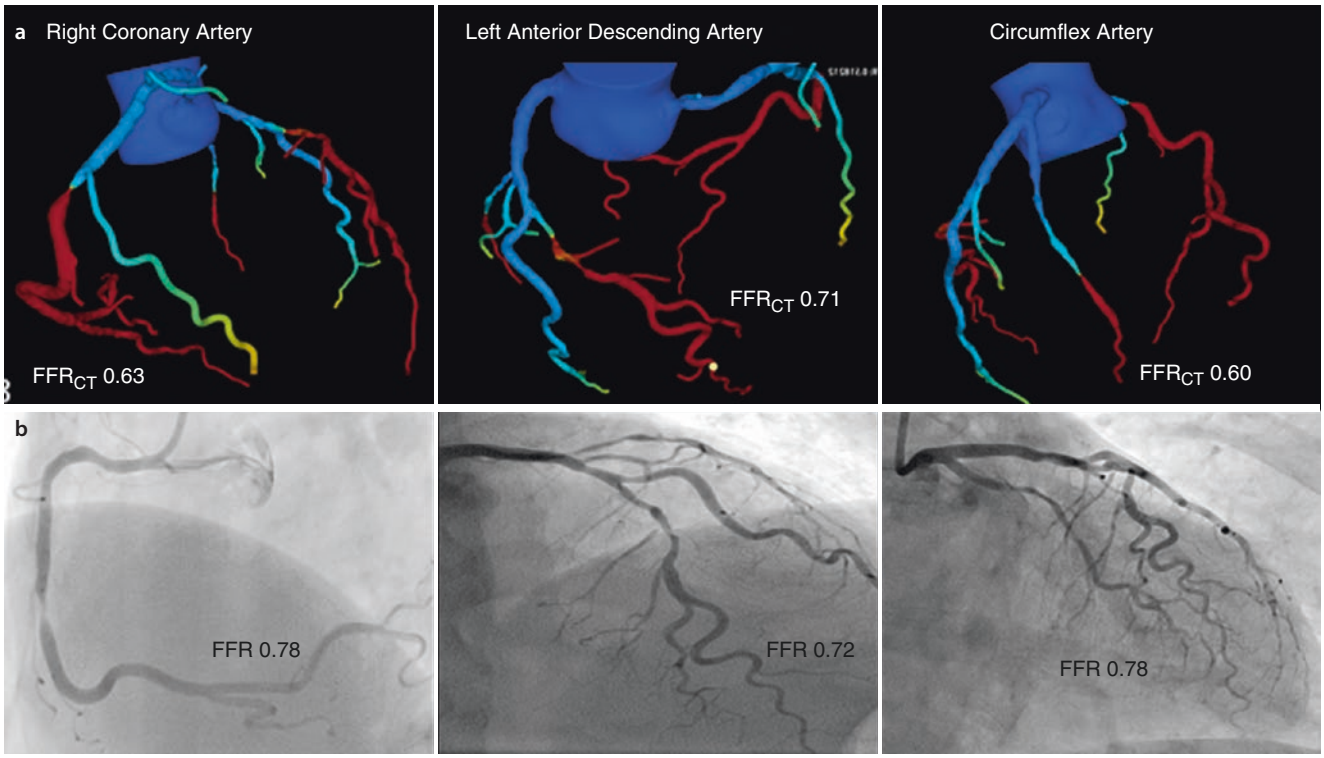


**Fig. 22.7** Clinical case 3. MSCT with FFRCT were performed before angiography and found an anatomical and functional 3 vessel disease. In the mid portion of the RCA a severe ischemic lesion was detected non-invasively with FFRCT and confirmed with an invasive FFR. In the mid LAD, a severe lesion with almost identical FFRCT and FFR. In the circumflex artery a severe ischemic lesion was identified by FFRCT and confirmed by invasive measurement of FFR. In this case, perfect agreement at the per-lesion level was found in a patient with multivessel disease

## 22.10 Glossary

**Allometry** Change in proportion of various parts of an object/organism as a consequence of growth

**Anisotropy** Having properties that differ according to the direction of measurement

**Impedance** Frequency analogue of resistance

**Lumped (model)** Zero-dimensional model

## References

1. Nieman K, Cademartiri F, Lemos PA, Raaijmakers R, Pattynama PM, de Feyter PJ. Reliable noninvasive coronary angiography with fast submillimeter multislice spiral computed tomography. Circulation. 2002;106(16):2051–4.
2. Arbab-Zadeh A, Hoe J. Quantification of coronary arterial stenoses by multidetector CT angiography in comparison with conventional angiography methods, caveats, and implications. JACC Cardiovasc Imaging. 2011;4(2):191–202.
3. Miller JM, Rochitte CE, Dewey M, Arbab-Zadeh A, Niinuma H, Gottlieb I, et al. Diagnostic performance of coronary angiography by 64-row CT. N Engl J Med. 2008;359(22):2324–36.
4. Douglas PS, Hoffmann U, Patel MR, Mark DB, Al-Khalidi HR, Cavanaugh B, et al. Outcomes of anatomical versus functional testing for coronary artery disease. N Engl J Med. 2015;372(14):1291–300.
5. investigators S-H. CT coronary angiography in patients with suspected angina due to coronary heart disease (SCOT-HEART): an open-label, parallel-group, multicentre trial. Lancet. 2015;385:2383–91.
6. Pijls NH, van Son JA, Kirkeeide RL, De Bruyne B, Gould KL. Experimental basis of determining maximum coronary, myocardial, and collateral blood flow by pressure measurements for assessing functional stenosis severity before and after percutaneous transluminal coronary angioplasty. Circulation. 1993;87(4):1354–67.
7. Pijls NH, van Schaardenburgh P, Manoharan G, Boersma E, Bech JW, van't Veer M, et al. Percutaneous coronary intervention of functionally nonsignificant stenosis: 5-year follow-up of the DEFER Study. J Am Coll Cardiol. 2007;49(21):2105–11.
8. Pijls NH, Fearon WF, Tonino PA, Siebert U, Ikeno F, Bornschein B, et al. Fractional flow reserve versus angiography for guiding percutaneous coronary intervention in patients with multivessel coronary artery disease: 2-year follow-up of the FAME (Fractional Flow Reserve Versus Angiography for Multivessel Evaluation) study. J Am Coll Cardiol. 2010;56(3):177–84.
9. Windecker S, Kolh P, Alfonso F, Collet JP, Cremer J, Falk V, et al. 2014 ESC/EACTS Guidelines on myocardial revascularization: the task force on myocardial revascularization of the European Society of Cardiology (ESC) and the European Association for Cardio-Thoracic Surgery (EACTS)Developed with the special contribution of the European Association of Percutaneous Cardiovascular Interventions (EAPCI). Eur Heart J. 2014;35(37):2541–619.
10. Min JK, Hachamovitch R, Rozanski A, Shaw LJ, Berman DS, Gibbons R. Clinical benefits of noninvasive testing: coronary computed tomography angiography as a test case. JACC Cardiovasc Imaging. 2010;3(3):305–15.
11. Schoenhagen P, Hachamovitch R, Achenbach S. Coronary CT angiography and comparative effectiveness research prognostic value of atherosclerotic disease burden in appropriately indicated clinical examinations. JACC Cardiovasc Imaging. 2011;4(5):492–5.
12. Williams MC, Reid JH, McKillop G, Weir NW, van Beek EJ, Uren NG, et al. Cardiac and coronary CT comprehensive imaging approach in the assessment of coronary heart disease. Heart. 2011;97(15):1198–205.

13. West GB, Brown JH, Enquist BJ. A general model for the origin of allometric scaling laws in biology. Science. 1997;276(5309):122–6.
14. Steele BN, Olufsen MS, Taylor CA. Fractal network model for simulating abdominal and lower extremity blood flow during resting and exercise conditions. Comput Methods Biomech Biomed Engin. 2007;10(1):39–51.
15. Murray CD. The physiological principle of minimum work: I. The vascular system and the cost of blood volume. Proc Natl Acad Sci U S A. 1926;12(3):207–14.
16. Hutchins GM, Miner MM, Boitnott JK. Vessel caliber and branch-angle of human coronary artery branch-points. Circ Res. 1976;38(6): 572–6.
17. Kamiya A, Togawa T. Adaptive regulation of wall shear stress to flow change in the canine carotid artery. Am J Physiol. 1980;239(1):H14–21.
18. Zarins CK, Zatina MA, Giddens DP, Ku DN, Glagov S. Shear stress regulation of artery lumen diameter in experimental atherogenesis. J Vasc Surg. 1987;5(3):413–20.
19. Zhou Y, Kassab GS, Molloi S. On the design of the coronary arterial tree: a generalization of Murray's law. Phys Med Biol. 1999;44(12):2929–45.
20. Zhou Y, Kassab GS, Molloi S. In vivo validation of the design rules of the coronary arteries and their application in the assessment of diffuse disease. Phys Med Biol. 2002;47(6):977–93.
21. Kim HJ, Vignon-Clementel IE, Figueroa CA, Jansen KE, Taylor CA. Developing computational methods for three-dimensional finite element simulations of coronary blood flow. Finite Elem Anal Des. 2010;46:514–25.
22. Müller J, Sahni O, Li X, Jansen KE, Shephard MS, Taylor CA. Anisotropic adaptive finite element method for modelling blood flow. Comput Methods Biomech Biomed Engin. 2005;8(5):295–305.
23. Sahni O, Müller J, Jansen KE, Shephard MS, Taylor CA. Efficient anisotropic adaptive discretization of the cardiovascular system. Comput Methods Appl Mech Engin. 2006;195:5634–55.
24. Sahni O, Jansen KE, Taylor CA, Shephard MS. Automated adaptive cardiovascular flow simulations. Eng Comput. 2009;25:25–36.
25. Kim HJ, Vignon-Clementel IE, Coogan JS, Figueroa CA, Jansen KE, Taylor CA. Patient-specific modeling of blood flow and pressure in human coronary arteries. Ann Biomed Eng. 2010;38(10):3195–209.
26. Kim HJ, Vignon-Clementel IE, Figueroa CA, LaDisa JF, Jansen KE, Feinstein JA, et al. On coupling a lumped parameter heart model and a three-dimensional finite element aorta model. Ann Biomed Eng. 2009;37(11):2153–69.
27. Min JK, Leipsic J, Pencina MJ, Berman DS, Koo BK, van Mieghem C, et al. Diagnostic accuracy of fractional flow reserve from anatomic CT angiography. JAMA. 2012;308(12):1237–45.
28. Koo BK, Erglis A, Doh JH, Daniels DV, Jegere S, Kim HS, et al. Diagnosis of ischemia-causing coronary stenoses by noninvasive fractional flow reserve computed from coronary computed tomographic angiograms. Results from the prospective multicenter DISCOVER-FLOW (Diagnosis of Ischemia-causing Stenoses obtained via Noninvasive Fractional Flow Reserve) study. J Am Coll Cardiol. 2011;58(19):1989–97.
29. Kim KH, Doh JH, Koo BK, Min JK, Erglis A, Yang HM, et al. A novel noninvasive technology for treatment planning using virtual coronary stenting and computed tomography-derived computed fractional flow reserve. JACC Cardiovasc Interv. 2014;7(1):72–8.
30. Tanaka K, Bezerra HG, Gaur S, Attizzani GF, Botker HE, Costa MA, et al. Comparison between Non-invasive (coronary computed tomography angiography derived) and invasive-fractional flow reserve in patients with serial stenoses within One coronary artery: a NXT trial substudy. Ann Biomed Eng. 2016;44(2):580–9.
31. Serruys PW, Morice MC, Kappetein AP, Colombo A, Holmes DR, Mack MJ, et al. Percutaneous coronary intervention versus coronary-artery bypass grafting for severe coronary artery disease. N Engl J Med. 2009;360(10):961–72.
32. Kerner A, Abadi S, Abergel E, Solomonica A, Aronson D, Roguin A, et al. Direct comparison between coronary computed tomography and invasive angiography for calculation of SYNTAX score. EuroIntervention. 2013;8:1428–34.
33. Papadopoulou SL, Girasis C, Dharampal A, Farooq V, Onuma Y, Rossi A, et al. CT-SYNTAX score: a feasibility and reproducibility Study. JACC Cardiovasc Imaging. 2013;6(3):413–5.
34. Farooq V, van Klaveren D, Steyerberg EW, Meliga E, Vergouwe Y, Chieffo A, et al. Anatomical and clinical characteristics to guide decision making between coronary artery bypass surgery and percutaneous coronary intervention for individual patients: development and validation of SYNTAX score II. Lancet. 2013;381(9867): 639–50.

# Supplementary Information




J. Escaned, J. Davies (eds.), *Physiological Assessment of Coronary Stenoses and the Microcirculation*,
DOI 10.1007/978-1-4471-5245-3

# Index

# D



# E



# F

# G



# H



# I

# L



# M



# N



# P



# R



# S



# T

# U



# V



# W